

**Relationships among the physical and  
chemical properties of soil, vegetation  
and land degradation in semi-arid  
environments**

**Jennifer Ann Dickie**

Thesis submitted to the University of Leicester  
for the degree of Doctor of Philosophy  
in the Department of Geography

2006

UMI Number: U231361

All rights reserved

INFORMATION TO ALL USERS

The quality of this reproduction is dependent upon the quality of the copy submitted.

In the unlikely event that the author did not send a complete manuscript and there are missing pages, these will be noted. Also, if material had to be removed, a note will indicate the deletion.



UMI U231361

Published by ProQuest LLC 2014. Copyright in the Dissertation held by the Author.  
Microform Edition © ProQuest LLC.

All rights reserved. This work is protected against  
unauthorized copying under Title 17, United States Code.



ProQuest LLC  
789 East Eisenhower Parkway  
P.O. Box 1346  
Ann Arbor, MI 48106-1346

**Relationships among the physical and chemical properties of soil, vegetation and land degradation in semi-arid environments.**



**Jennifer Ann Dickie**

Thesis submitted to the University of Leicester  
for the Degree of Doctor of Philosophy  
in the Department of Geography

2006

## **Abstract**

This study examines the spatial patterns of soil parameters to test the hypothesis that shrub encroachment initiates a change in scale of soil heterogeneity, which consequently influences a landscape's biotic and abiotic interactions and thus the susceptibility of soil to erosion. Grassland, shrubland and badland sites were established in two semi-arid environments; the Karoo, South Africa and the Sevilleta National Wildlife Refuge, New Mexico, U.S. 108 soil samples from each of the eleven 60m x 60m plots were analysed for bulk density, shear strength, texture, aggregate stability, organic matter content, pH, conductivity and available sodium, calcium, magnesium, potassium and phosphorus content. Geostatistical analyses determined that, at a scale representative of the vegetation community, the grassland landscape appeared relatively homogenous in its distribution of soil parameters. Shrublands, however, demonstrated an increase in heterogeneity of all soil parameters. Periodicity in the semi-variograms indicated that regular patterns across the landscape were evident for all parameters and thus likely to represent the differences between shrub and intershrub regions. Due to the complex plant-soil interactions, and the interactions amongst the soil parameters themselves, the cyclic patterns represent areas of high and low erodibility. More pronounced patterns were identified in the badlands. This indicates that, if the conditions are right, changes in plant-soil interactions caused by soil parameter redistribution in shrubland landscapes can exacerbate erosion leading to further degradation in the form of badlands. Comparisons between the two semi-arid regions suggest that although local variations in soil type and different species of vegetation will affect the intensity of the spatial response, the underlying patterns are similar at both locations and hence, potentially, at a global scale.



## TABLE OF CONTENTS

### **CHAPTER ONE: Introduction**

<b>1.1 Overall aim</b> _____	<b>1</b>
<b>1.2 Changing landscapes: the concept of desertification</b> _____	<b>3</b>
1.2.1 <i>Shrub encroachment and vegetation dynamics</i> _____	6
1.2.2 <i>Vegetation and soil property interactions</i> _____	7
1.2.3 <i>Badland development</i> _____	10
<b>1.3 Structure of thesis</b> _____	<b>12</b>

### **CHAPTER TWO: Literature Review**

#### **Understanding the complexities of vegetation change on soil properties and their effect on land degradation**

<b>2.1 Brief overview: the importance of vegetation</b> _____	<b>14</b>
<b>2.2 The physical and chemical properties of soil and their influence on the susceptibility of soil to erosion</b> _____	<b>18</b>
<b>2.3 The implications of changing spatial patterns of soil properties on soil erosion</b> _____	<b>28</b>
2.3.1 <i>The concept of heterogeneity</i> _____	28
2.3.2 <i>Implications of spatial heterogeneity on the erosional response of the landscape</i> _____	29
2.3.3 <i>A function of scale?</i> _____	36
<b>2.4 Summary and formulation of objectives</b> _____	<b>40</b>

### **CHAPTER THREE: Methodology**

#### **Description of the Study Area and Analysis Methods**

<b>3.1 Specific study area requirements</b> _____	<b>44</b>
<b>3.2 Description of the study area: The Karoo, South Africa</b> _____	<b>47</b>
3.2.1 <i>Vegetation change and historical legacies</i> _____	47
3.2.2 <i>Specific site description</i> _____	53



<b>3.3 Description of the study area: The Sevilleta National Wildlife Refuge, New Mexico</b>	60
<b>3.4 Sampling strategy for field studies</b>	66
<b>3.5 Physical Properties of Soil: Field and Laboratory Techniques</b>	71
3.5.1 <i>Shear Strength</i>	71
3.5.2 <i>Organic Matter Content of Soil</i>	72
3.5.3 <i>Dry Bulk Density</i>	73
3.5.4 <i>Moisture Content</i>	74
3.5.5 <i>Texture</i>	74
3.5.6 <i>Aggregate Stability</i>	76
<b>3.6 Chemical Properties of Soil: Field and Laboratory Techniques</b>	76
3.6.1 <i>pH</i>	76
3.6.2 <i>Soil Salinity and Conductivity</i>	77
3.6.3 <i>Nutrient Analysis</i>	78
<b>3.7 Statistical and Geostatistical Methods</b>	79
3.7.1 <i>Brief Overview</i>	79
3.7.2 <i>Calculation of the experimental semi-variogram</i>	83
3.7.3 <i>Variogram models</i>	85
<b>3.8 Summary</b>	89

## **CHAPTER FOUR: Results**

### **Grasslands: Analysis of the Spatial Continuity of Soil Properties**

<b>4.1 Introduction</b>	91
<b>4.2 Organic matter content</b>	93
4.2.1 <i>Results</i>	93
4.2.2 <i>Summary</i>	101
<b>4.3 Bulk density</b>	102
4.3.1 <i>Results</i>	102
4.3.2 <i>Summary</i>	111
<b>4.4 Soil Moisture</b>	111
4.4.1 <i>Results</i>	111



4.4.2 Summary	118
<b>4.5 Shear strength</b>	119
4.5.1 Results	119
4.5.2 Summary	127
<b>4.6 Particle-size distribution analysis</b>	128
4.6.1 Results	128
4.6.2 Summary	131
<b>4.7 Soil-aggregate stability</b>	132
4.7.1 Results	132
4.7.2 Summary	133
<b>4.8 pH</b>	134
4.8.1 Results	134
4.8.2 Summary	141
<b>4.9 Electrical conductivity</b>	141
4.9.1 Results	141
4.9.2 Summary	148
<b>4.10 Nutrient content analysis</b>	149
4.10.1 Results	150
4.10.2 Summary	175
<b>4.11 Key findings from the grassland plots</b>	177

## **CHAPTER FIVE: Results**

### **Shrublands: Analysis of the Spatial Continuity of Soil Properties**

<b>5.1 Introduction</b>	179
<b>5.2 Organic matter content</b>	181
5.2.1 Results	181
5.2.2 Summary	187
<b>5.3 Bulk density</b>	189
5.3.1 Results	189
5.3.2 Summary	197
<b>5.4 Soil Moisture</b>	197
5.4.1 Results	197



5.4.2 Summary	205
<b>5.5 Shear strength</b>	<b>206</b>
5.5.1 Results	206
5.5.2 Summary	213
<b>5.6 Soil-aggregate stability</b>	<b>214</b>
5.6.1 Results	214
5.6.2 Summary	215
<b>5.7 pH</b>	<b>215</b>
5.7.1 Results	215
5.7.2 Summary	222
<b>5.8 Electrical conductivity</b>	<b>223</b>
5.8.1 Results	223
5.8.2 Summary	229
<b>5.9 Nutrient content analysis</b>	<b>230</b>
5.9.1 Results	230
5.9.2 Summary	259
<b>5.10 Key findings from the shrubland plots</b>	<b>261</b>

## **CHAPTER SIX: Results**

### **Badlands: Analysis of the Spatial Continuity of Soil Properties**

<b>6.1 Introduction</b>	<b>263</b>
<b>6.2 Organic matter content</b>	<b>264</b>
6.2.1 Results	264
6.2.2 Summary	271
<b>6.3 Bulk density</b>	<b>272</b>
6.3.1 Results	272
6.3.2 Summary	279
<b>6.4 Soil Moisture</b>	<b>279</b>
6.4.1 Results	279
6.4.2 Summary	286
<b>6.5 Shear strength</b>	<b>287</b>
6.5.1 Results	287



6.5.2 Summary _____	294
<b>6.6 Particle-size distribution analysis _____</b>	<b>295</b>
6.6.1 Results _____	295
6.6.2 Summary _____	299
<b>6.7 Soil-aggregate stability _____</b>	<b>299</b>
6.7.1 Results _____	300
6.7.2 Summary _____	300
<b>6.8 pH _____</b>	<b>301</b>
6.8.1 Results _____	301
6.8.2 Summary _____	307
<b>6.9 Electrical conductivity _____</b>	<b>307</b>
6.9.1 Results _____	307
6.9.2 Summary _____	314
<b>6.10 Nutrient content analysis _____</b>	<b>315</b>
6.10.1 Results _____	315
6.10.2 Summary _____	341
<b>6.11 Key findings from the badland plots _____</b>	<b>342</b>

## **CHAPTER SEVEN: Discussion**

### **Changing Landscapes: the impact of vegetation change**

#### **7.1 Comparing soil parameter characteristics in grasslands and shrublands: a discussion on the impact of vegetation change**

7.1.1 *Grasslands and shrublands: a comparison of soil parameters* \_\_\_\_\_ 345

7.1.2 *Soil heterogeneity and vegetation type: changing spatial patterns or changing scale?* \_\_\_\_\_ 349

#### **7.2 The global applicability of soil parameter characteristics in semi-arid environments: a comparison between the Karoo, South Africa and the Sevilleta NWR, New Mexico**

7.2.1 *Comparison of soil properties between two semi-arid environments* \_\_\_\_\_ 358

7.2.2 *Spatial patterns: globally applicable or locally attributable?* \_ 361



**7.3 Badlands - a logical progression?**

7.3.1 <i>Badlands - a fair description? Characterising the soil properties in badlands and assessing the progressive nature of badland development</i> _____	366
7.3.2 <i>Identifying spatial patterns of soil properties in badlands and assessing the shrubland-badland connectivity</i> _____	370

**CHAPTER EIGHT: Discussion**

**Linking vegetation change and erosion: physical and chemical soil property interactions**

<b>8.1 <i>Vegetation change and the susceptibility of soil to erosion</i></b> __	<b>375</b>
<b>8.2 <i>The consequences for modelling</i></b> _____	<b>388</b>

**CHAPTER NINE: Conclusion** \_\_\_\_\_ 394

<b>Further work</b> _____	<b>401</b>
---------------------------	------------

## LIST OF FIGURES

### CHAPTER ONE

- Figure 1.1** A summary of the desertification process characteristic of some semi-arid environments \_\_\_\_\_ 5
- Figure 1.2** The basic interactions between vegetation, water movement and erosion on hillslopes, showing differences between shrub-dominated landscapes (upper) and grass-dominated landscapes (lower) \_\_\_\_\_ 8
- Figure 1.3** A conceptual model depicting some of the main interactions among some physical and chemical properties of soil and their effect on erosion \_\_\_\_\_ 10

### CHAPTER TWO

- Figure 2.1** Structural model, indicating the relative importance of vegetation cover and plant roots in controlling the intensity of several water erosion processes \_\_\_\_\_ 17
- Figure 2.2** Causal diagram summarising the erosion process in semi-arid environments \_\_\_\_\_ 31

### CHAPTER THREE

- Figure 3.1** Locations of the two study regions, The Karoo, South Africa and The Sevilleta National Wildlife Refuge, New Mexico \_\_\_\_\_ 46
- Figure 3.2** Perceptions of land degradation in South Africa from 1953-1993 showing the influence of (a) Acocks' 1953 expanding Karoo hypothesis on subsequent international syntheses such as those of (b) UNCOD (1977), (c) Dregne 1983 and (d) UNEP (1993) \_\_\_\_\_ 49
- Figure 3.3** a) Biomes of South Africa based on Acocks (1953) b) Biomes of the study region and surrounding districts of Graaff Reinet and Middelburg. The yellow circle depicts the study site \_\_\_\_\_ 54
- Figure 3.4** Photographs depicting different landscapes in the study region, located north of the Sneeuwberg Mountains in the Karoo, South Africa \_\_\_\_\_ 58
- Figure 3.5** Hypothesis linking causes, response functions and consequences of a biotic transition from grassland to shrubland \_\_\_\_\_ 61



<b>Figure 3.6</b> Average climate diagrams for the surrounding region, Albuquerque to the north and Socorro to the south (1989-2002). A site-specific climate diagram for the Sevilleta NWR is also presented including a summer/winter precipitation diagram, which highlights the characteristic summer monsoon season _____	63
<b>Figure 3.7</b> a) soil map of the Sevilleta National Wildlife Refuge b) vegetation map of Sevilleta National Wildlife Refuge _____	65
<b>Figure 3.8</b> An example of the nested sampling strategy employed in this study _____	67
<b>Figure 3.9</b> Plot locations and vegetation types for the Karoo fieldsite. (1: 50 000 3124DA Heydon) _____	68
<b>Figure 3.10</b> Plot locations and vegetation types for the Sevilleta NWR fieldsite _____	70
<b>Figure 3.11</b> Pre-processing stages and protocol for semi-variogram calculations _____	83
<b>Figure 3.12</b> Theoretical interpretations of semi-variograms, showing the proportion of variance found at increasing lag distances _____	86
<b>CHAPTER FOUR</b>	
<b>Figure 4.1</b> Boxplots representing the sample distribution of organic matter content in the grassland plots _____	93
<b>Figure 4.2</b> The means and standard deviations of organic matter content for each cell within the plots _____	96
<b>Figure 4.3</b> Semi-variograms of the organic matter content of the grassland plots _____	98
<b>Figure 4.4</b> Moran's I and Geary's C correlograms for the organic matter content of the grassland plots _____	100
<b>Figure 4.5</b> Boxplots representing the sample distribution of dry bulk density in the grassland plots _____	103
<b>Figure 4.6</b> The means and standard deviations of dry bulk density for each cell within the plots _____	106
<b>Figure 4.7</b> Modelled semi-variograms for the dry bulk density of grassland plots _____	108
<b>Figure 4.8</b> Moran's I and Geary's C correlograms for the dry bulk density of the grassland plots _____	110



<b>Figure 4.9</b> Boxplots representing the sample distribution of soil moisture in the grassland plots _____	112
<b>Figure 4.10</b> The means and standard deviations of percentage soil moisture for each cell within the plots _____	115
<b>Figure 4.11</b> Modelled semi-variograms for the soil moisture of grassland plots _____	116
<b>Figure 4.12</b> Moran's I and Geary's C correlograms for the soil moisture of the grassland plots _____	118
<b>Figure 4.13</b> Boxplots representing the sample distribution of soil shear strength in the grassland plots _____	120
<b>Figure 4.14</b> The means and standard deviations of soil shear strength for each cell within the plots _____	123
<b>Figure 4.15</b> Modelled semi-variograms for the soil shear strength of grassland plots _____	124
<b>Figure 4.16</b> Moran's I and Geary's C correlograms for the soil shear strength of the grassland plots _____	127
<b>Figure 4.17</b> Semi-variograms of the particle size distribution of a grassland plot _____	129
<b>Figure 4.18</b> Moran's I and Geary's C correlograms for the particle size distribution of the grassland plot _____	131
<b>Figure 4.19</b> The number of aggregates obtained from plots 1, 2 and 10 and the percentage weight loss after agitation in water _____	133
<b>Figure 4.20</b> Boxplots representing the sample distribution of soil pH in the grassland plots _____	134
<b>Figure 4.21</b> The means and standard deviations of soil pH for each cell within the plots _____	137
<b>Figure 4.22</b> Modelled semi-variograms for the pH of grassland plots _____	138
<b>Figure 4.23</b> Moran's I and Geary's C correlograms for the soil pH of the grassland plots _____	140
<b>Figure 4.24</b> Boxplots representing the sample distribution of soil conductivity in the grassland plots _____	142
<b>Figure 4.25</b> The means and standard deviations of soil conductivity for each cell within the plots _____	145



<b>Figure 4.26</b> Modelled semi-variograms for the conductivity of grassland plots _____	146
<b>Figure 4.27</b> Moran's I and Geary's C correlograms for the soil conductivity of the grassland plots _____	148
<b>Figure 4.28</b> Boxplots representing the sample distribution of available calcium in the grassland plots _____	150
<b>Figure 4.29</b> Modelled semi-variograms for the available calcium in grassland plots _____	152
<b>Figure 4.30</b> Moran's I and Geary's C correlograms for the available calcium in the grassland plots _____	154
<b>Figure 4.31</b> Boxplots representing the sample distribution of available potassium in the grassland plots _____	155
<b>Figure 4.32</b> Modelled semi-variograms for the available potassium in grassland plots _____	157
<b>Figure 4.33</b> Moran's I and Geary's C correlograms for the available potassium in the grassland plots _____	159
<b>Figure 4.34</b> Boxplots representing the sample distribution of available magnesium in the grassland plots _____	160
<b>Figure 4.35</b> Modelled semi-variograms for the available magnesium in grassland plots _____	162
<b>Figure 4.36</b> Moran's I and Geary's C correlograms for the available magnesium in the grassland plots _____	164
<b>Figure 4.37</b> Boxplots representing the sample distribution of available sodium in the grassland plots _____	165
<b>Figure 4.38</b> Modelled semi-variograms for the available sodium in grassland plots _____	167
<b>Figure 4.39</b> Moran's I and Geary's C correlograms for the available sodium in the grassland plots _____	169
<b>Figure 4.40</b> Boxplots representing the sample distribution of available phosphorus in the grassland plots _____	170
<b>Figure 4.41</b> Modelled semi-variograms for the available phosphorus in grassland plots _____	172
<b>Figure 4.42</b> Moran's I and Geary's C correlograms for the available phosphorus in the grassland plots _____	174



**CHAPTER FIVE**

<b>Figure 5.1</b> Boxplots representing the sample distribution of organic matter content in the shrubland plots _____	181
<b>Figure 5.2</b> The means and standard deviations of organic matter content for each cell within the plots _____	183
<b>Figure 5.3</b> Semi-variograms of the organic matter content of the shrubland plots _____	184
<b>Figure 5.4</b> Semi-variograms with connecting lines to show periodicity in organic matter content data in shrubland plots _____	185
<b>Figure 5.5</b> Moran's I and Geary's C correlograms for the organic matter content of the shrubland plots _____	187
<b>Figure 5.6</b> Boxplots representing the sample distribution of dry bulk density in the shrubland plots _____	189
<b>Figure 5.7</b> The means and standard deviations of dry bulk density for each cell within the plots _____	192
<b>Figure 5.8</b> Modelled semi-variograms for the dry bulk density of shrubland plots _____	193
<b>Figure 5.9</b> Semi-variograms with connecting lines to show periodicity in dry bulk density data in shrubland plots _____	195
<b>Figure 5.10</b> Moran's I and Geary's C correlograms for the dry bulk density of the shrubland plots _____	196
<b>Figure 5.11</b> Boxplots representing the sample distribution of soil moisture in the shrubland plots _____	198
<b>Figure 5.12</b> The means and standard deviations of soil moisture for each cell within the plots _____	201
<b>Figure 5.13</b> Modelled semi-variograms for the soil moisture of shrubland plots _____	202
<b>Figure 5.14</b> Semi-variograms with connecting lines to show periodicity in dry bulk density data in shrubland plots _____	203
<b>Figure 5.15</b> Moran's I and Geary's C correlograms for the soil moisture of the shrubland plots _____	205
<b>Figure 5.16</b> Boxplots representing the sample distribution of soil shear strength in the shrubland plots _____	206



<b>Figure 5.17</b> The means and standard deviations of soil shear strength for each cell within the plots _____	209
<b>Figure 5.18</b> Modelled semi-variograms for the soil shear strength of shrubland plots _____	210
<b>Figure 5.19</b> Semi-variograms with connecting lines to show periodicity in soil shear strength data in shrubland plots _____	211
<b>Figure 5.20</b> Moran's I and Geary's C correlograms for the soil shear strength of the shrubland plots _____	213
<b>Figure 5.21</b> The number of aggregates obtained from plots 3 and 5 and the percentage weight loss after agitation in water _____	214
<b>Figure 5.22</b> Boxplots representing the sample distribution of soil pH in the shrubland plots _____	216
<b>Figure 5.23</b> The means and standard deviations of soil pH for each cell within the plots _____	218
<b>Figure 5.24</b> Modelled semi-variograms for the pH of shrubland plots _____	219
<b>Figure 5.25</b> Semi-variograms with connecting lines to show periodicity in soil pH data in shrubland plots _____	220
<b>Figure 5.26</b> Moran's I and Geary's C correlograms for the soil pH of the shrubland plots _____	222
<b>Figure 5.27</b> Boxplots representing the sample distribution of soil conductivity in the shrubland plots _____	223
<b>Figure 5.28</b> The means and standard deviations of soil conductivity for each cell within the plots _____	225
<b>Figure 5.29</b> Modelled semi-variograms for the conductivity of shrubland plots _____	226
<b>Figure 5.30</b> Semi-variograms with connecting lines to show periodicity in soil conductivity data in shrubland plots _____	227
<b>Figure 5.31</b> Moran's I and Geary's C correlograms for the soil conductivity of the shrubland plots _____	229
<b>Figure 5.32</b> Boxplots representing the sample distribution of available calcium in the shrubland plots _____	231
<b>Figure 5.33</b> Modelled semi-variograms for the available calcium in shrubland plots _____	233



<b>Figure 5.34</b> Semi-variograms with connecting lines to show periodicity in the available calcium data in shrubland plots _____	234
<b>Figure 5.35</b> Moran's I and Geary's C correlograms for the available calcium in the shrubland plots _____	236
<b>Figure 5.36</b> Boxplots representing the sample distribution of available potassium in the shrubland plots _____	237
<b>Figure 5.37</b> Modelled semi-variograms for the available potassium in shrubland plots _____	239
<b>Figure 5.38</b> Semi-variograms with connecting lines to show periodicity in the available potassium data in shrubland plots _____	240
<b>Figure 5.39</b> Moran's I and Geary's C correlograms for the available potassium in the shrubland plots _____	242
<b>Figure 5.40</b> Boxplots representing the sample distribution of available magnesium in the shrubland plots _____	243
<b>Figure 5.41</b> Modelled semi-variograms for the available magnesium in shrubland plots _____	245
<b>Figure 5.42</b> Semi-variograms with connecting lines to show periodicity in the available magnesium data in shrubland plots _____	246
<b>Figure 5.43</b> Moran's I and Geary's C correlograms for the available magnesium in the shrubland plots _____	248
<b>Figure 5.44</b> Boxplots representing the sample distribution of available sodium in the shrubland plots _____	249
<b>Figure 5.45</b> Modelled semi-variograms for the available sodium in shrubland plots _____	251
<b>Figure 5.46</b> Semi-variograms with connecting lines to show periodicity in the available sodium data in shrubland plots _____	252
<b>Figure 5.47</b> Moran's I and Geary's C correlograms for the available sodium in the shrubland plots _____	253
<b>Figure 5.48</b> Boxplots representing the sample distribution of available phosphorus in the shrubland plots _____	254
<b>Figure 5.49</b> Modelled semi-variograms of the available phosphorus in shrubland plots _____	256
<b>Figure 5.50</b> Semi-variograms with connecting lines to show periodicity in the available phosphorus data in shrubland plots _____	257



<b>Figure 5.51</b> Moran's I and Geary's C correlograms for the available phosphorus in the shrubland plots _____	259
<b>CHAPTER SIX</b>	
<b>Figure 6.1</b> Boxplots representing the sample distribution of organic matter content in the badland plots _____	265
<b>Figure 6.2</b> The means and standard deviations of organic matter content for each cell within the plots _____	267
<b>Figure 6.3</b> Semi-variograms of the organic matter content of the badland plots _____	268
<b>Figure 6.4</b> Semi-variograms with connecting lines to show periodicity in organic matter content data in badland plots _____	269
<b>Figure 6.5</b> Moran's I and Geary's C correlograms for the organic matter content of the badland plots _____	271
<b>Figure 6.6</b> Boxplots representing the sample distribution of dry bulk density in the badland plots _____	273
<b>Figure 6.7</b> The means and standard deviations of dry bulk density for each cell within the plots _____	275
<b>Figure 6.8</b> Modelled semi-variograms for the dry bulk density of badland plots _____	276
<b>Figure 6.9</b> Semi-variograms with connecting lines to show periodicity in dry bulk density data in badland plots _____	277
<b>Figure 6.10</b> Moran's I and Geary's C correlograms for the dry bulk density of the badland plots _____	278
<b>Figure 6.11</b> Boxplots representing the sample distribution of soil moisture in the badland plots _____	280
<b>Figure 6.12</b> The means and standard deviations of soil moisture for each cell within the plots _____	282
<b>Figure 6.13</b> Modelled semi-variograms for the soil moisture of badland plots _____	283
<b>Figure 6.14</b> Semi-variograms with connecting lines to show periodicity in soil moisture data in badland plots _____	284
<b>Figure 6.15</b> Moran's I and Geary's C correlograms for the soil moisture of the badland plots _____	286



<b>Figure 6.16</b> Boxplots representing the sample distribution of soil shear strength in the badland plots _____	288
<b>Figure 6.17</b> The means and standard deviations of soil shear strength for each cell within the plots _____	290
<b>Figure 6.18</b> Semi-variograms of the soil shear strength of the badland plots _____	291
<b>Figure 6.19</b> Semi-variograms with connecting lines to show periodicity in soil shear strength data in badland plots _____	292
<b>Figure 6.20</b> Moran's I and Geary's C correlograms for the soil shear strength of the badland plots _____	294
<b>Figure 6.21</b> Semi-variograms of the particle size distribution of a badland plot _____	296
<b>Figure 6.22</b> Semi-variograms with connecting lines to show periodicity in the particle size distribution of a badland plot _____	297
<b>Figure 6.23</b> Moran's I and Geary's C correlograms for the particle size distribution of the badland plot _____	298
<b>Figure 6.24</b> The number of aggregates obtained from plot 6 and the percentage weight loss after agitation in water _____	300
<b>Figure 6.25</b> Boxplots representing the sample distribution of soil pH in the shrubland plots _____	301
<b>Figure 6.26</b> The means and standard deviations of soil pH for each cell within the plots _____	303
<b>Figure 6.27</b> Modelled semi-variograms for the pH of badland plots _____	304
<b>Figure 6.28</b> Semi-variograms with connecting lines to show periodicity in soil pH data in badland plots _____	305
<b>Figure 6.29</b> Moran's I and Geary's C correlograms for the soil pH of the badland plots _____	306
<b>Figure 6.30</b> Boxplots representing the sample distribution of soil conductivity in the badland plots _____	308
<b>Figure 6.31</b> The means and standard deviations of soil conductivity for each cell within the plots _____	310
<b>Figure 6.32</b> Modelled semi-variograms for the conductivity of badland plots _____	311



<b>Figure 6.33</b> Semi-variograms with connecting lines to show periodicity in soil conductivity data in badland plots _____	312
<b>Figure 6.34</b> Moran's I and Geary's C correlograms for the soil conductivity of the badland plots _____	314
<b>Figure 6.35</b> Boxplots representing the sample distribution of available calcium in the badland plots _____	316
<b>Figure 6.36</b> Modelled semi-variograms for the available calcium in badland plots _____	318
<b>Figure 6.37</b> Semi-variograms with connecting lines to show periodicity in the available calcium data in badland plots _____	319
<b>Figure 6.38</b> Moran's I and Geary's C correlograms for the available calcium in the badland plots _____	320
<b>Figure 6.39</b> Boxplots representing the sample distribution of available potassium in the shrubland plots _____	321
<b>Figure 6.40</b> Modelled semi-variograms for the available potassium in badland plots _____	323
<b>Figure 6.41</b> Semi-variograms with connecting lines to show periodicity in the available potassium data in badland plots _____	324
<b>Figure 6.42</b> Moran's I and Geary's C correlograms for the available potassium in the badland plots _____	325
<b>Figure 6.43</b> Boxplots representing the sample distribution of available magnesium in the badland plots _____	326
<b>Figure 6.44</b> Modelled semi-variograms for the available magnesium in badland plots _____	328
<b>Figure 6.45</b> Semi-variograms with connecting lines to show periodicity in the available magnesium data in badland plots _____	329
<b>Figure 6.46</b> Moran's I and Geary's C correlograms for the available magnesium in the badland plots _____	330
<b>Figure 6.47</b> Boxplots representing the sample distribution of available sodium in the badland plots _____	331
<b>Figure 6.48</b> Modelled semi-variograms for the available sodium in badland plots _____	333
<b>Figure 6.49</b> Semi-variograms with connecting lines to show periodicity in the available sodium data in shrubland plots _____	334



<b>Figure 6.50</b> Moran's I and Geary's C correlograms for the available sodium in the badland plots _____	335
<b>Figure 6.51</b> Boxplots representing the sample distribution of available phosphorus in the badland plots _____	336
<b>Figure 6.52</b> Modelled semi-variograms for the available phosphorus in badland plots _____	338
<b>Figure 6.53</b> Semi-variograms with connecting lines to show periodicity in the available phosphorus data in shrubland plots _____	339
<b>Figure 6.54</b> Moran's I and Geary's C correlograms for the available phosphorus in the badland plots _____	340

## CHAPTER EIGHT

<b>Figure 8.1</b> Conceptual model of processes, patterns and interactions connecting vegetation change to the susceptibility of soil to erosion in semi-arid environments _____	386
--	-----

## APPENDICES: CD

### Appendix 1

Grassland normality graphs  
Shrubland normality graphs  
Badland normality graphs

### Appendix 2

Shrubland ANOVA results  
Spearman's Rank correlation coefficient values

### Appendix 3

Grassland experimental semi-variograms  
Shrubland experimental semi-variograms  
Badland experimental semi-variograms

### Appendix 4

Photographs of the Karoo plots (South Africa)  
Photographs of the Sevilleta National Wildlife Refuge plots (New Mexico)



## LIST OF TABLES

### CHAPTER TWO

<b>Table 2.1</b> Mechanisms of vegetation dynamics (bold italics) and their variants (indented) recognized in a study of the Chihuahuan Desert _____	39
--	----

### CHAPTER THREE

<b>Table 3.1</b> Plot identification data for the Karoo plots _____	69
<b>Table 3.2</b> Plot identification data for the Sevilleta NWR plots _____	70
<b>Table 3.3</b> Effect of salinity on plants. Source: Soil and Plant Analysis Council Inc 1999 p. 60, 61 _____	78
<b>Table 3.4</b> Index of spatial dependence _____	87

### CHAPTER FOUR

<b>Table 4.1</b> Grassland plot identification data _____	92
<b>Table 4.2</b> Inter-plot comparisons of descriptive statistics: Organic matter content _____	94
<b>Table 4.3</b> Geostatistical analysis of organic matter content of grassland plots _____	97
<b>Table 4.4</b> Inter-plot comparisons of descriptive statistics: Dry bulk density (g cm <sup>-3</sup> ) _____	104
<b>Table 4.5</b> Geostatistical analysis of the dry bulk density of grassland plots _____	107
<b>Table 4.6</b> Inter-plot comparisons of descriptive statistics: Soil moisture (%) _____	113
<b>Table 4.7</b> Geostatistical analysis of the soil moisture of grassland plots _____	116
<b>Table 4.8</b> Inter-plot comparisons of descriptive statistics: Soil shear strength (kPa) _____	121
<b>Table 4.9</b> Geostatistical analysis of the soil shear strength of grassland plots _____	124
<b>Table 4.10</b> Inter-plot comparisons of descriptive statistics: Particle size distribution _____	128



<b>Table 4.11</b> Inter-plot comparisons of descriptive statistics: Soil pH_____	134
<b>Table 4.12</b> Geostatistical analysis of the soil pH of grassland plots_____	138
<b>Table 4.13</b> Inter-plot comparisons of descriptive statistics: Soil conductivity (dS m <sup>-1</sup> )_____	143
<b>Table 4.14</b> Geostatistical analysis of the soil conductivity of grassland plots_____	146
<b>Table 4.15</b> Inter-plot comparisons of descriptive statistics: Available calcium in ppm of soil_____	151
<b>Table 4.16</b> Geostatistical analysis of the available calcium of grassland plots_____	152
<b>Table 4.17</b> Inter-plot comparisons of descriptive statistics: Available potassium in ppm of soil_____	156
<b>Table 4.18</b> Geostatistical analysis of the available potassium in grassland plots_____	157
<b>Table 4.19</b> Inter-plot comparisons of descriptive statistics: Available magnesium in ppm of soil_____	161
<b>Table 4.20</b> Geostatistical analysis of the available magnesium in grassland plots_____	162
<b>Table 4.21</b> Inter-plot comparisons of descriptive statistics: Available sodium in ppm of soil_____	166
<b>Table 4.22</b> Geostatistical analysis of the available sodium in grassland plots_____	167
<b>Table 4.23</b> Inter-plot comparisons of descriptive statistics: Available phosphorus in ppm of soil_____	171
<b>Table 4.24</b> Geostatistical analysis of the available phosphorus in grassland plots_____	172
<b>CHAPTER FIVE</b>	
<b>Table 5.1</b> Shrubland plot identification data_____	180
<b>Table 5.2</b> Inter-plot comparisons of descriptive statistics: Organic matter content_____	182



<b>Table 5.3</b> Geostatistical analysis of organic matter content of shrubland plots_____	184
<b>Table 5.4</b> Inter-plot comparisons of descriptive statistics: Dry bulk density (g cm <sup>-3</sup> )_____	190
<b>Table 5.5</b> Geostatistical analysis of the dry bulk density of grassland plots_____	193
<b>Table 5.6</b> Inter-plot comparisons of descriptive statistics: Soil moisture (%) _____	199
<b>Table 5.7</b> Geostatistical analysis of the soil moisture of shrubland plots__	202
<b>Table 5.8</b> Inter-plot comparisons of descriptive statistics: Soil shear strength (kPa)_____	207
<b>Table 5.9</b> Geostatistical analysis of the soil shear strength of shrubland plots_____	210
<b>Table 5.10</b> Inter-plot comparisons of descriptive statistics: Soil pH_____	216
<b>Table 5.11</b> Geostatistical analysis of the soil pH of shrubland plots_____	219
<b>Table 5.12</b> Inter-plot comparisons of descriptive statistics: Soil conductivity (dS m <sup>-1</sup> )_____	224
<b>Table 5.13</b> Geostatistical analysis of the soil conductivity of shrubland plots_____	226
<b>Table 5.14</b> Inter-plot comparisons of descriptive statistics: Available calcium in ppm of soil _____	232
<b>Table 5.15</b> Geostatistical analysis of the available calcium of shrubland plots_____	233
<b>Table 5.16</b> Inter-plot comparisons of descriptive statistics: Available potassium in ppm of soil _____	238
<b>Table 5.17</b> Geostatistical analysis of the available potassium in shrubland plots_____	239
<b>Table 5.18</b> Inter-plot comparisons of descriptive statistics: Available magnesium in ppm of soil _____	243
<b>Table 5.19</b> Geostatistical analysis of the available magnesium in shrubland plots_____	244



<b>Table 5.20</b> Inter-plot comparisons of descriptive statistics: Available sodium in ppm of soil _____	250
<b>Table 5.21</b> Geostatistical analysis of the available sodium in shrubland plots _____	250
<b>Table 5.22</b> Inter-plot comparisons of descriptive statistics: Available phosphorus in ppm of soil _____	255
<b>Table 5.23</b> Geostatistical analysis of the available phosphorus in shrubland plots _____	256
<b>CHAPTER SIX</b>	
<b>Table 6.1</b> Inter-plot comparisons of descriptive statistics: Organic matter content _____	266
<b>Table 6.2</b> Geostatistical analysis of organic matter content of shrubland plots _____	268
<b>Table 6.3</b> Inter-plot comparisons of descriptive statistics: Dry bulk density (g cm <sup>-3</sup> ) _____	273
<b>Table 6.4</b> Inter-plot comparisons of descriptive statistics: Soil moisture (%) _____	281
<b>Table 6.5</b> Inter-plot comparisons of descriptive statistics: Soil shear strength (kPa) _____	289
<b>Table 6.6</b> Geostatistical analysis of the soil shear strength of badland plots _____	291
<b>Table 6.7</b> Inter-plot comparisons of descriptive statistics: Particle size distribution _____	295
<b>Table 6.8</b> Inter-plot comparisons of descriptive statistics: Soil pH _____	302
<b>Table 6.9</b> Inter-plot comparisons of descriptive statistics: Soil conductivity (dS m <sup>-1</sup> ) _____	308
<b>Table 6.10</b> Geostatistical analysis of the soil conductivity of badland plots _____	311
<b>Table 6.11</b> Inter-plot comparisons of descriptive statistics: Available calcium in ppm of soil _____	316
<b>Table 6.12</b> Geostatistical analysis of the available calcium of badland plots _____	317



<b>Table 6.13</b> Inter-plot comparisons of descriptive statistics: Available potassium in ppm of soil _____	322
<b>Table 6.14</b> Inter-plot comparisons of descriptive statistics: Available magnesium in ppm of soil _____	327
<b>Table 6.15</b> Geostatistical analysis of the available magnesium in badland plots _____	327
<b>Table 6.16</b> Inter-plot comparisons of descriptive statistics: Available sodium in ppm of soil _____	332
<b>Table 6.17</b> Inter-plot comparisons of descriptive statistics: Available phosphorus in ppm of soil _____	337
<b>CHAPTER SEVEN</b>	
<b>Table 7.1</b> Means and coefficients of variation [(SD + mean) x 100] of all the soil parameters from the combined grassland and shrubland plots _____	346
<b>Table 7.2</b> Mann-Whitney analysis between each soil parameter from the combined grassland and shrubland plots (the parameters in blue present significant results) _____	346
<b>Table 7.3</b> Minimum and maximum ranges of spatial autocorrelation derived from semi-variograms of soil parameters from grassland and shrubland plots _____	350
<b>Table 7.4</b> A comparison of the spatial autocorrelation values (in meters) of nutrients in semi-arid grasslands _____	355
<b>Table 7.5</b> A comparison of the spatial autocorrelation values (in meters) of nutrients in semi-arid grasslands _____	355
<b>Table 7.6</b> Means and coefficients of variation [(SD + mean) x 100] of all the soil parameters from the grassland and shrubland plots situated in the Karoo, S.A. and the Sevilleta NWR, N.M. _____	358
<b>Table 7.7</b> Mann-Whitney analysis of each soil parameter from the Karoo grassland and shrubland plots and the Sevilleta NWR grassland and shrubland plots (the parameters in blue present significant results) _____	359
<b>Table 7.8</b> Ranges of spatial autocorrelation (in meters) derived from semi-variograms for all shrubland and grassland plots in the Karoo and the Sevilleta NWR _____	374
<b>Table 7.9</b> Means and coefficients of variation [(SD + mean) x 100] of all the soil parameters from the combined grassland, shrubland and badlands plots in the Karoo _____	367



<b>Table 7.10</b> Mann-Whitney analysis between each soil parameter from the combined grassland, shrubland and badland plots (the parameters in blue present significant results) _____	368
<b>Table 7.11</b> Summary of particle sizes derived from grassland and shrubland environments in New Mexico. Where second values are given this indicate inter-vegetation areas apart from Müller where this indicates a second fieldsite _____	369
<b>Table 7.12</b> Ranges of spatial autocorrelation (in meters) derived from semi-variograms for all shrubland and badland plots in the Karoo _____	370
<b>CHAPTER EIGHT</b>	
<b>Table 8.1</b> F-values of Spearman's Rank correlation between soil parameters in grasslands, shrublands and badlands. _____	382

## **Acknowledgements**

I would like to express my gratitude to the many people who have supported me throughout my PhD experience.

Firstly, many thanks to my supervisor Professor Tony Parsons for his guidance, advice and patience, his assistance in the field and most importantly his ability to demonstrate his great culinary skills in even the most adverse of field conditions.

Many thanks to everyone in South Africa who made my fieldwork possible, including; Alf and Brenda James (Compassberg Farm) for their kindness, hospitality and advice on avoiding snakes and baboons, Dr. P. Boysen (Good Hope Farm) and John Curry (Eureka Farm and Highland Farm) for permitting us access to their land, and a special thanks to Peter Holmes and family for their generous hospitality in Cape Town. Assistance from colleagues and staff at the Sevilleta National Wildlife Refuge, New Mexico, was also much appreciated, particularly John DeWitt for his assistance with field supplies and logistical issues.

To everyone who has acted as my field assistant– without you I would not have been able to conduct this research. However, a special thanks to Graham Dickie for all his help in New Mexico, for creating a good balance of hard work and fun, but especially for being able to take orders from his little sister!

Last but not least, many thanks to all my family, friends and colleagues who have supported me throughout the highs and lows. Some of you have helped me solve problems and some of you have helped me forget about them, but all of you have been invaluable to my PhD experience!

*This research was funded by the Natural Environmental Research Council (NERC).*

## CHAPTER ONE

### Introduction

---

---

#### **1.1 Overall aim**

#### **1.2 Changing landscapes: the concept of desertification**

##### **1.2.1 Shrub encroachment and vegetation dynamics**

##### **1.2.2 Vegetation and soil property interactions**

##### **1.2.3 Badland development**

#### **1.3 Structure of thesis**

---

---

#### **1.1 Overall aim**

Land degradation and vegetation change are concurrent processes commonly associated with semi-arid regions. Vegetation change in these areas is predominantly in the form of a grassland-shrubland transition, a process that exacerbates soil erosion and can result in irreversible degradation known as desertification. Evidence of such transitions can be found at a global scale, documented in areas such as the Mediterranean (Martinez-Mena *et al.*, 1999; Bochet *et al.*, 1999; Maestre and Cortina, 2002), the American southwest (Buffington and Herbel, 1965; Gibbens *et al.*, 2005) and in many parts in Africa (Kraaij and Milton, 2006; Dean *et al.*, 1995; Hoffman *et al.*, 1999). This research has been undertaken to further the understanding of the changing landscapes in semi-arid environments through a detailed assessment of plant – soil feedback mechanisms. As well as being of scientific importance, this research area has social, economic and cultural context (Warren, 1998); loss of productive grassland to less palatable woody shrubland can have a severe impact on the economies of 'marginal' semi-arid lands. In general, these regions rely heavily on livestock

farming due to constraining climatic conditions and the low nutrient status associated with semi-arid landscapes. Consequently, from the agricultural viewpoint, vegetation change is often seen as a detrimental landscape process impacting on the sustainability and economic potential of land. Thus, vegetation change as a precursor of soil erosion is a subject that is becoming increasingly predominant in both research circles and public awareness.

Many studies have been undertaken in order to explain degradation processes ranging from determining rates of erosion and causal factors to building erosion prediction models. The over-simplified paradigm stating that land use and climatic variability control vegetation cover and vegetation cover controls erosion still dominates in the approach of addressing land degradation issues (Thornes, 2005). However, juxtaposing climate change and overgrazing as causal factors of increased erosion rates is problematic as it compounds the complexity of the controlling mechanisms, making it hard to differentiate between allogenic and autogenic drivers.

As a consequence of the spatial and temporal variations in climate and land use across dryland regions, quantifying and determining the rate of degradation is an ambiguous task. However, irrespective of the causes of degradation, a comprehension of the underlying processes is essential if land degradation and desertification in dryland systems are to be fully understood. Schlesinger *et al.*, (1996) propose an alternative method of measuring desertification by comparing soil nutrient heterogeneity between different vegetation structures based on the presumption that grasslands indicate a fine-scale distribution of soil resources and shrub ecosystems indicate a coarse-scale distribution. Whilst the spatial patterns of soil nutrients in drylands are well documented (Charley and West, 1975; Hook *et al.*, 1991; Tongway and Ludwig, 1994; Schlesinger *et al.*, 1996; Schlesinger and Pilmanis, 1998), as well as the effect of vegetation change on the physical properties of soil (Abrahams *et al.*, 1995; Parsons *et al.*, 1996; Wainwright *et al.*, 2000; Maestre and Cortina 2002) few have attempted to link both aspects of the process.

Undeniably, the mechanisms surrounding plant-soil interactions are such that the understanding of the relationship between the susceptibility of soil to erosion and vegetation change is complex. However, this research aims to address this issue by comparing the spatial patterns of the physical and chemical properties of soil between grassland, shrubland and badland areas, observing their interactions and assessing their influence on the susceptibility of soil to erosion.

## **1.2 Changing landscapes: the concept of desertification**

Increasing environmental awareness has raised the profile of desertification, a phenomenon commonly associated with the world's semi-arid regions. Drylands cover more than 50% of the land's surface (Asner and Heidebrecht, 2005) and support approximately 78% of the world's grazing capacity (Asner *et al.*, 2004). The degradation of drylands is therefore an issue of global concern impacting on the most extensive form of land use on the planet. Approximately one third of the earth's surface is thought to be affected by desertification (UNCDD, 2006) impacting more than one billion people in dryland regions throughout the world (UNCDD, 2006). The concept of desertification, however, is the subject of much debate (see Dean *et al.*, 1995) questioning not only the definition of the term but the causal factors and of more topical interest, the true extent of the phenomenon.

The multifaceted nature of desertification depicts that multidisciplinary approaches are used when addressing the problem. The implications of this are that both biophysical and socioeconomic use of the term encompasses a broad spectrum of definitions that cover a range of spatial and temporal scales. The term desertification portrays images of barren, desert-like conditions, consequently it is used as a driving force to increase the perception that the rate of environmental change is escalating in order to promote policy development (Thomas and Twyman, 2004). However, desertification was defined 1994 by the United Nations Convention to Combat Desertification (UNCCD) as 'land degradation in arid, semi-arid and dry subhumid areas resulting from various factors including climatic

variation and human activities'. Consequently, desertification is a general term used to describe land degradation ranging from a change in vegetation structure through to an expansion of desert areas. On the other hand, it is argued that a landscape cannot be described as 'desertified' unless the extent of degradation is such that recovery is not possible (Schlesinger *et al.*, 1990). The rationale behind this argument is that natural climatic cycles are evident throughout history in the form of alternating cycles of drought and rainfall, therefore a loss of productive agricultural land through drought cannot be classed as desertification if it recuperates after a rainfall cycle. Figure 1.1 summarises the desertification process characteristic of semi-arid environments, the photographs depicting some typical stages of degradation emphasise the dramatic landscape change that can be witnessed in dryland regions.

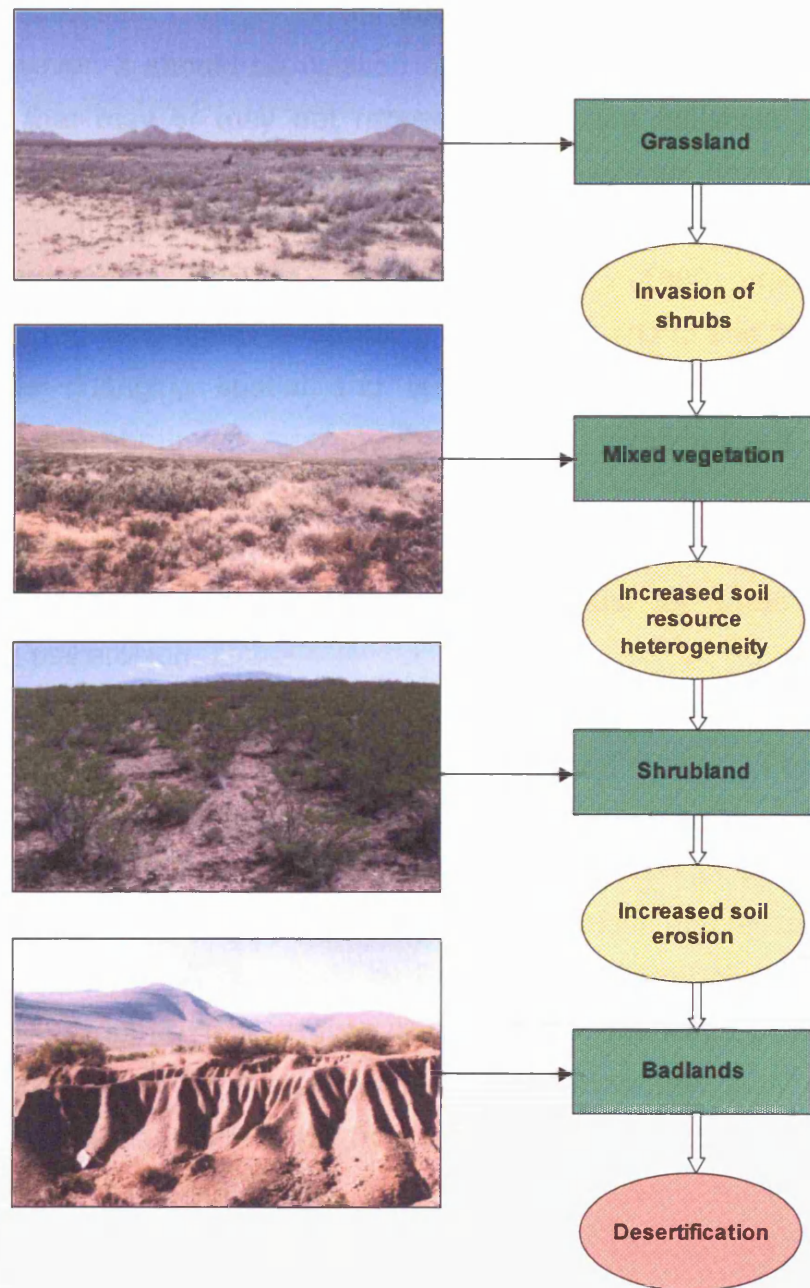


**Figure 1.1** A summary of the desertification process characteristic of some semi-arid environments.

### 1.2.1 Shrub encroachment and vegetation dynamics

Evidently, vegetation change is an instrumental factor in the desertification process, however, it should be classed as an intermediate stage indicating land degradation that may or may not recover rather than full-scale desertification. Notwithstanding the notion that vegetation change perhaps does not necessarily represent a uni-directional process, conceptual models of desertification consider this as a fundamental element. Schlesinger *et al.*, (1990) proposed that the framework surrounding the understanding of the semi-arid to arid transition should be based on changing spatial and temporal distributions of soil resources associated with shrub encroachment. It was hypothesised that various degradation processes could result in a change in the distribution of soil resources, from being relatively uniform in grassland systems to being more heterogeneous in nature thus increasing the potential for shrub invasion and exacerbating soil erosion.

Changes in the ecological status of dryland regions have been well documented (see Wiegand and Jeltsch, 2000). Conclusively, a series of similarities can be identified on a global scale both in the causal factors and in the changes of vegetation dynamics. A key study by Buffington and Herbel (1965) provides a comprehensive synopsis of vegetation change in the American Southwest over the past 150 years, noting the invasion of shrubs in areas previously dominated by productive grasslands. This study not only describes the observed transition of vegetation but also evaluates the factors likely to have induced the changes. Buffington and Herbel established that five main factors are accredited as influential mechanisms of vegetation change; climate change, grazing by domestic livestock, the effect of rodents, suppression of grassland fires and species competition. It was concluded, however, that the main instigating mechanism was not one attributable factor rather a complex combination of grazing practices and relatively short-term climate variations in the form of periodic droughts. A comparable study by Hoffman *et al.*, (1999) assesses the land degradation processes prevalent in the semi-arid regions of South Africa. Again, spatial and temporal variations in climate combined with detrimental grazing practices are

regarded as imperative in the disappearance of productive grasslands. Parallels can be drawn between these two studies emphasising the global importance of understanding this characteristic form of degradation in dryland regions.

### **1.2.2 Vegetation and soil property interactions**

Based on earlier work by Schlesinger *et al.*, (1996) on the spatial distribution of soil nutrients in desert ecosystems, Schlesinger and Pilmanis (1998) attempted to disaggregate plant-soil interactions. This study looked specifically at the spatial distribution of nutrients in a shrubland area and the subsequent development of high nutrient concentrations or 'islands of fertility' under shrub canopies. Geostatistical analyses showed that the distribution of nitrogen, phosphorus and potassium in the soil was strongly associated with the presence of shrubs. Hence, it is thought that once a shrub has established itself it becomes, to a certain extent, self-sustaining. A characteristic of these 'islands' is the build up of sediment under the shrub canopy, thought to form through a number of both physical and biological processes. Parsons *et al.*, (1992) attributed the formation of these mounds to differential rainsplash. An accumulation of sediment occurs under the shrub canopy as there is insufficient energy to remove the sediment deposited under the shrub (Wainwright *et al.*, 1999). In contrast, the exposed surrounding inter-shrub areas are further eroded. Combined with this effect is the build up of leaf litter, which accumulates under the shrubs. This net accumulation of litter gives rise to the so-called 'islands of fertility', as the subsequent decay redistributes nutrients back into the soil. Figure 1.2 illustrates the processes involved in the development of islands of fertility.

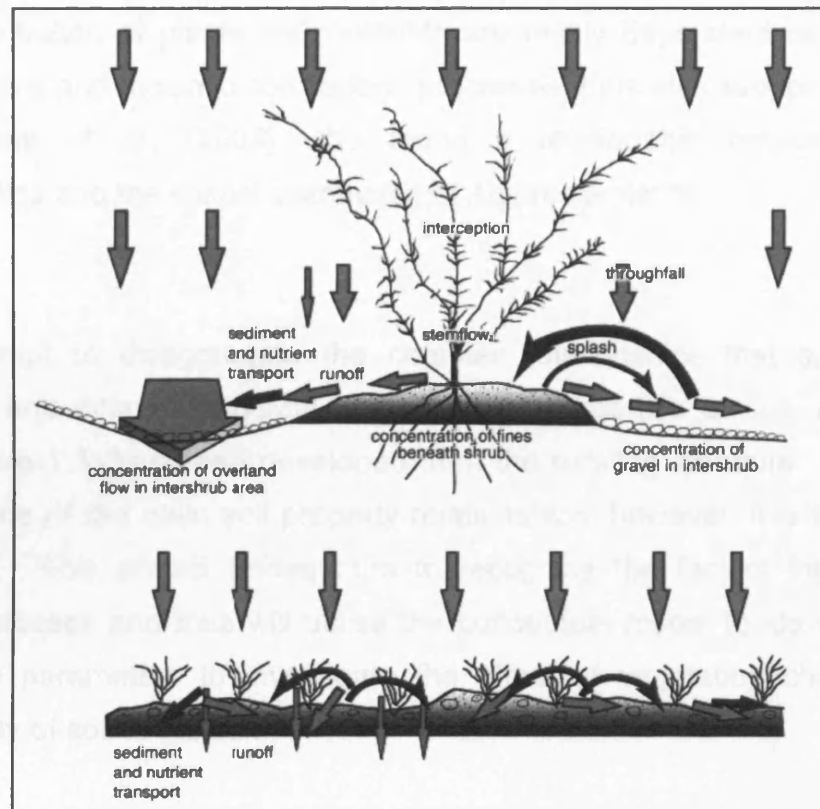


**Figure 1.2** The basic interactions between vegetation, water movement and erosion on hillslopes, showing differences between shrub-dominated landscapes (upper) and grass-dominated landscapes (lower).

Source: Wainwright et al. (2000) p.2922

Although these islands of fertility have been considered an instrumental factor concerning the decline in grasslands and exacerbation of soil erosion through the production of areas of preferential fertility and protective cover, largely neglected is the preferential distribution of other physical and chemical properties of soil that could be assumed to accompany a change in nutrient status. It is widely documented that soil structure, hence soil stability, is controlled by many factors (Gyssels and Poesen, 2003), therefore, only by investigating these other properties can the true effect of vegetation change on soil erodibility be understood. A study by Rietkerk *et al.*, (2002) touched this issue when investigating the fine-scale spatial distribution of plants and resources in the Sahel. It was hypothesised in this study that the distribution of annual plants would be spatially autocorrelated and thus, positively linked with the spatial patterns of

erodible soil particles, organic matter and nutrients. The conclusion was that the spatial distribution of plants and nutrients are highly dependent on soil surface characteristics and dynamic soil surface processes, thus also supporting evidence from Schenk *et al.*, (2003) who found a relationship between substrate characteristics and the spatial distribution of *Ambrosia* plants.

In an attempt to disaggregate the complex relationships that exist between vegetation and different physical and chemical properties of soil, a conceptual model (figure 1.3) has been developed from the existing literature. This model depicts some of the main soil property relationships, however, it is by no means exhaustive. This project endeavours to recognise the factors intrinsic to the erosional process and thus will utilise the conceptual model to identify the most appropriate parameters to investigate the effect of vegetation change on the susceptibility of soil to erosion.

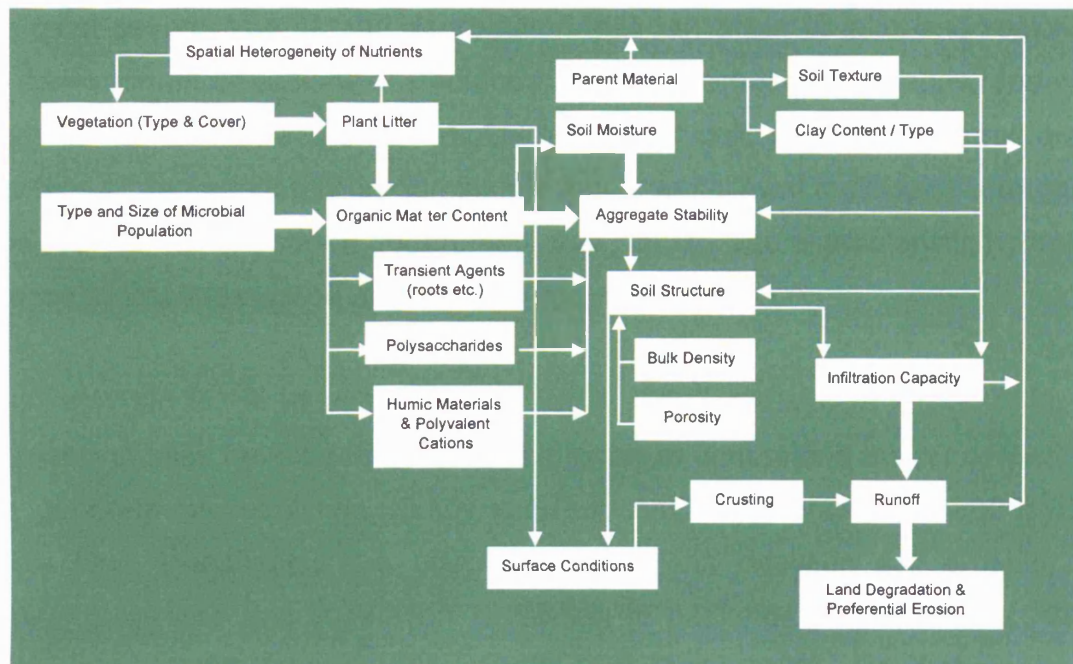


**Figure 1.3** A conceptual model depicting some of the main interactions among some physical and chemical properties of soil and their effect on erosion.

### 1.2.3 Badland development

This research endeavors to add another dimension to the vegetation change – soil erosion understanding. Although it is widely accepted that a grassland to shrubland transition is a form of land degradation, it is often presumed that when shrubs are established the dryland ecosystem has reached its climax or stable state. Ecological studies generally limit their focus to the processes preceding this ‘threshold’ in contrast to geomorphologists who consider this as part of the primary stages in the erosional process. Based on the idea proposed by Friedel (1991), this research intends to integrate the two disciplines, thus investigating changes in soil properties from the view that two process thresholds exist: the dominance of shrubs in an initially grassland landscape and a potentially irreversible change in the physical and chemical properties of soil leading to extensive degradation and desertification.

The most severe type of land degradation that can occur in semi-arid regions is the development of badlands. Badlands are highly eroded landscapes, sparse of vegetation and consisting of a complex network of gullies, rills and interrill areas. This type of degradation is predominantly found on colluvial footslopes with gullies developing in valley bottoms (Boardman *et al.*, 2003). The characteristic hydrology of these landscapes will be discussed in chapter 2.

Extensive studies have been conducted in order to understand the processes that may generate new badlands (Kirkby and Bull, 2000; Nogueras *et al.*, 2000) whilst others have investigated the effect of interactions between soil erosion, soil forming processes and vegetation in relation to badlands (Guardia *et al.*, 2000; Rienks *et al.*, 2000; Regues *et al.*, 2000; Torri *et al.*, 2000). Vegetation change has been attributed as one of the primary causal factors in the development of badlands, as rill and gully erosion often accompany the replacement of grassland by shrubland communities (Boardman *et al.*, 2003). However, the focus of many geomorphological studies of badlands tends towards the change in hydrological response as a factor of vegetation cover rather than how the autogenic response of plants may influence the susceptibility of soil to erosion through a change of soil resources. This research therefore considers not only how the physical and chemical properties of soil dictate the erosional response in badlands, but analyses the spatial patterns of soil properties. As a result, a continuum of data on the changing spatial patterns of soil characteristics will be achieved, starting at a grassland landscape and encompassing the transitions that finally lead to a desertified landscape. In addition, this data will provide a better understanding of badland systems as relatively little is known about the detailed spatial patterns of soil properties in this environment.

A detailed knowledge of the spatial distribution of physical and chemical properties of soil in badlands would be beneficial for a number of reasons, particularly for modelling purposes. Essentially these factors control the hydrological response of soil particles therefore the understanding of soil properties is considered a key theme of this research.

### **1.3 Structure of thesis**

The thesis is divided into nine chapters; the following section presents a brief summary of the structure of the thesis and its content.

The literature review presented in chapter two discusses the main concepts surrounding land degradation and desertification processes in semi-arid regions. This chapter provides a detailed account of the mechanisms involved in the erosional process and explains the complexity of plant-soil interactions. Essential to the understanding of this research is knowledge of how soil properties influence the susceptibility of soil to erosion; the interface of both physical and chemical properties with soil erodibility is reviewed and subsequently linked to the impact of vegetation change introduced in chapter one. In addition, this chapter introduces the concept of soil heterogeneity in relation to vegetation type by evaluating the differences in spatial patterns of soil properties across grasslands and shrublands. Central to this research is the argument concerning the influence of *scale* on soil heterogeneity; this chapter therefore discusses the initial evidence for this assumption and provides the rationale behind the research question, highlighting the need for an improved understanding of the mechanisms behind soil erosion.

A description of the study sites and analysis methods are given in chapter three. Firstly, an overview of the specific study areas and data requirements is presented, included is a description and geographical justification of the two study sites – the main study area, which is located in the Karoo region of South Africa and the secondary study site situated in the Sevilleta National Wildlife Refuge in New Mexico. The sampling strategy used to assess the spatial distribution of soil properties across the different vegetation communities is outlined and subsequently, a description of the field techniques and laboratory methods undertaken. Finally, an explanation of the statistical and geostatistical analysis used to quantify the spatial relationships of soil properties is provided.

Chapters four, five and six follow exactly the same structure themed around the grassland, shrubland and badland landscapes respectively. This layout is justified as it is hypothesised that the mechanisms underlying the erosional process, as a consequence of vegetation change, are characteristic of all semi-arid regions. Hence the spatial patterns in the Karoo should, in principle, mirror those in New Mexico. The validity of this hypothesis is considered a separate aspect of the research question and will therefore be discussed in detail in chapter seven. Chapters four to six are divided into eight main sections each one depicting a different soil property. In turn, each soil property is analysed statistically and spatially, the results are then summarised at the end of each section.

Although chapters four to six establish the spatial patterns of soil properties associated with each vegetation community, chapter seven attempts to integrate these findings. The effect of vegetation type on the spatial distribution of the physical and chemical properties of soil is discussed. These findings are advanced by discussing the idea of changing soil heterogeneity and debating the concept of scale. A comparison is made between the spatial patterns evident in the Karoo with those in New Mexico, thus putting the research into a more global context. This evidence is then put in context with respect to the main research question in chapter 8. An assessment of the impact of changing soil parameters, as a result of the aforementioned vegetation change, on the susceptibility of soil to erosion is made. The consequences of the findings on the future development of erosion prediction models and their global applicability are then discussed.

The final chapter provides a synopsis of the main findings of this research. The aim is reiterated and the associated conclusions stated. An evaluation of the global applicability of this research is provided with recommendations for future applications and development.

## CHAPTER TWO

# Understanding the complexities of vegetation change on soil properties and their effect on land degradation

---

---

### ***2.1 Brief overview: the importance of vegetation***

### ***2.2 The physical and chemical properties of soil and their influence on the susceptibility of soil to erosion***

### ***2.3 The implications of changing spatial patterns of soil properties on soil erosion***

#### ***2.3.1 The concept of heterogeneity***

#### ***2.3.2 Implications of spatial heterogeneity on the erosional response of the landscape***

#### ***2.3.3 A function of scale?***

### ***2.4 Summary and formulation of objectives***

---

---

### ***2.1 Brief overview: the importance of vegetation***

Vegetation change, as an intrinsic factor in the semi-arid erosional process, has been introduced in the previous chapter; this literature review considers the implications of this process by establishing the significance of relationships that exist between vegetation, surface soil characteristics and soil stability.

Plant-soil interactions have been briefly introduced in chapter one, explaining mainly the development of fertile mounds commonly found under shrubs in dryland regions, however, it is also important to look at processes on a larger scale and

thus by taking a holistic approach scientists have associated more general landscape characteristics with different vegetation types.

There is much literature documenting the significance of vegetation on the susceptibility of soil to erosion (Abrahams *et al.*, 1995; Prosser *et al.*, 1995; Parsons *et al.*, 1996; Schlesinger and Pilmanis, 1998; Havstad *et al.*, 1999; Kosmas *et al.*, 2000; Neave and Abrahams, 2002; Peters and Havstad, 2006), particularly in semi-arid environments where fragile boundaries exist not only between vegetation and erosion but also between the two dominant vegetation types, grasses and shrubs.

Evidence suggests that the hydrological response of semi-arid hillslopes is largely controlled by plant cover (Böhm and Gerold, 1995; Snelder and Bryan, 1995; Gutierrez and Hernandez, 1996; Rietkerk *et al.*, 2002). Vegetation type is therefore considered one of the most significant controlling variables of interrill runoff in semi-arid regions and as such, has been the focus of many studies (Abrahams *et al.*, 1995; Parsons *et al.*, 1996; Wainwright *et al.*, 2000).

Through comparisons of interrill runoff these studies have shown that shrublands display higher runoff coefficients than grasslands and as a result, erosion rates are increased. Abrahams *et al.*, (1995) and Parsons *et al.*, (1996) attributed these findings to a number of factors: 1) greater quantities of overland flow are attained in shrubland areas and achieve higher velocities in comparison to grasslands; 2) discontinuous canopy cover in shrub-dominated landscapes result in poor protection against raindrop impact in intershrub areas; and 3) shrubland soils may potentially be more susceptible to frost action due to the greater proportion of exposed soil. As a result, certain characteristics are associated with shrublands including an eroded A horizon, the formation of a desert pavement and the development of rills (Abrahams *et al.*, 1995). However, semi-arid grasslands are characteristically 'patchy' themselves, displaying mosaics of grassy tussocks and bare patches to varying degrees. Research has shown that within predominantly

grass landscapes there is preferential erosion in bare areas compared to high infiltration and low runoff rates within the vegetation patches (Cerdà, 1997).

Runoff and interrill erosion are associated with a critical level of plant cover and although disparities exist in defining this value e.g. 70% proposed by Lang (1979), 60% by Orr (1970) and 50% by Gifford (1985), aboveground biomass is considered an important factor in reducing the erosive impact of overland-flow (Gutierrez and Hernandez, 1996). Gyssels and Poesen (2003) found that an increase in shoot density resulted in an exponential decrease of runoff erosion rates. However, they also argue that the effectiveness of plant cover in reducing erosion by runoff is dependent on a number of factors including; plant canopy height and continuity, plant density, and the density of ground cover (Morgan, 1995) and therefore the effectiveness can vary significantly amongst species. This is particularly significant with respect to the difference in responses of grasslands and shrublands. In general, vegetation cover is greater in shrublands rather than grasslands in semi-arid environments (Wang, 2000). This implies that grasslands may display other vegetation characteristics that influence the erodibility of these landscapes and produce the lower erosion rates as found by Abrahams *et al.*, (1995) and Parsons *et al.*, (1996).

Gyssels and Poesen (2003) argue that while the impact of aboveground biomass on surface hydraulics and sediment movement has been well documented, equally important is the belowground biomass. Notwithstanding the fact that root systems are acknowledged as being beneficial to soil stability by providing mechanical reinforcement, only recently has the importance of root systems been investigated with respect to overland-flow induced erosion. Gyssels *et al.*, (2005) have compiled a review of the impact of plant roots on the erodibility of soil, in which the importance of root networks on soil properties are highlighted with specific reference to aggregate stability, infiltration capacity, bulk density, texture, organic matter content and chemical composition. Although roots provide the binding agents and organic matter needed to create stable aggregates, it is argued that the dominant erosion-reducing component is the dense root network or mat

associated with grass cover (Prosser *et al.*, 1995; Gyssels *et al.*, 2005). Evidence of this is provided by de Baets *et al.*, (2005) who confirmed the effectiveness of grass roots in reducing soil detachment rates through a quantitative study, emphasising the importance of a dense uniform root network and its positive influence on soil strength. This research builds on the suggestion by Gyssels and Poesen (2003) who state that fibrous lateral roots, a characteristic of grasses, are more effective at reducing erosion than shrub tap roots which cover a small surface area of the soil.

Gyssels *et al.*, (2005) summarise the relationships between vegetation cover, roots and erosional processes in figure 2.1. This diagram highlights that both cover and roots are important although their impact varies both spatially and temporally with respect to hillslope erosional processes. Scaling issues are therefore associated with vegetation-erosion interactions in semi-arid environments; the implications of this are discussed further in section 2.2.3.

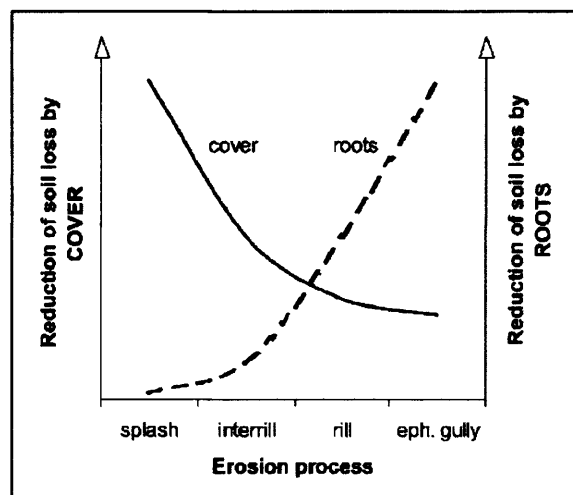


**Figure 2.1** Structural model, indicating the relative importance of vegetation cover and plant roots in controlling the intensity of several water erosion processes.

From: Gyssels *et al.*, (2005) p. 214

Despite the importance of the structural support provided by different vegetation communities on the stability of the landscape, complex plant-soil property interactions are such that they cannot be ignored in relation to the susceptibility of

soil to erosion. In order to fully understand the impact of vegetation change on erosion, an understanding of the behaviour of the underlying physical and chemical soil properties is needed.

## **2.2 The physical and chemical properties of soil and their influence on the susceptibility of soil to erosion**

Erodibility, a concept first formalised by Middleton (1930) is a generic term applied to the combination of soil properties thought to influence a soil's susceptibility to erosion. Since then, many studies have attempted to refine and develop the parameters thought to impact on a soil's erodibility (reviewed by Smith and Wischmeier, 1962) with the objective being to ascertain universally applicable indices (Bryan, 2000). Inasmuch as existing research has application in agricultural land practices and management, Bryan argues that, to date, research has provided little insight into hydrologic and geomorphic processes. Before the recent utilisation of 'naturally vegetated' experimental small-scale plots (Abrahams *et al.*, 1992; Parsons and Abrahams, 1992; Parsons *et al.*, 1996; Wainwright *et al.*, 2000), the majority of detailed soil erosion data was derived from studies on agricultural soils. A number of problems are associated with using this type of data to interpret processes occurring on naturally vegetated, undisturbed land. To a certain extent agricultural soils display artificial characteristics, for example, as a result of ploughing the soil profile will be homogenised and macropores destroyed, thus impacting on soil bulk density and consequently infiltration - a factor known to be a key controlling mechanism of overland flow behaviour. Plough-induced surface conditions significantly alter the hydrologic response of a landscape and when combined with the potential deterioration of soil structure and nutrient status, exaggerate the impact of particle detachment and transport.

As a result, the concept of soil erodibility, as defined from investigations conducted on agricultural land, provides an unrepresentative and unrealistic indicator of the susceptibility of soil to erosion on naturally vegetated hillslopes. In contrast,

quantitative soil data taken from the natural environment, representing both a variety of vegetation types and scales, would be invaluable to the understanding of the dynamics and influence of soil characteristics on the erodibility of soil in semi-arid environments. The subsequent discussion will outline the importance of different soil properties in relation to erosion, dealing with the physical properties of soil and chemical properties respectively.

Although conclusive evidence has provided a foundation for the widely accepted view that relationships exist between the susceptibility of soil to erosion and its physical and chemical nature, results indicate that no single soil property can be attributed as a dominant factor in the erosional response of a landscape. It can be argued that almost any soil property can have an influence on soil erodibility, whether it is direct or indirect, due to the complex interactions indicative of the natural environment.

As there is no single, measurable soil property available to fully represent a soil's erodibility, an assessment must be based on a number of different properties. Bryan (2000) states that due to the initial importance of the response of soil to rainfall, three properties are more influential than the others: soil aggregation, consistency and soil shear strength. Bryan argues that these properties override the significance of others due to their combined influence on "water movement, the distribution of erosive forces, and resistance to entrainment" (p11). This statement is the subject of debate, however, as Franzluebbbers (2002) attributes soil organic matter as a key indicator of soil quality due to the subsequent influence it has on soil aggregation and infiltration. Both statements are essentially true, although Franzluebbbers has attributed the primary soil condition as the controlling mechanism rather than the resultant secondary property. This type of inconsistency has implications on the development of spatially and temporally inclusive models of soil erosion (as described in section 2.3). Consequently, in order to fully explain the influence of physical properties of soil on erosion, basic soil-structure controlling properties need to be examined.

The term 'soil structure' encompasses a number of intrinsic soil properties but ultimately describes the arrangement and stabilisation of soil particles and pores formed by a variety of physical and biological actions (Rowell, 1994). Structure describes the porosity of the soil both between and within clustered soil particles, known as aggregates, and plays an instrumental role in determining a soils response to water through infiltration behaviour. Whereas variables such as porosity and soil bulk density can be used as indicators of structure, factors that influence soil structure include texture and organic matter content.

Soil texture is determined by the particle-size distribution associated with it and is a basic but fundamental characteristic of soil. The significance of texture can be attributed to the effects it has on the behaviour of soil by influencing other physical and chemical properties. For example, drainage and moisture content are dependent on not only the arrangement of particles (linked to soil structure) but also on the type of constituent particles. Fine textured, or clay-dominated soils do not transmit water well due to small pore sizes; on the other hand, they retain more chemicals than other textures due to surface properties of the clay particles. Coarse textured soil such as sand-dominated soils behave in the opposite way, displaying high transmission rates and water holding capacities although characteristically exhibit a low nutrient status.

Soil organic matter (SOM) content and texture are closely associated with respect to the structure of soil and its erodibility. The importance of organic matter accumulation with respect to vegetation patterns has been highlighted in chapter one regarding the development of 'islands of fertility' under shrubs (Parsons and Abrahams, 1992; Schlesinger and Pilmanis, 1998; Bochet *et al.*, 1999; Wainwright *et al.*, 1999; Wainwright *et al.*, 2000). Notwithstanding the obvious beneficial effect SOM has on soil fertility, there are many other favourable conditions induced by a high organic matter content, including; an increase in porosity and water-holding capacity, lower bulk density, increased cation exchange capacity, greater aggregation and increased aggregate stability (Christopher, 1996). Nevertheless, the stabilising effect of organic matter is not unbounded; thresholds have been

shown to exist as all soils have a limited ability to accumulate organic matter (Allison, 1973; Boix-Fayos *et al.*, 2001). These thresholds vary with soil type; poorly structured soils generally show a greater increase in stability with the addition of organic matter compared to well-structured soils. Although semi-arid soils are commonly associated with low SOM values, usually under 2% (Rowell, 1994), the stabilising qualities of organic matter may have a significant influence on spatial variability of soil stability in dryland landscapes. Due to the nature of the physio-chemical processes that are influenced by SOM, it can be hypothesised that if organic matter is spatially heterogeneous then the associated stabilising properties of soil will be equally heterogeneous.

Arguably one of the most important properties controlled by SOM, in relation to erosion, is soil aggregate stability. Although ultimately this can be classed as a physical property of soil, it is in fact the chemical properties of SOM and their interaction with soil particles that determine the stability of the aggregates. A conceptual model of the relationship between organic matter and aggregate stability was proposed by Tisdall and Oades (1982), three types of binding agents were attributed as responsible for the stability of aggregates; 1) transient agents of microbial and plant-derived polysaccharides, 2) temporary agents such as roots and hyphae and 3) persistent agents of aromatic humic materials which affect amorphous Al and Fe compounds and polyvalent cations (Christopher, 1996). The former two agents are thought to be responsible for the stability of macro-aggregates whereas the latter is thought to influence the stability of micro-aggregates.

The influence of aggregate stability on erosion was inferred by the splash and runoff entrainment relationships presented by Hjulstrom (1935) and Poesen (1981), indicating that aggregate size plays a critical role in soil erodibility. Bryan (2000), however, argues that the relationship was derived from material that was of uniform specific gravity where size and mass are directly related. Instead, Bryan argues that composite aggregates will display more complex relationships resulting in much greater variation in soil stability behaviour.

Boix-Fayos *et al.*, (2001) investigated this further through a study on the influence of soil properties on aggregation, using aggregate size and stability as indicators of land degradation. The results of this study indicate that the water stability of microaggregates is positively correlated with clay content whereas the stability of macroaggregates is dependent on organic matter content. However, this was found to be true only in soils where the SOM was greater than 5 or 6%, below this threshold aggregate stability displayed a more significant correlation with the carbonate content of the soil. Also emphasised was the care needed when interpreting aggregate size with respect to soil structure, stating that local characteristics must be considered as the presence of large aggregates does not always indicate an improved soil structure. The conclusion reached from this investigation indicates that although aggregate size distribution and stability cannot be considered as a unique erosion-determining parameter, it can be used as an indicator of land degradation.

Christopher (1996), however, suggests that when relating aggregate stability to organic matter content caution should be exercised as SOM behaviour can be diverse and can actually cause the dispersion of clay particles (Oades, 1984; Mbagwu *et al.*, 1993). Instead Christopher proposes that other factors such as soil pH should also be considered before direct inferences are made. Despite this, the applicability of aggregate stability as an indicator of a soil's susceptibility to runoff and erosion has continued to be investigated. One such study has been undertaken by Barthès and Roose (2002). The rationale behind this research was derived from the debate surrounding the degree of applicability of laboratory-based experiments; the argument being that relocated, sieved soil may not provide an accurate representation of the field phenomenon, a common problem in geomorphology. Through comparisons of top-soil aggregate stability and field-assessed soil susceptibility, Barthès and Roose validated aggregate stability as a relevant indicator of soil erodibility and provided evidence that laboratory-derived data correlates with those obtained from field investigations.

Léonard and Richard (2004) utilise this relationship albeit by a different approach to assess the susceptibility of soil to erosion. This research investigated soil shear strength as a means of estimating the critical shear stress of soil. As aggregate stability affects the cohesion and frictional resistance of soil, this, in addition to many other properties such as texture, organic matter content and bulk density have been related to critical shear stress values (Gilley *et al.*, 1993). Léonard and Richard present a synopsis of existing shear stress studies, drawing attention to gross inconsistencies evident throughout the datasets. Due to the variability of shear stress over a short-term temporal scale it is suggested that rather than using the aforementioned soil parameters to determine critical shear stress, mechanical properties of soil would present a more relevant method of assessment. However, results suggest that rather than total shear stress, a relationship exists between saturated soil shear strength and critical grain shear stress. This has implications for erosion prediction modelling as the majority of existing models deal only with total shear stress measurements.

Nevertheless, soil strength has been linked to a number of erosional processes including soil detachment (reviewed in Bouma and Imeson, 2000), rill initiation (Parsons and Wainwright, 2006) and surface sealing (Bradford *et al.*, 1992; Zhang *et al.*, 2001). Through an investigation of the applicability of a new method of shear strength measurement, in order to explain the processes of soil erosion and surface sealing, Zhang *et al.*, (2001) evaluated the influence of soil bulk density and soil moisture content on surface shear strength. The results indicated that bulk density and soil moisture have a significant impact on soil strength. The findings complement those presented by Nearing *et al.*, (1991), who stated that the tensile strength of soils decrease with decreasing bulk density and increasing water content. Huang *et al.*, (2002) on the other hand, focused on how hillslope position and moisture condition affect the generation of runoff and sediment production, but similarly attributed surface soil moisture as a controlling mechanism of erosion. In a study of the relationships between field indicators and erosion processes on badland surfaces, Bouma and Imeson (2000) also highlight the significance of soil moisture. The shear strength and vertical resistance of soil were found to be strongly reliant on the quantity of infiltrated water, thus it was

concluded that the relationship between soil moisture change and the behaviour of sediment concentration could potentially be used as a direct indicator of soil erodibility.

Bouma and Imeson's study also discusses the importance of chemical and mineralogical soil properties on erodibility. Although soil chemistry has obvious implications with respect to plant-available nutrients, soil solutes also play an instrumental role on the swelling and dispersive behaviour of clay particles. In studies where vegetation change is the focus, most are only concerned with plant-limiting nutrients and therefore do not interpret erosion by the direct effect of a redistribution of chemicals. Instead, they determine how the spatial discontinuation of nutrients affect the distribution of vegetation and subsequently, how this controls erosion through changes in the hydrological response of the landscape.

In contrast, the pronounced impact of soil chemistry on badland landscapes has been recognised by many (Bouma and Imeson, 2000; Rienks *et al.*, 2000; Vandekerckhove *et al.*, 2000). Two of the four major cations are largely responsible for the behaviour of clay particles, sodium ions ( $\text{Na}^+$ ) which cause clay particles to disperse thus exacerbating particle detachment, and calcium ions ( $\text{Ca}^{2+}$ ) which promote flocculation by providing a polyvalent bridge between clay particles and organic matter (Christopher, 1996; Wild, 2001). The two other major cations, potassium ( $\text{K}^+$ ) and magnesium ( $\text{Mg}^{2+}$ ) are also thought to influence the erodibility of soil although their effect is less clear. However, it is generally accepted that dispersibility decreases in the following order: Na, K, Mg, and Ca (Dexter and Chan, 1991).

The electrical conductivity (representing the soil salinity) and cation exchange capacity of a soil are commonly used as soil quality indicators, however, the sodicity of a soil is often considered a more relevant parameter to investigate with respect to erosion due to the dispersive nature of sodium ions (Pons *et al.*, 2000;

Mamedov *et al.*, 2002). Sodidity occurs when sodium salts accumulate, increasing the amount of exchangeable sodium. This is normally expressed as an exchangeable sodium percentage (ESP), which is a percentage of the total cation exchange capacity. A sodic soil is deemed as having > 15 per cent ESP (Rowell, 1994). Unlike salinity, the sodicity directly affects the structure of the soil (Pons *et al.*, 2000; Wright and Rajper, 2000; Mamedov *et al.*, 2002). An ESP measurement of between 10 and 15 is known to make clay particles swell and disperse thus causing a deterioration of the soil structure (Rowell, 1994; Pons *et al.*, 2000). Sodic soils are also alkaline, further adding to the deterioration of soil through the dispersal of soil organic matter. However, the damage caused by sodicity varies amongst soils, the sensitivity of the soil depending on many factors including: clay content, clay mineralogy, sesquioxide content, organic matter content, bulk density, exchangeable cations (particularly sodium), the soil solution concentration and pH (Rowell, 1994). A recent study by Vaidya and Pal (2002) also suggests that microtopographic differences influence the development of sodicity. However, the main implications of a high Na<sup>+</sup> content with respect to erosion is demonstrated through comparisons of non-sodic and sodic soils by Mamedov *et al.*, (2002). This investigation found that sodic soils produced runoff levels and velocities high enough to initiate rill erosion, which in association with raindrop detachment could significantly increase erosion.

The preceding discussion on the influence of the physical and chemical properties of soil is by no means exhaustive, however, it attempts to emphasise not only the importance of these properties but the complicated interactions that exist amongst them. Most studies conclude that it is inappropriate to use a single parameter as an indicator of soil erodibility and often highlight that anomalies in their data could be explained by investigating other soil properties.

Although the significance of vegetation on the structural stability of the soil has been shown (Prosser *et al.*, 1995; Gyssels *et al.*, 2005; de Baets *et al.*, 2005), the link between shrub invasion and an increase in erosion can be attributed to the complex relationships amongst the soil properties previously discussed.

Although they cannot be classed as discrete systems, shrub and intershrub areas display significantly different erosional response characteristics. These are largely controlled by edaphic factors, which in turn, are a consequence of plant-soil feedback mechanisms. Chapter one discusses the idea that shrubs are self-perpetuating systems that develop through the preferential accumulation of nutrient-rich litter. A brief outline of the distinctive hydrologic response involving rainsplash and the concentration of flow into intershrub areas is also provided. However, in order to fully understand why preferential erosion occurs in intershrub areas, further explanation is needed specific to the edaphic factors previously shown to affect a soil's susceptibility to erosion.

The microenvironments created by individual shrubs show an improved physical and chemical soil status in comparison to intershrub areas. These include: larger amounts of organic matter and nutrients, greater cation exchange capacities and aggregate stability, and lower pH, bulk density, penetration resistance and carbonate content values (Bochet *et al.*, 1999). These factors combine to increase the infiltration capacity of the soil under the shrub canopy thus decreasing runoff and improving the nutrient status of the soil by allowing the accumulation of litter and subsequently the leaching of available nutrients to the root zone. The improved soil chemistry also affects the erodibility of the soil by interacting with the increased quantities of organic matter thus producing more water stable aggregates.

In contrast, intershrub areas become increasingly susceptible to erosion through a lack of biotic activity (Schlesinger and Pilmanis, 1998). Overland flow, raindrop impact and an increased susceptibility to wind erosion (Okin *et al.*, 2006) combine to strip the A horizon from the intershrub areas, creating swales and gravel lags that constitute the desert pavement (Abrahams *et al.*, 1995). The surface crust is responsible for decreasing the infiltration capacity, increasing surface sealing and thus intensifying overland flow. The problem is exacerbated as the intershrub soil becomes more depleted of nutrients through increased runoff (Schlesinger and

Pilmanis, 1998; Schlesinger *et al.*, 1999; 2000) making it progressively more difficult for other vegetation types to become established.

An alternative explanation for the spatial variability of soil stability in semi-arid shrublands can be construed from the knowledge that a redistribution of nutrients accompanies vegetation change. Although nutrient patterns have been well documented in the literature with respect to shrubs and the development of 'islands of fertility', few have considered how this change in soil chemistry may directly affect a soil's susceptibility to erosion. An interesting observation was made by Bochet *et al.*, (1999) in their study of islands of fertility in southeast Spain. Significant levels of calcium ions were measured (due to gypsum in the region) in the intershrub areas. Due to its known flocculation-inducing abilities, the calcium content was attributed as the reason why aggregate stability values from under shrub canopies were similar to intershrub values. Schlesinger and Pilmanis (1998) on the other hand reported that sodium, among other nutrients, were found more frequently between shrubs. Such information implies that the redistribution of nutrients, calcium and sodium in particular, should be monitored not only with respect to plant availability but also in relation to the flocculation and dispersal behaviour of clay particles. In addition, Bochet *et al.*, (1999) state that under plant canopies soils are generally richer in sand and poorer in clay content, this would again imply that if both sodium content and clay content are concentrated in intershrub areas, increased erosion in these areas could be accounted for by augmented clay dispersal. It should be noted, however, that although the nutrient distribution of soil is controlled by a number of factors, it is primarily dictated by parent material, therefore regional differences will be evident both in grasslands and shrublands and thus should be taken into consideration when interpreting the results.

It can be argued that although soil chemistry, with regards to soil dispersibility, is considered significant in badland studies, shrubland investigations have largely ignored this aspect of the erosional process in preference to soil fertility studies. It is well documented that further degradation of shrublands can lead to the

formation of badlands thus it seems nonsensical that the consequences of a redistribution of nutrients with regards to soil chemistry-stability interactions has, to date, been largely overlooked.

## **2.3 The implications of changing spatial patterns of soil properties on soil erosion**

### **2.3.1 The concept of heterogeneity**

Shrubland landscapes are commonly described as heterogeneous in nature due to the development of intershrub and shrub units. As discussed previously, these areas display different characteristics in both their hydrologic response and physio-chemical nature. Conversely, grassland landscapes were initially regarded as relatively homogeneous, not only in plant cover but in all aspects relevant to erosion, including soil properties and overland flow characteristics. However, this perception has subsequently been re-evaluated as a result of fine-scale studies of grassland ecosystems (Hook *et al.*, 1991). It is currently proposed that rather than the simultaneous development of spatial heterogeneity with shrub encroachment, as initially suggested by Schlesinger *et al.*, (1990), it is thought that soil properties in grasslands also display spatially heterogeneous characteristics albeit at a micro-scale (Tongway and Ludwig, 1994; Schlesinger *et al.*, 1996).

The spatial patterns of soil properties, particularly in shrubland systems, have been of interest to multiple disciplines ranging from geomorphologists to ecologists. Whereas ecologists may be more interested in the effects on plant competition and diversity (Schenk *et al.*, 2003), the main motive for geomorphologists is the association between an increase in soil heterogeneity and the exacerbation of erosion potential of intershrub areas (Maestre and Cortina, 2002; Rietkerk *et al.*, 2002). In such studies the identification and quantification of spatial patterns is problematic as a result of the complex interactions and highly variable controlling factors. For example, Rango *et al.*, (2006) highlight the

importance of the precipitation regime on runoff in the Chihuahuan Desert, stating that topography and elevation in addition to local weather conditions are all accountable for the spatial distribution across the basin. These factors, in conjunction with the variations within and between soil and vegetation, result in a complex, multi-layer system of spatial patterns that make the disaggregation of independent variables very difficult.

The previous sections have highlighted the importance of aboveground and belowground biomass on the structural stability of a landscape as well as the interactions of soil parameters and their influence on the susceptibility of soil to erosion. This study therefore proposes that the significance of vegetation change on the potential degradation of the land can be linked to an increase in heterogeneous vegetation cover, and consequently, the spatial reorganisation of soil parameters. The hydrological processes and response of the landscape will reflect this spatial heterogeneity.

### **2.3.2 Implications of spatial heterogeneity on the erosional response of the landscape**

Chapter one briefly introduced the concept of the self-sustaining units or 'islands of fertility' evident in shrubland landscapes, emphasising the fundamental role vegetation plays in the hydrologic response of a landscape through its effect on rainsplash, overland flow and soil property redistribution. However, further explanation is necessary in order to understand the significance of the changing spatial patterns that accompany vegetation change and influence the susceptibility of soil to erosion. The importance of understanding the spatial patterns of soil properties at scales representative of vegetation communities is also highlighted with respect to the development and applicability of erosion prediction models.

A key component of the degradation process is the characteristic erosional response of semi-arid environments. Although many hillslope processes are prevalent in dryland landscapes two mechanisms are attributed as the main erosive agents responsible for instigating sediment detachment and transport, namely rainsplash and overland flow. In geomorphic terms, dryland erosional processes are commonly divided into two distinct components, interrill processes and rill erosion, which are primarily controlled by rainsplash and runoff respectively (Bryan, 2000). A conceptual model derived from the work of Meyer and Wischmeier (1969) recognises these mechanisms, dividing soil erosion into four sub-processes 1) soil detachment through rainfall; 2) transport by rainfall; 3) soil detachment through overland flow and 4) transport by overland flow. It is evident therefore, that the integration of hydrological and geomorphic concepts is necessary to explain the processes involved in land degradation and desertification.

The importance of overland flow has long been recognised in hillslope geomorphology. The key processes and interactions involving overland flow in semi-arid regions are summarised in figure 2.2. Two types of overland flow occur on hillslopes, saturation overland flow and Hortonian overland flow. Seasonal high-intensity rainfall events are responsible for Hortonian overland flow; a phenomenon that occurs when rainfall intensity exceeds soil infiltration capacity resulting in sheet erosion, this type of response is the most prevalent in semi-arid environments. Many overland flow studies focus on the importance of this process on soil erosion, or more specifically, its influence on rill initiation.

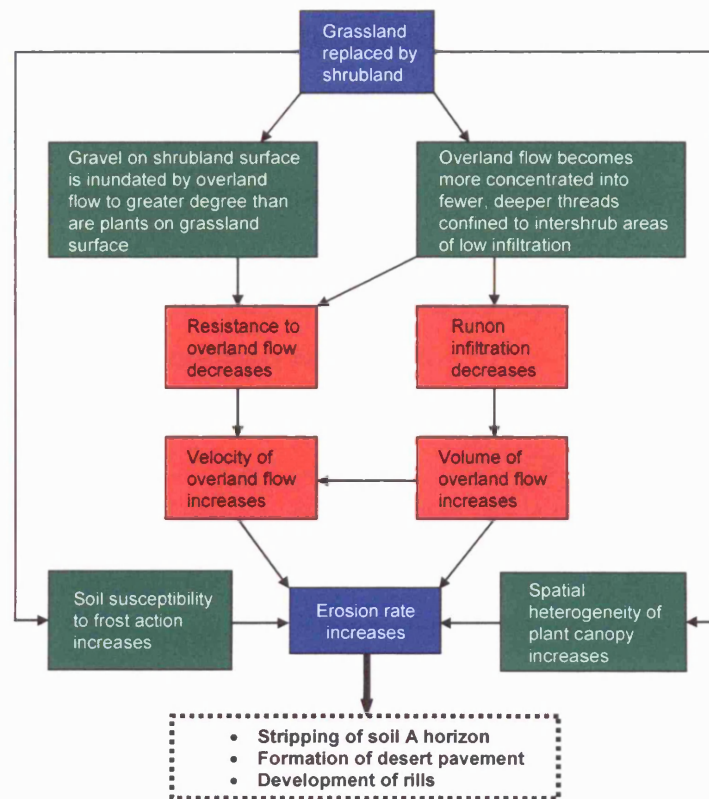


**Figure 2.2** Causal diagram summarising the erosion process in semi-arid environments

*Adapted from: Abrahams et al., (1995) p.47*

There is debate surrounding the instigating mechanisms of rill development. The question of causal factors was prominently raised by Horton (1945); after investigating the behaviour of runoff generation he concluded that an essentially uniform layer of water occurs on the slope surface thus simultaneously creating a uniform layer of erosion. Thus Horton concluded that rills would develop in areas where accidental concentrations of sheetflow occur. However, as Parsons and Wainwright (2006) argue, this statement contradicts Horton's own description of rills, where he states that they are "usually relatively uniform, closely spaced and nearly parallel" (p. 331), a regularity that would not be expected if the initiating mechanism is accidental. This problematic explanation has encouraged further investigation of rills although inconsistent results persist to impinge on progress. A significant discovery questions Horton's 'uniform sheetflow distribution' theory. Alternatively, this theory suggests that overland flow in fact consists of

anastomosing threads of deeper, faster flow (Parsons and Wainwright, 2006). This revelation prompted a study by Abrahams *et al.*, (1989) who undertook a quantitative investigation on the variability of overland flow depth. This research provided evidence of a negative exponential distribution for many of the observed distributions of depths. This evidence provided the basis of the idea that rill development could be explained by an increase in depth of overland flow where the shear resistance of the soil is undermined by the increased shear stress exerted on it through an increased flow depth.

An observation made by Parsons *et al.*, (1996) provided contradictory evidence to the initial findings of Abrahams *et al.*, (1989). Parsons *et al.* noted that shrubland hillslopes in the Walnut Gulch Experimental Watershed developed rills yet grasslands did not. The significance was that mean depths of flow in interrill areas, measured in a study of flow hydraulics on grassland and shrubland plots (Abrahams *et al.*, 1995), was shown to increase downslope on grasslands but not shrublands. This observation is exactly the opposite of what would be expected if the previous conclusion was correct (Parsons and Wainwright, 2006). The influence of overland flow on rill initiation has been acknowledged, however, with Parsons and Wainwright summarising four factors responsible for the activation of rills: 1) the probability of suitable conditions for turbulence in a distribution of flow depths; 2) the probability that the local soil shear strength will be exerted by the shear stress of a turbulent burst event; 3) the spatial distribution of soil shear strength and 4) the correlation between raindrop detachment and flow detachment.

Determination of the spatial patterns of soil properties can therefore be of significant importance in identifying areas that are sensitive to the potential initiation of rills.

One of the implications of the debate surrounding the mechanisms of rill initiation and development is that accurately predicting erosion through process-based

models is difficult. Existing prediction models, for example the Water Erosion Prediction Project (WEPP) (Lane and Nearing, 1989) and the European Soil Erosion Model (EUROSEM) (Morgan *et al.*, 1993) calculate the contributions of rill and interrill erosion separately, thus acknowledging that different mechanisms control particle detachment and transport in these areas. Nevertheless, some fundamental flaws are associated with models based on this conceptual framework. In particular, the assumption that rills are pre-existing and remain static throughout time is made. The consequence of ignoring the impact of rill development and the associated contribution to erosion is that total soil loss can be grossly underestimated (Favis-Mortlock *et al.*, 2000).

In contrast, Baird *et al.*, (1992) argue that the ability to develop models that can accurately predict erosion relies on the recognition that both rill and interrill areas are not separate entities, rather they represent inter-related parts of a dynamically evolving landscape. Therefore, in order to model erosion by overland flow and accurately be described as process-based, Parsons *et al.*, (1997) state that the possibility of dynamic changes from interrill to rill erosion must be incorporated into the model, thus accounting for the spatial variability of interrill overland flow.

An attempt to overcome such issues has been made through the development of distributed parameter models (Goodrich *et al.*, 1991; Moore and Grayson, 1991; Scoging *et al.*, 1992). The spatial variability of parameters are represented by applying a cell matrix over the runoff-producing area and employing a set of rules which dictate the path of flow, usually governed by topography (Parsons *et al.*, 1997). This approach was undertaken by Scoging (1992), who recognised that three key sets of decisions were fundamental to the development of a model representing hillslope erosion by overland flow. The first set of decisions establish the runoff generation through rainfall, surface materials and infiltration interactions; the second set deal with the flow path of water thus represent the hydraulics, temporal distribution and spatial concentration; and thirdly those which address the applicability of converting flow characteristics into erosion mechanics. Scoging (1992) and Scoging *et al.*, (1992) focused on the issues surrounding the first two

sets of decisions, highlighting the importance of scale, both spatially and temporally and ultimately the difficulty in producing models which are applicable to multiple scales. Nonetheless, the results derived from the developed model accurately predicted spatial variability in interrill flow, validated through observations made at the experimental runoff plots in the Walnut Gulch Experimental Watershed, Arizona. However, Grayson and Moore (1992) draw attention to a number of problems associated with distributed, physically based models stating that inasmuch as the models “provide us with an enormous amount of information and have the theoretical potential to provide a universal tool for the representation of hydrologic response...they are somewhat removed from reality” (p171).

Although modellers acknowledge the complexity of hillslope processes, the expectation that every process and hillslope characteristic could be incorporated into a process-based model is unrealistic. Baird (2004) emphasises the difficulties in conceptualising ‘real’ hillslope processes, demonstrating the inappropriate use of laboratory simulations and the problems associated with scale. However, it can be argued that without an understanding of the underlying mechanisms and characteristics, deterministic, process-based models will never be able to realistically represent the hydrologic response of a hillslope or accurately predict erosion.

An example can be drawn from Scoging’s (1992) model of overland flow; although acknowledging the fact that many factors influence overland flow, the model is only based on three key control variables: surface properties that influence infiltration and roughness; slope to determine flow route and a dynamic friction component. As a result of field-testing the model, Scoging *et al.*, (1992) identified that infiltration parameters derived from 1m by 1m plots did not represent infiltration processes at the main site, thus implying spatial variability and/or scaling issues. It seems relevant to highlight here that some of the most important controlling factors of infiltration and associated surface sealing are soil properties, for example, texture, porosity, soil moisture and structure (Franzluebbers, 2002).

Notwithstanding the fact that many authors have attempted to incorporate these factors into their models (de Lima, 1992; Lane *et al.*, 1992; Poesen, 1992; Schmidt, 1992) the intent appears to be on establishing knowledge of the overall spatial (and temporal) variations of overland flow characteristics and rill initiation rather than initially focusing on, and understanding, the distribution of the underlying variables, for example, those which control infiltration.

This issue was, to a certain extent, considered in a recent study of scaling approaches to modelling water, sediment and nutrient fluxes in semi-arid New Mexico (Müller, Unpublished thesis). Soil property measurements were taken from both grassland and shrubland plots at a number of different scales. The study considered the impact of the spatial variability of controlling soil parameters, concluding that this variability is significant in the scaling of hydrological/sediment transport models. The implications of this research highlight the need for a larger database of spatial data, over a variety of different scales as well as soil and vegetation types. Not only would this allow improved development of predictive models but a means of testing their applicability and accuracy.

It is important to gain an understanding of basic processes before attempting to explain the complex ones. This research therefore endeavours to gain a more comprehensive knowledge of the spatial patterns of soil properties and their influence on soil erosion. Although incorporating the findings of this work into a model is beyond the scope of this project, the potential application in the development of future process-based models may be significant.

### 2.3.3 A function of scale?

Imperative to the identification and understanding of spatial patterns in a landscape is the recognition of the impact of scale. Although early studies of plant communities have acknowledged the presence of spatial patterns e.g. (Greig-Smith, 1952; Kershaw, 1957), the realisation that the understanding of interactions between pattern and process depends on characterising spatial heterogeneity over a variety of scales is a relatively recent development (Wu *et al.*, 1997; Wainwright *et al.*, 1999; Wu *et al.*, 2000). This has been largely driven by the need to understand multi-scale processes for modelling purposes. Qi and Wu (1996, p39) stress the importance of scale issues by stating that, “pattern and scale are inseparable in theory and in reality. Pattern occurs on different scales, and scale affects pattern to be observed”.

Due to its multi-faceted nature, scale multiplicity plays a fundamental role in the understanding of land degradation processes. Recognition of scaling issues has now disseminated across many research areas, the three main disciplines with relevance to soil erosion being: geomorphology, hydrology and ecology. Although scientists have attempted to link spatio-temporal scale factors between geomorphic features and hydrologic processes, until recently, the integration of all three disciplines has been largely ignored. It is clear that a comprehensive understanding of vegetation change, as a mechanism of the degradation process, relies on interdisciplinary resolve over the dominant processes involved and the scaling issues associated with them.

Vegetation dynamics, soil property heterogeneity and erosional processes, the three key systems under investigation in this study, inherently operate on a number of levels and thus have encouraged the development of a hierarchical spatial framework. Although acknowledging that a continuum of scales is possible, Peters and Havstad (2006) identified five levels of hierarchy operating in semi-arid environments. The smallest unit of scale identified is at the plant – interplant level. A number of interacting processes operate at this scale, including:

the spatial redistribution of nutrients in shrublands resulting in the development of islands of fertility (Schlesinger *et al.*, 1990; Schlesinger *et al.*, 1996; Titus *et al.*, 2002); the preferential concentration of water under shrub canopies through mechanisms such as stemflow and throughfall (Rango *et al.*, 2006) and improved infiltration rates under canopies due to a reduction in raindrop impact and compaction (Schlesinger *et al.*, 1999; Wainwright *et al.*, 1999; Wainwright *et al.*, 2000). Following the plant-interplant level is the patch scale, used to describe the dynamics of a group of plants and their associated interplant zones. Such patches are usually characterised by several dominant species and can vary in size from several individuals to several hundred individuals. In Peters and Havstad's hierarchical framework the third scale of interest, patch mosaics, describe groups of patches dominated by different dominant species and inter-patch areas. Edaphically controlled ecological units, or groups of patch mosaics, combine to form the fourth scale, a landscape unit. Interacting landscape units form the final scale, defined as the geomorphic component. Parent material and landscape position are commonly the controlling factors at this scale.

Interactions within this spatial hierarchy are instrumental in controlling landscape dynamics. Connectivity factors interact across scales creating threshold behaviour and thus explain the variable and nonlinear spatial and temporal responses evident in semi-arid systems. Peters and Havstad (2006) suggest five connectivity factors are responsible for the redistribution of essential plant resources, both spatially and temporally, and thus influence the patterns and behaviour of vegetation in dryland regions. These factors are: 1) historical legacies, a term used to describe natural and anthropogenic impacts that have long-term consequences on ecosystem patterns and interactions; 2) the dynamic template, which portrays the spatial context and patterns inherent in ecological variables; 3) the redistribution of resources; 4) the feedbacks evident among vegetation, animals and soil; and 5) transport mechanisms including; fluvial, aeolian and animal influences.

In order to detect and interpret controlling mechanisms of vegetation dynamics in arid regions, Bestelmeyer *et al.*, (2006) highlight the need for the synthesis of spatially explicit, multi-temporal data. This study emphasises the dangers of potential misinterpretations of measurements taken at inappropriate scales. At too fine a scale, trends unrelated or opposite to those observed at a broader scale may be evident, whereas, at too coarse a scale significant fine-scale soil/vegetation changes may be missed, thus having a detrimental impact on remediation efforts. In response, Bestelmeyer *et al.*, propose that a classification of vegetation transition patterns can be used to aid the prediction of vegetation change at broad scales. This approach addresses the problems of scale and connectivity by basing the classifications on observations made at multiple scales of vegetation and soil patterns as well as considering cross-scale interactions. The mechanisms of vegetation change identified in their study of the Chihuahuan Desert are summarised in table 2.1. Although these are specific to one area, the general trends should, in principle, be transferable to similar semi-arid environments.

**Table 2.1** Mechanisms of vegetation dynamics (bold italics) and their variants (indented) recognized in a study of the Chihuahuan Desert. *Adapted from: Bestelmeyer et al., (2006) p.300*

Class	Criteria
<b><i>Stability</i></b>	<ul style="list-style-type: none"> <li>● Minimal change in size/cover or spatial position of plants over the time series.</li> </ul>
<b><i>Size oscillation</i></b> <b>Full size oscillation</b>	<ul style="list-style-type: none"> <li>● Both reduction and growth of canopy cover observed in the series. At least some of a plant's initial ramets maintain their spatial position over a time series, and initial ramets are the source for vegetative colonization of formerly or newly occupied areas.</li> </ul>
<b>Growth or decline</b>	<ul style="list-style-type: none"> <li>● Only one trend, either increase or decrease in plant canopy cover observed (e.g., a partial oscillation due to insufficient time).</li> </ul>
<b><i>Loss– reestablishment</i></b> <b>Full loss–reestablishment</b>	<ul style="list-style-type: none"> <li>● Death of individuals within a species or functional group is followed by or coupled with colonization by individuals of the same species or functional group in distinct spatial positions.</li> </ul>
<b>Establishment</b>	<ul style="list-style-type: none"> <li>● New propagules of existing species/functional groups appear in a field of view devoid of grasses, presumably due to colonization by seed or perhaps stolon for certain species.</li> </ul>
<b>Death (potential reestablishment)</b>	<ul style="list-style-type: none"> <li>● Plants die with no recruitment observed. This may be loss–reestablishment or loss- replacement pattern, but if there is no evidence of soil degradation or replacement, then loss–reestablishment is assumed.</li> </ul>
<b><i>Loss– replacement</i></b> <b>Full loss–replacement</b>	<ul style="list-style-type: none"> <li>● Death of individuals within a species or functional group that is followed by/coupled with colonization by individuals of a different functional group.</li> </ul>
<b>Death (little potential for reestablishment)</b>	<ul style="list-style-type: none"> <li>● Plants die with no recruitment. This may be loss–reestablishment or loss–replacement pattern. If there is evidence of soil degradation (i.e., erosion), then loss–replacement assumed.</li> </ul>
<b><i>Patch reorganization</i></b>	<ul style="list-style-type: none"> <li>● Death of individuals within a species or functional group that is coupled with colonization by individuals of the same or different species or functional group in other patches (i.e., coupled dynamics occur within an area44 m2). The coupling should indicate redistribution of resources. Usually detectable only with time sequences of landscape or aerial photos.</li> </ul>
<b><i>Cascading transition</i></b>	<ul style="list-style-type: none"> <li>● Death of individuals appears to be due to sand deposition from adjacent sites. Context indicating a cascade is apparent in aerial photographs or space-based imagery.</li> </ul>

## **2.4 Summary and formulation of objectives**

The mechanisms surrounding plant-soil interactions are such that the understanding of the relationship between the susceptibility of soil to erosion and vegetation change is complex. By comparing the spatial patterns of the physical and chemical properties of soil between grassland, shrubland and badland areas, this research aims to provide a more comprehensive understanding of the influence of vegetation dynamics on the susceptibility of soil to erosion.

In pursuit of understanding the mechanisms of land degradation geomorphologists have recognised that commonly, concurrent with shrub encroachment is the exacerbation of hillslope erosion. This process and its extent are dependent on a number of factors including soil type and surface conditions. This has promoted an inter-disciplinary approach to the investigation of land degradation and desertification in semi-arid environments. Although the instigating mechanisms of vegetation change are not yet fully understood, it is well recognised that the hydrological and erosional responses of a landscape are largely defined by vegetation type and structure. Consequently, grasslands, shrublands and badlands, the three dominant landcovers in semi-arid environments, each display distinct erosional characteristics.

Grassland landscapes may be less susceptible to erosion as a consequence of the more uniform structure of above and belowground biomass. Despite the percentage cover generally being higher in shrublands, the root and shoot structure of grass is a significant factor in semi-arid landscapes (Gyssels and Poesen, 2003; Gyssels *et al.*, 2005). In particular, the structural support provided by dense, fibrous root networks characteristic of grasses, in contrast to the tap roots of shrubs, has been shown to effectively reduce soil detachment rates (Gyssels and Poesen, 2003; de Baets, 2006).

Due to feedback mechanisms that exist between plant-soil systems, the pattern of vegetative cover is also associated with a similar distribution of plant resources (Schlesinger *et al.*, 1996; Schlesinger and Pilmanis, 1998; Ludwig *et al.*, 1999; Rietkerk *et al.*, 2002). In semi-arid environments grasslands are commonly deemed as having superior soil quality, this includes for example: higher organic matter content, greater aggregate stability and lower bulk densities. A uniform distribution of beneficial soil resources not only promotes better growing conditions for vegetation but also reduces soil erodibility by increasing infiltration capabilities. Interrill erosion is therefore reduced as a result of better surface conditions, reduced levels of runoff and lower runoff velocities. In addition, grasslands also discourage spatially concentrated flow thus rill initiation and development are minimised.

Plant-soil interactions become more pronounced during grassland to shrubland transitions. The self-perpetuating nature of shrubs promotes the spatial heterogeneity of soil resources, resulting in two inter-related but distinct systems: shrub and intershrub units. It is recognised that the hydrological response of these systems are significantly different and are thus treated as separate entities in most process-based erosion prediction models. Fine-scale studies of shrub ecosystems have shown that shrubs are, to a certain extent, self-sustaining. The discovery of the spatial autocorrelation of plant-limiting nutrients under shrub canopies initiated use of the term 'islands of fertility' (Schlesinger and Pilmanis, 1998). Although this mainly refers to the concentration of beneficial plant nutrients under the shrub canopy, it also encompasses other physical and chemical resources that support the growth and regeneration of shrubs. Improved soil qualities include: larger amounts of organic matter and available nutrients, greater cation exchange capacities and aggregate stability, lower pH, lower bulk densities and lower penetration resistance (Bochet *et al.*, 1999). These factors combine to increase the infiltration capacity of the soil under the shrub canopy thus decreasing runoff and improving the nutrient status of the soil by allowing the accumulation of litter and subsequently the leaching of available nutrients to the root zone.

Conversely, intershrub zones become increasingly susceptible to erosion through a lack of biotic activity (Schlesinger and Pilmanis, 1998). Overland flow, raindrop impact and an increased susceptibility to wind erosion combine to strip the A horizon from the intershrub areas thus aiding the development of a desert pavement (Abrahams *et al.*, 1995). As a result of the desert pavement, increased surface sealing and decreased infiltration intensifies overland flow and further exacerbates the erosion potential of intershrub areas.

Rather than instigating the spatial heterogeneity of soil resources, it is suggested that shrub encroachment simply amplifies fine-scale heterogeneity already present in grasslands (Hook *et al.*, 1991; Tongway and Ludwig, 1994; Schlesinger *et al.*, 1996; Ludwig *et al.*, 1999). This chapter has therefore introduced the concept that the spatial heterogeneity commonly associated with shrublands is, in reality, a function of scale (Schlesinger *et al.*, 1996). The importance of scale on pattern recognition in landscape dynamics is increasingly being emphasised, studies have been conducted on scales ranging from fine-scale at the plant-interplant level to broad-scale, which describes landscape and geomorphic units. Investigations to aid the understanding of broad-scale processes are largely driven by the economical needs of agricultural management, however, a comprehensive understanding of a landscape is impossible without considering the interactions within and between multi-scales characteristics. Wu *et al.*, (2000) highlight the ecological implications (thus also applicable to soil erodibility) of scale multiplicity, stating that: 1) landscapes may exhibit a scale hierarchy; 2) the scale of observation is significant, landscapes display distinctive spatial patterns at different scales as a result of different processes; 3) single scale observations are potentially inaccurate as the understanding of landscape dynamics relies on multiple-scale characterisation of spatial patterns and processes; and 4) models developed at a particular scale are unlikely to be applicable at other scales.

The feedbacks that exist between plant-soil characteristics suggest that in order to understand land degradation in semi-arid regions, firstly, the influence of soil properties on the susceptibility of soil to erosion should be understood. Secondly,

the effect of plant dynamics on soil must be investigated. This chapter has discussed the hydrologic responses of semi-arid landscapes under different vegetation covers and has provided a detailed discussion of the effects of different soil properties, both physical and chemical, on soil erodibility. The review of existing literature highlights the need for a broader understanding of erosion, linking vegetation change with not only soil properties of importance to plant sustainability but also to the erodibility potential. Although plant dynamics are known to vary both spatially and temporally, this study will focus on the spatial aspects of vegetation change and erosion; however, the study acknowledges the temporal aspect by investigating sites that represent different stages of the degradation process.

The aim of this research is therefore to investigate the relationships that may exist between vegetation change and land degradation. In order to address these issues three main objectives have been identified:

- 1) *To identify the spatial patterns of physical and chemical properties of soil in grassland, shrubland and badland landscapes.*
- 2) *To assess the impact of the spatial patterns on the susceptibility of soil to erosion.*
- 3) *To determine the importance of scale of measurement on the spatial patterns attributed to a landscape.*

## CHAPTER THREE

### Description of the Study Area and Analysis Methods

---

#### ***3.1 Specific study areas requirements***

#### ***3.2 Description of the study area: The Karoo, South Africa***

#### ***3.3 Description of the study area: Sevilleta, New Mexico***

#### ***3.4 Sampling strategy for field studies***

#### ***3.5 Physical Soil Properties: Field and laboratory techniques***

#### ***3.6 Chemical Soil Properties: Field and laboratory techniques***

#### ***3.7 Statistical and geostatistical methods***

#### ***3.8 Summary***

---

#### ***3.1 Specific study area requirements***

Whilst the drivers of land degradation, such as climatic and anthropogenic influences, have been investigated with respect to changes in the distribution of degraded land over time (e.g. Keay-Bright and Boardman, 2006), the intermediate processes of degradation have received little attention. This study proposes that vegetation change, induced by the aforementioned drivers, is significant in influencing the soil's susceptibility to erosion and thus plays an important role in the distribution of severely degraded land. Therefore, in order to assess the

influence of vegetation change on soil erodibility, two main field requirements were determined:

- To gain an understanding of the impact of shrub invasion, semi-arid sites that adequately represent both grassland and shrubland landscapes were required. By comparing the spatial patterns of soil properties from the two vegetation types, the impact of grass-shrub transitions on the susceptibility of soil to erosion can be assessed.
- As this study hypothesises that badlands can develop as a consequence of continuing soil parameter heterogeneity caused by shrubs, badland sites were also required. By investigating the spatial patterns of soil in this type of landscape, a better understanding of the semi-arid degradation process in its entirety would be achieved, rather than the disjointed nature of many existing studies of the erosional process.

The study therefore has to incorporate sites that sufficiently represent the different vegetation communities and the patterns of soil properties associated with them. An attempt to keep other environmental variables as constant as possible was also considered necessary to reduce any potential misinterpretation of the results.

Vegetation change in the semi-arid Karoo region of South Africa is well documented (e.g. Acocks, 1953; Dean *et al.*, 1995; Hoffman *et al.*, 1999) and as such was chosen as the study region for this investigation. A detailed account of the Karoo region is given in section 3.2, however, despite the majority of field requirements being met, the reconnaissance visit to the study area identified a potential problem in obtaining sufficient grassland data. Substantial shrub invasion has already occurred in this area, therefore adequate expanses of grassland were rare. Thus, in order to attain sufficient field data to address the objectives presented in chapter 2, an ancillary fieldsite was integrated into the project: The Sevilleta National Wildlife Refuge (NWR), New Mexico. Figure 3.1 presents the general locations of the two areas of interest.

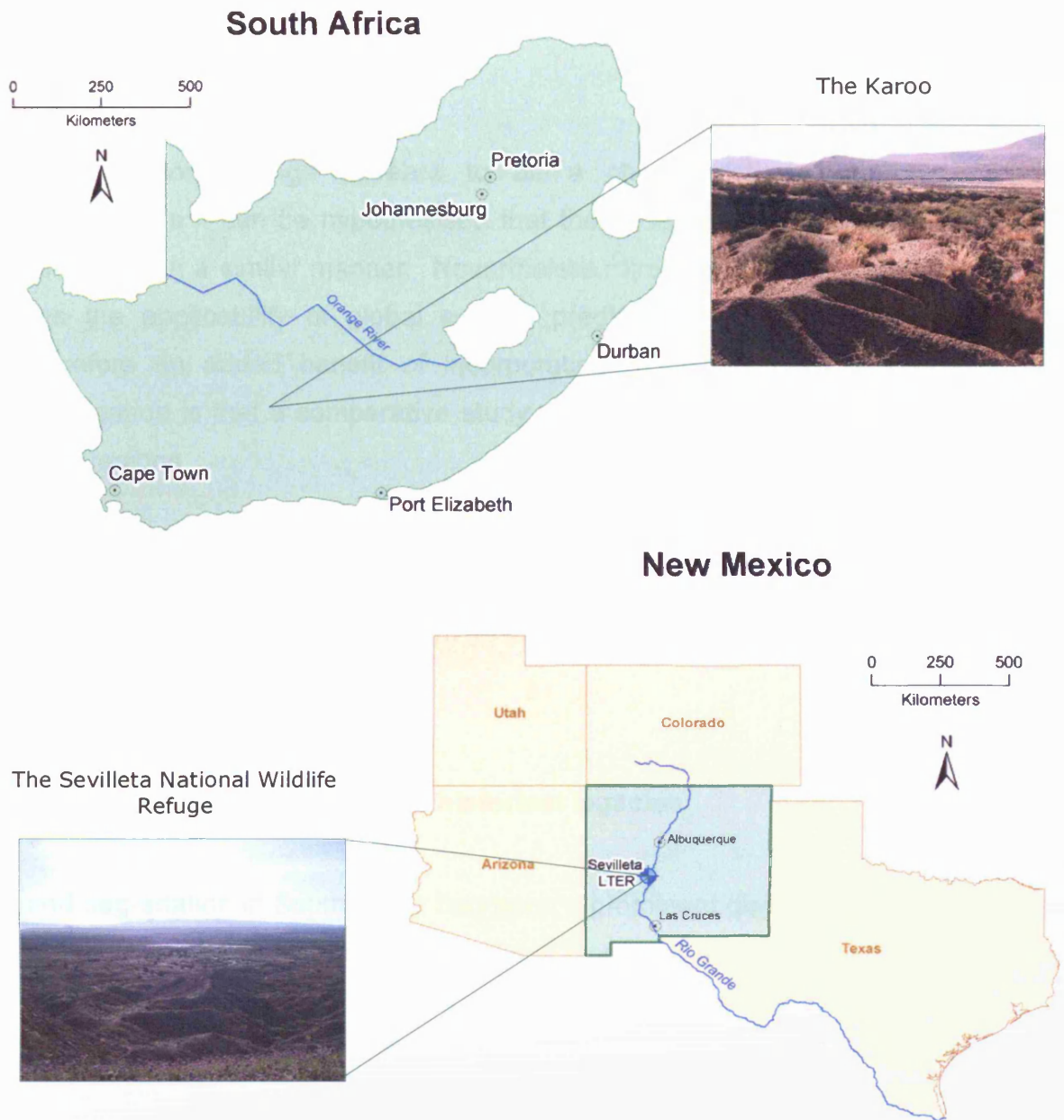


**Figure 3.1** Locations of the two study regions, The Karoo, South Africa and The Sevilleta National Wildlife Refuge, New Mexico.

The two sites display different characteristics of vegetation change. The Karoo landscape, as previously mentioned, is currently dominated by shrubland. Although some areas of grasslands still exist, these are relatively 'patchy' in nature and interspersed with invading shrubs. The Sevilleta NWR site will therefore allow the changes in soil parameter characteristics, induced by a grassland – shrubland transition, to be investigated more thoroughly. On the other hand, only the Karoo

exhibits areas of extensive degradation in the form of badlands, therefore this study region will mainly focus on the shrubland-badland interactions.

As vegetation change appears to be a characteristic of many semi-arid environments it can be hypothesised that the underlying controlling mechanisms will behave in a similar manner. Nevertheless, direct comparisons are scarce and thus the applicability of global erosion prediction models could be disputed. Therefore an added benefit of incorporating a second study region into the investigation is that a comparative study will also be carried out between the two study regions.

## ***3.2 Description of the study area: The Karoo, South Africa***

### **3.2.1 Vegetation change and historical legacies**

Land degradation in South Africa had been a prominent discourse for more than a century. According to the United Nations Convention to Combat Desertification (UNCCD) approximately 91% of South Africa is arid, semi-arid or sub-humid and thus classed as 'affected drylands'. A National Action Programme was ratified in 1997 and as a result an assessment of land degradation and desertification in South Africa was commissioned. Thus, in 1999, a document entitled 'A National Review of Land Degradation in South Africa' was published. This not only served to quantify the nationwide extent of degradation, but also, through an evaluation of the causes and consequences of land degradation, brought the implications of a changing landscape to worldwide attention.

The review raised many issues, encompassing both the biophysical nature of degradation and the socio-economic impact, two factors inherently interconnected.

Consequently, in South Africa, where 71% of the country is classed as commercial land (Hoffman, 1999), degradation can be considered an issue of national importance. The country's economic status relies on the sustainability of agricultural land and therefore the report investigated South Africa's historical and present-day agricultural practices with the view to assessing the applicability of mitigation policies and remediation methods. The impact of anthropogenic influences was also prominently debated, with particular emphasis on the long-term consequences of past agricultural practices.

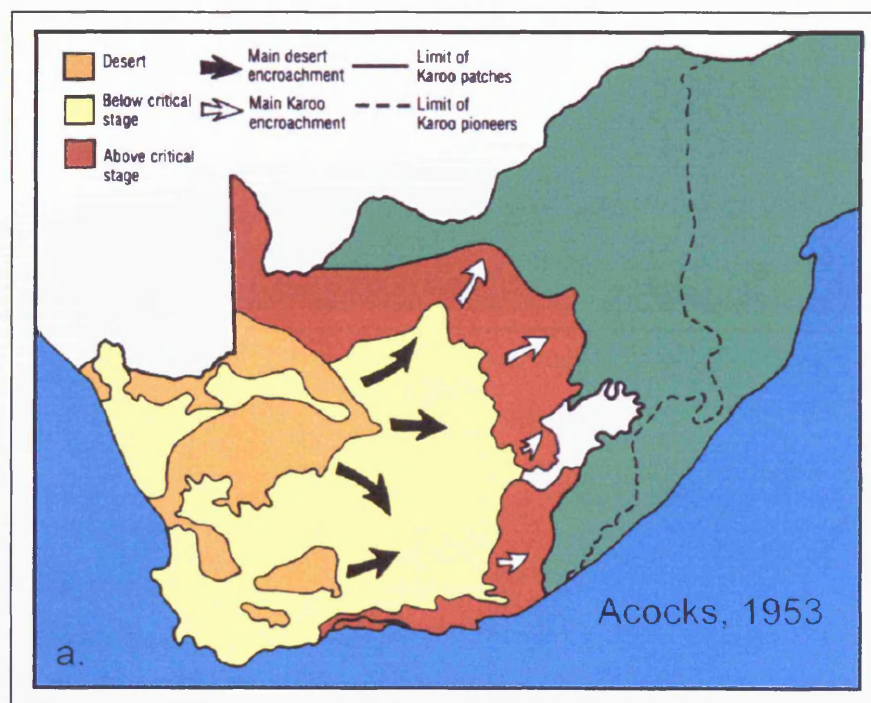
Although the overstocking of land, which was prevalent in the 18<sup>th</sup> and 19<sup>th</sup> centuries as a consequence of the European colonisation (Smith, 1999), is commonly attributed as being one of the instrumental causal factors of the exacerbation of land degradation in South Africa, the review concluded that this assumption is possibly misconstrued. Instead, it is suggested that notwithstanding the fact that the biophysical environment, climate and anthropogenic impacts all influence the degradation of land, ultimately it is the three key natural resources of water, soil and vegetation that determine the type and extent of the problem. It is highlighted that all three factors deserve equal status until the interactions and relationships among them all are better understood, thus it is a necessity that 'hierarchies of control, influence and interaction' are investigated.

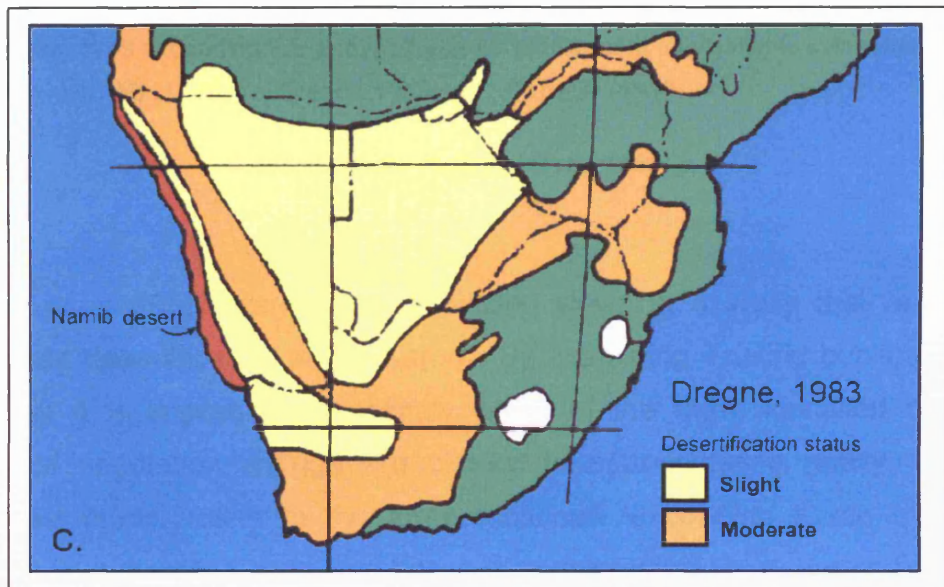
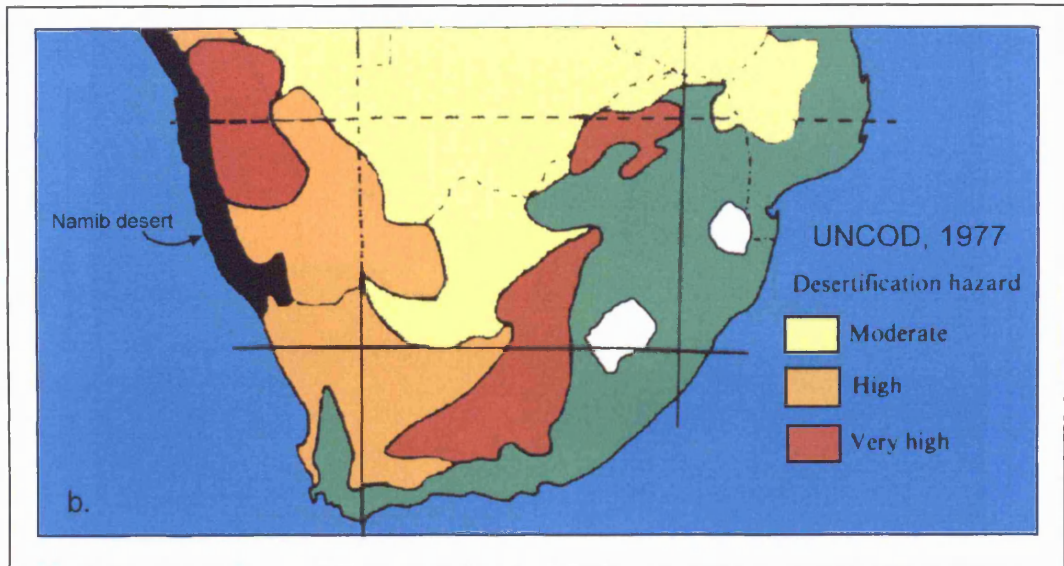
Central to the discussion on South Africa's land degradation status was, and still is, the debate surrounding the extent of desertification in the Karoo. Although increasing desiccation of South Africa was foreseen in the early 1900s, characterised by vegetation change in the eastern Karoo and considered a result of land-use practices, it was not until 1953 that the Karoo desertification hypothesis finally took form.

The expanding Karoo debate manifested after four maps depicting the distribution and vegetative state of South Africa were created by a biologist called John Acocks (1953). Firstly, the pristine vegetation condition of South Africa was

described, although this was based on a variety of other research and publications, no other vegetation map of this scale or detail previously existed. Before human intervention Acocks envisaged that the eastern Karoo was an area of predominantly perennial grasses, which existed in equilibrium with the prevailing climate. However, it is the second issue Acocks explored, that is considered a landmark in South Africa's environmental history.

As a result of colonial settlement, Acocks suggested that the eastern margins of the Karoo had expanded north eastwards and that the Karoo was irrefutably and relentlessly encroaching the Free State grasslands. A simplified version of Acock's desertification map is shown in figure 3.2a. Acock's powerful presentation of vegetation change was such that the view of desertification was predisposed to attributing historical landuse practices as the main causal factors. However, much debate continues to surround the veracity of the 'expanding Karoo hypothesis', with the extent, rate of change and causal factors being disputed to this day. In addition to Acocks vegetation map, figure 3.2 presents three alternative maps that illustrate the dynamic and subjective nature of both land degradation and people's opinions of this phenomenon.





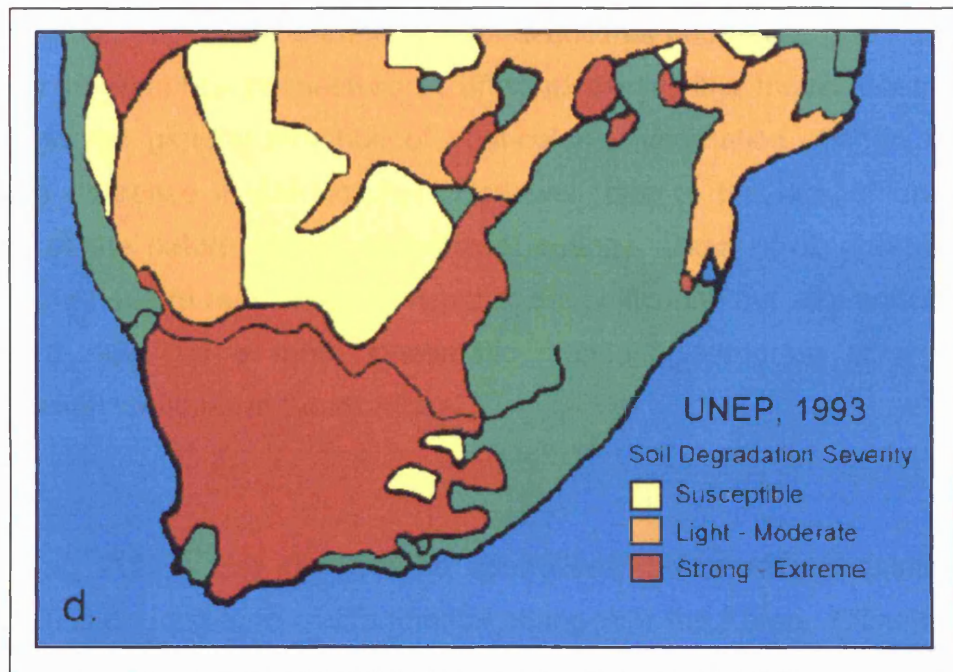


**Figure 3.2** Perceptions of land degradation in South Africa from 1953-1993 showing the influence of (a) Acocks' 1953 expanding Karoo hypothesis on subsequent international syntheses such as those of (b) UNCOD (1977), (c) Dregne 1983 and (d) UNEP (1993)

*Adapted from: Hoffman et al., (1999) p. 4*

Dean *et al.*, (1995) reiterate the conflicting views in a study that reviews and reassesses desertification in the Karoo. By examining existing publications they show that it is impossible to identify which of the three identified conceptual models of vegetation change are closest to approximating reality. The first conceptual model refers to the aforementioned 'expanding Karoo hypothesis', where it is suggested that the Karoo has expanded in a broad front north-eastwards in a unidirectional wave into the productive grasslands of the Free State. The second school of thought suggests that rather than a 'broad front' of vegetation change across the Karoo, vegetation change became apparent as a result of the amalgamation of degraded patches or mosaics over extensive areas and time. The third model considers the Karoo in a non-equilibrium state thus acknowledging the dynamic nature of vegetation in semi-arid environments. This model recognises the expansion of the Karoo but views this movement as 'pulses of migration' of karroid dwarf shrub species into grassland communities during

summer drought periods. Although it takes a conflicting view to the first model by suggesting that vegetation change is multi-directional and hence grasslands could potentially re-establish themselves in affected areas, this model does however accept that the general direction of post-colonial vegetation change has been towards a decrease in productivity. However, due to the lack of unequivocal evidence of the nature, extent and rate of change, Dean *et al.* (1995) not only highlight the need to re-think the concept of desertification but also concludes that there is a need for a more systematic monitoring program of a range of environmental variables in South Africa.

Dean *et al.*, (1995) also discuss the controversy surrounding the influence of climatic shifts on long-term environmental changes in the Karoo. Climate change, as a causal factor of vegetation change and land degradation, has been largely overshadowed by the supposed impact of humans and associated land management practices. However, evidence from Quaternary sedimentary sequences implies that vegetation change in the Karoo is not unusual, and simply portrays the response to a number of different climatic conditions which appear to have oscillated between moister and significantly more arid conditions than present day (Thomas *et al.*, 2002).

Notwithstanding the evidence that anthropogenic influences have played a significant role in the decline of productive land in the Karoo, and have led to people being described as 'proximal agents of desertification' (Meadows and Hoffman, 2002), evidence suggests that vegetation change is not necessarily caused by anthropogenic impacts. Fossil records show shifts in the grass:shrub ratio before human occupation in the Karoo and is thus attributed as a consequence of natural fluctuations in long-term rainfall patterns (Dean *et al.*, 1995).

### 3.2.2 Specific site description

The Karoo region encompasses more than 400 000km<sup>2</sup> of South Africa (Cowling *et al.*, 1986), and includes two biomes determined by different rainfall regimes: the winter-rainfall Succulent Karoo and the summer rainfall Nama-Karoo. The study region for this research is located within the Nama-Karoo biome where dwarf karroid shrubland typifies much of the environment (see figure 3.3). The specific field area is situated north of Kompasberg, the highest peak in the Sneeu Berg Mountain Range, which itself forms part of the Great Escarpment. This region feeds the upper catchment and headwaters of the Klein Seekoei River, a tributary of the Seekoei River, and drains in a northerly direction, eventually supplying the Orange River. An array of photographs of the Karoo fieldsite is depicted in figure 3.4 (at end of this section). The current landuse of this area is sheep grazing with limited areas of cultivation.

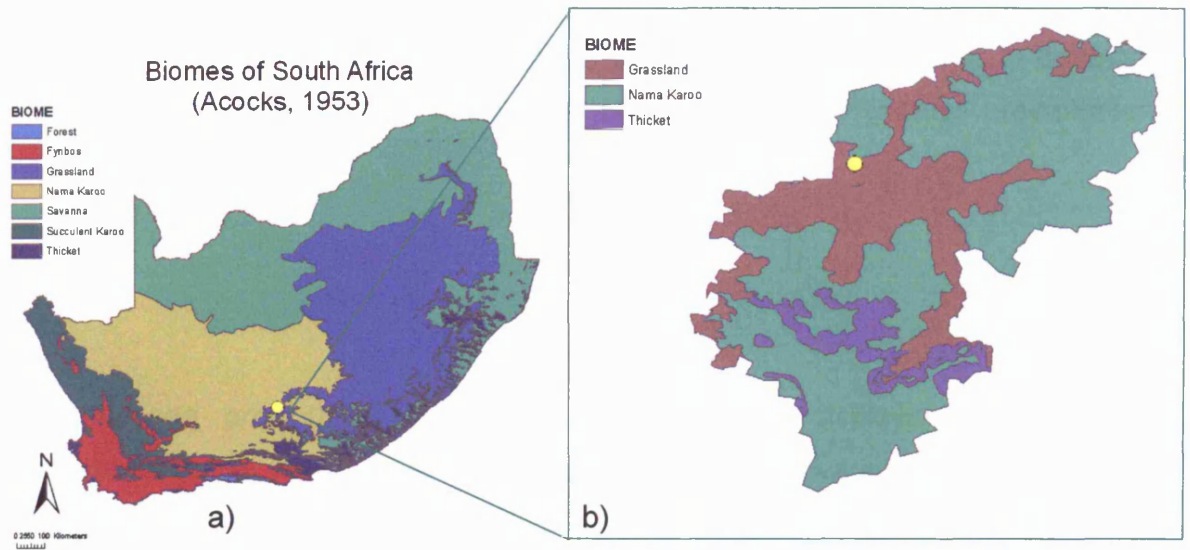


**Figure 3.3** a) Biomes of South Africa based on Acocks (1953) b) Biomes of the study region and surrounding districts of Graaff Reinet and Middelburg. The yellow circle depicts the study site.

### Geology

The geology of the study region is described as being Triassic Katberg Formation sandstone and mudstone of the upper Permian to Triassic Karoo Supergroup, capped by Jurassic dolerites (Watkeys, 1999; Boardman *et al.*, 2003). Dolerite tors therefore dominate the surrounding landscape, these comprise deeply weathered corestones in a matrix of red ferruginous sand. Horizontal bands of more-resistant sandstone and less-resistant shale are evident in the hillslopes whereas unconsolidated Quaternary sediment layers the valley floors, covering weak Balfour Formation mudstones, shales and sandstones (Boardman *et al.*, 2003).

### Soils

Karoo soils are considered typical of arid to semi-arid environments, displaying the full spectrum of soil development, including the preservation of palaeosols (Watkeys, 1999). In general, there is little organic material in the Karoo, thus an absence of an organic topsoil, or A horizon, is a common feature in the area. As a

result, soil formation is slow due to a lack of chemical and biological activity. However, increasing rainfall towards the east has allowed Duplex soils to develop, these are also found in the Sneeu Berg Mountains where greater precipitation occurs.

### *Climate*

As discussed previously, the climate of the Karoo displays some general characteristics, however, local conditions are extremely variable, largely due to altitudinal differences. The Sneeu Berg Mountains are located within the eastern region of the Warm Temperate Zone (Sugden, 1989). Diurnal and seasonal temperatures show large fluctuations, a summer maxima c. 30° and winter minima of below -10°C having been recorded (Schulze, 1980). In winter, snow is common in the higher altitudes as a result of the west to east movement of cold fronts. In late summer (March) a rainfall peak is evident and is associated with convectional thunderstorms common in the summer months.

Boardman *et al.*, (2003) reviewed rainfall data from two locations specific to the study area and found that mean annual rainfall was higher in both cases (517mm and 433mm) than was reported by Schultz (1980) who stated that the region receives 346mm annual rainfall. Although the reason for this may be due to locational differences, Boardman *et al.* state that there is no evidence that rainfall in the study region has varied significantly during the late 19<sup>th</sup> and 20<sup>th</sup> centuries. However, more notable is evidence of multidecadal variability; periodicities between 16 and 20 years have been identified relating to alternating wet and dry phases in the area.

### *Vegetation*

Acocks (1988) classified the Karoo as Karroid *Merxmuellera* Mountain veld in the higher altitudes and False Upper Karoo in the valleys. Many synonymous descriptions have been published, including Low and Rebelo's (1996)

classification of Southeastern Mountain Grassveld and Eastern Mixed Nama Karoo. However, the general term of Karroid scrub is often associated with the study region, an area where grasslands are scarce and degradation is evident.

Roux and Theron (1987) describe the Karoo as 'a vast tension zone located between the summer rainfall grasslands and the winter rainfall succulent shrublands' (p.60). Such is the vastness of the Karoo and the variety of climatic regimes that span the area, characterising the vegetation is difficult. Generally, it is observed that less palatable species are best adapted to the harsh conditions therefore replace the palatable species during droughts or as a consequence of overgrazing.

Cowling *et al.*, (1986) on the other hand highlight the importance of soil development on determining prevailing species. Where the A horizon exists, usually consisting of a sandy loam, grass cover such as *Aristida* and *Eragrostis* species can establish itself. However, in the absence of an A horizon as a consequence of erosion, specialised plant species root in the B horizon. These plants are not limited by the dry, compact nature of the B horizon and include species such as *Salsola*, *Zygophyllum incrustatum* and *Nestlera* (Cowling *et al.*, 1986). Further degradation through sheetwash and splash erosion will result in the B horizon surface becoming worn down and smooth, here species such as *Lycium cinereum* and *Eriocephalus spinescens* frequently dominate (Boardman *et al.*, 2003).

### *Badlands*

Extensive badlands are evident within the study region and as such are considered a fundamental element of the degradation processes that characterise this area. Badlands commonly develop on colluvial footslopes of usually less than 10 degrees (Boardman *et al.*, 2003) and comprise a dense gully network inter-dispersed with non-degraded, gently sloping interfluvial partitions. Both the gully

systems and interfluvial areas are relatively unvegetated with only the most resistant shrub species able to survive the harsh conditions. The badlands in this area are classed as incipient badlands due to their scale of incision; at present this is approximately 1 - 2m (Boardman *et al.*, 2003). The initial development of major gullies in the area is thought to be a consequence of vegetation change caused by the European settlers using the area as a routeway, however, evidence suggests that these gullies were active until at least the 1960s (Boardman *et al.*, 2003). No obvious evidence exists to suggest that the major gullies are presently active, nevertheless, the continually eroding smaller-scale rills are conducive to forming the badland landscapes that have become a characteristic of this semi-arid environment.

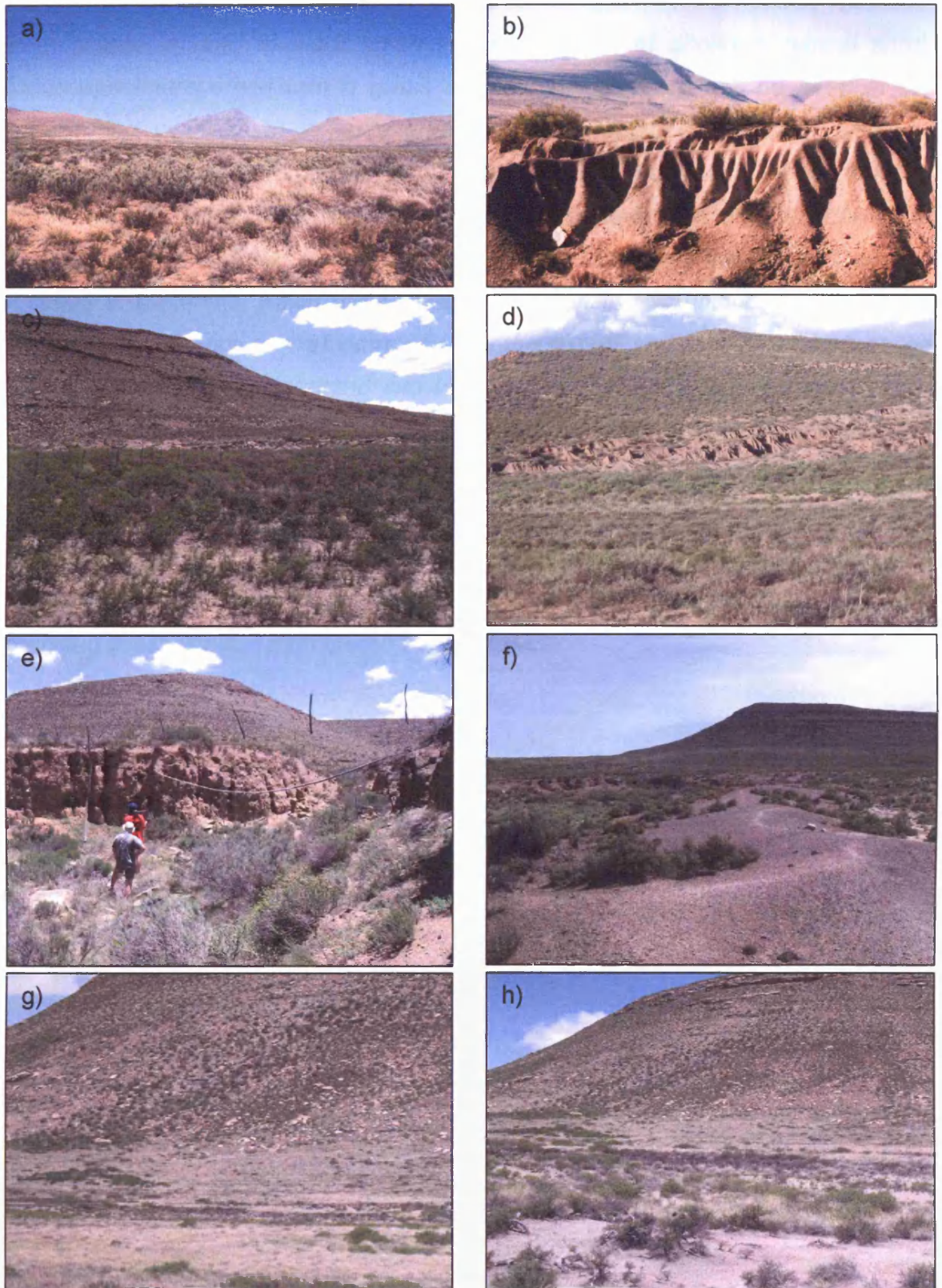


**Figure 3.4** Photographs depicting different landscapes in the study region, located north of the Sneeuwberg Mountains in the Karoo, South Africa.

*Figure 3.4 shows a number of typical landscapes in the Karoo fieldsite. Photographs a) and b) were taken in winter (Aug); a) shows a typical shrub landscape interspersed with a grass species, Kompasberg can be seen in the background whereas b) is an example of the undulating, sparsely vegetated badlands in the study region. Photograph c) depicts the landscape surrounding plots 3 and 4. In the foreground, shrublands can be seen to typify the locality and the bare intershrub areas are evident. Photograph d) shows the typical footslope location of badlands, which have developed within the shrubland landscape. A 'hanging fence' shown in e) demonstrates the extent and rate of erosion in the recent years. Another badland site is shown in f), here it is evident that local wildlife/livestock utilise the bare interfluvial areas and thus possibly exacerbate the erosion problem in badland landscapes. A grassland landscape in the Karoo is depicted in g); this is one of the largest extents of grassland in this area and clearly demonstrates the scarcity of grass in this region. Finally, h) portrays a mixed vegetation site where shrubs are generally prevalent, however, more resistant grass species intersperse the landscape.*

### **3.3 Description of the study area: The Sevilleta National Wildlife Refuge, New Mexico**

#### **General background**

The second study area is located in the American Southwest. The field site is situated within The Sevilleta National Wildlife Refuge (Sevilleta NWR), in the Socorro County of central New Mexico.

Vegetation change in the American Southwest has been well documented (Buffington and Herbel, 1965; Peters, 2002; Gibbens *et al.*, 2005) and typifies the land degradation characteristics of semi-arid environments. The causes and consequences of land degradation in this area have been discussed in detail in the previous chapters, but on a superficial level, portrays a less complex picture of degradation than the Karoo site. At present, only grassland-shrubland transitions have occurred, there is no evidence of badland development.

The Sevilleta NWR was chosen as the ancillary site to the Karoo for a number of reasons. This 100 000ha area, situated in the central Rio Grande Basin, consists of a junction of four biomes: the Great Plains Grassland to the north, the Great Basin Shrub-steppe to the west, the Chihuahuan Desert to the south and finally, the Montane Coniferous Forest in the upper elevations. As a result, a major research program exists in this area, which is dedicated to examining the biome transition zones. The Sevilleta Long Term Ecological Research program (LTER) has allowed a wide range of research to be continually conducted in this region and thus extensive resources and research history exist for this area. This area has restricted access so no grazing or agricultural practices are carried out in this study region.

The aim of the LTER is “to understand the causes and consequences of biotic transition zones on ecosystem, structure and function” (LTER Data, 2006), with particular reference to the impact of climate variability and change. The basis of the research is therefore to view the seemingly disparate transition zones as being conceptually linked and hence considered as one system. Therefore, rather than being site-specific, research is considered in a broader context, thus allowing a more comprehensive understanding of system processes and drivers. In order to do this, a number of commonalities and differences among the systems are being investigated. It is thought that parallel hypotheses exist between the different transition zones. An example of the grass to shrub transition is given in figure 3.5, however, parallels have been identified for other transitions such as the transition from woodland to grassland as a consequence of regional drought (LTER Data, 2006).

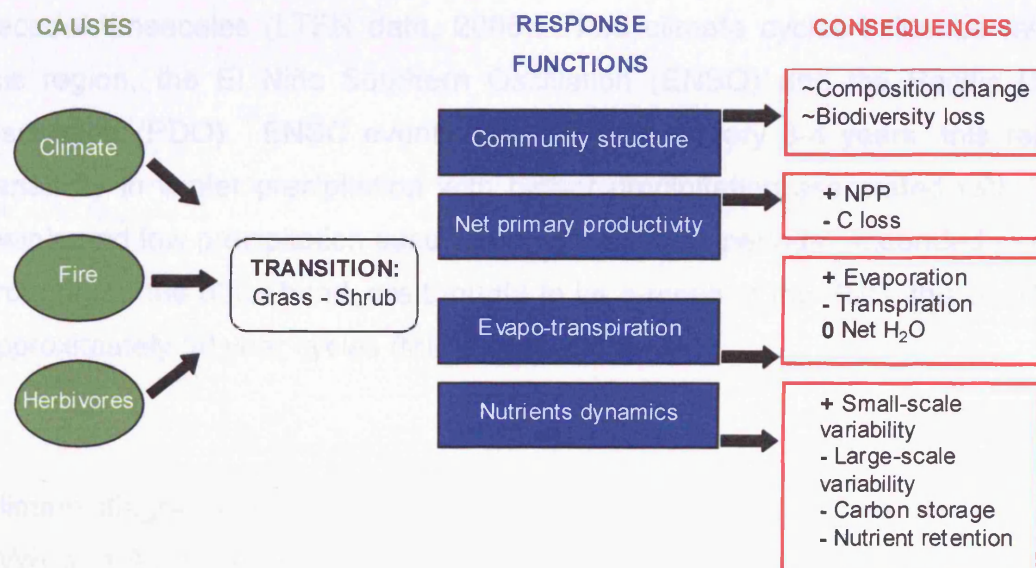


**Figure 3.5** Hypothesis linking causes, response functions and consequences of a biotic transition from grassland to shrubland.

*Adapted from Sevilleta LTER data (2006)*  
 (<http://sevilleta.unm.edu/>)

This research site is therefore an ideal location for gaining ancillary data on grassland to shrubland vegetation dynamics and will be utilised to aid the understanding of the questions raised in this thesis. Existing research, specific to

the sites chosen in the Sevilleta NWR, will be beneficial to this project by providing alternative explanations for some of the processes, which due to time constraints, cannot be investigated in this research. This site therefore allows an investigation into whether parallels exist not only at different transition zones but also between processes in semi-arid environments across the globe.

### *Climate*

High temperatures, low humidity and high variability characterise the climate of the Sevilleta region. This is thought to be a consequence of the site being located in the boundary between several major air mass zones (LTER data, 2006).

Precipitation inputs in central New Mexico vary seasonally, annually and on decadal timescales (LTER data, 2006). Two climate cycles influence rainfall in this region, the El Niño Southern Oscillation (ENSO) and the Pacific Decadal Oscillation (PDO). ENSO events typically occur every 3-4 years, this regulates variability in winter precipitation with higher precipitation associated with El Niño events and low precipitation associated with La Niña periods. Extended periods of drought, on the other hand, are thought to be a result of the PDO, this oscillates in approximately 50 year cycles (Milne *et al.*, 2003).

Climate diagrams for the Sevilleta NWR, Socorro, 20km south of the Sevilleta NWR and Albuquerque, 60 km north are presented in figure 3.6, these show that the region is moisture deficient for most of the year. However, this area displays highly variable annual and seasonal rainfall patterns. Figure 3.6 also presents rainfall data collected from a meteorological station on the Sevilleta NWR and demonstrates the year to year climatic variations. The site, on average, receives approximately 250mm of precipitation annually, 60% of which occurs during the summer monsoon season (Jun-Sept). Between 1989-2002, on-site meteorological data shows the mean annual temperature to be 13.2°C, with a winter (Jan) minima of 1.6°C and a summer (Jul) maxima of 25.1°C (LTER data, 2006).

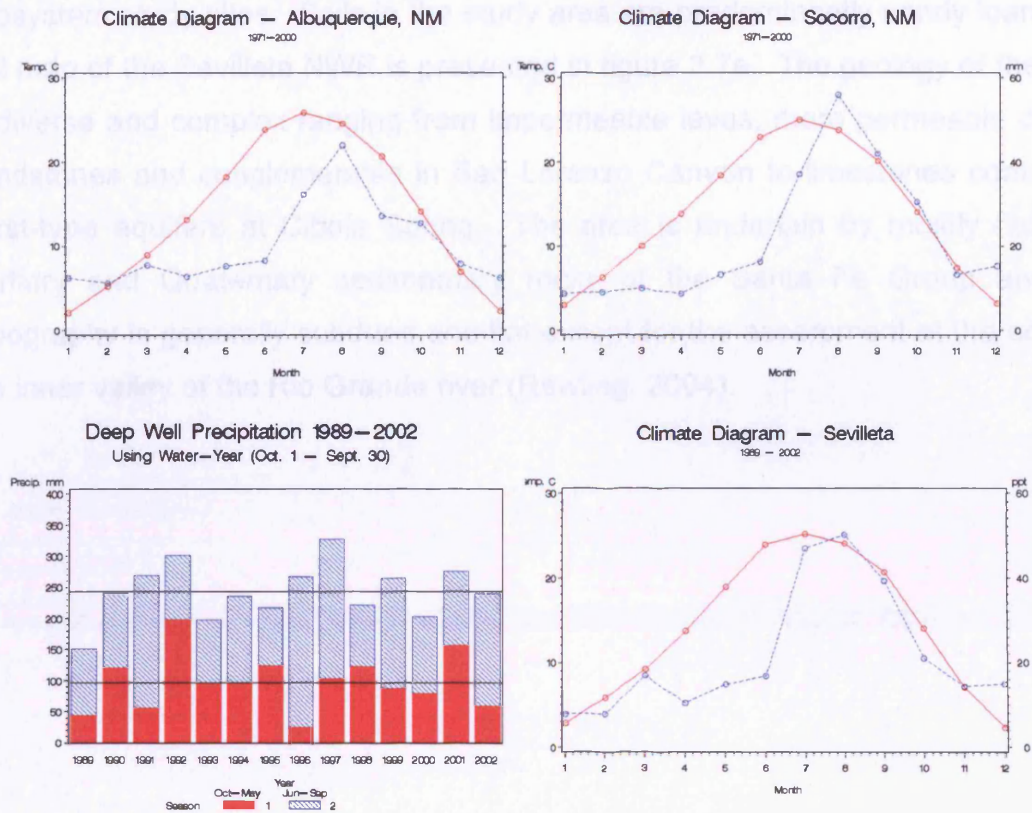


**Figure 3.6** Average climate diagrams for the surrounding region, Albuquerque to the north and Socorro to the south (1989-2002). A site-specific climate diagram for the Sevilleta NWR is also presented including a summer/winter precipitation diagram, which highlights the characteristic summer monsoon season.

Source: LTER data (2006)  
(<http://sevilleta.unm.edu>)

### *Vegetation, soil and geology*

Vegetation change in this area is predominantly from blue grama (*Bouteloua gracilis*) grasslands to Chihuahuan desert vegetation, which includes black grama (*Bouteloua eriopoda*) grassland and creosotebush (*Larrea tridentata*) shrubland. Unlike the vegetation in the Karoo, these three species form comparatively monodominant patches and thus form relatively abrupt transition zones. A detailed vegetation map of the Sevilleta NWR is provided in figure 3.7b highlighting the biome diversity in the area.

Nutrient deficient soils characterise the transition zones. In a study by Zak *et al.*, (1994) a grassland site in the Sevilleta displayed the lowest total soil nitrogen,

lowest nitrogen mineralisation rate and lowest soil carbon levels of 13 cross-ecosystem study sites. Soils in the study area are predominantly sandy loams. A soil map of the Sevilleta NWR is presented in figure 3.7a. The geology of the area is diverse and complex ranging from impermeable lavas, more permeable coarse sandstones and conglomerates in San Lorenzo Canyon to limestones containing karst-type aquifers at Cibola Spring. The area is underlain by mostly flat-lying Tertiary and Quaternary sedimentary rocks of the Santa Fe Group and the topography is generally subdued and flat except for the escarpment at the edge of the inner valley of the Rio Grande river (Rawling, 2004).

## 3.4 Sampling strategy for field studies

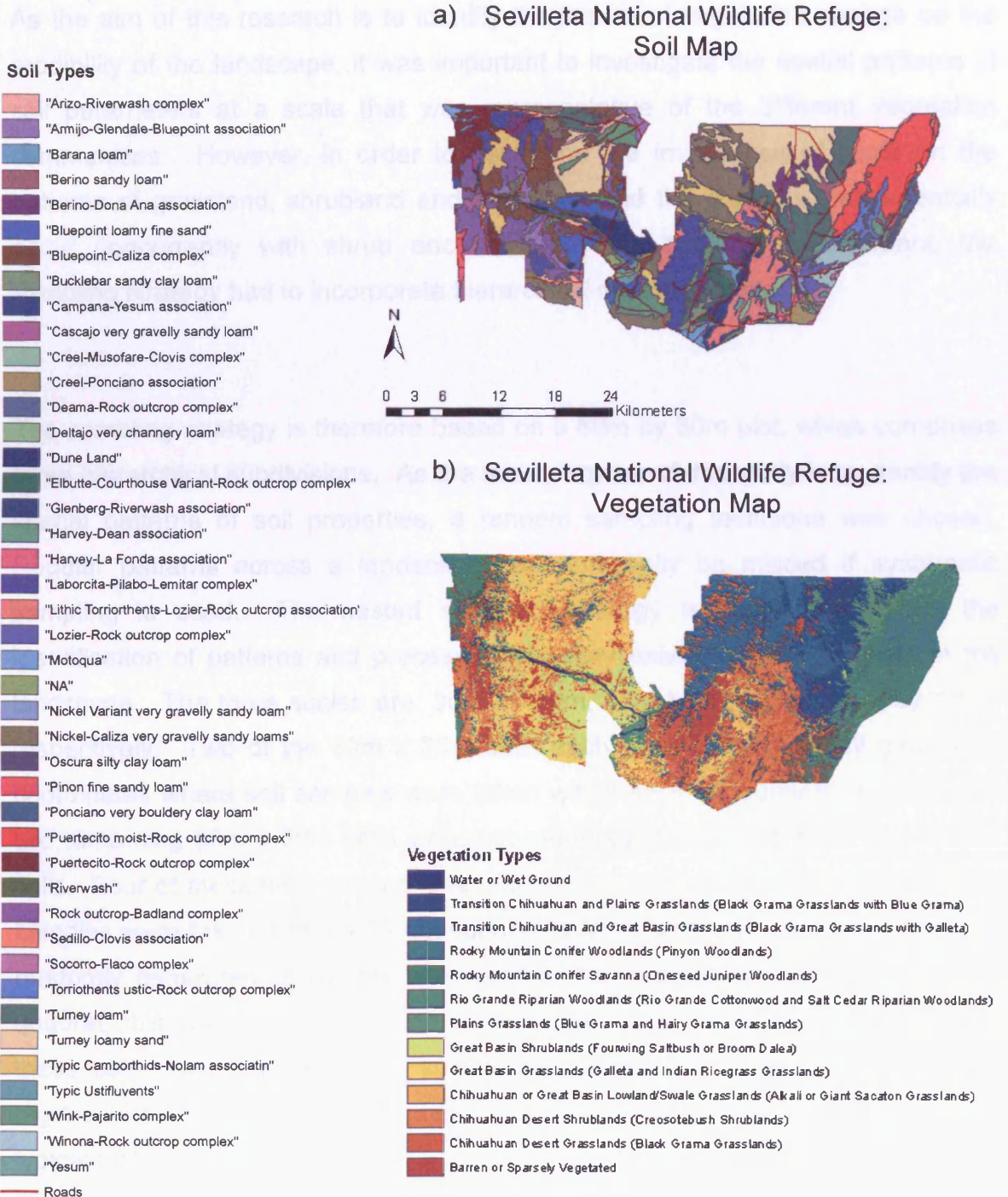


**Figure 3.7** a) soil map of the Sevilleta National Wildlife Refuge b) vegetation map of Sevilleta National Wildlife Refuge

Source: LTER data  
(<http://sevilleta.unm.edu/>)

### **3.4 Sampling strategy for field studies**

As the aim of this research is to identify the impact of vegetation change on the erodibility of the landscape, it was important to investigate the spatial patterns of soil parameters at a scale that was representative of the different vegetation communities. However, in order to determine the importance of scale on the patterns of grassland, shrubland and badlands, and the changes that potentially occur concurrently with shrub encroachment and badland development, the sampling strategy had to incorporate hierarchical measurements.

The sampling strategy is therefore based on a 60m by 60m plot, which comprises three hierarchical subdivisions. As the main purpose of this study is to identify the spatial patterns of soil properties, a random sampling technique was chosen. Regular patterns across a landscape can potentially be missed if systematic sampling is used. The nested sampling strategy is used to assist in the identification of patterns and processes that may exist at different scales in the landscape. The three scales are: 30m by 30m, 10m by 10m and 1.5m by 1.5m, respectively. Two of the 30m x 30m cells each have nine randomly generated coordinates where soil samples were taken within a 15 cm support. Each of the two remaining 30m x 30m cells were subsequently divided into nine 10m x 10m cells. Four of these cells contain nine randomly generated coordinates where soil samples were taken within a 15 cm support. Within six of the 10m x 10m cells, a randomly generated coordinate was used as the origin point of a 1.5m x 1.5m quadrat; this was divided into nine 0.5m x 0.5m cells. The centroid of each of these cells was considered the sample point, therefore a systematic sampling regime was undertaken at this scale. Figure 3.8 shows a schematic diagram of a typical plot layout.

In total, 108 samples were obtained from each plot. Where sample locations fell on areas that were impossible to sample e.g. aardvark burrows or on bedrock, a set of additional randomly generated locations was used.

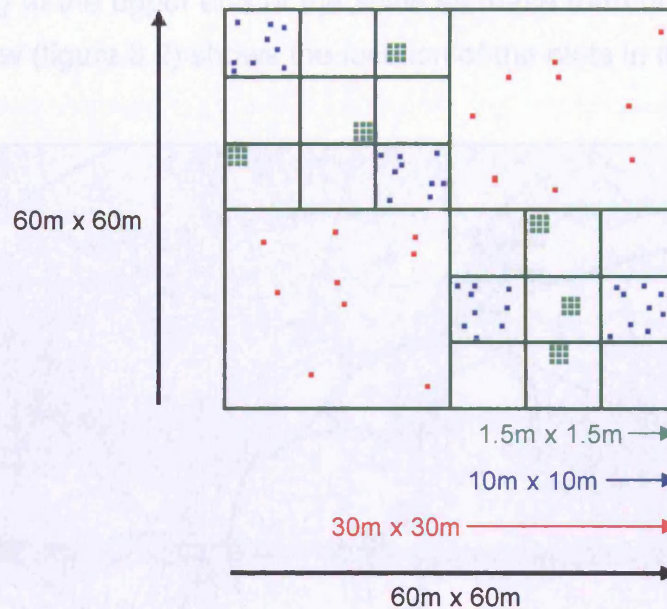


**Figure 3.8** An example of the nested sampling strategy employed in this study

The sampling strategy and scales measured were based on the methods used by Müller (Unpublished thesis), who conducted similar work on the Jornada Experimental Range, New Mexico. This site is also a LTER site and is situated approximately 170km south of the Sevilleta NWR in the Chihuahuan Desert. It is the intention that, by utilising a similar sampling strategy, a future collaboration of the two data sets will be made.

Fieldwork was undertaken in the Karoo in the early summer, between the months of November and December 2003, before the start of the summer rainfall regime. The plot locations were identified through visual inspection. Care was taken to avoid areas affected by anthropogenic influences, including: areas that had recently been burnt due to the effect it has on vegetation dynamics and nutrient cycles, areas that had been ploughed resulting in the artificial redistribution of nutrients, and areas that varied greatly in past grazing densities. The topography of the plots was not measured specifically but care was taken to keep this factor

as constant as possible both within and across the plots. In the Karoo, the slope angle of the plots generally ranged from 5-10 degrees, with the badlands (plots 4, 6 and 7) being at the upper end of the scale as these form on colluvial footslopes. The map below (figure 3.9) shows the location of the plots in the Karoo fieldsite.



- |                  |                  |
|------------------|------------------|
| ● Grassland site | ● Shrubland site |
| ● Mixed site     | ● Badland site   |

**Figure 3.9** Plot locations and vegetation types for the Karoo fieldsite. (1: 50 000 3124DA Heydon)

In total, seven plots were measured in the Karoo, representing the different vegetation types and thus stages of land degradation. The plot numbers and the associated vegetation types can be seen in table 3.1. These plot numbers will be referred to throughout the thesis. Only one grassland plot (2) was measured in the Karoo due to the absence of expanses of pure grassland. Instead, a mixed plot

was also measured. Although grass was the dominant vegetation type, a substantial number of shrubs were present in this plot, approximately 30% of the plot could be classed as shrubland. This provides an indication of spatial patterns of soil properties during the initial stages of shrub encroachment. Two shrubland plots that were considered to characterise the shrubland communities were measured. As no badlands are present in the Sevilleta NWR, three badland plots were measured in the Karoo. Photographs depicting the different plots can be found in appendix 4, where photographs of the general landscape do not exist (e.g. plot 1), ground cover photographs are provided.

**Table 3.1** Plot identification data for the Karoo plots

Plot number	Vegetation type
1	<b>Mixed vegetation</b> (Grass/shrub)
2	<b>Grassland</b> (e.g Karroid <i>Merxmuellera</i> )
3	<b>Shrubland</b> (Mixed Karroid shrubs e.g. <i>Acacia karroo</i> )
4	<b>Badlands</b>
5	<b>Shrubland</b> (Mixed Karroid shrubs e.g. <i>Acacia karroo</i> )
6	<b>Badlands</b>
7	<b>Badlands</b>

Fieldwork in the Sevilleta NWR was carried out between April and May 2004, again, avoiding the rainfall season of June to September. The same site selection protocol as before was used. The exact plot locations are shown in figure 3.10.

In total, four plots were measured in the Sevilleta NWR, representing the grassland and shrubland vegetation communities. The plot numbers and the associated vegetation types can be seen in table 3.2. These plot numbers will be referred to throughout the thesis. Photographs of the four Sevilleta NWR plots can be found in appendix 4. Again, the topography of the plots was not measured specifically but care was taken to keep this factor as constant as possible both within and across the plots. In the Sevilleta NWR, the slope angle of the plots was generally less than 5 degrees.

## 3.5 Physical Properties of Soil: Field and Laboratory Techniques

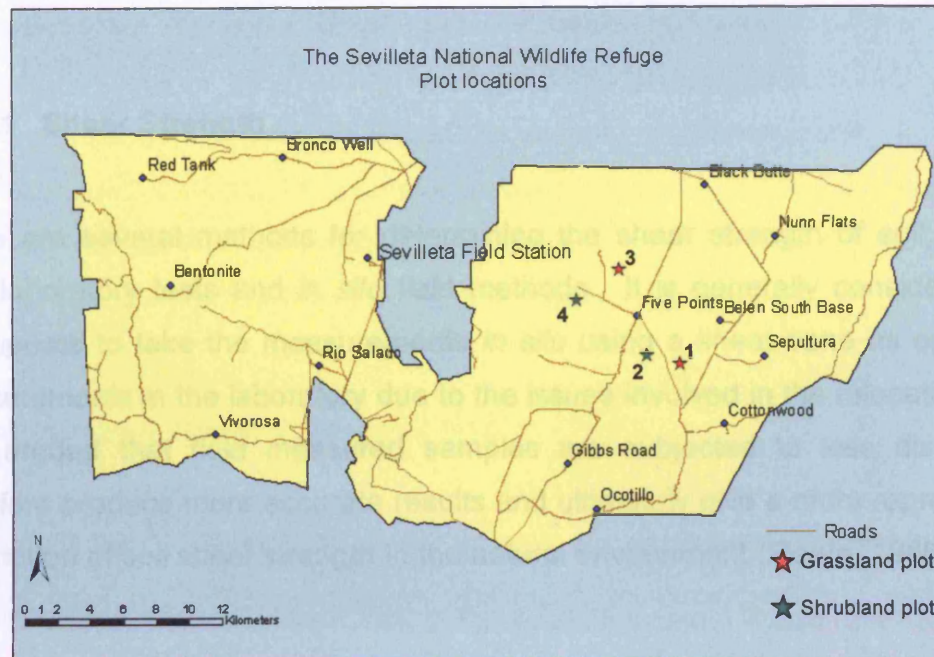


Figure 3.10 Plot locations and vegetation types for the Sevilleta NWR fieldsite.

Table 3.2 Plot identification data for the Sevilleta NWR plots

Plot number	Vegetation type
8	Grassland (Black grama: <i>Bouteloua eriopoda</i> )
9	Shrubland (Creosotebush: <i>Larrea tridentate</i> )
10	Grassland (Black grama: <i>Bouteloua eriopoda</i> )
11	Shrubland (Creosotebush: <i>Larrea tridentate</i> )

At each sample site a groundcover photograph was taken for future reference, a shear strength and bulk density measurement were taken and a second soil sample was collected for laboratory analysis.

### 3.5 Physical Properties of Soil: Field and Laboratory Techniques

#### 3.5.1 Shear Strength

There are several methods for determining the shear strength of soil, including both laboratory tests and *in situ* field methods. It is generally considered more appropriate to take the measurements *in situ* using a shear vane as opposed to measurements in the laboratory due to the issues involved in the relocation of soil. It is argued that field measured samples are subjected to less disturbances therefore produce more accurate results and ultimately give a more representative description of soil shear strength in the natural environment (Flaate, 1966).

In this study a field-based determination of shear strength was undertaken. The shear strength of the soil was measured using a Pilcon hand-held shear vane. The surface shear strength was determined by inserting a shear vane with a 33mm diameter into the ground to the depth of 50mm, the full length of the vane blades. The shear vane was then rotated at a speed equivalent of approximately 1 revolution per minute until the soil sheared. A direct measurement in kPa was taken from the vane. The range of measurement was increased by inserting the vane 25mm into the soil, half the height of the blade. The following equation (3.1) was used to convert the data:

#### Equation 3.1

$$S_u = \frac{T}{\pi \left[ \left( D^2 H / 2 \right) + \left( D^3 / 6 \right) \right]}$$

Where  $S_u$ : shear strength (kPa)  
 $T$ : torque (Nm)  
 $D$ : diameter (m)  
 $H$ : height (m)

Source: Flaate (1966) p. 23

To avoid biased results involving the positioning of the vane, a system was undertaken that involved alternating the sampling site between adjacent samples at a set distance of 15cm either at a 0° or 180° angle from the sample origin. Where the ground was impenetrable, as evident in badland sites, these points were assigned a maximum value. As soil moisture must be considered when interpreting shear strength results, the recent rainfall conditions for each plot were noted. These can be found in the relevant results chapters.

### **3.5.2 Organic Matter Content of Soil**

A measure of the chemically active organic matter rather than the total carbon content of the soil was required for this study. This encompasses both the humus and organic residues in soil, its relevance related to soil genesis and fertility (Jackson, 1958).

Total organic matter (OM) content of the soil was determined using the loss-on-ignition (LOI) method. The soil used to measure the OM content was obtained from the same sample used to measure the soil bulk density. This measurement was taken from the top 8cm of soil. In order to provide a representative sample the soil was mixed thoroughly and a 10g sub-sample was used to obtain the OM content. This technique involves ashing the OM in a muffle furnace and is preferred to extraction methods as it removes organics that are tightly bound to soil particles without changing soil composition (Rowell, 1994). Results obtained by the LOI procedure have proved comparable to those obtained by both the dichromate wet-oxidation method and by carbon analysers (Soil and Plant Analysis Council, Inc 1999 (2000)). However, it should be noted that the LOI procedure provides only an approximation of OM content, inevitably producing an overestimation, especially in soils with a high clay content. Sandy soils are less affected but soils containing more clay and sesquioxides will lose 'structural' water between the ashing temperatures of 105° C and 500° C (Rowell, 1994). Therefore, the methodology of the LOI procedure varies, largely involving the

ashing temperatures used, these can range from 360°C (Schulte *et al.*, 1991) to 850°C (Ball, 1964).

In this study the procedure given by Rowell (1994) was used. The organic matter content was determined by drying the soil at a temperature of 105°C. A subsample was then placed in a crucible and weighed before being placed in a furnace at 500°C for 12 hours. The crucible was then reweighed to give the mass of the ignited soil. The following expression (3.2) was used to determine the percentage organic matter content:

**Equation 3.2**

$$\text{Loss-on-ignition} = \frac{(\text{mass of oven-dry soil} - \text{mass of ignited soil})}{\text{Mass of oven-dry soil}} \times 100$$

### 3.5.3 Dry Bulk Density

In the field, bulk density samples were acquired using a guide plate, driving tool and cylinder. The guide plate is placed on the surface of the soil and the cylinder is driven vertically into to the ground. Care is taken to minimise compaction and disturbance in order to retain the natural structure of the soil. The cylinder is then removed from the ground and excess soil is trimmed from either end. The soil surface must be flush with the ends of the cylinder since the sample has to be of a known volume. In this case, the measurement was taken from the top 8cm of soil and the bulk density tin had a volume of 100cm<sup>3</sup>. To avoid biased results involving the positioning of the cylinder, a system was undertaken that involved alternating the sampling site between adjacent samples at a set distance of 15cm either at 90° or 270° from the sample origin. Where the ground was impenetrable with the cylinder, as evident in a few cases at badland sites, these points were classified as 'no data'.

The soil samples were sealed in polythene bags to allow the bulk density and moisture content of the soil to be measured simultaneously. In the laboratory, the moist samples were weighed and then dried for 12 hours at a temperature of 105°C; the oven-dried soil was then re-weighed. Bulk density was calculated using equation 3.3.

**Equation 3.3**

$$\text{Bulk Density} = \text{Mass of oven dry soil} / \text{volume of soil cylinder (100cm}^3\text{)}$$

**3.5.4 Moisture Content**

The water content of the soil for every sample point was measured from a sealed soil sample brought back from the field. The soil used to measure the moisture content was the same sample used to measure the soil bulk density. This measurement was taken from the top 8cm of soil. Details of the rainfall conditions prior to the sampling can be found in the appropriate results chapters. The moist samples were weighed and then dried for 12 hours at a temperature of 105°C; the oven-dried soil was then re-weighed. Soil moisture was calculated using equation 3.4.

**Equation 3.4**

$$\text{Soil Moisture (\%)} = \frac{\text{Mass of moist soil} - \text{Mass of dry sample}}{\text{Mass of dry sample}} \times 100$$

**3.5.5 Texture**

Soil texture is typically given as a percentage of total soil mass occupied by a given size fraction (Eshel *et al.*, 2004). In simple terms, soils are generally

allocated to a textural class according to the content of sand, silt and clay particles. There are a number of classification systems, the two most commonly used being the USDA system and the European system. The classification is based not on the type of minerals present but the effect that particles of different sizes have on the physical and chemical properties of the soil.

There are numerous methods used to determine particle size distribution, traditional, such as: sieving, sedimentation, pipette and hydrometer methods and comparatively modern techniques, such as laser diffraction and optical modelling. A critique of methods is given by Eshel *et al.* (2004), who conclude that due to the heterogeneous nature of soil particles in both shape and density, the determination of particle size distribution, whichever method used, is at best an estimate. However, in a study by Buurman *et al.* (1997) it was determined that although a standard correlation between the classic pipette method and laser diffraction has not been established, laser diffraction provides reproducible results ideal for spatial comparisons of samples. In addition, the continuous distribution curves and amount of information available on the fine fractions make this method an appealing one.

All techniques appear to have their own advantages and disadvantages and thus the technique used is individual to the user's circumstances and/or needs. Due to the large sample size and time constraints imposed in this study the laser diffraction method was chosen. This has the advantages of a high rate of sample turnover as well as the need for only a small amount of sample for measurement. Reliability, reproducibility and analysis speed all contribute to the benefits of this method.

Semi-arid soils are notably low in organic matter content and thus its removal for particle sizing is, in some cases, considered unnecessary. However, through a visual inspection it was deemed necessary to implement a pre-treatment method in this case. Due to time constraints the hydrogen peroxide removal technique

was not applicable, therefore organic matter removal by the loss-on-ignition method (as described before) was undertaken. To avoid the cementing of soil particles the samples were treated at a lower temperature of 450°C for 12 hours. Dispersal techniques were also employed to minimise this risk, these included the use of a dispersant agent, sodium hexametaphosphate and ultrasonics.

### **3.5.6 Aggregate Stability**

Aggregate stability was measured using the sample taken for nutrient analysis. A sample taken to the depth of approximately 6cm and 100g was taken at each of the 108 sample sites for all 11 plots. The whole soil sample was passed through an 11mm and an 8mm sieve. Aggregates that passed through the 11mm sieve but not the 8 mm sieve were collected. Care was taken to discard pieces of crusting due to the known differences in formation and water-stability behaviour compared to normal aggregates. Ideally 8 aggregates were analysed, however, when this was not possible the available aggregates were analysed and the number recorded. The total weight of the dry aggregates was measured. The aggregates were then placed in the 8mm sieve and submerged in water. A reciprocal shaker was used to agitate the aggregates for a total of 2 minutes at a speed setting of 2.1rps. The remaining soil/aggregates in the 8mm sieve were collected and dried before reweighing. The percentage weight loss was then calculated.

## **3.6 Chemical Properties of Soil: Field and Laboratory Techniques**

### **3.6.1 pH**

The soil pH was measured using a subsample taken after the bulk density was measured. This measurement was taken from the top 8cm of soil. In order to

provide a representative sample the soil was mixed thoroughly and a 10g sub-sample was used to obtain the soil pH. Many different techniques including both *in situ* and laboratory methods are employed to determine pH depending on the output required. In this study the soil pH was measured in the laboratory using a Sartorius PP-25 bench-top pH meter. Due to the large sample size and related time constraints it was decided that the procedure most appropriate to determine the pH was that of a 1:1 water to soil suspension. A full description can be found in Soil and Plant Analysis Council Inc 1999 (2000). Accurate measurements of soil pH are difficult to obtain depending on both soil characteristics and the measurement technique undertaken. To reduce potential error three measurements per sample were taken and the average calculated. In addition, it has been noted that in neutral and alkaline soil suspensions, a stabilised reading takes longer to achieve. Therefore a minimum of a 30 second stabilisation time was implicated as suggested by Rowell (1994).

### **3.6.2 Soil Salinity and Conductivity**

The electrical conductivity (EC), also known as the specific conductance, was measured from the same sub-sample the pH reading was taken from. EC can be measured using a variety of techniques, the most common being the soil-paste extract method. However, a 1:2 soil to water extraction method outlined by Soil and Plant Analysis Council Inc 1999 (2000) has been found to be applicable in a variety of soils. Therefore, although the specific conductance values from a 1:2 extract method are not comparable with those from a soil-paste extract method, it was decided that due to the large sample size and the fact that this is a comparative study, the 1:2 soil to water extraction would be used.

The EC was measured following the pH by increasing the water to soil ratio from 1:1 to 1:2. A Sartorius PP-25 bench-top conductivity meter was used. To reduce potential error three measurements per sample were taken and the average calculated. Table 3.3 was used to determine the impact of soil salinity on vegetation, for further details refer to the SSSA Book Series 3: Soil Testing and Plant Analysis (Westerman, 1990).

**Table 3.3** Effect of salinity on plants.

dSm <sup>-1</sup> at 25°C	Effects
<0.40	Non-saline. Most crops will grow quite well
0.40-0.80	Very slightly saline. Relatively safe for plants, long dry spells may draw salts up to near the surface and damage plants
0.81-1.20	Moderately saline. Only salt tolerant plants can survive
>1.20	Saline. Few plants will survive

Source: Soil and Plant Analysis Council Inc 1999 (2000) p. 60, 61

### 3.6.3 Nutrient Analysis

A sample of 100g was taken from approximately the top 6cm of soil at each of the 108 sample sites for all 11 plots. The samples were air-dried in the field and packaged in paper bags to rule out potential contamination. As the nutrient sample could not be taken from the exact position of the bulk density sample, a system was undertaken that involved alternating the bulk density location and the nutrient sampling site. This system was also implemented to avoid biased results. Samples were taken at a fixed distance of 15cm either at 90° or 270° from the sample origin. Although the position of sample area varied only slightly it may be important in later studies to know the vegetation type the sample was taken from. In the present study the plot is classified as only one generic vegetation type, however, if micro-scale studies are to be undertaken or underlying patterns in the data are found, this ancillary data is available.

In the laboratory each sample was air-dried and passed through a 2mm sieve. The major cations; magnesium, calcium, potassium and sodium as well as phosphorus were extracted using the Mehlich No. 3 extraction method as described in the Soil Analysis Handbook of Reference Methods (Soil and Plant Analysis Council, Inc. 1999, 2000). This method was used as it has been found to

be applicable to a range of soils as well as correlating well with Mehlich No. 1, Mehlich No.2 and the ammonium acetate extraction method. The levels of nutrients were determined using an ICP-AES.

### **3.7 Statistical and Geostatistical Methods**

#### **3.7.1 Brief Overview**

An integral aspect of this research was to determine the spatial patterns of soil resources across different vegetation communities. However, as a consequence of the multi-faceted nature of the environment, a complex series of processes and interactions exist. Each process itself could potentially operate at different scales simultaneously, in a non-linear way, and with local positive feedback (Webster and Oliver, 2001). As a result, the outcome can be so complex that variation appears to be random. A deterministic description of the distribution of soil properties is therefore not applicable.

In contrast, geostatistics address the issues associated with the complex and highly variable parameters that define soil through the recognition of the influence of scale and the impact of autocorrelation. Geostatistical techniques allow the spatial variation of soil to be described quantitatively, unsampled points can be predicted and error margins defined.

The benefits and progressive nature of geostatistics, particularly its application in soil science, has been discussed in detail by many, such as: Goovaerts (1999), Brus and Gruijter (1997) and Webster and Oliver, (2001). Furthermore, many examples of how geostatistics have been utilised in soil studies exist; ranging from its use in defining the spatial variability of nutrients in soil (Schlesinger *et al.*, 1996; González *et al.*, 1996) and general soil properties (Sun *et al.*, 2003; Carroll and

Oliver, 2005; Western *et al.*, 1998) to identifying spatial relationships among soil properties and weed populations (Gaston *et al.*, 2003). Geostatistical analysis is considered a fundamental tool in soil science, and is therefore used to evaluate and characterise the spatial patterns of the soil parameters in this study.

In order to fully understand the characteristics and spatial patterns of soil properties a number of different statistical techniques have been applied to the data. Both intra-plot and inter-plot comparisons were made, contributing to the overall assessment of soil characteristics in semi-arid landscapes. These statistical results were calculated for each soil parameter; a detailed description and the purpose of each test are as follows:

*a) Test of normality, descriptive statistics and inter-plot analysis*

The normality of the data was investigated using histograms and descriptive statistics. Due to the large quantity of datasets the histograms can be found in appendix 1, boxplots of the four grassland plots have been provided within the chapter for summary purposes.

The reason for testing the normality of each parameter is two-fold. Firstly, it provides an indication of the general distribution of data and allows the identification of outliers. Secondly, it provides an indication of the applicability of geostatistics to the dataset and thus the pre-processing techniques that may need to be carried out before the analysis. If the data are skewed then the data may need to be transformed and/or outliers removed. Extreme values are potentially caused by measurement errors both in the field and in the laboratory. However, caution has to be exercised when removing outliers, particularly in semi-arid environments which are commonly found to display a wide range of values. As with all statistical, and particularly geostatistical, analyses it is important to consider the underlying physical processes and any prior knowledge about the region when manipulating data (Webster and Oliver, 2001). A protocol for the removal of outliers was determined. Due to the adverse impact on the

geostatistical analysis, the removal of outliers was only considered if the distribution was classed as highly skewed. A maximum of three values could be removed. If the removal of these values did not improve the skewness of the data then transformations were performed. The removal of the outliers in favour of transforming the data was justified as transformed data affects the comparability of the final results.

Summary statistics were calculated using Minitab versions 13 and 14. These basic descriptive statistics are used to assess the general characteristics of the datasets including the central tendency, dispersion and shape of the frequency distribution. Inter-plot comparisons are made with particular attention paid to the mean, range and coefficients of variation, which are used to summarise the general variability of the datasets. The original datasets are used for the descriptive and statistical investigations.

*b) Analysis of variance (ANOVA) tests and two-sample T-tests*

Following the descriptive statistics, the parameter in question is then subject to inter-plot comparisons using either an analysis of variance test (ANOVA) or a two-sample T-test. Although some datasets were identified as being skewed, these tests are considered to be relatively robust against non-normal distributions therefore the original datasets are used to calculate the aforementioned statistics.

The ANOVA test is used to analyse statistically whether the parameter values across all the plots differ significantly or, in statistical terms, whether the samples come from a populations with similar distributions. If there are significant differences among the plots, within plot variability would be expected to be much smaller than the between plot variability giving a *large* F value. The latter test is used to identify statistically whether significant differences exist between the parameters derived from the plots located in South Africa and similarly whether significant differences exist between the plots located in New Mexico. These tests

have been undertaken to assess the influence of geographical location on the mean values of parameters from each plot. All statistics are tested at a significance level of 0.05.

*c) Intra-plot variation*

In order to visualise the distribution of data within each plot at a more detailed level, the means and standard deviations of each cell were calculated and plotted. Also, the cells within each of the three spatial scales (1.5 x 1.5m, 10 X 10m and 30 x 30m) are highlighted in order to assess whether scale of measurement strongly influences the spread of data, thus having implications on future sampling strategies.

*d) Geostatistical analysis*

The geostatistical analysis was used to quantify the spatial variability of the soil properties. For each parameter the geostatistical analysis was divided into three parts; the first and main analysis was the semi-variogram, then follows the Geary's C and Moran's I statistics, respectively. Three different geostatistical methods are utilised in order to derive the most appropriate conclusions about the spatial structures as it is well documented that no single method is completely reliable (Dale *et al.*, 2002; Perry *et al.*, 2002). However, before any geostatistical analysis was carried out a number of pre-processing stages had to be implemented. The pre-processing stages are summarised in stages i) to iii) of figure 3.11.

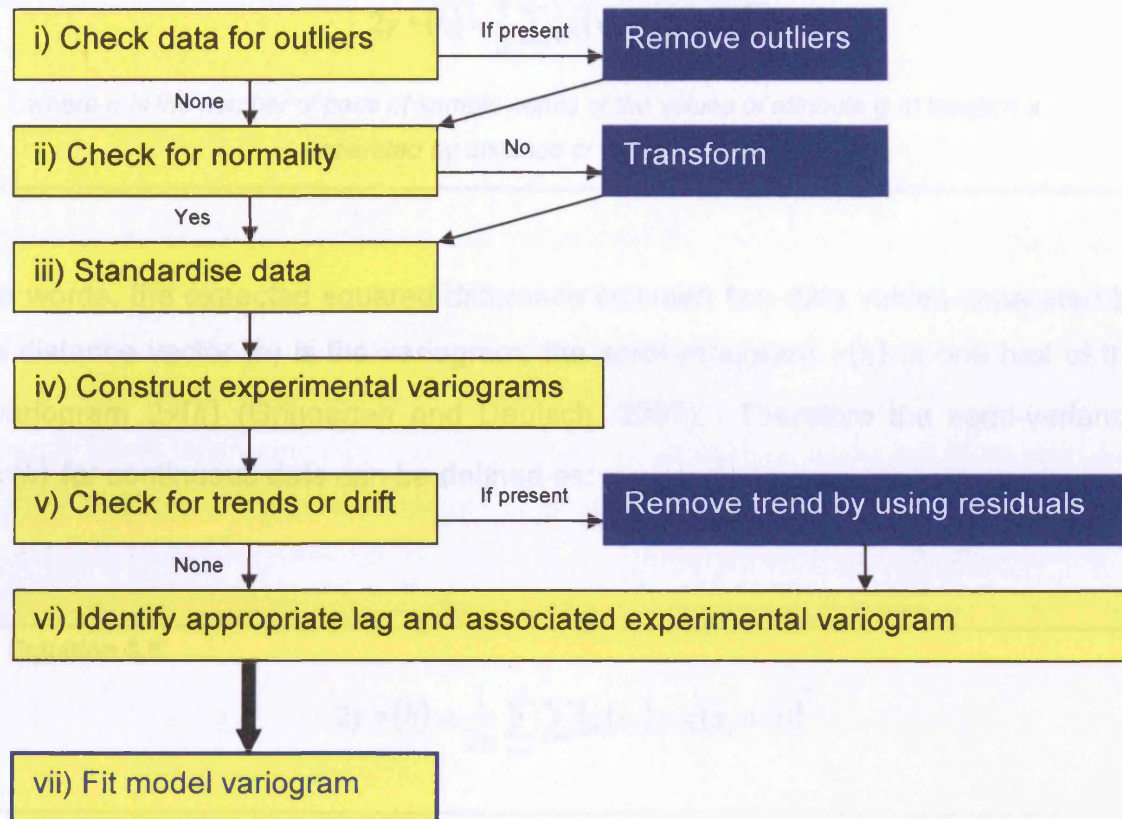


Figure 3.11 Pre-processing stages and protocol for semi-variogram calculations

### 3.7.2 Calculation of the experimental semi-variogram

Experimental semi-variograms were calculated in order to define the spatial continuity of the soil parameters of interest. The semi-variogram shows the average variance found in comparisons of samples taken at increasing distance from one another (Schlesinger *et al.*, 1996). The nested sampling strategy was therefore designed and developed with the knowledge that different soil parameters may operate at different scales and thus incorporated fine to broad-scale measurements across the 60m x 60m plot (as discussed in section 3.4).

The experimental variogram is defined as:

**Equation 3.4**

$$2\gamma^*(h) = \frac{1}{n} \sum [g(x) - g(x+h)]^2$$

where  $n$  is the number of pairs of sample points of the values of attribute  $g$  at location  $x$  separated by distance or lag interval  $h$ .

In words, the expected squared difference between two data values separated by a distance vector ( $h$ ) is the variogram; the *semi*-variogram  $\gamma(h)$  is one half of the variogram  $2\gamma(h)$  (Gringarten and Deutsch, 2001). Therefore the semi-variance  $\gamma(h)$  for continuous data can be defined as:

**Equation 3.5**

$$2\gamma^*(h) = \frac{1}{2n} \sum_{n=i}^n \sum [g(x_i) - g(x_i + h)]^2$$

The experimental semi-variograms were calculated using VARIOWIN software (Pannatier, 1996). As VARIOWIN does not permit the use of irregular lag distances in the construction of a semivariogram, 8 semivariograms were created for every parameter from each of the 11 plots using different lag distances. These were: 0.5m, 1.0m, 2.0m, 3.0m, 4.0m, 4.5m, 5.0m and 6.0m. The lag distance demonstrating the clearest spatial structure was then chosen. However, the other semivariograms, particularly those created using the smallest lag distances, assisted in the interpretation of the data and the application of the most appropriate model, these can be found in appendix 3.

The experimental variograms were also used to identify the presence of drift in the datasets. If the variance continued to increase without reaching a sill, the data was analysed for trends by calculating and mapping the focal mean using ArcGIS

vs 9.0 software. If drift was identified, this was removed by calculating the residuals; this dataset was then used for all geostatistical analyses.

### 3.7.3 Variogram models

In order to interpret an experimental variogram, the data must be fitted to a theoretical model. One of the most controversial topics in geostatistics is the debate surrounding the methods of choosing and fitting variogram models to the data. Two main methods are commonly employed to fit the models, manually, by visual inspection and mathematically, using 'black-box' software (Webster and Oliver, 2001). However, Webster and Oliver highlight that both methods are associated with a number of difficulties for a number of reasons, including:

- i) The accuracy of the observed semivariances is not constant.
- ii) The variation may be anisotropic.
- iii) The plotted semi-variogram may display much point-to-point fluctuation.
- iv) Most models are non-linear in one or more parameters.

For these reasons Webster and Oliver recommend a procedure that involves both visual inspection and statistical fitting. A number of different models exist, including: the spherical, Gaussian, exponential and linear models. Figure 3.12 demonstrates some of these models.

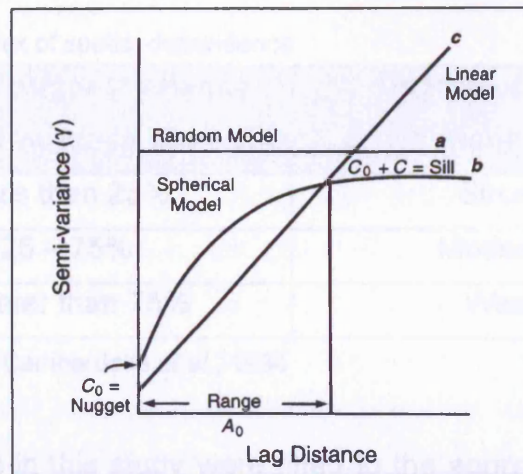


**Figure 3.12** Theoretical interpretations of semi-variograms, showing the proportion of variance found at increasing lag distances. Curve *a* is expected when soil properties are randomly distributed. Curve *b* is expected when soil properties show spatial autocorrelation over a range ( $A_0$ ) and independence beyond that distance. Curve *c* depicts a large-scale trend in the distribution of soil properties, but no local pattern within the scale of sampling.

Source: Schlesinger *et al.*, (1996) p. 365

If the data are randomly distributed, little change in the semi-variance will be witnessed with increasing distance. Thus, the total sample variance will be found at all scales of sampling and the semi-variogram will be essentially flat, demonstrated by curve *a* (Schlesinger *et al.*, 1996). If a pattern in the data exists, firstly the semi-variogram will rise reflecting autocorrelation. The curve will then level off indicating the distance at which the samples become independent, this is known as the *sill* as demonstrated by curve *b*. The range ( $A_0$ ) of the semi-variogram determines the scale of the spatial pattern existing in the measured parameter. The *nugget* value ( $C_0$ ) at zero lag distance, indicates the variance that exists at a finer scale than the sampled area. A high nugget value suggests that most variance occurs over short distances and a high nugget to sill ratio indicates the presence of a random pattern in the measured parameter (Schlesinger *et al.*, 1996). The ratio of nugget variance ( $C_0$ ) to sill variance ( $C_0 + C_1$ ) therefore provides an indication of the extent of spatial dependence. Cambardella *et al.*, (1994) suggest an index to define the degree of spatial dependence based on the nugget-to-sill ratio (table 3.4).

**Table 3.4** Index of spatial dependence

Ratio of nugget variance ( $C_0$ ) to sill variance ( $C_0 + C_1$ )	Degree of spatial dependence
Less than 25%	Strong
25 – 75%	Moderate
Greater than 75%	Weak

Adapted from Cambardella *et al.*, 1994

The semi-variograms in this study were fitted to the appropriate models using the 'manual' function in the VARIOWIN software (Pannatier, 1996). This method was chosen as Olea (1999) and Wackernagel (2003) argue that visual fitting is more appropriate for the detection of underlying structure as automatic fitting fails to consider the influence of outliers. The processes undertaken to reach this stage are summarised in figure 3.13.

The semi-variogram graphs and the statistics derived are presented for all plots. Although many researchers are only interested in the statistics, the general form of the graphs also provides an indication of the spatial patterns in the landscape, especially those that may be considered overly complicated to model but exist none the less.

Where periodicity was evident in the datasets, the closest model was applied to data to derive a range of spatial autocorrelation. However, where strong periodicity was displayed, the semi-variance data was also presented the form of a graph with connecting lines. This allowed the wavelengths to be analysed to derive whether or not the spatial patterns of the soil parameters correspond to the expected patterns caused by shrub and intershrub areas. The implications of these patterns are discussed in chapters 7 and 8.

e) *Geostatistical analysis: Moran's I and Geary's C statistics*

Due to the debate surrounding the reliability of geostatistical techniques, it is recommended that more than one measure of spatial autocorrelation is implemented to assess the spatial patterns of a property (Dale *et al.*, 2002; Perry *et al.*, 2002). Arguably one of the most debated aspects of semi-variograms is the impact of sample size. Therefore, in acknowledging the relatively small sample sizes used in this project, a more robust measure of spatial autocorrelation with respect to sample size was applied to the data, the Moran's I statistic. Both statistics were calculated using the RookCase software (Sawada, 1999). In addition, a squared-difference coefficient was calculated, called the Geary's C statistic. This was chosen because of its similarity to the semi-variogram. The same data were used to calculate all three measures of spatial autocorrelation to allow comparisons to be made between the techniques. The Moran's I and Geary's C statistics are presented in graphical form, called a correlogram, using the same lag distances used for the semi-variograms. As each plot was best represented by different lag distances a key is provided for each graph to indicate the true lag on the standardised scale.

The conceptual and mathematical relationships that exist among methods of spatial analysis are described in detail by Dale *et al.*, (2002). However, the relationship that exists between Moran's I and Geary's C is such that, in principle, the two graphical outputs should mirror each other. Interpretation is based on the following:

<b>Moran's I</b>		<b>Geary's C</b>	<b><u>Interpretation</u></b>
$I > -1/(n-1)$	Positive Spatial Autocorrelation	$C < 1$	<ul style="list-style-type: none"> <li>• Spatial clustering of high and/or low values</li> </ul>
$I < -1/(n-1)$	Negative Spatial Autocorrelation	$C > 1$	<ul style="list-style-type: none"> <li>• Checkerboard pattern</li> </ul>

Adapted from: Anselin (08/08/2006)

In particular, these graphs are used to assess whether periodicity is evident in the data. Due to software and time restrictions this type of output cannot be modelled from the experimental variograms but if periodicity is evident from all three statistical methods further conclusions can be drawn from the data. Unfortunately the correlograms do not differentiate between clustering of high and low values therefore interpretation has to be carried out with caution.

### **3.8 Summary**

An overview detailing the specific field requirements for this study has been presented. Two semi-arid study regions have been identified as being representative of the characteristic degradation processes, specifically vegetation change in the form of grassland to shrubland transitions. In the Karoo, extensive grasslands are rare and karroid dwarf shrubs dominate the landscape, interspersed with areas of dense rill networks that are collectively known as badlands. Much debate surrounds the definition, extent, causal factors and consequences of degradation in the Karoo and as such, a better understanding of the underlying processes of degradation in this region is required. Due to the absence of extensive grasslands in the Karoo, an auxiliary site was incorporated into the study. The Sevilleta National Wildlife Refuge, a LTER site, was chosen as the area is currently undergoing a grassland-shrubland transition. Grasslands are still prevalent but extensive areas are under threat of shrub invasion.

Detailed site descriptions are provided for both fieldsites, including; soil, vegetation and climatic characteristics as well as a brief landuse history of the area. In total, 11 plots were constructed to fully represent the spectrum of vegetation communities and thus the different stages of land degradation evident in semi-arid environments. A nested sampling strategy was developed to aid the identification of spatial patterns of soil parameters at a range of spatial scales. A total of 108 samples per plot were collected and a number of physical and chemical properties were measured.

The principles behind the identification of spatial patterns using geostatistical analysis were outlined and the justification for its applicability presented. Notwithstanding the fact that the use of geostatistics does not substitute field-sampling itself, it provides a useful tool that permits the identification of spatial patterns in the landscape and the scales at which they exist.

#### 4.1 Introduction

#### 4.2 Organic matter content

#### 4.3 Bulk density

#### 4.4 Soil moisture

#### 4.5 Shear strength

#### 4.6 Particle-size distribution analysis

#### 4.7 Soil-aggregate stability

#### 4.8 pH

#### 4.9 Electrical conductivity

#### 4.10 Nutrient content analysis

#### 4.11 Key Findings

#### 4.1 Introduction

## CHAPTER FOUR

### Grasslands:

#### Analysis of the Spatial Continuity of Soil Properties

---

##### 4.1 Introduction

##### 4.2 Organic matter content

##### 4.3 Bulk density

##### 4.4 Soil moisture

##### 4.5 Shear strength

##### 4.6 Particle-size distribution analysis

##### 4.7 Soil-aggregate stability

##### 4.8 pH

##### 4.9 Electrical conductivity

##### 4.10 Nutrient content analysis

##### 4.11 Key findings

---

##### 4.1 Introduction

This chapter presents the results and discussion of the spatial distribution of soil parameters derived from plots classified as grasslands. The chapter investigates the notion that grassland landscapes are traditionally considered homogeneous, both in vegetation cover and the associated grassland soil parameters (Schlesinger *et al.*, 1990). More recently, however, it has been suggested that contrary to being homogenous, grasslands exhibit heterogeneous spatial patterns albeit at smaller scales than those displayed by shrubland landscapes (Hook *et al.*, 1991; Schlesinger *et al.*, 1996).

Four plots in total have been investigated including three grassland plots and a mixed vegetation plot. The mixed vegetation plot has been included in this chapter as the grass to shrub ratio marginally favours a grassland classification. Table 4.1 indicates the plot number that will be referred to throughout the chapter, the associated vegetation type and study region.

**Table 4.1** Grassland plot identification data

Plot number	Vegetation Type	Study Region
1	Mixed	Karoo
2	Grassland	Karoo
8	Grassland	Sevilleta NWR
10	Grassland	Sevilleta NWR

As it is hypothesised that the mechanisms underlying the erosional process, as a consequence of vegetation change, are characteristic of all semi-arid regions the spatial patterns in the Karoo should, in principle, mirror those in New Mexico. Although the applicability of this hypothesis will be investigated statistically in this chapter, comparisons will only be made on an individual soil parameter basis. The validity of this hypothesis is considered a separate aspect of the research question and will therefore be discussed in detail in chapter seven.

Due to the large data set and interrelated nature of the study the chapter has been structured in such a way that each soil parameter is dealt with in turn. Therefore, for each parameter, a separate summary will follow the results of the four plots. An overview will be provided at the end of the chapter summarising the key findings.

## 4.2 Organic matter content

### 4.2.1 Results:

#### a) Test of normality, descriptive statistics and inter-plot variation

The frequency distributions displayed by the boxplots (figure 4.1) show that the datasets from all plots are positively skewed. Plots 1 and 2 are considered to be highly positively skewed as the skewness values are greater than 1 (see table 4.2). More outliers are displayed in the Karoo datasets and all are evident at the upper end of the measurement scale.

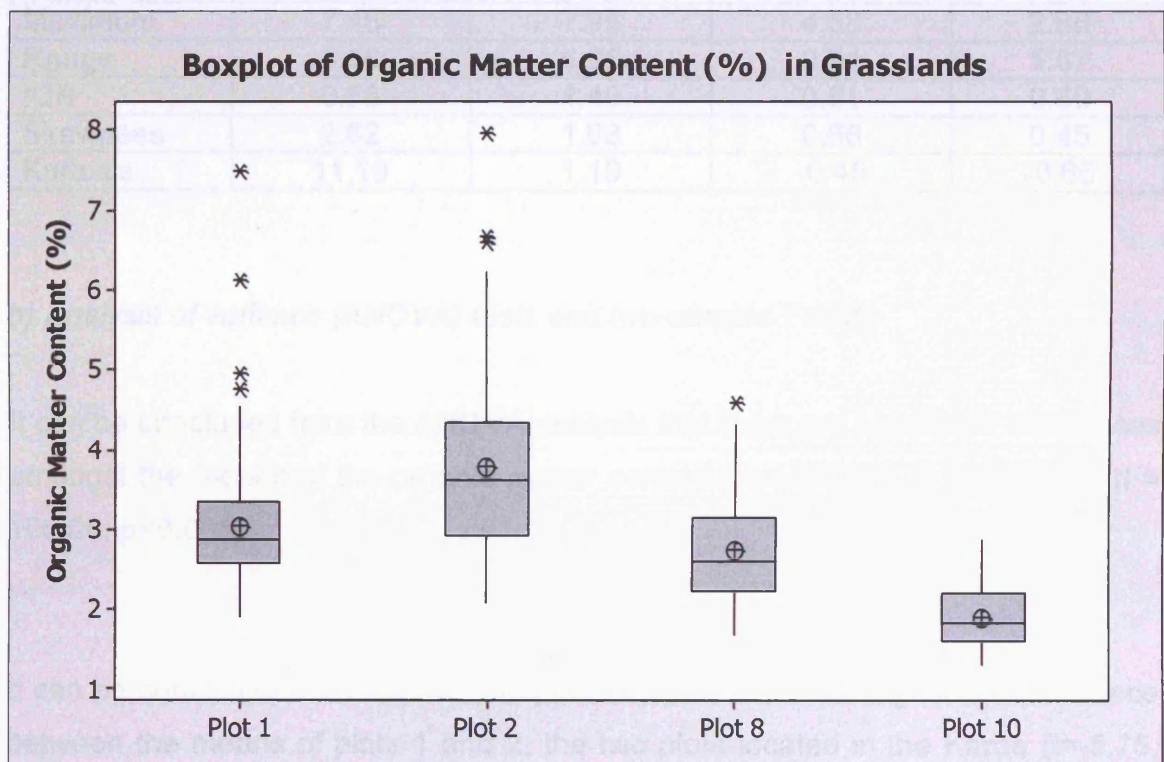


**Figure 4.1** Boxplots representing the sample distribution of organic matter content in the grassland plots.

Inter-plot comparisons of the descriptive statistics can be seen in table 4.2. The two plots with the highest mean values and greatest ranges are plots 1 and 2, the two plots situated in the Karoo, South Africa. Interestingly, the coefficient of variation (Coef Var) values, which are an index of the overall plot variation relative to the mean, do not vary greatly across the different plots.

**Table 4.2** Inter-plot comparisons of descriptive statistics: Organic matter content

Descriptive Statistic	Plot 1 (Mixed)	Plot 2 (Grassland)	Plot 8 (Grassland)	Plot 10 (Grassland)
<b>Mean</b>	<b>3.05</b>	<b>3.80</b>	<b>2.74</b>	<b>1.92</b>
Median	2.88	3.61	2.59	1.84
SE of Mean	0.07	0.11	0.07	0.04
St Dev	0.77	1.11	0.71	0.37
Variance	0.60	1.24	0.50	0.13
<b>Coef Var</b>	<b>25.40</b>	<b>29.27</b>	<b>25.75</b>	<b>19.14</b>
Minimum	1.90	2.07	1.67	1.31
Maximum	7.48	7.95	4.58	2.88
<b>Range</b>	<b>5.58</b>	<b>5.88</b>	<b>2.91</b>	<b>1.57</b>
IQR	0.78	1.40	0.91	0.60
Skewness	2.62	1.08	0.66	0.45
Kurtosis	11.19	1.19	-0.49	-0.66

*b) Analysis of variance (ANOVA) tests and two-sample T-tests*

It can be concluded from the ANOVA analysis that there are significant differences amongst the means of the organic matter content from plots 1, 2, 8 and 10. ( $F=106.06$ ,  $p<0.005$ ).

It can be concluded from the two-sample t-test that there is a significant difference between the means of plots 1 and 2, the two plots located in the Karoo ( $t=-5.75$ ,  $p<0.005$ ). Similarly, there is a significant difference between the means of plots 8 and 10, the two plots located in the Sevilleta NWR ( $t=10.79$ ,  $p<0.005$ ).

*c) Intra-plot variation*

Examination of the means and standard deviations at each spatial scale (figure 4.2) do not show any significant characteristics that applicable to all the plots. Therefore the initial results suggest that the sample distribution of organic matter content is not significantly affected by the scale of sampling in a plot scale study. On a basic level these results imply that each grassland plot displays a relatively homogenous organic matter content, however geostatistical analysis will investigate this on a more comprehensive level.

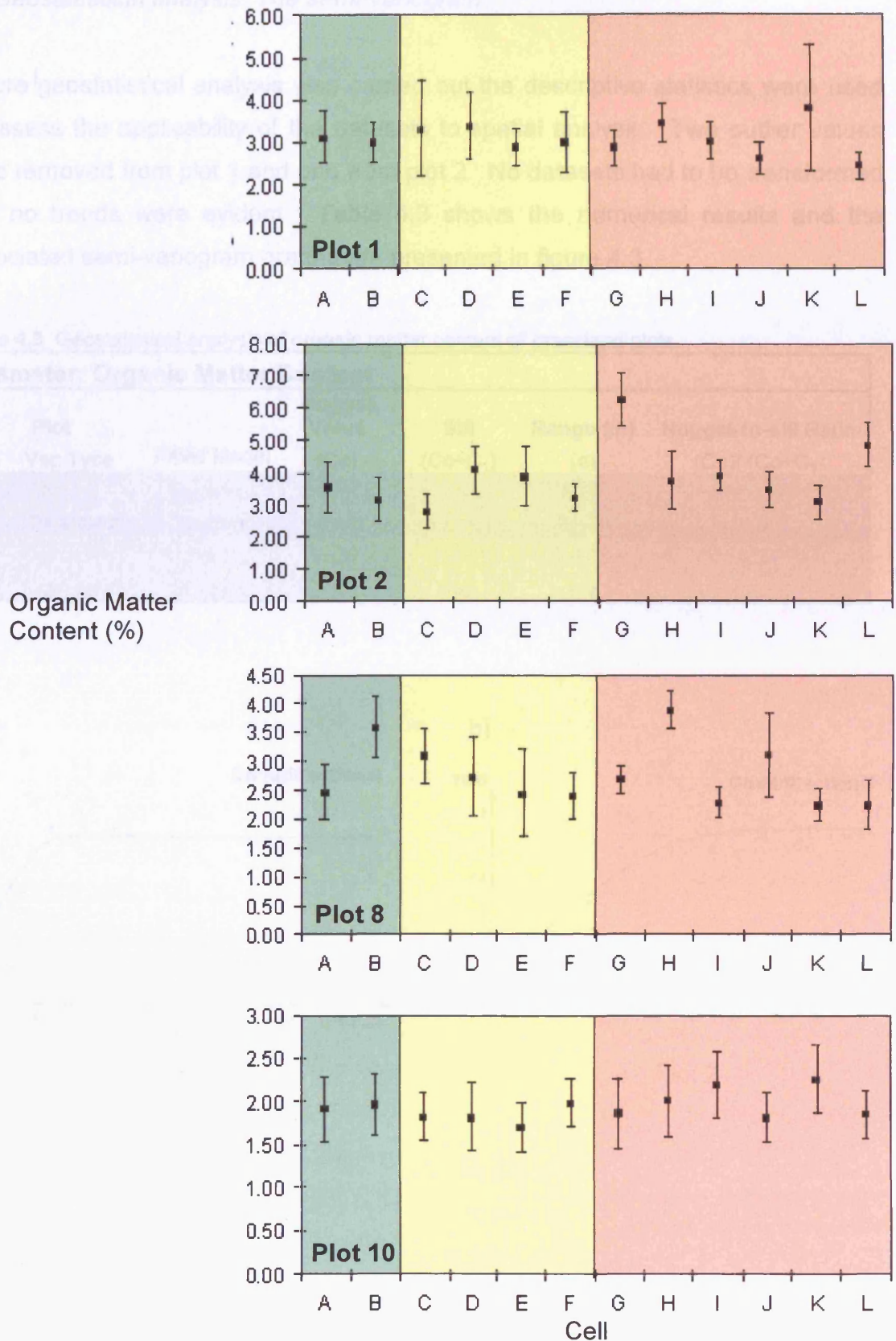


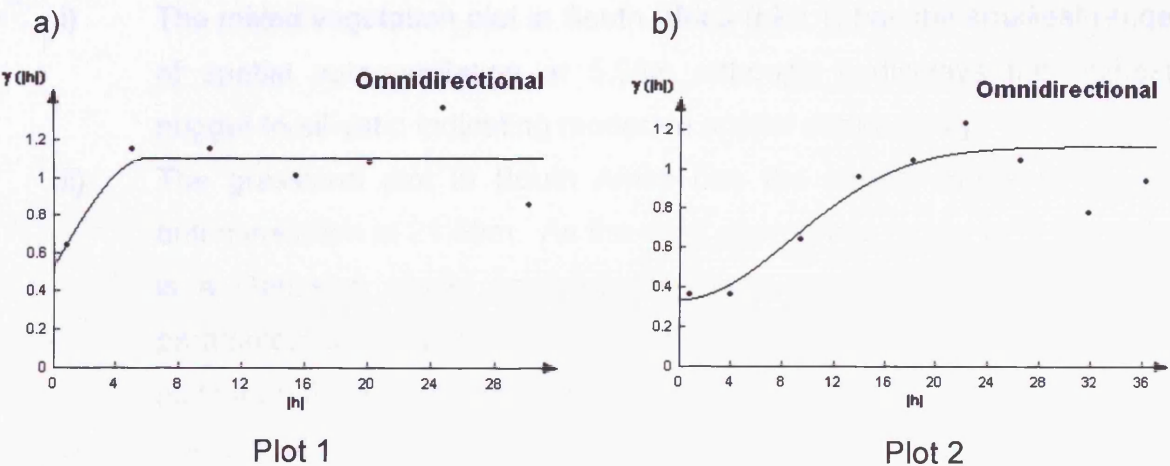
**Figure 4.2** The means and standard deviations of organic matter content for each cell within the plots. Green represents the 30 x 30m cells, yellow represents the 10 x 10m cells and pink represents 1.5 x 1.5m cells.

d) Geostatistical analysis: The semi-variogram

Before geostatistical analysis was carried out the descriptive statistics were used to assess the applicability of the datasets to spatial analysis. Two outlier values were removed from plot 1 and one from plot 2. No datasets had to be transformed and no trends were evident. Table 4.3 shows the numerical results and the associated semi-variogram graphs are presented in figure 4.3.

**Table 4.3** Geostatistical analysis of organic matter content of grassland plots

<b>Parameter: Organic Matter Content</b>						
No.	Plot	Fitted Model	Nugget Value ( $C_0$ )	Sill ( $C_0+C_1$ )	Range (m) (a)	Nugget-to-sill Ratio ( $C_0$ )/ ( $C_0+C_1$ )
1	Mixed	Spherical	0.53	1.11	<b>5.98</b>	<b>0.48</b>
2	Grassland	Gaussian	0.34	1.12	<b>21.09</b>	<b>0.30</b>
8	Grassland	Spherical	0.25	1.01	<b>14.06</b>	<b>0.25</b>
10	Grassland	Nugget	1.00	na	na	na



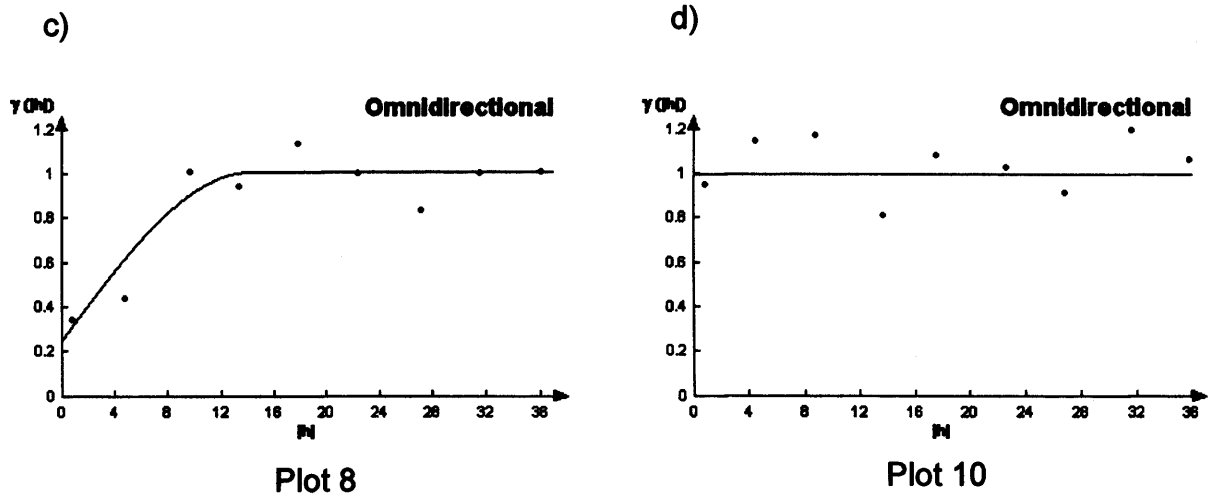


**Figure 4.3** Semi-variograms of the organic matter content of the grassland plots. Plots 1 and 2 (a & b) are situated in the Karoo, S. A. and plots 8 and 10 (c & d) are situated in the Sevilleta, NWR, N. M.

The results are as follows:

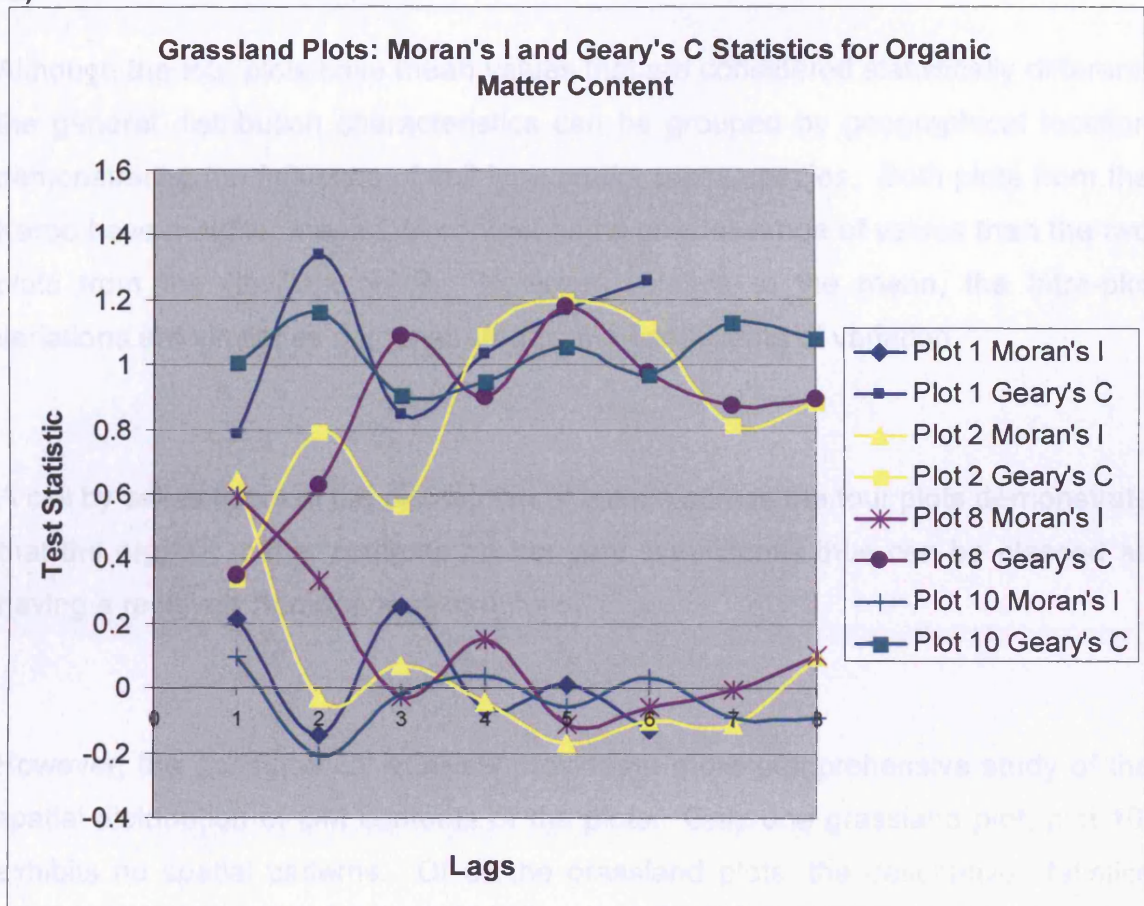
- i) The mixed vegetation plot in South Africa (plot 1) has the smallest range of spatial autocorrelation at 5.98m although it displays the highest nugget-to-sill-ratio indicating moderate spatial dependency.
- ii) The grassland plot in South Africa has the largest range of spatial autocorrelation at 21.09m. As the most appropriate model to fit this data is a Gaussian model comparisons made with other models spatial parameters are inappropriate. However, this itself indicates that the two plots from the Karoo exhibit different characteristics.
- iii) The two plots in New Mexico vary significantly. Plot 8 has a range of 14.06m whereas plot 10 is best represented by a pure nugget model indicating a random pattern among the data.
- iv) There are no obvious characteristics that indicate a typical spatial structure for grassland plots in either the Karoo or the Sevilleta NWR.

**e) Geostatistical analysis: Moran's I and Geary's C statistics**

The results are as follows: (see figure 4.4)

- i) The Moran's I and Geary's C correlograms mirror each other relatively well, this increases confidence in the results.
- ii) The Geary's C analysis, which is closely related to the semi-variogram shows that plot 1 exhibits evidence of spatial clustering until lag 2 (5 > to <= 10m). This coincides with the range of 5.98m given by the semi-variogram. Spatial clustering is also suggested at lag 3 (10 > to <= 15m), this is evident in the semi-variogram but is not as prominent. As this statistic does not differentiate between high and low cluster values exact interpretation of this is difficult, however, it may signify a bare patch in the ground cover resulting in a low organic matter content.
- iii) Plots 2 and 8 are relatively well represented by the Geary's C statistics, the results appear to be comparable to those of the semi-variogram.
- iv) Plot 10 shows undulation above and below 1 on the Geary's C scale indicating that although the semi-variogram classes this as a random pattern, periodicity may exist suggesting 'patchiness' in the distribution of organic matter.

a)



b)

Lag increment codes	Plot 1	Plots 2, 8, 10
1	0 > to <= 5	0 > to <= 4.5
2	5 > to <= 10	4.5 > to <= 9
3	10 > to <= 15	9 > to <= 13.5
4	15 > to <= 20	13.5 > to <= 18
5	20 > to <= 25	18 > to <= 22.5
6	25 > to <= 30	22.5 > to <= 27
7		27 > to <= 31.5
8		31.5 > to <= 36

**Figure 4.4** a) Moran's I and Geary's C correlograms for the organic matter content of the grassland plots. b) provides the key to the lag increments used in the correlograms for each plot.

### 4.2.2 Summary

Although the four plots have mean values that are considered statistically different, the general distribution characteristics can be grouped by geographical location demonstrating the influence of soil type and/or grass species. Both plots from the Karoo have a higher mean OM content and a greater range of values than the two plots from the Sevilleta NWR. However, relative to the mean, the intra-plot variations are similar as demonstrated by the coefficients of variation.

A cell by cell account of the distribution of values across the four plots demonstrate that the organic matter contents do not vary significantly thus can be classed as having a relatively homogenous structure.

However, the geostatistical analysis provides a more comprehensive study of the spatial distribution of OM contents of the plots. Only one grassland plot, plot 10, exhibits no spatial patterns. Of all the grassland plots, the descriptive statistics identified this plot as having the least variation, therefore we can be reasonably confident that this interpretation is correct. In contrast, spatial patterns were evident in plots 1, 2 and 8. Plot 1, the mixed vegetation plot has the smallest range of spatial autocorrelation at 5.98m whereas plots 2 and 8 has larger ranges of 21.09m and 14.06m, respectively.

Plot 2, the pure grassland plot located in the Karoo, has a considerably larger range of spatial autocorrelation than plot 1 and a stronger spatial correlation according to the nugget-to-sill ratio. As a considerable number of shrubs were identified in plot 1, this finding may be an initial indication of the influence of shrubs, their promotion of shorter ranges of spatial autocorrelation and thus increased spatial heterogeneity amongst soil parameters. According to Cambardella and Karlen (1999) a low nugget-to-sill ratio combined with a small range indicates a patchy distribution thus supporting this interpretation.

Comparisons between the two Sevilleta NWR sites indicate that although the two grassland sites appear to be similar visually, the spatial structures of organic matter content are different. Plot 8 displays obvious spatial autocorrelation (14.06m) whereas plot 10 is best represented by a pure nugget model. Despite this, some periodicity is evident in plot 10's semi-variogram implying regular patterns of organic matter content exist across the plot.

### **4.3 Bulk density**

#### **4.3.1 Results**

##### *a) Test of normality, descriptive statistics and inter-plot variation*

Negatively skewed distributions are evident in plots 1 and 2 whereas plots 8 and 10 can be classed as having normal distributions (figure 4.5). Both plots 1 and 2, the two plots located in the Karoo, display outliers at the lowest end of the scale of measurement whereas plots 8 and 10, located in the Sevilleta NWR, display outliers at the upper end of the scale of measurement.

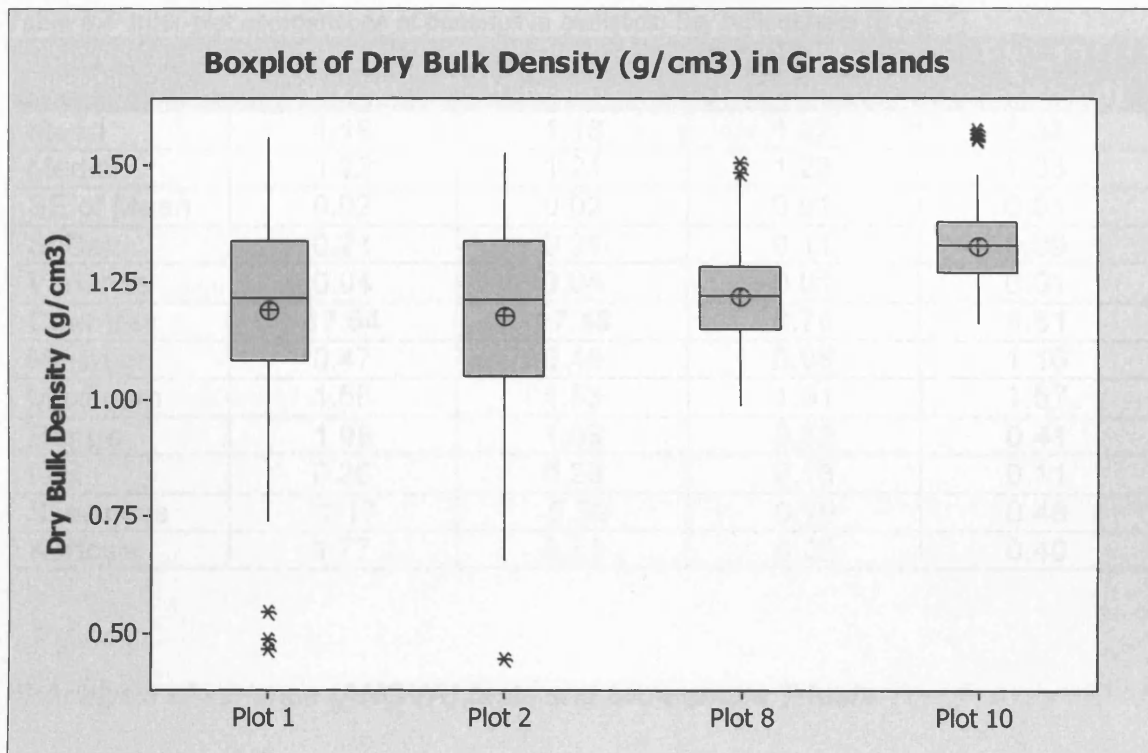


Figure 4.5 Boxplots representing the sample distribution of dry bulk density in the grassland plots.

Both the boxplots and the descriptive statistics (table 4.4) demonstrate that although the mean and median values of all four plots are relatively similar, the distribution of data varies. There is consistency in the maximum values found from each plot but plots 1 and 2 appear to have a much lower minimum bulk density than plots 8 and 10. The coefficient of variation values reflect these differences; plots 1 and 2, situated into the Karoo, South Africa have values of 17.64% and 17.48% respectively, values that are at least double the coefficient of variation values of plots 8 and 10, which are situated in the Sevilleta NWR, New Mexico.

Table 4.4 Inter-plot comparisons of descriptive statistics: Dry bulk density ( $\text{g cm}^{-3}$ )

Descriptive Statistic	Plot 1 (Mixed)	Plot 2 (Grassland)	Plot 8 (Grassland)	Plot 10 (Grassland)
<b>Mean</b>	<b>1.19</b>	<b>1.18</b>	<b>1.22</b>	<b>1.33</b>
Median	1.22	1.21	1.22	1.33
SE of Mean	0.02	0.02	0.01	0.01
St Dev	0.21	0.21	0.11	0.09
Variance	0.04	0.04	0.01	0.01
<b>Coef Var</b>	<b>17.64</b>	<b>17.48</b>	<b>8.76</b>	<b>6.61</b>
Minimum	0.47	0.45	0.98	1.16
Maximum	1.56	1.53	1.51	1.57
<b>Range</b>	<b>1.09</b>	<b>1.08</b>	<b>0.52</b>	<b>0.41</b>
IQR	0.26	0.29	0.13	0.11
Skewness	-1.17	-0.69	0.19	0.46
Kurtosis	1.77	0.53	0.22	0.40

*b) Analysis of variance (ANOVA) tests and two-sample T-tests*

It can be concluded from the ANOVA analysis that there are significant differences amongst the means of the organic matter content from plots 1, 2, 8 and 10. ( $F=18.86$ ,  $p<0.005$ ).

It can be concluded from the two-sample t-test that there is a no significant difference between the means of plots 1 and 2, the two plots located in the Karoo ( $t=0.49$ ,  $p=0.668$ ). However, there is a significant difference between the means of plots 8 and 10, the two plots located in the Sevilleta NWR ( $t=-8.10$ ,  $p<0.005$ ).

*c) Intra-plot variation*

A number of observations have been made from studying the mean values and standard deviations of each cell for each plot (figure 4.6).

- i) The cells representing the largest scale of measurement (30 x 30m) in plot 1 have the highest mean values of dry bulk density but the smallest

standard deviations. The cells representing the two other scales (10 x 10m and 1.5 x 1.5m) do not vary significantly.

- ii) The general trend of mean dry bulk densities from plot 2 is that as the scale of measurement increases the mean value increases. Although the cells representing the smallest scale display the greatest variation in mean values and standard deviations.
- iii) Plots 8 and 10 display similar characteristics across all three scales of measurement. Less variation in the mean values and standard deviations are evident than in the Karoo plots (1 and 2). However, in both plots there is significant variation in mean values and standard deviations between the two cells representing the largest scale, 30 x 30m.

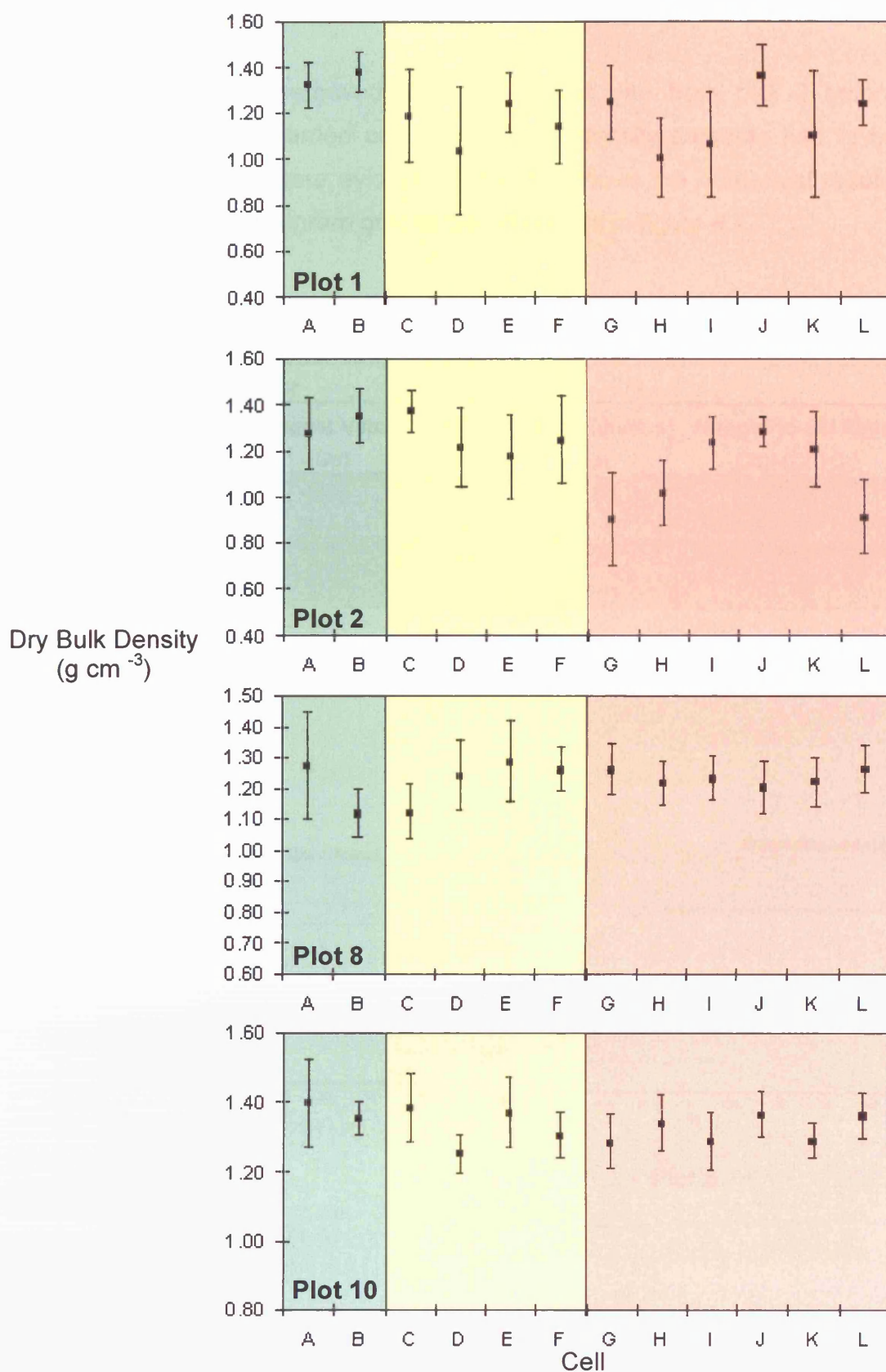


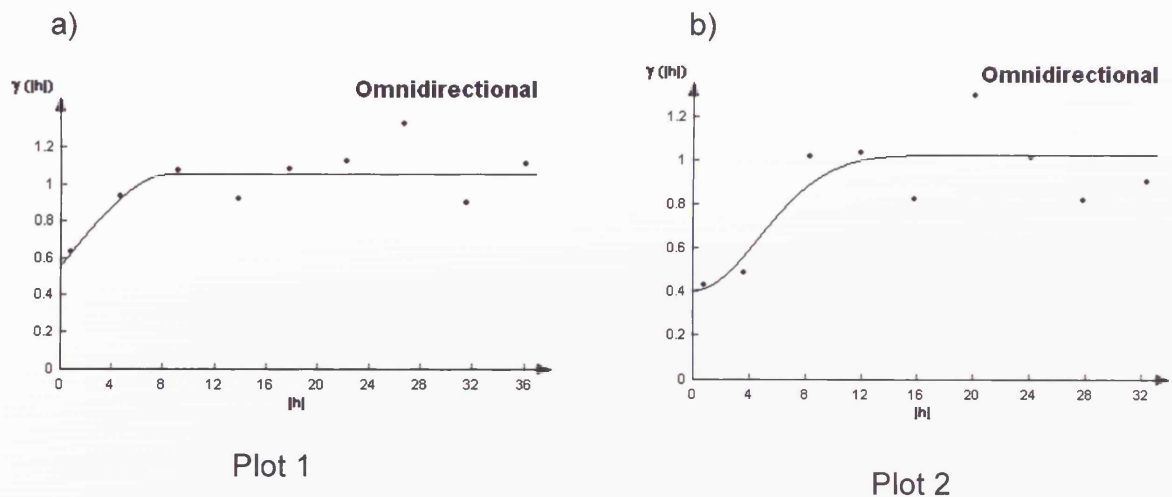
**Figure 4.6** The means and standard deviations of dry bulk density for each cell within the plots. Green represents the 30 x 30m cells, yellow represents the 10 x 10m cells and pink represents 1.5 x 1.5m cells.

## d) Geostatistical analysis: The semi-variogram

Three outlier values were removed from plot 1 and one from plot 2 before geostatistical analysis was carried out. No dry bulk density datasets had to be transformed and no trends were evident. Table 4.5 shows the numerical results and the associated semi-variogram graphs are presented in figure 4.7.

**Table 4.5** Geostatistical analysis of the dry bulk density of grassland plots

Parameter: Dry Bulk Density						
Plot No.	Veg Type	Fitted Model	Nugget Value (Co)	Sill (Co+C <sub>1</sub> )	Range (meters) (a)	Nugget-to-sill Ratio (Co)/(Co+C <sub>1</sub> )
1	Mixed	Spherical	0.56	1.06	8.60	0.53
2	Grassland	Gaussian	0.41	1.03	11.55	0.40
8	Grassland	Spherical	0.34	1.24	6.60	0.32
10	Grassland	Spherical	0.63	1.01	9.30	0.62



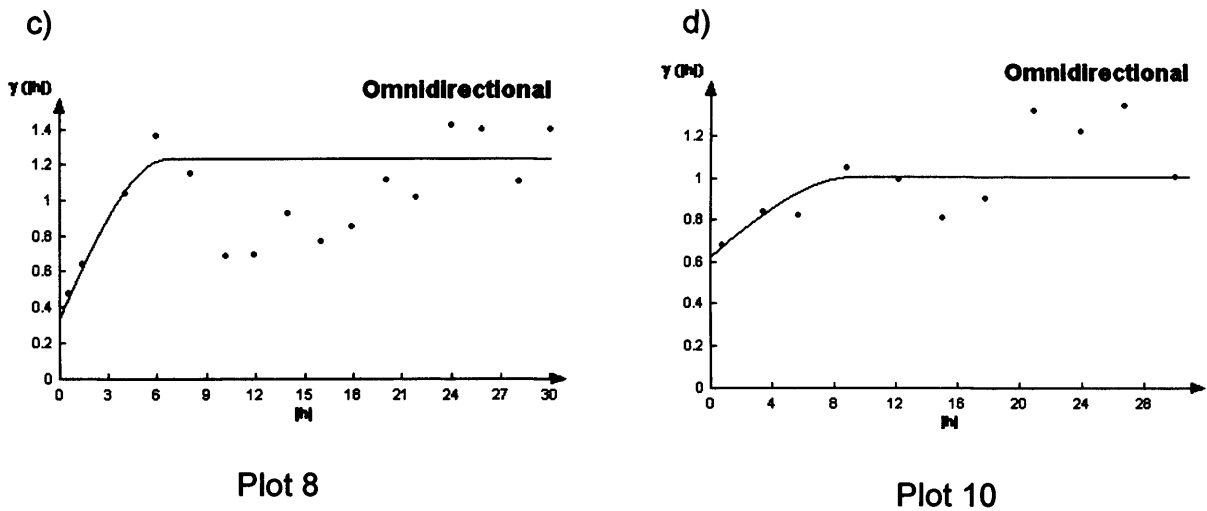


**Figure 4.7** Modelled semi-variograms for the dry bulk density of grassland plots.

The results are as follows:

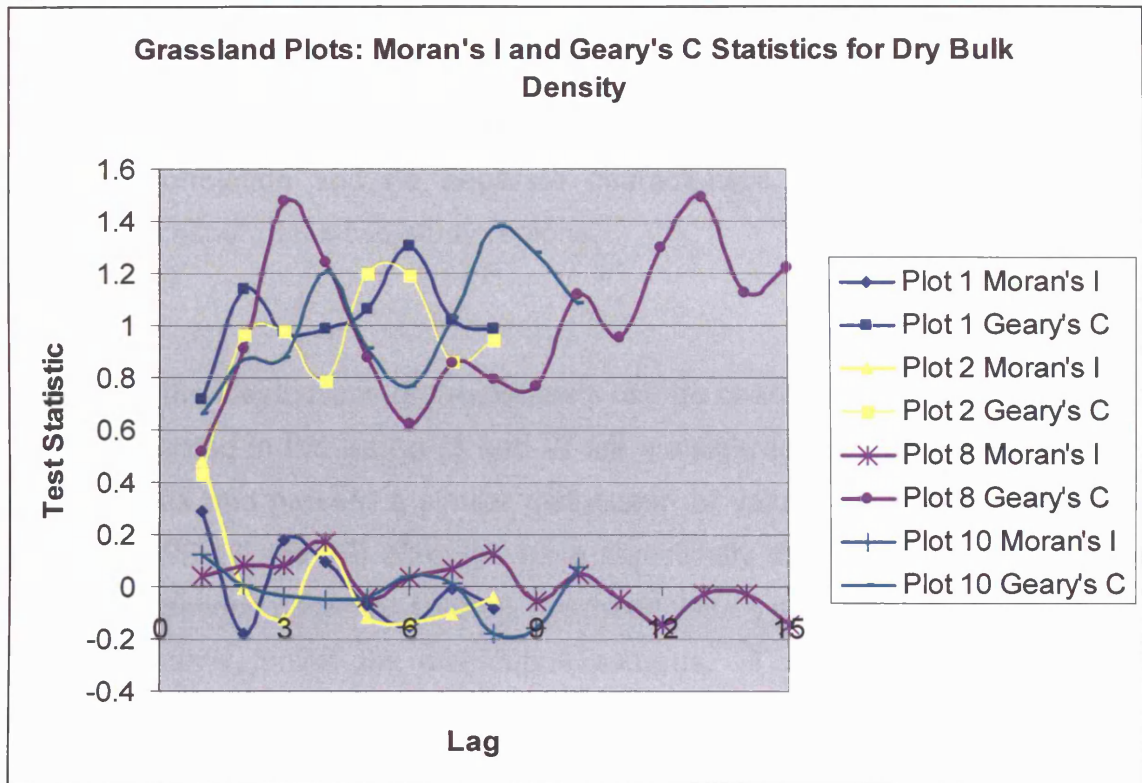
- i) The spatial autocorrelation ranges of dry bulk density vary from 6.60m to 11.55m and all nugget-to-sill ratios suggest moderate spatial dependency.
- ii) All plots except plot 2 were best represented by a spherical model. A Gaussian model was fitted to the data from plot 2.
- iii) Plot 8 displays evidence of a significant 'hole effect'. Although this is ignored with respect to fitting a model due to the complexities involved it can be seen in the data points shown in graph c. This is thought to be caused by patches in vegetation cover.
- iv) There are no distinct spatial characteristics evident with respect to the geographical location of the plots.

*e) Geostatistical analysis: Moran's I and Geary's C statistics*

The results are as follows: (see figure 4.8)

- i) Comparisons made between the Moran's I and the Geary's C correlograms show that plots 1 and 2 produce comparable results, whereas plots 8 and 10 show a weaker relationship between the two statistics, particularly at the shorter lag distances. This suggests more confidence can be placed in the results of the first two plots. However, this observation may just reflect the Moran's I test's response to the hole effect evident in plot 8 and to a lesser degree in plot 10.
- ii) The Geary's C analysis shows that the ranges of spatial autocorrelation calculated by the semi-variogram are similar to the distances derived from the correlograms for all four plots.
- iii) The 'hole effect' evident in plot 8 is well represented by the Geary's C correlogram. Although it does not differentiate between clusters high and low values, the graph can be seen to fall below 1 between the distances of approximately 8m to 22m lag distances signifying a clustering of values. This corresponds to results produced by the semi-variogram (c).

a)



b)

Lag increment codes	Plot 1	Plot 2	Plot 8	Plot 10
1	0 > to <= 4.5	0 > to <= 4	0 > to <= 2	0 > to <= 3
2	4.5 > to <= 9	4 > to <= 8	2 > to <= 4	3 > to <= 6
3	9 > to <= 13.5	8 > to <= 12	4 > to <= 6	6 > to <= 9
4	13.5 > to <= 18	12 > to <= 16	6 > to <= 8	9 > to <= 12
5	18 > to <= 22.5	16 > to <= 20	8 > to <= 10	12 > to <= 15
6	22.5 > to <= 27	20 > to <= 24	10 > to <= 12	15 > to <= 18
7	27 > to <= 31.5	24 > to <= 28	12 > to <= 14	18 > to <= 21
8	31.5 > to <= 36	28 > to <= 32	14 > to <= 16	21 > to <= 24
9			16 > to <= 18	24 > to <= 27
10			18 > to <= 20	27 > to <= 30
11			20 > to <= 22	
12			22 > to <= 24	
13			24 > to <= 26	
14			26 > to <= 28	
15			28 > to <= 30	

Figure 4.8 a) Moran's I and Geary's C correlograms for the dry bulk density of the grassland plots. b) provides the key to the lag increments used in the correlograms for each plot.

### **4.3.2 Summary**

All four plots displayed evidence of spatial autocorrelation, the ranges of influence spanning from 6.60m to 11.55m. The nugget-to-sill ratios all suggest moderate levels of correlation and no separate characteristic spatial patterns can be attributed to either of the two study regions.

In contrast, the distributions of the datasets can be characterised by location. The two plots located in the Karoo (1 and 2) are considered to have the same mean bulk densities and present a similar distribution of values. The two plots in the Sevilleta NWR (8 and 10) although have statistically different means, also have similar distributions patterns. Overall, the mean values across the four plots do not vary significantly, unlike the distribution patterns. The greater spread of bulk density values in the Karoo may be related to the species of grass present in this region or the texture of the soil, however, it can be concluded that although the range of bulk density values may vary within a plot, this does not appear to interfere with the spatial patterns evident in the grassland landscapes.

## **4.4 Soil Moisture**

### **4.4.1 Results**

Soil moisture measurements are strongly influenced by the antecedent rainfall conditions of the area, thus making comparisons among the absolute values of the plots difficult. Although detailed rainfall data are not available, a record of the weather conditions was kept throughout the fieldwork period. Dry conditions leading up to and during measurement of plots 2, 8 and 10 were recorded, however, heavy rain was observed shortly before plot 1 was measured. Therefore, as climatic conditions cannot be standardised, inter-plot comparisons of the absolute values will not be discussed. However, due to the complex relationships that exist among soil properties it is important to know the soil

moisture content in order to interpret results derived from other soil parameters. As all the data are standardised for the geostatistical analysis, comparisons among the spatial characteristics are possible.

*a) Test of normality, descriptive statistics and inter-plot variation*

The boxplots in figure 4.9 show that plot 1 follows a normal distribution whereas plots 2, 8 and 10 are all highly positively skewed. All plots except plot 1 display evidence of outliers, which are only evident at the upper end of the scale of measurement.

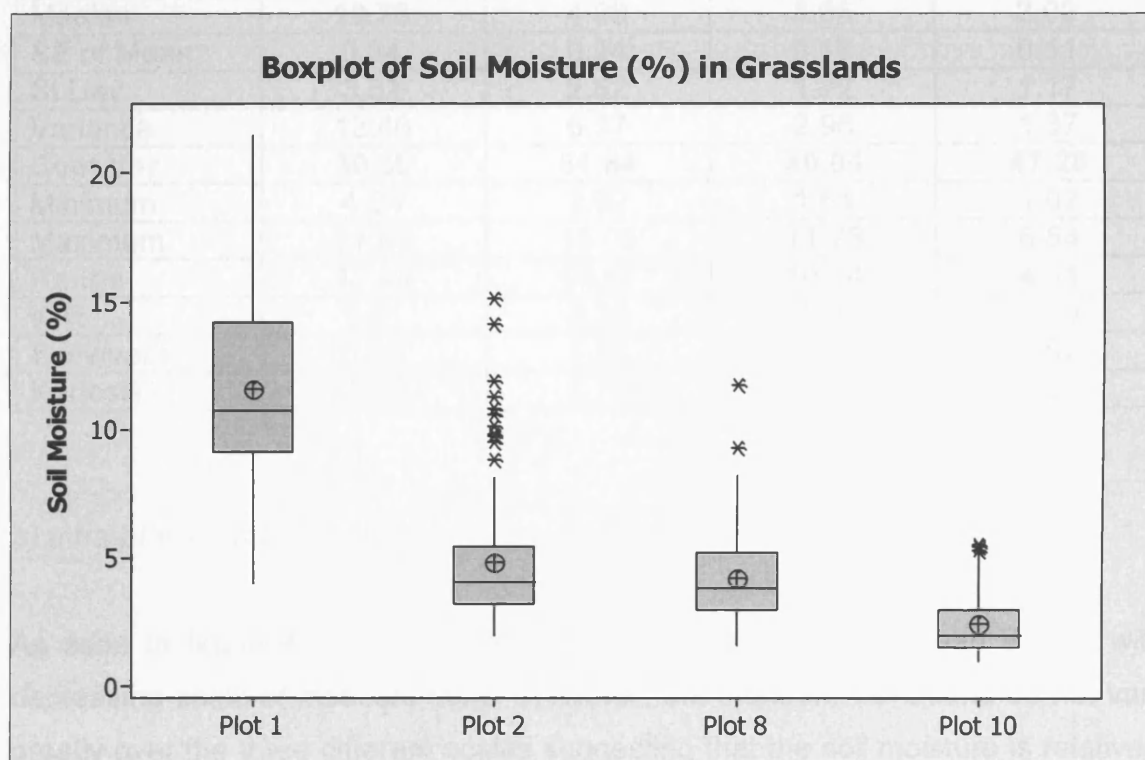


**Figure 4.9** Boxplots representing the sample distribution of soil moisture in the grassland plots.

The descriptive statistics in table 4.6 show that the mean value of plot 1 is significantly higher than the other three plots, the range of values is wider and it displays a higher maximum and minimum value. The coefficient variation values show that relative to the mean, plot 2 shows the greatest within-plot variation. Plots 8 and 10 also display high coefficients of variation values whereas plot 1

shows the least variation relative to its mean. As discussed before, comparisons made among plots are not appropriate, however, due to the spatial and temporal similarities of the measurements taken from plots 8 and 10, observations can be made with caution. Plot 10, a grassland plot in the Seville NWR, has the lowest soil moisture content of all four plots and its mean is approximately half that of plot 8. Although this may be a response to the period of time since the last localised rain event it may also reflect a difference in soil type or quality compared to plot 8.

**Table 4.6** Inter-plot comparisons of descriptive statistics: Soil moisture (%)

Descriptive Statistic	Plot 1 (Mixed)	Plot 2 (Grassland)	Plot 8 (Grassland)	Plot 10 (Grassland)
<b>Mean</b>	<b>11.59</b>	<b>4.89</b>	<b>4.30</b>	<b>2.48</b>
Median	10.78	4.09	3.85	2.02
SE of Mean	0.34	0.24	0.17	0.11
St Dev	3.52	2.52	1.72	1.17
Variance	12.40	6.37	2.96	1.37
<b>Coef Var</b>	<b>30.39</b>	<b>51.64</b>	<b>40.04</b>	<b>47.28</b>
Minimum	4.04	2.02	1.64	1.02
Maximum	21.48	15.09	11.78	5.54
<b>Range</b>	<b>17.44</b>	<b>13.07</b>	<b>10.14</b>	<b>4.51</b>
IQR	5.01	2.20	2.20	1.49
Skewness	0.45	1.89	1.26	1.02
Kurtosis	-0.22	3.79	2.64	0.05

#### *b) Intra-plot variation*

As seen in figure 4.10, plot 1 shows a general decrease in mean values with decreasing scale of measurement. However, the standard deviations do not vary greatly over the three different scales suggesting that the soil moisture is relatively uniform across the whole plot and the scale of measurement would not significantly influence the results. Plot 2 shows the opposite trend; as the scale of measurement decreases the mean value of the cell generally increases. The standard deviations of the means vary greatly, particularly when comparing the largest cells with the smallest cells. The samples within the 1.5 x 1.5m cells generally have greater standard deviations than the 30 x 30m cells. This is the opposite response to the one expected if spatial autocorrelation is present. Plot 8

exhibits a large amount of variation across and within the three scales of measurement. The results from the 1.5 x 1.5m cells in particular indicate the large variation of soil moisture measurements. Half the cells show relatively little variation among the sample values whereas the other half vary greatly. This may indicate the influence of another factor such as slope or another soil parameter. Plot 10 displays a similar pattern of variation to plot 8. In general, the greatest amount of variation is displayed in the largest cell, 30 x 30m and the most consistent results are derived from the 10m x 10m cells.

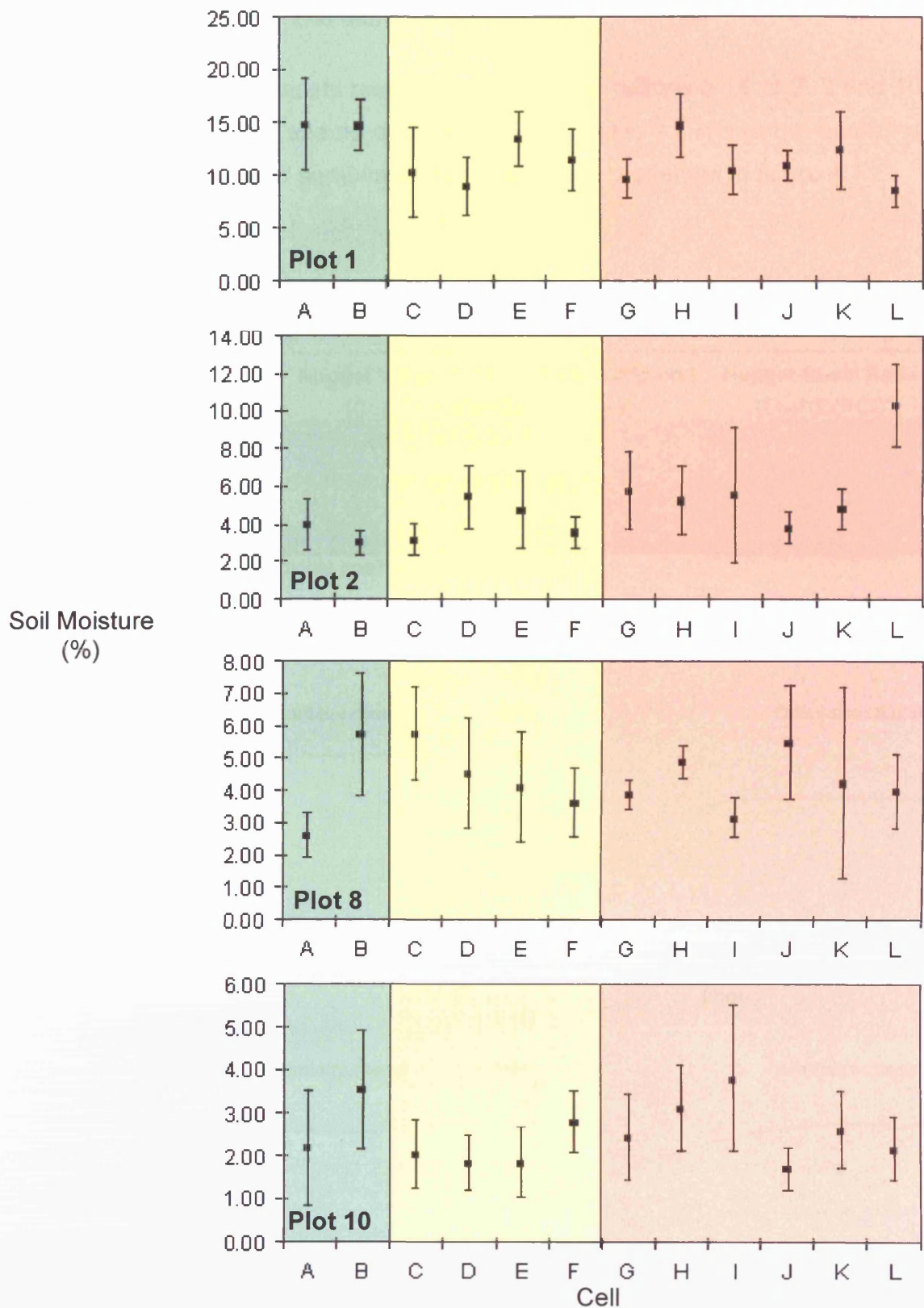


**Figure 4.10** The means and standard deviations of percentage soil moisture for each cell within the plots. Green represents the 30 x 30m cells, yellow represents the 10 x 10m cells and pink represents 1.5 x 1.5m cells.

d) Geostatistical analysis: The semi-variogram

Pre-processing of the datasets resulted in log transformations of plots 2, 8 and 10. No trends were identified and no outliers removed. Table 4.7 shows the numerical results and the associated semi-variogram graphs are presented in figure 4.11.

**Table 4.7** Geostatistical analysis of the soil moisture of grassland plots

Parameter: Soil Moisture						
Plot No.	Veg Type	Fitted Model	Nugget Value (Co)	Sill (Co+C <sub>1</sub> )	Range (meters) (a)	Nugget-to-sill Ratio (Co)/(Co+C <sub>1</sub> )
1	Mixed	Spherical	0.42	0.76	16.17	0.55
2	Grassland*	Spherical	0.41	0.94	19.47	0.44
8	Grassland*	Spherical	0.59	1.01	10.73	0.58
10	Grassland*	Spherical	0.60	1.07	25.11	0.56

\*Log transformed data due to highly positively skewed data

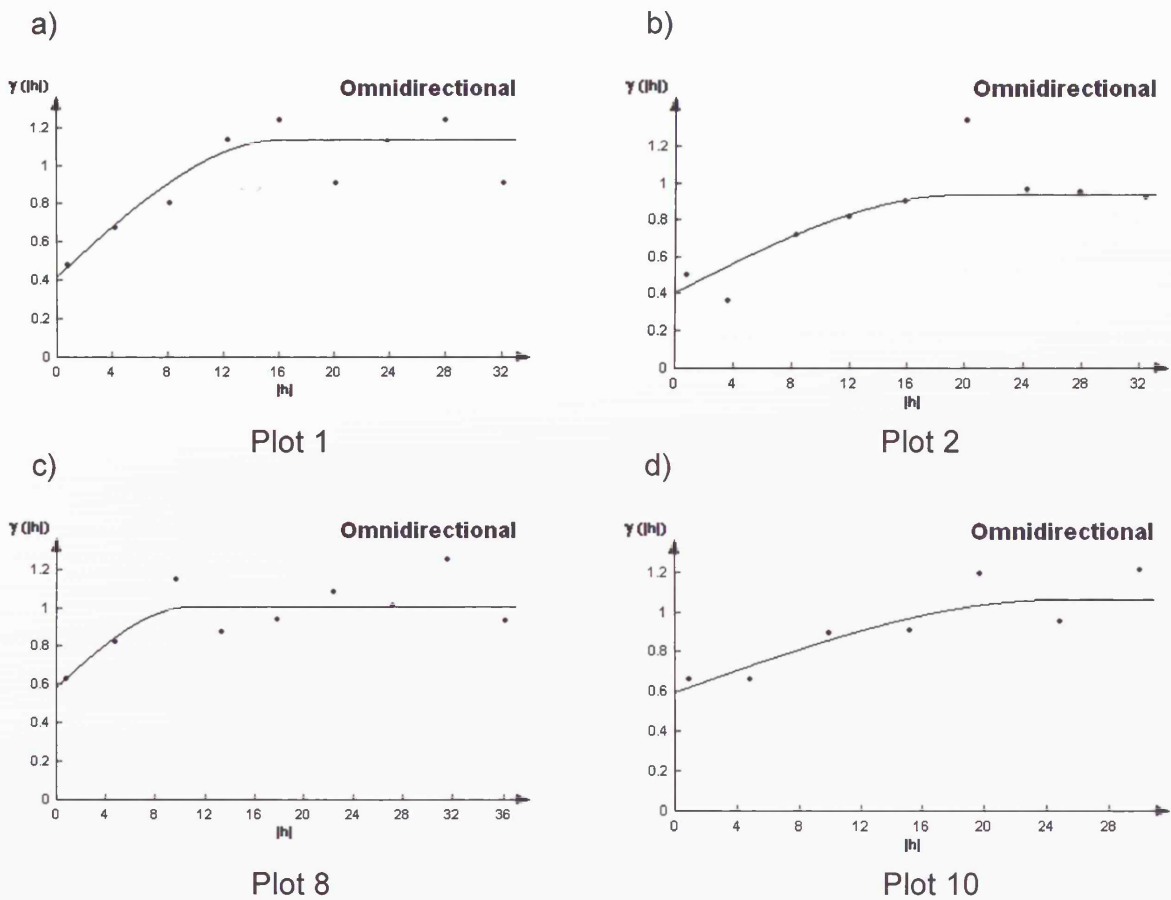


**Figure 4.11** Modelled semi-variograms for the soil moisture of grassland plots.

The results are as follows:

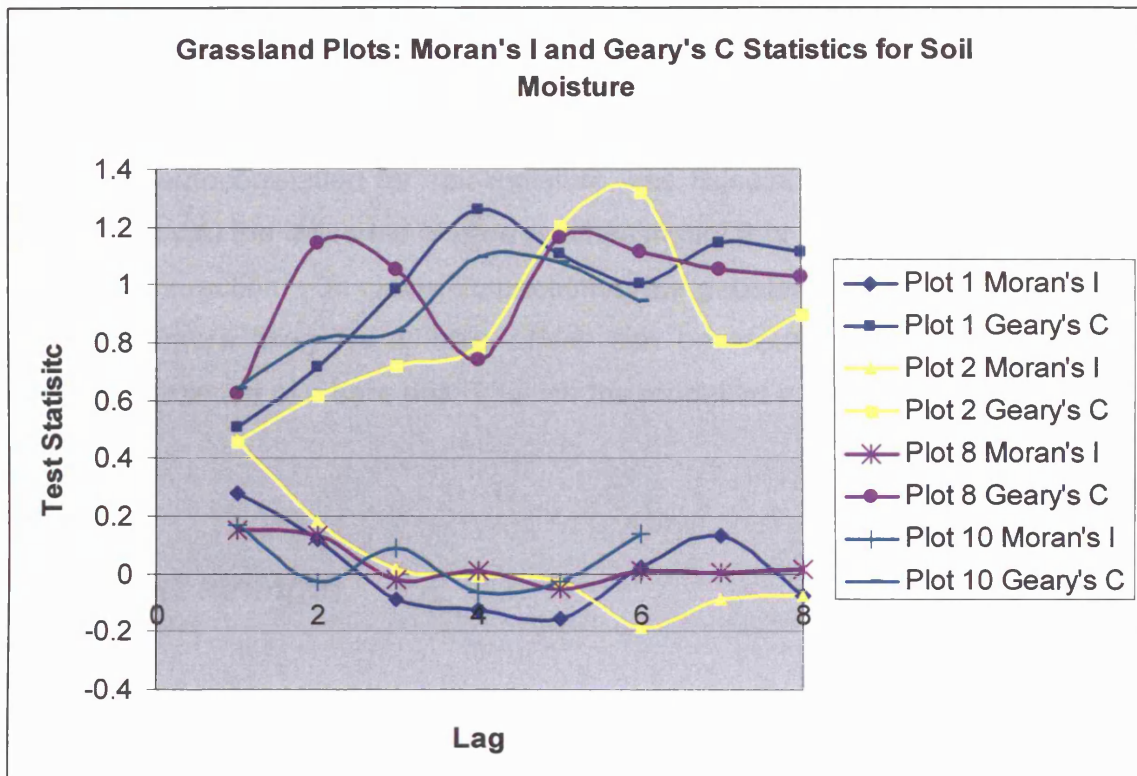
- i) The spatial autocorrelation ranges of soil moisture vary from 10.73m to 25.11m and all nugget-to-sill ratios suggest moderate spatial dependency.
- ii) All plots were best represented by a spherical model.
- iii) Plots 8 and 10, the two plots considered the most similar with respect to location and time of moisture sampling, show the greatest difference in range of spatial autocorrelation.
- iv) There are no distinct spatial characteristics evident with respect to the geographical location of the plots.

*e) Geostatistical analysis: Moran's I and Geary's C statistics*

The results are as follows: (see figure 4.12)

- i) The Moran's I and Geary's C correlograms mirror each other relatively well, providing confidence in these results.
- ii) The ranges of spatial autocorrelation calculated by the Geary's C analysis, however, are consistently lower than the ranges calculated using the semi-variograms. This suggests that a margin of error should be considered when interpreting the soil moisture semi-variogram results.
- iii) A cluster has been identified in plot 8 between lag distances of approximately 9m and 18m, contradicting the previously reported range of spatial autocorrelation of 10.73m. However, because the semi-variogram analysis largely ignores the 'hole effect' this may explain the discrepancy in results.
- iv) There is also evidence of a cluster in plot 2 starting at a lag distance of 22m and continuing indefinitely.

a)



b)

Lag increment codes	Plot 1 & 2	Plot 8	Plot 10
1	0 > to <= 4	0 > to <= 4.5	0 > to <= 5
2	4 > to <= 8	4.5 > to <= 9	5 > to <= 10
3	8 > to <= 12	9 > to <= 13.5	10 > to <= 15
4	12 > to <= 16	13.5 > to <= 18	15 > to <= 20
5	16 > to <= 20	18 > to <= 22.5	20 > to <= 25
6	20 > to <= 24	22.5 > to <= 27	25 > to <= 30
7	24 > to <= 28	27 > to <= 31.5	
8	28 > to <= 32	31.5 > to <= 36	

**Figure 4.12** a) Moran's I and Geary's C correlograms for the soil moisture of the grassland plots. b) provides the key to the lag increments used in the correlograms for each plot.

#### 4.4.2 Summary

All grassland plots demonstrate large ranges of spatial autocorrelation, from 10.73m to 25.11m and nugget-to-sill values that suggest all show moderate spatial correlation. Due to the variation in vegetation structures, differences in the mean values are to be expected between the plots from the Karoo i.e. plot 1 is a mixed

vegetation plot and plot 2 a pure grassland plot, yet the large disparity between the ranges of influence evident between the plots in the Sevilleta NWR are surprising. These plots are considered to be the most similar of the four plots- in location, vegetation cover and type, however, a difference of nearly 15m between the ranges of autocorrelation for soil moisture was calculated. This can possibly be explained by a) the influence of bare patches in plot 8 or b) different underlying soil processes in action. On closer inspection of the geostatistical results, explanation a) seems more likely as a 'hole effect' can be identified. This indicates the possible presence of a bare patch, which the modelled variogram ignores.

## **4.5 Shear strength**

### **4.5.1 Results:**

#### *a) Test of normality, descriptive statistics and inter-plot variation*

The frequency distributions displayed by the boxplots (figure 4.13) show that the shear strength data are relatively varied across the plots. Plot 1 is very slightly positively skewed, plot 2 is negatively skewed and plots 8 and 10 are both positively skewed. Plots 1 and 2 do not display any outliers whereas high extreme values are evident in the two Sevilleta NWR plots.

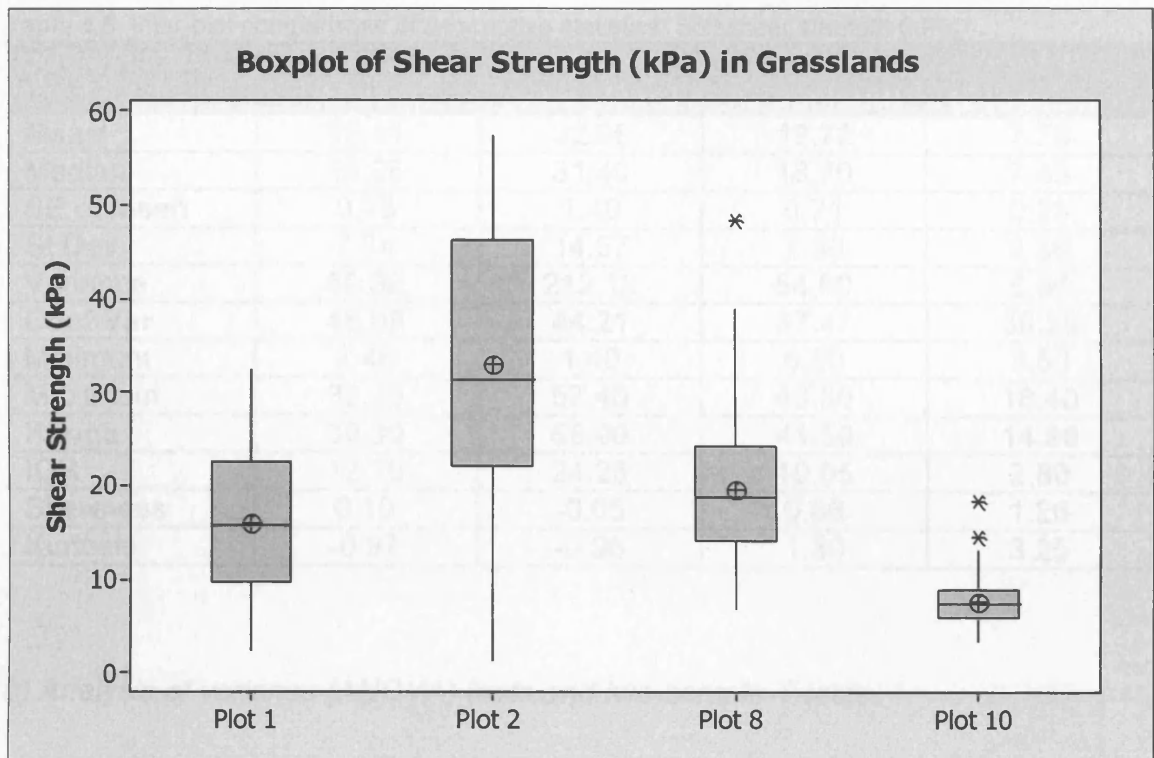


**Figure 4.13** Boxplots representing the sample distribution of soil shear strength in the grassland plots.

Initial inspection of inter-plot variation displayed by the descriptive statistics (table 4.8) shows that the shear strength values of the plots show no consistency across the four plots or even within the two study regions. It can be seen that the mean values vary greatly, for example plot 10 has a relatively low mean shear strength (7.78 kPa) with the smallest range of values (14.9 kPa) whereas plot 2 has the greatest mean shear strength (32.96 kPa) and range (56.0 kPa). However, relative to their mean, plot 1 and 2 demonstrate the greatest amount of intra-plot variation.

**Table 4.8** Inter-plot comparisons of descriptive statistics: Soil shear strength (kPa)

Descriptive Statistic	Plot 1 (Mixed)	Plot 2 (Grassland)	Plot 8 (Grassland)	Plot 10 (Grassland)
<b>Mean</b>	<b>16.11</b>	<b>32.96</b>	<b>19.72</b>	<b>7.78</b>
Median	15.85	31.40	18.70	7.45
SE of Mean	0.75	1.40	0.71	0.23
St Dev	7.74	14.57	7.39	2.36
Variance	59.98	212.13	54.60	5.56
<b>Coef Var</b>	<b>48.09</b>	<b>44.21</b>	<b>37.47</b>	<b>30.29</b>
Minimum	2.40	1.40	6.80	3.50
Maximum	32.40	57.40	48.30	18.40
<b>Range</b>	<b>30.00</b>	<b>56.00</b>	<b>41.50</b>	<b>14.90</b>
IQR	12.70	24.25	10.05	2.80
Skewness	0.10	-0.05	0.86	1.26
Kurtosis	-0.97	-0.96	1.30	3.25

*b) Analysis of variance (ANOVA) tests and two-sample T-tests*

It can be concluded from the ANOVA analysis that there are significant differences amongst the means of the organic matter content from plots 1, 2, 8 and 10. ( $F=142.72$ ,  $p<0.005$ ).

It can be concluded from the two-sample t-test that there is a significant difference between the means of plots 1 and 2, the two plots located in the Karoo ( $t=-10.61$ ,  $p<0.005$ ). Similarly, there is a significant difference between the means of plots 8 and 10, the two plots located in the Sevilleta NWR ( $t=15.99$ ,  $p<0.005$ ).

*c) Intra-plot variance*

The intra-plot analysis (figure 4.14) shows that plots 1 and 2 demonstrate a wide spread of shear strength values both within each cell and across the plot as a whole. The scale of measurement does not appear to impact the variability of results. Plots 8 and 10 exhibit less variation of the mean across the plots and the standard deviations of each cell are, in general, considerably less than plots 1 and 2. The two latter plots also display evidence of more variation in shear strength

values at the largest scale of measurement. This indicates that the soil shear strength in these plots may be spatially related.

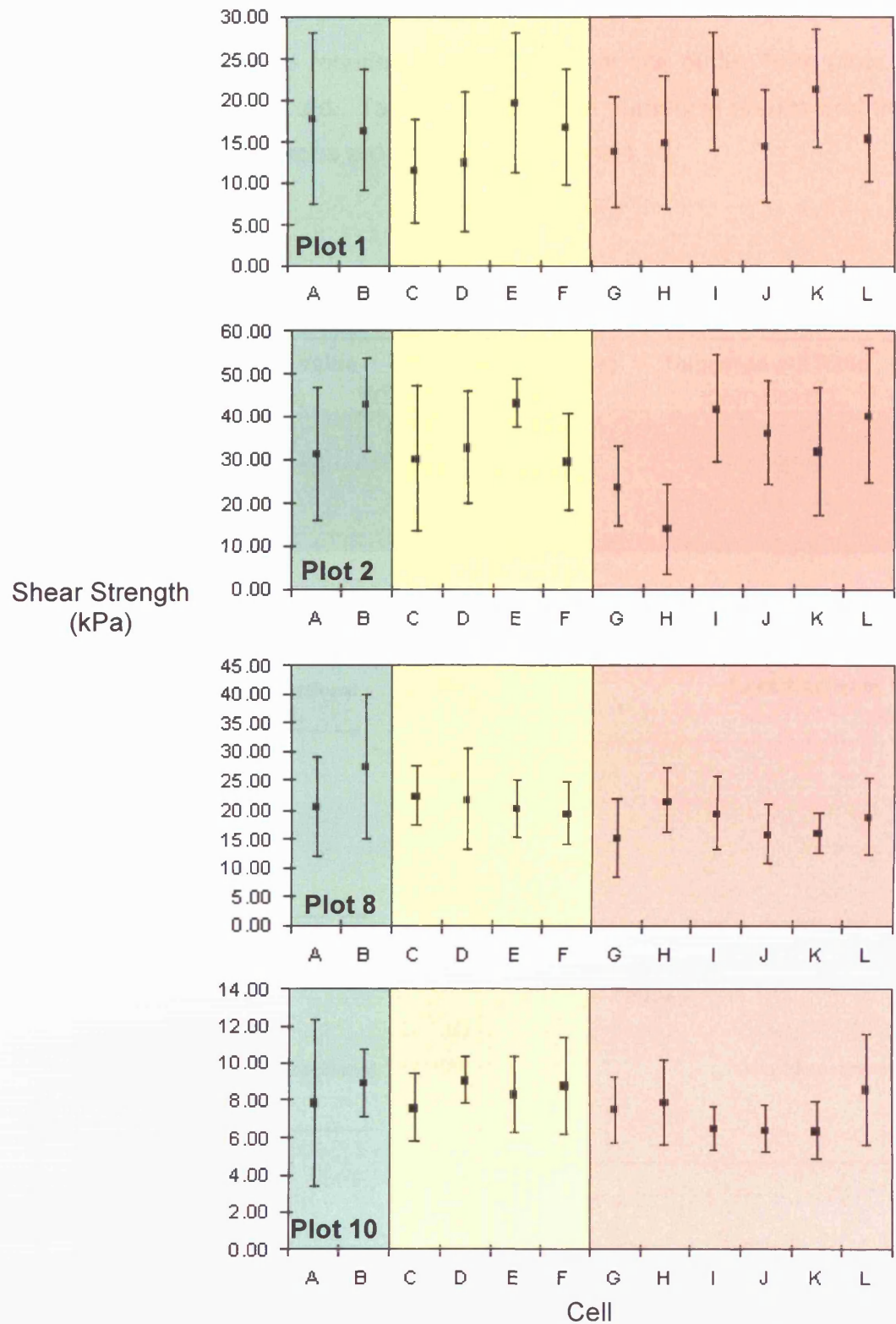


**Figure 4.14** The means and standard deviations of soil shear strength for each cell within the plots. Green represents the 30 x 30m cells, yellow represents the 10 x 10m cells and pink represents 1.5 x 1.5m cells.

## d) Geostatistical analysis: The semi-variogram

Pre-processing of the datasets resulted in the removal of one outlier from plots 8 and 10. No trends were detected. Table 4.9 shows the numerical results and the associated semi-variogram graphs are presented in figure 4.15.

**Table 4.9** Geostatistical analysis of the soil shear strength of grassland plots

Parameter: Shear Strength						
Plot			Nugget Value	Sill	Range (meters)	Nugget-to-sill Ratio
No.	Veg Type	Fitted Model	( $C_0$ )	( $C_0+C_1$ )	(a)	( $C_0$ )/ ( $C_0+C_1$ )
1	Mixed	Spherical	0.78	1.07	8.51	0.73
2	Grassland	Gaussian	0.73	1.00	9.24	0.73
8	Grassland	Spherical	0.57	1.13	17.16	0.50
10	Grassland	Nugget	1.00	na	na	na

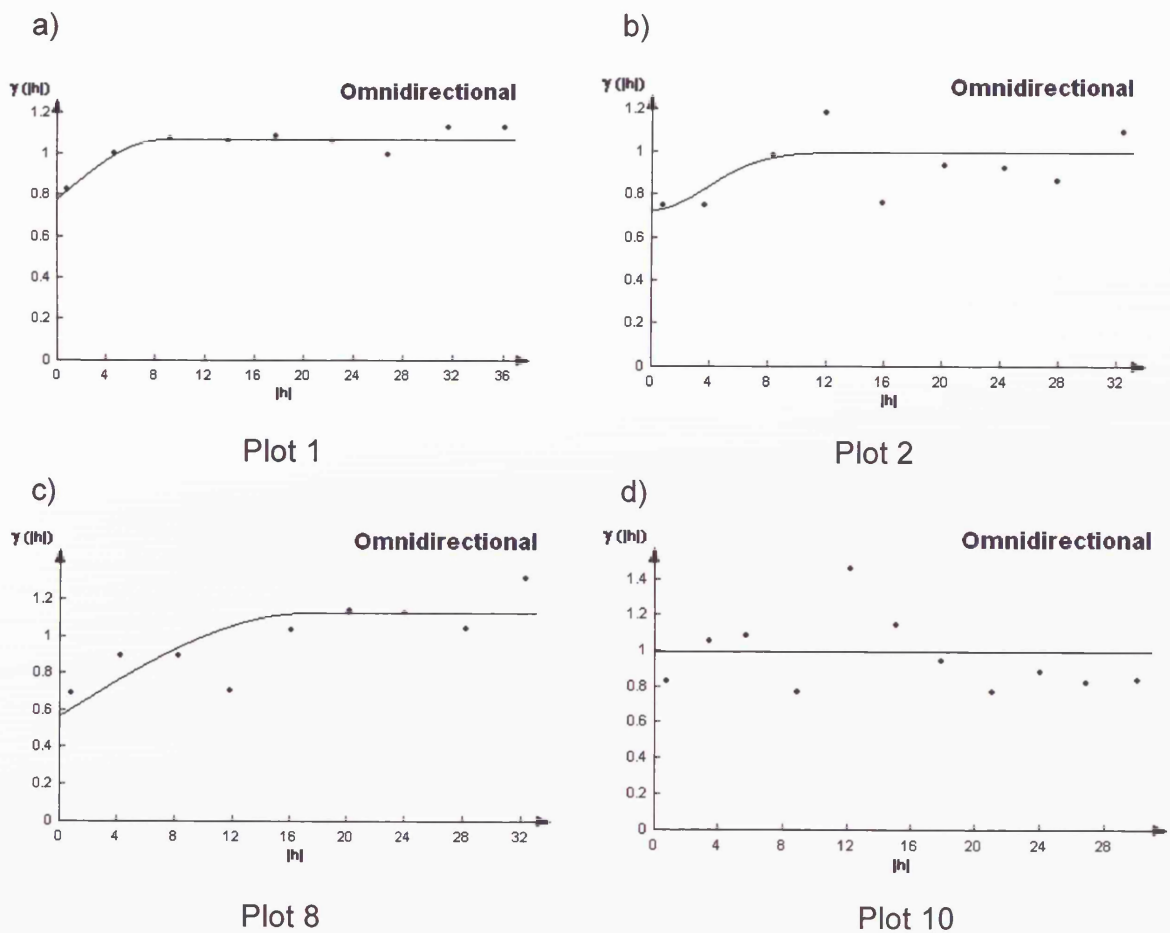


**Figure 4.15** Modelled semi-variograms for the soil shear strength of grassland plots.

The results are as follows:

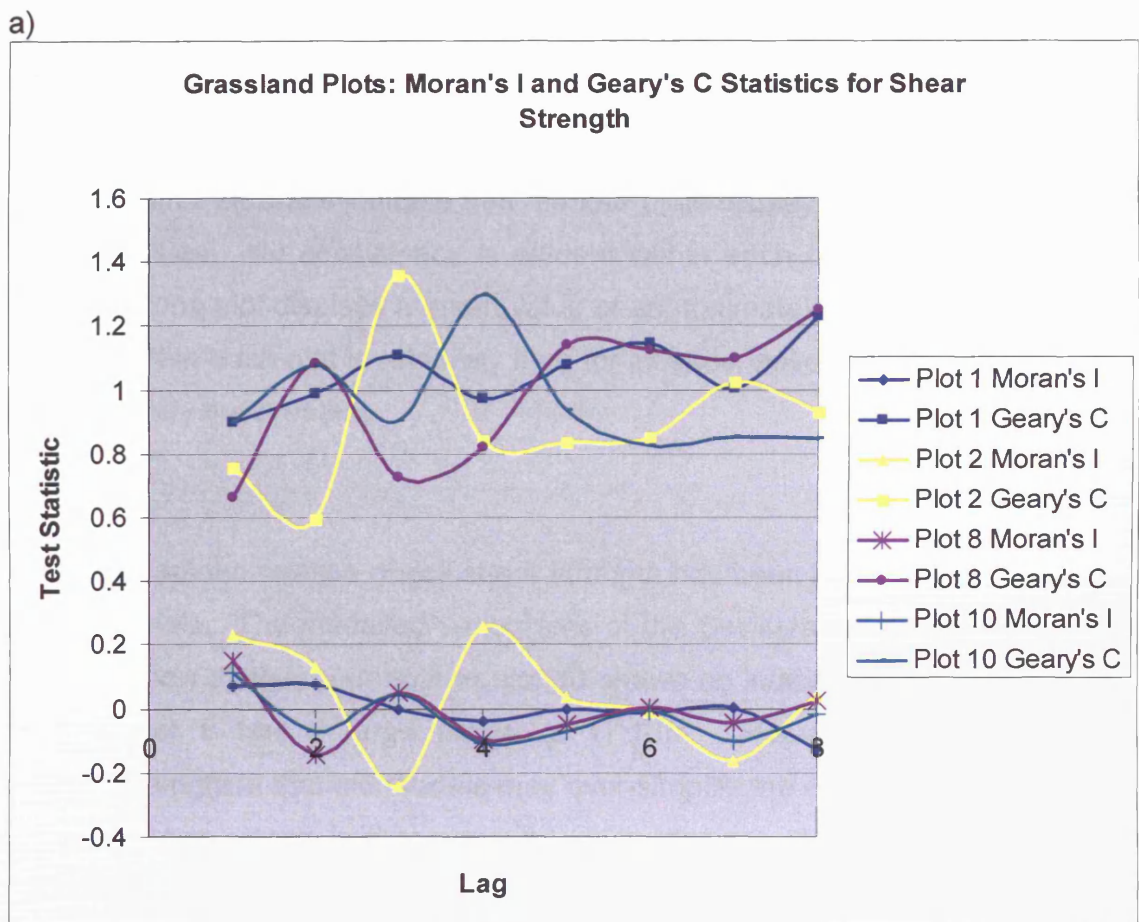
- i) The spatial autocorrelation ranges of soil shear strength vary from 8.51m to 17.16m.
- ii) The data from plot 10 was best represented by a 'pure nugget' model suggesting a random pattern of soil shear strength.
- iii) Plots 1 and 8 were best represented by a spherical model. A Gaussian model was fitted to the data from plot 2.
- iv) Evidence of a 'hole effect' can be seen in plot 8. Although this is not modelled due to the complexities involved it can be seen in the data points shown in graph c between approximately the 8m and 16m lags. This is thought to be caused by patches in vegetation cover.
- v) Plots 1 and 2, the two Karoo plots have similar ranges of autocorrelation, both of which are approximately half the range of the Sevilleta NWR plot (8). However, the nugget-to-sill ratios of plot 1 and 2 are significantly higher than plot 8 suggesting weaker spatial dependency at these plots.
- vi) Using simple models plot 10 has been best described as displaying a random pattern, however, by studying the semi-variogram (figure 4.15) plot 10 shows evidence of the 'hole effect' and a possible decrease in variance with increasing lag distance. This suggests the influence of patches or perhaps a 'checkerboard' pattern of shear strength.

*e) Geostatistical analysis: Moran's I and Geary's C statistics*

The results are as follows: (see figure 4.16)

- i) The Moran's I and Geary's C correlograms mirror each other relatively well, providing confidence in these results.
- ii) The results derived from the Geary's C correlograms are similar to those produced by the semi-variograms for plot 1, 2 and 8.

- iii) The general pattern of the correlograms produced for plot 2 are different to those exhibited by the other plots, this is reflected in the usage of a Gaussian model in the semi-variogram analysis.
- iv) The close fluctuation above and below 1 indicates that plot 10 could be classed as having a random pattern of soil shear strength. However, starting at a lag distance of 16m the correlograms indicate evidence of clustering. This could be caused by the influence of another trend that is greater than the maximum scale measured in this study.



b)

Lag increment codes	Plot 1	Plot 2, 8 & 10
1	0 > to ≤ 4.5	0 > to ≤ 4
2	4.5 > to ≤ 9	4 > to ≤ 8
3	9 > to ≤ 13.5	8 > to ≤ 12
4	13.5 > to ≤ 18	12 > to ≤ 16
5	18 > to ≤ 22.5	16 > to ≤ 20
6	22.5 > to ≤ 27	20 > to ≤ 24
7	27 > to ≤ 31.5	24 > to ≤ 28
8	31.5 > to ≤ 36	28 > to ≤ 32

**Figure 4.16** a) Moran's I and Geary's C correlograms for the soil shear strength of the grassland plots. b) provides the key to the lag increments used in the correlograms for each plot.

#### 4.5.2 Summary

The descriptive statistics indicate that the four plots display a wide variety of shear strength values. No consistency is evident within each of the study regions; in both cases one plot displays a mean value of approximately double the other. The variation within each plot is relatively high for all sites, nevertheless, the plots from the Karoo vary the greatest.

The spatial autocorrelation of soil shear strength has been identified in three of the grassland plots. The modelled variograms of the Sevilleta NWR sites reveal that the distribution of shear strength in plot 10 shows no indication of spatial patterns whereas plot 8 has a large range of 17.16m. However, the experimental variograms suggest that the models may over-simplify the structures and therefore less confidence placed in these results. Nevertheless the nugget-to-sill ratio of plot 8 suggests that moderate spatial dependency is evident. The two plots from the Karoo, however, have similar ranges of correlation (8.51m and 9.24m), both of which are considerably less than the Sevilleta NWR plot. Despite the shorter ranges, weak spatial correlation is associated with these plots, indicated by the high nugget-to-sill ratios.

## 4.6 Particle-size distribution analysis

### 4.6.1 Results

#### a) Descriptive statistics

Due to time constraints it was only possible to measure the particle size distribution of one grassland plot. The descriptive statistics of plot 2 are shown in table 4.10.

**Table 4.10** Inter-plot comparisons of descriptive statistics: Particle size distribution

Descriptive Statistic	Clay	Silt	Sand
Mean	0.72	19.79	79.50
Median	0.70	18.19	81.09
SE of Mean	0.02	0.71	0.73
St Dev	0.22	7.24	7.44
Variance	0.05	52.47	55.41
Coef Var	30.56	36.58	9.36
Minimum	0.00	5.38	58.69
Maximum	1.24	40.07	94.62
Range	1.24	34.69	35.93
IQR	0.29	10.44	10.78
Skewness	-0.19	0.54	-0.53
Kurtosis	1.10	-0.21	-0.20

#### b) Geostatistical analysis: The semi-variogram and Moran's I and Geary's C correlograms

No outliers were removed from any of the plots and no transformations were performed before geostatistical analysis was carried out. None of the datasets could be modelled using the simple models available, thus only the experimental semi-variogram graphs are presented (figure 4.17).

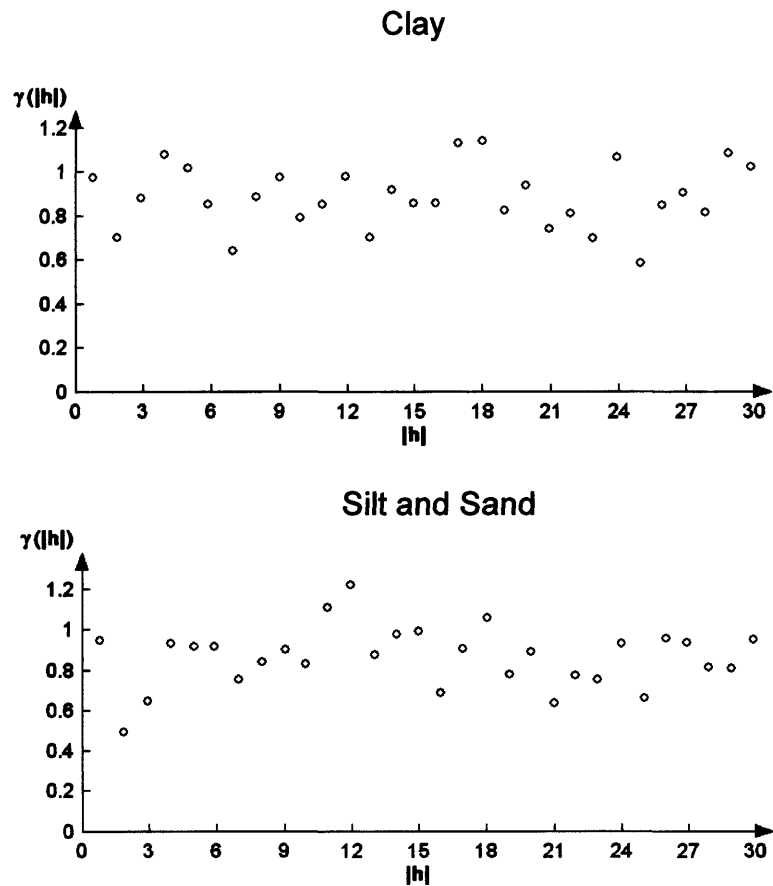
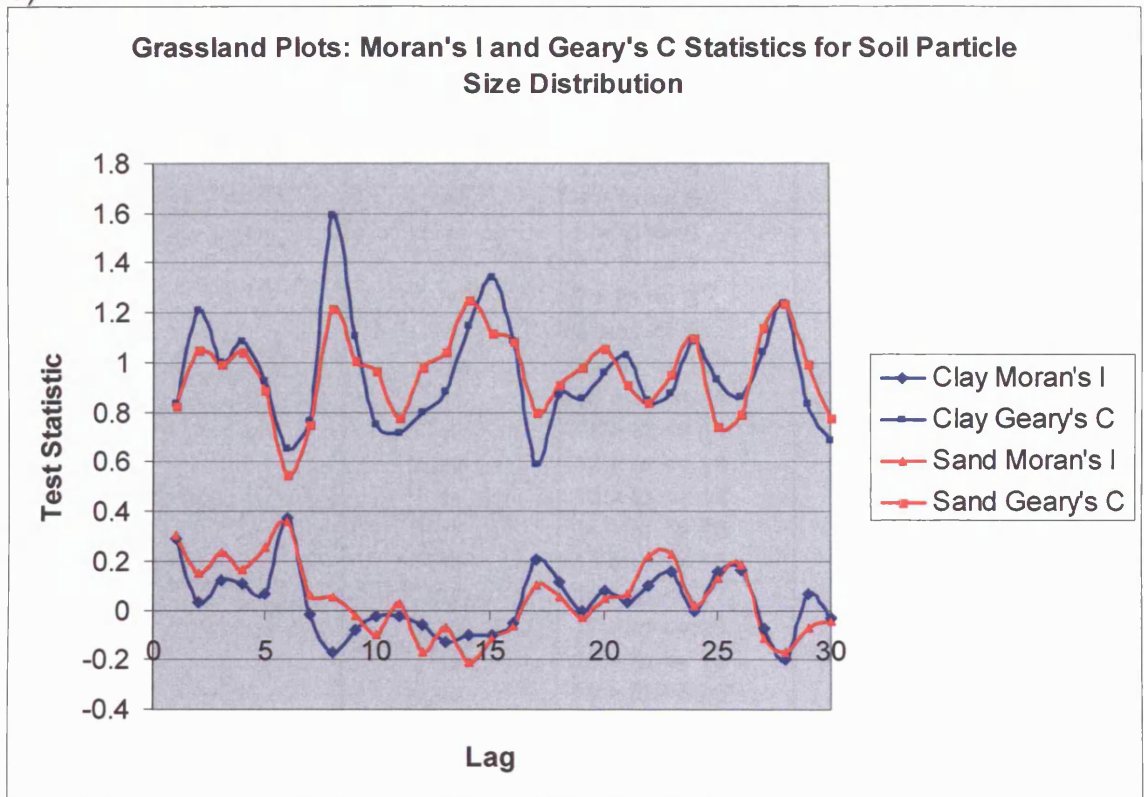


**Figure 4.17** Semi-variograms of the particle size distribution of a grassland plot.

The results are as follows:

- i) The experimental variograms show that the datasets are best represented by a pure nugget model indicating that no significant spatial patterns are evident.
- ii) However, the clay content variogram demonstrates some evidence of periodicity.
- iii) Relatively regular fluctuation in the data is also evident in the Moran's I and Geary's C correlograms (figure 4.18) suggesting some spatial patterns may exist.

a)



b)

Lag increment codes	Clay and Sand
1	0 > to <= 1
2	1 > to <= 2
3	2 > to <= 3
4	3 > to <= 4
5	4 > to <= 5
6	5 > to <= 6
7	6 > to <= 7
8	7 > to <= 8
9	8 > to <= 9
10	9 > to <= 10
11	10 > to <= 11
12	11 > to <= 12
13	12 > to <= 13
14	13 > to <= 14
15	14 > to <= 15
16	15 > to <= 16
17	16 > to <= 17
18	17 > to <= 18
19	18 > to <= 19
20	19 > to <= 20
21	20 > to <= 21
22	21 > to <= 22
23	22 > to <= 23
24	23 > to <= 24
25	24 > to <= 25
26	25 > to <= 26
27	26 > to <= 27
28	27 > to <= 28
29	28 > to <= 29
30	29 > to <= 30

**Figure 4.18** a) Moran's I and Geary's C correlograms for the particle size distribution of the grassland plot. b) provides the key to the lag increments used in the correlograms for each plot.

#### 4.6.2 Summary

According to the British classification of soil texture, plot 2 can be classed as having a loamy sand texture. Although no spatial autocorrelation can be identified from the experimental variograms of particle sizes across the grassland plot, there is evidence in the clay content variogram of periodicity. Relatively regular wavelengths are produced by the Geary's C correlogram and are seen to a lesser

degree in the Moran's I. These patterns suggest that some spatial organisation of particle size may occur in grassland landscapes.

#### **4.7 Soil-aggregate stability**

Unfortunately the technique employed to measure soil aggregate stability (see chapter 3) did not produced adequate datasets to allow the application of spatial statistics. All samples from the 108 locations for plots 1, 2 and 10 were sieved in order to collect aggregates for measurement, however not all samples contained a sufficient quality or quantity of aggregates. Plot 10 in particular provided a very poor dataset thus due to the similarities in soil texture with plot 8, combined with the time constraints in place, a decision was made not to measure the aggregate stability of plot 8. However, the lack of aggregates in the samples itself is an indicator of the strength of the soil; this will be discussed further in chapter 8.

##### **4.7.1 Results**

From figure 4.19 a number of observations can be made about the aggregate stability of soil in the three semi-arid mixed and grassland plots:

- i) In all cases the number of adequate aggregates obtained from the samples was low, less than 50% of the total samples per plot contained suitable aggregates.
- ii) Out of 108 samples, plot 10 (Sevilleta, NWR) only had 5 samples containing suitable aggregates. This suggests that the soil structure is very weak. However, of the 5 samples measured, only 1 dispersed completely and the four others lost only a maximum of 40% of their total weight.
- iii) Plot 1, the mixed vegetation plot situated in the Karoo, S.A. had significantly more measurable aggregates, however, these were largely

unstable with over 40% of the samples losing more than 50% of their total weight after agitation and 23% dispersing completely.

- iv) Plot 2, the grassland plot situated in the Karoo, S.A. had the most samples and also the most stable aggregates. No aggregate samples dispersed completely and more than 70% of the total samples only lost 10% of their total weight.

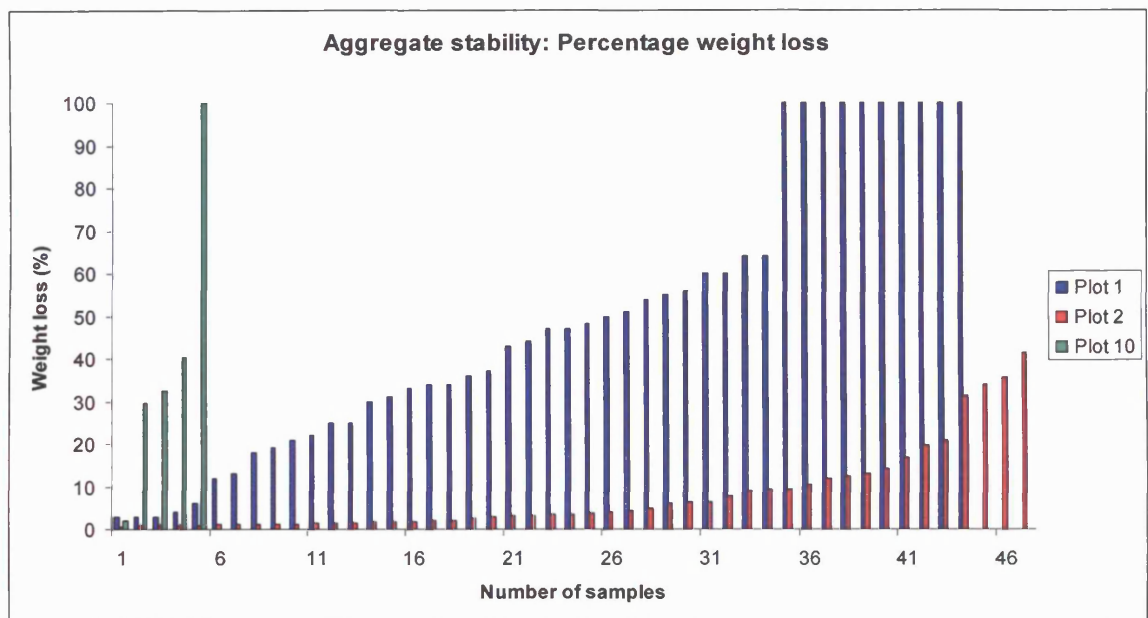


**Figure 4.19** The number of aggregates obtained from plots 1, 2 and 10 and the percentage weight loss after agitation in water.

#### 4.7.2 Summary

Using aggregate stability as an indicator of the erodibility of the soil, the results suggest that the pure grassland plot in the Karoo (plot 2) is the most stable. This plot has both the greatest quantity of aggregates and the most stable aggregates. In contrast plot 10, situated in the Sevilleita NWR, reveals a soil with a weak structure. Very few aggregates were obtained and those which were measured were found to be highly unstable.

Unfortunately these results cannot be compared to those derived from different studies due to inconsistencies in sampling methods.

## 4.8 pH

### 4.8.1 Results

#### a) Descriptive statistics, descriptive statistics and inter-plot variation

No characteristic population distribution is evident for soil pH (figure 4.20). Plot 1 can be classed as a normal distribution, plot 2 is positively skewed and plots 8 and 10 are negatively skewed. Although by taking an average of three soil pH readings it is hoped that measurement error is reduced, a number of extreme values are evident. The distribution of plot 10 in particular is strongly influenced by such values.

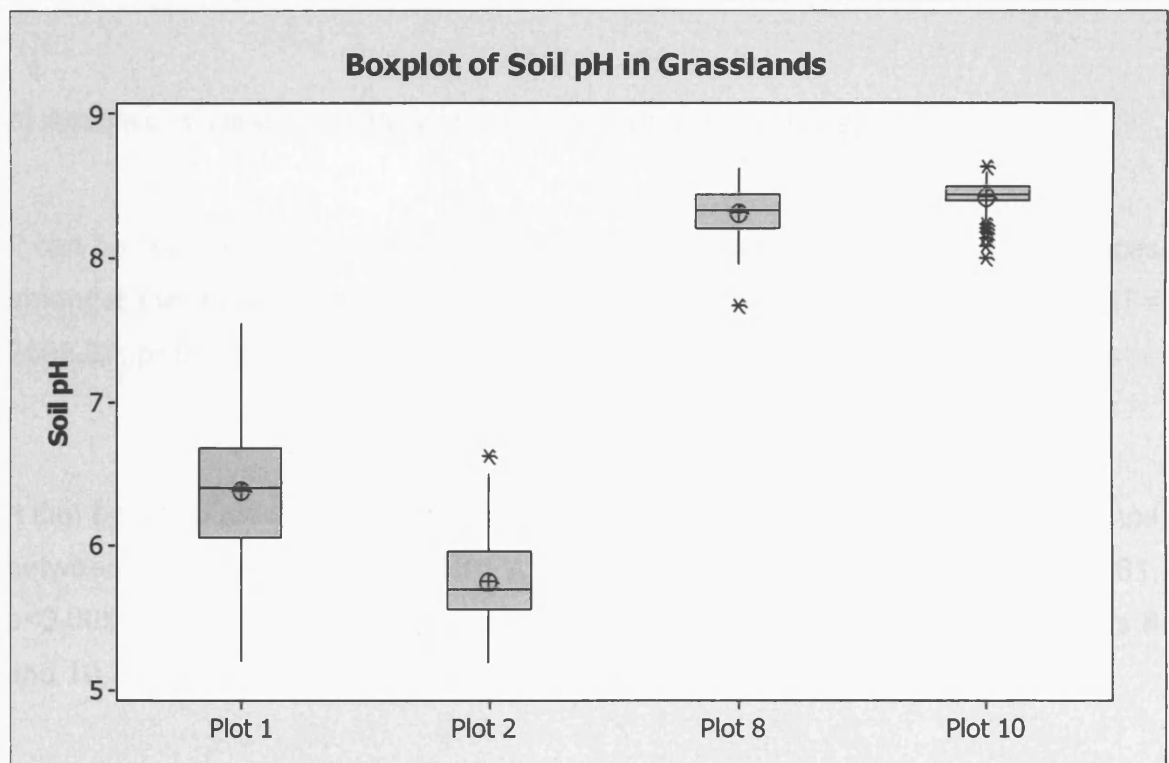


Figure 4.20 Boxplots representing the sample distribution of soil pH in the grassland plots.

The descriptive statistics show a difference between the pH values from the Karoo sites and the sites from the Sevilleta NWR. Table 4.11 shows that the soils from the Karoo are acidic (< pH7) whereas the soils from the Sevilleta NWR are alkali (>pH7). The coefficient of variance and range values show that pH values within plots 8 and 10 fluctuate significantly less than plots 1 and 2.

**Table 4.11** Inter-plot comparisons of descriptive statistics: Soil pH

Descriptive Statistic	Plot 1 (Mixed)	Plot 2 (Grassland)	Plot 8 (Grassland)	Plot 10 (Grassland)
Mean	6.40	5.76	8.32	8.44
Median	6.41	5.70	8.34	8.45
SE of Mean	0.04	0.03	0.02	0.01
St Dev	0.44	0.29	0.17	0.10
Variance	0.19	0.08	0.03	0.01
Coef Var	6.90	5.04	2.00	1.17
Minimum	5.20	5.20	7.68	8.01
Maximum	7.56	6.63	8.62	8.64
Range	2.35	1.43	0.95	0.63
IQR	0.62	0.40	0.23	0.09
Skewness	-0.09	0.62	-0.88	-1.61
Kurtosis	-0.04	0.12	1.06	4.45

*b) Analysis of variance (ANOVA) tests and two-sample T-tests*

It can be concluded from the ANOVA analysis that there are significant differences amongst the means of the organic matter content from plots 1, 2, 8 and 10. ( $F=2509.27$ ,  $p<0.005$ ).

It can be concluded from the two-sample t-test that there is a significant difference between the means of plots 1 and 2, the two plots located in the Karoo ( $t=12.61$ ,  $p<0.005$ ). Similarly, there is a significant difference between the means of plots 8 and 10, the two plots located in the Sevilleta NWR ( $t=-6.45$ ,  $p<0.005$ ).

*c) Intra-plot variation*

The plots do not demonstrate any significant characteristics in their cell by cell variability across the three scales of measurement (see figure 4.21). In all cases the measurements taken in the smallest quadrats show a similar spread of data to those taken from the largest quadrats. Where the variation is great this would suggest that soil pH may display a 'checkerboard' pattern across the 60 x 60m plots i.e. plots 1, 2 and 8. Where the variation is small this would suggest that no spatial patterns exist i.e. plot 10.

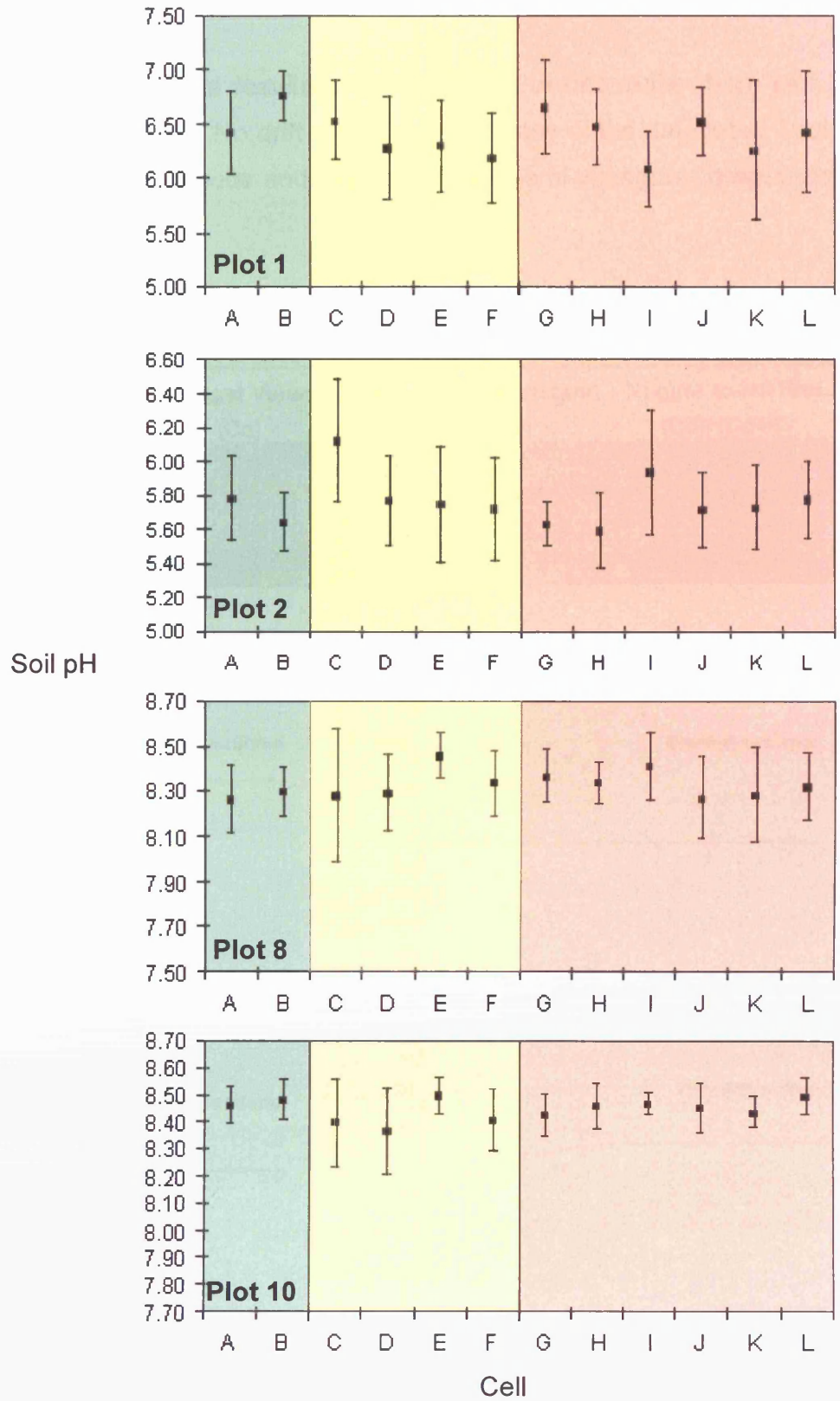


**Figure 4.21** The means and standard deviations of soil pH for each cell within the plots. Green represents the 30 x 30m cells, yellow represents the 10 x 10m cells and pink represents 1.5 x 1.5m cells.

d) Geostatistical analysis: The semi-variogram

Pre-processing of the datasets resulted in the removal of one outlier from plot 8 and two outliers from plot 10. No drift was identified in any of the datasets. Table 4.12 shows the numerical results and the associated semi-variogram graphs are presented in figure 4.22.

Table 4.12 Geostatistical analysis of the soil pH of grassland plots

Parameter: pH						
Plot No.	Veg Type	Fitted Model	Nugget Value	Sill	Range (meters)	Nugget-to-sill Ratio
			(Co)	(Co+C <sub>1</sub> )	(a)	(Co)/(Co+C <sub>1</sub> )
1	Mixed	Nugget	1.00	na	na	na
2	Grassland	Nugget	1.00	na	na	na
8	Grassland	Nugget	1.00	na	na	na
10	Grassland	Spherical	0.80	0.30	16.56	0.73

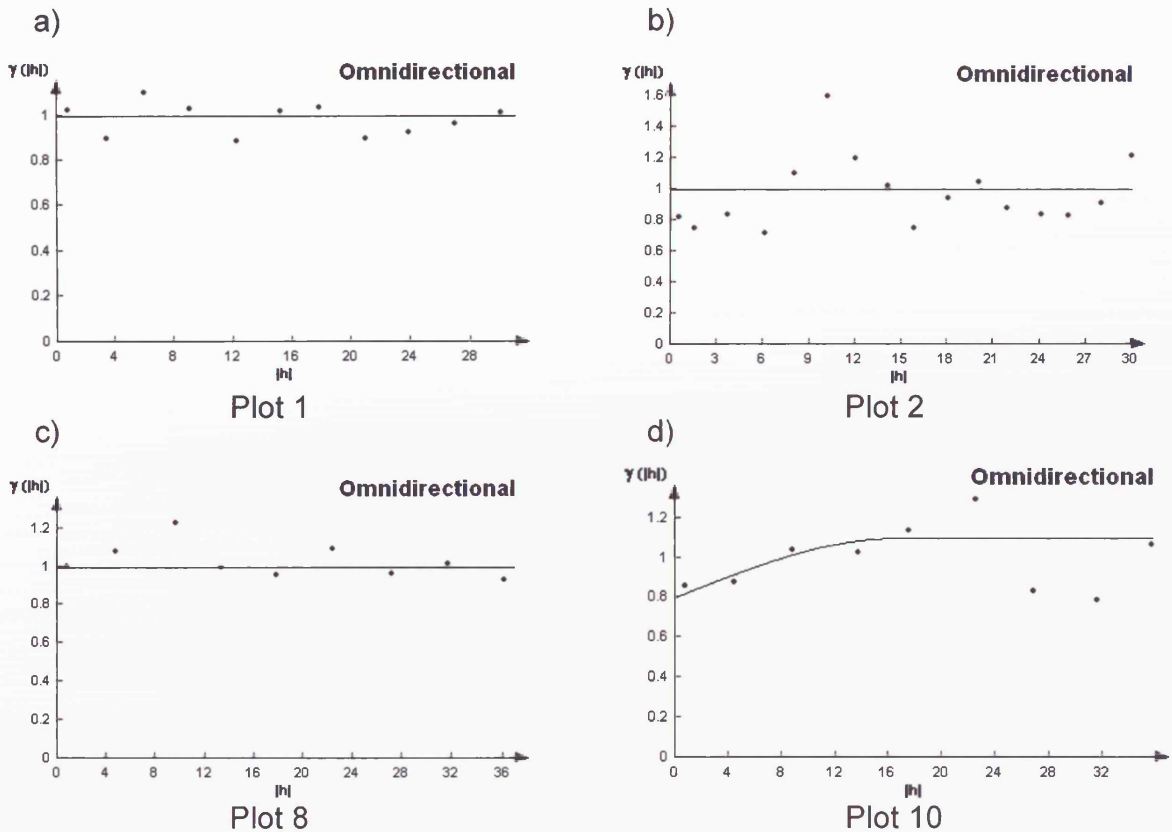


Figure 4.22 Modelled semi-variograms for the pH of grassland plots.

The results are as follows:

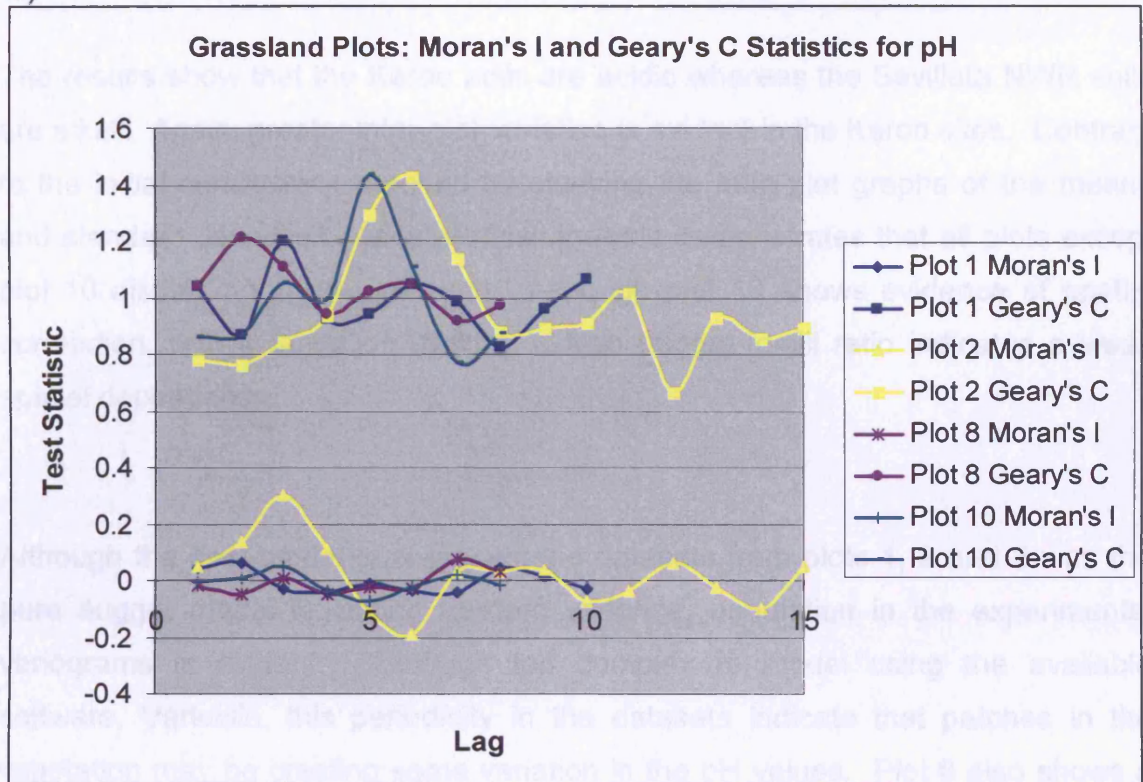
- i) Only plot 10 demonstrates spatial autocorrelation of soil pH with a range of 16.56m.
- ii) Plots 1, 2 and 8 were best represented by a 'pure nugget' model suggesting no spatial patterns exist for soil pH.
- iii) This suggests that pH can generally be considered as homogenous across grasslands at the scales of measurement used in this study.
- iv) A nugget-to-sill ratio of 0.73 suggests that moderate to weak spatial dependency describes the results derived for plot 10.
- v) Using simple models plots 1, 2 and 8 have been best described as displaying no spatial pattern. However, by studying the semi-variograms all three show some evidence of periodicity and plot 8 also shows a slight decrease in variance with increasing lag distance. This suggests that some spatial pattern may exist, perhaps varying scales of the 'checkerboard' pattern.

*e) Geostatistical analysis: Moran's I and Geary's C statistics*

The results are as follows:

- i) The undulating nature of the semi-variograms are mirrored in the correlograms.
- ii) The results of plots 1 and 10 are considered to be relatively comparable to the interpretations made from the semi-variograms.
- iii) Both the Geary's C and Moran's I correlograms show that clustering occurs with an increase in lag distance in plot 8 thus backing up the suggestion that a 'checkerboard' pattern may exist.
- iv) The results for plot 2 suggest that clustering occurs across most lag distances indicating no particular spatial pattern, however, between lag distances of approximately 8m and 12m large differences among the values exist. This is also reflected in the semi-variogram. This peak may also indicate the influence of 'patches' in the plot.

a)



b)

Lag increment codes	Plot 1	Plot 2	Plot 8 & 10
1	0 > to ≤ 3	0 > to ≤ 2	0 > to ≤ 4.5
2	3 > to ≤ 6	2 > to ≤ 4	4.5 > to ≤ 9
3	6 > to ≤ 9	4 > to ≤ 6	9 > to ≤ 13.5
4	9 > to ≤ 12	6 > to ≤ 8	13.5 > to ≤ 18
5	12 > to ≤ 15	8 > to ≤ 10	18 > to ≤ 22.5
6	15 > to ≤ 18	10 > to ≤ 12	22.5 > to ≤ 27
7	18 > to ≤ 21	12 > to ≤ 14	27 > to ≤ 31.5
8	21 > to ≤ 24	14 > to ≤ 16	31.5 > to ≤ 36
9	24 > to ≤ 27	16 > to ≤ 18	
10	27 > to ≤ 30	18 > to ≤ 20	
11		20 > to ≤ 22	
12		22 > to ≤ 24	
13		24 > to ≤ 26	
14		26 > to ≤ 28	
15		28 > to ≤ 30	

**Figure 4.23** a) Moran's I and Geary's C correlograms for the soil pH of the grassland plots. b) provides the key to the lag increments used in the correlograms for each plot.

### **4.8.2 Summary**

The results show that the Karoo soils are acidic whereas the Sevilleta NWR soils are alkali. Again, greater inter-plot variation is evident in the Karoo sites. Contrary to the initial conclusions reached by studying the intra-plot graphs of the means and standard deviations, geostatistical analysis demonstrates that all plots except plot 10 display no spatial patterns. Although plot 10 shows evidence of spatial correlation, with a range of 16.58m, a high nugget-to-sill ratio indicates a weak spatial dependency.

Although the best model to represent the datasets from plots 1, 2 and 8 was the pure nugget model indicating random variance, undulation in the experimental variograms is evident. Although too complex to model using the available software, Variowin, this periodicity in the datasets indicate that patches in the vegetation may be creating some variation in the pH values. Plot 8 also shows a slight decrease in variance with increasing lag distance. This suggests that the soil pH may be displaying evidence of a 'checkerboard' pattern.

## **4.9 Electrical conductivity**

### **4.9.1 Results**

#### *a) Test of normality, descriptive statistics and inter-plot variation*

The frequency distributions displayed by the boxplots (figure 4.24) show that the datasets from all plots display varying degrees of positively skewed distributions. However, the skew of plot 10 is weak and can therefore be classed as having a normal distribution. Extreme values are only evident at the upper region of the scale.

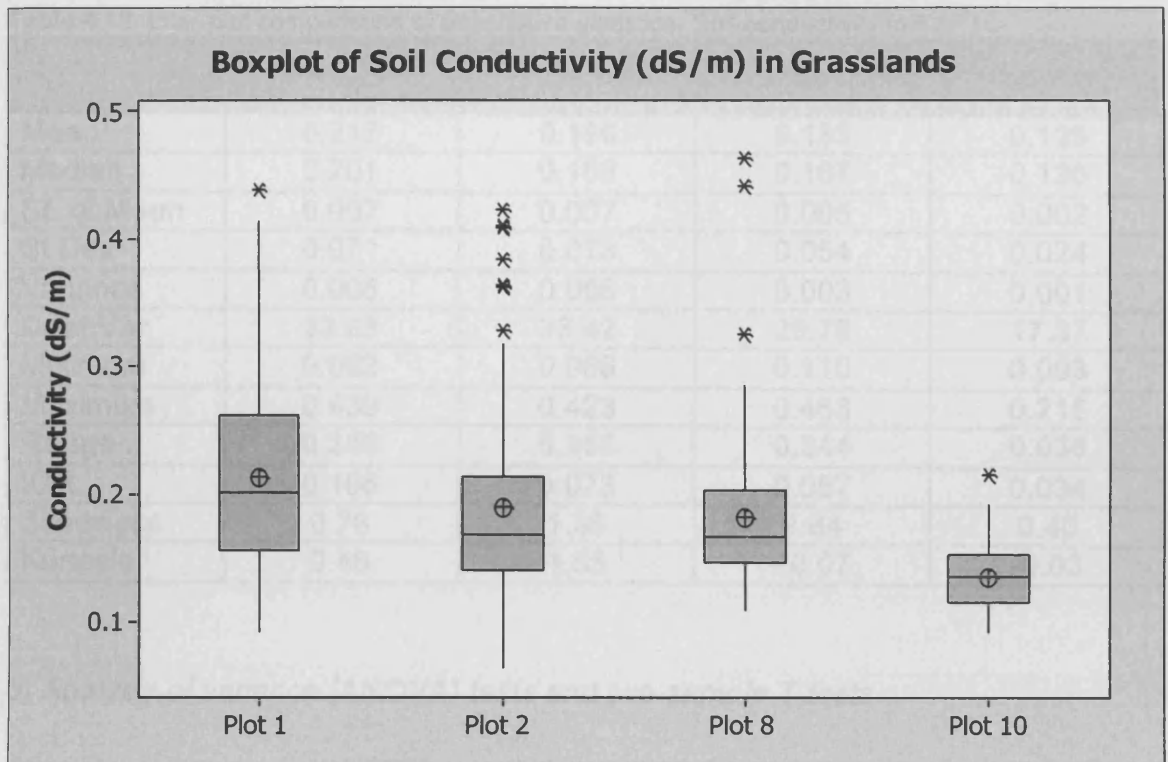


**Figure 4.24** Boxplots representing the sample distribution of soil conductivity in the grassland plots.

Inter-plot comparisons (table 4.13) show that the mean conductivity values of plots 1 and 2 are greater than plots 8 and 10, albeit by a small amount. The data from plot 10 appears to vary the least, evident from the coefficient of variance and range values whereas the three other plots appear to have relatively similar sample population distributions.

**Table 4.13** Inter-plot comparisons of descriptive statistics: Soil conductivity (dS m<sup>-1</sup>)

Descriptive Statistic	Plot 1 (Mixed)	Plot 2 (Grassland)	Plot 8 (Grassland)	Plot 10 (Grassland)
<b>Mean</b>	<b>0.213</b>	<b>0.190</b>	<b>0.183</b>	<b>0.136</b>
Median	0.201	0.168	0.167	0.136
SE of Mean	0.007	0.007	0.005	0.002
St Dev	0.071	0.073	0.054	0.024
Variance	0.005	0.005	0.003	0.001
<b>Coef Var</b>	<b>33.63</b>	<b>38.42</b>	<b>29.78</b>	<b>17.37</b>
Minimum	0.092	0.066	0.110	0.093
Maximum	0.439	0.423	0.463	0.215
<b>Range</b>	<b>0.346</b>	<b>0.358</b>	<b>0.344</b>	<b>0.036</b>
IQR	0.106	0.073	0.057	0.034
Skewness	0.78	1.35	2.64	0.40
Kurtosis	0.46	1.55	10.07	-0.03

*b) Analysis of variance (ANOVA) tests and two-sample T-tests*

It can be concluded from the ANOVA analysis that there are significant differences amongst the means of the organic matter content from plots 1, 2, 8 and 10. ( $F=31.72$ ,  $p<0.005$ ).

It can be concluded from the two-sample t-test that there is a significant difference between the means of plots 1 and 2, the two plots located in the Karoo ( $t=2.34$ ,  $p=0.021$ ). Similarly, there is a significant difference between the means of plots 8 and 10, the two plots located in the Sevilleta NWR ( $t=5.58$ ,  $p<0.005$ ).

*c) Intra-plot variation*

As seen in figure 4.25, the graph of plot 1 shows that the measurements taken in the smallest quadrats display a similar amount of variation in data to those taken from the largest quadrats. This would suggest that the soil conductivity distribution is relatively uniform. Plot 2 shows evidence of a fluctuating mean across the cells as well as high and low levels of variation within cells of the same scale. This may indicate the presence of patches, a larger scale checkerboard pattern. Apart from

cell H in plot 8, both plots 8 and 10 do not show much fluctuation in the means or the standard deviations across the cells. This suggests that the conductivity of these plots will probably not display any spatial patterns.

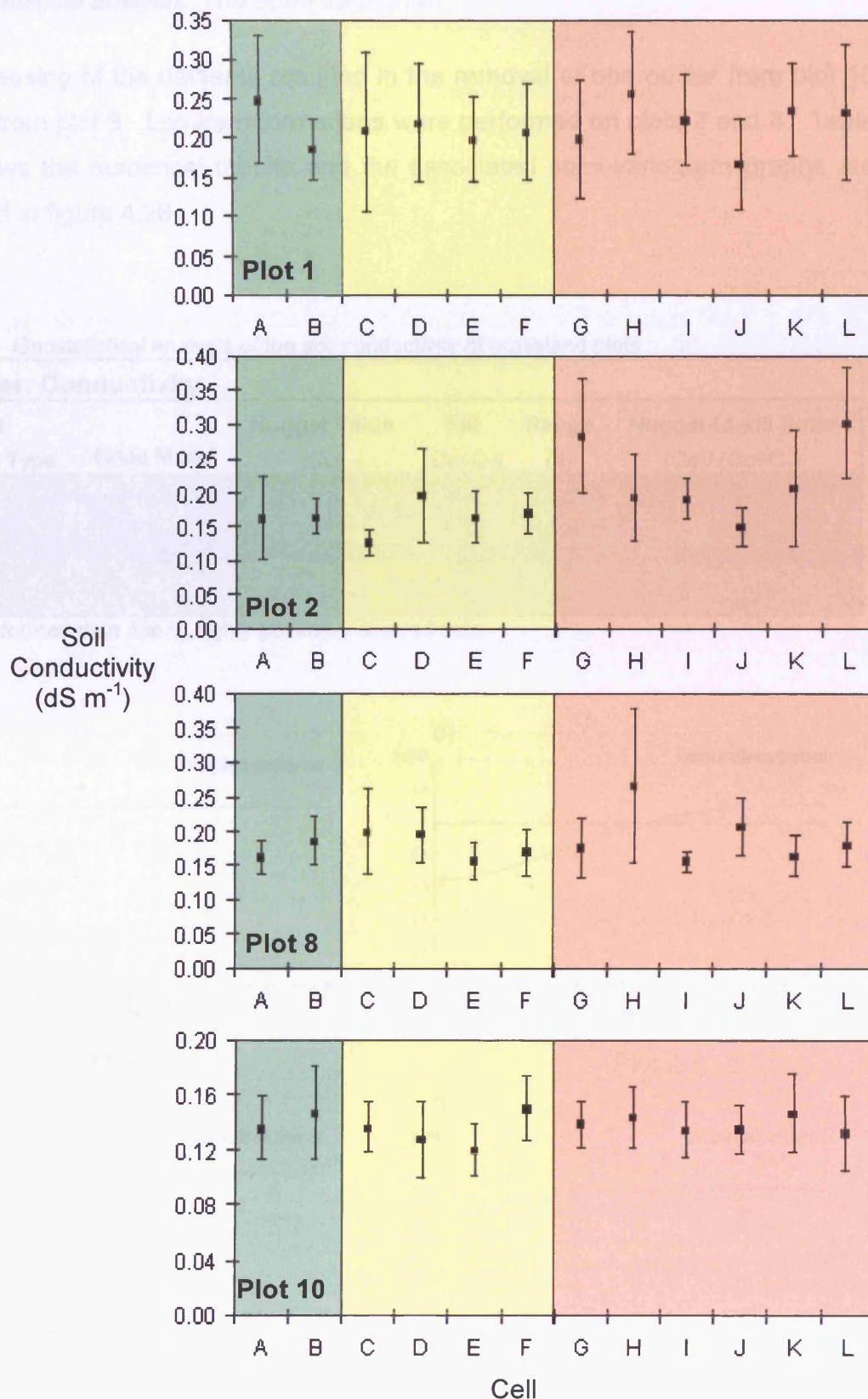


**Figure 4.25** The means and standard deviations of soil conductivity for each cell within the plots. Green represents the 30 x 30m cells, yellow represents the 10 x 10m cells and pink represents 1.5 x 1.5m cells.

d) Geostatistical analysis: The semi-variogram

Pre-processing of the datasets resulted in the removal of one outlier from plot 10 and two from plot 8. Log transformations were performed on plots 2 and 8. Table 4.14 shows the numerical results and the associated semi-variogram graphs are presented in figure 4.26.

**Table 4.14** Geostatistical analysis of the soil conductivity of grassland plots

Parameter: Conductivity						
Plot No.	Veg Type	Fitted Model	Nugget Value (Co)	Sill (Co+C <sub>1</sub> )	Range (a)	Nugget-to-sill Ratio (Co)/(Co+C <sub>1</sub> )
1	Mixed	Nugget	1.00	na	na	na
2	Grassland*	Gaussian	0.65	1.18	19.47	0.55
8	Grassland*	Nugget	1.00	na	na	na
10	Grassland	Nugget	1.00	na	na	na

\* Log transformed data due to highly positively skewed data

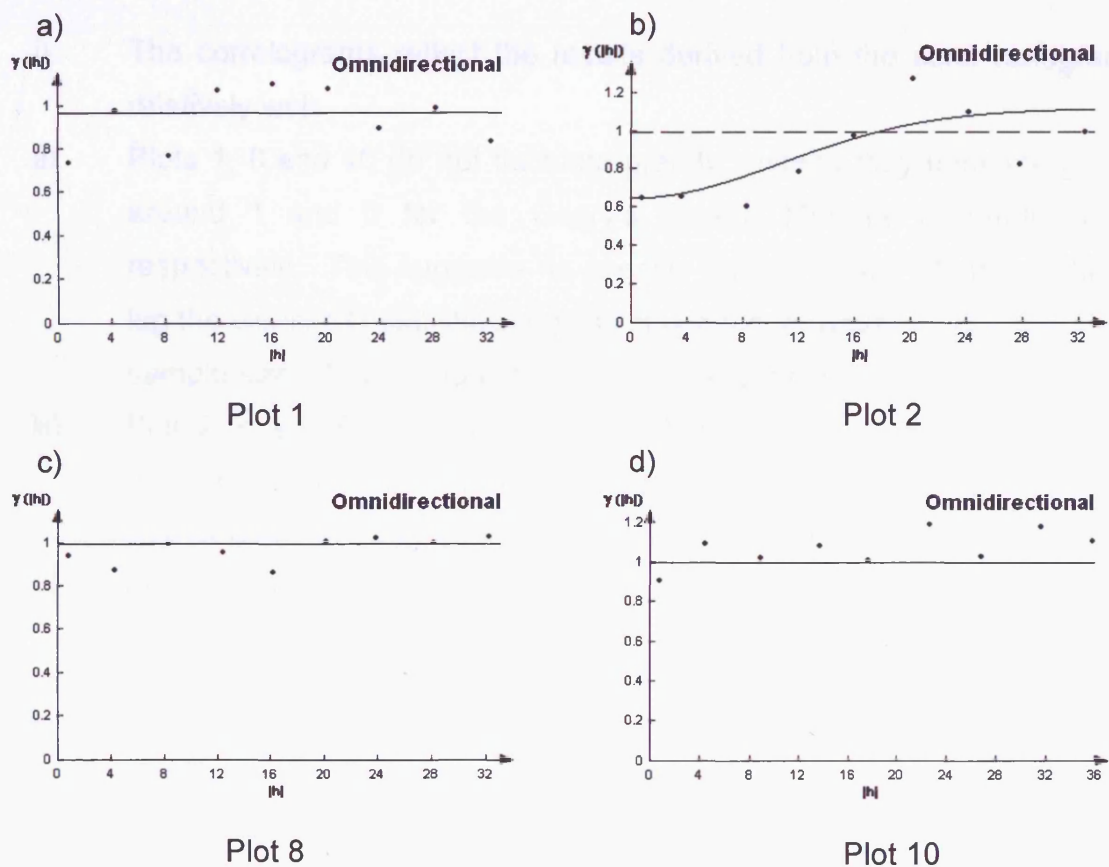


**Figure 4.26** Modelled semi-variograms for the conductivity of grassland plots.

The results are as follows:

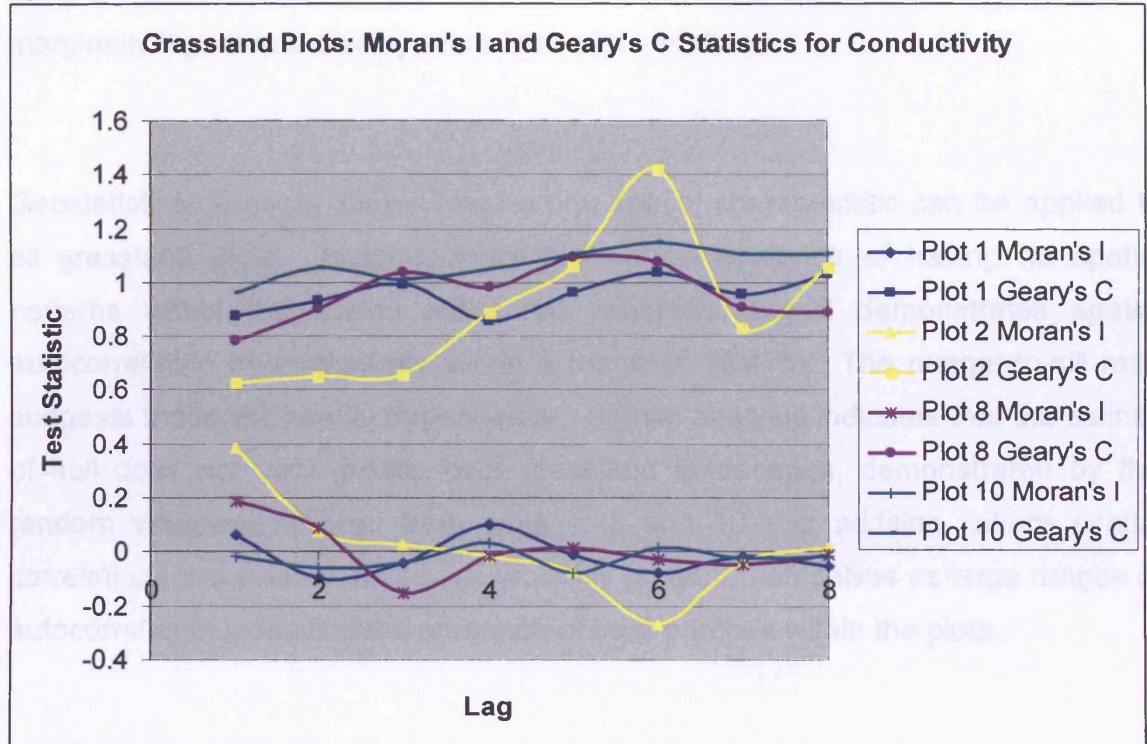
- i) Only plot 2 demonstrates spatial autocorrelation of soil conductivity with a range of 19.47m.
- ii) A nugget-to-sill ratio of 0.55 suggests that moderate spatial dependency describes the results derived for plot 2.
- iii) Plots 1, 8 and 10 were best represented by a 'pure nugget' model suggesting no spatial patterns are evident for soil conductivity.
- iv) This suggests that, in general, conductivity can be considered as homogenous across grasslands at the scales of measurement used in this study.

*e) Geostatistical analysis: Moran's I and Geary's C statistics*

The results are as follows: (see figure 4.27)

- i) The correlograms reflect the results derived from the semi-variograms relatively well.
- ii) Plots 1, 8 and 10 do not fluctuate greatly, instead they undulate gently around 1 and 0 for the Geary's C and Moran's I correlograms, respectively. This suggests no specific pattern exists. At the smallest lag the Geary's C statistic suggests clustering, however, due to the small sample size interpretation of this should be done with caution.
- iii) Plot 2 is significantly different from the other plots, clustering is the predominant pattern across the different lag distances. The range of spatial autocorrelation derived from the semi-variogram coincides with the peak in the Geary's C correlogram.

a)



b)

Lag increment codes	Plot 1, 2 & 8	Plot 10
1	0 > to <= 4	0 > to <= 4.5
2	4 > to <= 8	4.5 > to <= 9
3	8 > to <= 12	9 > to <= 13.5
4	12 > to <= 16	13.5 > to <= 18
5	16 > to <= 20	18 > to <= 22.5
6	20 > to <= 24	22.5 > to <= 27
7	24 > to <= 28	27 > to <= 31.5
8	28 > to <= 32	31.5 > to <= 36

**Figure 4.27** a) Moran's I and Geary's C correlograms for the soil conductivity of the grassland plots. b) provides the key to the lag increments used in the correlograms for each plot.

## 4.9.2 Summary

Different methods of measuring conductivity are available making comparisons amongst studies difficult. However, according to the Soil and Plant Analysis

Council Inc.,1999 (2000) the results derived from all plots in this study can be classed as 'non-saline'. The mean values of conductivity from all the plots are relatively similar although the mean values from the Karoo plots (1 and 2) are marginally higher and display more intra-plot variation.

Geostatistical analysis shows that no one spatial characteristic can be applied to all grassland plots. Instead, three plots show evidence of having no spatial patterns within the scales measured, whereas plot 2 demonstrates spatial autocorrelation of conductivity within a range of 19.47m. The nugget-to-sill ratio suggests moderate spatial dependency. Spatial analysis indicates that the salinity of soil does not vary greatly over grassland landscapes, demonstrated by the random variances derived from plots 1, 8 and 10. In addition, where spatial correlations are evident, these will probably present themselves as large ranges of autocorrelation indicating the presence of bare patches within the plots.

#### ***4.10 Nutrient content analysis***

The nutrient status of the soil was assessed by analysing the available phosphorus content and the following cations; calcium, sodium, magnesium and potassium (in ppm of soil). Refer to chapter 3 for the extraction technique and methodology. Due to some obvious anomalies in the output datasets, as a result of machine error, the results presented here have been filtered and some data points removed. Plots 2 and 10 were unaffected but sample size for plots 1 and 8 have been reduced to 106 and 105, respectively. The normality, descriptive statistics, inter-plot variation and geostatistical results will be presented for each nutrient, followed by an overall discussion at the end of the section.

#### 4.10.1 Results:

##### Calcium

##### a) Test of normality, descriptive statistics and inter-plot variation

The boxplots in figure 4.28 show that plot 1 displays a highly positively skewed distribution, the data from plot 2 follows a slightly positively skewed distribution and plots 8 and 10 are both negatively skewed. Outliers are evident in all datasets except plot 2. These are evident at the upper end of the scale for plot 1 and the lower end of the scale for plots 8 and 10.

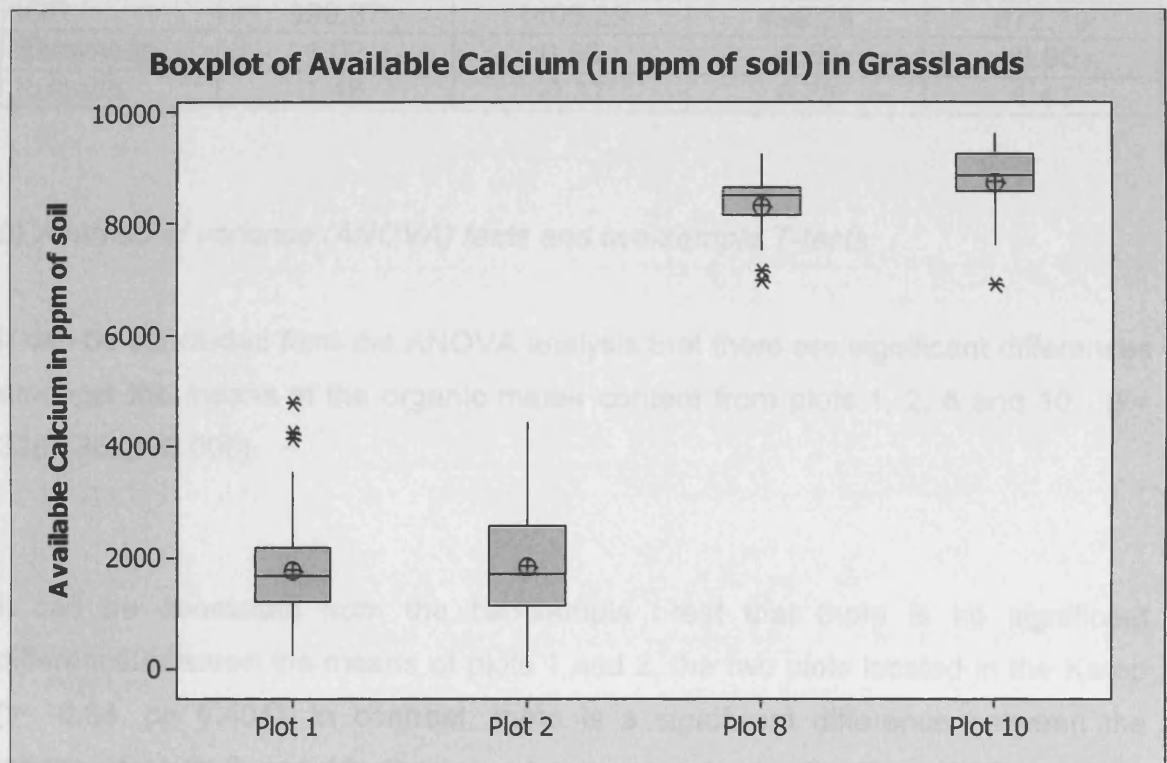


**Figure 4.28** Boxplots representing the sample distribution of available calcium in the grassland plots.

Inter-plot analysis (table 4.15) shows that there is a significant difference in the available calcium content between the sites in the Karoo, South Africa and the sites in the Sevilleta NWR, New Mexico. Available calcium is significantly higher in

the Sevilleta NWR. The ranges of values within these plots are also lower than the sites situated in the Karoo.

**Table 4.15** Inter-plot comparisons of descriptive statistics: Available calcium in ppm of soil

Descriptive Statistic	Plot 1 (Mixed)	Plot 2 (Grassland)	Plot 8 (Grassland)	Plot 10 (Grassland)
<b>Mean</b>	<b>1767.23</b>	<b>1869.28</b>	<b>8420.68</b>	<b>8856.71</b>
Median	1668.03	1715.51	8505.21	8887.63
SE of Mean	83.73	88.71	42.13	46.75
St Dev	862.08	921.92	431.71	485.81
Variance	743174	849936	186374	236010
<b>Coef Var</b>	<b>48.55</b>	<b>49.32</b>	<b>10.58</b>	<b>5.49</b>
Minimum	229.28	33.21	6999.51	6924.47
Maximum	4767.11	4421.62	9253.39	9606.20
<b>Range</b>	<b>4537.83</b>	<b>4388.41</b>	<b>2253.88</b>	<b>2681.73</b>
IQR	990.37	1405.29	499.26	672.79
Skewness	1.02	0.56	-0.65	-0.90
Kurtosis	1.46	-0.37	0.73	1.43

*b) Analysis of variance (ANOVA) tests and two-sample T-tests*

It can be concluded from the ANOVA analysis that there are significant differences amongst the means of the organic matter content from plots 1, 2, 8 and 10. ( $F=3287.35$ ,  $p<0.005$ ).

It can be concluded from the two-sample t-test that there is no significant difference between the means of plots 1 and 2, the two plots located in the Karoo ( $t= -0.84$ ,  $p= 0.404$ ). In contrast, there is a significant difference between the means of plots 8 and 10, the two plots located in the Sevilleta NWR ( $t=-6.93$ ,  $p<0.005$ ).

*c) Geostatistical analysis: The semi-variogram*

The distribution of plot 1 was identified as being highly positively skewed thus the dataset was transformed using a log transformation, no other datasets were

transformed. Table 4.16 shows the numerical results and the associated semi-variogram graphs are presented in figure 4.29.

**Table 4.16** Geostatistical analysis of the available calcium of grassland plots

Parameter: Calcium							
No.	Plot	Veg Type	Fitted Model	Nugget Value	Sill	Range	
				(Co)	(Co+C <sub>1</sub> )	(a)	Nugget-to-sill Ratio (Co)/(Co+C <sub>1</sub> )
1	Mixed*		Nugget	1.00	na	na	na
2	Grassland		Spherical	0.47	0.94	10.50	0.50
8	Grassland		Nugget	1.00	na	na	na
10	Grassland		Spherical	0.50	1.26	19.84	0.40

\*Log transformed data due to highly positively skewed data

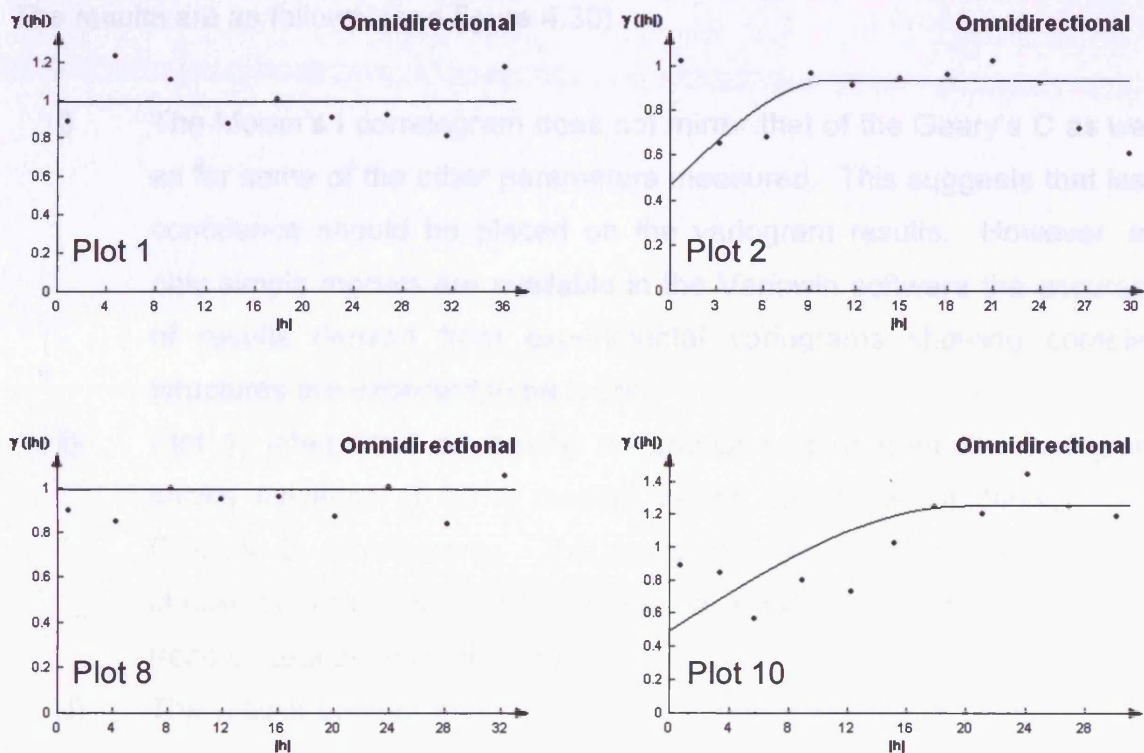


**Figure 4.29** Modelled semi-variograms for the available calcium in grassland plots.

The results are as follows:

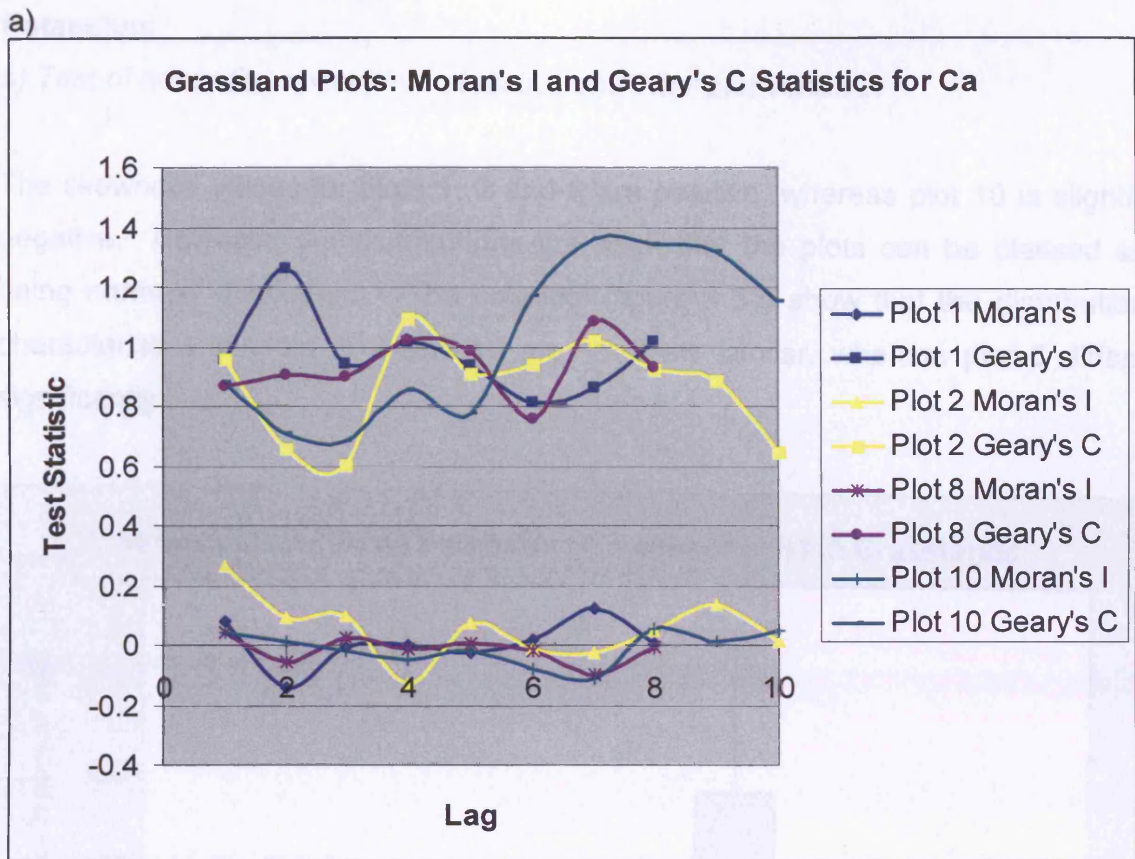
- i) Plots 1 and 8 are best represented by a 'pure nugget' model. This suggests that the distribution of available calcium does not follow any spatial patterns.

- ii) Plots 2 and 10, both modelled by a spherical model, show evidence of spatial autocorrelation. The ranges of autocorrelation are 10.50m and 19.84m respectively.
- iii) The nugget-to-sill ratios indicate that the available calcium in both plots show moderate levels of spatial dependency.
- iv) The experimental data of plots 2 and 10 exhibit evidence of 'hole effects' suggesting that large patches may be found within the plots.

*d) Geostatistical analysis: Moran's I and Geary's C statistics*

The results are as follows: (see figure 4.30)

- i) The Moran's I correlogram does not mirror that of the Geary's C as well as for some of the other parameters measured. This suggests that less confidence should be placed on the variogram results. However, as only simple models are available in the Variowin software the accuracy of results derived from experimental variograms showing complex structures are expected to be lower.
- ii) Plot 1, interpreted as having no spatial pattern from the variogram shows evidence of some random values and some clustering in the Geary's C correlogram. This suggests that calcium may follow a checkerboard pattern; this may also be evident in the slight downward trend of data points in the variogram.
- iii) The results derived from the Geary's C correlograms for plots 2, 8 and 10 seem to be consistent with those derived from the variograms.



b)

Lag increment codes	Plot 1	Plot 2 & 10	Plot 8
1	0 > to ≤ 4.5	0 > to ≤ 3	0 > to ≤ 4
2	4.5 > to ≤ 9	3 > to ≤ 6	4 > to ≤ 8
3	9 > to ≤ 13.5	6 > to ≤ 9	8 > to ≤ 12
4	13.5 > to ≤ 18	9 > to ≤ 12	12 > to ≤ 16
5	18 > to ≤ 22.5	12 > to ≤ 15	16 > to ≤ 20
6	22.5 > to ≤ 27	15 > to ≤ 18	20 > to ≤ 24
7	27 > to ≤ 31.5	18 > to ≤ 21	24 > to ≤ 28
8	31.5 > to ≤ 36	21 > to ≤ 24	28 > to ≤ 32
9		24 > to ≤ 27	
10		27 > to ≤ 30	

**Figure 4.30** a) Moran's I and Geary's C correlograms for the available calcium in the grassland plots. b) provides the key to the lag increments used in the correlograms for each plot.

## Potassium

### a) Test of normality, descriptive statistics and inter-plot variation

The skewness values for plots 1, 2 and 8 are positive, whereas plot 10 is slightly negative. However, the distributions are such that the plots can be classed as being normally distributed. The boxplots (figure 4.31) show that the distribution characteristics of plots 1, 2 and 10 are relatively similar, whereas plot 8 differs significantly.

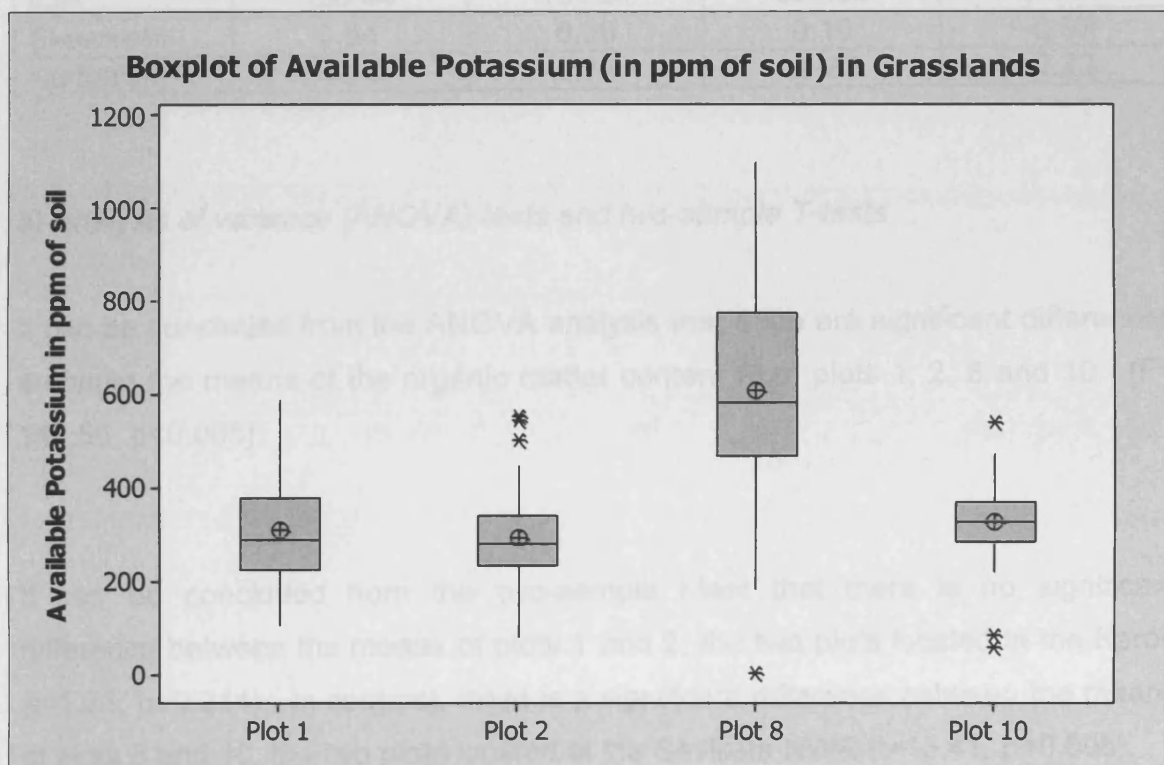


**Figure 4.31** Boxplots representing the sample distribution of available potassium in the grassland plots.

The mean of plot 8 can be seen to be approximately double those found in plots 1, 2 and 10 (table 4.17). The range of values in plot 8 is also significantly greater than the other three plots. Even if the lowest value, potentially an error, is removed this plot displays very different distribution characteristics to the other grassland plots.

**Table 4.17** Inter-plot comparisons of descriptive statistics: Available potassium in ppm of soil

Descriptive Statistic	Plot 1 (Mixed)	Plot 2 (Grassland)	Plot 8 (Grassland)	Plot 10 (Grassland)
<b>Mean</b>	<b>310.91</b>	<b>293.92</b>	<b>613.87</b>	<b>331.51</b>
Median	291.16	281.20	583.16	328.78
SE of Mean	11.00	8.07	20.23	5.83
St Dev	113.26	83.89	207.33	60.56
Variance	12827.4	7037.61	42987.20	3667.49
<b>Coef Var</b>	<b>36.26</b>	<b>28.54</b>	<b>34.27</b>	<b>18.27</b>
Minimum	104.33	80.80	5.72	84.66
Maximum	585.31	551.58	1097.78	541.48
<b>Range</b>	<b>480.98</b>	<b>470.78</b>	<b>1092.06</b>	<b>456.82</b>
IQR	156.44	104.51	304.35	80.45
Skewness	0.54	0.56	0.10	-0.07
Kurtosis	-0.29	0.72	-0.23	-0.23

*b) Analysis of variance (ANOVA) tests and two-sample T-tests*

It can be concluded from the ANOVA analysis that there are significant differences amongst the means of the organic matter content from plots 1, 2, 8 and 10. ( $F=147.55$ ,  $p<0.005$ ).

It can be concluded from the two-sample t-test that there is no significant difference between the means of plots 1 and 2, the two plots located in the Karoo ( $t=1.25$ ,  $p=0.214$ ). In contrast, there is a significant difference between the means of plots 8 and 10, the two plots located in the Sevilleta NWR ( $t=13.41$ ,  $p<0.005$ ).

*c) Geostatistical analysis: The semi-variogram*

No outliers were removed from any of the plots and no transformations were performed before geostatistical analysis was carried out. Table 4.18 shows the numerical results and the associated semi-variogram graphs are presented in figure 4.32.

Table 4.18 Geostatistical analysis of the available potassium in grassland plots

Parameter: Potassium						
Plot No.	Veg Type	Fitted Model	Nugget Value (Co)	Sill (Co+C <sub>1</sub> )	Range (a)	Nugget-to-sill Ratio (Co)/(Co+C <sub>1</sub> )
1	Mixed	Nugget	1.00	na	na	na
2	Grassland	Nugget	1.00	na	na	na
8	Grassland	Spherical	0.44	0.62	12.58	0.42
10	Grassland	Spherical	0.50	0.47	16.74	0.52

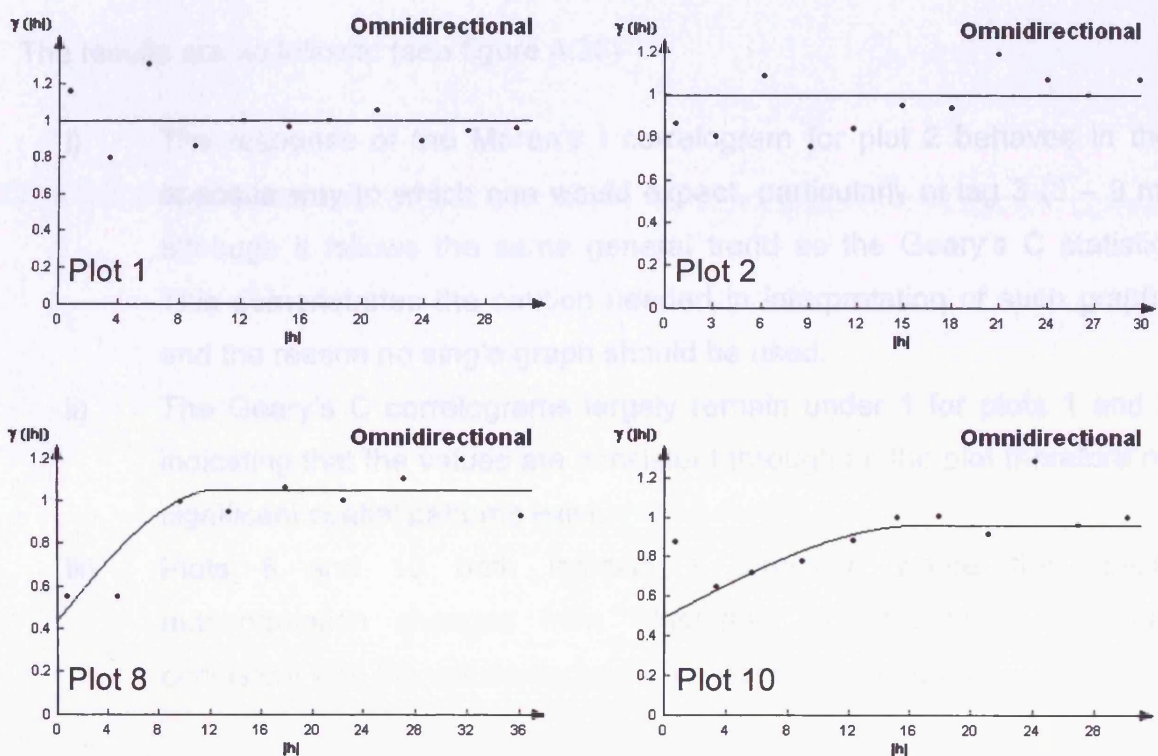


Figure 4.32 Modelled semi-variograms for the available potassium in grassland plots.

The results are as follows:

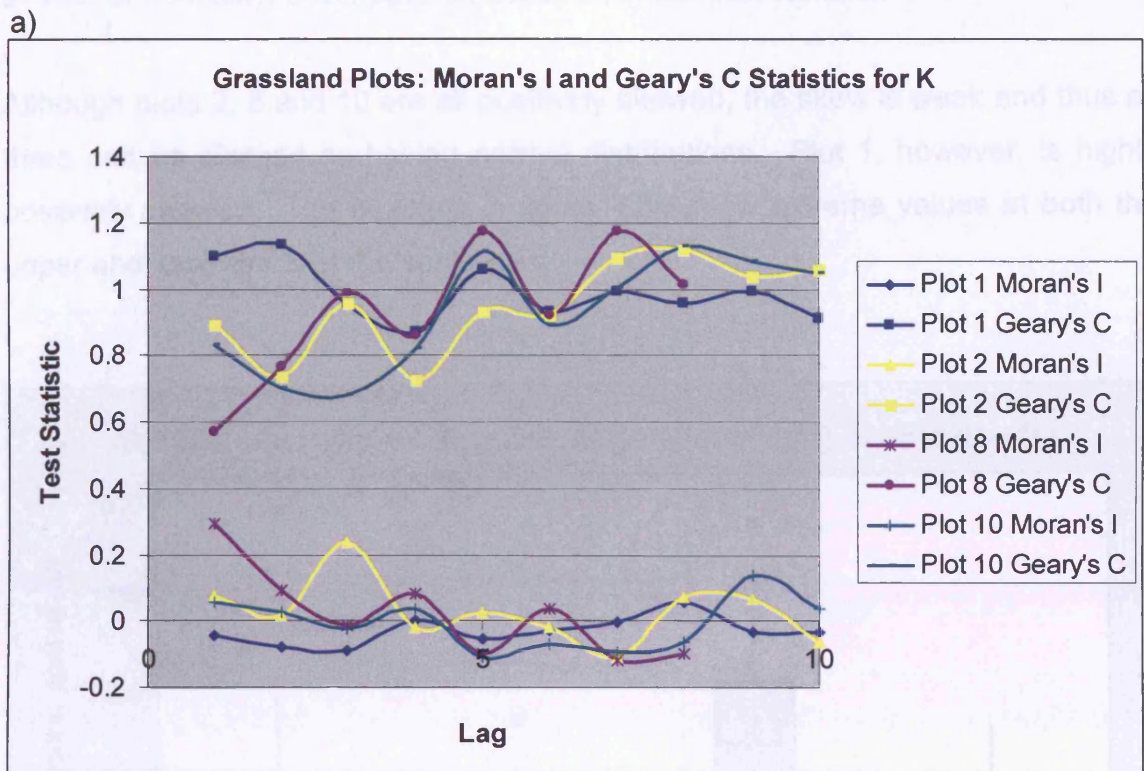
- i) Plots 1 and 2 are best represented by a 'pure nugget' model. This suggests that the distribution of available potassium does not follow any spatial patterns.

- ii) Plots 8 and 10, both modelled by a spherical model, show evidence of spatial autocorrelation. The ranges of autocorrelation are 12.58m and 16.74m respectively.
- iii) The nugget-to-sill ratios indicate that the available potassium in both plots show moderate levels of spatial dependency.

*e) Geostatistical analysis: Moran's I and Geary's C statistics*

The results are as follows: (see figure 4.33)

- i) The response of the Moran's I correlogram for plot 2 behaves in the opposite way to which one would expect, particularly at lag 3 (8 – 9 m) although it follows the same general trend as the Geary's C statistic. This demonstrates the caution needed in interpretation of such graphs and the reason no single graph should be used.
- ii) The Geary's C correlograms largely remain under 1 for plots 1 and 2 indicating that the values are consistent throughout the plot therefore no significant spatial patterns exist.
- iii) Plots 8 and 10 both indicate a threshold where the spatial autocorrelation changes from 'clustering' to 'random'. Both are consistent with the values derived from the semi-variograms.



b)

Lag increment codes	Plot 1, 2 & 10	Plot 8
1	0 > to ≤ 3	0 > to ≤ 4.5
2	3 > to ≤ 6	4.5 > to ≤ 9
3	6 > to ≤ 9	9 > to ≤ 13.5
4	9 > to ≤ 12	13.5 > to ≤ 18
5	12 > to ≤ 15	18 > to ≤ 22.5
6	15 > to ≤ 18	22.5 > to ≤ 27
7	18 > to ≤ 21	27 > to ≤ 31.5
8	21 > to ≤ 24	31.5 > to ≤ 36
9	24 > to ≤ 27	
10	27 > to ≤ 30	

**Figure 4.33** a) Moran's I and Geary's C correlograms for the available potassium in the grassland plots. b) provides the key to the lag increments used in the correlograms for each plot.

## Magnesium

### a) Test of normality, descriptive statistics and inter-plot variation

Although plots 2, 8 and 10 are all positively skewed, the skew is weak and thus all three can be classed as having normal distributions. Plot 1, however, is highly positively skewed. The boxplots in figure 4.34 show extreme values at both the upper and lower ends of the scale exist.

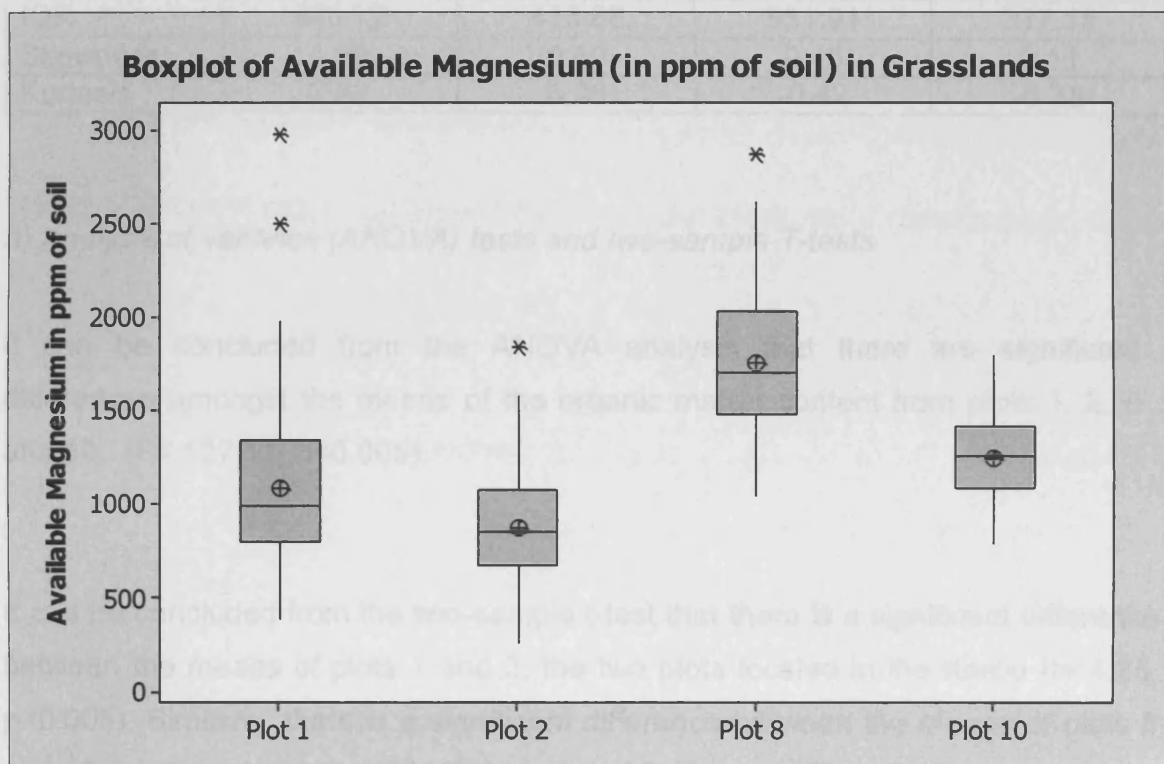


**Figure 4.34** Boxplots representing the sample distribution of available magnesium in the grassland plots.

The two plots from the Karoo have lower mean values of available magnesium than the Sevilleta NWR plots (table 4.19). However, the ranges of distributions vary across the two regions with plot 10 presenting the smallest variation in values and plot 1 presenting the greatest. Nevertheless, if the outliers are discounted the distributions of the four plots appear relatively similar.

**Table 4.19** Inter-plot comparisons of descriptive statistics: Available magnesium in ppm of soil

Descriptive Statistic	Plot 1 (Mixed)	Plot 2 (Grassland)	Plot 8 (Grassland)	Plot 10 (Grassland)
<b>Mean</b>	<b>1099.80</b>	<b>887.02</b>	<b>1768.50</b>	<b>1257.96</b>
Median	997.73	860.55	1701.46	1260.54
SE of Mean	42.14	27.12	38.89	20.73
St Dev	433.81	281.79	398.51	215.40
Variance	188189	79405.60	158806	46398.20
<b>Coef Var</b>	<b>39.26</b>	<b>31.77</b>	<b>23.71</b>	<b>17.12</b>
Minimum	386.19	267.77	1049.43	796.56
Maximum	2978.07	1843.61	2870.87	1795.89
<b>Range</b>	<b>2591.88</b>	<b>1575.84</b>	<b>1821.44</b>	<b>999.33</b>
IQR	540.72	415.68	551.91	317.15
Skewness	1.20	0.50	0.45	0.11
Kurtosis	2.82	0.36	-0.42	-0.38

*b) Analysis of variance (ANOVA) tests and two-sample T-tests*

It can be concluded from the ANOVA analysis that there are significant differences amongst the means of the organic matter content from plots 1, 2, 8 and 10. ( $F = 127.17$ ,  $p < 0.005$ ).

It can be concluded from the two-sample t-test that there is a significant difference between the means of plots 1 and 2, the two plots located in the Karoo ( $t = 4.25$ ,  $p < 0.005$ ). Similarly, there is a significant difference between the means of plots 8 and 10, the two plots located in the Sevilleta NWR ( $t = 11.58$ ,  $p < 0.005$ ).

*c) Geostatistical analysis: The semi-variogram*

No outliers were removed from any of the datasets. However, the data from plot 1 was log transformed. Table 4.20 shows the numerical results and the associated semi-variogram graphs are presented in figure 4.35.

Table 4.20 Geostatistical analysis of the available magnesium in grassland plots

Parameter: Magnesium						
Plot No.	Vegetation Type	Fitted Model	Nugget Value (Co)	Sill (Co+C <sub>1</sub> )	Range (a)	Nugget-to-sill Ratio (Co)/(Co+C <sub>1</sub> )
1	Mixed*	Spherical	0.60	0.97	16.12	0.62
2	Grassland	Nugget	1.00	na	na	na
8	Grassland	Spherical	0.41	1.22	12.95	0.34
10	Grassland	Nugget	1.00	na	na	na

\*Log transformed data due to highly positively skewed data

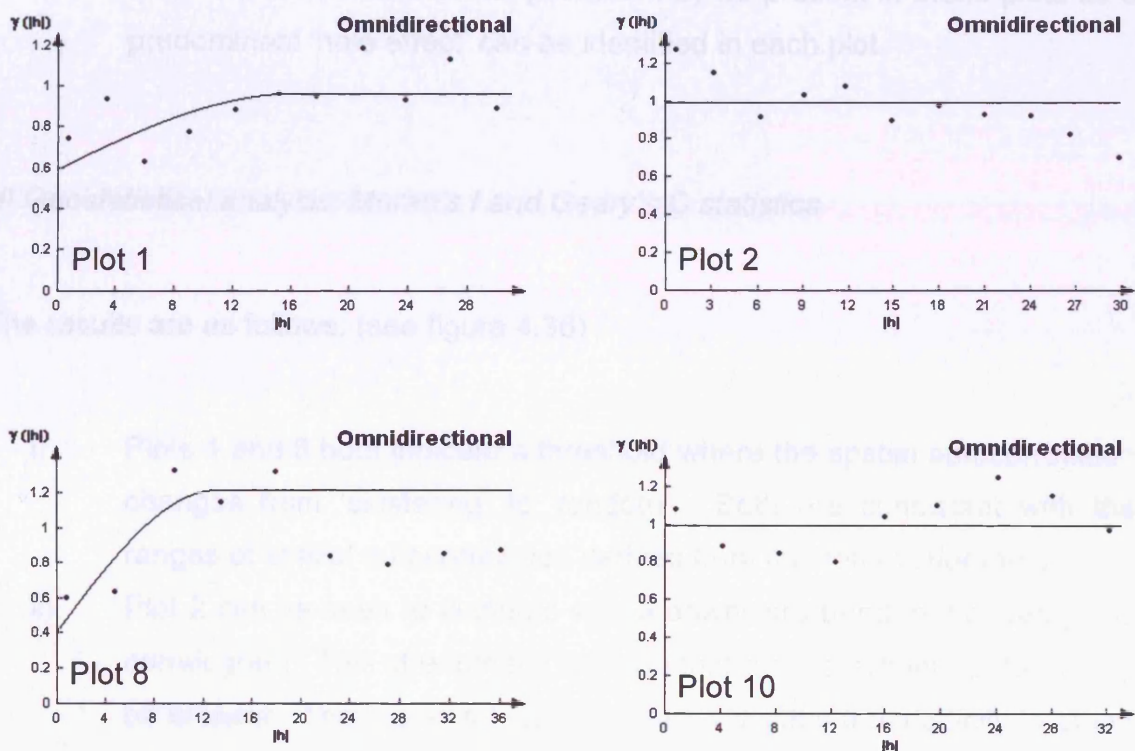


Figure 4.35 Modelled semi-variograms for the available magnesium in grassland plots.

The results are as follows:

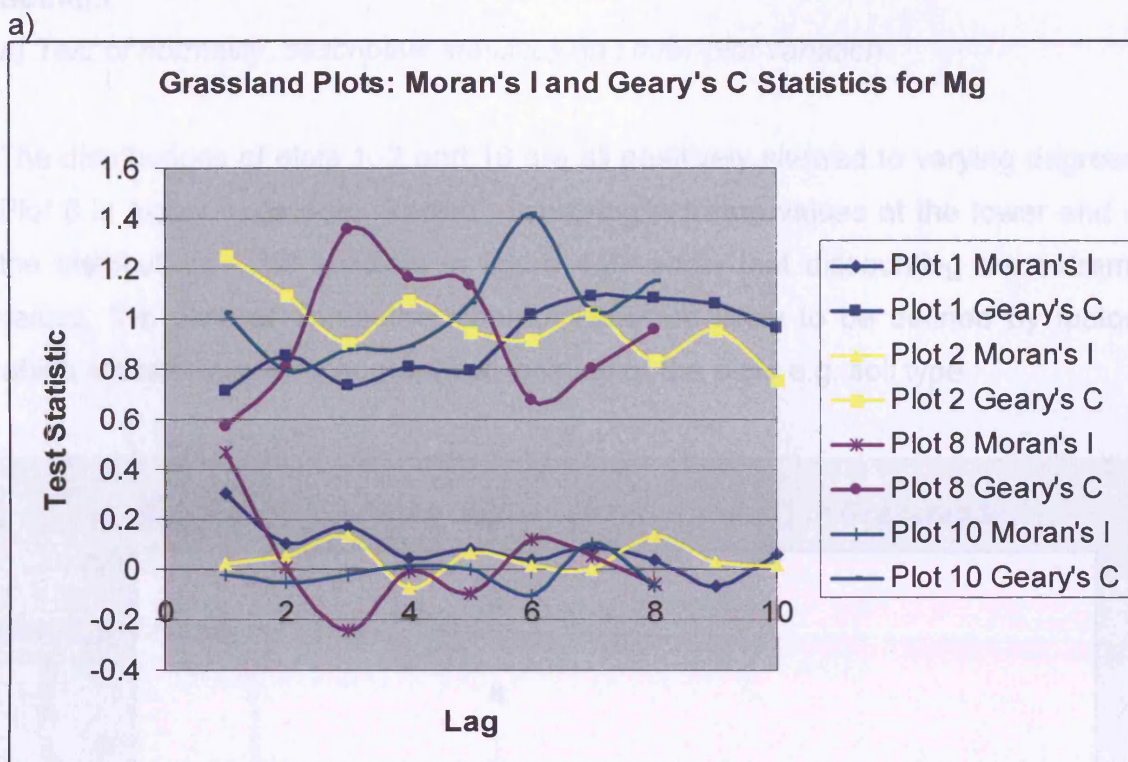
- i) Plots 2 and 10 are best represented by a 'pure nugget' model. This suggests that the distribution of available magnesium does not follow any spatial patterns.
- ii) Plots 1 and 8, both modelled by a spherical model, show evidence of spatial autocorrelation. The ranges of autocorrelation are 16.12m and 12.95m respectively.

- iii) The nugget-to-sill ratios indicate that the available magnesium in both plots show moderate levels of spatial dependency although plot 1 has a value approximately double that of plot 8 suggesting that spatial dependency is weaker in plot 1.
- iv) Plot 2, although best modelled by a pure nugget model, shows a definite decrease in variance with an increase in lag distance. This suggests the distribution of available magnesium may present itself in a 'checkerboard' pattern.
- v) Plots 8 and 10 indicate that patches may be present in these plots as a predominant 'hole effect' can be identified in each plot.

**d) Geostatistical analysis: Moran's I and Geary's C statistics**

The results are as follows: (see figure 4.36)

- i) Plots 1 and 8 both indicate a threshold where the spatial autocorrelation changes from 'clustering' to 'random'. Both are consistent with the ranges of spatial autocorrelation derived from the semi-variograms.
- ii) Plot 2 can be seen to fluctuate with a downward trend in the Geary's C correlogram. This strengthens the idea that a checkerboard pattern may be present. The Moran's I statistics also indicates a periodicity in areas of correlation and no correlation.
- iii) Significant areas of 'random' values can be identified in plots 8 and 10. Again, these further the evidence of the suggestion that large patches are present in these plots.



b)

Lag increment codes	Plot 1 & 2	Plot 8	Plot 10
1	0 > to ≤ 3	0 > to ≤ 4.5	0 > to ≤ 4
2	3 > to ≤ 6	4.5 > to ≤ 9	4 > to ≤ 8
3	6 > to ≤ 9	9 > to ≤ 13.5	8 > to ≤ 12
4	9 > to ≤ 12	13.5 > to ≤ 18	12 > to ≤ 16
5	12 > to ≤ 15	18 > to ≤ 22.5	16 > to ≤ 20
6	15 > to ≤ 18	22.5 > to ≤ 27	20 > to ≤ 24
7	18 > to ≤ 21	27 > to ≤ 31.5	24 > to ≤ 28
8	21 > to ≤ 24	31.5 > to ≤ 36	28 > to ≤ 32
9	24 > to ≤ 27		
10	27 > to ≤ 30		

**Figure 4.36** a) Moran's I and Geary's C correlograms for the available magnesium in the grassland plots. b) provides the key to the lag increments used in the correlograms for each plot.

## Sodium

### a) Test of normality, descriptive statistics and inter-plot variation

The distributions of plots 1, 2 and 10 are all positively skewed to varying degrees. Plot 8 is highly negatively skewed, displaying extreme values at the lower end of the distribution. The boxplots in figure 4.37 show that discounting the extreme values, the general distribution characteristic are likely to be defined by factors which characterise the geographical location of the plots e.g. soil type.

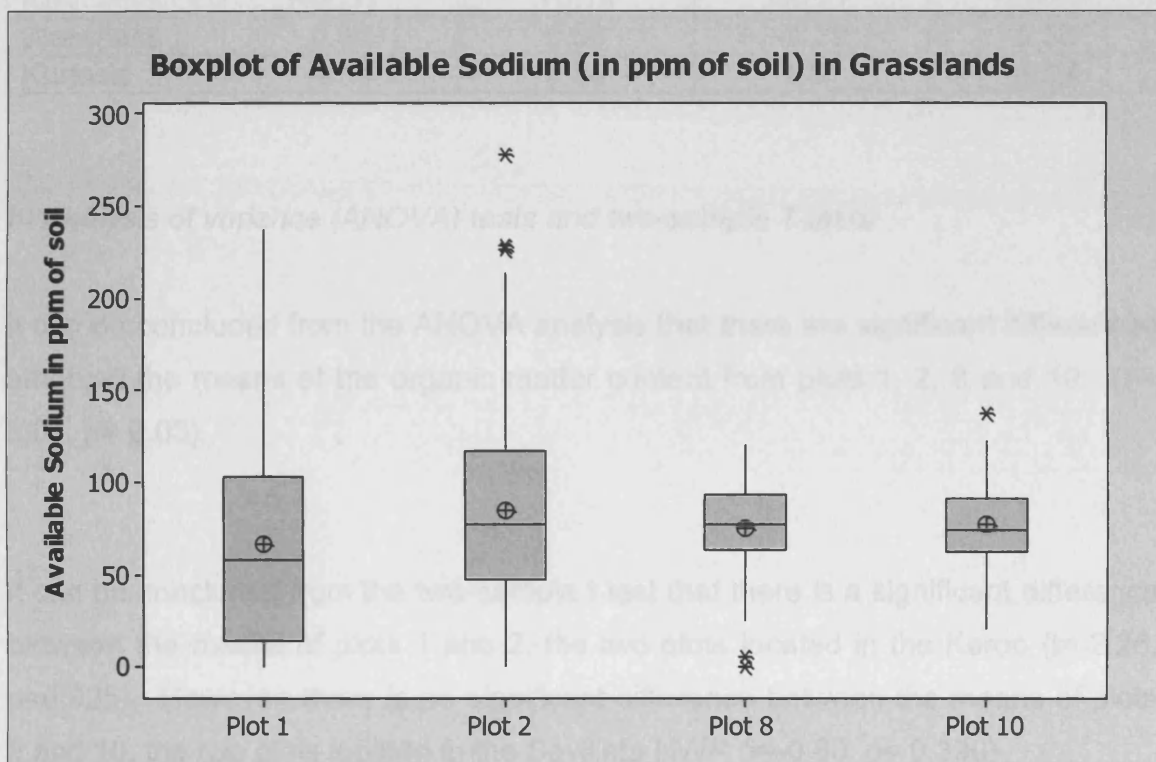


**Figure 4.37** Boxplots representing the sample distribution of available sodium in the grassland plots.

Although the distributions appear to vary between the two study regions, the mean values of available sodium do not (table 4.21). Nevertheless, although plots 1 and 2 represent the lowest and highest values of the four plots, overall the variation across the four plots is not significant.

**Table 4.21** Inter-plot comparisons of descriptive statistics: Available sodium in ppm of soil

Descriptive Statistic	Plot 1 (Mixed)	Plot 2 (Grassland)	Plot 8 (Grassland)	Plot 10 (Grassland)
<b>Mean</b>	<b>66.45</b>	<b>84.98</b>	<b>75.22</b>	<b>78.05</b>
Median	54.87	77.92	78.05	74.11
SE of Mean	5.88	5.73	2.62	1.99
St Dev	60.58	59.52	26.80	20.72
Variance	3670.16	3542.76	718.18	429.39
<b>Coef Var</b>	<b>90.74</b>	<b>70.04</b>	<b>35.63</b>	<b>26.55</b>
Minimum	0.00	0.00	0.00	43.87
Maximum	237.42	277.52	120.53	137.29
<b>Range</b>	<b>237.42</b>	<b>277.52</b>	<b>120.53</b>	<b>93.42</b>
IQR	92.31	70.19	30.21	28.05
Skewness	0.80	0.68	-1.29	0.55
Kurtosis	-0.14	0.38	1.91	-0.34

*b) Analysis of variance (ANOVA) tests and two-sample T-tests*

It can be concluded from the ANOVA analysis that there are significant differences amongst the means of the organic matter content from plots 1, 2, 8 and 10. ( $F=3.01$ ,  $p=0.03$ ).

It can be concluded from the two-sample t-test that there is a significant difference between the means of plots 1 and 2, the two plots located in the Karoo ( $t=-2.26$ ,  $p=0.025$ ). However, there is no significant difference between the means of plots 8 and 10, the two plots located in the Sevilleta NWR ( $t=-0.86$ ,  $p=0.390$ ).

*c) Geostatistical analysis: The semi-variogram*

No transformations were needed for plots 1, 2 and 10. However, as the distribution of data from plot 8 was highly negatively skewed, the data was transformed using a squared transformation. Although this technique has implications on the comparability of the data, none of the semi-variograms could be modelled therefore this issue was not important. Table 4.22 shows the

numerical results and the associated semi-variogram graphs are presented in figure 4.38.

**Table 4.22** Geostatistical analysis of the available sodium in grassland plots

Parameter: Sodium						
No.	Plot	Fitted Model	Nugget Value (Co)	Sill (Co+C <sub>1</sub> )	Range (a)	Nugget-to-sill Ratio (Co)/(Co+C <sub>1</sub> )
1	Mixed	Nugget	1.00	na	na	na
2	Grassland	Nugget	1.00	na	na	na
8	Grassland**	Nugget	1.00	na	na	na
10	Grassland	Nugget	1.00	na	na	na

\*\* Squared transformed data due to highly negatively skewed data

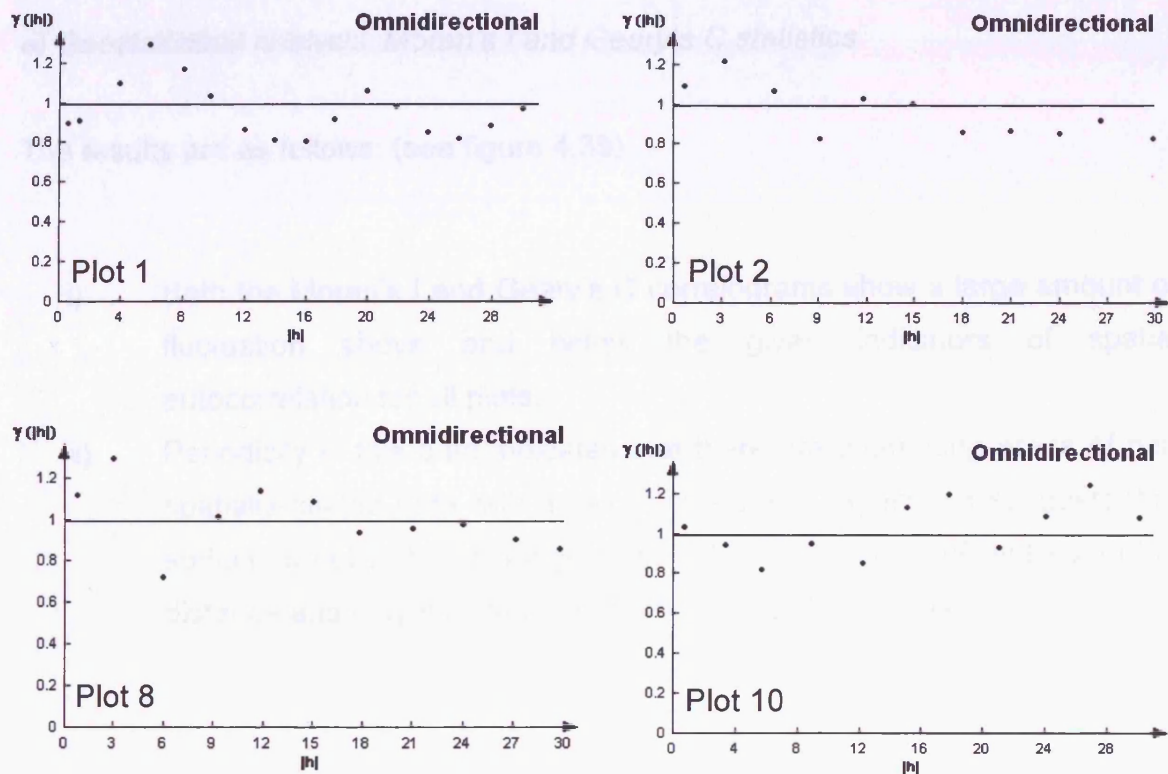


**Figure 4.38** Modelled semi-variograms for the available sodium in grassland plots.

The results are as follows:

- i) No spatial autocorrelation was identified for available sodium in any of the plots. A pure nugget model was fitted to all variograms suggesting

that no patterns are evident thus the sodium content of soil is homogenous across the 60m x 60m plots.

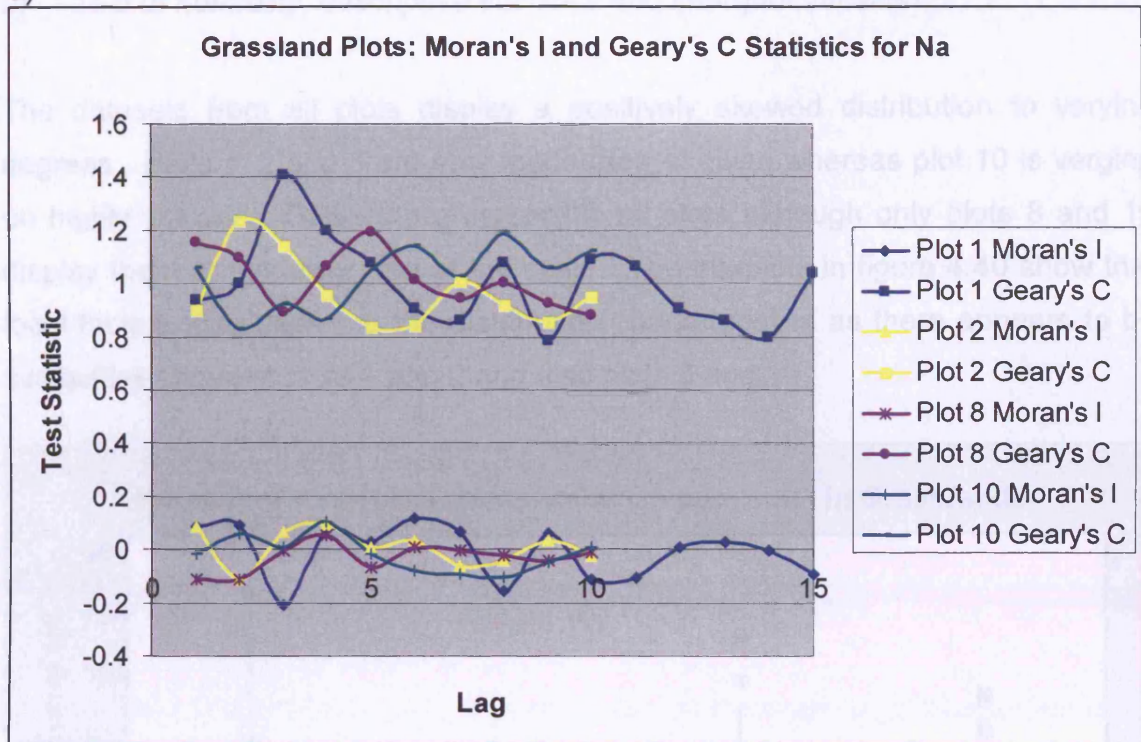
- ii) However, a closer inspection of the variograms themselves suggests that the pure nugget model has over-simplified the data and contrary to the initial findings, some patterns may exist.
- iii) This is particularly evident in plot 1 where a definite periodicity in variance is identifiable.
- iv) In addition, plots 1, 2 and 8 also exhibit a slight downward trend in variance with increasing lag distances. This suggests that sodium may also follow a checkerboard pattern across the landscape.

***e) Geostatistical analysis: Moran's I and Geary's C statistics***

The results are as follows: (see figure 4.39)

- i) Both the Moran's I and Geary's C correlograms show a large amount of fluctuation above and below the given indicators of spatial autocorrelation for all plots.
- ii) Periodicity in this data indicates that there are alternating areas of non spatially-related data with areas of clustering. Again this suggests that sodium is not in fact homogenous, rather it varies significantly with lag distance and may indicate the presence of a checkerboard pattern.

a)



b)

Lag increment codes	Plot 1	Plot 2, 8 & 10
1	0 > to ≤ 2	0 > to ≤ 3
2	2 > to ≤ 4	3 > to ≤ 6
3	4 > to ≤ 6	6 > to ≤ 9
4	6 > to ≤ 8	9 > to ≤ 12
5	8 > to ≤ 10	12 > to ≤ 15
6	10 > to ≤ 12	15 > to ≤ 18
7	12 > to ≤ 14	18 > to ≤ 21
8	14 > to ≤ 16	21 > to ≤ 24
9	16 > to ≤ 18	24 > to ≤ 27
10	18 > to ≤ 20	27 > to ≤ 30
11	20 > to ≤ 22	
12	22 > to ≤ 24	
13	24 > to ≤ 26	
14	26 > to ≤ 28	
15	28 > to ≤ 30	

**Figure 4.39** a) Moran's I and Geary's C correlograms for the available sodium in the grassland plots. b) provides the key to the lag increments used in the correlograms for each plot.

## Phosphorus

### a) Test of normality, descriptive statistics and inter-plot variation

The datasets from all plots display a positively skewed distribution to varying degrees. Plots 1, 2 and 8 are only moderately skewed whereas plot 10 is verging on highly skewed. Outliers are present in all plots although only plots 8 and 10 display them at the lower end of the scale. The boxplots in figure 4.40 show that local factors may influence the distribution characteristics as there appears to be similarities between plots 1 and 2 and also plots 8 and 10.

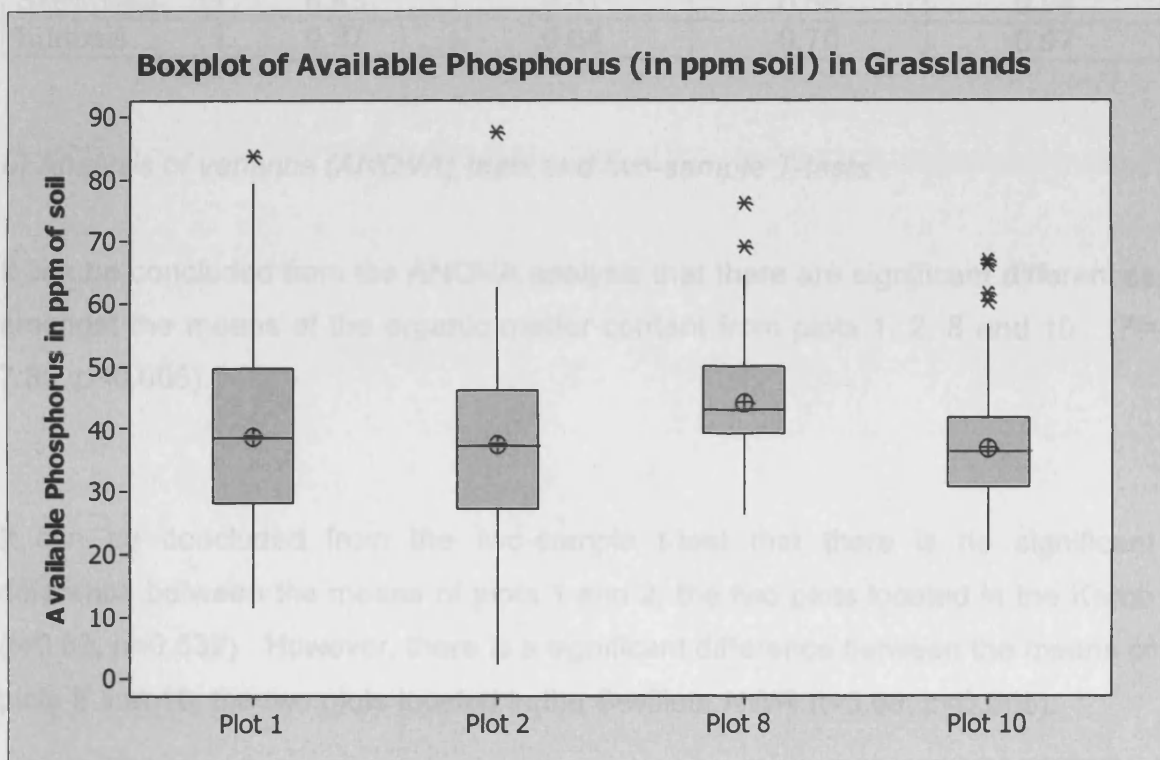


**Figure 4.40** Boxplots representing the sample distribution of available phosphorus in the grassland plots.

The descriptive statistics (see table 4.23) show that although the variability of phosphorus is greater in the Karoo plots, the mean value remains relatively constant across all four plots.

**Table 4.23** Inter-plot comparisons of descriptive statistics: Available phosphorus in ppm of soil

Descriptive Statistic	Plot 1 (Mixed)	Plot 2 (Grassland)	Plot 8 (Grassland)	Plot 10 (Grassland)
<b>Mean</b>	<b>39.13</b>	<b>37.92</b>	<b>44.42</b>	<b>37.20</b>
Median	38.63	37.28	42.83	36.30
SE of Mean	1.43	1.30	0.89	0.90
St Dev	14.73	13.55	9.17	9.36
Variance	216.98	183.55	84.02	87.70
<b>Coef Var</b>	<b>27.47</b>	<b>35.73</b>	<b>22.00</b>	<b>25.17</b>
Minimum	11.60	2.40	26.18	20.55
Maximum	83.63	87.34	75.93	66.97
<b>Range</b>	<b>72.03</b>	<b>84.94</b>	<b>49.74</b>	<b>46.41</b>
IQR	21.35	19.24	10.77	10.82
Skewness	0.43	0.37	0.56	0.94
Kurtosis	0.37	0.64	0.70	0.97

*b) Analysis of variance (ANOVA) tests and two-sample T-tests*

It can be concluded from the ANOVA analysis that there are significant differences amongst the means of the organic matter content from plots 1, 2, 8 and 10. ( $F=7.89$ ,  $p<0.005$ ).

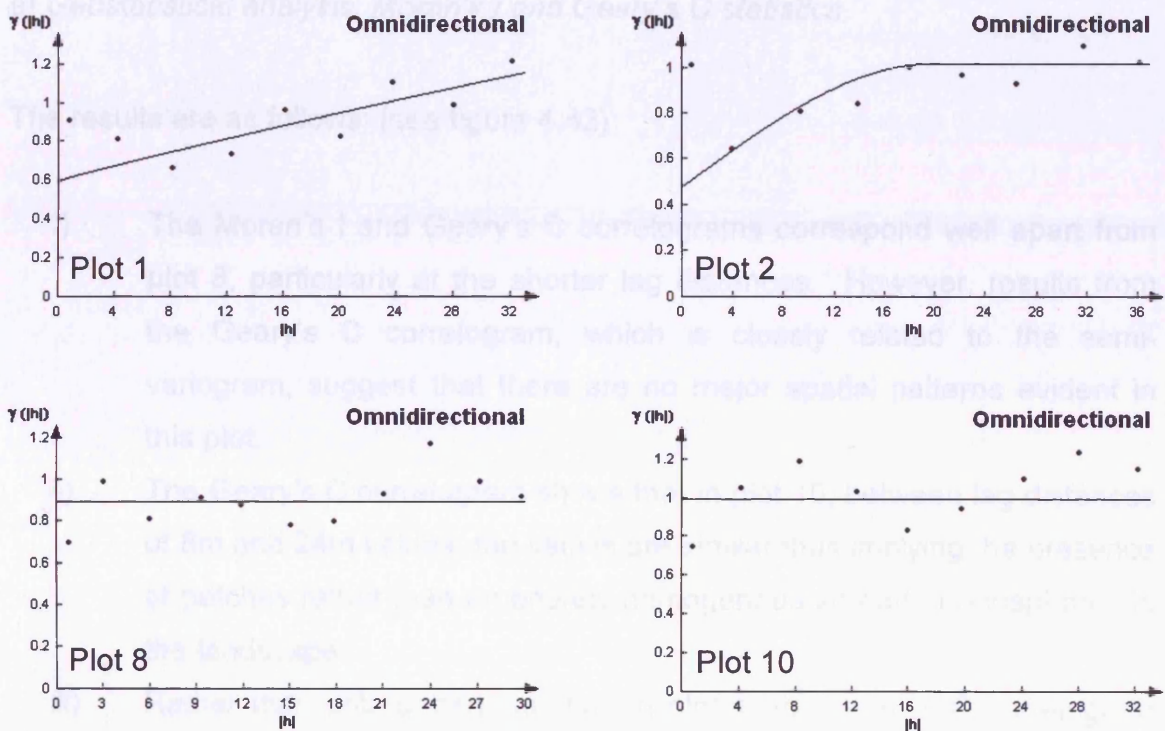
It can be concluded from the two-sample t-test that there is no significant difference between the means of plots 1 and 2, the two plots located in the Karoo ( $t=0.63$ ,  $p=0.532$ ). However, there is a significant difference between the means of plots 8 and 10, the two plots located in the Sevilleta NWR ( $t=5.69$ ,  $p<0.005$ ).

*c) Geostatistical analysis: The semi-variogram*

No outliers were removed from any of the plots and no transformations were performed before geostatistical analysis was carried out. Table 4.24 shows the numerical results and the associated semi-variogram graphs are presented in figure 4.41.

**Table 4.24** Geostatistical analysis of the available phosphorus in grassland plots

Parameter: Phosphorus						
Plot		Fitted Model	Nugget Value	Sill	Range	Nugget-to-sill Ratio
No.	Veg Type		(Co)	(Co+C <sub>1</sub> )	(a)	(Co)/(Co+C <sub>1</sub> )
1	Mixed	Power	0.60	na	na	na
2	Grassland	Spherical	0.48	1.02	19.61	0.47
8	Grassland	Nugget	1.00	na	na	na
10	Grassland	Nugget	1.00	na	na	na

**Figure 4.41** Modelled semi-variograms for the available phosphorus in grassland plots.

The results are as follows:

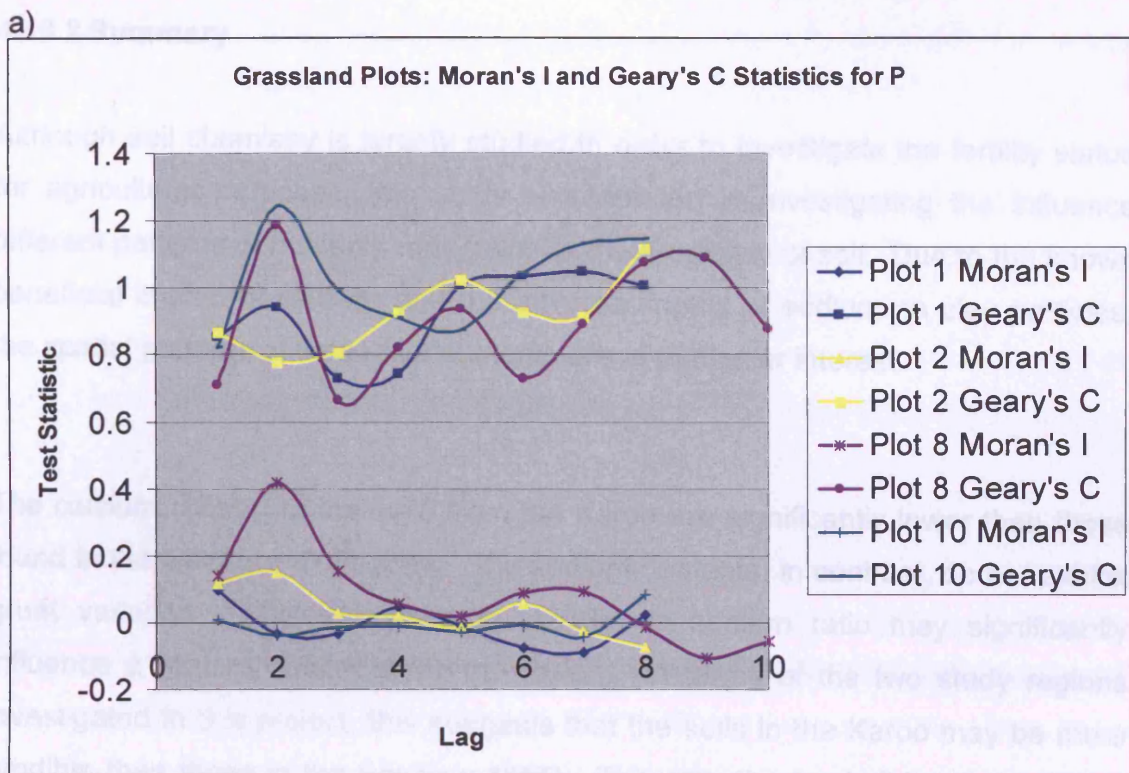
- i) Plots 8 and 10 are best represented by a 'pure nugget' model. This suggests that the distribution of available phosphorus does not follow any spatial patterns.
- ii) Plot 2 is modelled by a spherical model and shows evidence of spatial autocorrelation. The range of autocorrelation is 19.61m.
- iii) The nugget-to-sill ratio indicates that the available phosphorus shows a moderate level of spatial dependency.

- iv) Plot 1 has been fitted with a power function as the variance does not reach a sill. This is described as unbounded random variation.
- vi) Although best modelled by a pure nugget model, plots 8 and 10 show evidence of periodicity indicating the presence of patches in the landscape rather than a purely homogenous cover suggested by the pure nugget model.

**e) Geostatistical analysis: Moran's I and Geary's C statistics**

The results are as follows: (see figure 4.42)

- i) The Moran's I and Geary's C correlograms correspond well apart from plot 8, particularly at the shorter lag distances. However, results from the Geary's C correlogram, which is closely related to the semi-variogram, suggest that there are no major spatial patterns evident in this plot.
- ii) The Geary's C correlogram shows that in plot 10, between lag distances of 8m and 24m values, the values are similar thus implying the presence of patches rather than an entirely homogenous spread of phosphorus in the landscape.
- iii) Rather than unbounded variation in plot 1, the Geary's C correlogram suggests that a sill is reached at a range of approximately 16 to 20m.



b)

Lag increment codes	Plot 1 & 10	Plot 2	Plot 8
1	0 > to ≤ 4	0 > to ≤ 4.5	0 > to ≤ 3
2	4 > to ≤ 8	4.5 > to ≤ 9	3 > to ≤ 6
3	8 > to ≤ 12	9 > to ≤ 13.5	6 > to ≤ 9
4	12 > to ≤ 16	13.5 > to ≤ 18	9 > to ≤ 12
5	16 > to ≤ 20	18 > to ≤ 22.5	12 > to ≤ 15
6	20 > to ≤ 24	22.5 > to ≤ 27	15 > to ≤ 18
7	24 > to ≤ 28	27 > to ≤ 31.5	18 > to ≤ 21
8	28 > to ≤ 32	31.5 > to ≤ 36	21 > to ≤ 24
9			24 > to ≤ 27
10			27 > to ≤ 30

Figure 4.42 a) Moran's I and Geary's C correlograms for the available phosphorus in the grassland plots. b) provides the key to the lag increments used in the correlograms for each plot.

#### 4.10.2 Summary

Although soil chemistry is largely studied in order to investigate the fertility status for agricultural purposes, this study is interested in investigating the influence different patterns of nutrients may have on the erodibility of soil. Due to the known beneficial impact of calcium and the adverse impact of sodium on clay particles, the spatial patterns of these two nutrients are of particular interest.

The calcium content of the soils from the Karoo are significantly lower than those found in the Sevilleta NWR sites. The sodium contents, in contrast, do not exhibit great variation. This difference in calcium to sodium ratio may significantly influence a regions susceptibility to erosion. In terms of the two study regions investigated in this project, this suggests that the soils in the Karoo may be more erodible than those in the Sevilleta NWR. This hypothesis shall be discussed in more detail in chapter 7.

Detailed investigation of the spatial properties of calcium and sodium also produced some interesting findings. Although significant differences in quantities of calcium were measured between the two study regions, no characteristic spatial patterns were identified. Conversely, sodium produced results indicating that no spatial patterns exist in any of the plots. However, by investigating the geostatistical results further, i.e. analysing the experimental variograms rather than the possibly over-simplified modelled variograms, periodicity in the variance of all plots can be seen. In addition, a general downward trend of variance with increasing lag distances is evident. Although there is uncertainty surrounding the interpretation of these phenomena, two possible explanations exist: a) that the periodicity is indicative of autocorrelation between patches (e.g. Radeloff *et al.*, 2000) or b) a pattern in the sodium distribution does exist, taking the form of a checkerboard i.e. a fine-scale pattern of high and low values.

The phosphorus content is similar in both study regions, however, the spatial patterns differ. Plots 1 and 2, the Karoo plots, were modelled by a power model and a spherical model, respectively. However, dips in the variance are evident suggesting that the plots may be exhibiting evidence of 'patches' in the landscape. Plots 8 and 10, in contrast, have been modelled using a pure nugget model signifying that no spatial patterns exist. Although this was the most representative model, periodicity is evident in both plots suggesting that the phosphorus content fluctuates in a regular manner across the Sevilleta NWR grassland plots.

The available magnesium content is lower in the Karoo, however, no characteristic spatial patterns are evident for either of the two study regions. The spatial structures of this nutrient are complex. Plot 2 displays a fluctuating downward trend in variance whereas plots 8 and 10 show evidence of periodicity. The simple models used here are unlikely to be accurately representing the spatial distribution of magnesium.

Available potassium, in contrast, appears to be homogenous across plots 1 and 2. Although ranges of spatial autocorrelation were derived from plots 8 and 10, the values are reasonably large indicating that the distribution of available potassium in these plots can also be classed as being relatively uniform. Plots 1, 2 and 10 produced similar mean contents whereas plot 8 was significantly higher. This would indicate that available potassium may be controlled by other soil parameters rather than vegetation type.

#### **4.11 Key findings from the grassland plots**

- The mean contents of each soil parameter from the 4 grassland plots were compared, for all parameters the values were shown to be statistically different.
- The soil parameters of the two Karoo plots appear to be statistically more similar than the two Sevilleta NWR plots. Between the two Karoo plots, bulk density, available calcium, potassium and phosphorus were similar, whereas only the available sodium content was similar in the two Sevilleta NWR plots.
- Significant differences in soil pH were evident between the two study regions. The Karoo plots are classed as being acidic whereas the Sevilleta NWR plots are alkali.
- Of the plots that demonstrated spatial autocorrelation, the ranges are as follows:
  - Organic Matter: 5.98m – 21.09m
  - Dry bulk density: 6.60m – 11.55m
  - Soil moisture: 10.73m – 25.11m
  - Shear strength: 8.51m – 17.16m
  - Particle size: none determined
  - pH: 16.56m
  - Conductivity: 19.47m
  - Calcium: 10.50m – 19.84m
  - Magnesium: 12.95m – 16.12m
  - Potassium: 12.58m – 16.74m
  - Sodium: none determined
  - Phosphorus: 19.61m
- No fine-scale spatial patterns are evident in the ranges of spatial autocorrelation derived for soil parameters from grasslands. However, this may be a function of scale as the minimum lag distance calculated was

0.5m. Insufficient data was derived at this lag distance in order to accurately interpret patterns at this scale.

- The large ranges and number of 'pure nugget' results suggest that the soil parameters in grasslands are relatively homogenous.
- However, the 'hole effect' was identified in all three pure grassland plots 2, 8 and 10. The parameters that displayed this characteristic were:

Plot 1 – Available phosphorus

Plot 2 – Available calcium and phosphorus

Plot 8 – Bulk density, shear strength and available magnesium

Plot 10 – Shear strength, available calcium and available magnesium.

This phenomenon indicates that the grasslands exhibit 'patchy' spatial patterns in the landscape.

- Cyclic patterns are evident in some semi-variograms, this indicates that the properties are heterogeneous in their distribution across the grassland landscape. The parameters that display this pattern are: the clay content, pH, available sodium and available phosphorus.
- A decrease in variance with an increasing lag distance was identified in the semi-variograms of shear strength, pH, available magnesium and available sodium. This may indicate that these properties are distributed in a checkerboard pattern.

The relationships among the soil parameters will be investigated further in chapters 7 and 8, followed by a detailed interpretation and discussion of the results.

## CHAPTER FIVE

### Shrublands:

#### Analysis of the Spatial Continuity of Soil Properties

---

---

##### **5.1 Introduction**

##### **5.2 Organic matter content**

##### **5.3 Bulk density**

##### **5.4 Soil moisture**

##### **5.5 Shear strength**

##### **5.6 Soil-aggregate stability**

##### **5.7 pH**

##### **5.8 Electrical conductivity**

##### **5.9 Nutrient content analysis**

##### **5.10 Key findings**

---

---

##### **5.1 Introduction**

This chapter presents the results and discussion of the spatial distribution of soil parameters derived from plots classified as shrublands. The chapter investigates the notion that shrubland landscapes are traditionally considered heterogeneous, both in vegetation cover and the associated shrubland soil parameters (Schlesinger *et al.*, 1996; Bochet *et al.*, 1999; Titus *et al.*, (2002).

The structure of this chapter will follow that of chapter 4. Table 5.1 indicates the plot number that will be referred to throughout the chapter, the associated vegetation type and study region.

**Table 5.1** Shrubland plot identification data

Plot number	Vegetation Type	Study Region
3	Shrubland (Mixed types)	Karoo
5	Shrubland (Mixed types)	Karoo
9	Shrubland (Creosotebush)	Sevilleta NWR
11	Shrubland (Creosotebush)	Sevilleta NWR

In some cases the experimental variograms cannot be modelled. These datasets show a downward trend in variance with increasing lag distances. Even a pure nugget model cannot be applied to this type of data. Despite this, these datasets should not be dismissed, as a downward trend possibly signifies the presence of a checkerboard pattern. Although these variograms cannot be modelled, the experimental variograms are presented to show the spatial distribution.

Analysis of variance (ANOVA) tests were conducted to determine whether the parameter values across all four grassland plots differ significantly. As all soil parameters produced the same results, it can be concluded that the samples from the four plots come from populations with significantly different distributions. These results will therefore not be repeated throughout the chapter. The p-values and F-statistics can be found in the appendix 2.

## 5.2 Organic matter content

### 5.2.1 Results:

#### a) Test of normality, descriptive statistics and inter-plot variation

The frequency distributions displayed by the boxplots (figure 5.1) show that the datasets from all the plots are positively skewed, however, this is weak in plot 11 and can therefore be classed as having a normal distribution. Plots 3 and 5 are considered to be highly positively skewed as the skewness values are greater than 1 (see table 5.2). Outliers are evident in all datasets.

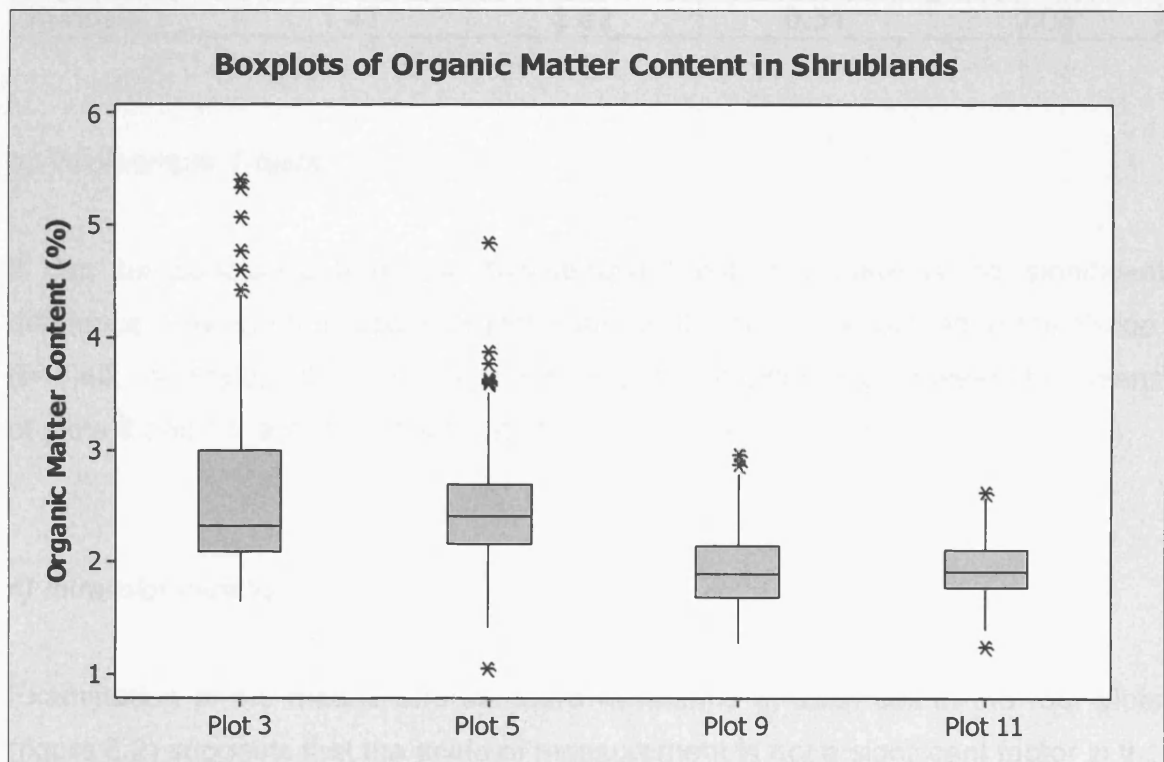


Figure 5.1 Boxplots representing the sample distribution of organic matter content in the shrubland plots.

Inter-plot comparisons of the descriptive statistics can be seen in table 5.2. The two plots with the highest mean values and greatest ranges are plots 3 and 5, the two plots situated in the Karoo, South Africa. The coefficient of variation values

also indicate that the plots with the greatest variation relative to the mean are the two situated in the Karoo.

**Table 5.2** Inter-plot comparisons of descriptive statistics: Organic matter content

Descriptive Statistic	Plot 3 (Karoo)	Plot 5 (Karoo)	Plot 9 (Sevilleta)	Plot 11 (Sevilleta)
Mean	2.64	2.50	1.93	1.94
Median	2.32	2.41	1.90	1.93
SE of Mean	0.08	0.05	0.03	0.02
St Dev	0.86	0.55	0.34	0.25
Variance	0.73	0.31	0.12	0.06
<b>Coef Var</b>	<b>32.43</b>	<b>22.09</b>	<b>17.69</b>	<b>13.13</b>
Minimum	1.65	1.05	1.28	1.25
Maximum	5.41	4.86	2.97	2.63
<b>Range</b>	<b>3.76</b>	<b>3.81</b>	<b>1.69</b>	<b>1.37</b>
IQR	0.91	0.54	0.47	0.33
Skewness	1.39	1.00	0.64	0.15
Kurtosis	1.47	2.82	0.51	0.08

#### *b) Two-sample T-tests*

It can be concluded from the two-sample t-test that there is no significant difference between the means of plot 3 and 5, the two plots located in the Karoo. ( $t = 1.40$ ,  $p = 0.162$ ). Similarly, there is no significant difference between the means of plots 9 and 11, the two plots located in the Sevilleta NWR ( $t = -0.19$ ,  $p = 0.849$ ).

#### *c) Intra-plot variation*

Examination of the means and standard deviations of each cell in the four plots (figure 5.2) suggests that the scale of measurement is not a significant factor in the characterisation of organic matter content of soil. All plots demonstrate little variation across the three spatial scales. On a basic level these results imply that each shrubland plot displays a relatively homogenous organic matter content, however, geostatistical analysis will investigate this on a more comprehensive level.

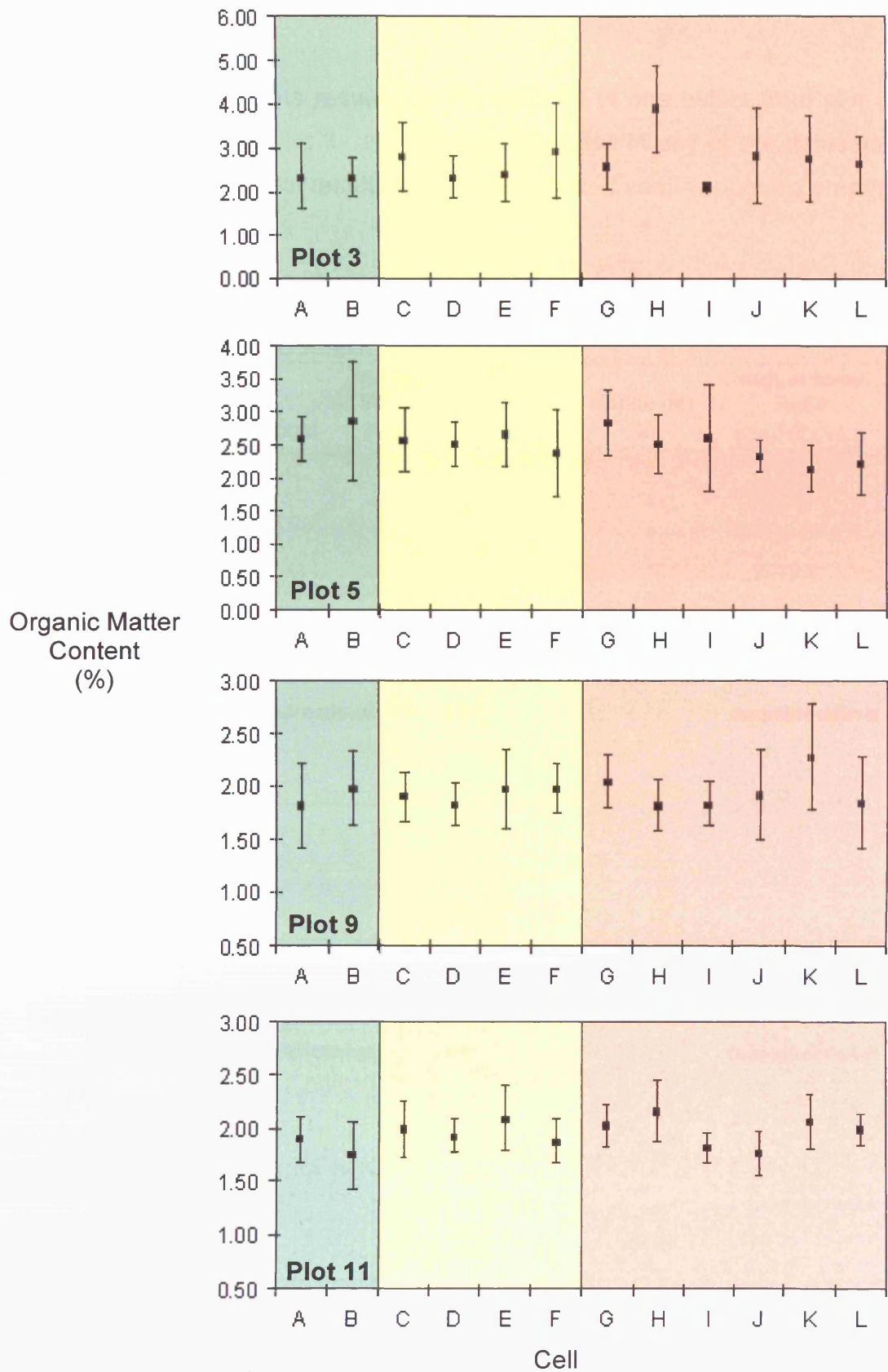


**Figure 5.2** The means and standard deviations of organic matter content for each cell within the plots. Green represents the 30 x 30m cells, yellow represents the 10 x 10m cells and pink represents 1.5 x 1.5m cells.

d) Geostatistical analysis: The semi-variogram

Pre-processing of the datasets resulted in the removal of one outlier from plot 5 and a log transformation of plot 3. No drift was identified in any of the datasets. Table 5.3 shows the numerical results and the associated semi-variogram graphs are presented in figure 5.3.

**Table 5.3** Geostatistical analysis of organic matter content of shrubland plots

Parameter: Organic Matter Content						
No.	Plot Location	Fitted Model	Nugget Value (Co)	Sill (Co+C <sub>1</sub> )	Range (m) (a)	Nugget-to-sill Ratio (Co)/(Co+C <sub>1</sub> )
3	Karoo*	Spherical	0.7	1.10	4.5	0.64
5	Karoo	Nugget	1.00	na	na	na
9	Sevilleta NWR	None	na	na	na	na
11	Sevilleta NWR	Nugget	1.00	na	na	na

\* Log transformed data due to highly positively skewed data

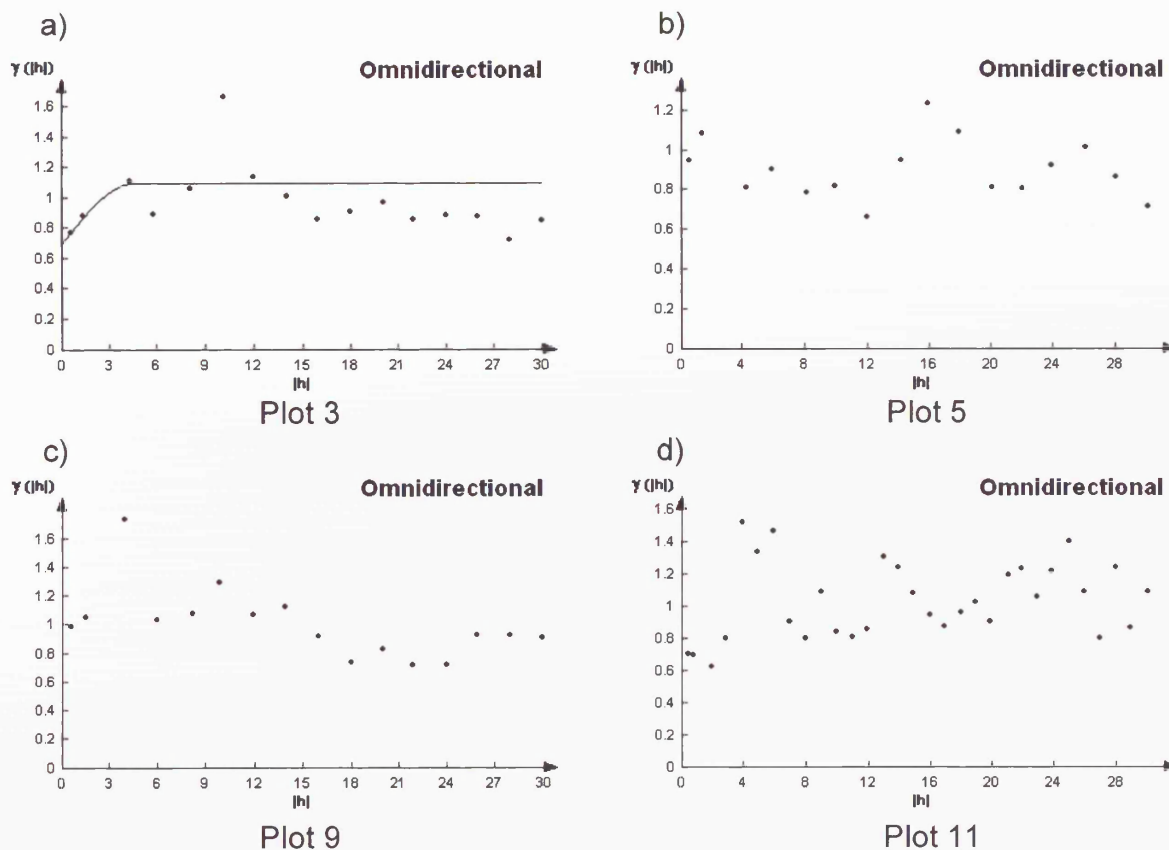


**Figure 5.3** Semi-variograms of the organic matter content of the shrubland plots.

The results are as follows:

- i) Only plot 3 shows evidence of spatial autocorrelation with a range of 4.5m. Although the nugget-to-sill ratio indicates a moderate spatial dependency it also shows evidence of a downward trend in variance with an increasing lag.
- ii) Plots 5 and 11 are best represented by the pure nugget model indicating that no spatial patterns are evident, however, some evidence of periodicity is present in both these plots suggesting that the pure nugget model may not be a true representation of the patterns in these plots.
- i) Plot 9 has not been modelled due to the obvious downward trend in variance with an increasing lag distance. It is thought that this represents a checkerboard pattern in the dataset.
- ii) The two plots from the Sevilleleta NWR (9 and 11) both show a great increase in variance at a lag distance of approximately 4m.
- iii) Examining the periodicity in the data (figure 5.4) all plots excluding plot 5 follow a similar wave pattern, albeit with different amplitudes of variance, until a lag distance of approximately 12m.

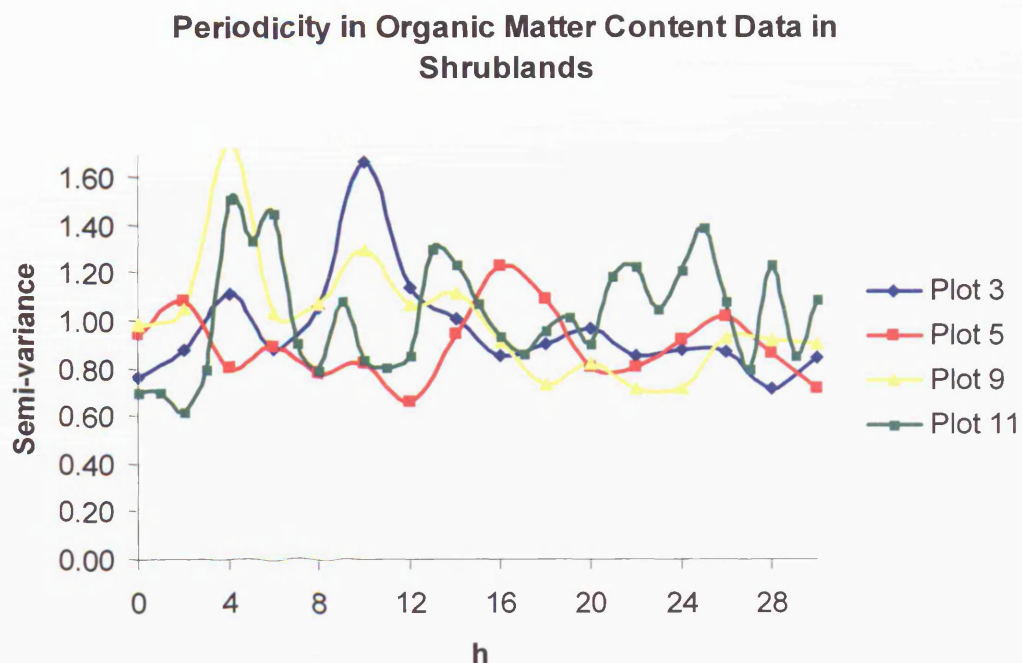


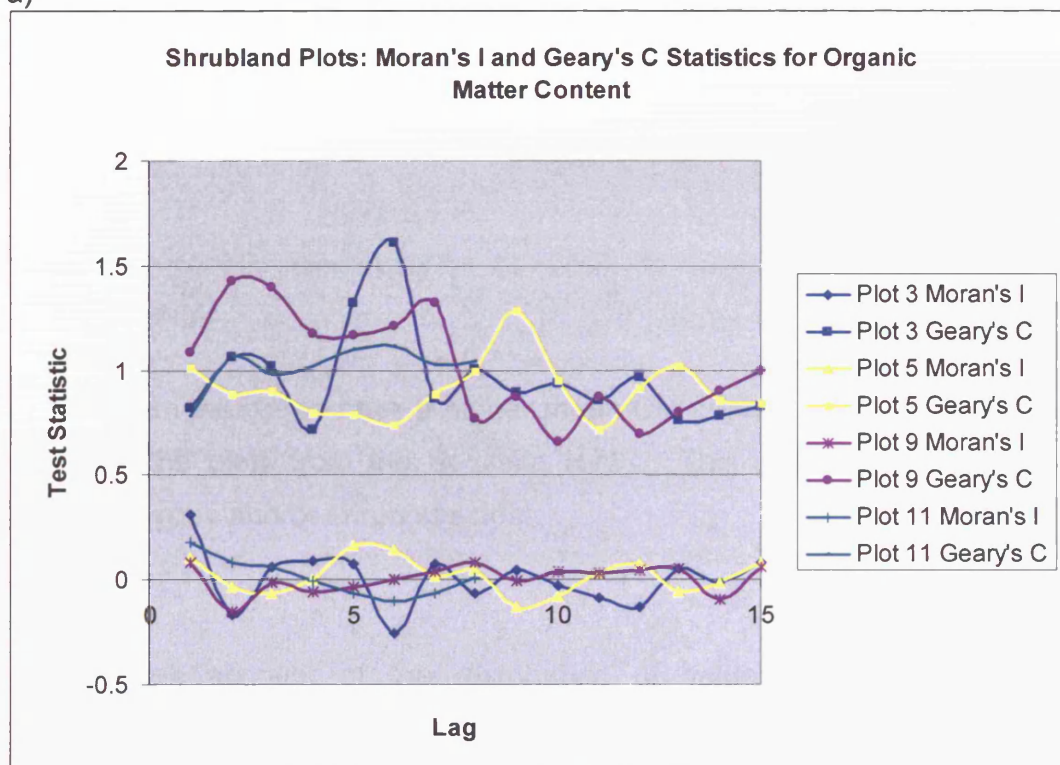
**Figure 5.4** Semi-variograms with connecting lines to show periodicity in organic matter content data in shrubland plots.

## e) Geostatistical analysis: Moran's I and Geary's C statistics

The results are as follows: (see figure 5.5)

- i) Comparisons made between the Moran's I and Geary's C statistics show that the results mirror each other relatively well, this increases the confidence in the results.
- ii) The Geary's C analysis indicates that both plots 3 and 11 show a range of spatial autocorrelation of approximately 4m. In general, plot 3 shows evidence of clustering although between lag distances of approximately 7m and 12m the Geary's C statistics suggests random patterns are present. This corresponds to the semi-variogram results.
- iii) Plot 5 appears to show that clustering is evident at most lag distances. Although periodicity is evident, only lag distances between 14m and 20m are considered not to be spatially related.
- iv) Plot 9 highlights the issue surrounding modelling this dataset. At lag distances smaller than 14m, the correlograms suggest that the samples are not spatially related whereas after this threshold the correlogram falls below 1 suggesting that clustering is present.

a)



b)

Lag increment codes	Plot 3, 5 & 9	Plot 11
1	0 > to <= 2	0 > to <= 1
2	2 > to <= 4	1 > to <= 2
3	4 > to <= 6	2 > to <= 3
4	6 > to <= 8	3 > to <= 4
5	8 > to <= 10	4 > to <= 5
6	10 > to <= 12	5 > to <= 6
7	12 > to <= 14	6 > to <= 7
8	14 > to <= 16	7 > to <= 8
9	16 > to <= 18	8 > to <= 9
10	18 > to <= 20	9 > to <= 10
11	20 > to <= 22	10 > to <= 11
12	22 > to <= 24	11 > to <= 12
13	24 > to <= 26	12 > to <= 13
14	26 > to <= 28	13 > to <= 14
15	28 > to <= 30	14 > to <= 15
16		15 > to <= 16
17		16 > to <= 17
18		17 > to <= 18
19		18 > to <= 19
20		19 > to <= 20
21		20 > to <= 21
22		21 > to <= 22
23		22 > to <= 23
24		23 > to <= 24
25		24 > to <= 25
26		25 > to <= 26
27		26 > to <= 27
28		27 > to <= 28
29		28 > to <= 29
30		29 > to <= 30

**Figure 5.5** a) Moran's I and Geary's C correlograms for the organic matter content of the shrubland plots. b) provides the key to the lag increments used in the correlograms for each plot.

### 5.2.2 Summary

Both plots from the Karoo have a higher mean OM content and a greater range of values than the plots from the Sevilleta NWR. This may be a function of the different soil types and/or shrub species.

A cell by cell account of the distribution of values across the four plots demonstrates a marginally increased intra-plot variation in the two Karoo plots and

relatively little variation in the Sevilleta NWR plots. In general, the intra-plot variation is not significant across the three spatial scales indicating a homogenous distribution.

The geostatistical analysis reflects these conclusions as only plot 3 in the Karoo showed evidence of spatial autocorrelation. A range of 4.5m was determined; this value is too large to be attributed to the shrub zone but may represent the inter-shrub zone. The OM contents of plots 5 and 11 were considered to be homogeneous whereas plot 9 could not be represented by a simple model due to a downward trend in variance with an increasing lag.

However, as only simple geostatistical models are being utilised in this study, observations made from the experimental semi-variograms are also considered to be important. A significant observation is that at a lag distance of approximately 4m all plots except plot 5 show an increase in variance thus suggesting that it is not only plot 3 that shows signs of spatial autocorrelation.

The complex structures in the shrubland datasets make the interpretation difficult, plots 3 and 9 show a definite decrease in variance with increasing lag distances suggesting the presence of checkerboard patterns. In addition, periodicity is present in most plots. This cyclic behaviour could represent the differences between shrub and intershub zones and suggests that scale of measurement is important when characterising the spatial distribution of organic matter content in shrublands. The implications of these findings will be discussed further in chapter 7.

### 5.3 Bulk density

#### 5.3.1 Results

##### a) Test of normality, descriptive statistics and inter-plot variation

The frequency distributions displayed by the boxplots (figure 5.6) show that the datasets from all plots are negatively skewed to varying degrees. Plot 5 can be considered as having a normal distribution as the skew is not significant. Outliers are evident in all datasets.

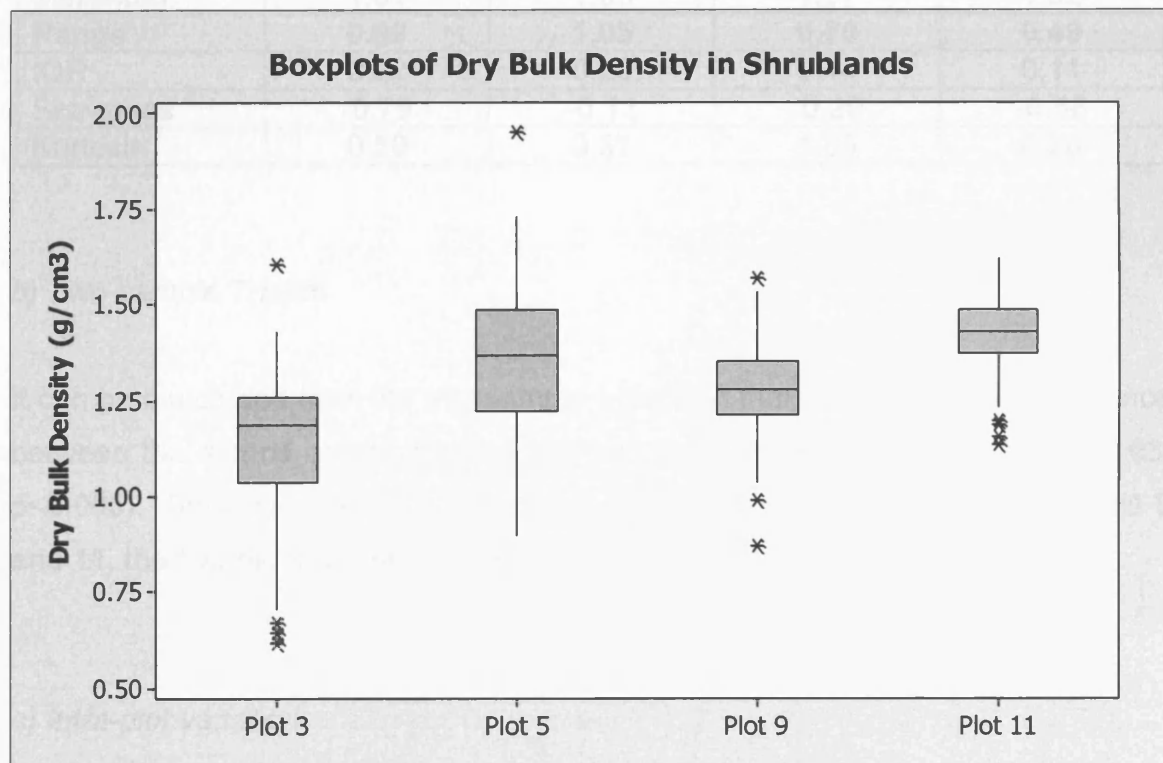


**Figure 5.6** Boxplots representing the sample distribution of dry bulk density in the shrubland plots.

Both the boxplots and the descriptive statistics (table 5.4) demonstrate some interesting differences amongst the four plots. Although the mean and median values of all four plots are relatively similar, the distribution of data varies. The coefficient of variation values reflect these differences; plots 3 and 5 have values of 16.63% and 14.17% respectively, values that are approximately double the

coefficient of variation values of plots 9 and 11. As plots 3 and 5 are situated in the Karoo, South Africa and plots 9 and 11 are situated in the Sevilleta NWR, New Mexico, this demonstrates the influence of the local conditions such as soil type.

**Table 5.4** Inter-plot comparisons of descriptive statistics: Dry bulk density ( $\text{g cm}^{-3}$ )

Descriptive Statistic	Plot 3 (Karoo)	Plot 5 (Karoo)	Plot 9 (Sevilleta)	Plot 11 (Sevilleta)
<b>Mean</b>	<b>1.14</b>	<b>1.35</b>	<b>1.28</b>	<b>1.42</b>
Median	1.19	1.37	1.28	1.43
SE of Mean	0.02	0.02	0.01	0.01
St Dev	0.19	0.19	0.12	0.10
Variance	0.04	0.04	0.01	0.01
<b>Coef Var</b>	<b>16.63</b>	<b>14.17</b>	<b>9.07</b>	<b>6.93</b>
Minimum	0.62	0.90	0.87	1.13
Maximum	1.61	1.95	1.57	1.62
<b>Range</b>	<b>0.99</b>	<b>1.05</b>	<b>0.70</b>	<b>0.49</b>
IQR	0.22	0.26	0.14	0.11
Skewness	-0.79	-0.13	-0.29	-0.58
Kurtosis	0.50	0.37	1.05	0.20

#### *b) Two-sample T-tests*

It can be concluded from the two-sample t-test that there is a significant difference between the means of plot 3 and 5, the two plots located in the Karoo. ( $t = -7.93$ ,  $p < 0.005$ ). Similarly, there is a significant difference between the means of plots 9 and 11, the two plots located in the Sevilleta NWR ( $t = -9.42$ ,  $p < 0.005$ ).

#### *c) Intra-plot variation*

Intra-plot analysis shows that the mean values of all the cells in each plot do not vary greatly (figure 5.7). Similarly, the standard deviations of plots 3 and 11 do not demonstrate great variability across the cells suggesting that the scale of measurement is not a significant factor in the characterisation of dry bulk density in these plots. Plot 5, in contrast, shows that the standard deviation increases as the scale of measurement increases. This suggests that the distribution of bulk density is not homogenous and some spatial autocorrelation may exist.

Controversially, plot 9 demonstrates the opposite trend; as the scale of measurement increases the standard deviation decreases. This indicates that samples close together vary greatly whereas samples located at greater distances are more similar in value.

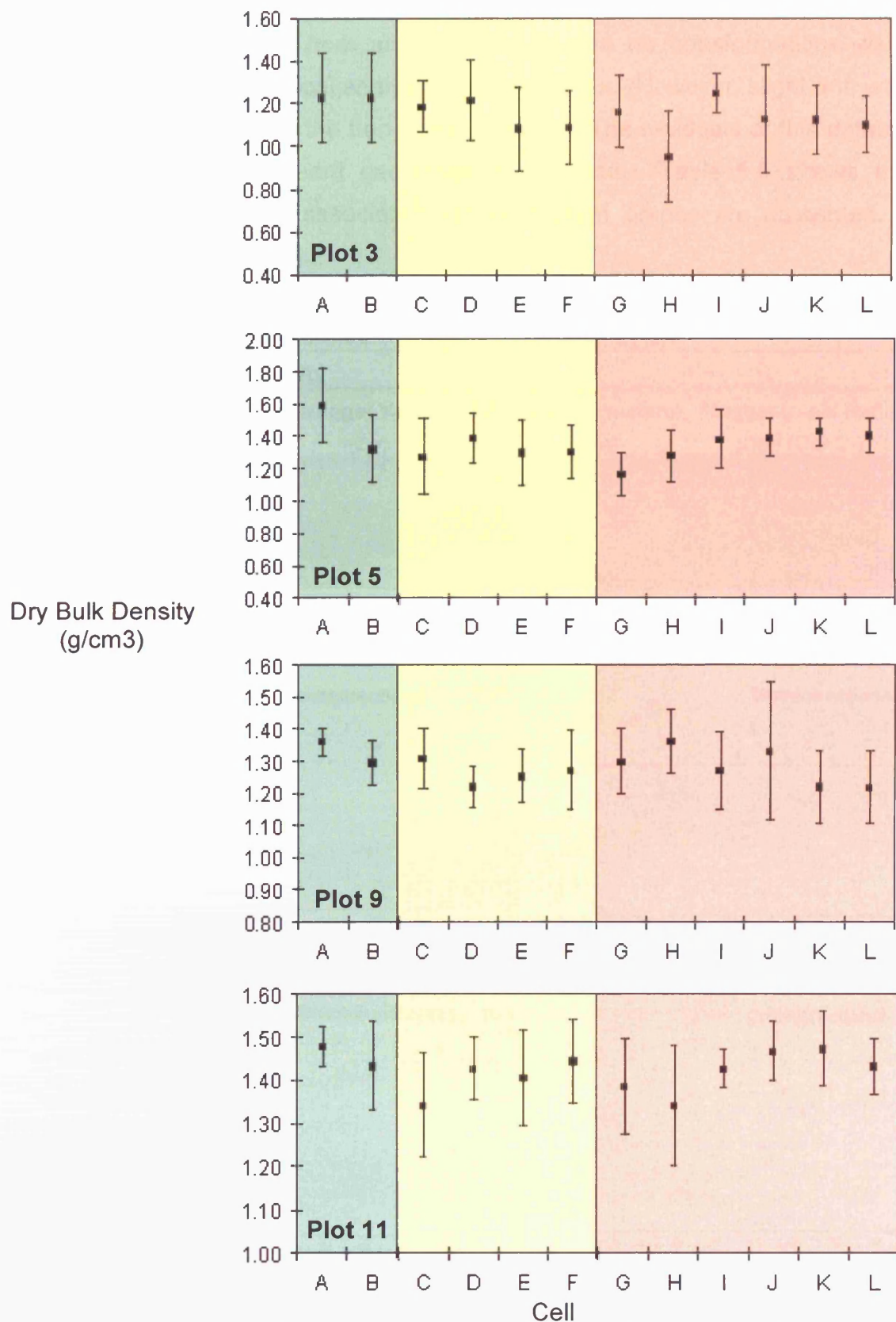


**Figure 5.7** The means and standard deviations of dry bulk density for each cell within the plots. Green represents the 30 x 30m cells, yellow represents the 10 x 10m cells and pink represents 1.5 x 1.5m cells.

d) Geostatistical analysis: The semi-variogram

No outliers were removed from any of the plots and no transformations were performed before geostatistical analysis was carried out. However, slight drift was identified in plot 5 therefore the trend was removed. The residuals of this dataset were used for all subsequent geostatistical analyses. Table 5.5 shows the numerical results and the associated semi-variogram graphs are presented in figure 5.8.

**Table 5.5** Geostatistical analysis of the dry bulk density of grassland plots

Parameter: Dry Bulk Density						
Plot No.	Plot Location	Fitted Model	Nugget Value (Co)	Sill (Co+C <sub>1</sub> )	Range (meters) (a)	Nugget-to-sill Ratio (Co)/(Co+C <sub>1</sub> )
3	Karoo	Nugget	1.00	na	Na	na
5	Karoo	Spherical	0.46	0.89	6.82	0.52
9	Sevilleta NWR	Nugget	1.00	na	Na	na
11	Sevilleta NWR	Nugget	1.00	na	Na	na

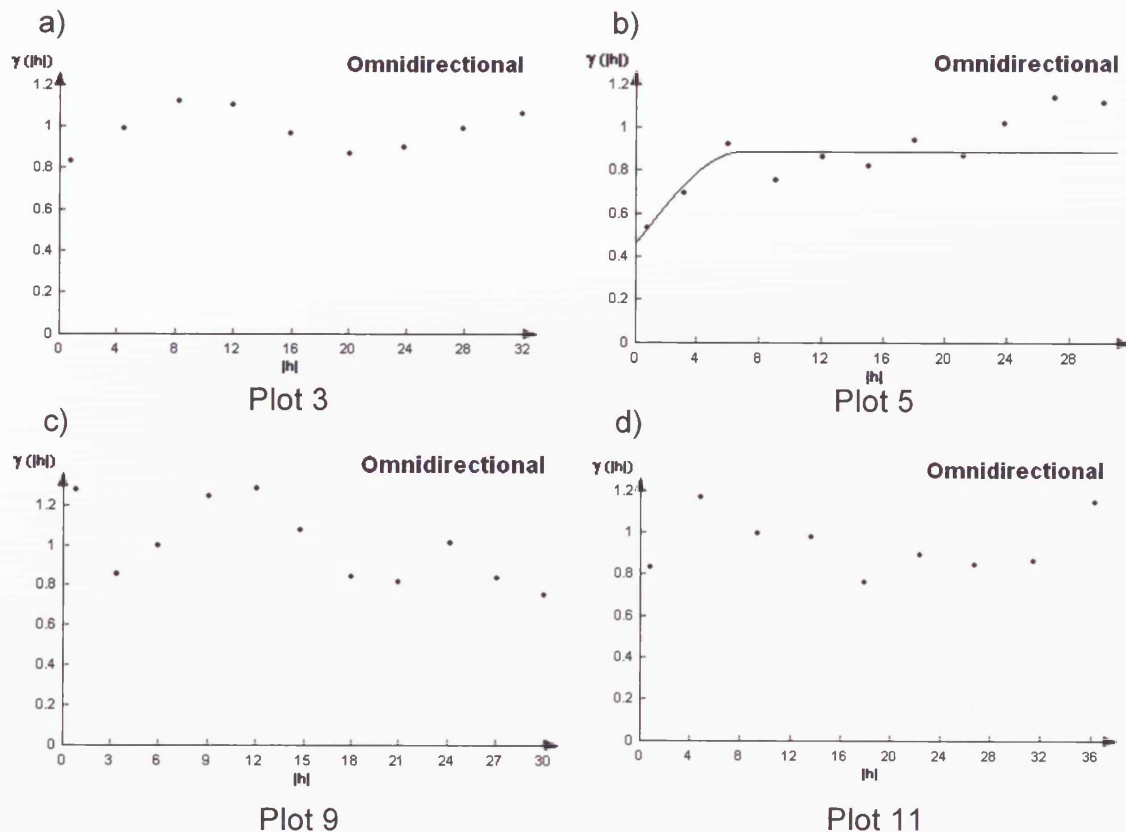


**Figure 5.8** Modelled semi-variograms for the dry bulk density of shrubland plots.

The results are as follows:

- i) Only plot 5 shows evidence of spatial autocorrelation with a range of 6.82m. The nugget-to-sill ratio indicates a moderate spatial dependency.
- ii) Plots 3, 9 and 11 are best represented by the pure nugget model indicating that no spatial patterns are evident, however, some evidence of periodicity is present in these plots suggesting that the pure nugget model may not be a true representation of the patterns of dry bulk density in these plots.
- iii) Plot 9 shows a downward trend in variance with an increasing lag distance. It is thought that this represents a checkerboard pattern in the dataset.
- iv) Plots 3 and 9 both show evidence of periodicity, however, if this is ignored and only the first 3 or 4 lags are investigated it may be argued that sills are reached producing ranges of spatial autocorrelation of approximately 9m in both cases.
- v) Through the examination of the periodicity in the data (figure 5.9) it can be concluded that although plot 9 has a shorter wavelength, in general, plots 3, 9 and 11 follow a similar wave pattern.

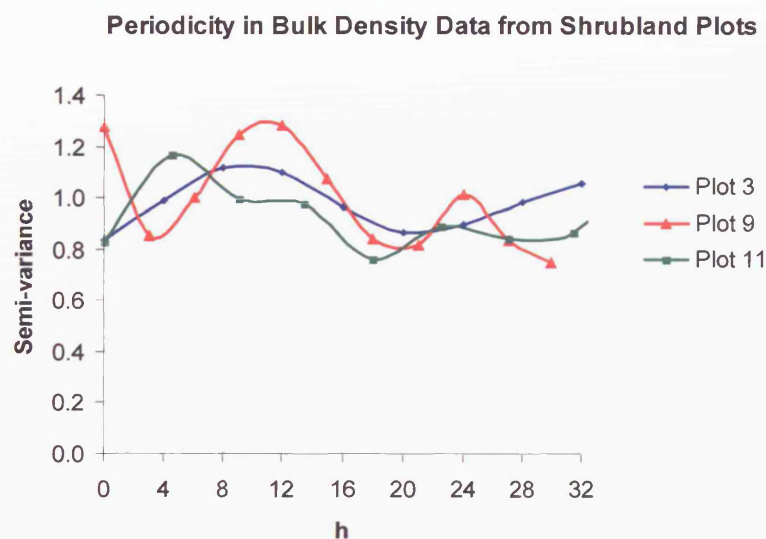


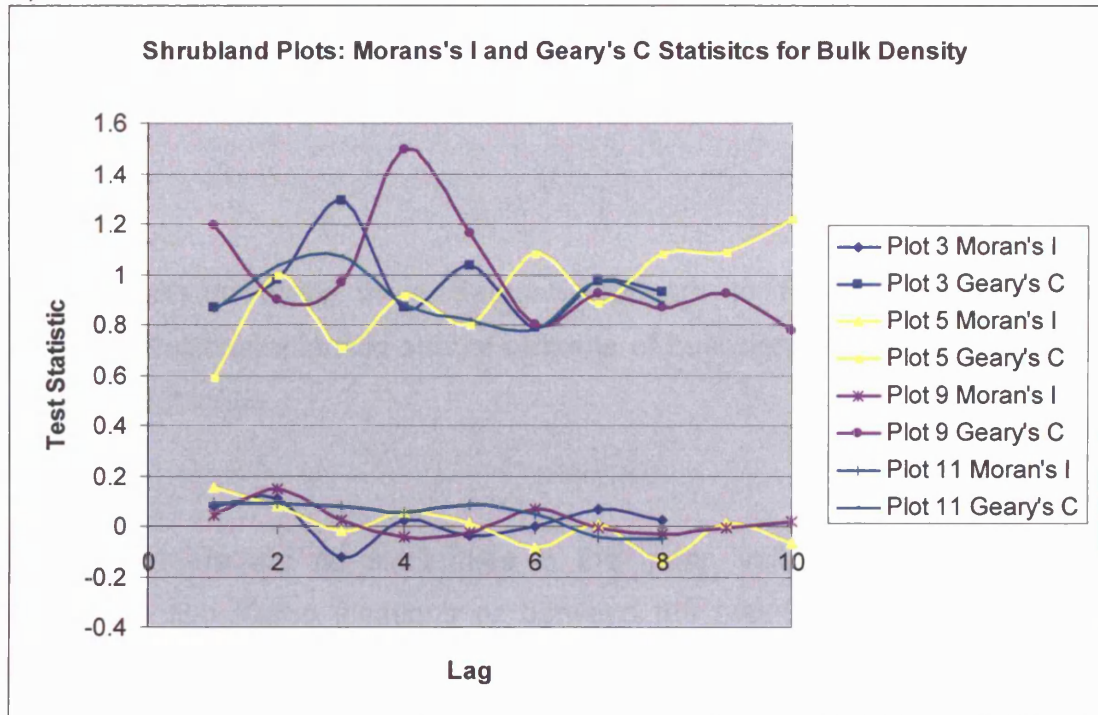
**Figure 5.9** Semi-variograms with connecting lines to show periodicity in dry bulk density data in shrubland plots.

**e) Geostatistical analysis: Moran's I and Geary's C statistics**

The results are as follows: (see figure 5.10)

- i) Comparisons made between the Moran's I and Geary's C statistics show that the results from the Moran's I correlogram produce a much weaker signal than the Geary's C. Some variation between the two types of correlograms is evident suggesting that caution should be exercised when interpreting the results, particularly with plots 9 and 11.
- ii) Interpretation of the Geary's C analysis indicates that plots 3, 9 and 11 show evidence of spatial correlation, clustering is evident at ranges less than approximately 4 - 8m, 8 - 12m and 4.5 - 9m, respectively.
- iii) Although the Geary's C correlogram suggests that a range may exist for plot 11, the Moran's I correlogram suggests the nugget model may be more appropriate as clustering is evident in the majority of lag distances.
- iv) Plot 5 demonstrates a range much greater than that determined by the semi-variogram. The correlograms suggest a range of 12 – 15m rather than a range of 6.82m derived from the semi-variogram.

a)



b)

Lag increment codes	Plot 3	Plot 5 & 9	Plot 11
1	0 > to <= 4	0 > to <= 3	0 > to <= 4.5
2	4 > to <= 8	3 > to <= 6	4.5 > to <= 9
3	8 > to <= 12	6 > to <= 9	9 > to <= 13.5
4	12 > to <= 16	9 > to <= 12	13.5 > to <= 18
5	16 > to <= 20	12 > to <= 15	18 > to <= 22.5
6	20 > to <= 24	15 > to <= 18	22.5 > to <= 27
7	24 > to <= 28	18 > to <= 21	27 > to <= 31.5
8	28 > to <= 32	21 > to <= 24	31.5 > to <= 36
9		24 > to <= 27	
10		27 > to <= 30	

**Figure 5.10** a) Moran's I and Geary's C correlograms for the dry bulk density of the shrubland plots. b) provides the key to the lag increments used in the correlograms for each plot.

### 5.3.2 Summary

Only plot 5, situated in the Karoo, demonstrates spatial autocorrelation with a range of 6.82m and a nugget-to-sill ratio of 0.52. Despite the fact that pure nugget

models have been applied to plots 3, 9 and 11, implying that no spatial patterns are present, some evidence of periodicity is present indicating that a pure nugget model may not be a true representation of the patterns of dry bulk density in these plots.

The periodicity in these three datasets appears to follow a similar pattern suggesting that characteristic spatial patterns of bulk density may indeed exist in semi-arid shrublands.

Statistically, there are no similarities in the mean values of dry bulk density between the two Karoo locations or between the two Sevilleta NWR locations implying that bulk density is site specific and thus influenced by many factors. Although the coefficients of variation values indicate more intra-plot variation within the Karoo plots, the cell by cell account demonstrates that these variations are not significant. The conclusions derived from the cell by cell variations for plots 5 and 9 correspond to those derived from the semi-variograms. Plot 5 demonstrates spatial autocorrelation and plot 9 displays a decrease in variance with increasing lag distance.

## **5.4 Soil Moisture**

### **5.4.1 Results**

As discussed in chapter 4, the antecedent weather conditions must be considered when interpreting the soil moisture results. Although detailed rainfall data are not available, a record of the weather conditions was kept throughout the fieldwork period. In the Karoo, dry conditions leading up to and during measurement of plot 3 were recorded, however, showery conditions were observed prior to the measurement of plot 5. In the Sevilleta NWR, light showers were also observed

prior to the measurement of plot 9 and 11, some localised rain was also experienced during the measurement of plot 11.

a) *Test of normality, descriptive statistics and inter-plot variation*

The frequency distributions displayed by the boxplots (figure 5.11) show that the datasets from all plots are positively skewed. Plot 11 is considered to be highly positively skewed as the skewness value is greater than 1 (see table 5.6). Outliers are evident in all datasets except the dataset from plot 3. In all cases the outliers are at the upper end of the measurements.

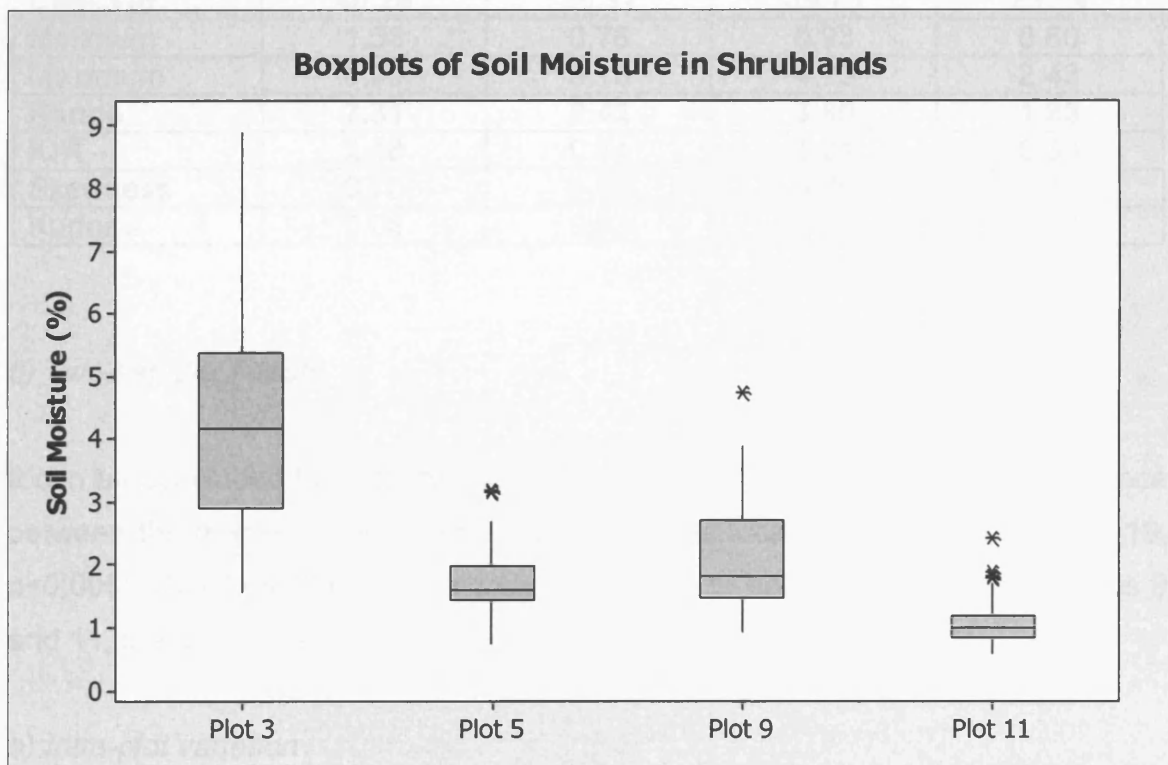


Figure 5.11 Boxplots representing the sample distribution of soil moisture in the shrubland plots.

Plot 3, situated in the Karoo, has the greatest mean value, coefficient of variation and range of all four plots. Plot 9, located in the Sevilleta NWR, has the second

highest mean value. Although this plot has a mean value and range that are approximately half that of plot 3, relative to the mean this plot demonstrates a similar amount of within-plot variation to plot 3. Plot 5 (Karoo) and plot 11 (Sevilleta NWR) have similar distributions including similar means, ranges and coefficient of variation values.

**Table 5.6** Inter-plot comparisons of descriptive statistics: Soil moisture (%)

Descriptive Statistic	Plot 3 (Karoo)	Plot 5 (Karoo)	Plot 9 (Sevilleta)	Plot 11 (Sevilleta)
Mean	4.32	1.69	2.08	1.08
Median	4.18	1.60	1.82	0.99
SE of Mean	0.17	0.04	0.08	0.03
St Dev	1.74	0.46	0.83	0.31
Variance	3.02	0.21	0.69	0.10
Coef Var	40.24	26.97	39.73	29.04
Minimum	1.58	0.76	0.93	0.60
Maximum	8.90	3.18	4.73	2.43
Range	7.31	2.42	3.80	1.83
IQR	2.48	0.54	1.21	0.34
Skewness	0.70	0.61	0.86	1.43
Kurtosis	0.04	0.93	-0.08	2.64

#### *b) Two-sample T-tests*

It can be concluded from the two-sample t-test that there is a significant difference between the means of plot 3 and 5, the two plots located in the Karoo ( $t= 15.19$ ,  $p<0.005$ ). Similarly, there is a significant difference between the means of plots 9 and 11, the two plots located in the Sevilleta NWR ( $t= 11.84$ ,  $p<0.005$ ).

#### *b) Intra-plot variation*

Examination of the means and standard deviations of each cell in the four plots (figure 5.12) suggests that although variation is evident, the scale of measurement is not a significant factor in the characterisation of soil moisture. In general, both plots 5 and 9 demonstrate a similar amount of variation across the three spatial scales. Plot 9 appears to have the most constant means and standard deviations

whereas plot 11 shows the greatest variation in soil moisture across the different spatial scales. Plots 3 and 11 both demonstrate significant variation among the six cells representing the smallest scale of measurement (1.5m x 1.5m). The varying distributions of data from cells of the same size suggest that some spatial patterns may exist. Geostatistical analysis will investigate this on a more comprehensive level.

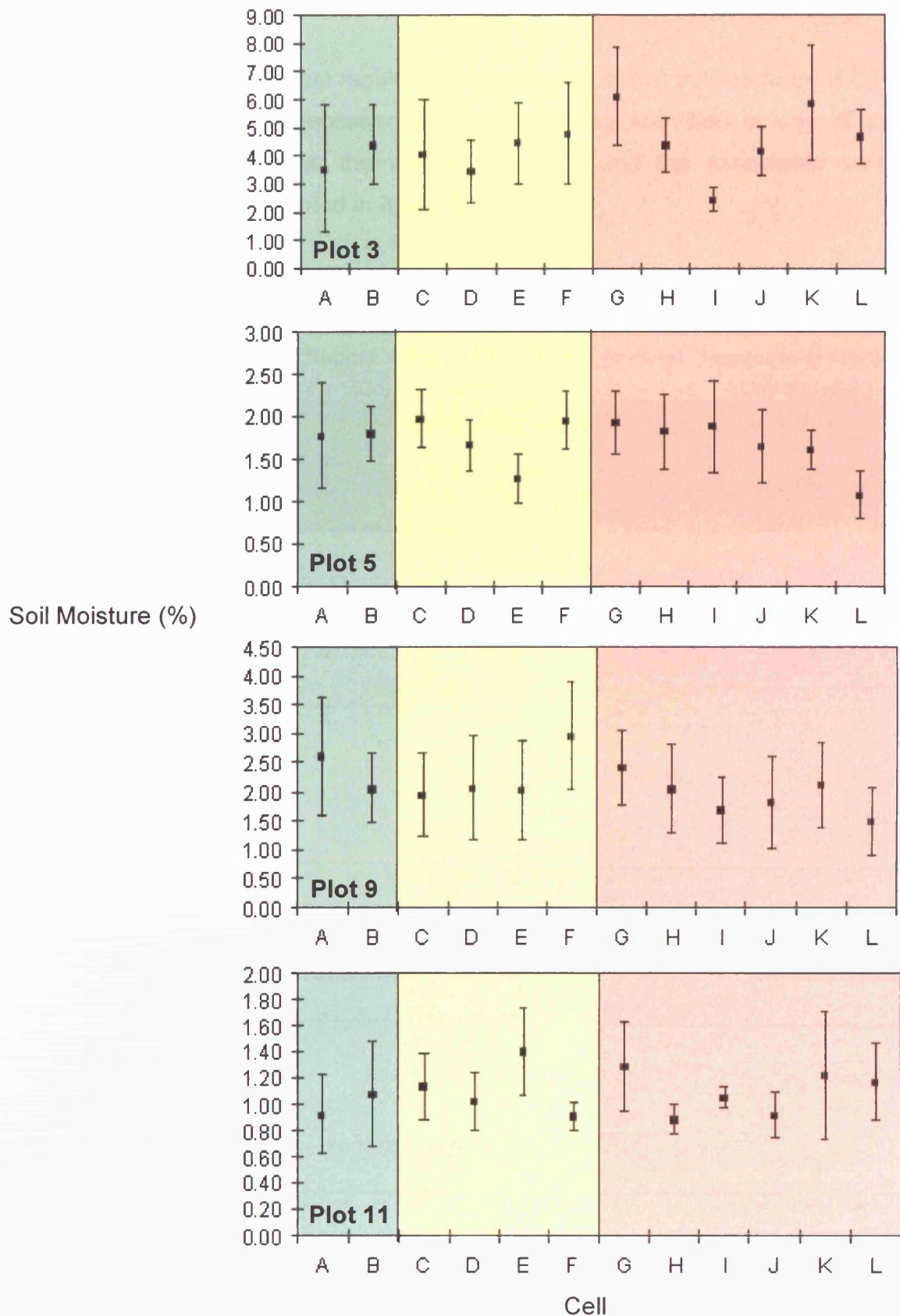


**Figure 5.12** The means and standard deviations of soil moisture for each cell within the plots. Green represents the 30 x 30m cells, yellow represents the 10 x 10m cells and pink represents 1.5 x 1.5m cells.

d) Geostatistical analysis: The semi-variogram

Pre-processing of the datasets resulted in the removal of two outliers from plot 11. No transformations were necessary and no drift was identified in any of the datasets. Table 5.7 shows the numerical results and the associated semi-variogram graphs are presented in figure 5.13.

**Table 5.7** Geostatistical analysis of the soil moisture of shrubland plots

Parameter: Soil Moisture						
No.	Plot Location	Fitted Model	Nugget Value (Co)	Sill (Co+C <sub>1</sub> )	Range (meters) (a)	Nugget-to-sill Ratio (Co)/(Co+C <sub>1</sub> )
3	Karoo	Spherical	0.50	1.05	6.60	0.48
5	Karoo	Spherical	0.57	0.96	15.84	0.59
9	Sevilleta NWR	Spherical	0.58	1.19	9.60	0.49
11	Sevilleta NWR	Spherical	0.39	1.17	7.44	0.33

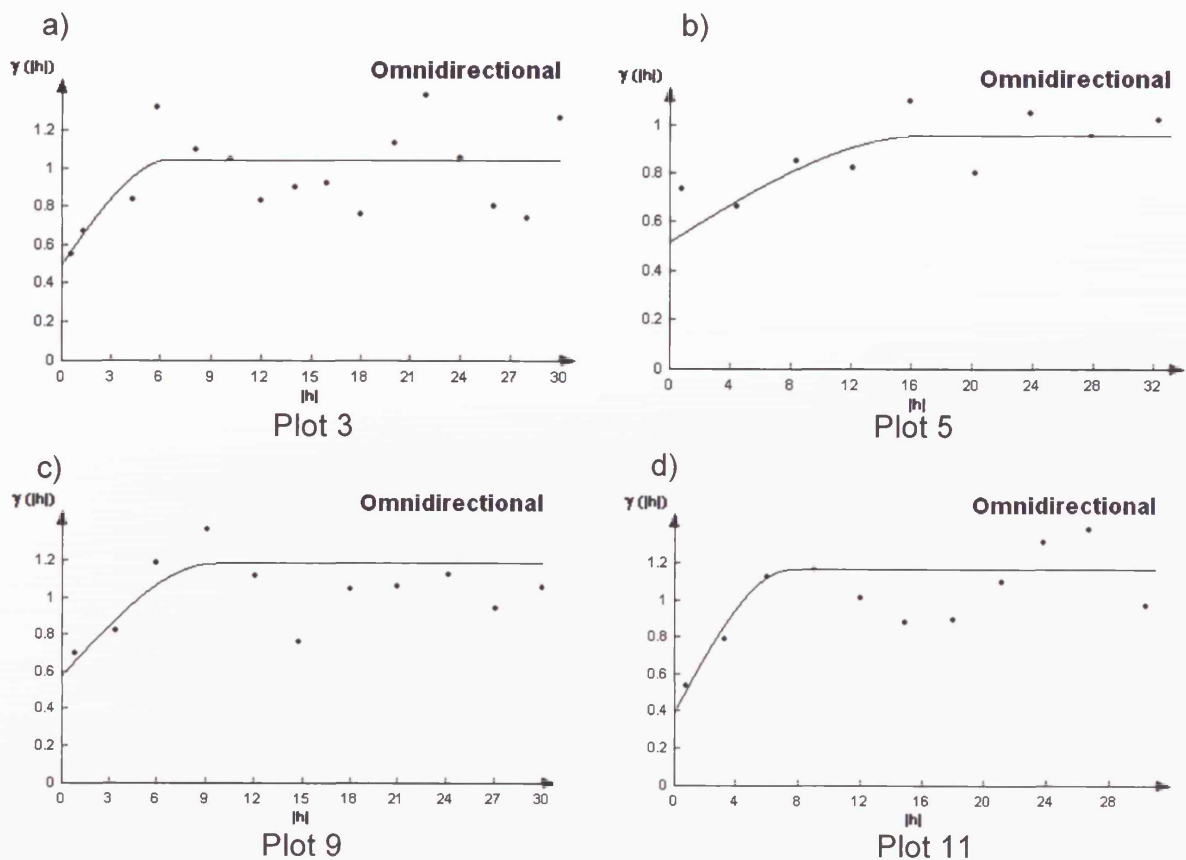


**Figure 5.13** Modelled semi-variograms for the soil moisture of shrubland plots.

The results are as follows:

- i) The spatial autocorrelation ranges of soil moisture vary from 6.60m to 15.84m and all nugget-to-sill ratios suggest moderate spatial dependency.
- ii) All plots were best represented by a spherical model.
- iii) Plots 3, 9 and 11 show elements of periodicity. Nevertheless, it is suggested that, particularly in the cases of plots 9 and 11, greater lag distances should be included before a firm conclusion is reached.
- iv) Regarding the ranges of spatial autocorrelation, there are no distinct characteristics evident with respect to the two different geographical locations of the plots.
- v) The three datasets identified as possibly demonstrating periodicity (figure 5.14) appear to have similar wavelength patterns.

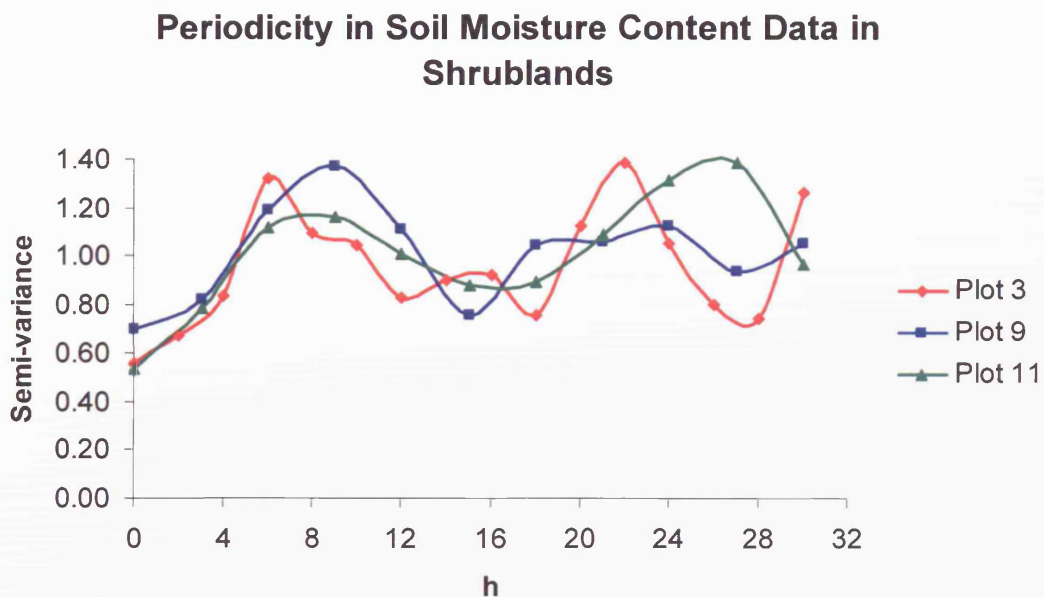


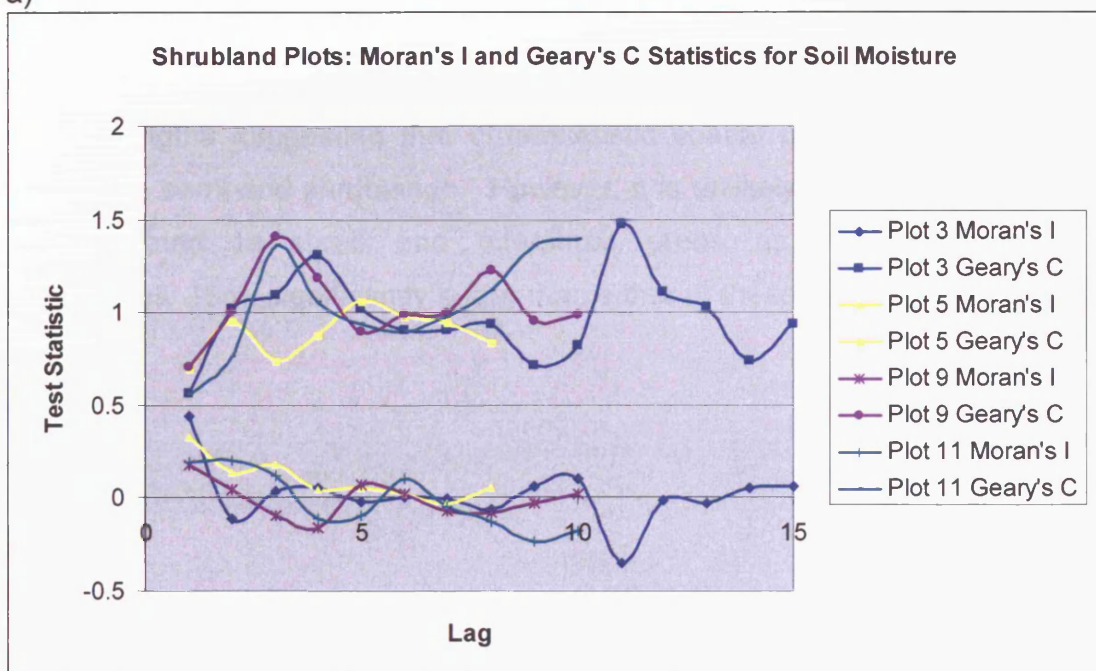
**Figure 5.14** Semi-variograms with connecting lines to show periodicity in dry bulk density data in shrubland plots.

e) Geostatistical analysis: Moran's I and Geary's C statistics

The results are as follows: (see figure 5.15)

- i) Comparisons made between the Moran's I and Geary's C statistics show that the results mirror each other relatively well; this increases the confidence in the results.
- ii) The Geary's C analysis indicates that both plots 3 and 9 show ranges of spatial autocorrelation that are slightly less than those calculated by the semi-variograms.
- iii) The ranges of autocorrelation evident in plots 5 and 11, calculated from the semi-variograms, correspond with the results derived from the Geary's C correlogram.
- iv) Although it is not as obvious in the Moran's I correlogram, the Geary's C correlogram shows that plot 5 behaves differently to the other plots. The Geary's C statistics show that at most lag distances spatial clustering exists. In addition, the test statistic at the lag distance at which the semi-variogram suggests is the threshold of spatial autocorrelation is weak. This decreases the confidence in the results derived from this plot.

a)



b)

Lag increment codes	Plot 3	Plot 5 & 9	Plot 11
1	0 > to <= 2	0 > to <= 4	0 > to <= 3
2	2 > to <= 4	4 > to <= 8	3 > to <= 6
3	4 > to <= 6	8 > to <= 12	6 > to <= 9
4	6 > to <= 8	12 > to <= 16	9 > to <= 12
5	8 > to <= 10	16 > to <= 20	12 > to <= 15
6	10 > to <= 12	20 > to <= 24	15 > to <= 18
7	12 > to <= 14	24 > to <= 28	18 > to <= 21
8	14 > to <= 16	28 > to <= 32	21 > to <= 24
9	16 > to <= 18		24 > to <= 27
10	18 > to <= 20		27 > to <= 30
11	20 > to <= 22		
12	22 > to <= 24		
13	24 > to <= 26		
14	26 > to <= 28		
15	28 > to <= 30		

**Figure 5.15** a) Moran's I and Geary's C correlograms for the soil moisture of the shrubland plots. b) provides the key to the lag increments used in the correlograms for each plot.

#### 5.4.2 Summary

All shrubland plots demonstrate spatial autocorrelation, ranging from 6.60m to 15.84m. The nugget-to-sill values suggest that all show moderate spatial correlation. Study location does not appear to influence the ranges greatly as plots 5 (Karoo) and 9 (Sevilleta NWR) exhibit the two greatest values. Although models were applied to plots 3, 9 and 11, the datasets of all three plots display fluctuating variances. A comparison of the cyclic behaviour shows a similarity in the wavelengths suggesting that characteristic spatial patterns of soil moisture may exist in semi-arid shrublands. However, it is unlikely that this pattern can be directly related to shrub and intershrub areas as the wavelengths are approximately 16m, significantly larger than either of these areas.

## 5.5 Shear strength

### 5.5.1 Results:

#### a) Test of normality, descriptive statistics and inter-plot variation

The frequency distributions displayed by the boxplots (figure 5.16) show that the datasets from all plots are positively skewed. Plots 3, 5 and 9 are considered to be highly positively skewed as the skewness values are greater than 1 (see table 5.8). Plot 11, in contrast, can be considered as having a normal distribution as the skew is not significant. Outliers are evident in these three datasets. The boxplots show the distributions of the plots can be grouped by geographical location; the two plots from the Karoo (3 & 5) have greater distributions than both the Sevilleleta plots (9 & 11).

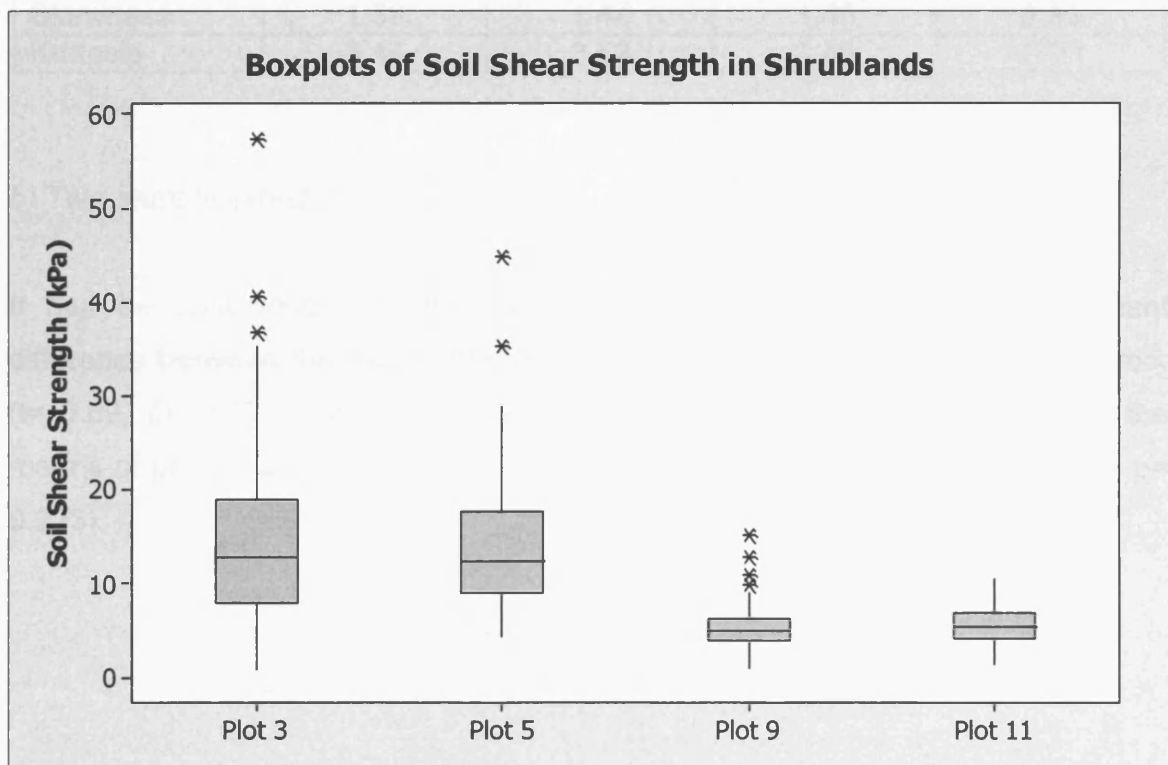


Figure 5.16 Boxplots representing the sample distribution of soil shear strength in the shrubland plots.

The mean soil shear strength of both the plots from the Sevilleta NWR are less than half those derived from the two plots in the Karoo. In addition, the ranges of both the Karoo plots are significantly greater than those found in the Sevilleta NWR. Although the Karoo plots have higher coefficients of variation, plots 9 and 11 from the Sevilleta NWR have similar values to plot 5. Therefore, relative to the mean, the variation within plots 5, 9 and 11 do not differ significantly.

**Table 5.8** Inter-plot comparisons of descriptive statistics: Soil shear strength (kPa)

Descriptive Statistic	Plot 3 (Karoo)	Plot 5 (Karoo)	Plot 9 (Sevilleta)	Plot 11 (Sevilleta)
<b>Mean</b>	<b>14.74</b>	<b>13.98</b>	<b>5.30</b>	<b>5.65</b>
Median	12.95	12.35	5.00	5.45
SE of Mean	0.90	0.65	0.22	0.18
St Dev	9.32	6.75	2.27	1.89
Variance	86.89	45.53	5.15	3.57
<b>Coef Var</b>	<b>63.24</b>	<b>48.28</b>	<b>42.83</b>	<b>33.45</b>
Minimum	0.80	4.40	1.00	1.40
Maximum	57.40	44.80	15.20	10.50
<b>Range</b>	<b>56.60</b>	<b>40.40</b>	<b>14.20</b>	<b>9.10</b>
IQR	11.00	8.73	2.30	2.88
Skewness	1.39	1.44	1.40	0.39
Kurtosis	3.44	3.52	3.49	-0.21

#### *b) Two-sample T-tests*

It can be concluded from the two-sample t-test that there is no significant difference between the means of plot 3 and 5, the two plots located in the Karoo. ( $t = 0.69$ ,  $p = 0.491$ ). Similarly, there is a no significant difference between the means of plots 9 and 11, the two plots located in the Sevilleta NWR ( $t = -1.22$ ,  $p = 0.223$ ).

*c) Intra-plot variation*

Plot 3 demonstrates a wide spread of mean shear strength values both within each cell and across the plot as a whole (see figure 5.17). However, the range of shear strength values is particularly evident in cells representing the smallest spatial scale (1.5 x 1.5 m). Interestingly, the two cells representing the largest scale (30 x 30m) show similar mean values and standard deviations. Plot 5, in contrast, demonstrates less variation in both the mean values and standard deviations across the plot. However, the plot does show greater variation in the means at the largest scale of measurement. As plots 3 and 5 are located in the Karoo the graphs suggest that the spatial patterns may differ and therefore characteristic patterns of soil shear strength may not exist for the study region. Plot 9, from the Sevilleta NWR, demonstrates significant variation among the six cells representing the smallest scale of measurement (1.5m x 1.5m) whereas the cells representing the largest spatial scale have similar means and standard deviations. The varying distributions of data from cells of the same size suggest that some spatial patterns may exist. In contrast, plot 11 shows less variation in the means and standard deviations at the smallest scale and significant differences between both the means and standard deviations from the two cells at the largest spatial scale. Again this suggests that no characteristic patterns of soil shear strength may exist for each of the study regions.



d) Geostatistical analysis: The semi-variogram

Pre-processing of the datasets resulted in the removal of one outlier from plots 3 and 5 and two outliers from plot 9. No transformations were necessary; however, drift was identified in the data from plot 5. This was removed and subsequent geostatistical analysis was carried out using the residuals. Table 5.9 shows the numerical results and the associated semi-variogram graphs are presented in figure 5.18.

Table 5.9 Geostatistical analysis of the soil shear strength of shrubland plots

Parameter: Shear Strength						
No.	Plot	Fitted Model	Nugget Value (Co)	Sill (Co+C <sub>1</sub> )	Range (meters) (a)	Nugget-to-sill Ratio (Co)/(Co+C <sub>1</sub> )
3	Karoo	Nugget	1.00	na	Na	na
5	Karoo	Power	0.63	Power: 0.52	Slope: 0.06	
9	Sevilleta NWR	Spherical	0.61	0.96	4.20	0.64
11	Sevilleta NWR	Spherical	0.60	1.07	9.61	0.56

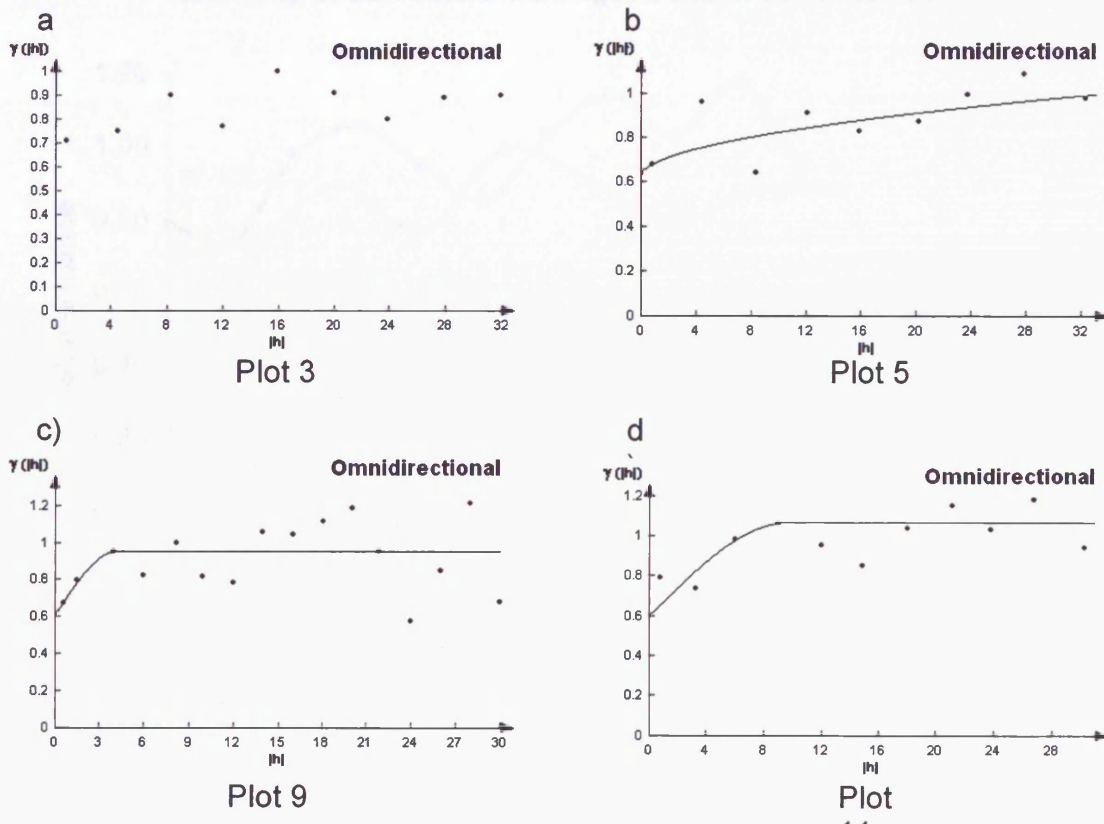
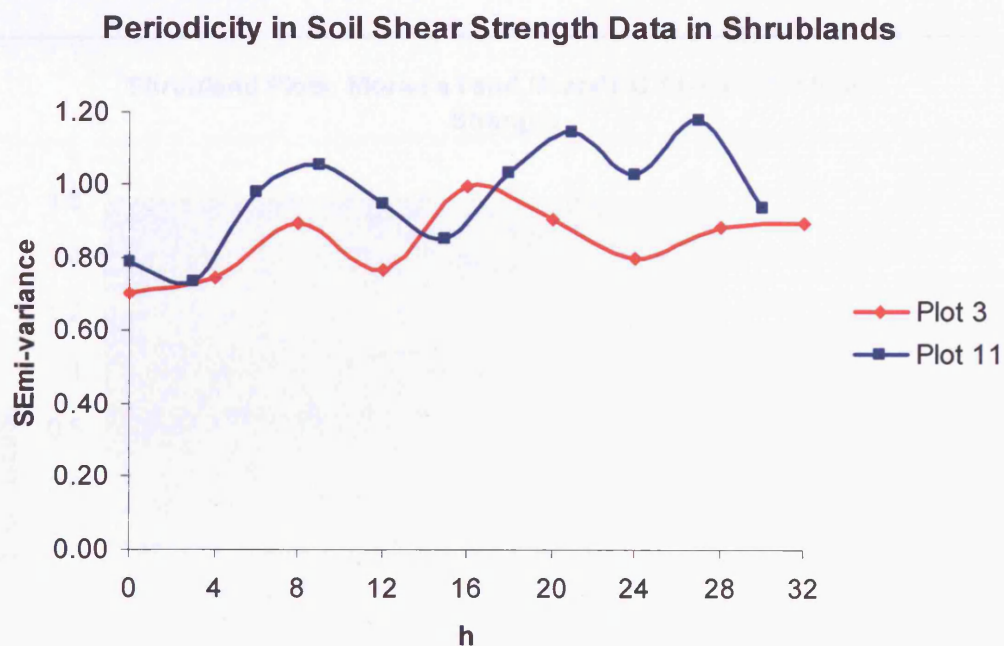


Figure 5.18 Modelled semi-variograms for the soil shear strength of shrubland plots.

The results are as follows:

- i) The two plots from the Sevilleta NWR, plots 9 and 11, show ranges of spatial autocorrelation of 4.20m and 9.61m, respectively.
- ii) The data from both these plots were best represented by a spherical model and both show moderate spatial dependency.
- iii) A pure nugget model was used to describe the data derived from plot 1.
- iv) Although the residuals were used to calculate the semi-variogram for plot 5 and upward trend was still apparent therefore a power model has been applied to the data. No sill is reached thus no range of spatial autocorrelation is evident.
- v) Plots 3 and 11 show evidence of periodicity (figure 5.19). Although the wavelengths do not match exactly, both peak for the first time at a lag distance of 9m.

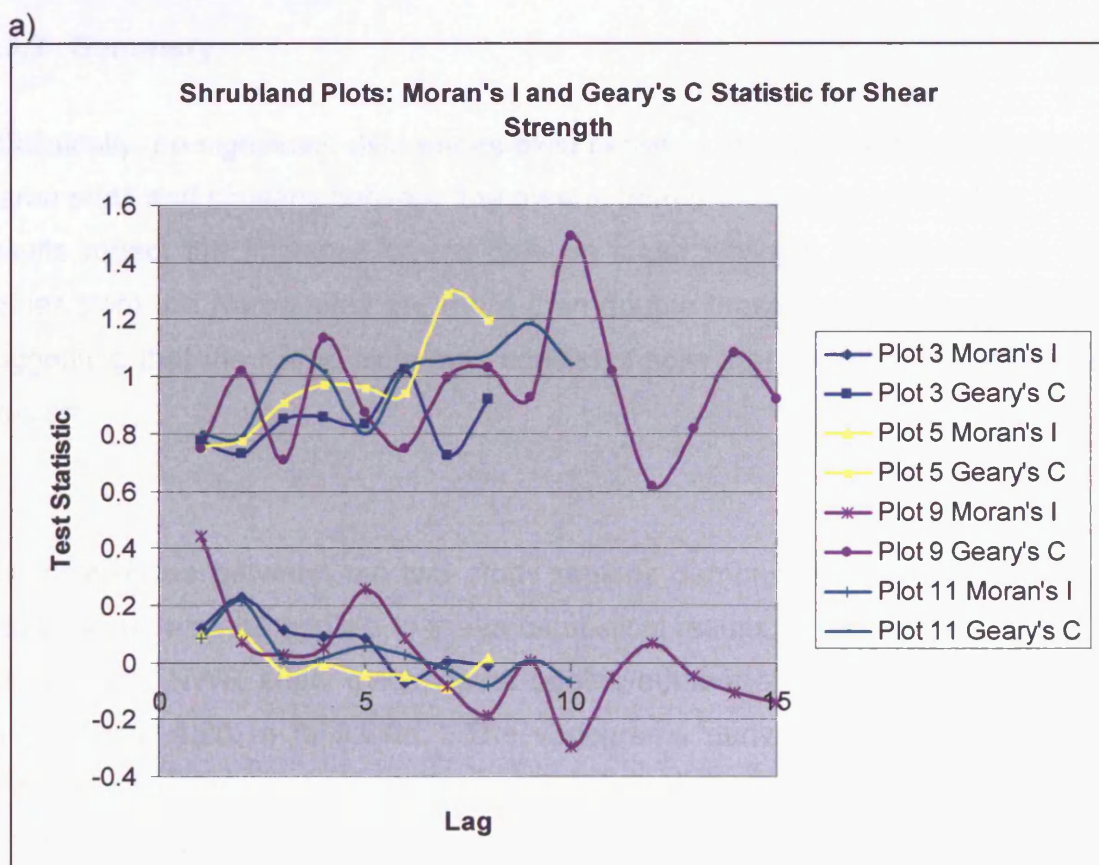


**Figure 5.19** Semi-variograms with connecting lines to show periodicity in soil shear strength data in shrubland plots.

e) Geostatistical analysis: Moran's I and Geary's C statistics

The results are as follows: (see figure 5.20)

- i) At the smaller lag distances the Moran's I and Geary's C statistics do not correspond as well as they have done for other soil parameters. This is particularly evident for plot 9.
- ii) The Geary's C correlogram, however, produces results that correspond to the ranges of spatial autocorrelation for plots 9 and 11 derived from the semi-variograms.
- iii) The Geary's C correlograms of plots 3 and 5 suggest that it is possible ranges may exist, both between lag distances of 20 and 24m. However, it appears that this is more likely to be true of plot 5 as the significance of the test statistic of plot 3 is low.



b)

Lag increment codes	Plot 3 & 5	Plot 9	Plot 11
1	0 > to <= 4	0 > to <= 2	0 > to <= 3
2	4 > to <= 8	2 > to <= 4	3 > to <= 6
3	8 > to <= 12	4 > to <= 6	6 > to <= 9
4	12 > to <= 16	6 > to <= 8	9 > to <= 12
5	16 > to <= 20	8 > to <= 10	12 > to <= 15
6	20 > to <= 24	10 > to <= 12	15 > to <= 18
7	24 > to <= 28	12 > to <= 14	18 > to <= 21
8	28 > to <= 32	14 > to <= 16	21 > to <= 24
9		16 > to <= 18	24 > to <= 27
10		18 > to <= 20	27 > to <= 30
11		20 > to <= 22	
12		22 > to <= 24	
13		24 > to <= 26	
14		26 > to <= 28	
15		28 > to <= 30	

**Figure 5.20** a) Moran's I and Geary's C correlograms for the soil shear strength of the shrubland plots. b) provides the key to the lag increments used in the correlograms for each plot.

### 5.5.2 Summary

Statistically, no significant differences exist between the mean values from the two Karoo plots and similarly between the means from the Sevilleta NWR plots. These results reflect the influence of soil type on shear strength measurements. The values from the Karoo sites are more than double those from the Sevilleta NWR suggesting that the Karoo plots may consist of soils that are more resistant to soil erosion.

The differences between the two study regions demonstrated by the descriptive statistics can also be applied to the geostatistical results. The two plots located in the Sevilleta NWR show evidence of spatial autocorrelation despite the ranges varying from 4.20 m to 9.61m. The variograms derived from the Karoo data, however, do not reach a sill. A power function was applied to plot 5 representing a variance that continually increases with an increasing lag distance. Although a pure nugget model being applied to plot 3 thus indicating random variance, a slight upward trend is also evident in this plot albeit weaker than plot 5.

## 5.6 Soil-aggregate stability

The problems associated with the technique employed to measure the aggregate stability has been discussed in chapter 4. Two plots were chosen to represent the shrublands from each of the study regions, plot 5 from the Karoo and plot 9 from the Sevilleta NWR.

### 5.6.1 Results

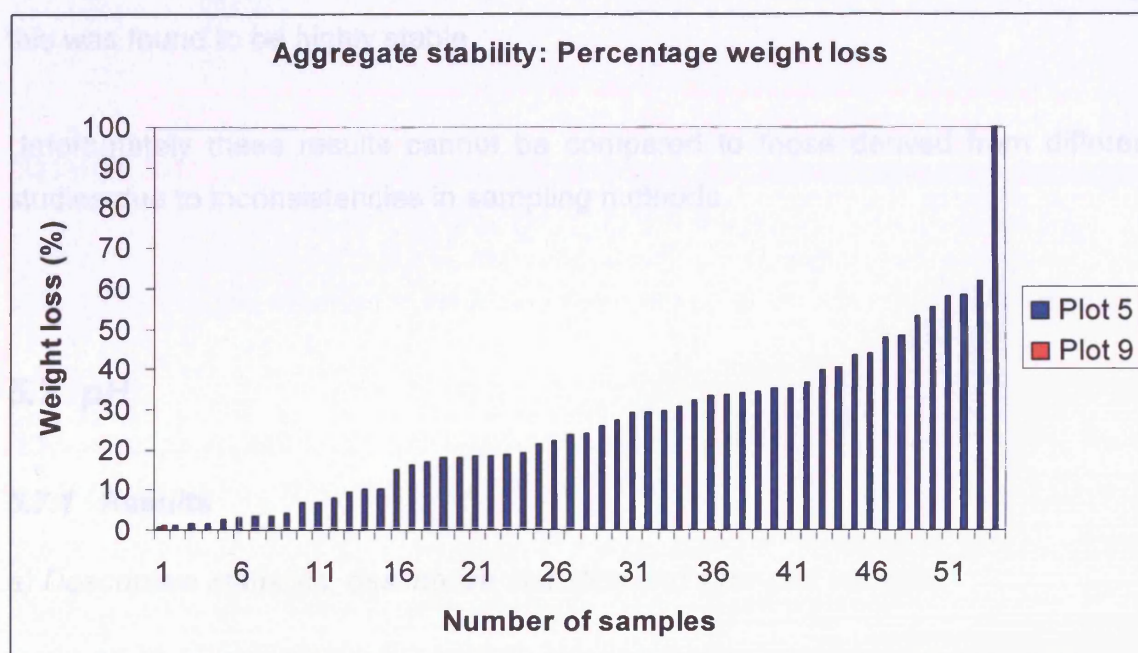


**Figure 5.21** The number of aggregates obtained from plots 3 and 5 and the percentage weight loss after agitation in water.

From figure 5.21 a number of observations can be made about the aggregate stability of soil in the two semi-arid shrubland plots:

- i) Out of 108 samples, plot 9 (Sevilleta, NWR) only had 1 sample containing suitable aggregates. This suggests that the soil structure is very weak. However, this one sample was very stable.
- ii) Plot 5, situated in the Karoo, S.A. had significantly more measurable aggregates. Nearly 90% of the aggregate samples lost less than 50% of

their total weight and nearly 30% only lost 10% of their total weight. Only one sample dispersed completely.

### 5.6.2 Summary

The shrubland plot located in the Karoo (plot 5) is the most stable. This plot had significantly more measurable aggregates, most of which were relatively stable. In contrast, the soil from plot 9, situated in the Sevilleta NWR, has an extremely weak structure. Only one suitable sample was obtained from a total of 108, although this was found to be highly stable.

Unfortunately these results cannot be compared to those derived from different studies due to inconsistencies in sampling methods.

## 5.7 pH

### 5.7.1 Results

#### *a) Descriptive statistics, descriptive statistics and inter-plot variation*

The frequency distributions displayed by the boxplots (figure 5.22) show that plot 3 is positively skewed, plot 5 can be classed as a normal distribution and the two plots from the Sevilleta NWR, plots 9 and 11, are negatively skewed. Outliers are evident in all datasets. Although by taking an average of three soil pH readings it is hoped that measurement error is reduced, a number of extreme values are evident. The distributions of plots 9 and 11 in particular are strongly influenced by such values.

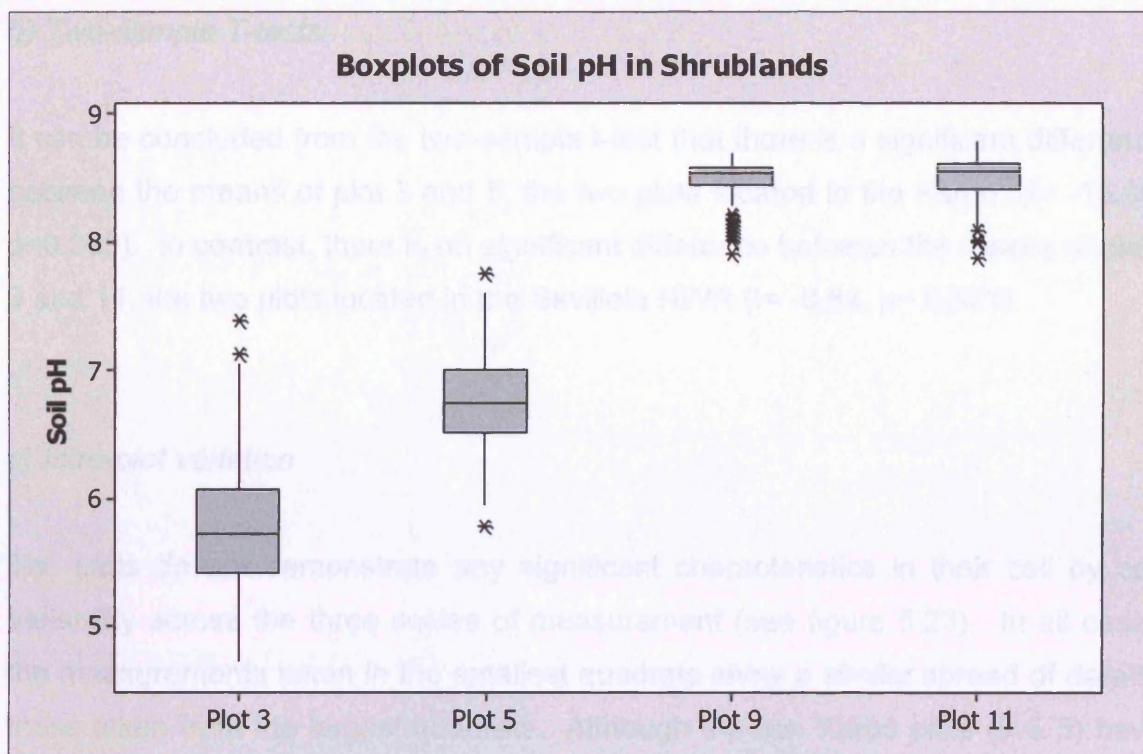


Figure 5.22 Boxplots representing the sample distribution of soil pH in the shrubland plots.

The descriptive statistics show a difference between the pH values from the Karoo sites and the sites from the Sevilleta NWR. Table 5.10 shows that the soils from the Karoo are acidic ( $< \text{pH}7$ ) whereas the soils from the Sevilleta NWR are alkaline ( $> \text{pH}7$ ). The coefficient of variance and range values show that pH values within plots 9 and 11 fluctuate significantly less than plots 1 and 2.

Table 5.10 Inter-plot comparisons of descriptive statistics: Soil pH

Descriptive Statistic	Plot 3 (Karoo)	Plot 5 (Karoo)	Plot 9 (Sevilleta)	Plot 11 (Sevilleta)
Mean	5.79	6.75	8.48	8.50
Median	5.73	6.74	8.53	8.55
SE of Mean	0.05	0.03	0.01	0.02
St Dev	0.55	0.35	0.15	0.18
Variance	0.30	0.12	0.02	0.03
Coef Var	9.46	5.21	1.74	2.11
Minimum	4.73	5.78	7.91	7.88
Maximum	7.38	7.75	8.69	8.77
Range	2.65	1.96	0.78	0.89
IQR	0.66	0.48	0.14	0.20
Skewness	0.57	0.11	-1.70	-1.25
Kurtosis	0.07	0.45	3.01	1.58

***b) Two-sample T-tests***

It can be concluded from the two-sample t-test that there is a significant difference between the means of plot 3 and 5, the two plots located in the Karoo. ( $t = -15.30$ ,  $p < 0.005$ ). In contrast, there is no significant difference between the means of plots 9 and 11, the two plots located in the Sevilleta NWR ( $t = -0.64$ ,  $p = 0.521$ ).

***c) Intra-plot variation***

The plots do not demonstrate any significant characteristics in their cell by cell variability across the three scales of measurement (see figure 5.23). In all cases the measurements taken in the smallest quadrats show a similar spread of data to those taken from the largest quadrats. Although the two Karoo plots (3 & 5) have an overall greater variability in values within the cells, the Sevilleta NWR plots (9 & 11) demonstrate greater variation among the cells. However, variability does not appear to be influenced by the scale of measurement. This may indicate that spatial autocorrelation of soil pH is more likely to be evident in the Sevilleta NWR plots.

### Geostatistical analysis: The semi-variogram

Pre-processing of the data from plot 1 was carried out and the results and the associated

Table 5.11 Geostatistical Parameter: pH

Plot

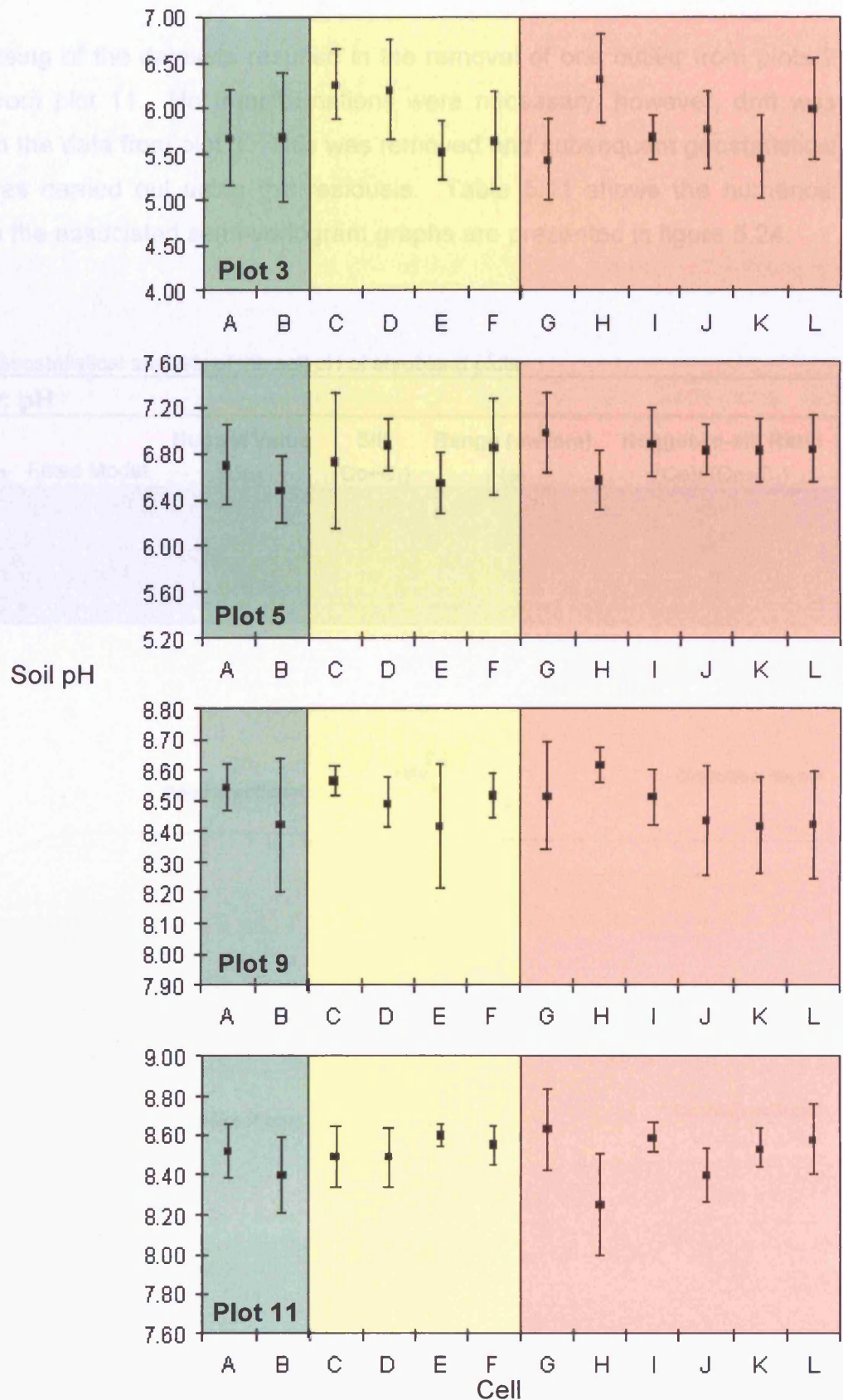


**Figure 5.23** The means and standard deviations of soil pH for each cell within the plots. Green represents the 30 x 30m cells, yellow represents the 10 x 10m cells and pink represents 1.5 x 1.5m cells.

## d) Geostatistical analysis: The semi-variogram

Pre-processing of the datasets resulted in the removal of one outlier from plots 9 and four from plot 11. No transformations were necessary; however, drift was identified in the data from plot 3. This was removed and subsequent geostatistical analysis was carried out using the residuals. Table 5.11 shows the numerical results and the associated semi-variogram graphs are presented in figure 5.24.

Table 5.11 Geostatistical analysis of the soil pH of shrubland plots

Parameter: pH						
Plot No.	Location	Fitted Model	Nugget Value (Co)	Sill (Co+C <sub>1</sub> )	Range (meters) (a)	Nugget-to-sill Ratio (Co)/(Co+C <sub>1</sub> )
3	Karoo	Spherical	0.65	1.06	15.54	0.61
5	Karoo	Spherical	0.60	1.01	5.89	0.59
9	Sevilleta	None	na	na	na	na
11	Sevilleta	None	na	na	na	na

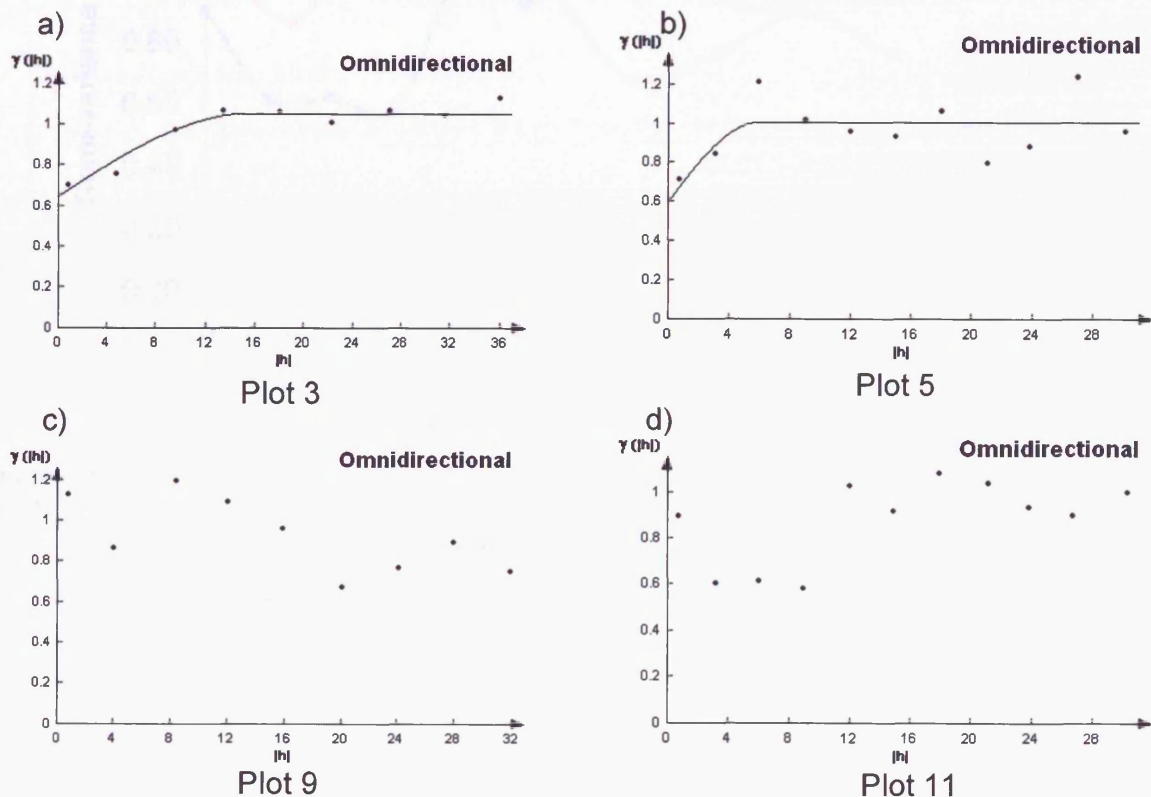
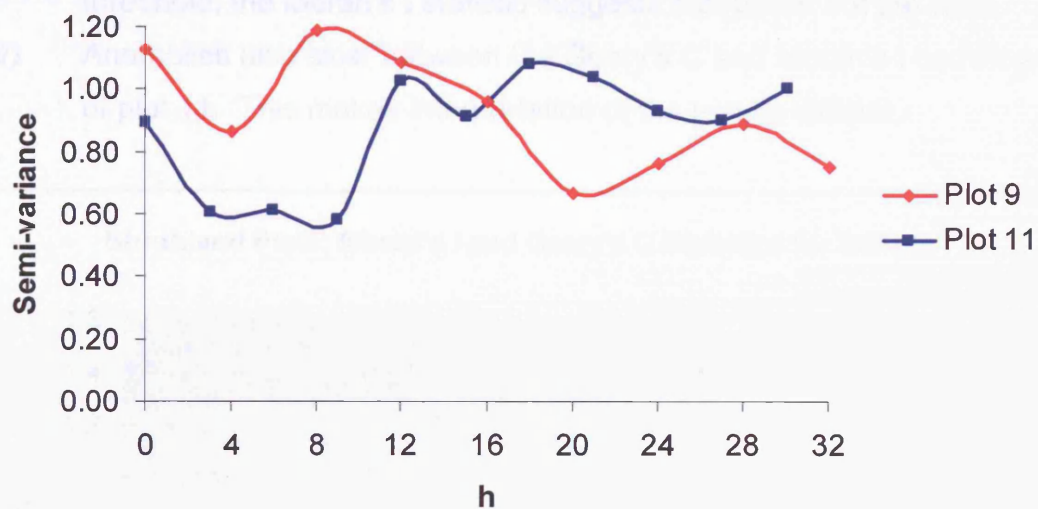


Figure 5.24 Modelled semi-variograms for the pH of shrubland plots.

The results are as follows:

- i) The two plots from the Karoo (3 & 5) demonstrate spatial autocorrelation of soil pH with ranges of 15.54m and 5.89m, respectively.
- ii) A spherical model was applied to the two modelled plots; nugget-to-sill ratios of 0.61 and 0.59 suggest that moderate to weak spatial dependency describes plots 3 and 5.
- iii) Plots 9 and 11, located in the Sevilleta NWR have not been modelled as none of the simple models were deemed appropriate.
- iv) Both the semi-variogram and the periodicity graph (figure 5.25) of plot 9 demonstrate a downward trend of variance with increasing lag distances.
- v) Plot 11 may be illustrating the 'hole effect' at the smaller lag distances, the variance appears to reach a sill at a range of approximately 12m.

Periodicity in pH Data in Shrublands

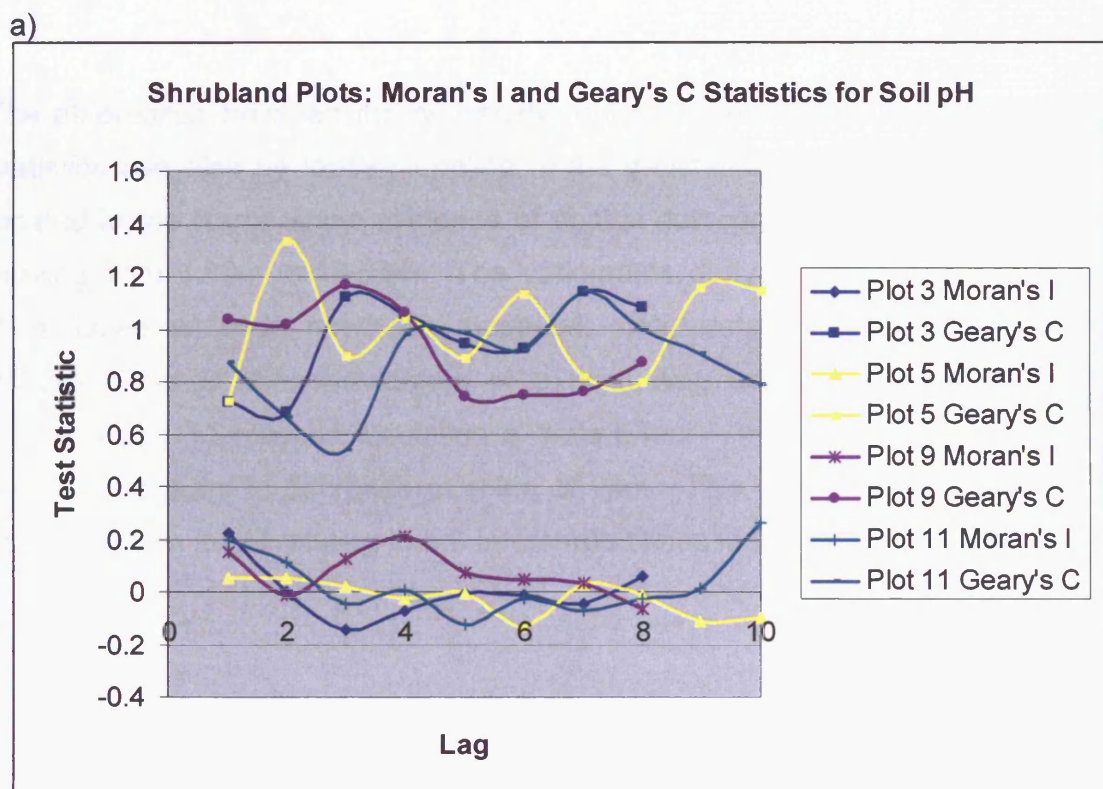


**Figure 5.25** Semi-variograms with connecting lines to show periodicity in soil pH data in shrubland plots.

e) *Geostatistical analysis: Moran's I and Geary's C statistics*

The results are as follows: (see figure 5.26)

- i) Comparisons made between the Moran's I and Geary's C statistics show that the results from the Moran's I correlogram produce a much weaker signal than the Geary's C. Some variation between the two types of correlograms is evident suggesting that caution should be exercised when interpreting the results.
- ii) Interpretation of the Geary's C analysis indicates that plots 3 and 5 show evidence of spatial correlation, clustering is evident at ranges less than approximately 9 - 13.5m and 1.5 - 3m, respectively. Both these ranges are approximately 2m less than those estimated by the semi-variogram.
- iii) Although the Geary's C correlogram suggests that the pH in plot 9 shows no spatial autocorrelation at lag distances less than 12 - 16m and then shows evidence of spatial clustering at lags greater than this threshold, the Moran's I statistic suggests that this is not the case.
- iv) Anomalies also exist between the Geary's C and Moran's I correlograms of plot 11. This makes interpretation of the results difficult.



b)

Lag increment codes	Plot 3	Plot 5 & 11	Plot 9
1	0 > to <= 4.5	0 > to <= 3	0 > to <= 4
2	4.5 > to <= 9	3 > to <= 6	4 > to <= 8
3	9 > to <= 13.5	6 > to <= 9	8 > to <= 12
4	13.5 > to <= 18	9 > to <= 12	12 > to <= 16
5	18 > to <= 22.5	12 > to <= 15	16 > to <= 20
6	22.5 > to <= 27	15 > to <= 18	20 > to <= 24
7	27 > to <= 31.5	18 > to <= 21	24 > to <= 28
8	31.5 > to <= 36	21 > to <= 24	28 > to <= 32
9		24 > to <= 27	
10		27 > to <= 30	

**Figure 5.26** a) Moran's I and Geary's C correlograms for the soil pH of the shrubland plots. b) provides the key to the lag increments used in the correlograms for each plot.

### 5.7.2 Summary

Again the shrubland results show that the Karoo soils are acidic whereas the Sevilleta NWR soils are alkaline. However, statistical evidence suggests that the mean values of the two Karoo plots are different whereas no significant differences exist between the two means from the Sevilleta NWR sites.

The differences between the two study regions demonstrated by the descriptive statistics can also be loosely applied to the geostatistical results. The two plots located in the Karoo show evidence of spatial autocorrelation despite the ranges varying from 5.89m to 15.54m. The variograms derived from the Sevilleta NWR data, however, have not been modelled. Interpretation of these two plots is difficult. Plot 9 shows evidence of a fluctuating downward trend in variance whereas plot 11 may be exhibiting a 'hole effect'. In both cases, however, the variance appears to decrease at a lag of ~4m. This may indicate some level of spatial pattern in pH relating to the intershrub zones in the Sevilleta NWR.

## 5.8 Electrical conductivity

### 5.8.1 Results

#### a) Test of normality, descriptive statistics and inter-plot variation

The frequency distributions displayed by the boxplots (figure 5.27) show that the datasets from all plots are positively skewed. Plots 3, 9 and 11 are considered to be highly positively skewed as the skewness values are greater than 1 (see table 5.12). Outliers are evident in all datasets and are only present at the upper region of the scale.

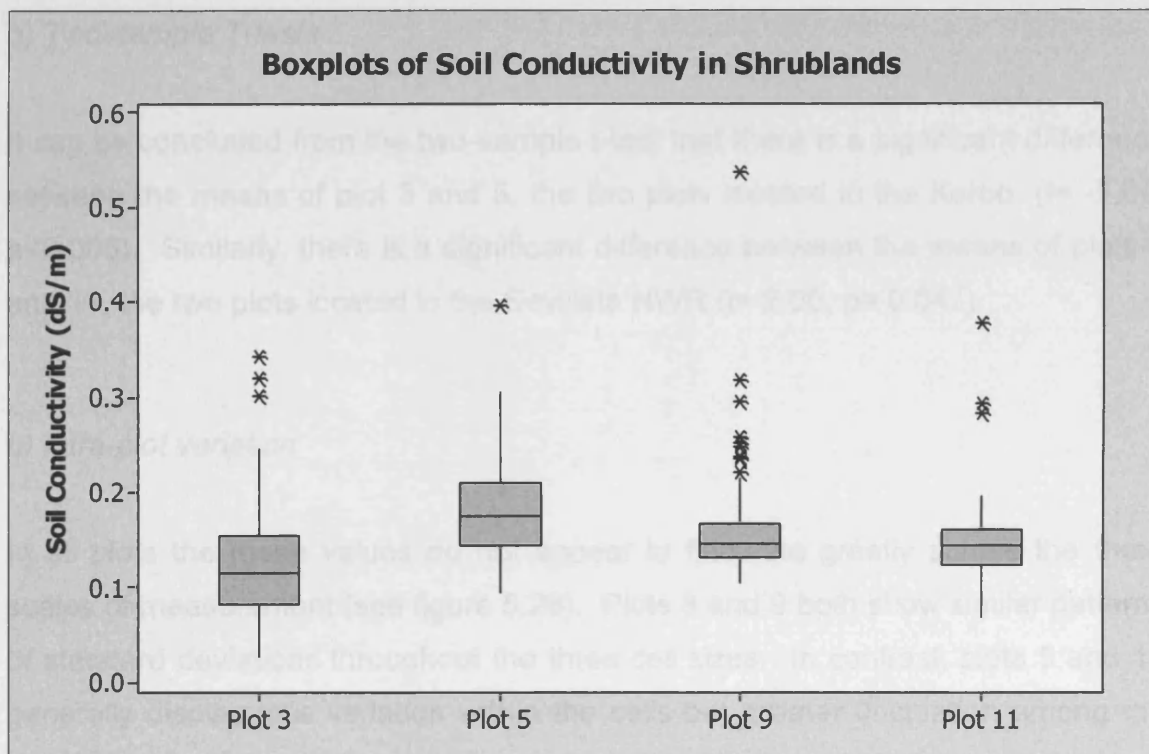


**Figure 5.27** Boxplots representing the sample distribution of soil conductivity in the shrubland plots.

Inter-plot comparisons (table 5.12) show that the mean values of conductivity are similar in all the plots. No significant differences in the descriptive statistics are evident between the Karoo plots and the Sevilleta plots suggesting that both regions have relatively similar distribution characteristics.

**Table 5.12** Inter-plot comparisons of descriptive statistics: Soil conductivity ( $\text{dS m}^{-1}$ )

Descriptive Statistic	Plot 3 (Karoo)	Plot 5 (Karoo)	Plot 9 (Sevilleta)	Plot 11 (Sevilleta)
Mean	0.13	0.18	0.16	0.15
Median	0.12	0.18	0.15	0.14
SE of Mean	0.01	0.00	0.01	0.00
St Dev	0.06	0.05	0.05	0.04
Variance	0.00	0.00	0.00	0.00
Coef Var	45.95	28.37	32.77	27.59
Minimum	0.03	0.10	0.11	0.07
Maximum	0.34	0.40	0.54	0.38
Range	0.32	0.30	0.43	0.31
IQR	0.07	0.07	0.03	0.04
Skewness	1.36	0.94	4.28	2.36
Kurtosis	2.54	1.86	26.34	11.54

#### b) Two-sample T-tests

It can be concluded from the two-sample t-test that there is a significant difference between the means of plot 3 and 5, the two plots located in the Karoo. ( $t = -7.60$ ,  $p < 0.005$ ). Similarly, there is a significant difference between the means of plots 9 and 11, the two plots located in the Sevilleta NWR ( $t = 2.00$ ,  $p = 0.047$ ).

#### b) Intra-plot variation

In all plots the mean values do not appear to fluctuate greatly across the three scales of measurement (see figure 5.28). Plots 3 and 9 both show similar patterns of standard deviations throughout the three cell sizes. In contrast, plots 5 and 11 generally display less variation within the cells but greater fluctuation among the cells. However, this does not appear to be related to the scale of measurement.

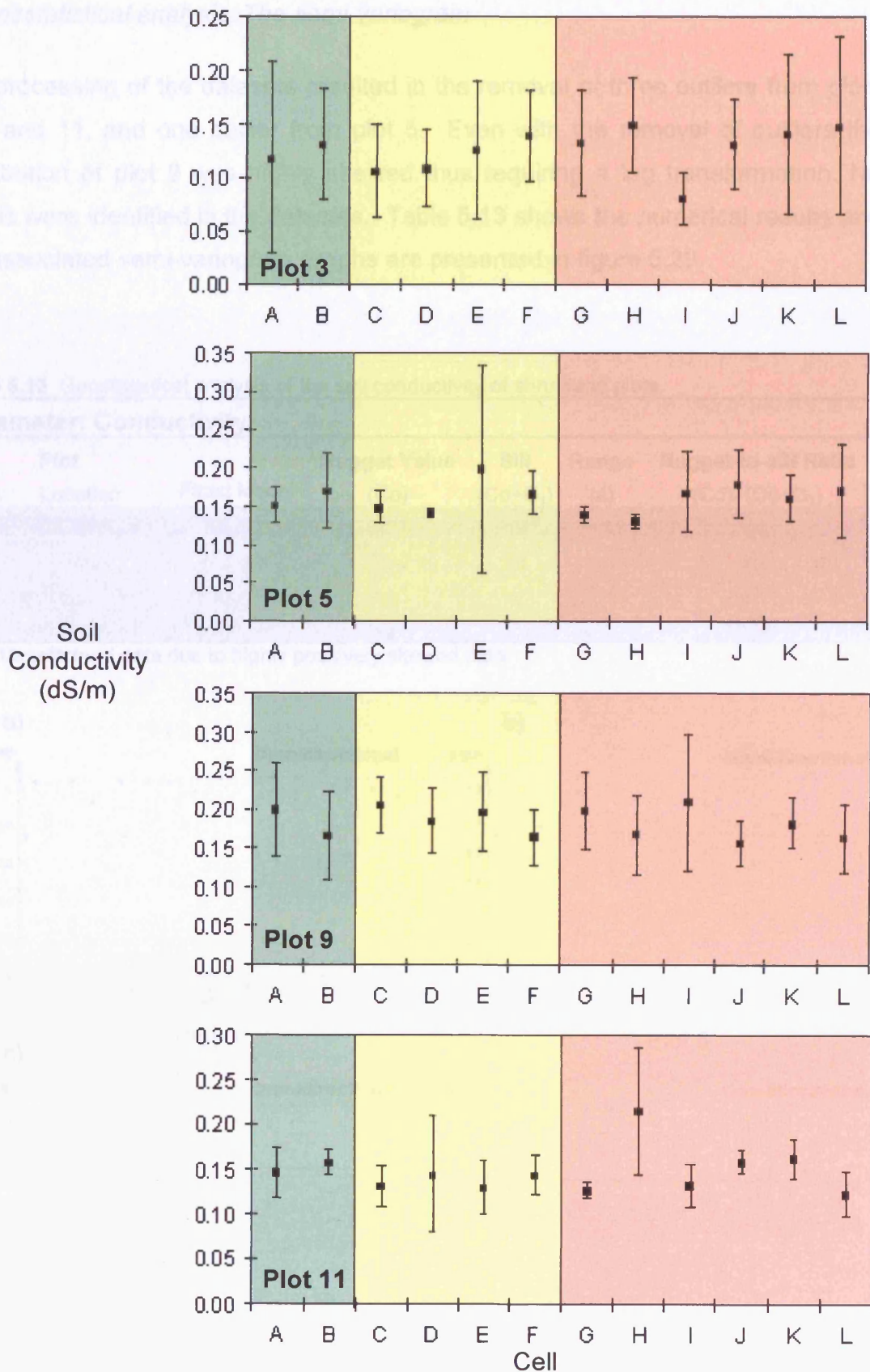


**Figure 5.28** The means and standard deviations of soil conductivity for each cell within the plots. Green represents the 30 x 30m cells, yellow represents the 10 x 10m cells and pink represents 1.5 x 1.5m cells.

## d) Geostatistical analysis: The semi-variogram

Pre-processing of the datasets resulted in the removal of three outliers from plots 3, 9 and 11, and one outlier from plot 5. Even with the removal of outliers the distribution of plot 9 was highly skewed thus requiring a log transformation. No trends were identified in the datasets. Table 5.13 shows the numerical results and the associated semi-variogram graphs are presented in figure 5.29.

Table 5.13 Geostatistical analysis of the soil conductivity of shrubland plots

Parameter: Conductivity						
No.	Plot Location	Fitted Model	Nugget Value (Co)	Sill (Co+C <sub>1</sub> )	Range (a)	Nugget-to-sill Ratio (Co)/(Co+C <sub>1</sub> )
3	Karoo	Nugget	1.00	na	na	na
5	Karoo	Nugget	1.00	na	na	na
9	Sevilleta NWR*	Spherical	0.56	0.91	8.1	0.62
11	Sevilleta NWR	Spherical	0.31	1.10	5.27	0.28

\* Log transformed data due to highly positively skewed data

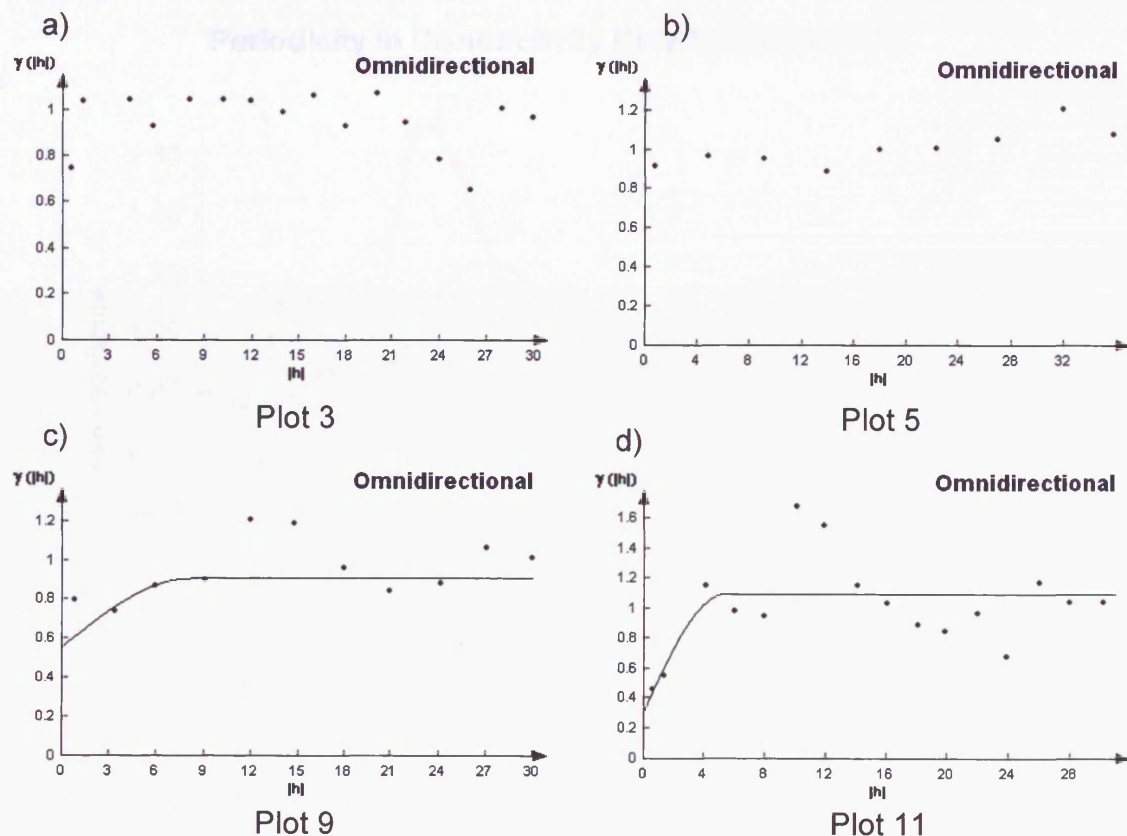
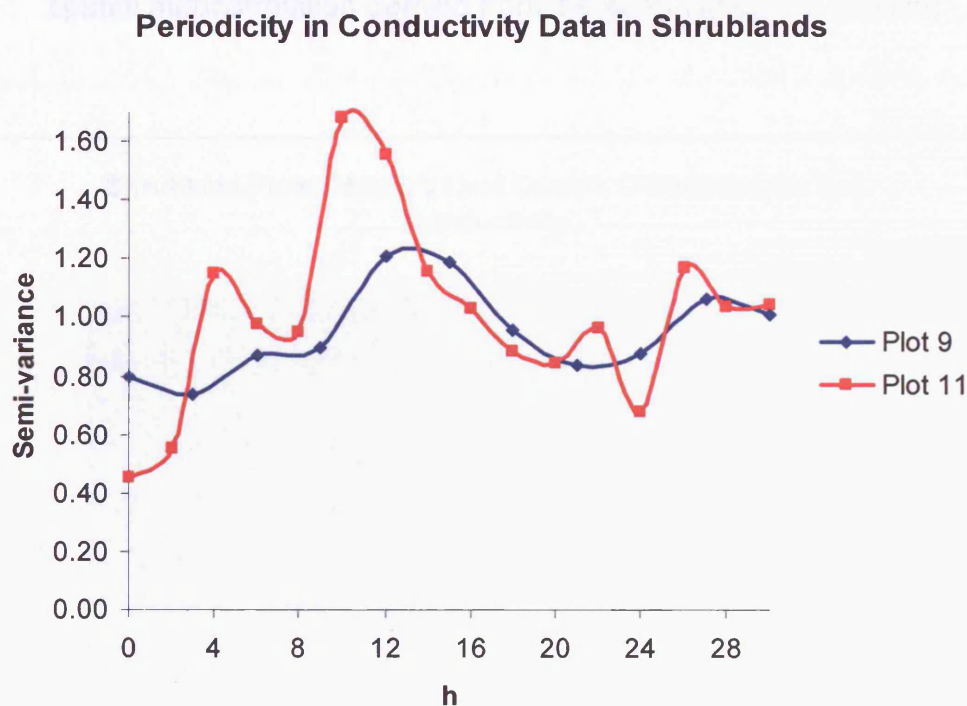


Figure 5.29 Modelled semi-variograms for the conductivity of shrubland plots.

The results are as follows:

- i) The two plots located in the Karoo, plots 3 and 5, were best represented by a pure nugget model indicating no spatial autocorrelation is present.
- ii) The two plots located in the Sevilleta NWR, plots 9 and 11, demonstrate spatial autocorrelation ranges of 8.1m and 5.27m, respectively. In both cases a spherical model was applied.
- iii) A nugget-to-sill ratio of 0.62 suggests that moderate to weak spatial dependency describes the results from plot 9, whereas a ratio of 0.28 suggests that a moderate to strong spatial dependency describes the results derived for plot 11.
- iv) Although plots 9 and 11 have been modelled, the experimental data indicates that some elements of periodicity may be evident. Figure 5.30 displays this fluctuation; both plots appear to follow approximately the same pattern.



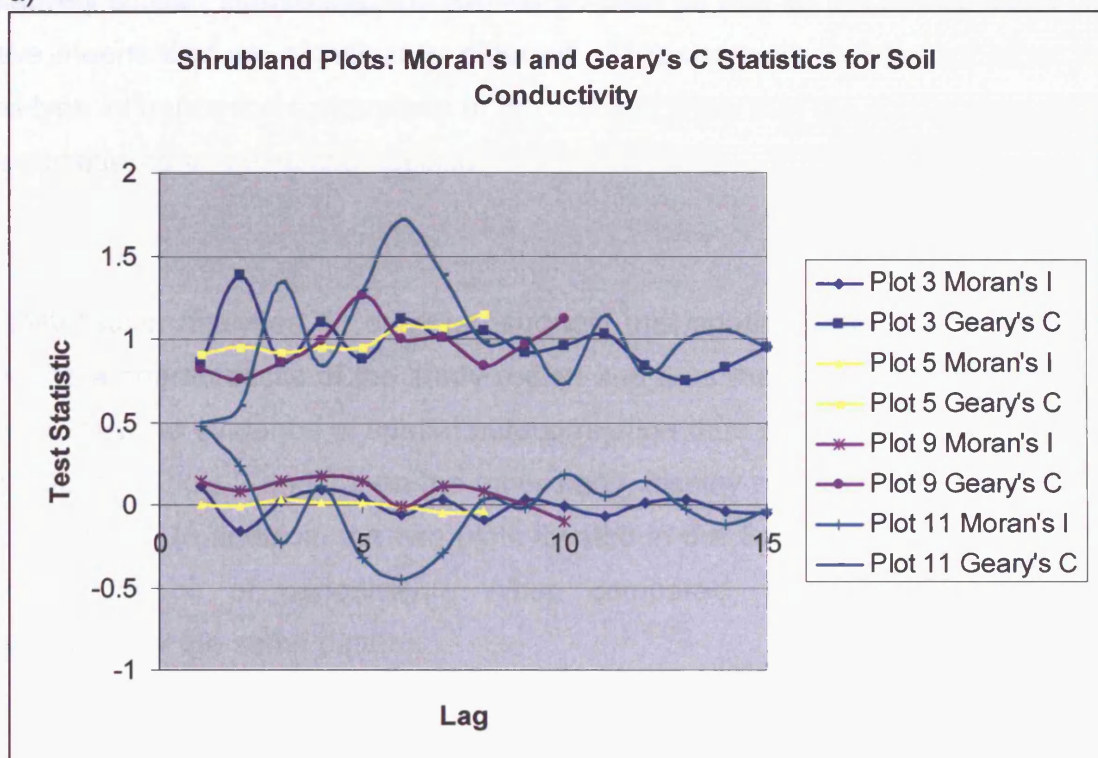
**Figure 5.30** Semi-variograms with connecting lines to show periodicity in soil conductivity data in shrubland plots.

e) *Geostatistical analysis: Moran's I and Geary's C statistics*

The results are as follows (see figure 5.31):

- i) Comparisons made between the Moran's I and Geary's C statistics show that the results mirror each other relatively well, this increases the confidence in the results.
- ii) The Geary's C analysis indicates that both plot 3 and 5 demonstrate no significant signs of spatial patterns, this corresponds to the semi-variogram results.
- iii) The Geary's C correlogram for plot 9 suggests that spatial clustering occurs until a lag distance of approximately 9m, this is comparable to the results derived from the semi-variogram, which suggested a range of 8.1m. However, the Moran's I correlogram does not correspond to this finding.
- iv) Both correlograms agree that in plot 11 spatial clustering occurs at lag distances less than 4 - 6m. This finding corresponds to the range of spatial autocorrelation derived from the semi-variogram (5.27m).

a)



b)

Lag increment codes	Plot 3 & 11	Plot 5	Plot 9
1	0 > to <= 2	0 > to <= 4.5	0 > to <= 3
2	2 > to <= 4	4.5 > to <= 9	3 > to <= 6
3	4 > to <= 6	9 > to <= 13.5	6 > to <= 9
4	6 > to <= 8	13.5 > to <= 18	9 > to <= 12
5	8 > to <= 10	18 > to <= 22.5	12 > to <= 15
6	10 > to <= 12	22.5 > to <= 27	15 > to <= 18
7	12 > to <= 14	27 > to <= 31.5	18 > to <= 21
8	14 > to <= 16	31.5 > to <= 36	21 > to <= 24
9	16 > to <= 18		24 > to <= 27
10	18 > to <= 20		27 > to <= 30
11	20 > to <= 22		
12	22 > to <= 24		
13	24 > to <= 26		
14	26 > to <= 28		
15	28 > to <= 30		

**Figure 5.31** a) Moran's I and Geary's C correlograms for the soil conductivity of the shrubland plots. b) provides the key to the lag increments used in the correlograms for each plot.

### 5.8.2 Summary

Despite the mean values of conductivity from all the plots appearing to be relatively similar, statistically, the two Karoo plots as well as the two Sevilleta plots have means that are significantly different. This suggests that factors other than soil type influence the conductivity of the soil and imply that the conductivity should be considered as being site specific.

Geostatistical analyses, in contrast, suggest that spatial patterns of conductivity may be a characteristic of the study region and thus the local conditions. Plots 3 and 5 show no evidence of spatial autocorrelation thus suggesting a homogenous distribution. Plots 9 and 11, on the other hand, display ranges of 8.1m and 5.27m, respectively. In addition, the two plots located in the Sevilleta NWR demonstrate some evidence of periodicity. When compared, these fluctuations follow approximately the same pattern.

## **5.9 Nutrient content analysis**

Due to some obvious anomalies in the output datasets, as a result of machine error, the results presented here have been filtered and some data points removed. Of the shrubland plots only plot 9 was affected thus the sample size was reduced to 105.

### **5.9.1 Results:**

#### **Calcium**

##### *a) Test of normality, descriptive statistics and inter-plot variation*

The frequency distributions displayed by the boxplots (figure 5.32) show that plot 3 displays a highly positively skewed distribution whereas plots 5, 9 and 11 are negatively skewed. Plots 9 and 11 are considered to be highly negatively skewed as their skewness values are less than -1 (see table 5.14). Outliers are evident in all datasets except plot 5. These are evident at the upper end of the scale for plot 3 and the lower end of the scale for plots 9 and 11.

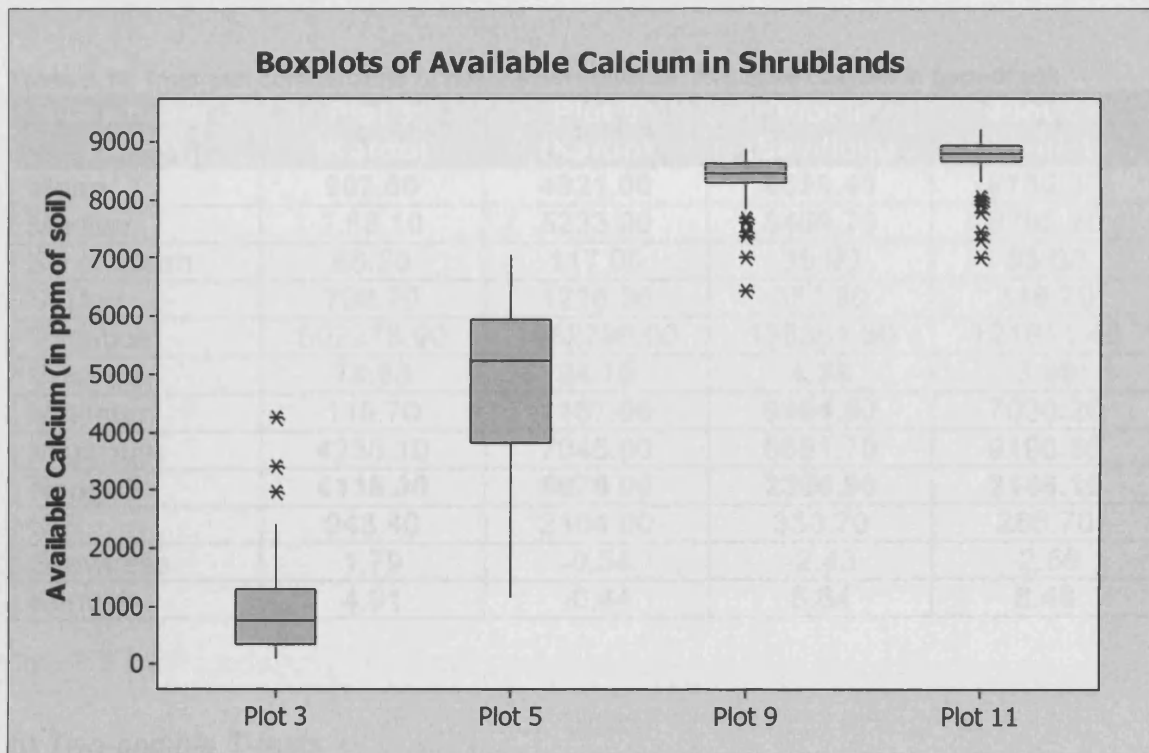


**Figure 5.32** Boxplots representing the sample distribution of available calcium in the shrubland plots.

Inter-plot analysis shows that there is a significant difference in the available calcium content between the sites in the Karoo, South Africa and the sites in the Sevilleta NWR, New Mexico. Available calcium is significantly higher in the Sevilleta NWR, this is a characteristic of the soil type. The ranges of values and the variation within these plots are also lower than the sites situated in the Karoo. Notwithstanding these geographical differences, the mean values derived from the two Karoo plots vary greatly compared to the two means derived from the Sevilleta NWR plots. Significant differences in the coefficient of variation values are also evident in the Karoo plots.

**Table 5.14** Inter-plot comparisons of descriptive statistics: Available calcium in ppm of soil

Descriptive Statistic	Plot 3 (Karoo)	Plot 5 (Karoo)	Plot 9 (Sevilleta)	Plot 11 (Sevilleta)
Mean	<b>907.60</b>	<b>4921.00</b>	<b>8399.40</b>	<b>8736.30</b>
Median	7.68.10	5233.00	8469.70	8785.20
SE of Mean	68.20	117.00	35.90	33.60
St Dev	708.70	1218.00	367.90	348.70
Variance	502278.90	1482786.00	135361.30	121611.40
Coef Var	<b>78.08</b>	<b>24.75</b>	<b>4.38</b>	<b>3.99</b>
Minimum	119.70	1167.00	6454.80	7030.20
Maximum	4238.10	7045.00	8851.70	9196.30
Range	<b>4118.30</b>	<b>5878.00</b>	<b>2396.90</b>	<b>2166.10</b>
IQR	943.40	2104.00	330.70	286.70
Skewness	1.79	-0.54	-2.43	-2.56
Kurtosis	4.91	-0.44	8.64	8.48

#### b) Two-sample T-tests

It can be concluded from the two-sample t-test that there is a significant difference between the means of plot 3 and 5, the two plots located in the Karoo. ( $t = -29.60$ ,  $p < 0.005$ ). Similarly, there is a significant difference between the means of plots 9 and 11, the two plots located in the Sevilleta NWR ( $t = -6.86$ ,  $p < 0.005$ ).

#### c) Geostatistical analysis: The semi-variogram

Pre-processing of the datasets resulted in the removal of one outlier from plot 3 and four outliers from plots 9 and 11. Even with the removal of the outlier the distribution of plot 3 was highly skewed thus requiring a log transformation. No trends were identified in the datasets. Table 5.15 shows the numerical results and the associated semi-variogram graphs are presented in figure 5.33.

**Table 5.15** Geostatistical analysis of the available calcium of shrubland plots

Parameter: Calcium						
No.	Plot Location	Fitted Model	Nugget Value (Co)	Sill (Co+C <sub>1</sub> )	Range (a)	Nugget-to-sill Ratio (Co)/(Co+C <sub>1</sub> )
3	Karoo*	None	na	na	na	na
5	Karoo	Nugget	1.00	na	na	na
9	Sevilleta NWR	Spherical	0.60	1.08	6.60	0.56
11	Sevilleta NWR	Nugget	1.00	na	na	na

\* Log transformed data due to highly positively skewed data

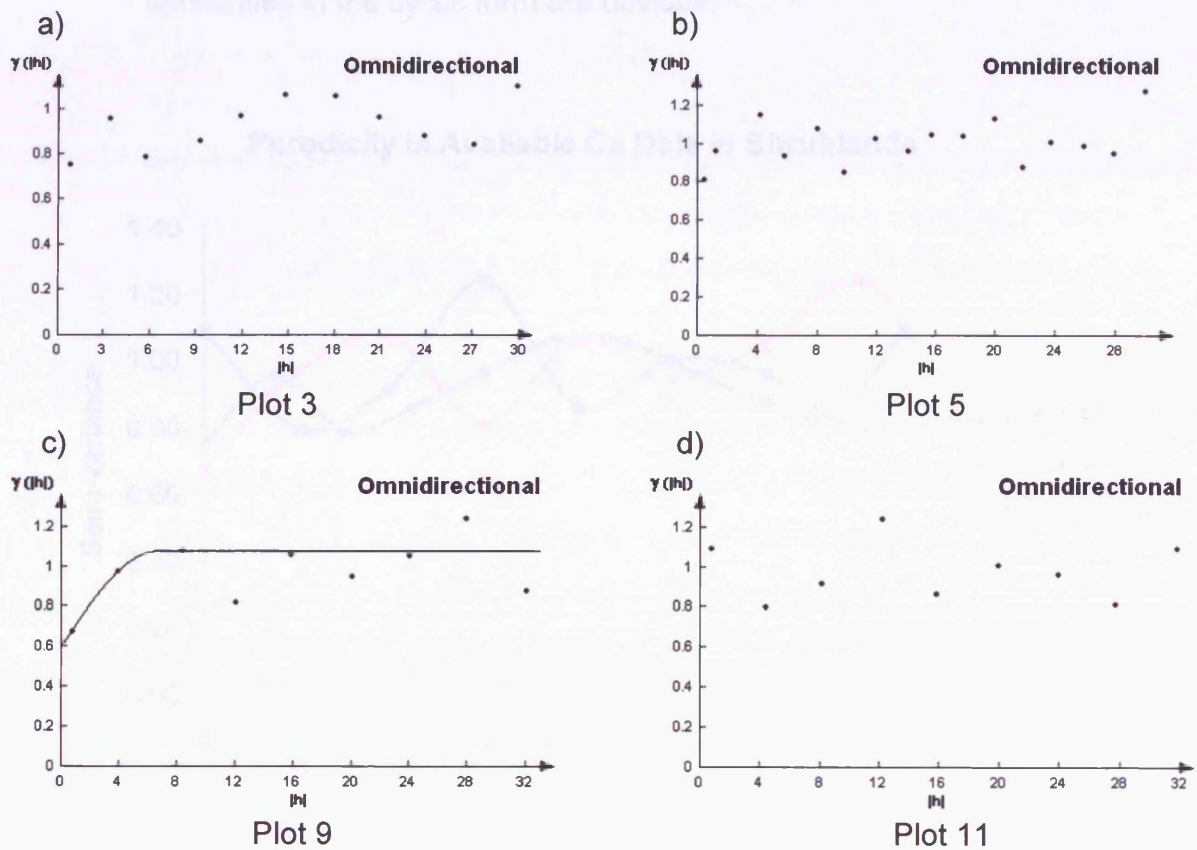


**Figure 5.33** Modelled semi-variograms for the available calcium in shrubland plots.

The results are as follows:

- i) Plots 5 and 11 are best represented by a 'pure nugget' model. This suggests that the distribution of available calcium does not follow any spatial patterns.

- ii) Plot 9, modelled by a spherical model, shows evidence of spatial autocorrelation. The range of autocorrelation for available calcium is 6.60m.
- iii) The nugget-to-sill ratio indicates that plot 9 shows moderate levels of spatial dependency.
- iv) None of the simple models were thought to adequately model plot 3 as periodicity in the dataset is evident.
- v) Although plot 9 has been modelled and plot 11 has not, some periodicity is thought to be evident in both datasets (fig 5.34). However, no similarities in the cyclic form are obvious.

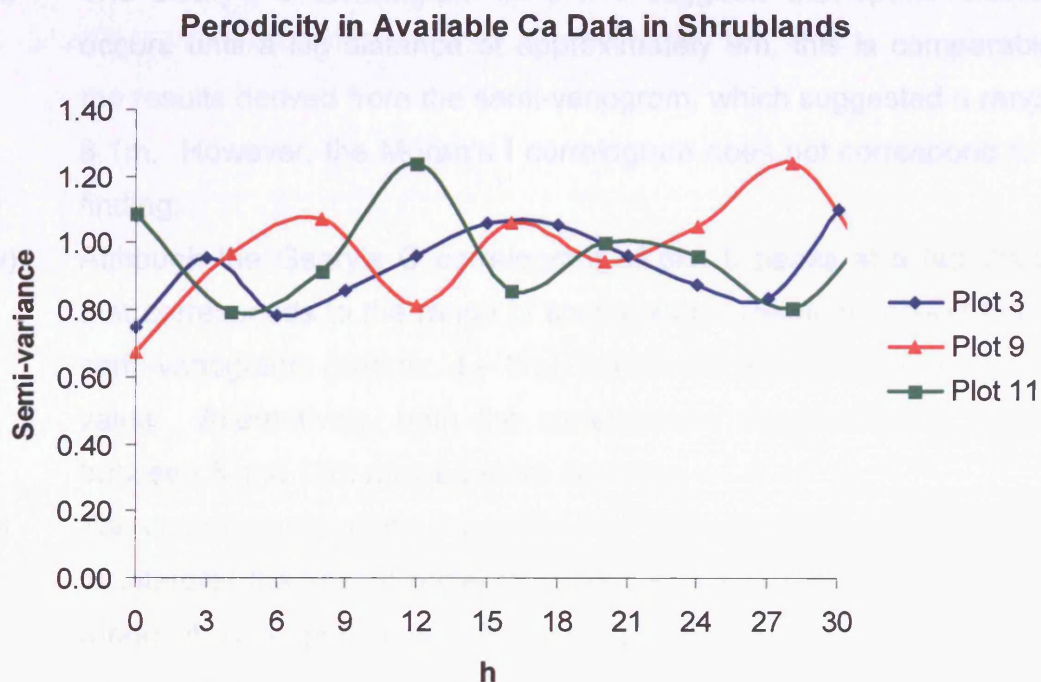


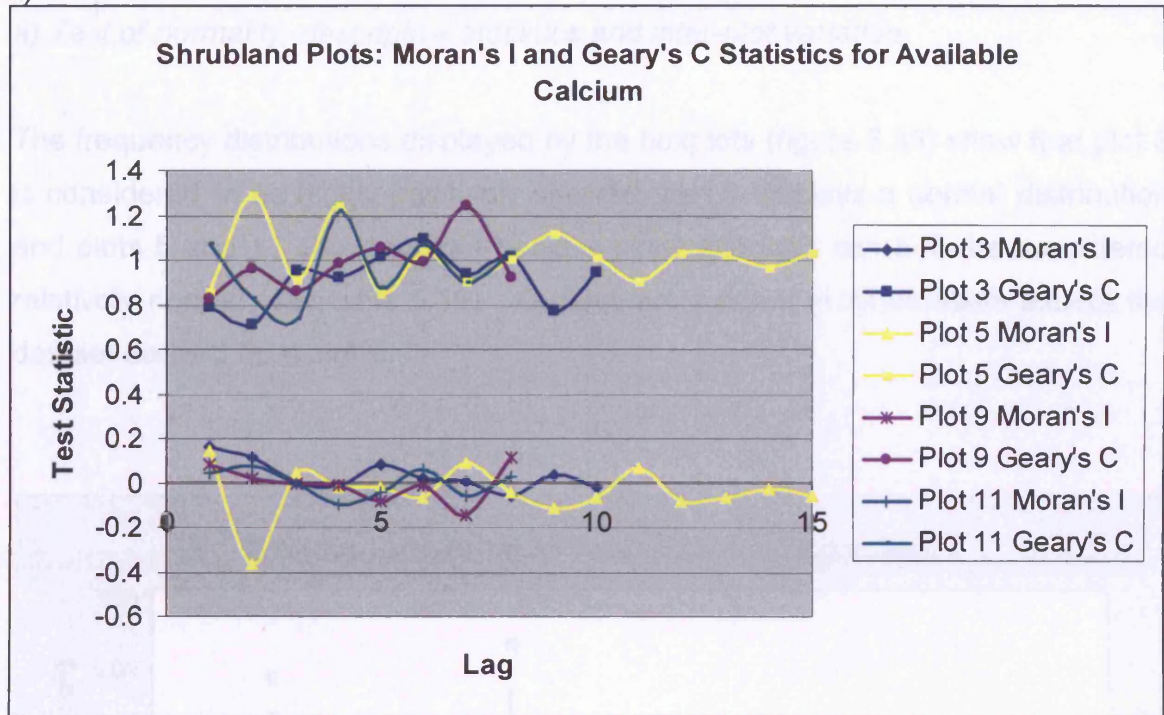
**Figure 5.34** Semi-variograms with connecting lines to show periodicity in the available calcium data in shrubland plots.

***d) Geostatistical analysis: Moran's I and Geary's C statistics***

The results are as follows: (see figure 5.35)

- i) Comparisons made between the Moran's I and Geary's C statistics show that the results mirror each other relatively well, this increases the confidence in the results.
- ii) The Geary's C analysis indicates that both plot 5 and 11 demonstrate no significant signs of spatial patterns, this corresponds to the semi-variogram results.
- iii) The Geary's C correlogram for plot 9 suggests that spatial clustering occurs until a lag distance of approximately 9m, this is comparable to the results derived from the semi-variogram, which suggested a range of 8.1m. However, the Moran's I correlogram does not correspond to this finding.
- iv) Although the Geary's C correlogram of plot 9 peaks at a lag distance that corresponds to the range of spatial autocorrelation derived from the semi-variograms (approx. 4 – 8m), it does not appear to be a significant value. Alternatively, both the correlograms suggest that a range of between 8 and 12m may be more accurate.
- v) The correlograms of plot 3 indicate two different results making it difficult to interpret the spatial patterns. The Geary's C results suggest that a range of 12 – 15m may exist, corresponding to the main peak in the semi-variogram. The Moran's I results, however, suggest that a range of 6 – 9 m may exist.

a)



b)

Lag increment codes	Plot 3	Plot 5	Plot 9 & 11
1	0 > to ≤ 3	0 > to ≤ 2	0 > to ≤ 4
2	3 > to ≤ 6	2 > to ≤ 4	4 > to ≤ 8
3	6 > to ≤ 9	4 > to ≤ 6	8 > to ≤ 12
4	9 > to ≤ 12	6 > to ≤ 8	12 > to ≤ 16
5	12 > to ≤ 15	8 > to ≤ 10	16 > to ≤ 20
6	15 > to ≤ 18	10 > to ≤ 12	20 > to ≤ 24
7	18 > to ≤ 21	12 > to ≤ 14	24 > to ≤ 28
8	21 > to ≤ 24	14 > to ≤ 16	28 > to ≤ 32
9	24 > to ≤ 27	16 > to ≤ 18	
10	27 > to ≤ 30	18 > to ≤ 20	
11		20 > to ≤ 22	
12		22 > to ≤ 24	
13		24 > to ≤ 26	
14		26 > to ≤ 28	
15		28 > to ≤ 30	

**Figure 5.35** a) Moran's I and Geary's C correlograms for the available calcium in the shrubland plots. b) provides the key to the lag increments used in the correlograms for each plot.

## Potassium

### a) Test of normality, descriptive statistics and inter-plot variation

The frequency distributions displayed by the boxplots (figure 5.36) show that plot 3 is considered to be highly positively skewed, plot 9 displays a normal distribution and plots 5 and 11 show a slight positive skew although can both be considered relatively normal (see table 5.16). Outliers are evident in all datasets except the dataset derived from plot 9.

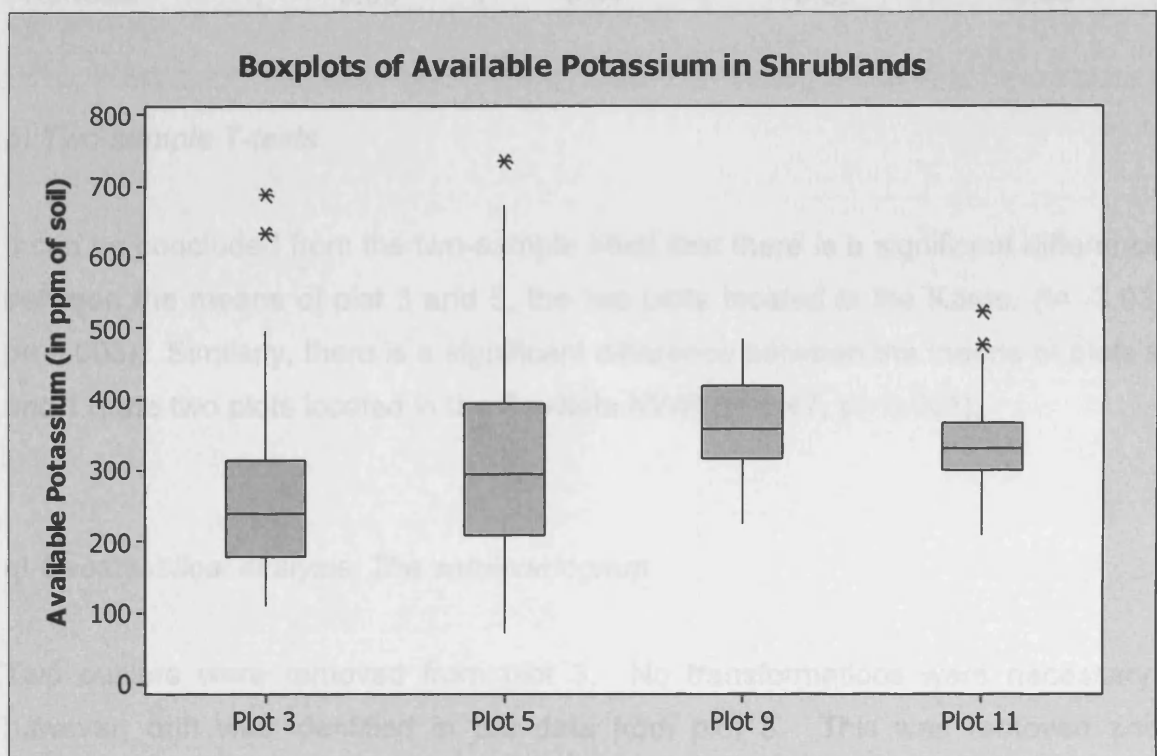


**Figure 5.36** Boxplots representing the sample distribution of available potassium in the shrubland plots.

Although the mean values do not vary greatly across the four plots, the distribution characteristics do. The ranges of the Karoo plots, for example, are approximately double those of the Sevilleta NWR plots. Similarly, the coefficients of variation values indicate that relative to the mean, the Karoo plots display a greater amount of sample variation than the Sevilleta NWR plots.

**Table 5.16** Inter-plot comparisons of descriptive statistics: Available potassium in ppm of soil

Descriptive Statistic	Plot 3 (Karoo)	Plot 5 (Karoo)	Plot 9 (Sevilleta)	Plot 11 (Sevilleta)
Mean	257.77	306.50	362.37	334.58
Median	240.49	295.60	358.63	331.47
SE of Mean	9.95	12.60	6.14	5.15
St Dev	103.42	131.10	62.90	53.56
Variance	10696.69	17184.80	3955.92	2868.48
Coef Var	40.12	42.77	17.36	16.01
Minimum	109.92	71.60	226.00	209.90
Maximum	688.94	737.00	485.96	523.44
Range	579.02	665.40	259.95	313.54
IQR	135.31	185.50	102.06	65.48
Skewness	1.38	0.65	-0.07	0.47
Kurtosis	3.09	0.44	-0.85	0.93

### b) Two-sample T-tests

It can be concluded from the two-sample t-test that there is a significant difference between the means of plot 3 and 5, the two plots located in the Karoo. ( $t = -3.03$ ,  $p = 0.003$ ). Similarly, there is a significant difference between the means of plots 9 and 11, the two plots located in the Sevilleta NWR ( $t = 3.47$ ,  $p = 0.001$ ).

### c) Geostatistical analysis: The semi-variogram

Two outliers were removed from plot 3. No transformations were necessary; however, drift was identified in the data from plot 5. This was removed and subsequent geostatistical analysis was carried out using the residuals. Table 5.17 shows the numerical results and the associated semi-variogram graphs are presented in figure 5.37.

Table 5.17 Geostatistical analysis of the available potassium in shrubland plots

Parameter: Potassium						
No.	Plot Location	Fitted Model	Nugget Value (Co)	Sill (Co+C <sub>1</sub> )	Range (a)	Nugget-to-sill Ratio (Co)/(Co+C <sub>1</sub> )
3	Karoo	Nugget	1.00	na	na	na
5	Karoo	Gaussian	0.77	1.21	31.44	0.64
9	Sevilleta NWR	Spherical	0.23	0.75	7.5	0.31
11	Sevilleta NWR	Spherical	0.31	1.10	8.06	0.28

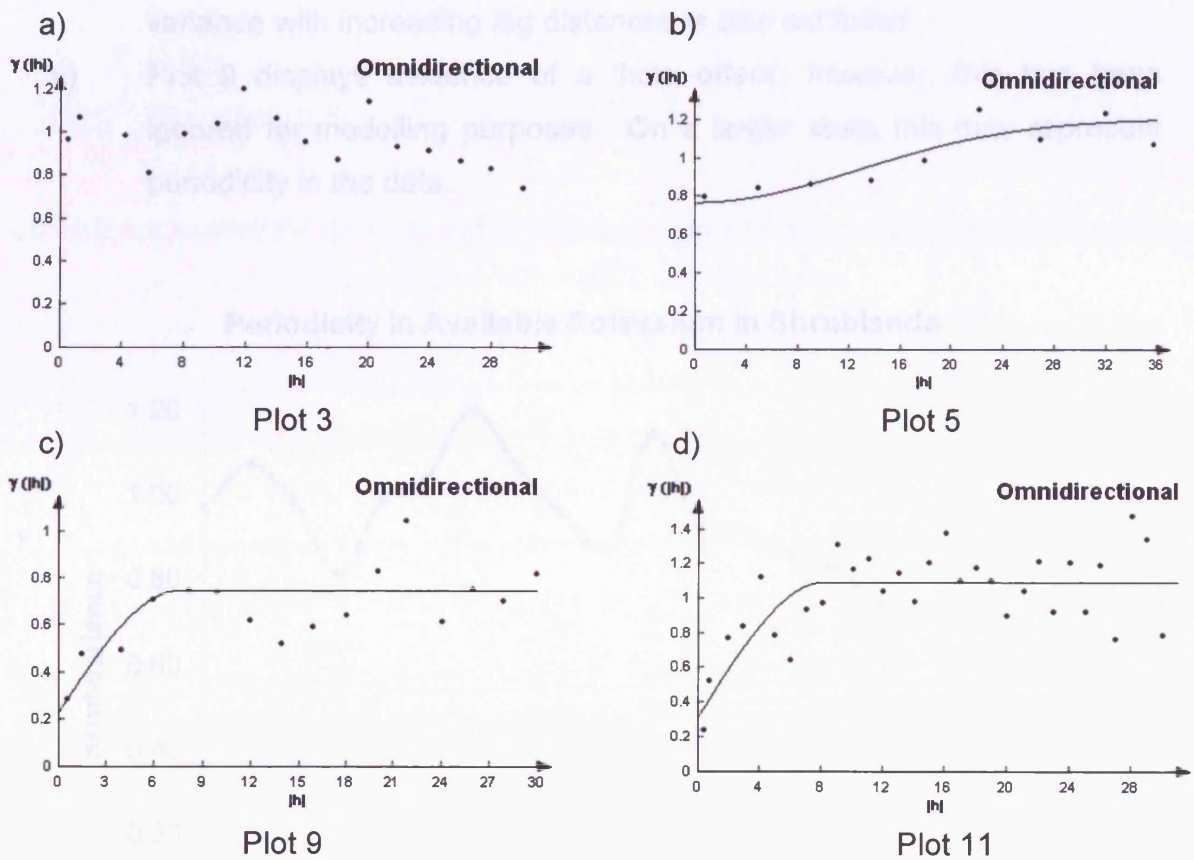


Figure 5.37 Modelled semi-variograms for the available potassium in shrubland plots.

The results are as follows:

- i) Plot 3 is best represented by a 'pure nugget' model. This suggests that the distribution of available potassium does not follow any spatial patterns.
- ii) Plots 5, represented by a Gaussian model, shows evidence of spatial autocorrelation. The range of autocorrelation for available potassium is

31.44m and the nugget-to-sill ratio indicates moderate to weak spatial dependency.

- iii) The two plots from the Sevilleta NWR (plots 9 & 11) also show evidence of spatial autocorrelation, the ranges being 7.5m and 8.06m. The nugget-to-sill ratios indicate moderate to strong spatial dependency in both cases.
- iv) Although plot 3 was represented by a pure nugget model, some periodicity is thought to be evident (figure 5.38). A downward trend in variance with increasing lag distances is also exhibited.
- v) Plot 9 displays evidence of a 'hole effect', however, this has been ignored for modelling purposes. On a larger scale this may represent periodicity in the data.

#### Periodicity in Available Potassium in Shrublands

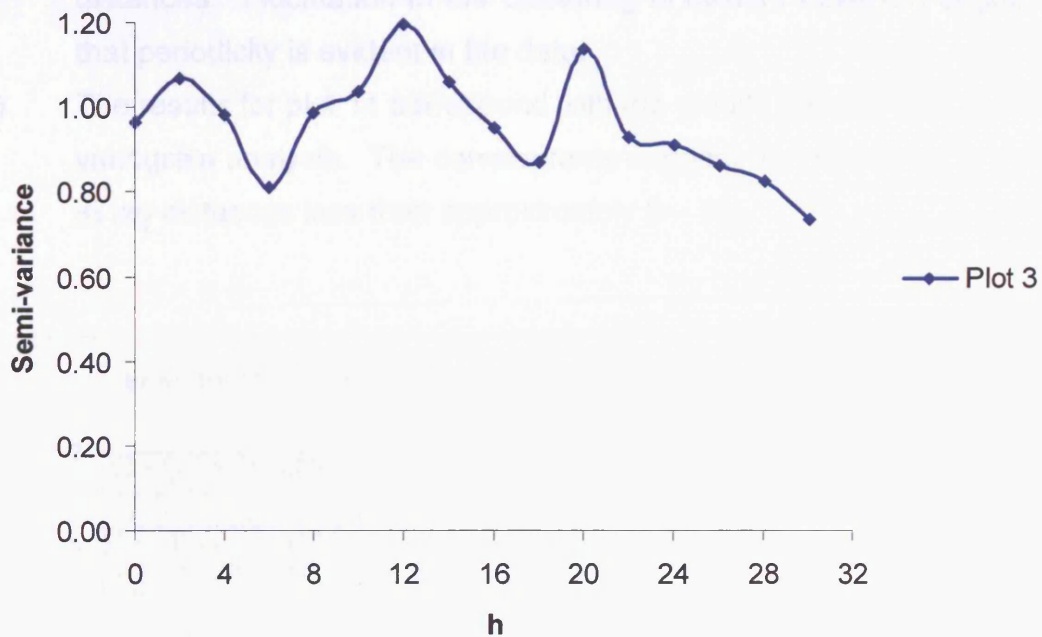
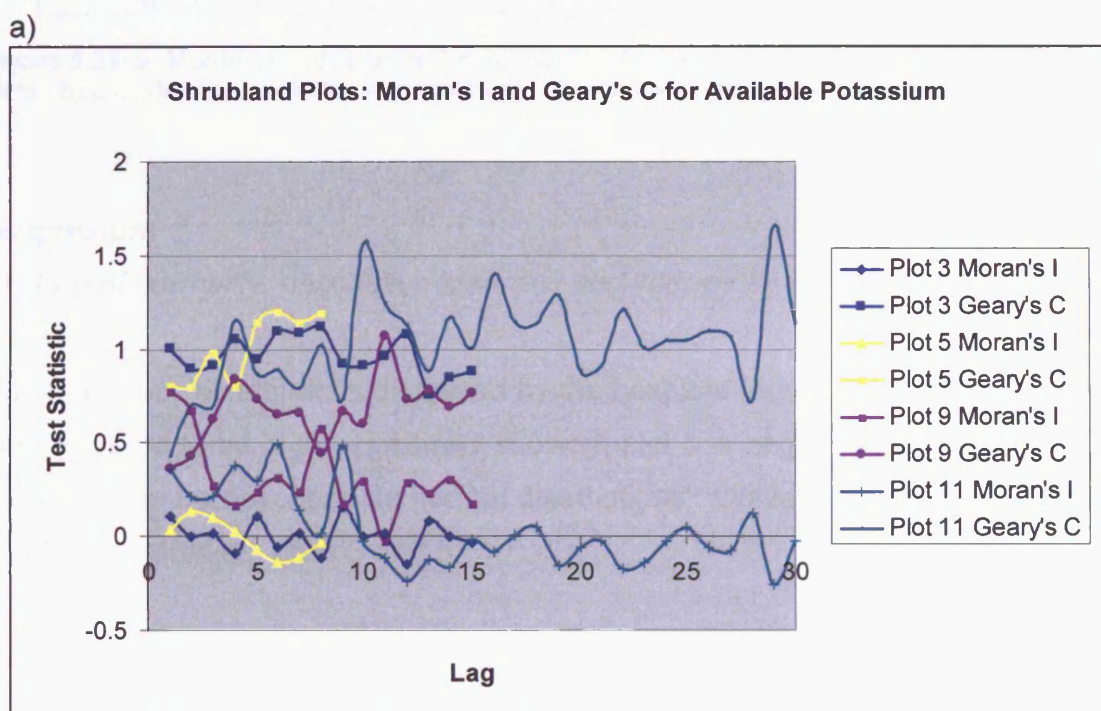


**Figure 5.38** Semi-variograms with connecting lines to show periodicity in the available potassium data in shrubland plots.

e) Geostatistical analysis: Moran's I and Geary's C statistics

The results are as follows: (see figure 5.39)

- i) Comparisons made between the Moran's I and Geary's C statistics show that the results mirror each other relatively well, this increases the confidence in the results.
- ii) The Geary's C analysis indicates that plot 3 demonstrates no significant signs of a spatial pattern, this corresponds to the semi-variogram results.
- iii) The correlograms suggest that plot 5 has a range less than that calculated by the semi-variogram. A range of approximately 18 – 22.5m is indicated by both the Geary's C and Moran's I statistics rather than 31.44m indicated by the semi-variogram analysis.
- iv) The correlograms indicate that clustering occurs in plot 9 at most lag distances. Fluctuation in the clustering is evident however, suggesting that periodicity is evident in the data.
- v) The results for plot 11 correspond with the results derived from the semi-variogram analysis. The correlograms suggest that clustering is evident at lag distances less than approximately 8 – 9m.



b)

Lag increment codes	Plot 3	Plot 5	Plot 9	Plot 11
1	0 > to ≤ 2	0 > to ≤ 4.5	0 > to ≤ 2	0 > to ≤ 1
2	2 > to ≤ 4	4.5 > to ≤ 9	2 > to ≤ 4	1 > to ≤ 2
3	4 > to ≤ 6	9 > to ≤ 13.5	4 > to ≤ 6	2 > to ≤ 3
4	6 > to ≤ 8	13.5 > to ≤ 18	6 > to ≤ 8	3 > to ≤ 4
5	8 > to ≤ 10	18 > to ≤ 22.5	8 > to ≤ 10	4 > to ≤ 5
6	10 > to ≤ 12	22.5 > to ≤ 27	10 > to ≤ 12	5 > to ≤ 6
7	12 > to ≤ 14	27 > to ≤ 31.5	12 > to ≤ 14	6 > to ≤ 7
8	14 > to ≤ 16	31.5 > to ≤ 36	14 > to ≤ 16	7 > to ≤ 8
9	16 > to ≤ 18		16 > to ≤ 18	8 > to ≤ 9
10	18 > to ≤ 20		18 > to ≤ 20	9 > to ≤ 10
11	20 > to ≤ 22		20 > to ≤ 22	10 > to ≤ 11
12	22 > to ≤ 24		22 > to ≤ 24	11 > to ≤ 12
13	24 > to ≤ 26		24 > to ≤ 26	12 > to ≤ 13
14	26 > to ≤ 28		26 > to ≤ 28	13 > to ≤ 14
15	28 > to ≤ 30		28 > to ≤ 30	14 > to ≤ 15
16				15 > to ≤ 16
17				16 > to ≤ 17
18				17 > to ≤ 18
19				18 > to ≤ 19
20				19 > to ≤ 20
21				20 > to ≤ 21
22				21 > to ≤ 22
23				22 > to ≤ 23
24				23 > to ≤ 24
25				24 > to ≤ 25
26				25 > to ≤ 26
27				26 > to ≤ 27
28				27 > to ≤ 28
29				28 > to ≤ 29
30				29 > to ≤ 30

**Figure 5.39** a) Moran's I and Geary's C correlograms for the available potassium in the shrubland plots. b) provides the key to the lag increments used in the correlograms for each plot.

## Magnesium

### a) Test of normality, descriptive statistics and inter-plot variation

The frequency distributions displayed by the boxplots (figure 5.40) show that plot 3 is considered to be highly positively skewed, plot 5 is negatively skewed and plots 9 and 11 can be described as normal distributions. Outliers are evident in only the two Karoo datasets, plots 3 and 5.

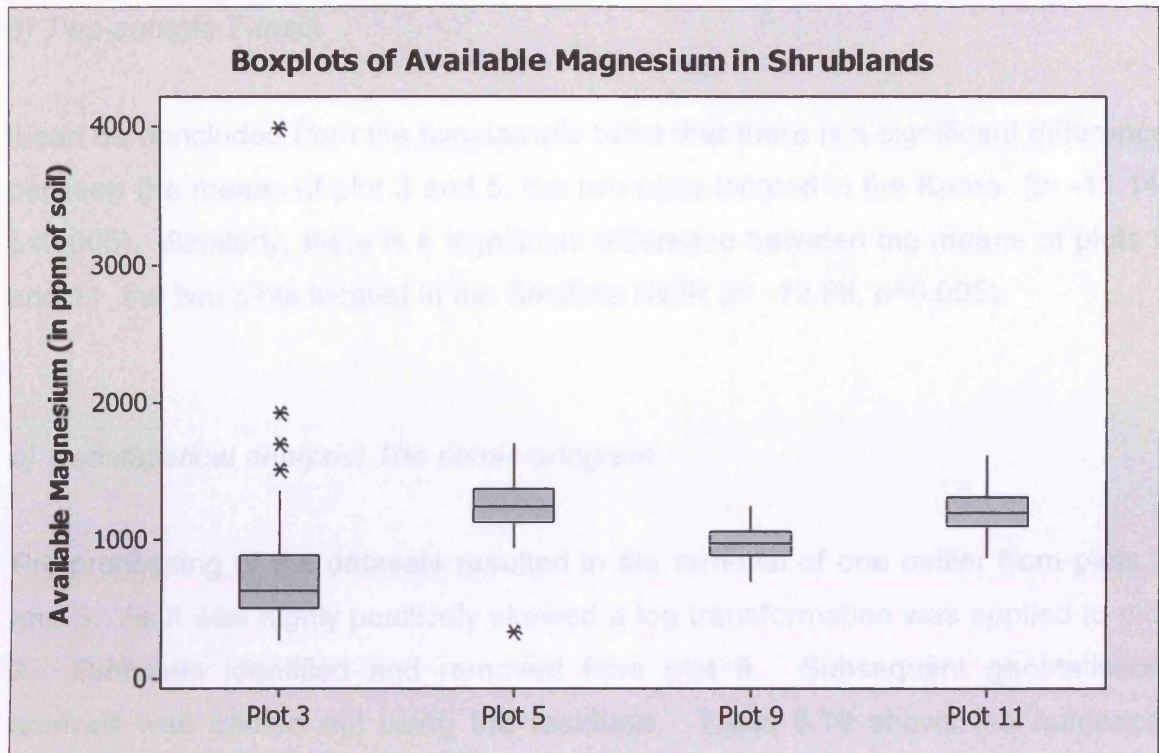


**Figure 5.40** Boxplots representing the sample distribution of available magnesium in the shrubland plots.

The two Karoo plots display both the highest and lowest mean values of all four plots (see table 5.18). However, greater sample ranges are evident in the Karoo. Interestingly, plots 5, 9 and 11 all show similar levels of inter-plot variation but plot 3 displays significantly greater variation.

**Table 5.18** Inter-plot comparisons of descriptive statistics: Available magnesium in ppm of soil

Descriptive Statistic	Plot 3 (Karoo)	Plot 5 (Karoo)	Plot 9 (Sevilleta)	Plot 11 (Sevilleta)
Mean	747.60	1243.70	974.00	1210.10
Median	637.80	1239.90	975.40	1204.30
SE of Mean	40.90	17.50	12.50	13.40
St Dev	425.60	181.50	127.90	139.40
Variance	181098.50	32925.60	16359.50	19443.40
Coef Var	56.92	14.59	13.13	11.52
Minimum	277.90	339.70	709.50	878.70
Maximum	3993.10	1706.50	1243.30	1615.50
Range	3715.20	1366.80	533.80	736.80
IQR	385.60	230.70	171.50	206.80
Skewness	4.59	-0.87	-0.06	0.03
Kurtosis	31.54	4.77	-0.48	-0.19

### b) Two-sample T-tests

It can be concluded from the two-sample t-test that there is a significant difference between the means of plot 3 and 5, the two plots located in the Karoo. ( $t = -11.14$ ,  $p < 0.005$ ). Similarly, there is a significant difference between the means of plots 9 and 11, the two plots located in the Sevilleta NWR ( $t = -12.88$ ,  $p < 0.005$ ).

### c) Geostatistical analysis: The semi-variogram

Pre-processing of the datasets resulted in the removal of one outlier from plots 3 and 5. As it was highly positively skewed a log transformation was applied to plot 3. Drift was identified and removed from plot 9. Subsequent geostatistical analysis was carried out using the residuals. Table 5.19 shows the numerical results and the associated semi-variogram graphs are presented in figure 5.41.

**Table 5.19** Geostatistical analysis of the available magnesium in shrubland plots

<b>Parameter: Magnesium</b>						
No.	Vegetation Type	Fitted Model	Nugget Value (Co)	Sill (Co+C <sub>1</sub> )	Range (a)	Nugget-to-sill Ratio (Co)/(Co+C <sub>1</sub> )
3	Karoo*	Spherical	0.29	0.82	<b>21.43</b>	<b>0.35</b>
5	Karoo	Spherical	0.31	0.87	<b>8.68</b>	<b>0.36</b>
9	Sevilleta NWR	Power	0.59	Power: 0.71	<b>Slope: 0.06</b>	<b>na</b>
11	Sevilleta NWR	Spherical	0.55	0.87	<b>5.58</b>	<b>0.63</b>

\* Log transformed data due to highly positively skewed data

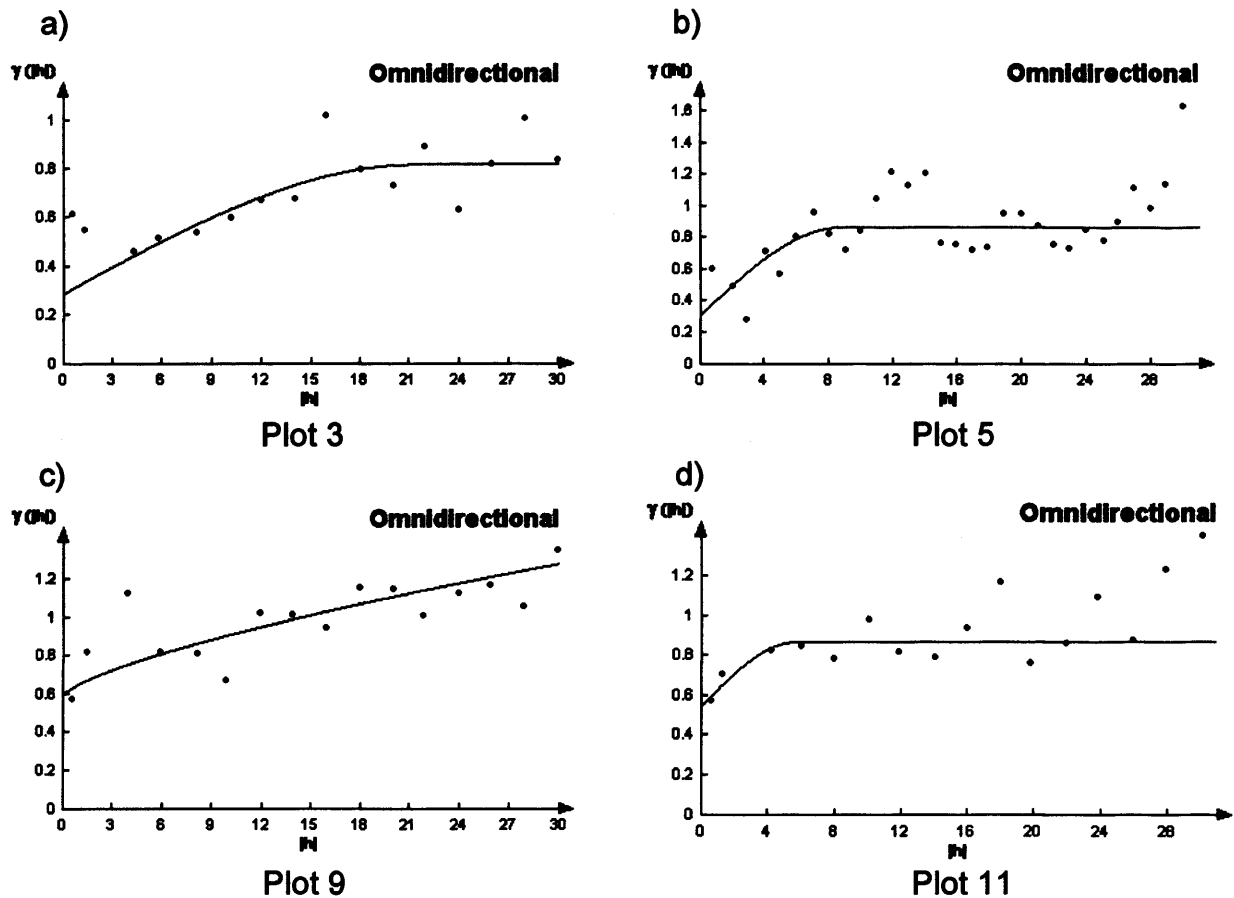


**Figure 5.41** Modelled semi-variograms for the available magnesium in shrubland plots.

The results are as follows:

- i) Plots 3, 5 and 11 show evidence of spatial autocorrelation. All three plots were best represented by a spherical model and show ranges of 21.43m, 8.68m and 5.58m, respectively.
- ii) The nugget-to-sill ratios suggest that plots 3 and 5 show moderate to strong spatial dependency whereas plot 11 demonstrates moderate to weak spatial dependency.
- iii) Even after any potential drift was removed plot 9 demonstrated an increasing variance with increasing lag distances. This data was therefore best represented by a power model.

- iv) When plotted to analyse the periodicity (figure 5.42) it can be seen that this upward trend is evident in plots 5, 9 and 11 and therefore may be a characteristic of available magnesium in semi-arid environments.

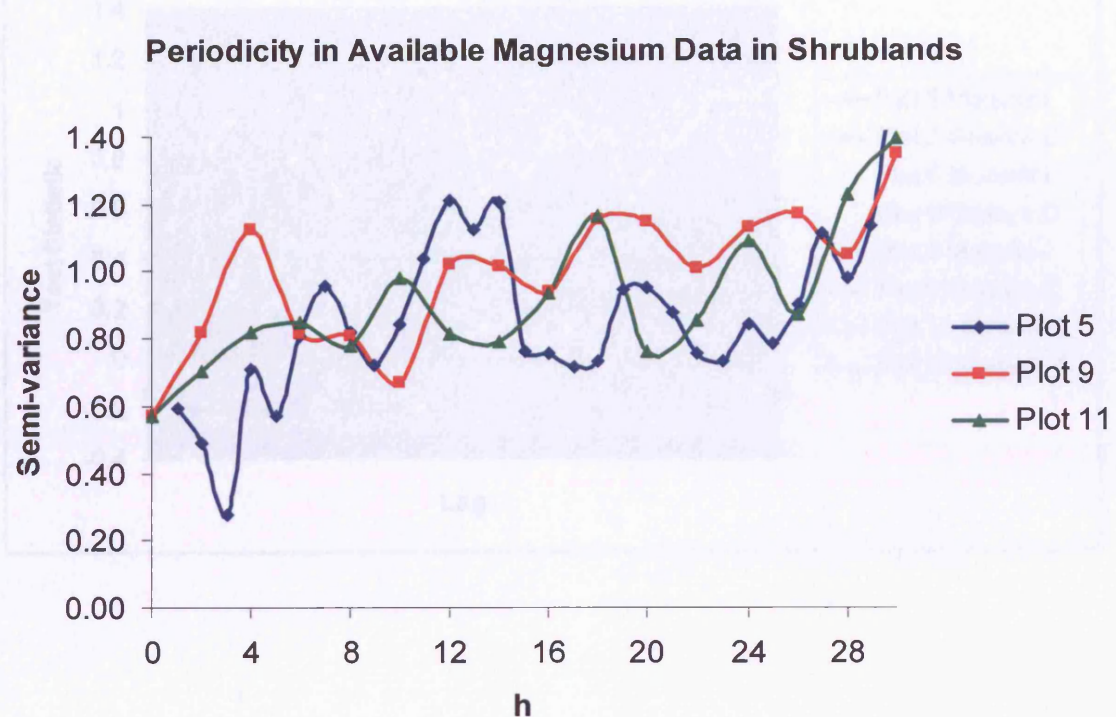


**Figure 5.42** Semi-variograms with connecting lines to show periodicity in the available magnesium data in shrubland plots.

*d) Geostatistical analysis: Moran's I and Geary's C statistics*

The results are as follows: (see figure 5.43)

- i) Comparisons made between the Moran's I and Geary's C statistics show that the results mirror each other relatively well, this increases the confidence in the results.
- ii) Interpretation of the correlograms appears to underestimate the possible ranges of spatial relationships compared to those calculated from the semi-variogram analysis with perhaps the exception of plot 5.
- iii) Compared to the power model applied to plot 9, the correlograms suggest that spatial correlation may exist near the smallest scale of measurement. A range of 2 – 4m can be derived from these results.

a)

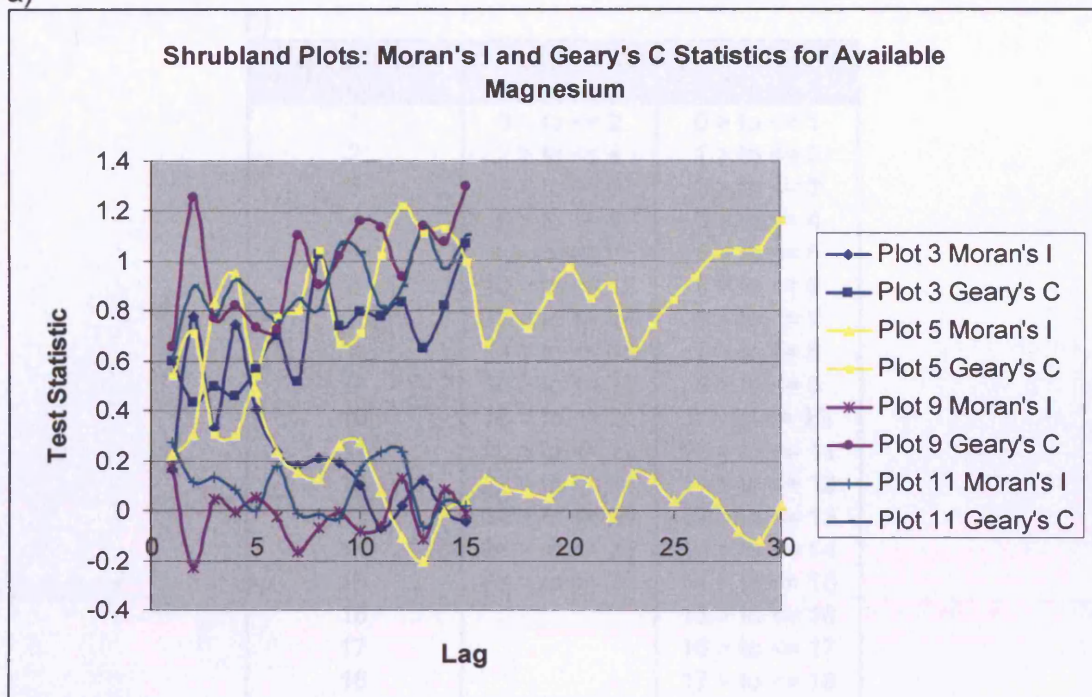


Figure 5.33. Moran's I and Geary's C statistics for available magnesium in shrubland plots 3, 5, 9, and 11.

Shrubland

Plot 3

Plot 5

Plot 9

Plot 11

b)

Lag increment codes	Plot 3, 9 & 11	Plot 5
1	0 > to <= 2	0 > to <= 1
2	2 > to <= 4	1 > to <= 2
3	4 > to <= 6	2 > to <= 3
4	6 > to <= 8	3 > to <= 4
5	8 > to <= 10	4 > to <= 5
6	10 > to <= 12	5 > to <= 6
7	12 > to <= 14	6 > to <= 7
8	14 > to <= 16	7 > to <= 8
9	16 > to <= 18	8 > to <= 9
10	18 > to <= 20	9 > to <= 10
11	20 > to <= 22	10 > to <= 11
12	22 > to <= 24	11 > to <= 12
13	24 > to <= 26	12 > to <= 13
14	26 > to <= 28	13 > to <= 14
15	28 > to <= 30	14 > to <= 15
16		15 > to <= 16
17		16 > to <= 17
18		17 > to <= 18
19		18 > to <= 19
20		19 > to <= 20
21		20 > to <= 21
22		21 > to <= 22
23		22 > to <= 23
24		23 > to <= 24
25		24 > to <= 25
26		25 > to <= 26
27		26 > to <= 27
28		27 > to <= 28
29		28 > to <= 29
30		29 > to <= 30

**Figure 5.43** a) Moran's I and Geary's C correlograms for the available magnesium in the shrubland plots. b) provides the key to the lag increments used in the correlograms for each plot.

## Sodium

### a) Test of normality, descriptive statistics and inter-plot variation

The frequency distributions displayed by the boxplots (figure 5.44) show that the datasets from all plots are positively skewed to varying degrees. Plot 3 is considered to be highly positively skewed whereas plots 5 and 9 are only slightly skewed and therefore can be considered as normal distributions. Outliers are

evident in all datasets except the dataset from plot 5. In all cases the outliers are at the upper end of the measurements.

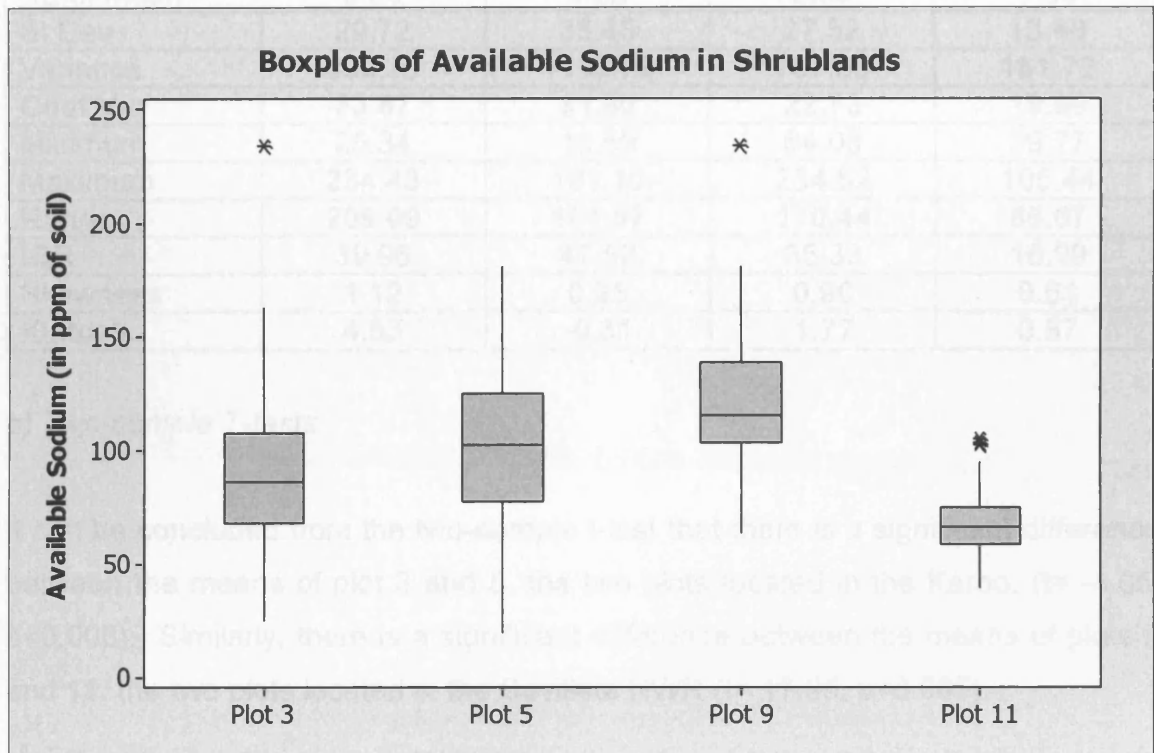


**Figure 5.44** Boxplots representing the sample distribution of available sodium in the shrubland plots.

The two Sevilleleta NWR plots display both the highest and lowest mean values of all four plots (see table 5.20). However, greater coefficients of variation values are evident in the Karoo although these do not vary significantly from those measured in the Sevilleleta NWR.

**Table 5.20** Inter-plot comparisons of descriptive statistics: Available sodium in ppm of soil

Descriptive Statistic	Plot 3 (Karoo)	Plot 5 (Karoo)	Plot 9 (Sevilleleta)	Plot 11 (Sevilleleta)
Mean	87.75	105.17	121.08	67.53
Median	86.37	102.80	115.24	66.29
SE of Mean	2.86	3.22	2.69	1.30
St Dev	29.72	33.45	27.52	13.48
Variance	883.36	1118.72	757.56	181.72
Coef Var	33.87	31.80	22.73	19.96
Minimum	25.34	19.59	64.08	39.77
Maximum	234.43	181.16	234.52	105.44
Range	209.09	161.57	170.44	65.67
IQR	39.96	47.52	35.33	16.99
Skewness	1.12	0.28	0.90	0.61
Kurtosis	4.63	-0.31	1.77	0.57

*b) Two-sample T-tests*

It can be concluded from the two-sample t-test that there is a significant difference between the means of plot 3 and 5, the two plots located in the Karoo. ( $t = -4.05$ ,  $p < 0.005$ ). Similarly, there is a significant difference between the means of plots 9 and 11, the two plots located in the Sevilleleta NWR ( $t = 17.95$ ,  $p < 0.005$ ).

*c) Geostatistical analysis: The semi-variogram*

Pre-processing of the datasets resulted in the removal of one outlier from plots 3 and 9. No transformations were necessary and no drift was identified in the datasets. Table 5.21 shows the numerical results and the associated semi-variogram graphs are presented in figure 5.45.

**Table 5.21** Geostatistical analysis of the available sodium in shrubland plots

Parameter: Sodium						
No.	Plot		Nugget Value	Sill	Range	Nugget-to-sill Ratio
	Vegetation Type	Fitted Model	(Co)	(Co+C <sub>1</sub> )	(a)	(Co)/(Co+C <sub>1</sub> )
1	Karoo	Nugget	1.00	na	na	na
2	Karoo	None	na	na	na	na
8	Sevilleleta NWR	None	na	na	na	na
10	Sevilleleta NWR	Nugget	1.00	na	na	na

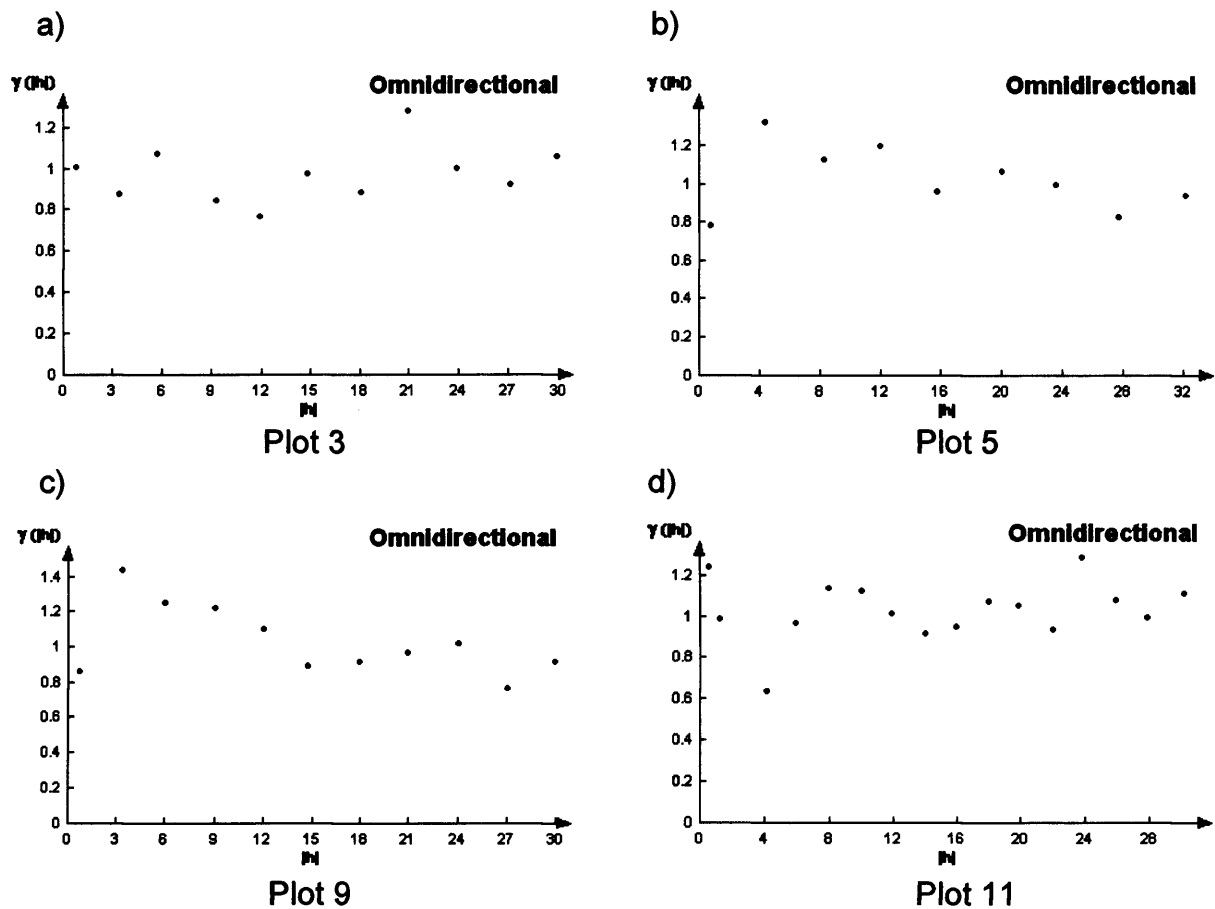


**Figure 5.45** Modelled semi-variograms for the available sodium in shrubland plots.

The results are as follows:

- i) No spatial autocorrelation was identified for available sodium in any of the plots.
- ii) A pure nugget model was fitted to plots 3 and 11 suggesting that no patterns are evident.
- iii) No simple models were considered to represent plots 5 and 9 adequately. However, a closer inspection of the variograms themselves suggests that some patterns may exist.
- iv) Plots 5 and 9 exhibit a downward trend in variance with increasing lag distances. This suggests that sodium may follow a checkerboard pattern across the landscape. These two plots can be seen to follow a similar pattern in figure 5.46
- v) Some cyclic behaviour is evident in all the plots although the behaviour of plots 5 and 9 appears to be similar and plots 3 and 11 are relatively

similar. This is interesting as one would expect the two plots from the same study region to be more similar rather than the grouping that is apparent.

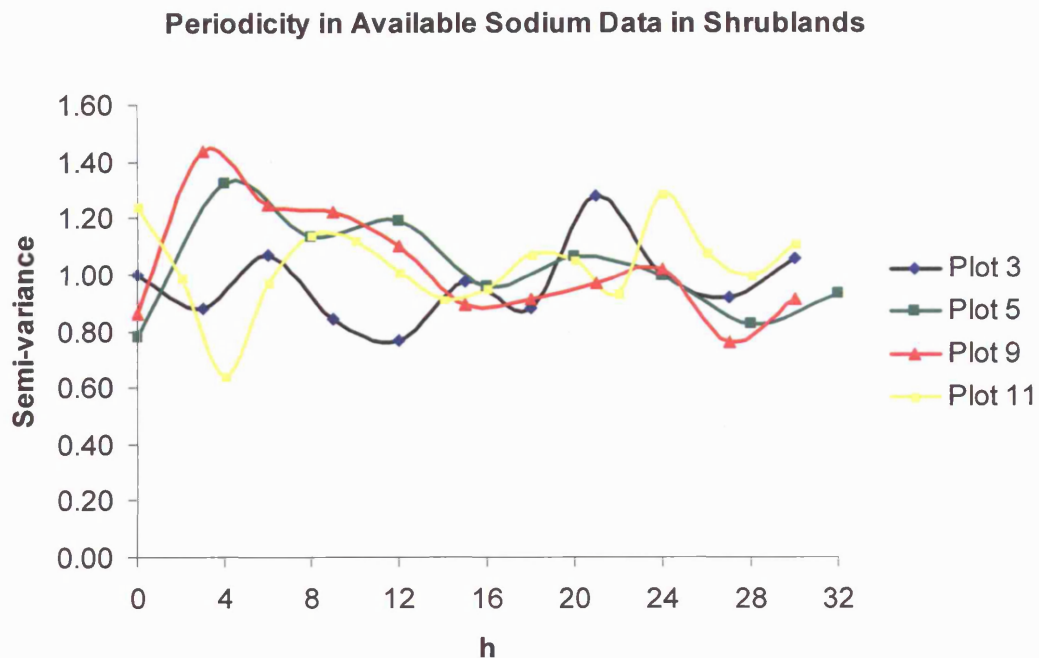


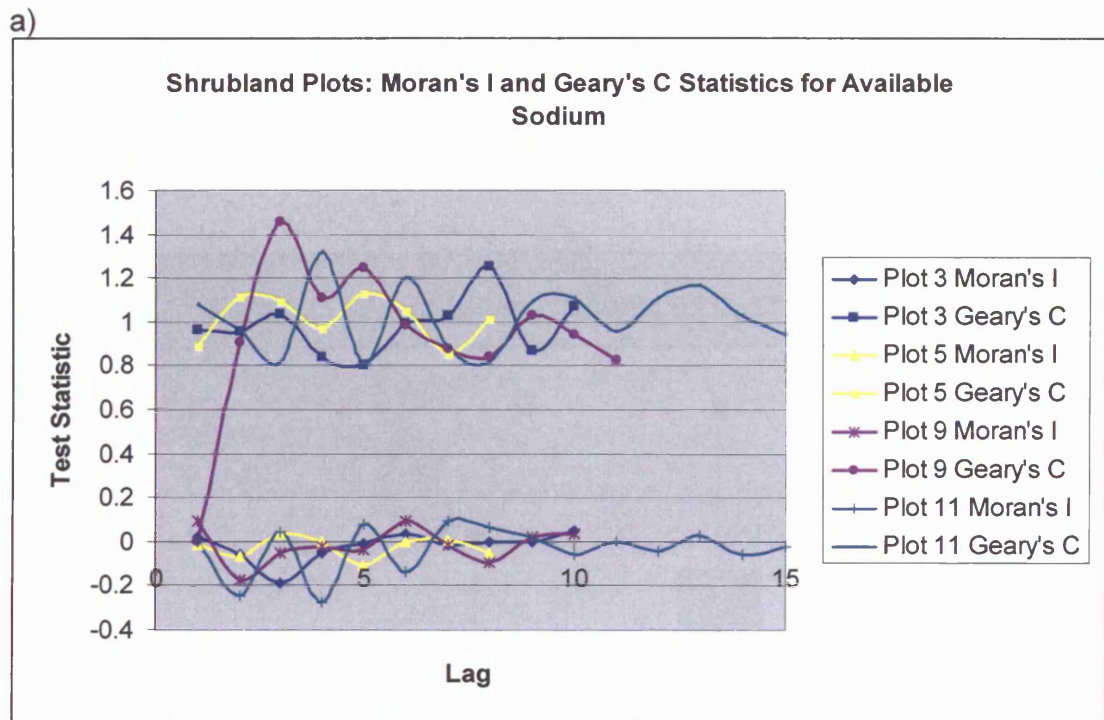
**Figure 5.46** Semi-variograms with connecting lines to show periodicity in the available sodium data in shrubland plots.

*e) Geostatistical analysis: Moran's I and Geary's C statistics*

The results are as follows: (see figure 5.47)

- i) Comparisons made between the Moran's I and Geary's C statistics show that the results mirror each other relatively well, this increases the confidence in the results.
- ii) The Geary's C correlogram shows that both plots 3 and 11 seem to fluctuate equally above and below 1 indicating that, although periodicity may be evident, the nugget model applied to the semi-variogram analysis is appropriate.
- iii) The downward trends of plots 5 and 9 observed in the semi-variograms, can be identified in the Geary's C correlogram, although the response of

plot 5 is relatively weak. Interpretation from the Moran's I correlogram would point to the presence of random patterns.



b)

Lag increment codes	Plot 3 & 9	Plot 5	Plot 11
1	0 > to <= 3	0 > to <= 4	0 > to <= 2
2	3 > to <= 6	4 > to <= 8	2 > to <= 4
3	6 > to <= 9	8 > to <= 12	4 > to <= 6
4	9 > to <= 12	12 > to <= 16	6 > to <= 8
5	12 > to <= 15	16 > to <= 20	8 > to <= 10
6	15 > to <= 18	20 > to <= 24	10 > to <= 12
7	18 > to <= 21	24 > to <= 28	12 > to <= 14
8	21 > to <= 24	28 > to <= 32	14 > to <= 16
9	24 > to <= 27		16 > to <= 18
10	27 > to <= 30		18 > to <= 20
11			20 > to <= 22
12			22 > to <= 24
13			24 > to <= 26
14			26 > to <= 28
15			28 > to <= 30

**Figure 5.47** a) Moran's I and Geary's C correlograms for the available sodium in the shrubland plots. b) provides the key to the lag increments used in the correlograms for each plot.

## Phosphorus

### a) Test of normality, descriptive statistics and inter-plot variation

The frequency distributions displayed by the boxplots (figure 5.48) show that the datasets from plots 5 and 11 are positively skewed whereas plots 3 and 9 can be described as having normal distributions. Outliers are evident in all datasets except the dataset from plot 3.

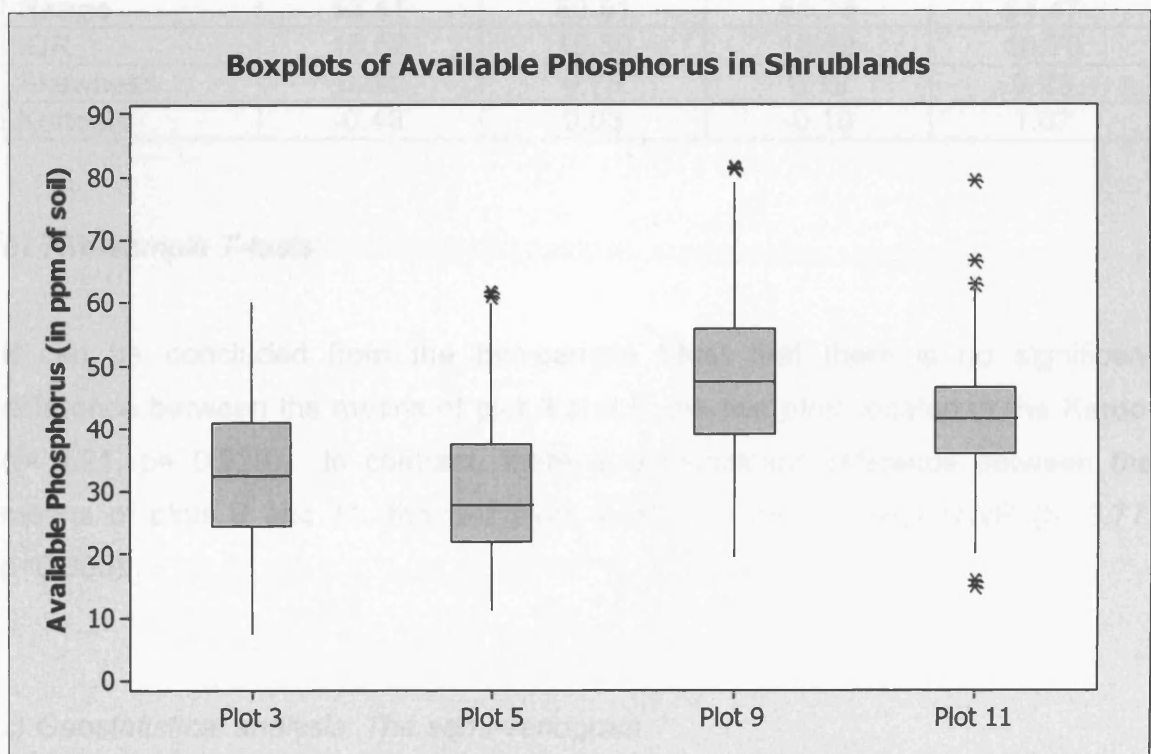


**Figure 5.48** Boxplots representing the sample distribution of available phosphorus in the shrubland plots.

Higher mean values of available phosphorus are evident in the two Sevilleta NWR plots (9 & 11) (see table 5.22). Within each study region the mean values are similar, demonstrating the influence of the soil type and/or the shrub species. The ranges of available phosphorus are greater in the Sevilleta NWR plots, however, higher coefficient of variation values are evident in the two Karoo plots. In general, the four plots do not vary significantly in their distribution characteristics.

**Table 5.22** Inter-plot comparisons of descriptive statistics: Available phosphorus in ppm of soil

Descriptive Statistic	Plot 3 (Karoo)	Plot 5 (Karoo)	Plot 9 (Sevilleta)	Plot 11 (Sevilleta)
Mean	32.65	30.65	47.51	41.34
Median	32.64	28.11	47.42	41.53
SE of Mean	1.15	1.19	1.32	0.98
St Dev	12.00	12.40	13.51	10.13
Variance	144.07	153.86	182.39	102.66
Coef Var	36.76	40.47	28.42	24.51
Minimum	7.53	11.25	19.69	14.90
Maximum	60.04	61.76	81.44	79.38
Range	52.51	50.51	61.75	64.47
IQR	16.52	15.30	16.62	10.70
Skewness	0.04	0.79	0.19	0.23
Kurtosis	-0.48	0.03	-0.10	1.67

### b) Two-sample T-tests

It can be concluded from the two-sample t-test that there is no significant difference between the means of plot 3 and 5, the two plots located in the Karoo. ( $t = 1.21$ ,  $p = 0.229$ ). In contrast, there is a significant difference between the means of plots 9 and 11, the two plots located in the Sevilleta NWR ( $t = 3.77$ ,  $p < 0.005$ ).

### c) Geostatistical analysis: The semi-variogram

No outliers were removed from any of the plots, no transformations were necessary and no drift was identified. Table 5.23 shows the numerical results and the associated semi-variogram graphs are presented in figure 5.49.

Table 5.23 Geostatistical analysis of the available phosphorus in shrubland plots

Parameter: Phosphorus						
No.	Plot Location	Fitted Model	Nugget Value (Co)	Sill (Co+C <sub>1</sub> )	Range (a)	Nugget-to-sill Ratio (Co)/(Co+C <sub>1</sub> )
3	Karoo	Spherical	0.20	0.85	8.37	0.24
5	Karoo	Spherical	0.46	0.94	5.27	0.49
9	Sevilleta NWR	Spherical	0.30	0.79	8.40	0.58
11	Sevilleta NWR	Nugget	1.00	na	na	na

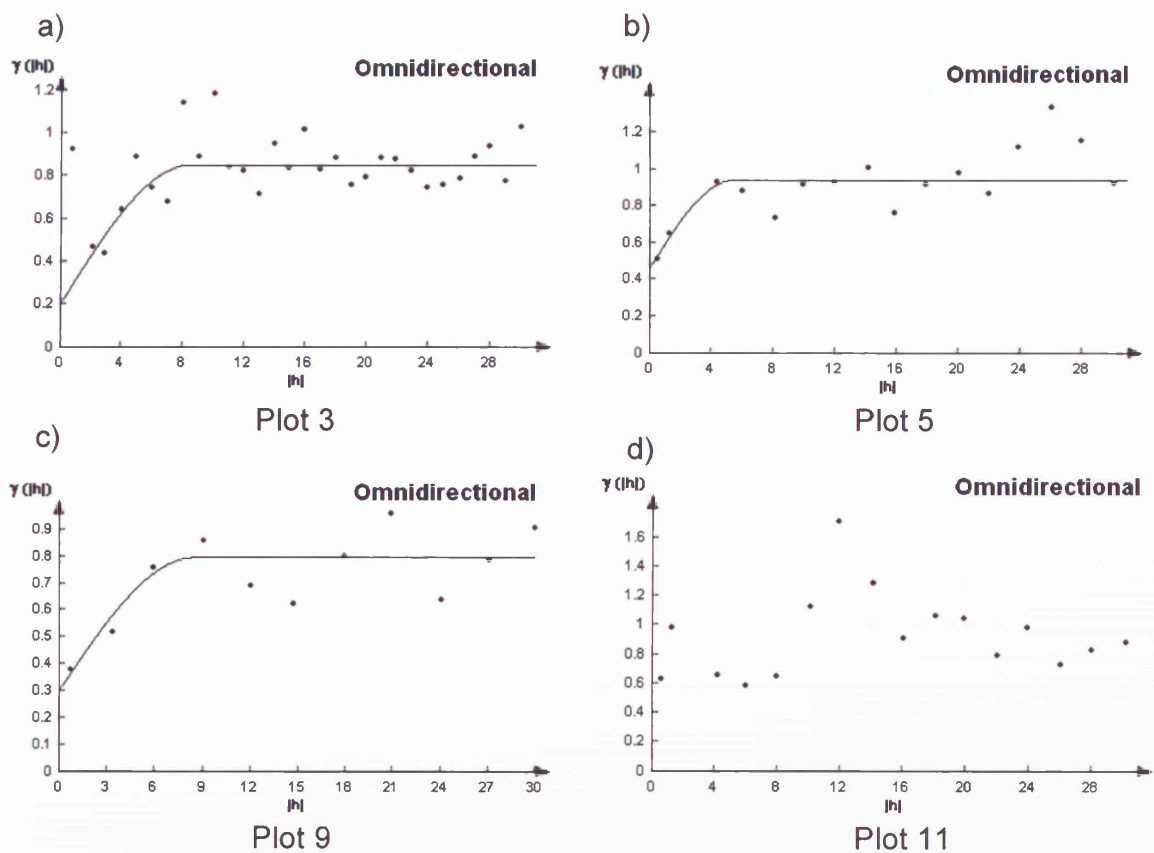
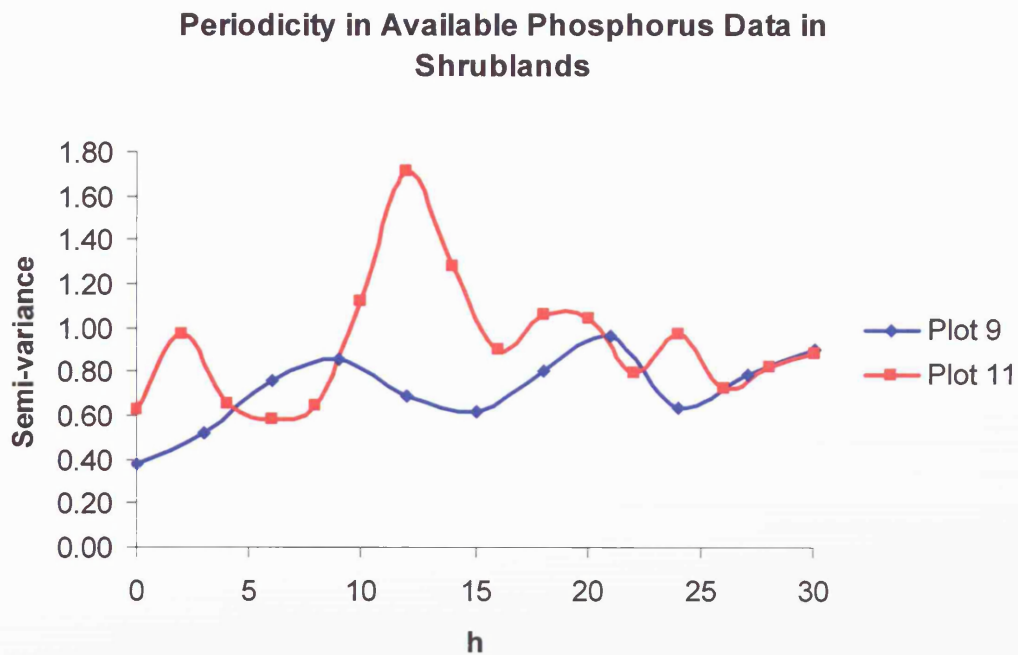


Figure 5.49 Modelled semi-variograms of the available phosphorus in shrubland plots.

The results are as follows:

- Spatial autocorrelation of available phosphorus was identified in plots 3, 5 and 9. All were best represented by a spherical model and the ranges were 8.37m, 5.27m and 8.40m, respectively.

- ii) Plot 3 was considered to show a strong spatial dependency with a nugget-to-sill ratio of 0.24, where both plots 5 and 9 show moderate spatial dependency.
- iii) A pure nugget model was applied to plot 11, which suggests no spatial patterns exist. However, a large peak is identifiable in the experimental variogram that implies this plot may be demonstrating the 'hole effect' or large scale periodicity. This can be seen in figure 5.50.
- iv) Although a model was applied to plot 9, strong periodicity is evident (figure 5.50). Some weak periodicity may be present in plots 3 and 5, however, this has not been included in the graph as it is not considered to be significant.



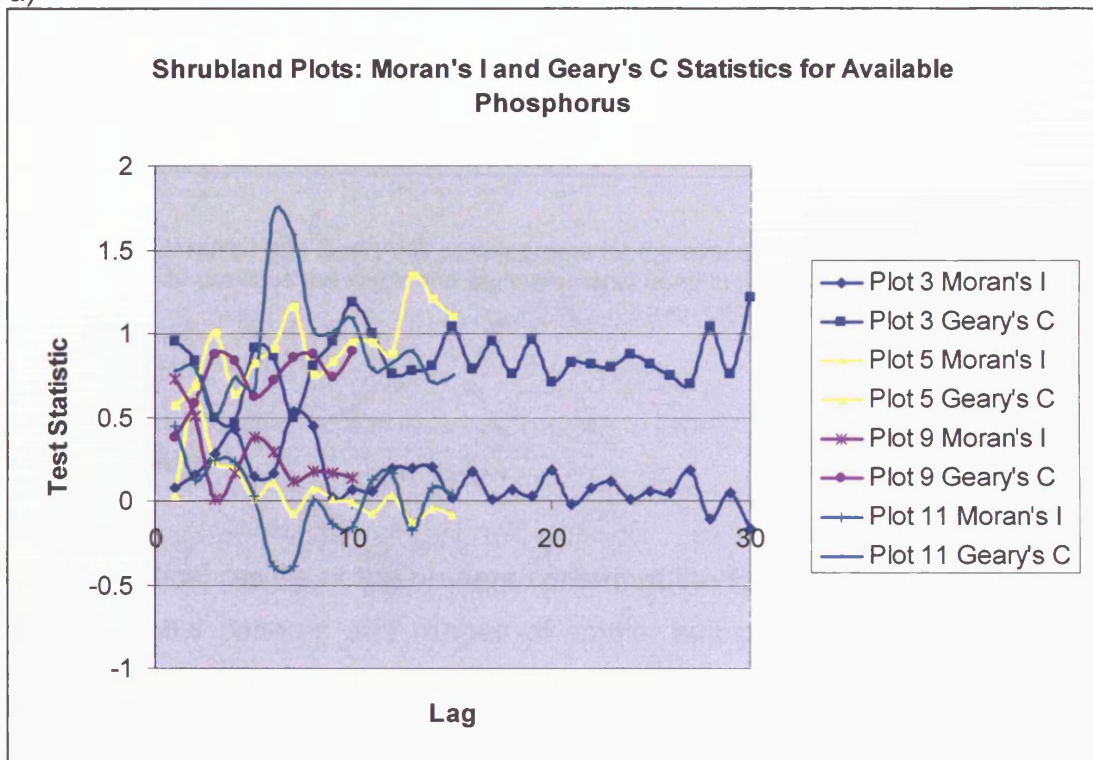
**Figure 5.50** Semi-variograms with connecting lines to show periodicity in the available phosphorus data in shrubland plots.

e) Geostatistical analysis: Moran's I and Geary's C statistics

The results are as follows: (see figure 5.51)

- i) Comparisons made between the Moran's I and Geary's C statistics show that the results mirror each other relatively well with the exception of the smaller lag distances of plot 5.
- ii) The interpretation of the correlograms generally produced comparative results to those derived from the semi-variogram.
- iii) The Geary's C correlogram suggests that plot 9 displays clustering at all lag distances only to varying degrees, however, the Moran's I correlogram indicates that between 6 and 9m random spatial patterns are evident. This result coincides with that derived from the semi-variogram.
- iv) The correlograms indicate that a range of between 8 and 10m may be applicable to plot 11.

a)



b)

Lag increment codes	Plot 3	Plot 5 & 11	Plot 9
1	0 > to <= 1	0 > to <= 2	0 > to <= 3
2	1 > to <= 2	2 > to <= 4	3 > to <= 6
3	2 > to <= 3	4 > to <= 6	6 > to <= 9
4	3 > to <= 4	6 > to <= 8	9 > to <= 12
5	4 > to <= 5	8 > to <= 10	12 > to <= 15
6	5 > to <= 6	10 > to <= 12	15 > to <= 18
7	6 > to <= 7	12 > to <= 14	18 > to <= 21
8	7 > to <= 8	14 > to <= 16	21 > to <= 24
9	8 > to <= 9	16 > to <= 18	24 > to <= 27
10	9 > to <= 10	18 > to <= 20	27 > to <= 30
11	10 > to <= 11	20 > to <= 22	
12	11 > to <= 12	22 > to <= 24	
13	12 > to <= 13	24 > to <= 26	
14	13 > to <= 14	26 > to <= 28	
15	14 > to <= 15	28 > to <= 30	
16	15 > to <= 16		
17	16 > to <= 17		
18	17 > to <= 18		
19	18 > to <= 19		
20	19 > to <= 20		
21	20 > to <= 21		
22	21 > to <= 22		
23	22 > to <= 23		
24	23 > to <= 24		
25	24 > to <= 25		
26	25 > to <= 26		
27	26 > to <= 27		
28	27 > to <= 28		
29	28 > to <= 29		
30	29 > to <= 30		

**Figure 5.51** a) Moran's I and Geary's C correlograms for the available phosphorus in the shrubland plots. b) provides the key to the lag increments used in the correlograms for each plot.

### 5.9.2 Summary

The geostatistical results of the nutrient content of the four shrubland plots show a variety of spatial patterns and ranges of spatial autocorrelation. Where spatial autocorrelation is evident, only two ranges are greater than 9m and none are less than 5m. However, six results were classed as having random patterns and three were not modelled as a result of a downward trend in variance with an increasing lag distance. It is thought that this trend may indicate a checkerboard pattern in

the data. No nutrients demonstrate consistent results across all four plots, although phosphorus shows similar ranges of autocorrelation across three of the plots and the magnesium contents show a similar pattern of increasing variance.

Potassium is the only nutrient that demonstrates spatial patterns that may be related to the geographical location; the Sevilleta NWR plots have ranges of 7.5m (plot 9) and 8.06m (plot 11) whereas the Karoo plots demonstrate no spatial pattern (plot 3) and a range of >30m (plot 5), which can be classed as having no spatial pattern as it is greater than the largest scale of interest.

The results derived for the available sodium show that two plots (1 and 10) display no spatial patterns but two plots (5 and 9) possibly exhibit a checkerboard pattern. In view of these results, it is suggested that a fine-scale checkerboard pattern (<0.5m) of high and low sodium values may exist in shrubland landscapes. As this range is less than the minimum scale of interest in this research, further field analysis would have to be undertaken to test this hypothesis. This may be important with respect to the erodibility of soil due to the dispersive effect of sodium on clay particles.

In contrast to sodium, the available calcium, also potentially important in the susceptibility of soil to erosion, exhibits significant differences between the two study regions. The calcium contents of the soils from the Karoo are significantly lower than those found in the Sevilleta NWR sites. This difference in calcium to sodium ratio may significantly influence a regions susceptibility to erosion. In terms of the two study regions investigated in this project, this suggests that the soils in the Karoo may be more erodible than those in the Sevilleta NWR. This hypothesis shall be discussed in more detail in chapter 7. In terms of spatial autocorrelation, calcium does not produce consistent results, however, periodicity is evident in the majority of plots, this cyclic behaviour suggests that calcium varies between shrub and intershrub areas.

### **5.10 Key findings from the shrubland plots**

- Complex spatial structures are evident for many of the shrubland soil parameters, thus making it difficult to represent them accurately with the simple models utilised in this study. Where possible the most representative models have been applied, however, fluctuation of the variance suggests that these models may be misrepresenting the spatial patterns evident in shrublands.
- However, the shorter lag distances are generally more important in determining whether spatial autocorrelation exists therefore if the variance fluctuates at the larger lags this is considered less important.
- Periodicity is evident in many of the shrubland datasets; this is thought to represent the heterogeneity caused by differences in soil parameter between shrub and intershrub areas.
- The periodicity in the data suggests that the scale of measurement is important when determining the spatial patterns of soil parameters in semi-arid shrublands.
- A decrease in variance with an increasing lag distance is displayed by some of the plots for organic matter content, bulk density, soil pH and available potassium and sodium. This would suggest a checkerboard pattern is present.
- Of the plots that demonstrated spatial autocorrelation, the ranges are as follows:

- Organic Matter: 4.5m
  - Dry bulk density: 6.82m
  - Soil moisture: 6.60m – 15.84m
  - Shear strength: 4.20 – 9.61m
  - pH: 5.89 – 15.54m
  - Conductivity: 5.27 – 8.10m
  - Calcium: 6.60m
  - Magnesium: 5.58 – 21.43m
  - Potassium: 7.5m – 31.44m
  - Sodium: none determined
  - Phosphorus: 5.27 – 8.40m
- 
- The parameters that show evidence of having mean values specific to each of the study regions are: organic matter content, shear strength, soil pH, available calcium and available phosphorus.
  - The parameters that show evidence of having distribution characteristics specific to the study region are: organic matter content, bulk density, shear strength, soil pH, and available calcium, potassium and phosphorus.
  - Available calcium and soil pH demonstrate the most significant differences between the Karoo and Sevilleta NWR plots. These differences reflect the characteristics of the two soil types. This must be considered when interpreting the results of the other soil parameters.

The relationships among the soil parameters will be investigated further in chapters 7 and 8, followed by a detailed interpretation and discussion of the results.

## CHAPTER SIX

### Badlands:

#### Analysis of the Spatial Continuity of Soil Properties

---

---

##### ***6.1 Introduction***

##### ***6.2 Organic matter content***

##### ***6.3 Bulk density***

##### ***6.4 Soil moisture***

##### ***6.5 Shear strength***

##### ***6.6 Particle-size distribution analysis***

##### ***6.7 Soil-aggregate stability***

##### ***6.8 pH***

##### ***6.9 Electrical conductivity***

##### ***6.10 Nutrient content analysis***

##### ***6.11 Key findings***

---

---

##### ***6.1 Introduction***

This chapter presents the results and a brief discussion of the spatial distribution of soil parameters derived from plots classed as badlands.

This chapter will follow the same structure as the previous two chapters. Refer to sections 4.1 for a detailed explanation of the analysis presented here.

In contrast to the grassland and shrubland data, no comparisons can be made between badland datasets from the two study regions as this type of landscape is not present in the Sevilleta NWR, New Mexico. Thus, in order to gain as much understanding of these landscapes as possible, three plots were measured in the Karoo, South Africa: plots 4, 6 and 7.

As with the shrubland data, it is not possible to model some of the experimental variograms, these variograms are presented nonetheless along with the reasons why they are considered unsuitable for modelling purposes.

In addition, it should be noted that the spatial analyses of plots 4 and 7 vary from the grassland and shrubland investigations regarding the scale of measurement. As a consequence of the nature of badland development, the gully networks characteristically form across footslopes in the Karoo thus making it more practical, in some cases, to have plots of 30m x 120m rather than 60 x 60m. This allows the majority of the plot to encompass the gullied landscape rather than the surrounding shrublands. Plot 6 follows the conventional plot layout as this was a substantial area of badlands and was therefore adequately represented within the 60 x 60m plot. As a result of the change in plot layout, the maximum lag distance was increased from 30m to 60m.

## **6.2 Organic matter content**

### **6.2.1 Results:**

#### *a) Test of normality, descriptive statistics and inter-plot variation*

The frequency distributions displayed by the boxplots (figure 6.1) show that the datasets from all the plots are positively skewed, however, the skew of plot 4's data is weak and can therefore be classed as having a normal distribution. Plots 6

and 7 are considered to be highly positively skewed as the skewness values are greater than 1 (see table 6.1). Outliers are evident in all datasets.

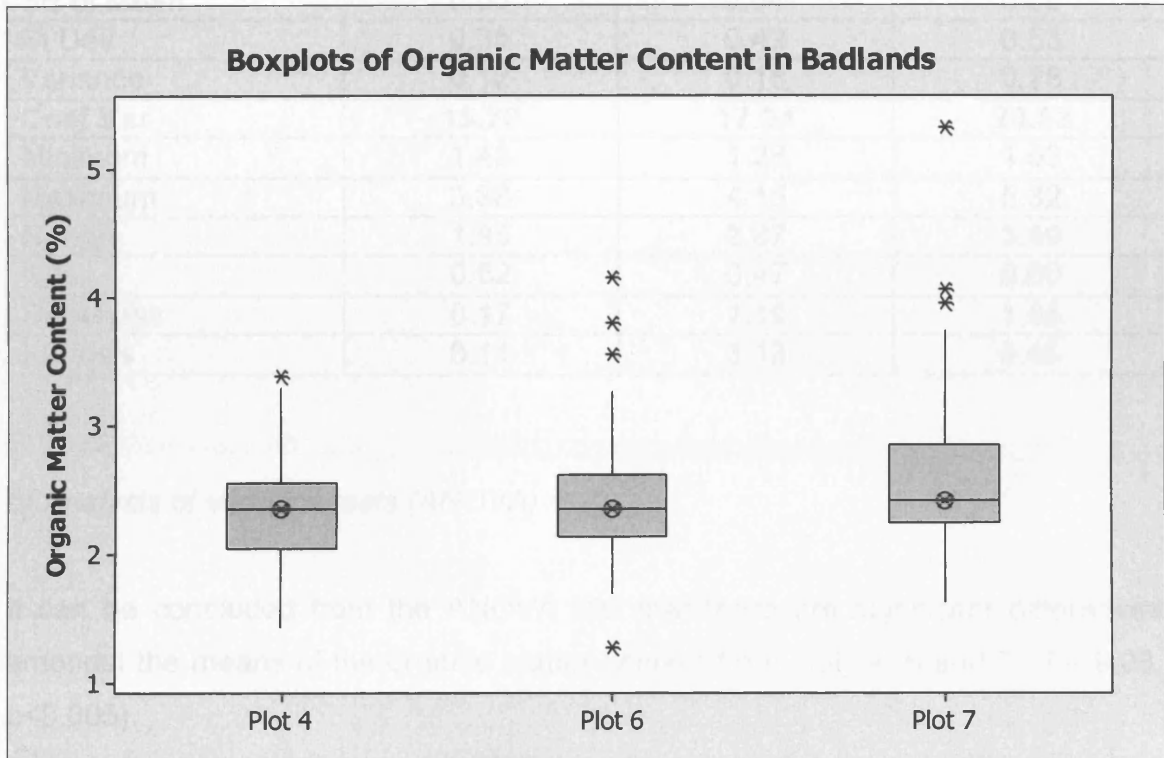


**Figure 6.1** Boxplots representing the sample distribution of organic matter content in the badland plots.

Inter-plot comparisons of the descriptive statistics can be seen in table 6.1. The three plots have similar mean values, ranges and coefficient of variation values. However, plot 7 demonstrates the greatest variation relative to the mean and plot 4 shows the least intra-plot variation.

**Table 6.1** Inter-plot comparisons of descriptive statistics: Organic matter content

Descriptive Statistic	Plot 4 (Karoo)	Plot 6 (Karoo)	Plot 7 (Karoo)
<b>Mean</b>	<b>2.32</b>	<b>2.41</b>	<b>2.57</b>
Median	2.34	2.34	2.41
SE of Mean	0.03	0.04	0.05
St Dev	0.35	0.42	0.53
Variance	0.12	0.18	0.28
<b>Coef Var</b>	<b>15.20</b>	<b>17.34</b>	<b>20.52</b>
Minimum	1.43	1.28	1.63
Maximum	3.38	4.15	5.32
<b>Range</b>	<b>1.95</b>	<b>2.87</b>	<b>3.69</b>
IQR	0.52	0.47	0.60
Skewness	0.17	1.19	1.85
Kurtosis	0.11	3.18	6.45

*b) Analysis of variance tests (ANOVA)*

It can be concluded from the ANOVA test that there are significant differences amongst the means of the organic matter content from plots 4, 6 and 7. ( $F= 9.08$ ,  $p<0.005$ ).

*c) Intra-plot variation*

Examination of the means and standard deviations of each cell in the three plots (figure 6.2) suggests that the scale of measurement may be a significant factor in the characterisation of organic matter content of soil. At the smallest scale of measurement (1.5m x 1.5m), plots 6 and 7 in particular, demonstrate significant differences in amount of variation within each of the cells. At the largest cell size (30m x 30m) the amounts of variation are similar although the means vary. This would suggest that some spatial patterns exist for organic matter content in badland landscapes.

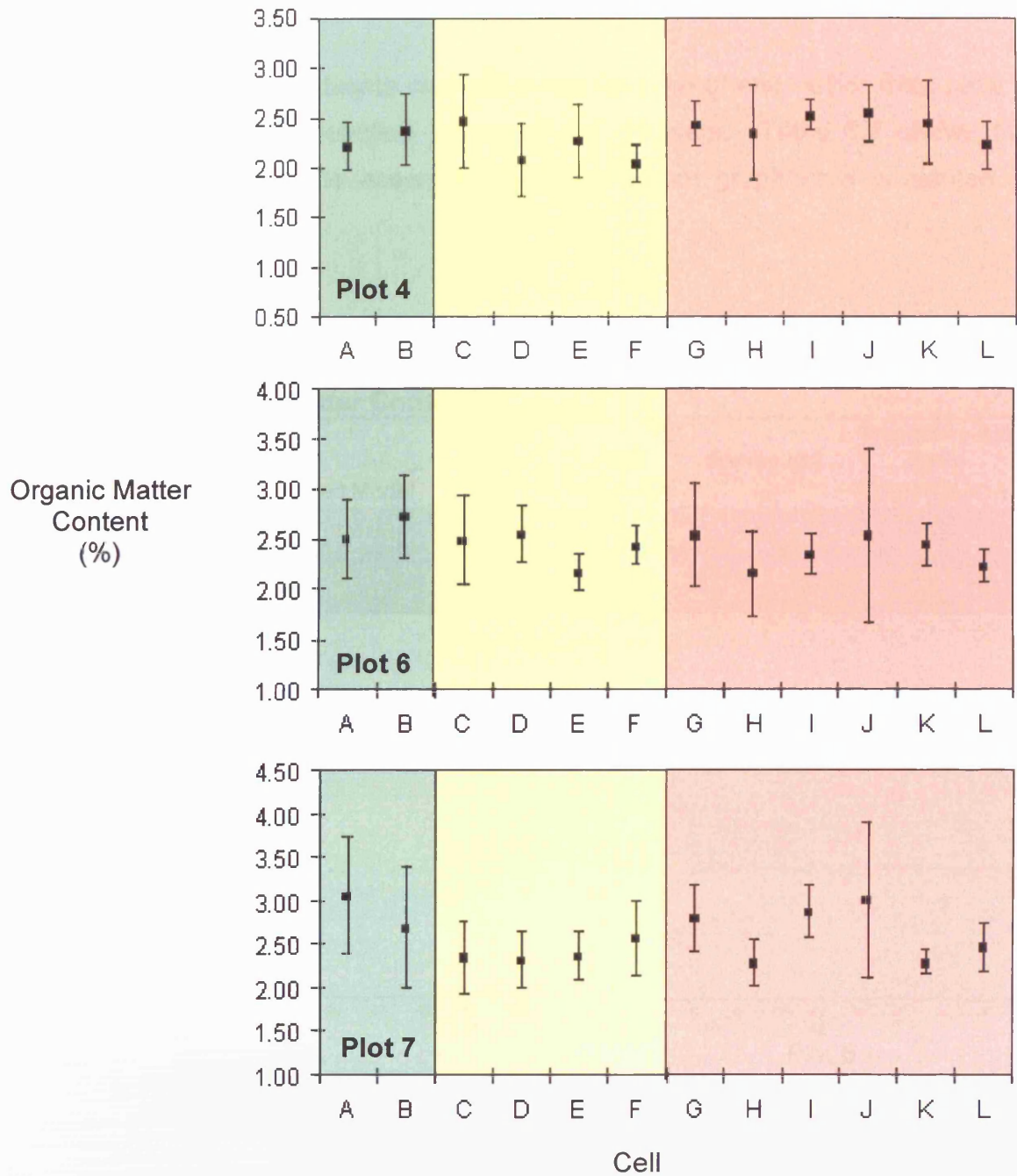


**Figure 6.2** The means and standard deviations of organic matter content for each cell within the plots. Green represents the 30 x 30m cells, yellow represents the 10 x 10m cells and pink represents 1.5 x 1.5m cells.

d) *Geostatistical analysis: The semi-variogram*

Pre-processing of the datasets resulted in the removal of one outlier from plots 6 and 7. No drift was identified in any of the datasets. Table 6.2 shows the numerical results and the associated semi-variogram graphs are presented in figure 6.3.

**Table 6.2** Geostatistical analysis of organic matter content of shrubland plots

<b>Parameter: Organic Matter Content</b>						
No.	Plot Location	Fitted Model	Nugget Value (Co)	Sill (Co+C <sub>1</sub> )	Range (m) (a)	Nugget-to-sill Ratio (Co)/(Co+C <sub>1</sub> )
4	Karoo	na	na	na	na	na
6	Karoo	Spherical	0.07	1.00	7.20	0.07
7	Karoo	Spherical	0.31	0.75	7.48	0.41

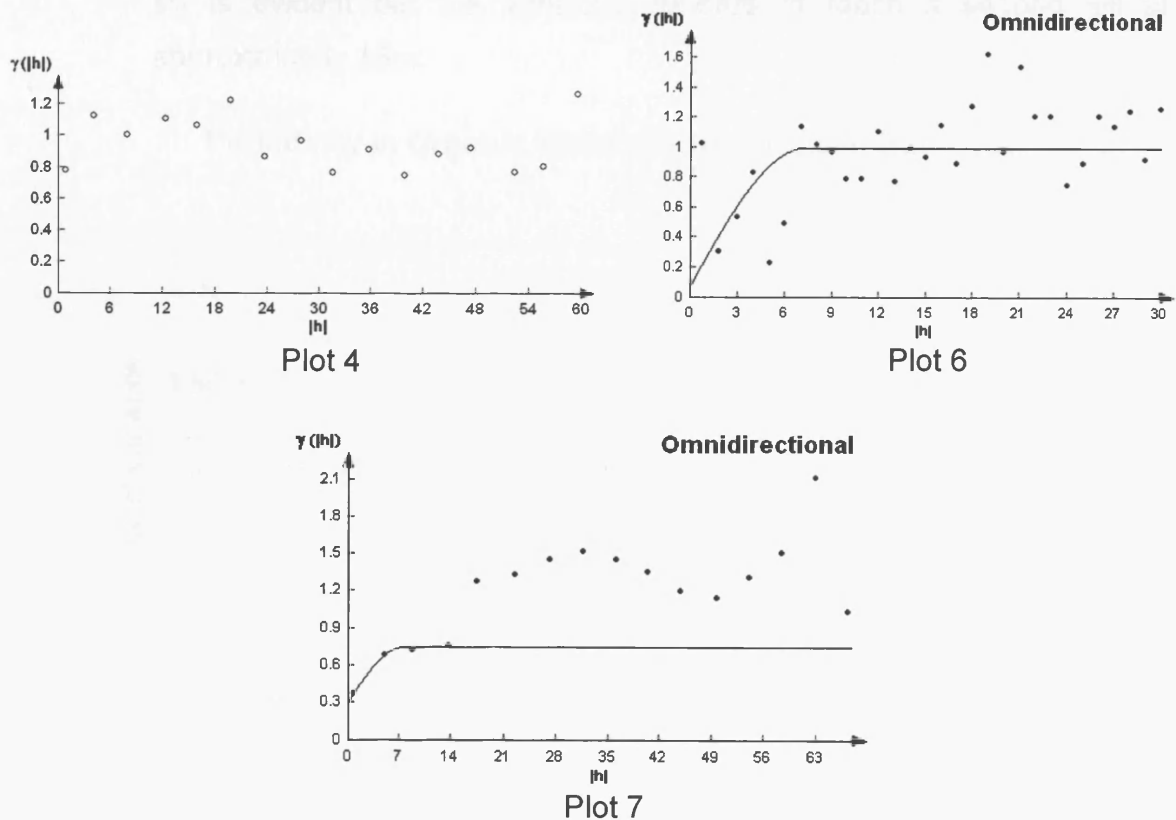


**Figure 6.3** Semi-variograms of the organic matter content of the badland plots.

The results are as follows:

- i) Plots 6 and 7 show evidence of spatial autocorrelation. Both have been modelled with a spherical model and the nugget-to-sill ratios indicate strong and moderate spatial dependency, respectively. The ranges are similar for both plots, although plot 7, which has a larger maximum lag as a result of the change in plot layout, shows that although a sill is reached at approximately 7m, periodicity is evident in the variance suggesting larger-scale patterns exist in this landscape.
- ii) Plot 4, in contrast, could not be accurately represented by a model. The most accurate simple model would be a pure nugget model thus suggesting no spatial patterns exist. However, this variogram displays a fluctuating downward trend in variance with an increasing lag distance. This may represent a checkerboard pattern in organic matter content. The periodicity of plot 4 can be seen in figure 6.4.
- iii) Figure 6.4 also shows the complex spatial structure of plot 7. The first sill is evident but the variance appears to reach a second sill at approximately 18m.

**Periodicity in Organic Matter Content Data in Badlands**

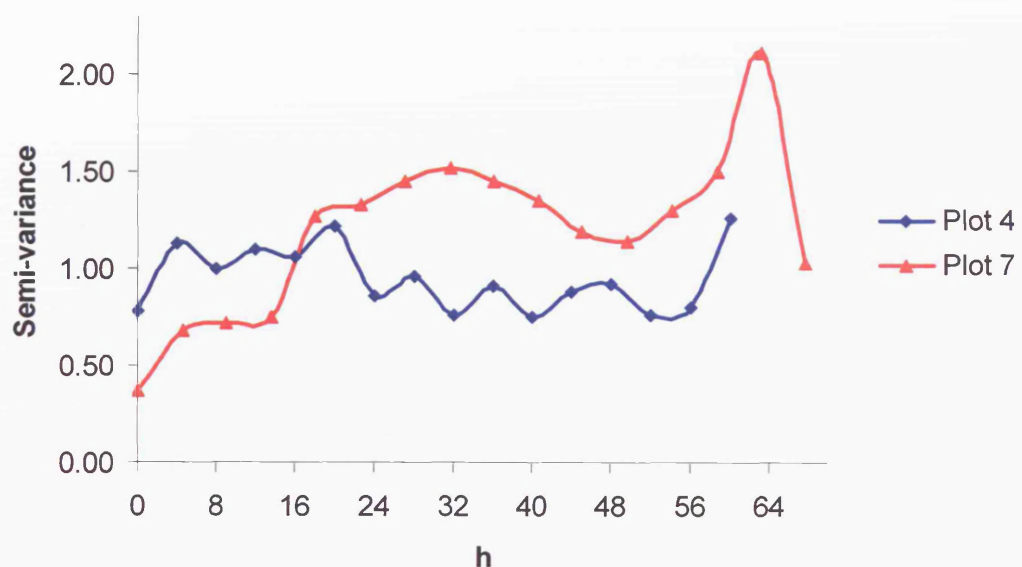
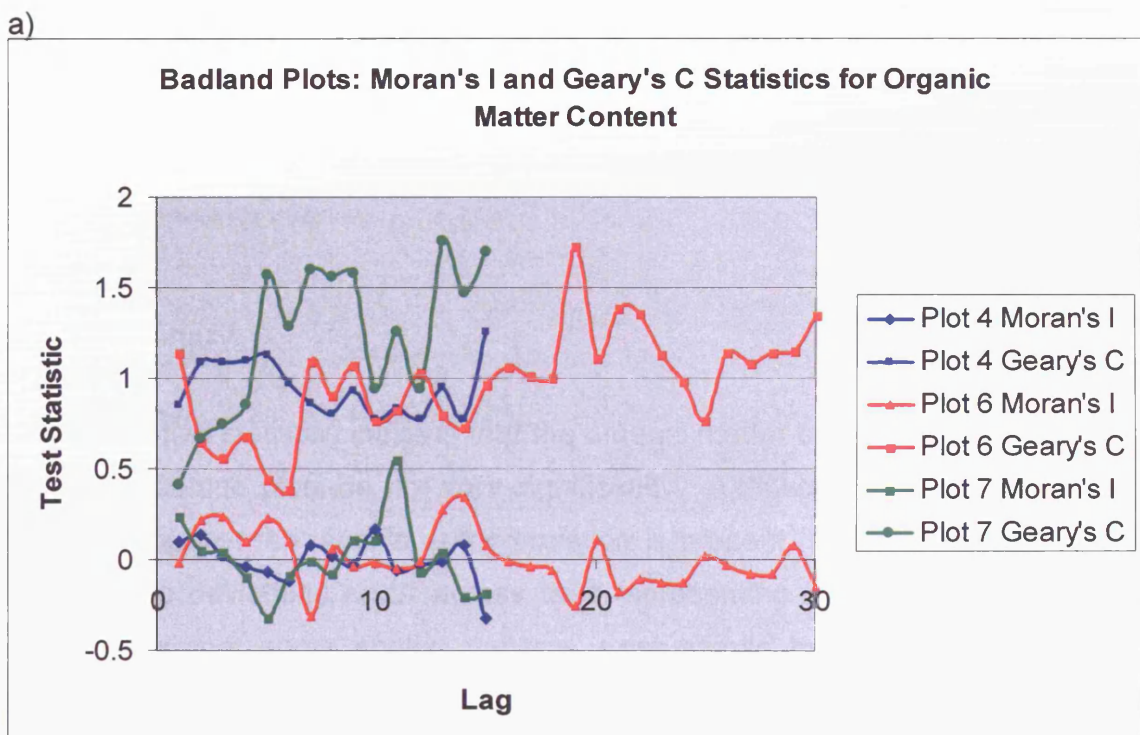


**Figure 6.4** Semi-variograms with connecting lines to show periodicity in organic matter content data in badland plots.

e) *Geostatistical analysis: Moran's I and Geary's C statistics*

The results are as follows: (see figure 6.5)

- i) Comparisons made between the Moran's I and Geary's C statistics show that the results mirror each other relatively well, this increases the confidence in the results.
- ii) Both the Moran's I and the Geary's C analyses indicate that plot 4 generally displays a random pattern, although the Geary's C correlogram shows that between lags of approximately 18 and 54m the samples show evidence of various levels of clustering. This corresponds to the semi-variogram results.
- iii) Evidence from both the Moran's I and Geary's C statistics correspond to the variogram results produced for plot 6. A change in spatial structure is present at a lag distance of approximately 6 -7 m.
- iv) In contrast to the variogram results, the two correlograms suggest that the most significant change in spatial structure in plot 7 occurs at a lag distance of approximately 18m. This is the second sill identified in the variograms.



b)

Lag increment codes	Plot 4	Plot 6	Plot 7
1	0 > to <= 4	0 > to <= 1	0 > to <= 4.5
2	4 > to <= 8	1 > to <= 2	4.5 > to <= 9
3	8 > to <= 12	2 > to <= 3	9 > to <= 13.5
4	12 > to <= 16	3 > to <= 4	13.5 > to <= 18
5	16 > to <= 20	4 > to <= 5	18 > to <= 22.5
6	20 > to <= 24	5 > to <= 6	22.5 > to <= 27
7	24 > to <= 28	6 > to <= 7	27 > to <= 31.5
8	28 > to <= 32	7 > to <= 8	31.5 > to <= 36
9	32 > to <= 36	8 > to <= 9	36 > to <= 40.5
10	36 > to <= 40	9 > to <= 10	40.5 > to <= 45
11	40 > to <= 44	10 > to <= 11	45 > to <= 49.5
12	44 > to <= 48	11 > to <= 12	49.5 > to <= 54
13	48 > to <= 52	12 > to <= 13	54 > to <= 58.5
14	52 > to <= 56	13 > to <= 14	58.5 > to <= 63
15	56 > to <= 60	14 > to <= 15	63 > to <= 67.5
16		15 > to <= 16	
17		16 > to <= 17	
18		17 > to <= 18	
19		18 > to <= 19	
20		19 > to <= 20	
21		20 > to <= 21	
22		21 > to <= 22	
23		22 > to <= 23	
24		23 > to <= 24	
25		24 > to <= 25	
26		25 > to <= 26	
27		26 > to <= 27	
28		27 > to <= 28	
29		28 > to <= 29	
30		29 > to <= 30	

**Figure 6.5** a) Moran's I and Geary's C correlograms for the organic matter content of the badland plots. b) provides the key to the lag increments used in the correlograms for each plot.

### 6.2.2 Summary

The descriptive statistics indicate that the organic matter contents of the soils from the three badland plots do not vary significantly. Although the intra-plot analysis does not suggest that spatial autocorrelation is present, significant differences in the standard deviations occur across cells representing the same spatial scales. This implies that some spatial patterns exist across badland landscapes and therefore the scale of measurement is potentially important.

The geostatistical analyses confirm these conclusions. Two plots (6 and 7) demonstrate evidence of spatial autocorrelation; the ranges derived were both approximately 7m. However, these two plots have different maximum lag distances; 30m and 60m, respectively. Clear periodicity can be seen in the data from plot 7, the plot with the greater scale of measurement, thus suggesting that the derived range values are actually only representing part of the spatial structure and not adequately representing the true spatial patterns of organic matter content across a badland landscape.

Plot 4, in contrast, presents another spatial pattern. This variogram displays a fluctuating downward trend in variance with an increasing lag distance. This may represent a checkerboard pattern in organic matter content. However, another explanation may be that this plot is also only representing part of a larger-scale cyclic pattern.

### **6.3 Bulk density**

#### **6.3.1 Results**

##### *a) Test of normality, descriptive statistics and inter-plot variation*

The frequency distributions displayed by the boxplots (figure 6.6) show that plot 4 can be considered as having a normal distribution, plot 6 is moderately negatively skewed and plot 7 is moderately positively skewed. Outliers at both the top and bottom of the scale are evident in plots 6 and 7.

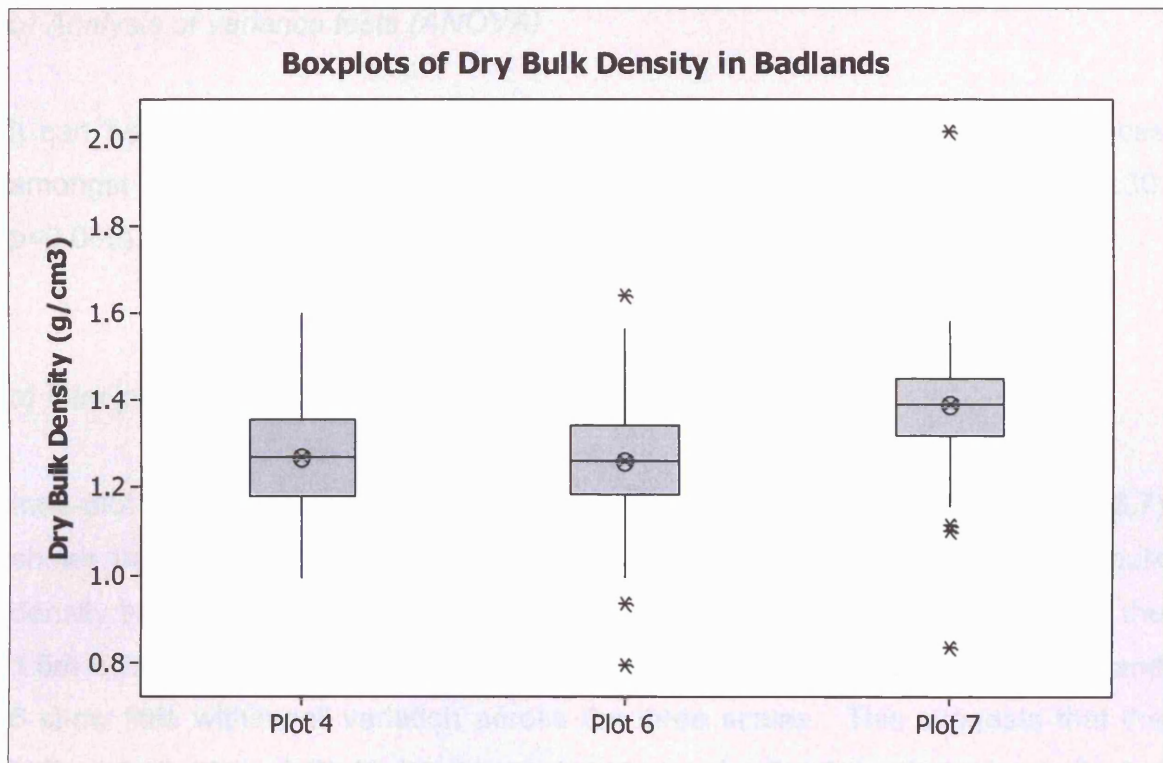


**Figure 6.6** Boxplots representing the sample distribution of dry bulk density in the badland plots.

The descriptive statistics show that the mean bulk density values are relatively similar for all three plots but particularly between plots 4 and 6. Plot 7 has a marginally higher mean bulk density and range but, relative to the mean, the variation within the plot is slightly less than plots 4 and 6.

**Table 6.3** Inter-plot comparisons of descriptive statistics: Dry bulk density ( $\text{g cm}^{-3}$ )

Descriptive Statistic	Plot 4 (Karoo)	Plot 6 (Karoo)	Plot 7 (Karoo)
Mean	1.27	1.26	1.38
Median	1.27	1.26	1.39
SE of Mean	0.01	0.01	0.01
St Dev	0.14	0.13	0.13
Variance	0.02	0.02	0.02
Coef Var	10.97	10.38	9.53
Minimum	0.99	0.80	0.83
Maximum	1.60	1.64	2.01
Range	0.61	0.84	1.18
IQR	0.18	0.16	0.13
Skewness	0.21	-0.3	0.16
Kurtosis	-0.31	1.33	6.62

*b) Analysis of variance tests (ANOVA)*

It can be concluded from the ANOVA test that there are significant differences amongst the means of the dry bulk density from plots 4, 6 and 7. ( $F= 26.30$ ,  $p<0.005$ ).

*c) Intra-plot variation*

Intra-plot analysis using the means and standard deviations of the cells (figure 6.7) shows that the scale of measurement does not appear to be significant for bulk density in badlands. Only plot 7 shows greater differences in variation within the 1.5m x 1.5m cells compared to the other scales of measurement. Both plots 4 and 6 show little within-cell variation across the three scales. This suggests that the bulk density is relatively homogenous across badland landscapes. Spatial analysis will investigate this to a more comprehensive level.

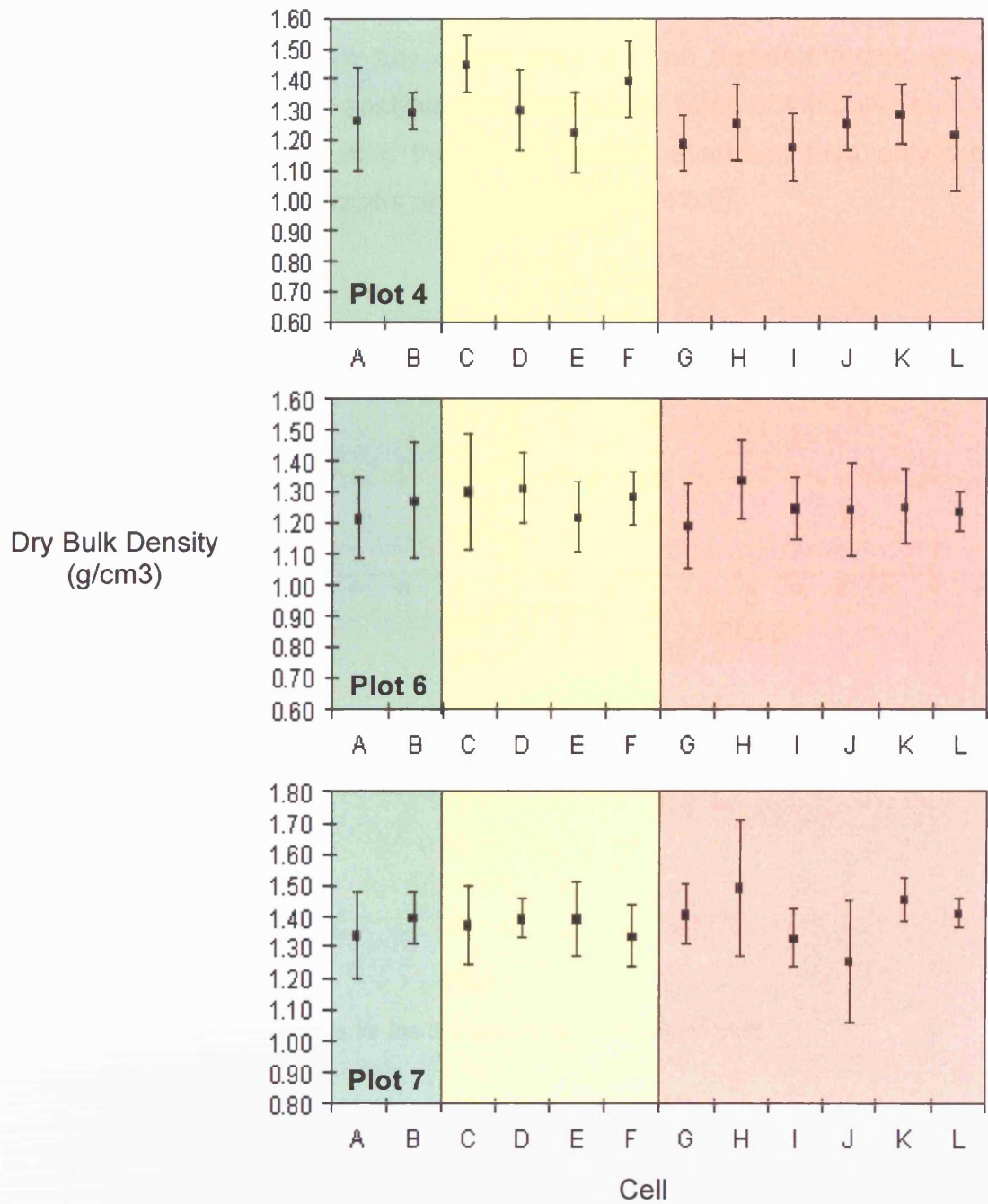


**Figure 6.7** The means and standard deviations of dry bulk density for each cell within the plots. Green represents the 30 x 30m cells, yellow represents the 10 x 10m cells and pink represents 1.5 x 1.5m cells

*d) Geostatistical analysis: The semi-variogram*

No outliers were removed from any of the plots and no transformations were performed before geostatistical analysis was carried out. None of the bulk density datasets could be modelled using the simple models available, thus only the experimental semi-variogram graphs are presented (figure 6.8).

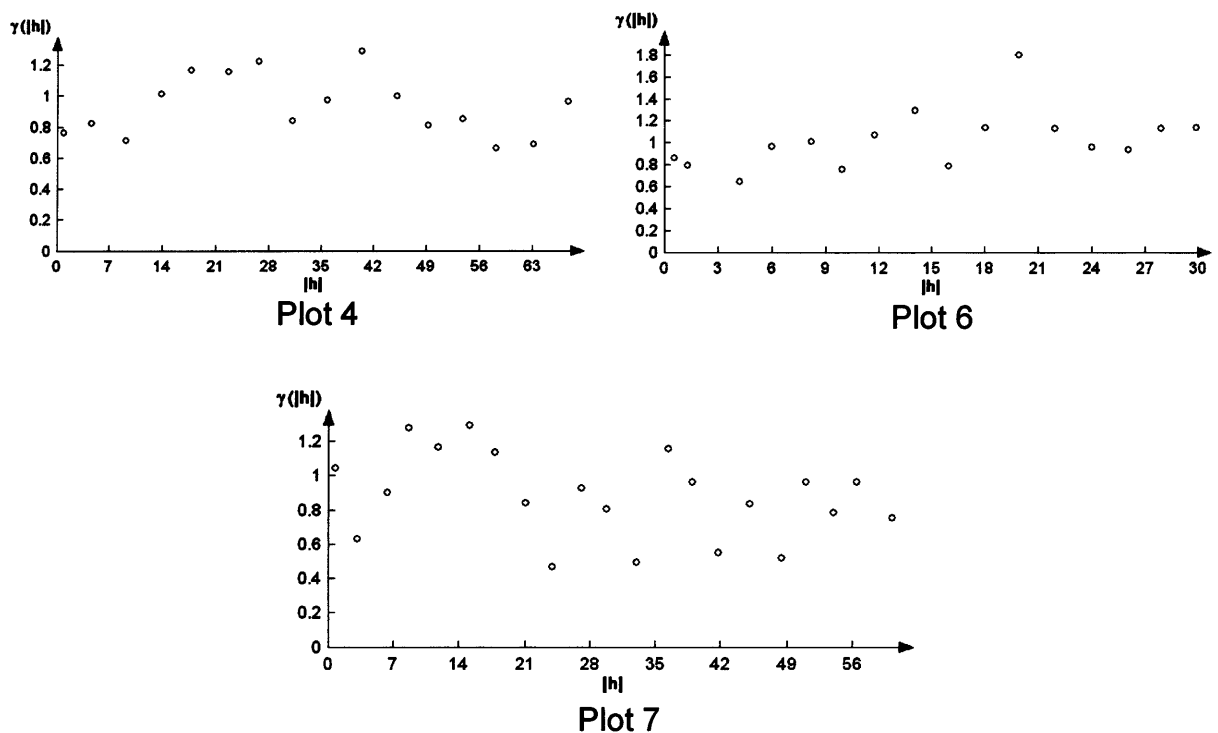


**Figure 6.8** Modelled semi-variograms for the dry bulk density of badland plots.

The results are as follows:

- i) The experimental variograms show that none of the datasets can be represented by simple models. If the data is considered very generally, a nugget model could be applied but for this study this model does not accurately represent the spatial patterns in this landscape.
- ii) Although plots 4 and 7 represent a larger scale of measurement than plot 6, all three plots show some evidence of cyclic behaviour. This can be seen in figure 6.9.

- iii) Plots 4 and 7 display a slight downward trend of variance with increasing lag distances.

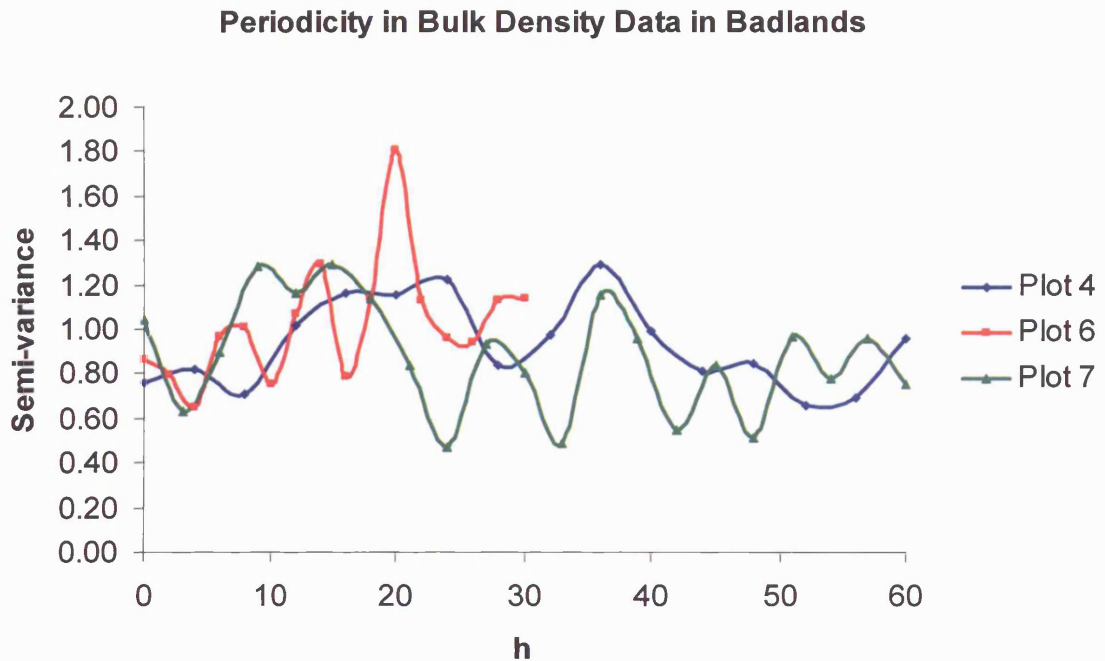


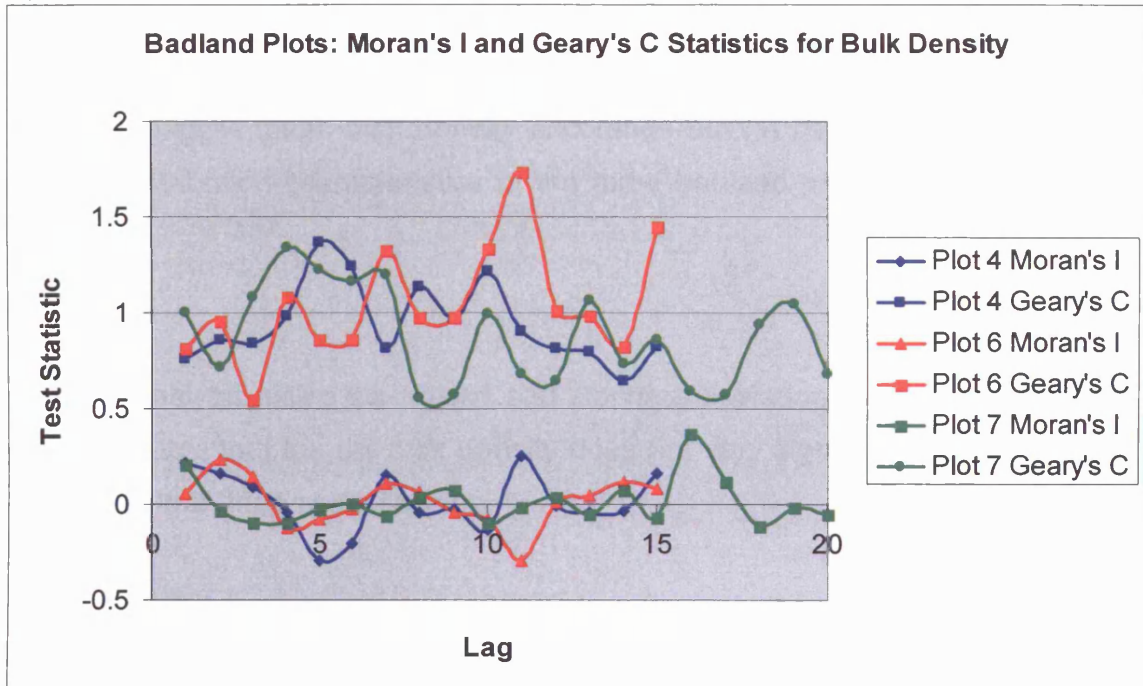
**Figure 6.9** Semi-variograms with connecting lines to show periodicity in dry bulk density data in badland plots.

e) *Geostatistical analysis: Moran's I and Geary's C statistics*

The results are as follows: (see figure 6.10)

- i) Comparisons made between the Moran's I and Geary's C statistics show that the results from the Moran's I correlogram produce a much weaker signal than the Geary's C for plots 6 and 7. Some variation between the two types of correlograms is evident suggesting that caution should be exercised when interpreting the results. Plot 4, in contrast, is well represented by both correlograms.
- ii) The cyclic nature of bulk density in the three badland plots is evident in both correlograms.

a)



b)

Lag increment codes	Plot 4	Plot 6	Plot 7
1	0 > to <= 4.5	0 > to <= 2	0 > to <= 3
2	4.5 > to <= 9	2 > to <= 4	3 > to <= 6
3	9 > to <= 13.5	4 > to <= 6	6 > to <= 9
4	13.5 > to <= 18	6 > to <= 8	9 > to <= 12
5	18 > to <= 22.5	8 > to <= 10	12 > to <= 15
6	22.5 > to <= 27	10 > to <= 12	15 > to <= 18
7	27 > to <= 31.5	12 > to <= 14	18 > to <= 21
8	31.5 > to <= 36	14 > to <= 16	21 > to <= 24
9	36 > to <= 40.5	16 > to <= 18	24 > to <= 27
10	40.5 > to <= 45	18 > to <= 20	27 > to <= 30
11	45 > to <= 49.5	20 > to <= 22	30 > to <= 33
12	49.5 > to <= 54	22 > to <= 24	33 > to <= 36
13	54 > to <= 58.5	24 > to <= 26	36 > to <= 39
14	58.5 > to <= 63	26 > to <= 28	39 > to <= 42
15	63 > to <= 67.5	28 > to <= 30	42 > to <= 45
16			45 > to <= 48
17			48 > to <= 51
18			51 > to <= 54
19			54 > to <= 57
20			57 > to <= 60

Figure 6.10 a) Moran's I and Geary's C correlograms for the dry bulk density of the badland plots. b) provides the key to the lag increments used in the correlograms for each plot.

### **6.3.2 Summary**

The mean bulk density values are relatively similar for all three plots. Plot 7 has a marginally higher mean bulk density and range but, in general, it can be argued that the distribution characteristics of the three badland plots are not significantly different.

Intra-plot analysis, using the means and standard deviations of each cell within the plots, indicates that the dry bulk density does not vary significantly across each of the plots or the three spatial scales.

None of the experimental variograms were considered to be accurately represented by the simple models available in the software used in this study. If the data is considered very generally, a nugget model could be applied but because periodicity is evident in all three plots, classifying the distribution of bulk density as random would be inaccurate.

## **6.4 Soil Moisture**

### **6.4.1 Results**

As previously discussed, the antecedent weather conditions must be considered when interpreting the soil moisture results. Fine weather conditions were recorded before and during the measurement of plot 4. Similar conditions were observed before the measurement of plot 6, however, light rainfall was experienced during the sampling of this plot. In contrast, a large thunderstorm and heavy rainfall occurred the day before plot 7 was sampled, 11mm of precipitation was recorded.

a) *Test of normality, descriptive statistics and inter-plot variation*

The frequency distributions displayed by the boxplots (figure 6.11) show that the datasets from all plots are highly positively skewed. Outliers are evident in all datasets and in all cases the outliers are at the upper end of the measurements.

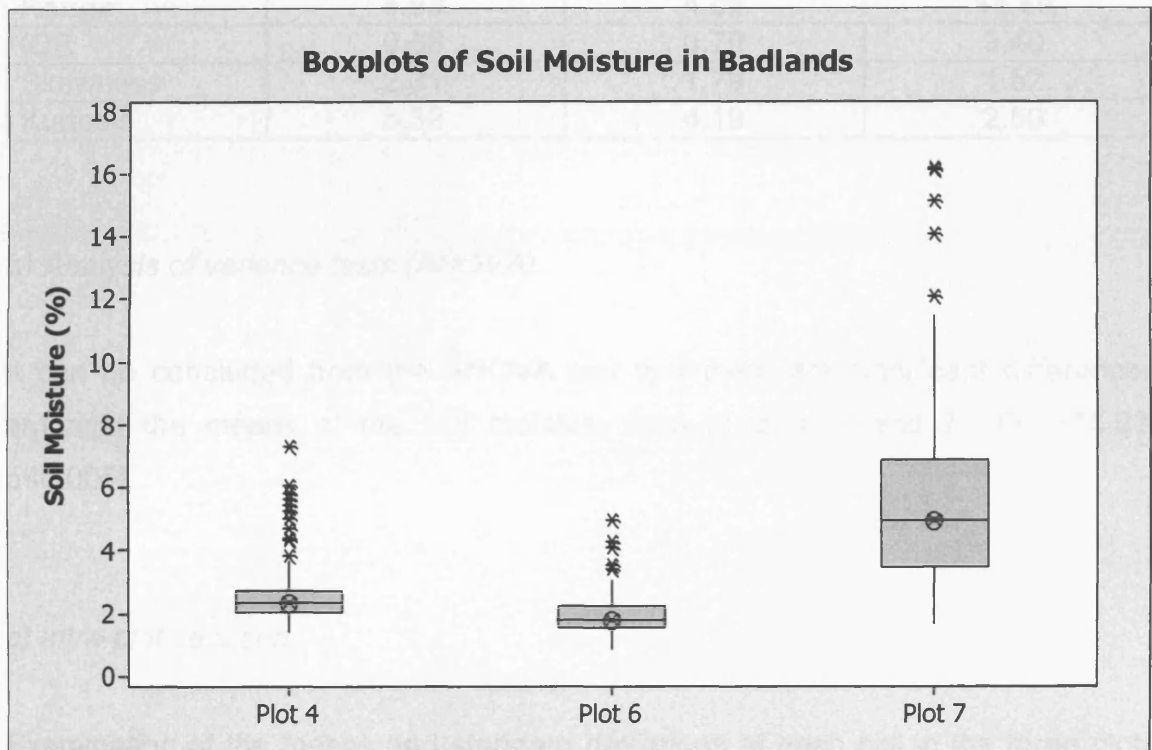


Figure 6.11 Boxplots representing the sample distribution of soil moisture in the badland plots.

Plots 4 and 6 demonstrate similar distribution characteristics. In contrast, plot 7 displays a mean value of approximately double those of plots 4 and 6. The range of soil moisture values is significantly greater in plot 7 and as a consequence the coefficient of variation is also higher.

**Table 6.4** Inter-plot comparisons of descriptive statistics: Soil moisture (%)

Descriptive Statistic	Plot 4 (Karoo)	Plot 6 (Karoo)	Plot 7 (Karoo)
<b>Mean</b>	<b>2.66</b>	<b>2.00</b>	<b>5.67</b>
Median	2.33	1.78	4.94
SE of Mean	0.10	0.07	0.29
St Dev	1.05	0.68	3.03
Variance	1.11	0.46	9.17
<b>Coef Var</b>	<b>39.59</b>	<b>33.86</b>	<b>53.38</b>
Minimum	1.41	0.89	1.70
Maximum	7.34	4.98	16.19
<b>Range</b>	<b>5.93</b>	<b>4.09</b>	<b>14.50</b>
IQR	0.68	0.70	3.40
Skewness	2.31	1.79	1.52
Kurtosis	5.39	4.19	2.50

*b) Analysis of variance tests (ANOVA)*

It can be concluded from the ANOVA test that there are significant differences amongst the means of the soil moisture from plots 4, 6 and 7. ( $F= 115.63$ ,  $p<0.005$ ).

*c) Intra-plot variation*

Examination of the means and standard deviations of each cell in the three plots (figure 6.12) suggests that no specific distribution characteristics of soil moisture can be applied to all badlands. Plot 4 demonstrates relatively similar means and small standard deviations across the three spatial scales apart from three cells. Plot 6 demonstrates higher mean values and greater within-plot variation in the 30 x 30m cells, at the smallest scale the means and standard deviations are less, apart from cell I. Plot 7 also displays one 1.5 x 1.5m cell that has a significantly higher mean value and greater within-plot variation. These results imply that the response of soil moisture is site-specific.

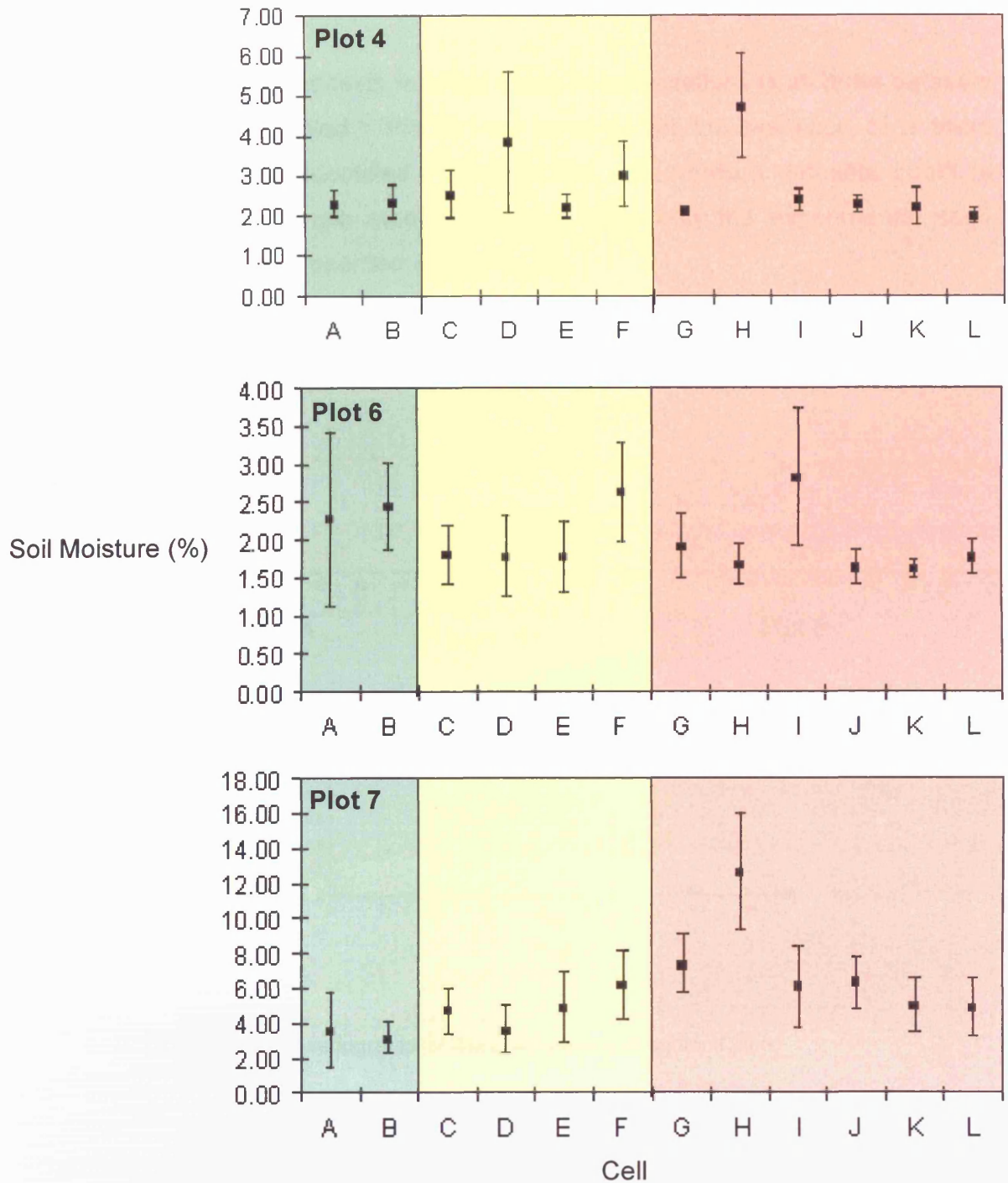


**Figure 6.12** The means and standard deviations of soil moisture for each cell within the plots. Green represents the 30 x 30m cells, yellow represents the 10 x 10m cells and pink represents 1.5 x 1.5m cells.

*d) Geostatistical analysis: The semi-variogram*

Pre-processing of the datasets resulted in log transformations of all three datasets. No outliers were removed. Plot 6 was checked for the presence of a trend, although no drift was identified. None of the soil moisture datasets could be modelled using the simple models available, thus only the experimental semi-variogram graphs are presented (figure 6.13).

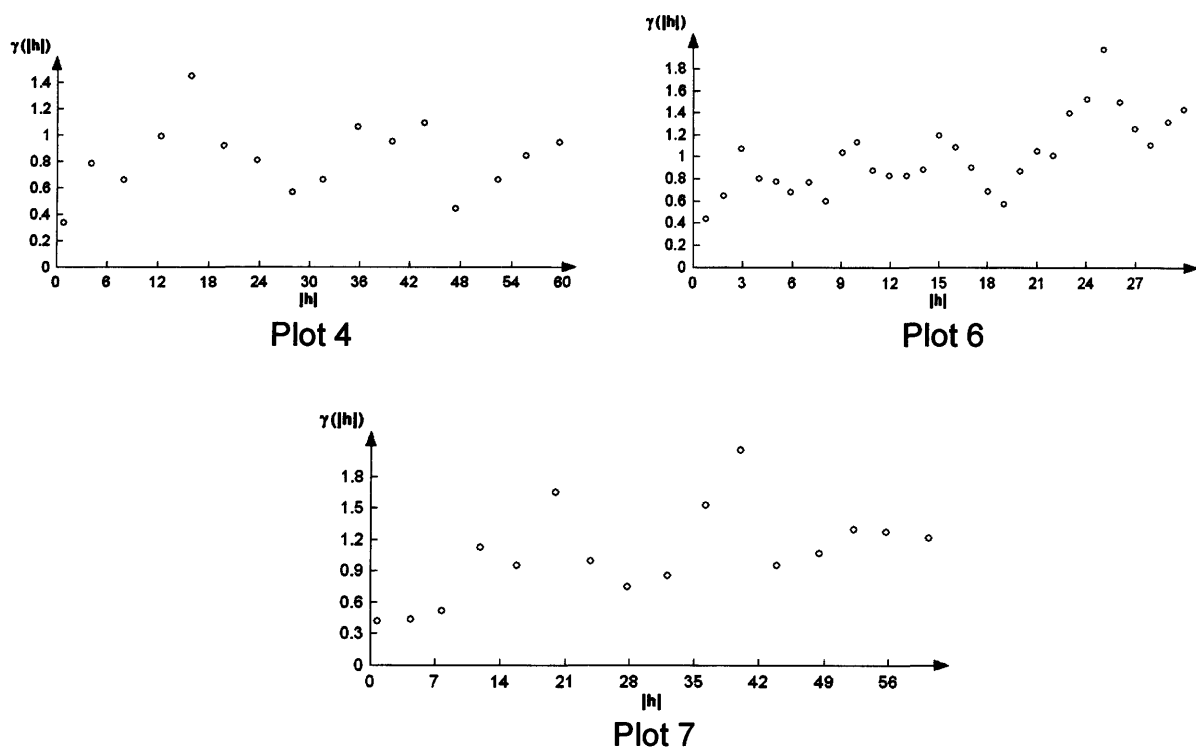


**Figure 6.13** Modelled semi-variograms for the soil moisture of badland plots.

The results are as follows:

- i) The experimental variograms show that none of the datasets can be represented by simple models. If the data is considered very generally, a nugget model could be applied but for this study this model does not accurately represent the spatial patterns in this landscape.

- ii) Although plots 4 and 7 represent a larger scale of measurement than plot 6, all three plots show some evidence of cyclic behaviour. This can be seen in figure 6.14.
- iii) Plots 4 and 7, the two plots with comparable scales of measurement, show similar cyclic patterns. Two main peaks can be identified at similar lag distances. This is clearly seen in figure 6.14.
- iv) The fluctuation evident in the variance of plot 6 suggests that small-scale patterns are present in badlands.

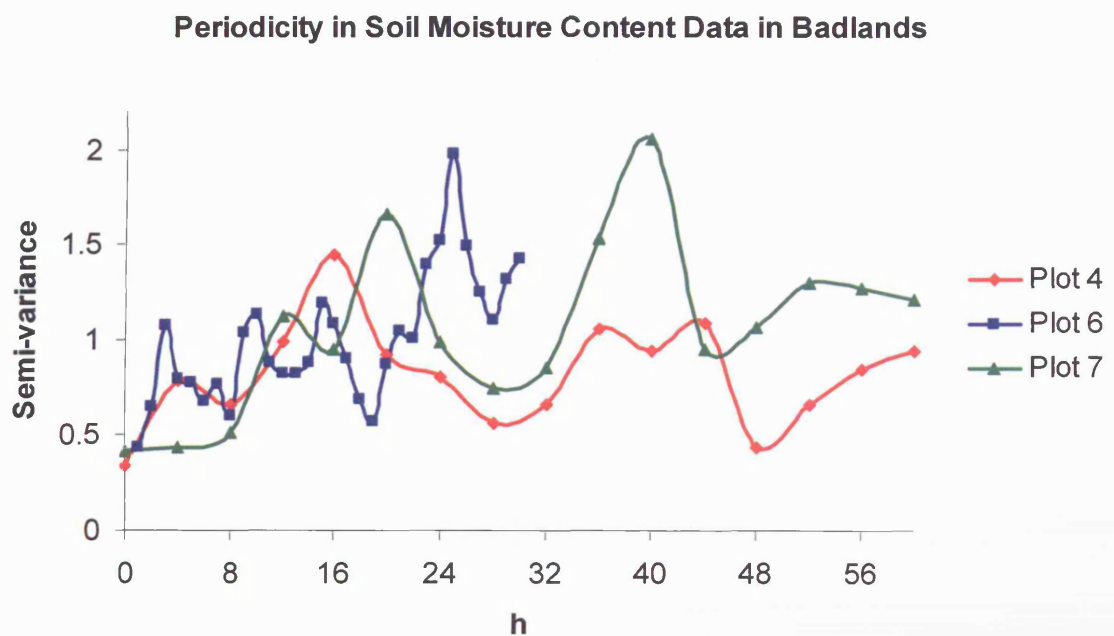


**Figure 6.14** Semi-variograms with connecting lines to show periodicity in soil moisture data in badland plots.

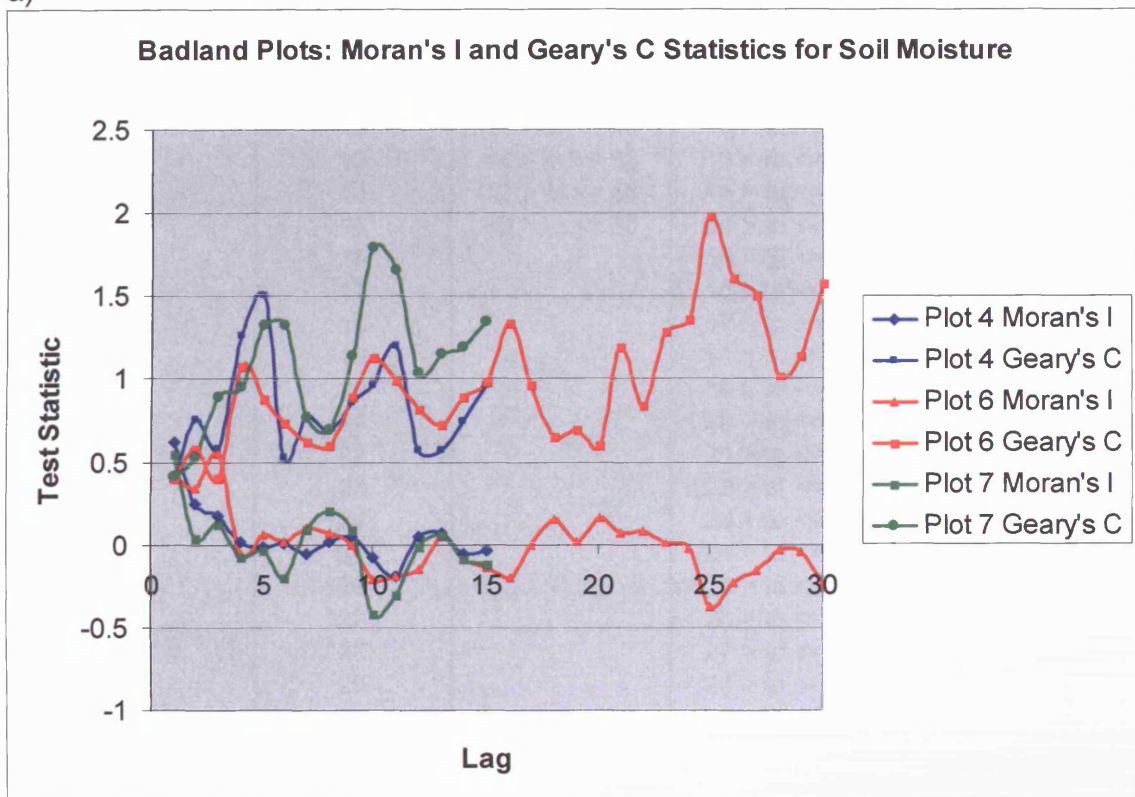
*e) Geostatistical analysis: Moran's I and Geary's C statistics*

The results are as follows: (see figure 6.15)

- i) Comparisons made between the Moran's I and Geary's C statistics show that the results mirror each other relatively well; this increases the confidence in the results.

- ii) The similarities between the spatial patterns of plots 4 and 7 can clearly be seen in the two correlograms.
- iii) The small-scale periodicity seen in the variograms of plot 6 is evident in the correlograms. However, the change of spatial structure appears to be weaker than those identified in plots 4 and 7.

a)



b)

Lag increment codes	Plot 4 & 7	Plot 6
1	0 > to <= 4	0 > to <= 1
2	4 > to <= 8	1 > to <= 2
3	8 > to <= 12	2 > to <= 3
4	12 > to <= 16	3 > to <= 4
5	16 > to <= 20	4 > to <= 5
6	20 > to <= 24	5 > to <= 6
7	24 > to <= 28	6 > to <= 7
8	28 > to <= 32	7 > to <= 8
9	32 > to <= 36	8 > to <= 9
10	36 > to <= 40	9 > to <= 10
11	40 > to <= 44	10 > to <= 11
12	44 > to <= 48	11 > to <= 12
13	48 > to <= 52	12 > to <= 13
14	52 > to <= 56	13 > to <= 14
15	56 > to <= 60	14 > to <= 15
16		15 > to <= 16
17		16 > to <= 17
18		17 > to <= 18
19		18 > to <= 19
20		19 > to <= 20
21		20 > to <= 21
22		21 > to <= 22
23		22 > to <= 23
24		23 > to <= 24
25		24 > to <= 25
26		25 > to <= 26
27		26 > to <= 27
28		27 > to <= 28
29		28 > to <= 29
30		29 > to <= 30

**Figure 6.15** a) Moran's I and Geary's C correlograms for the soil moisture of the badland plots. b) provides the key to the lag increments used in the correlograms for each plot.

### 6.4.2 Summary

Although the distribution characteristics of plots 4 and 6 are similar, the significant differences that exist between these two plots and plot 7 indicate that no characteristic distribution can be applied to all badland plots. This is largely due to the relationship between soil moisture and antecedent weather conditions. The intra-plot analysis provides further evidence that the results of soil moisture measurements are site specific.

Despite the descriptive statistics indicating that the response of the plots are site specific, the geostatistical analysis suggests that the spatial patterns of soil moisture are similar in the three badland plots. Although no obvious spatial autocorrelation has been identified, cyclic patterns are evident in all three plots. Despite plot 6 being measured at a different scale, in general, the wavelengths are similar to those of plots 4 and 7. However, smaller scale fluctuation is also evident in plot 6, this suggests that a number of patterns may be in operation at different scales throughout badland landscapes.

## **6.5 Shear strength**

### **6.5.1 Results:**

#### *a) Test of normality, descriptive statistics and inter-plot variation*

The frequency distributions displayed by the boxplots (figure 6.16) show that the datasets from plots 6 and 7 are highly positively skewed. In contrast, plot 4 is negatively skewed. The distribution of plot 4 is therefore significantly different from those of plots 6 and 7. This is a result of the median of plot 4 being the maximum value of soil shear strength. This has occurred as a maximum value of 55.5 kPa was applied to sample sites that were impenetrable with the shear vane. Outliers are only evident in plot 6.

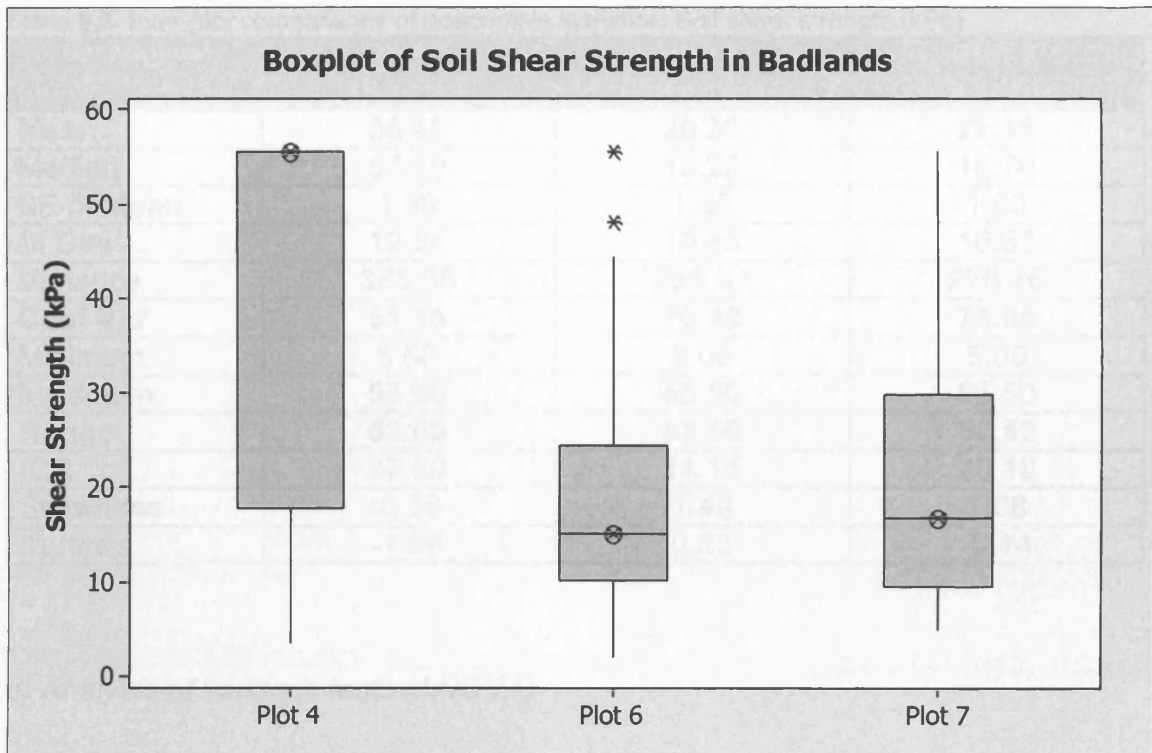


**Figure 6.16** Boxplots representing the sample distribution of soil shear strength in the badland plots.

Inter-plot comparisons of the descriptive statistics can be seen in table 6.5. The distribution characteristics of plots 6 and 7 are very similar. Although plot 4 has a similar range of shear strength values, the mean is almost double those of plots 6 and 7. However, the coefficient of variation shows that, relative to the mean, the variability of shear strength values is less than in the two other plots. This is likely to be a consequence of a greater occurrence of ground impenetrability in plot 4.

**Table 6.5** Inter-plot comparisons of descriptive statistics: Soil shear strength (kPa)

Descriptive Statistic	Plot 4 (Karoo)	Plot 6 (Karoo)	Plot 7 (Karoo)
<b>Mean</b>	<b>38.40</b>	<b>20.36</b>	<b>22.15</b>
Median	55.50	15.20	16.70
SE of Mean	1.89	1.48	1.60
St Dev	19.64	15.35	16.62
Variance	385.86	235.67	276.26
<b>Coef Var</b>	<b>51.15</b>	<b>75.42</b>	<b>75.05</b>
Minimum	3.50	2.00	5.00
Maximum	55.50	55.50	55.50
<b>Range</b>	<b>52.00</b>	<b>53.50</b>	<b>50.50</b>
IQR	37.60	14.15	20.18
Skewness	-0.39	1.40	1.08
Kurtosis	-1.68	0.83	-0.14

*b) Analysis of variance tests (ANOVA)*

It can be concluded from the ANOVA test that there are significant differences amongst the means of the soil shear strength from plots 4, 6 and 7. ( $F = 35.69$ ,  $p < 0.005$ ).

*c) Intra-plot variation*

The intra-plot analysis of the means and standard deviations of each cell (table 6.17) show that the shear strength of soil varies greatly across each of the three plots. Both the mean values and standard deviations of the cells from the same spatial scales display no specific characteristics. However, the large variation across and within the cells suggest that some spatial patterns may exist and that spatial analysis is needed to determine the nature of these patterns.

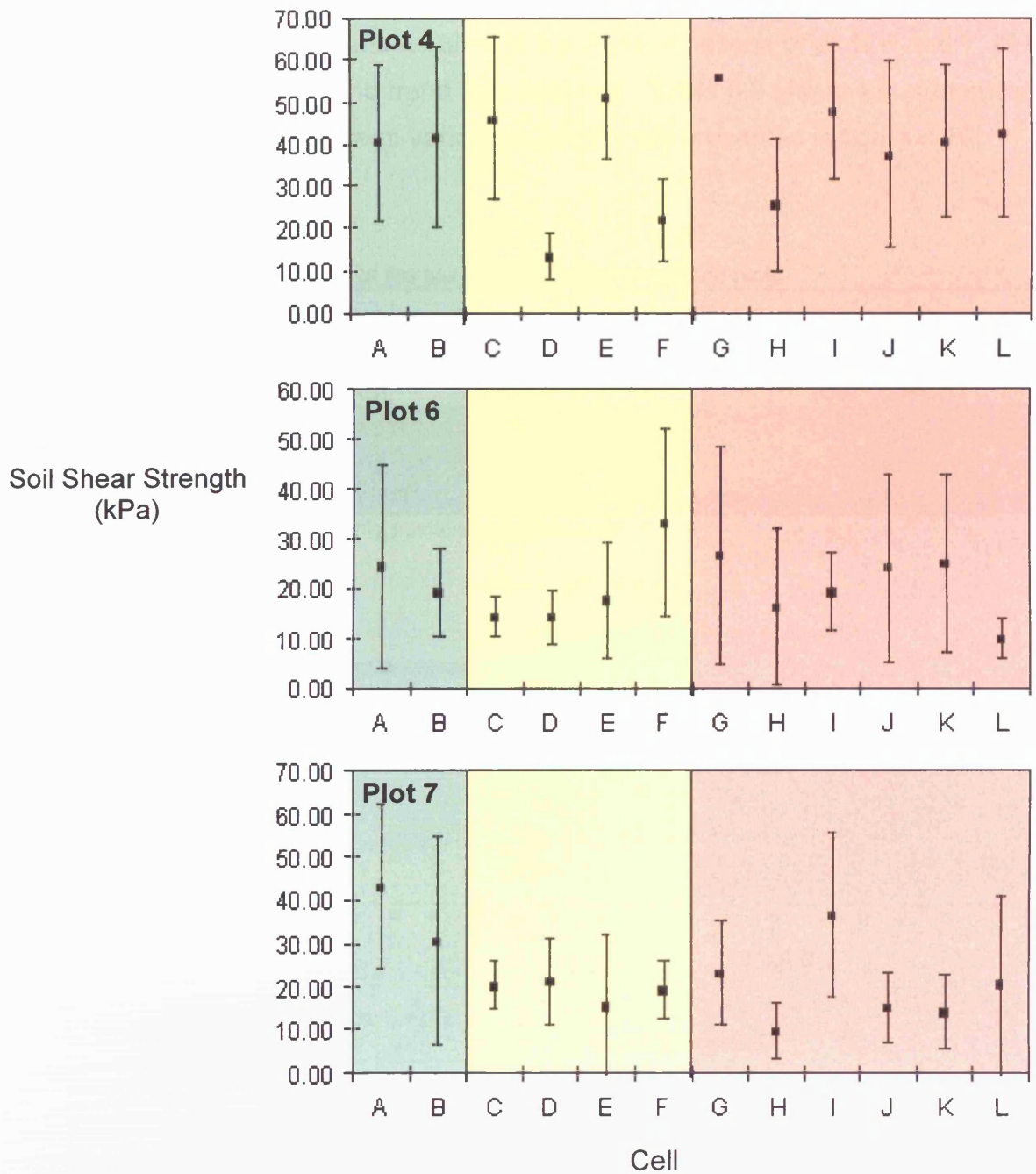


**Figure 6.17** The means and standard deviations of soil shear strength for each cell within the plots. Green represents the 30 x 30m cells, yellow represents the 10 x 10m cells and pink represents 1.5 x 1.5m cells.

## d) Geostatistical analysis: The semi-variogram

Pre-processing of the datasets resulted in log transformations of plots 6 and 7. No outliers were removed and no trend was detected. Table 6.6 shows the numerical results and the associated semi-variogram graphs are presented in figure 6.18.

**Table 6.6** Geostatistical analysis of the soil shear strength of badland plots

Parameter: Shear Strength						
Plot No.	Location	Fitted Model	Nugget Value (Co)	Sill (Co+C <sub>1</sub> )	Range (meters) (a)	Nugget-to-sill Ratio (Co)/(Co+C <sub>1</sub> )
4	Karoo	Spherical	0.50	1.11	16.62	0.45
6	Karoo*	Nugget	na	na	na	na
7	Karoo*	Spherical	0.55	1.06	14.03	0.52

\* Log transformed data due to highly positively skewed data

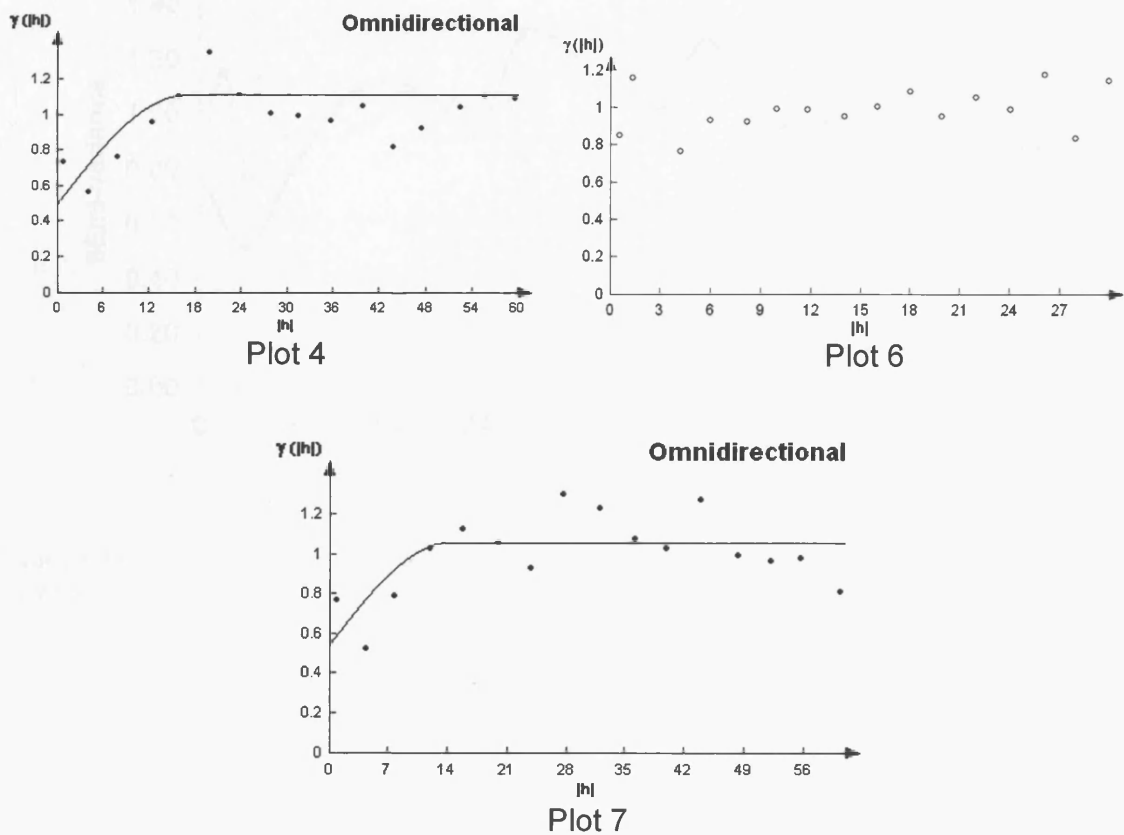


**Figure 6.18** Semi-variograms of the soil shear strength of the badland plots.

The results are as follows:

- i) Plots 4 and 7 show ranges of spatial autocorrelation of 16.62m and 14.03m, respectively.
- ii) The data from both these plots were best represented by a spherical model and both show moderate spatial dependency.
- iii) A pure nugget model best describes the data derived from plot 6.
- iv) Plot 6 may be displaying some smaller-scale cyclic behaviour whereas plot 7 shows evidence of periodicity on a larger scale, (figure 6.19). This indicates that the scale of measurement is a significant factor when determining spatial patterns in a landscape.

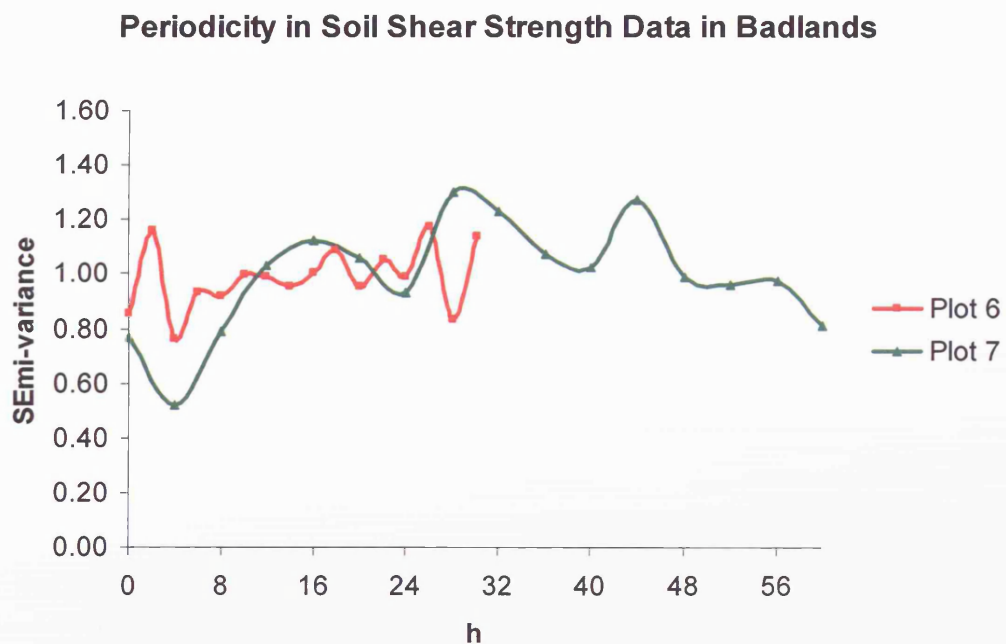


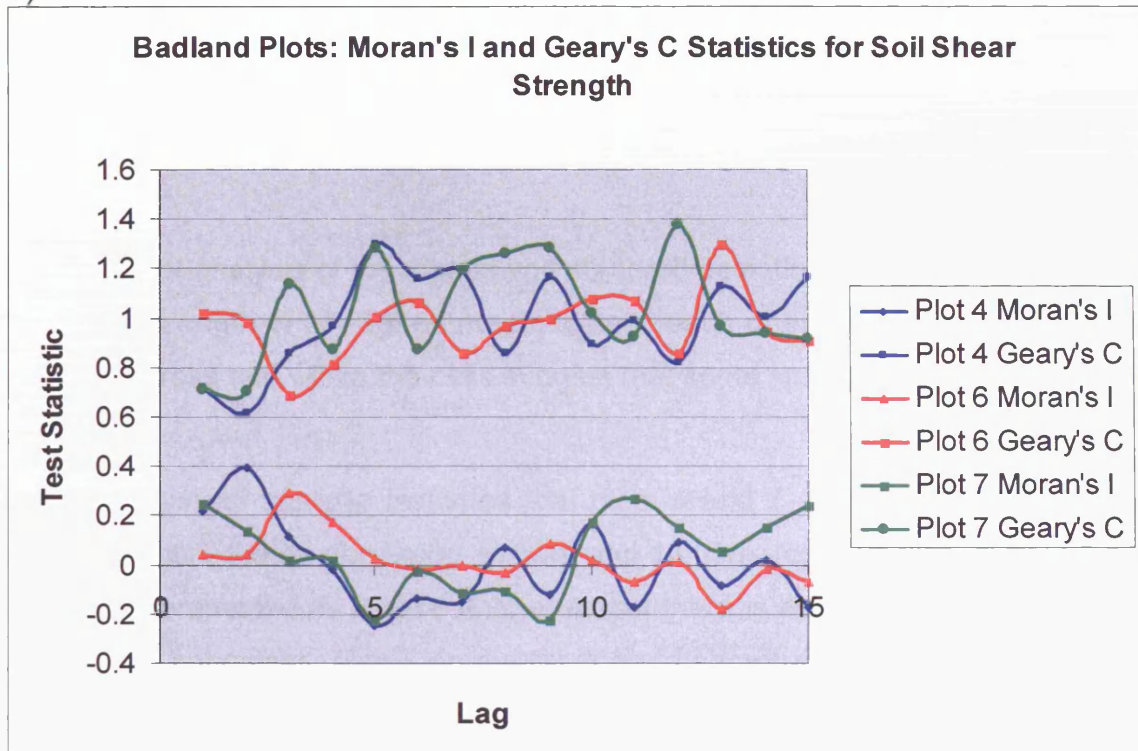
**Figure 6.19** Semi-variograms with connecting lines to show periodicity in soil shear strength data in badland plots.

## e) Geostatistical analysis: Moran's I and Geary's C statistics

The results are as follows: (see figure 6.20)

- i) Comparisons made between the Moran's I and Geary's C statistics show that the results mirror each other relatively well, this increases the confidence in the results.
- ii) The results from the correlograms suggest that there is a change in spatial structure at lags of approximately 16m and 12m for plots 4 and 7, respectively. The results for plot 4 are similar to those produced by the semi-variogram, however, the correlograms for plot 7 suggest a range that is slightly less than previously predicted.
- iii) All three plots show fluctuation in the spatial structures; these are more pronounced in the correlograms than the fluctuating variances in the variograms, particularly the dataset derived from plot 4.
- iv) Plot 6 displays less fluctuation than plots 4 and 7 suggesting that the periodicity is weaker and thus the datasets may be adequately represented by a pure nugget model.

a)



b)

Lag increment codes	Plot 4 & 7	Plot 6
1	0 > to ≤ 4	0 > to ≤ 2
2	4 > to ≤ 8	2 > to ≤ 4
3	8 > to ≤ 12	4 > to ≤ 6
4	12 > to ≤ 16	6 > to ≤ 8
5	16 > to ≤ 20	8 > to ≤ 10
6	20 > to ≤ 24	10 > to ≤ 12
7	24 > to ≤ 28	12 > to ≤ 14
8	28 > to ≤ 32	14 > to ≤ 16
9	32 > to ≤ 36	16 > to ≤ 18
10	36 > to ≤ 40	18 > to ≤ 20
11	40 > to ≤ 44	20 > to ≤ 22
12	44 > to ≤ 48	22 > to ≤ 24
13	48 > to ≤ 52	24 > to ≤ 26
14	52 > to ≤ 56	26 > to ≤ 28
15	56 > to ≤ 60	28 > to ≤ 30

**Figure 6.20** a) Moran's I and Geary's C correlograms for the soil shear strength of the badland plots. b) provides the key to the lag increments used in the correlograms for each plot.

### 6.5.2 Summary

The descriptive statistics indicate that whilst the distribution characteristics of plots 6 and 7 are similar, plot 4 has a significantly higher mean value and a smaller coefficient of variation. The distribution characteristics of plot 4 have potentially been influenced by the fact that a maximum shear strength was applied to sample locations that were impenetrable with the shear vane.

The intra-plot analysis of the means and standard deviations of each cell show that the shear strength of soil varies greatly across each of the three plots. The large variation across and within the cells suggest that some spatial patterns may exist.

The geostatistical analysis indicates that plots 4 and 7 show evidence of spatial autocorrelation, the ranges being 16.62m and 14.03m, respectively. Although plot 6 is best represented by a pure nugget model there is some evidence of smaller-scale cyclic behaviour. Plot 7 on the other hand shows evidence of periodicity on a larger scale. This indicates that the scale of measurement is potentially a

significant factor when determining spatial patterns of shear strength in badland landscapes.

## 6.6 Particle-size distribution analysis

### 6.6.1 Results

#### a) Descriptive statistics

Due to time constraints it was only possible to measure the particle size distribution of one badland plot. The descriptive statistics of plot 6 are shown in table 6.7

**Table 6.7** Inter-plot comparisons of descriptive statistics: Particle size distribution

Descriptive Statistic	Plot 6 Clay	Plot 6 Silt	Plot 6 Sand
<b>Mean</b>	<b>0.47</b>	<b>8.10</b>	<b>91.43</b>
Median	0.44	8.10	91.51
SE of Mean	0.02	0.33	0.35
St Dev	0.19	3.40	3.56
Variance	0.04	11.54	12.70
<b>Coef Var</b>	<b>40.25</b>	<b>42.00</b>	<b>3.89</b>
Minimum	0.13	1.84	82.84
Maximum	1.04	16.23	98.01
<b>Range</b>	<b>0.91</b>	<b>14.38</b>	<b>15.18</b>
IQR	0.22	4.29	4.36
Skewness	0.83	0.42	-0.43
Kurtosis	0.69	-0.18	-0.17

#### b) Geostatistical analysis: The semi-variogram and Moran's I and Geary's C correlograms

No outliers were removed from any of the plots and no transformations were performed before geostatistical analysis was carried out. None of the datasets could be modelled using the simple models available, thus only the experimental semi-variogram graphs are presented (figure 6.21).

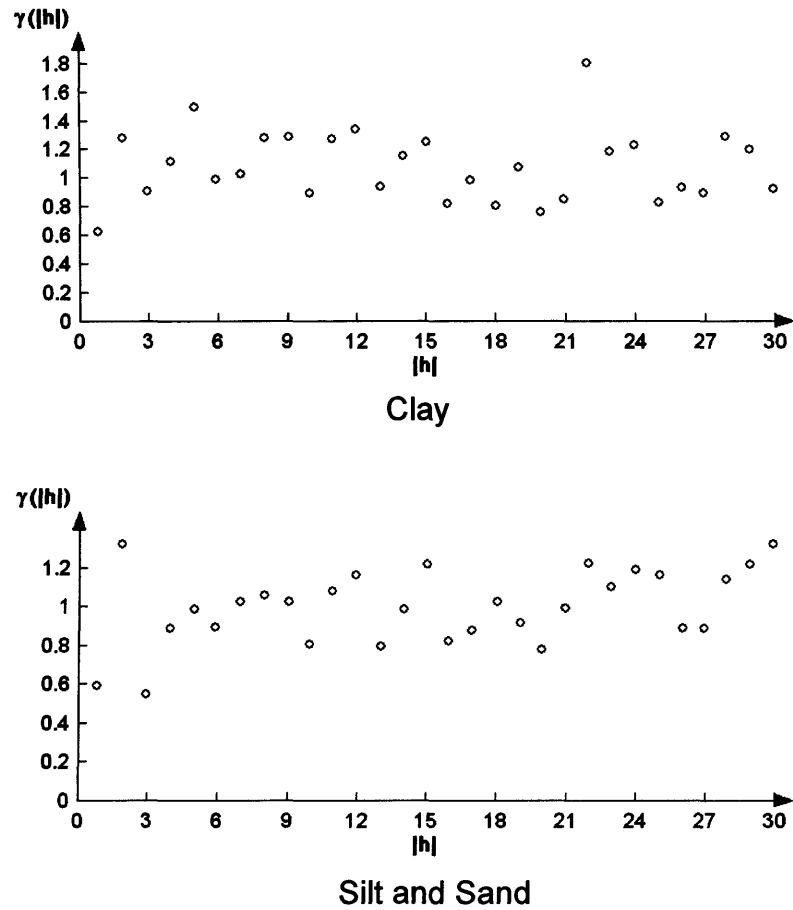


**Figure 6.21** Semi-variograms of the particle size distribution of a badland plot.

The results are as follows:

- i) The experimental variograms show that the datasets are best represented by a pure nugget model indicating that no significant spatial patterns are evident.
- ii) However, figure 6.22 shows that periodicity is evident thus suggesting that particle size distribution fluctuates in a regular fashion across badland landscapes.

- iii) The clay semi-variogram shows some evidence of a decrease in variance with increasing lag. This may represent a checkerboard pattern, however, it may be reflecting part of a larger-scale periodicity.
- iv) The Moran's I and Geary's C correlograms (figure 6.23) also display evidence of fluctuating changes in the spatial structure and thus correspond to the findings derived from the semi-variograms.

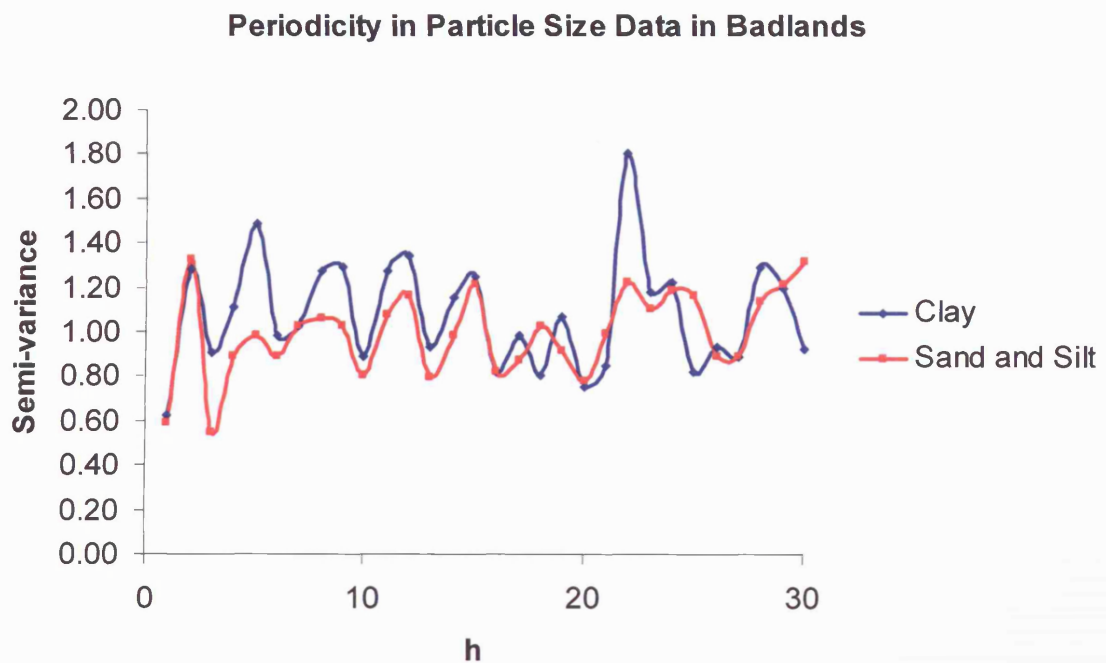
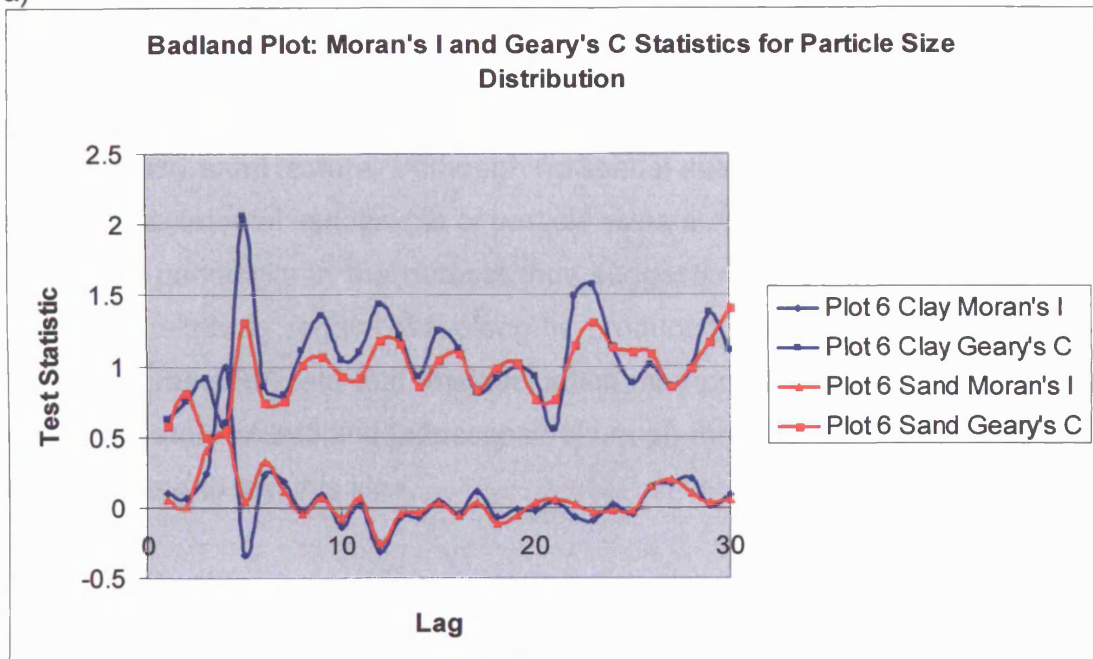


**Figure 6.22** Semi-variograms with connecting lines to show periodicity in the particle size distribution of a badland plot.

a)



b)

Lag increment codes	Clay and Sand
1	0 > to <= 1
2	1 > to <= 2
3	2 > to <= 3
4	3 > to <= 4
5	4 > to <= 5
6	5 > to <= 6
7	6 > to <= 7
8	7 > to <= 8
9	8 > to <= 9
10	9 > to <= 10
11	10 > to <= 11
12	11 > to <= 12
13	12 > to <= 13
14	13 > to <= 14
15	14 > to <= 15
16	15 > to <= 16
17	16 > to <= 17
18	17 > to <= 18
19	18 > to <= 19
20	19 > to <= 20
21	20 > to <= 21
22	21 > to <= 22
23	22 > to <= 23
24	23 > to <= 24
25	24 > to <= 25
26	25 > to <= 26
27	26 > to <= 27
28	27 > to <= 28
29	28 > to <= 29
30	29 > to <= 30

**Figure 6.23** a) Moran's I and Geary's C correlograms for the particle size distribution of the badland plot. b) provides the key to the lag increments used in the correlograms for each plot.

### **6.6.2 Summary**

According to the British classification of soil texture, plot 6 can be classed as having a loamy sand texture. Although no spatial autocorrelation can be identified from the experimental variograms of particle sizes across the badland plot, there is evidence of periodicity in the dataset thus suggesting that some spatial patterns exist. The relatively regular wavelengths produced across both the variograms and correlograms indicate that this fluctuation may potentially be a function of the undulating nature of badland landscapes although more badland plots will have to be investigated to test this idea.

### **6.7 *Soil-aggregate stability***

The problems associated with the technique employed to measure the aggregate stability has been discussed in chapter 4 (section 4.7). Due to time constraints, the aggregate stability of only one badland plot from the Karoo was measured, plot 6.

### 6.7.1 Results

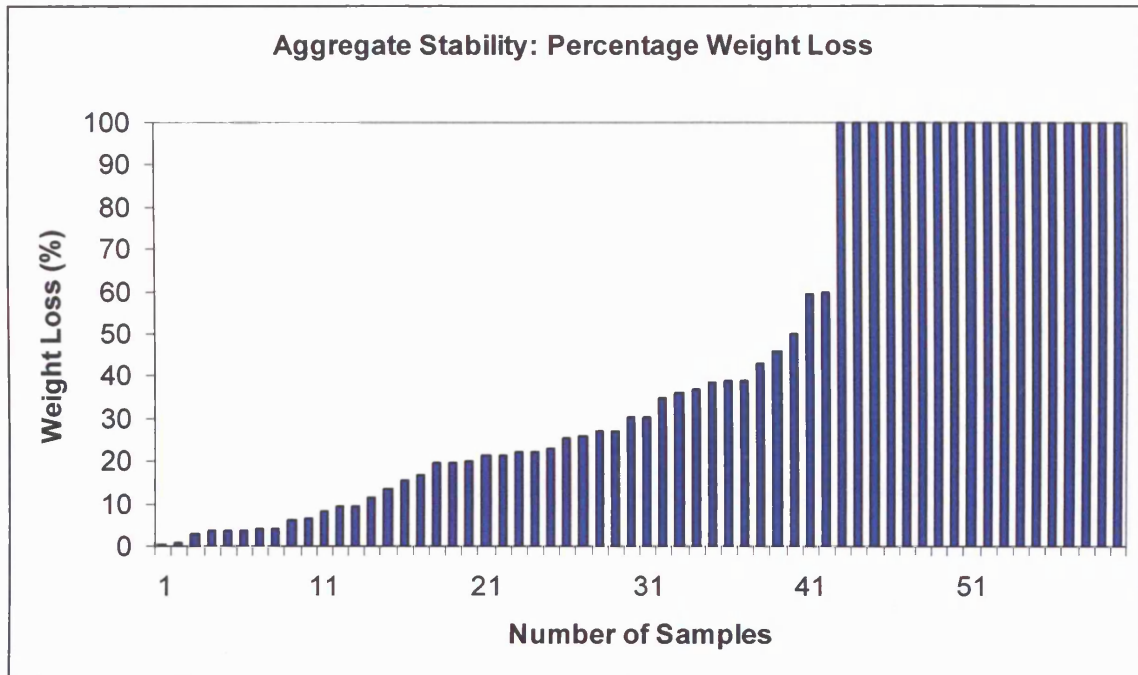


**Figure 6.24** The number of aggregates obtained from plot 6 and the percentage weight loss after agitation in water.

From figure 6.24 a number of observations can be made about the aggregate stability of soil in the badland plot:

- i) Out of 108 samples, plot 6 had 60 samples containing suitable aggregates.
- ii) Approximately 67% of the aggregate samples lost less than 50% of their total weight and just over 20% only lost 10% of their total weight. However, 30% of all samples were dispersed completely.

### 6.7.2 Summary

The aggregate stability of plot 6 appears to be relatively variable. More than half the samples from the badland plot provided suitable aggregates for measurement. However, approximately a third of these samples dispersed completely indicating that some aggregates are extremely unstable. In contrast, just over 20% of the

aggregates proved to be relatively stable, losing only 10% of their total weight. This suggests that aggregate stability may vary spatially, however, due to the lack of measurable aggregates geostatistical analysis cannot be carried out in this case.

## 6.8 pH

### 6.8.1 Results

#### a) Descriptive statistics, descriptive statistics and inter-plot variation

The frequency distributions displayed by the boxplots (figure 6.25) show that plots 4 and 6 are slightly positively skewed, however, the skews are weak and can therefore be considered as having normal distributions. Plot 7 has a negatively skewed distribution. Outliers are present in all three plots.

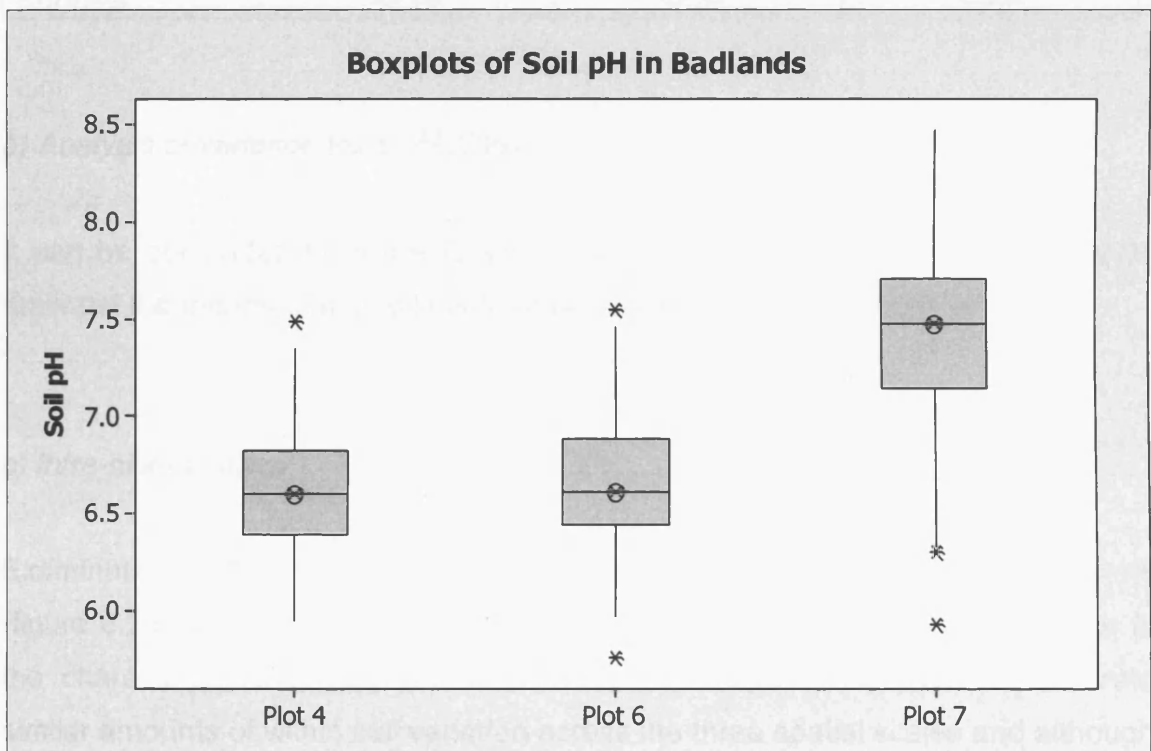


Figure 6.25 Boxplots representing the sample distribution of soil pH in the shrubland plots.

The descriptive statistics show that differences exist amongst the soil pH values from the three badland plots. Table 6.8 shows that the soils from plots 4 and 6 are acidic (< pH7) whereas the soil from plot 7 can be considered as slightly alkali (>pH7). The coefficient of variance and range values show that pH values within plots 4 and 6 fluctuate less than plot 7.

**Table 6.8** Inter-plot comparisons of descriptive statistics: Soil pH

Descriptive Statistic	Plot 4 (Karoo)	Plot 6 (Karoo)	Plot 7 (Karoo)
<b>Mean</b>	<b>6.62</b>	<b>6.65</b>	<b>7.42</b>
Median	6.60	6.62	7.48
SE of Mean	0.03	0.03	0.05
St Dev	0.31	0.31	0.49
Variance	0.10	0.10	0.24
<b>Coef Var</b>	<b>4.69</b>	<b>4.71</b>	<b>6.62</b>
Minimum	5.95	5.76	5.93
Maximum	7.49	7.55	8.47
<b>Range</b>	<b>1.54</b>	<b>1.79</b>	<b>2.54</b>
IQR	0.43	0.44	0.56
Skewness	0.30	0.15	-0.43
Kurtosis	-0.14	0.37	0.49

#### *b) Analysis of variance tests (ANOVA)*

It can be concluded from the ANOVA test that there are significant differences amongst the means of the soil pH from plots 4, 6 and 7. ( $F= 153.27$ ,  $p<0.005$ ).

#### *c) Intra-plot variation*

Examination of the means and standard deviations of each cell in the three plots (figure 6.26) suggests that the scale of measurement is not a significant factor in the characterisation of soil pH in badland landscapes. All plots demonstrate similar amounts of within cell variation across the three spatial scales and although the mean values do vary across the cells, they do not display any characteristics specific to the scale of measurement. As no significant variation is evident across

the plots, the results suggest that soil pH is relatively homogenous across badland landscapes.

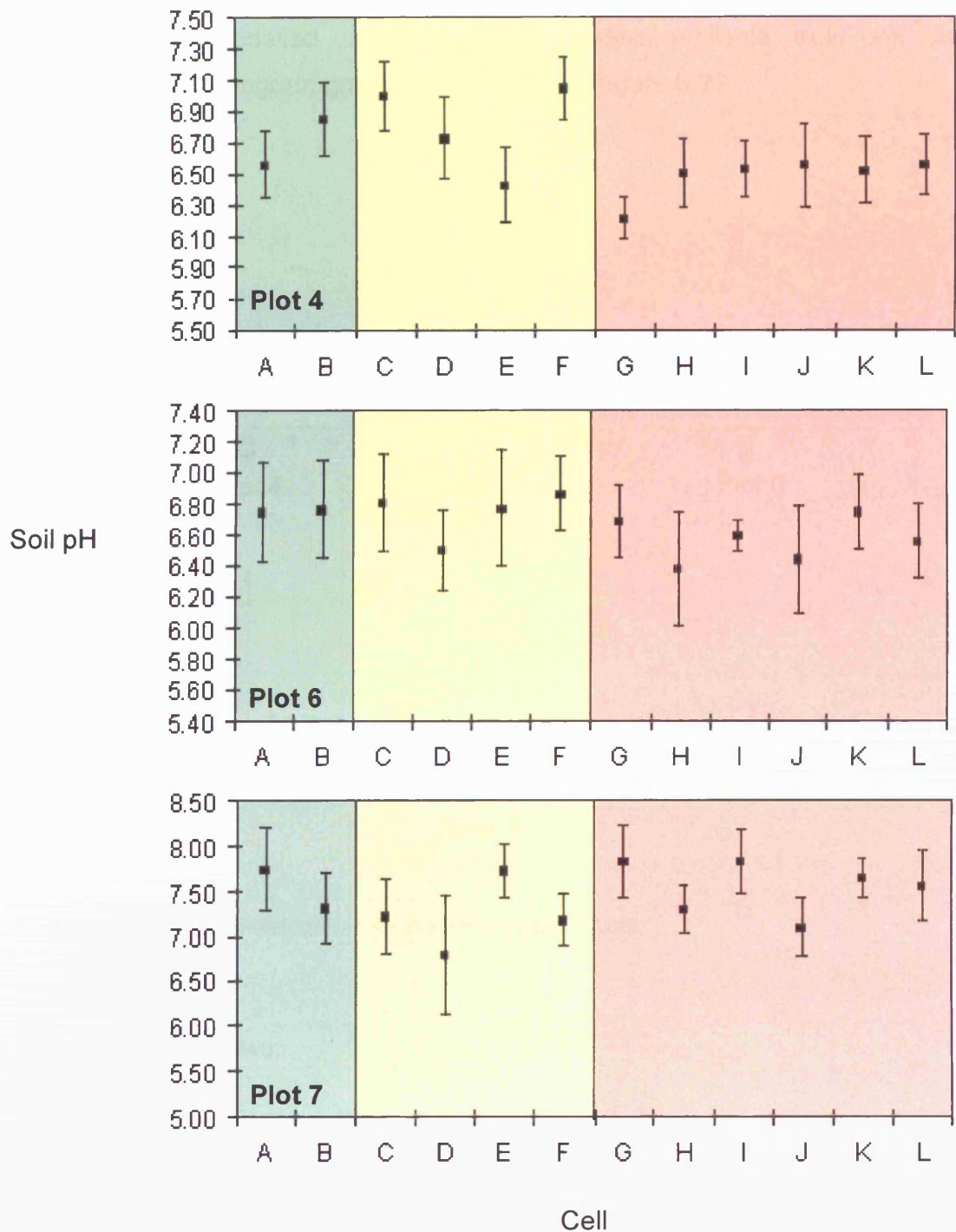


**Figure 6.26** The means and standard deviations of soil pH for each cell within the plots. Green represents the 30 x 30m cells, yellow represents the 10 x 10m cells and pink represents 1.5 x 1.5m cells.

d) *Geostatistical analysis: The semi-variogram*

No outliers were removed from any of the plots and no transformations were performed before geostatistical analysis was carried out. None of the soil pH datasets could be modelled using the simple models available, thus only the experimental semi-variogram graphs are presented (figure 6.27).

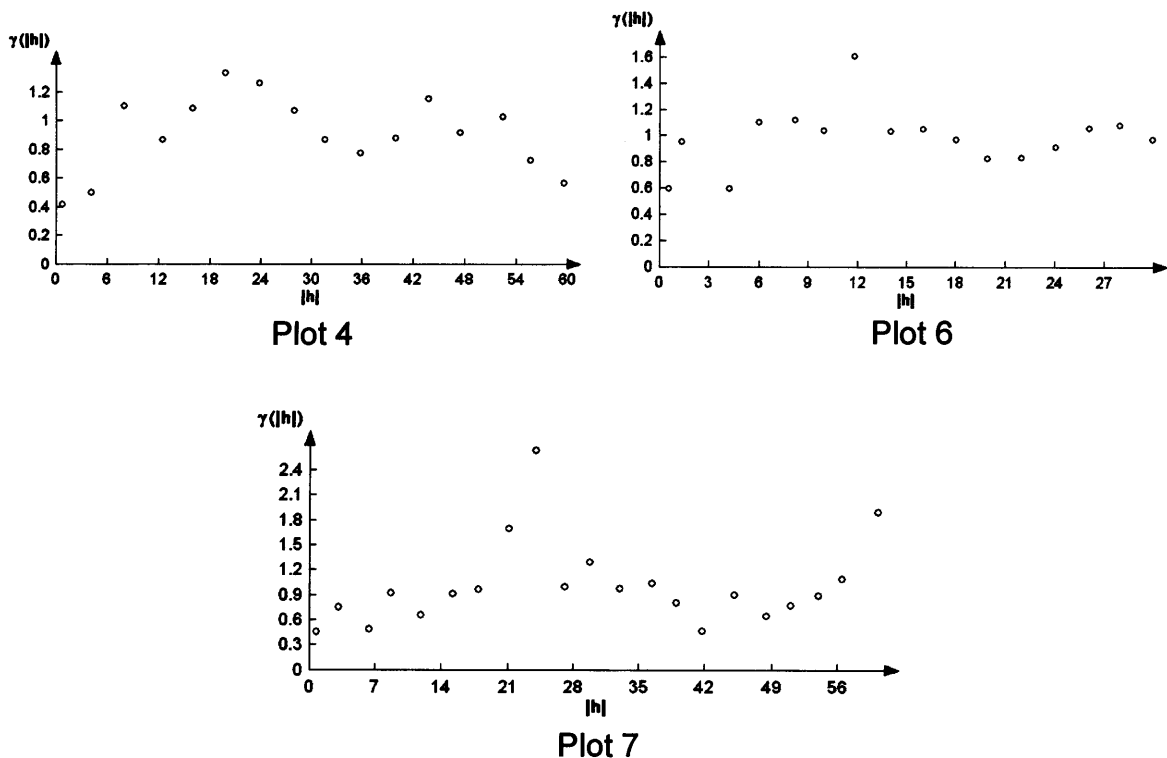


**Figure 6.27** Modelled semi-variograms for the pH of badland plots.

The results are as follows:

- i) The experimental variograms show that none of the datasets can be represented by simple models.
- ii) Although plots 4 and 6 represent different scales of measurement, both show evidence of cyclic behaviour. This can be seen in figure 6.28.

- iii) Plot 7 shows evidence of peaks that may represent periodicity, although this is difficult to determine at this scale. Some small scale periodicity may also be evident in plot 7, this is more obvious in figure 6.28.

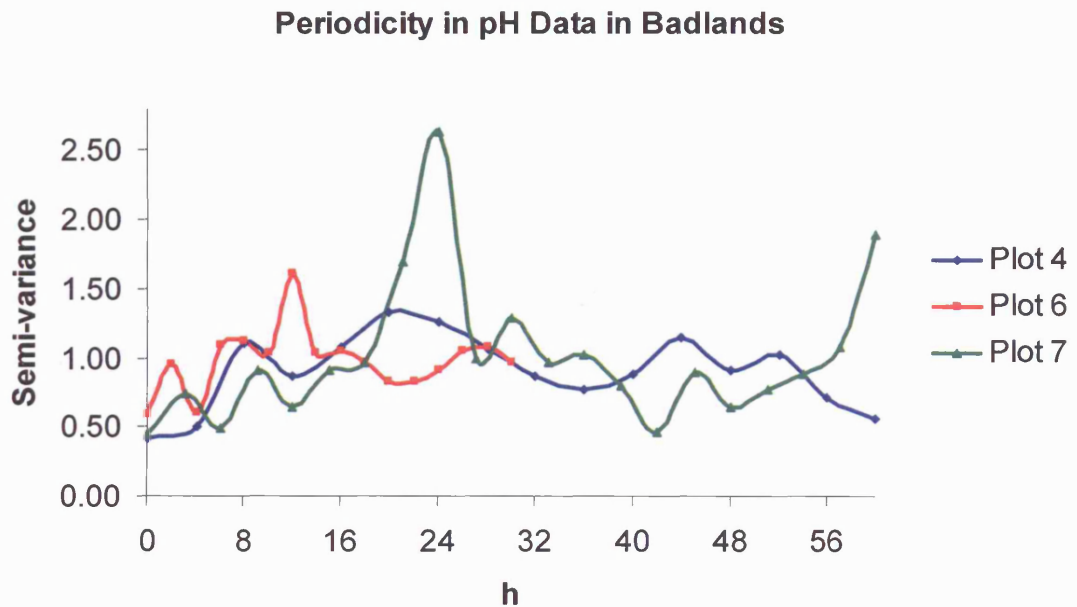


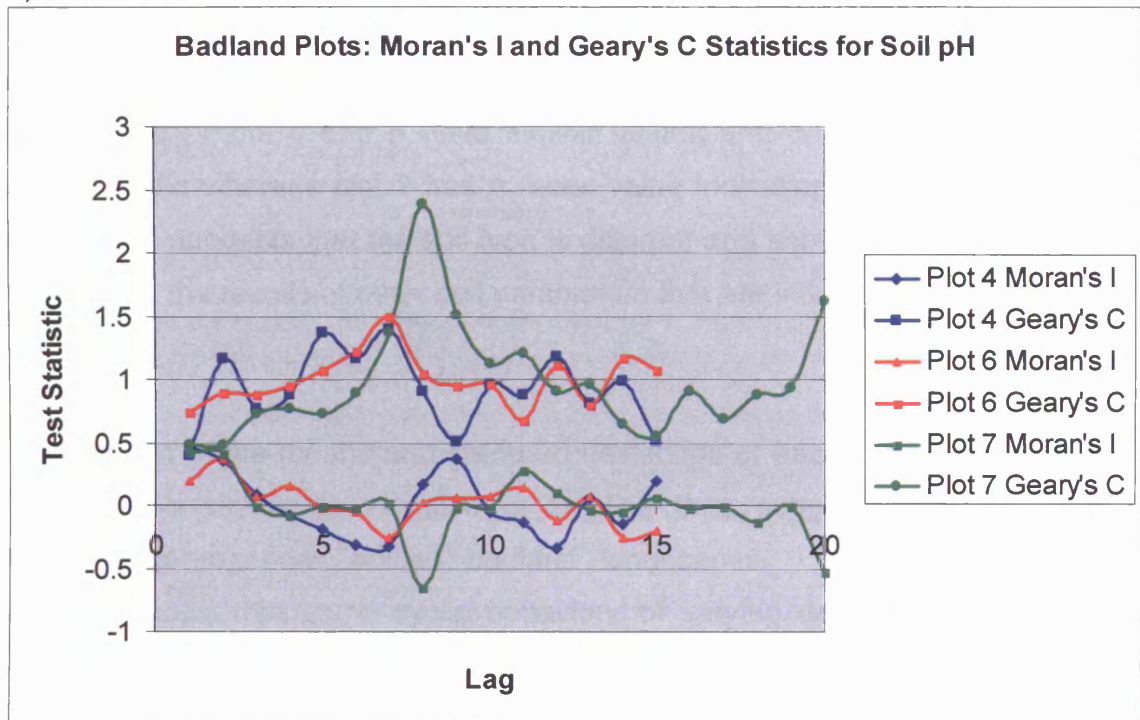
**Figure 6.28** Semi-variograms with connecting lines to show periodicity in soil pH data in badland plots.

e) *Geostatistical analysis: Moran's I and Geary's C statistics*

The results are as follows: (see figure 6.29)

- i) Some variation between the two types of correlograms at the shorter lags is evident suggesting that caution should be exercised when interpreting these results.
- ii) All three datasets show fluctuation in spatial structure across the plots.
- iii) Fluctuation in the results produced for plot four are more pronounced in the correlograms than in the semi-variogram.
- iv) The correlograms suggest more cyclic behaviour is evident in the larger lag distances for plot 6, however, the semi-variograms show the opposite; the periodicity is more obvious at the shorter lags.

a)



b)

Lag increment codes	Plot 4	Plot 6	Plot 7
1	0 > to <= 4	0 > to <= 2	0 > to <= 3
2	4 > to <= 8	2 > to <= 4	3 > to <= 6
3	8 > to <= 12	4 > to <= 6	6 > to <= 9
4	12 > to <= 16	6 > to <= 8	9 > to <= 12
5	16 > to <= 20	8 > to <= 10	12 > to <= 15
6	20 > to <= 24	10 > to <= 12	15 > to <= 18
7	24 > to <= 28	12 > to <= 14	18 > to <= 21
8	28 > to <= 32	14 > to <= 16	21 > to <= 24
9	32 > to <= 36	16 > to <= 18	24 > to <= 27
10	36 > to <= 40	18 > to <= 20	27 > to <= 30
11	40 > to <= 44	20 > to <= 22	30 > to <= 33
12	44 > to <= 48	22 > to <= 24	33 > to <= 36
13	48 > to <= 52	24 > to <= 26	36 > to <= 39
14	52 > to <= 56	26 > to <= 28	39 > to <= 42
15	56 > to <= 60	28 > to <= 30	42 > to <= 45
16			45 > to <= 48
17			48 > to <= 51
18			51 > to <= 54
19			54 > to <= 57
20			57 > to <= 60

**Figure 6.29** a) Moran's I and Geary's C correlograms for the soil pH of the badland plots. b) provides the key to the lag increments used in the correlograms for each plot.

### **6.8.2 Summary**

Some interesting differences in the mean pH values from the three badland plots are evident. Plots 4 and 6 have similar values and can be classed as being slightly acidic whereas plot 7 has a mean value indicating that the soil is slightly alkali. This suggests that the soil type is different and should be considered when interpreting the results of other soil parameters that are influenced by the pH.

Examination of the means and standard deviations of each cell in the three plots suggests no significant variation is evident, thus suggesting that soil pH is relatively homogenous across badland landscapes. However, geostatistical analysis shows that some cyclic behaviour of varying degrees is evident in all three plots. This indicates that although no obvious spatial autocorrelation is identifiable, some spatial patterns exist.

## **6.9 *Electrical conductivity***

### **6.9.1 Results**

#### *a) Test of normality, descriptive statistics and inter-plot variation*

The frequency distributions displayed by the boxplots (figure 6.30) show that the datasets from all plots are highly positively skewed. Many outliers are evident in all datasets and are only present at the upper region of the scale.

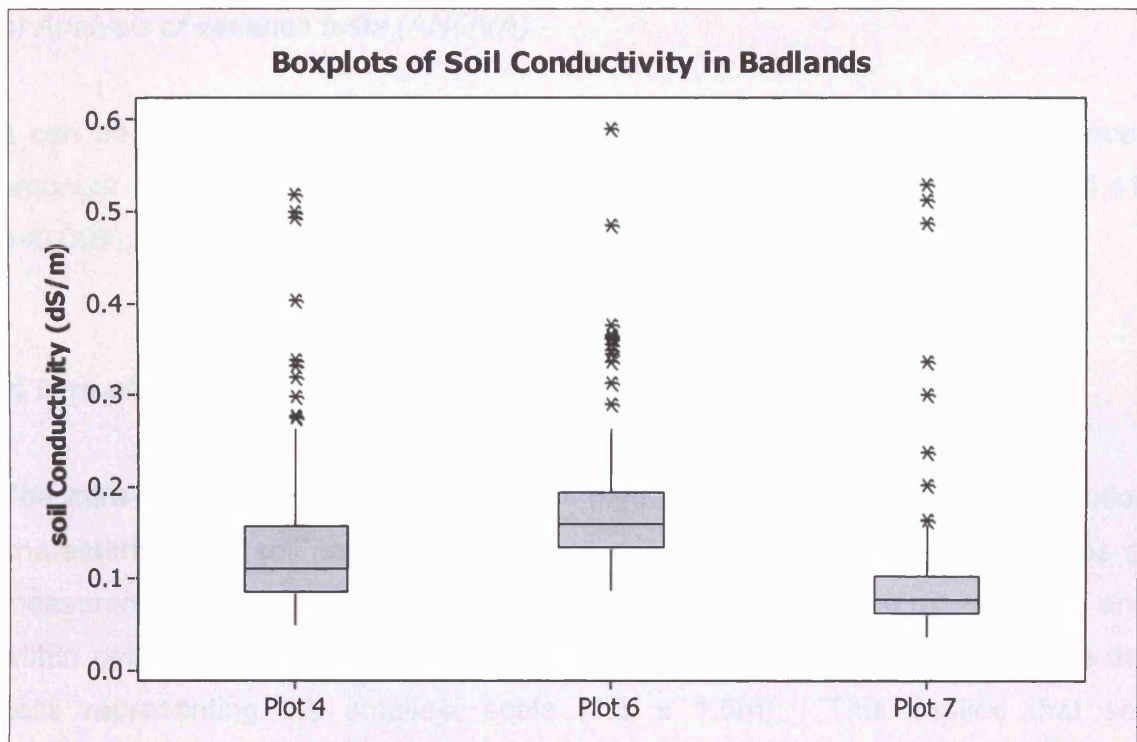


Figure 6.30 Boxplots representing the sample distribution of soil conductivity in the badland plots.

Inter-plot comparisons (table 6.9) show that the mean values of conductivity from the three badland plots vary considerably despite having similar ranges. Plot 6 has the highest mean value but the lowest coefficient of variation. Plot 7, on the other hand, has the lowest mean value but the greatest amount of within-plot variability.

Table 6.9 Inter-plot comparisons of descriptive statistics: Soil conductivity ( $\text{dS m}^{-1}$ )

Descriptive Statistic	Plot 4 (Karoo)	Plot 6 (Karoo)	Plot 7 (Karoo)
Mean	0.14	0.18	0.10
Median	0.11	0.16	0.08
SE of Mean	0.01	0.01	0.01
St Dev	0.09	0.09	0.08
Variance	0.008	0.007	0.007
Coef Var	64.86	47.04	83.43
Minimum	0.05	0.09	0.04
Maximum	0.52	0.60	0.53
Range	0.47	0.50	0.49
IQR	0.07	0.069	0.04
Skewness	2.39	2.36	3.78
Kurtosis	6.37	6.23	15.45

***b) Analysis of variance tests (ANOVA)***

It can be concluded from the ANOVA test that there are significant differences amongst the means of the soil conductivity from plots 4, 6 and 7. ( $F= 24.41$ ,  $p<0.005$ ).

***c) Intra-plot variation***

The intra-plot analysis of the three plots (figure 6.31) shows that the distribution characteristics of soil conductivity are site specific. At the two largest scales of measurement, plot 4 demonstrates differences amongst both the mean values and within cell variation. Significantly less variation is evident across and within the cells representing the smallest scale (1.5 x 1.5m). This implies that soil conductivity may display spatial autocorrelation. Plot 6, in contrast, displays no considerable differences across the three spatial scales, suggesting the scale of measurement is not significant and no spatial patterns exist. Plot 7 shows a different distribution again. The two largest cells display higher means and greater within cell variability. Apart for two 1.5 x 1.5m cells, all other cells display significantly lower means and standard deviations. The distribution of this plot implies that spatial patterns of conductivity may be present, although these are site specific and a function of features in the landscape.

of Geostatistical analysis: The semi-variogram

Pre-processing of

No. of cells

ndividual results

Figure 6.32

Table 6.10 Geostatistical

Parameter: Conductivity

No. of cells

No. of cells

Log transformation

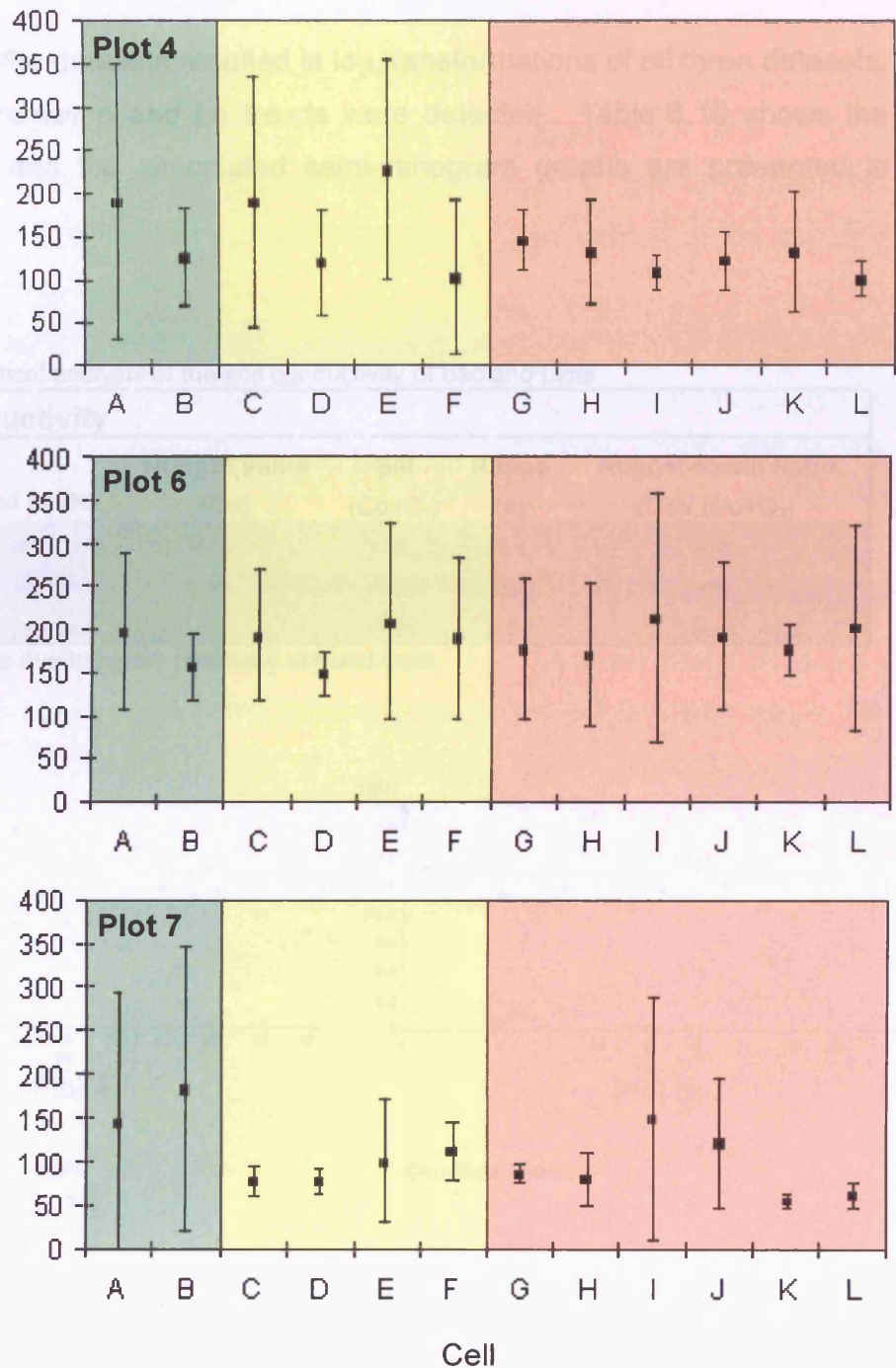


**Figure 6.31** The means and standard deviations of soil conductivity for each cell within the plots. Green represents the 30 x 30m cells, yellow represents the 10 x 10m cells and pink represents 1.5 x 1.5m cells.

d) Geostatistical analysis: The semi-variogram

Pre-processing of the datasets resulted in log transformations of all three datasets. No outliers were removed and no trends were detected. Table 6.10 shows the numerical results and the associated semi-variogram graphs are presented in figure 6.32.

**Table 6.10** Geostatistical analysis of the soil conductivity of badland plots

Parameter: Conductivity						
No.	Plot	Fitted Model	Nugget Value ( $C_0$ )	Sill ( $C_0+C_1$ )	Range ( $a$ )	Nugget-to-sill Ratio ( $C_0$ )/ ( $C_0+C_1$ )
4	na*	na	na	na	na	na
6	na*	na	na	na	na	na
7	Karoo*	Spherical	0.42	0.99	8.54	0.42

\* Log transformed data due to highly positively skewed data

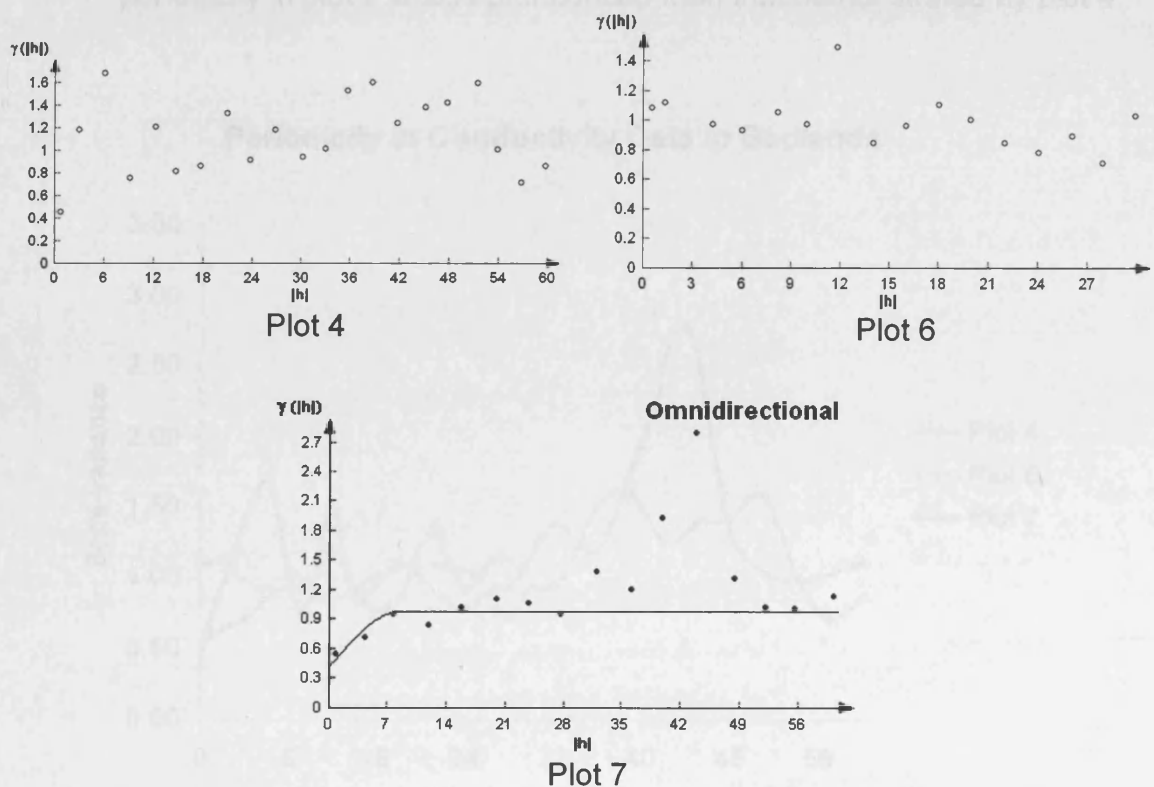


**Figure 6.32** Modelled semi-variograms for the conductivity of badland plots.

The results are as follows:

- i) Only plot 7 demonstrates spatial autocorrelation, with a range of 8.54m. A spherical model was applied and the nugget-to-sill ratio of 0.42 suggests that moderate spatial dependency can be used to describe the results. However, this plot also displays a large peak at a lag distance of approximately 45m.
- ii) Plots 4 and 6, in contrast, could not be accurately represented by a model. The most accurate simple model would be a pure nugget model thus suggesting no spatial patterns exist. However, these variograms display evidence of periodicity and therefore suggests some spatial patterns exist (see figure 6.33).
- iii) Plot 6 also demonstrates a fluctuating downward trend in variance with an increasing lag distance. This may represent a checkerboard pattern.
- iv) Although plots 4 and 7 are measured using the same spatial scale, the periodicity in plot 7 is less pronounced than that demonstrated by plot 4.

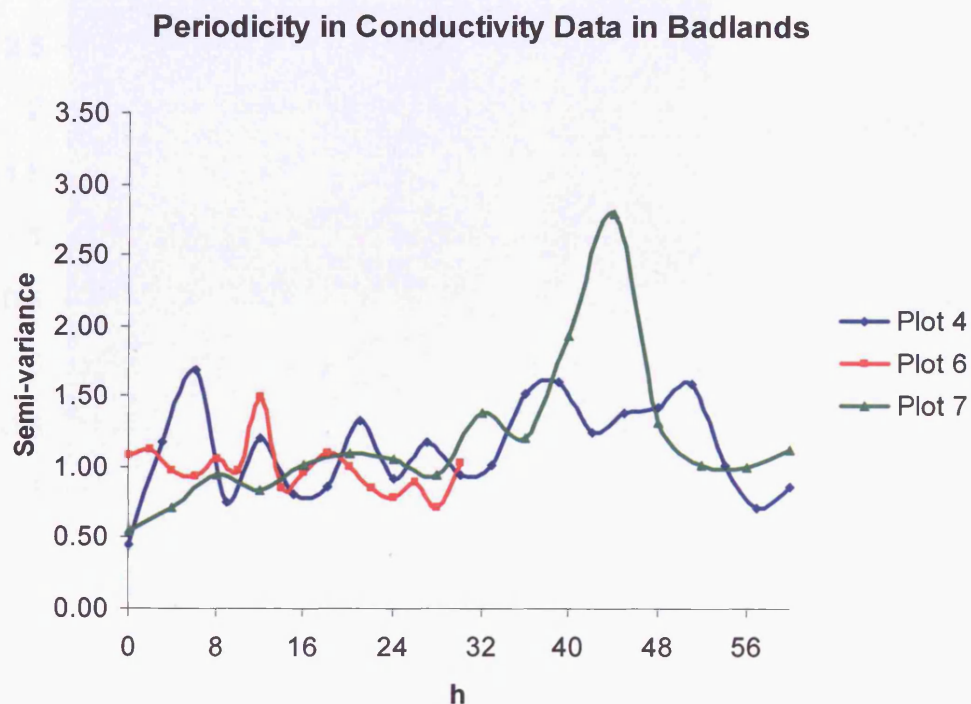


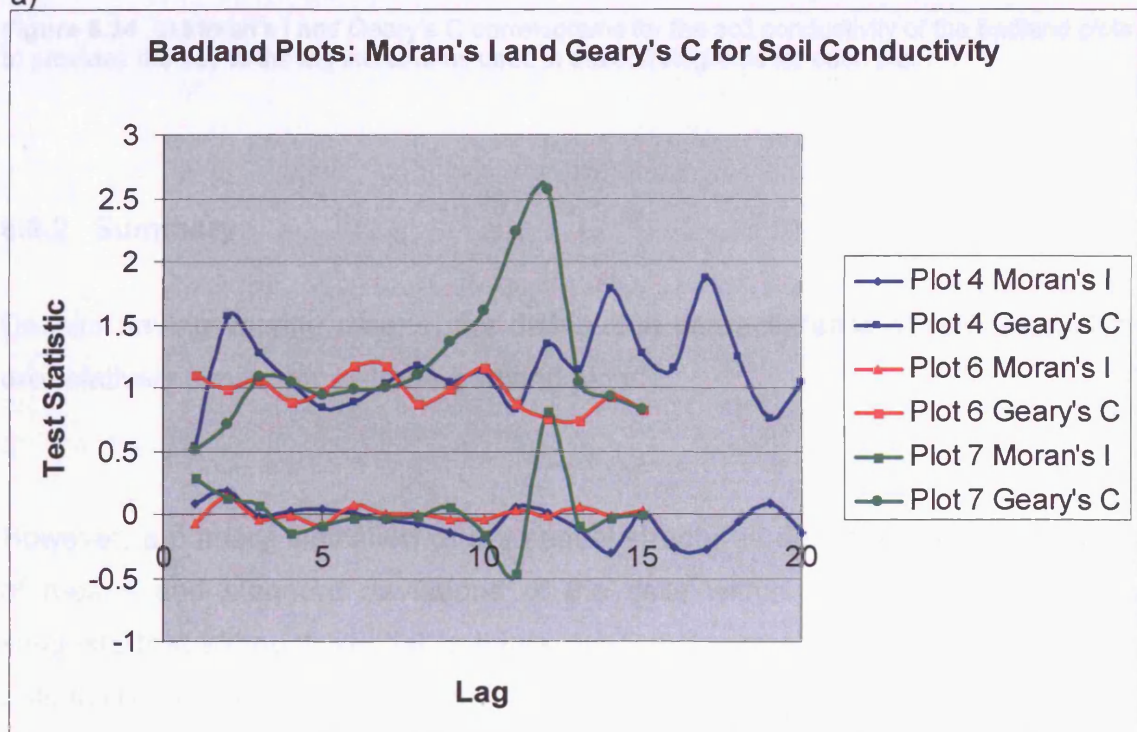
**Figure 6.33** Semi-variograms with connecting lines to show periodicity in soil conductivity data in badland plots.

e) *Geostatistical analysis: Moran's I and Geary's C statistics*

The results are as follows (see figure 6.34):

- i) Some variation between the two types of correlograms is evident suggesting that caution should be exercised when interpreting these results.
- ii) Fluctuation in the results produced for all three plots are less pronounced in the correlograms than in the semi-variograms, particularly for plots 4 and 7 and at the smaller lag distances.
- iii) For plot 6, the Geary's C correlogram shows the slight cyclic downward trend evident in the semi-variogram, however, the Moran's I correlogram suggests that no spatial patterns exist.

a)



b)

Lag increment codes	Plot 4	Plot 6	Plot 7
1	0 > to <= 3	0 > to <= 1	0 > to <= 4
2	3 > to <= 6	1 > to <= 2	4 > to <= 8
3	6 > to <= 9	2 > to <= 3	8 > to <= 12
4	9 > to <= 12	3 > to <= 4	12 > to <= 16
5	12 > to <= 15	4 > to <= 5	16 > to <= 20
6	15 > to <= 18	5 > to <= 6	20 > to <= 24
7	18 > to <= 21	6 > to <= 7	24 > to <= 28
8	21 > to <= 24	7 > to <= 8	28 > to <= 32
9	24 > to <= 27	8 > to <= 9	32 > to <= 36
10	27 > to <= 30	9 > to <= 10	36 > to <= 40
11	30 > to <= 33	10 > to <= 11	40 > to <= 44
12	33 > to <= 36	11 > to <= 12	44 > to <= 48
13	36 > to <= 39	12 > to <= 13	48 > to <= 52
14	39 > to <= 42	13 > to <= 14	52 > to <= 56
15	42 > to <= 45	14 > to <= 15	56 > to <= 60
16	45 > to <= 48		
17	48 > to <= 51		
18	51 > to <= 54		
19	54 > to <= 57		
20	57 > to <= 60		

**Figure 6.34** a) Moran's I and Geary's C correlograms for the soil conductivity of the badland plots. b) provides the key to the lag increments used in the correlograms for each plot.

## 6.9.2 Summary

Despite having varying means, the distribution characteristics of soil conductivity are relatively similar for all three badland plots.

However, a cursory indication of the spatial structures derived from the variability of means and standard deviations of the cells within each of the three plots suggests that although spatial patterns exist, they are site specific and therefore potentially a function of features in the landscape.

The geostatistical analysis provides further evidence that the spatial patterns of soil conductivity are site specific with each plot displaying a different spatial response. Only plot 7 demonstrates spatial autocorrelation, with a range of 8.54m.

Plots 4 and 6, in contrast, could not be accurately represented by a model. Nevertheless, these variograms display evidence of periodicity thus suggesting that some spatial patterns exist. Plot 6 also demonstrates a fluctuating downward trend in variance with an increasing lag distance, which may represent a checkerboard distribution.

### **6.10 Nutrient content analysis**

Due to some obvious anomalies in the output datasets, as a result of machine error, the results presented here have been filtered and some data points removed. Of the badland plots only plot 7 was affected thus the sample size was reduced to 106.

#### **6.10.1 Results:**

##### **Calcium**

##### *a) Test of normality, descriptive statistics and inter-plot variation*

The frequency distributions displayed by the boxplots (figure 6.35) show that all plots are positively skewed, however, the skew of plot 6 is weak and therefore can be considered as having a normal distribution. Outliers are only evident in plot 4.

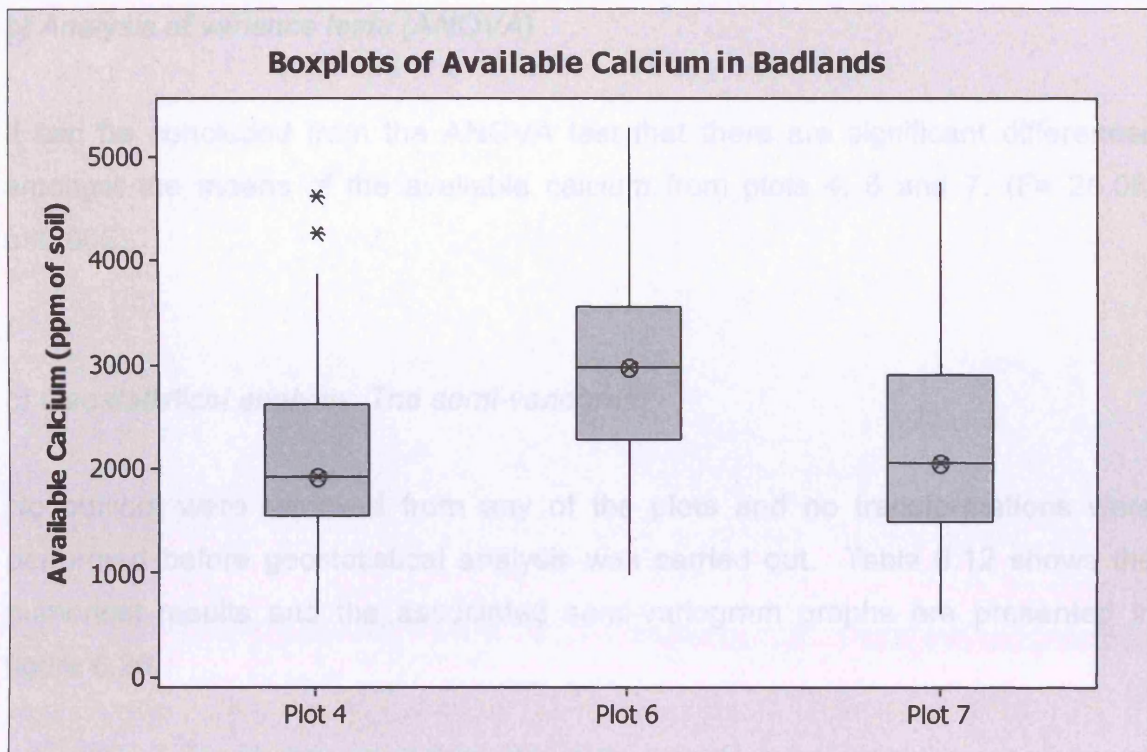


**Figure 6.35** Boxplots representing the sample distribution of available calcium in the badland plots.

The distribution characteristics of available calcium are similar for all three badland plots. Plot 6 has the highest mean value and the greatest range, although the coefficient of variation shows that, relative to the mean, plot 6 has the least intra-plot variability. The greatest within plot variation is found in plot 7.

**Table 6.11** Inter-plot comparisons of descriptive statistics: Available calcium in ppm of soil

Descriptive Statistic	Plot 4 (Karoo)	Plot 6 (Karoo)	Plot 7 (Karoo)
<b>Mean</b>	<b>2118.70</b>	<b>2934.70</b>	<b>2246.70</b>
Median	1927.80	2968.50	2056.40
SE of Mean	76.50	91.20	95.00
St Dev	794.60	948.30	977.70
Variance	631461.80	899178.60	955826.80
<b>Coef Var</b>	<b>37.51</b>	<b>32.31</b>	<b>43.52</b>
Minimum	614.00	997.50	621.90
Maximum	4616.00	5276.20	4758.30
<b>Range</b>	<b>4002.00</b>	<b>4278.70</b>	<b>4136.40</b>
IQR	1061.30	1274.40	1402.70
Skewness	0.78	0.11	0.62
Kurtosis	0.21	-0.31	-0.13

*b) Analysis of variance tests (ANOVA)*

It can be concluded from the ANOVA test that there are significant differences amongst the means of the available calcium from plots 4, 6 and 7. ( $F= 25.08$ ,  $p<0.005$ ).

*c) Geostatistical analysis: The semi-variogram*

No outliers were removed from any of the plots and no transformations were performed before geostatistical analysis was carried out. Table 6.12 shows the numerical results and the associated semi-variogram graphs are presented in figure 6.36.

**Table 6.12** Geostatistical analysis of the available calcium of badland plots

<b>Parameter: Calcium</b>						
Plot		Fitted Model	Nugget Value	Sill	Range	Nugget-to-sill Ratio
No.	Location		(Co)	(Co+C <sub>1</sub> )	(a)	(Co)/(Co+C <sub>1</sub> )
4	Karoo	na	na	na	na	na
6	Karoo	Spherical	0.59	1.12	4.8	0.53
7	Karoo	Spherical	0.44	1.25	27.45	0.35

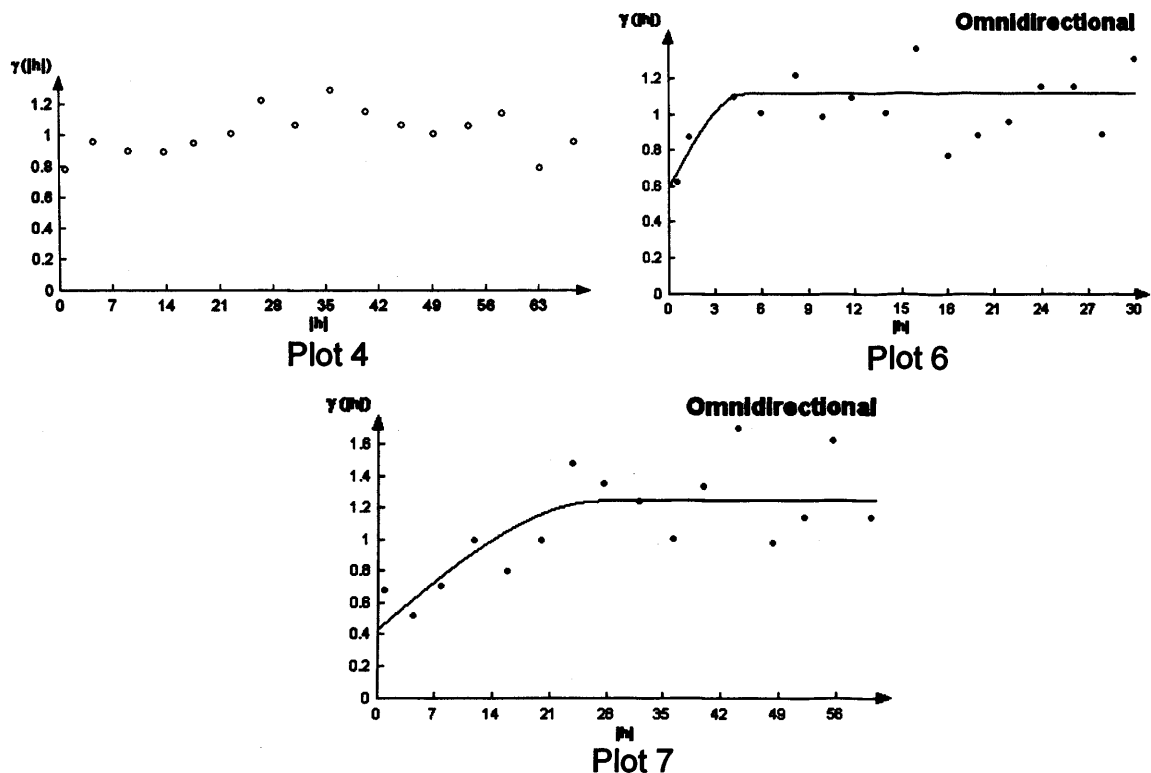


**Figure 6.36** Modelled semi-variograms for the available calcium in badland plots.

The results are as follows:

- i) Plots 6 and 7 show evidence of spatial autocorrelation with ranges of 4.8m and 27.45m, respectively. In both cases the nugget-to-sill ratios indicate a moderate spatial dependency.
- ii) Plot 4 is best represented by the pure nugget model indicating that no spatial patterns are evident, however, some evidence of periodicity is present suggesting that the pure nugget model may not be a true representation of the pattern in this plot.
- iii) Examining the periodicity in the three datasets (figure 6.37) suggests that scale of measurement may be important when attempting to identify spatial patterns in available calcium. Smaller wavelengths are evident in the results from plot 6, which has a maximum lag of 30m, whereas a much larger average wavelength is evident in the results derived from plot 7, which has a maximum lag of 60m.

### Periodicity in Available Ca Data in Badlands

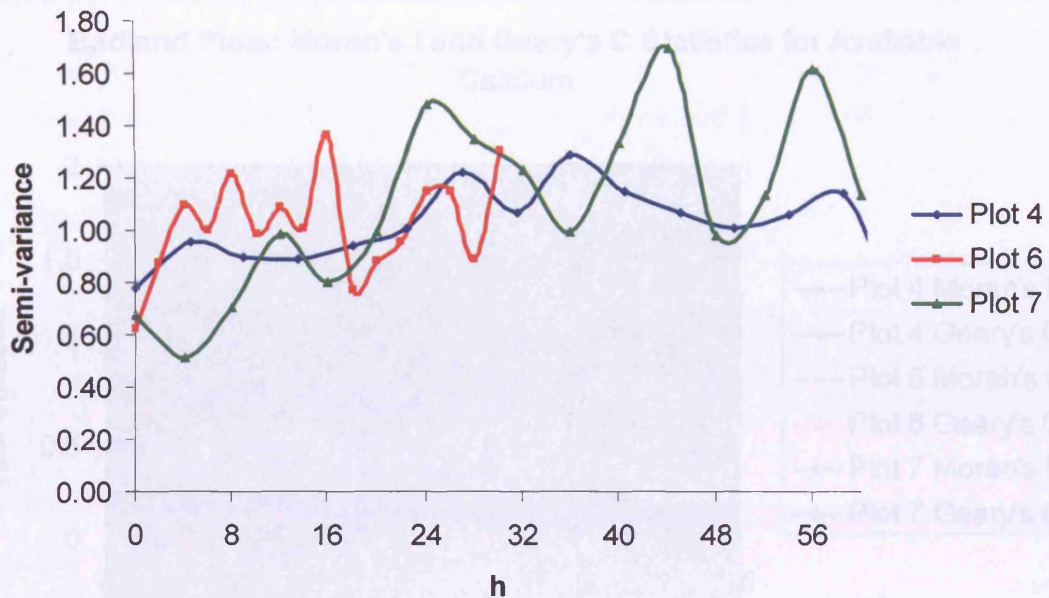


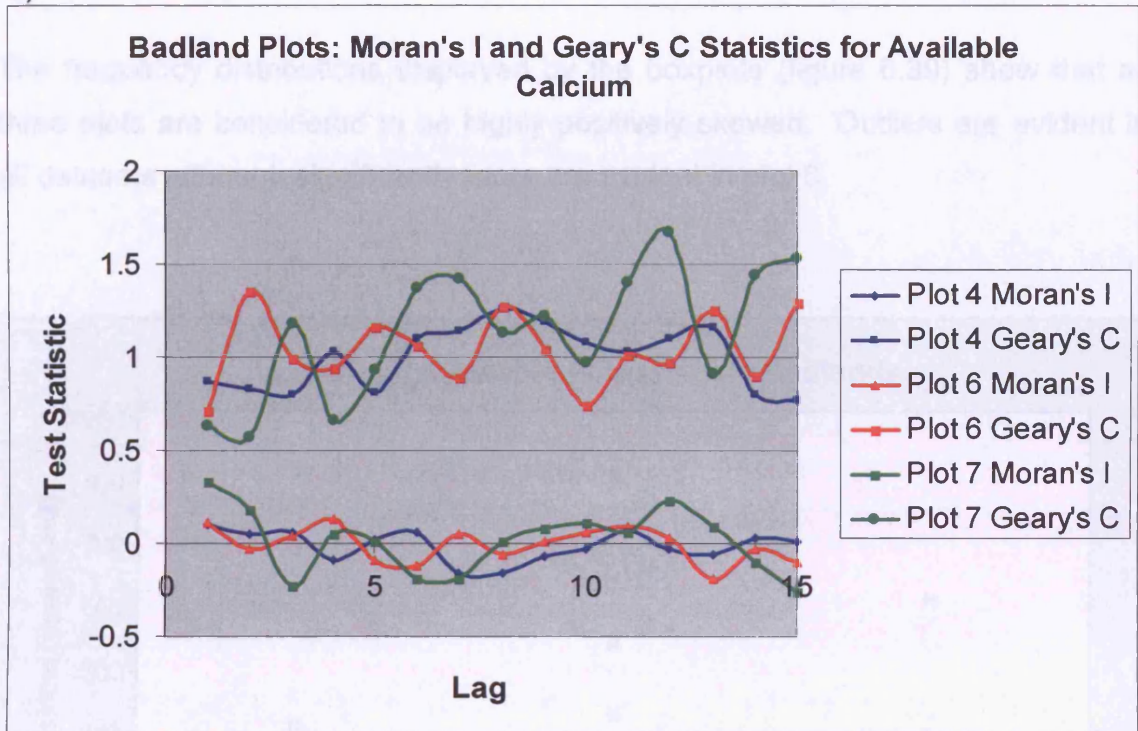
**Figure 6.37** Semi-variograms with connecting lines to show periodicity in the available calcium data in badland plots.

#### d) Geostatistical analysis: Moran's I and Geary's C statistics

The results are as follows: (see figure 6.38)

- i) Although the Moran's I and Geary's C correlograms correspond relatively well, the results do not reflect the same ranges of spatial autocorrelation derived from the semi-variograms.
- ii) Interpretation of plots 6 and 7 are difficult. Although the fluctuating nature of the data can be seen in the Geary's C correlogram, demonstrating that the spatial structures are changing, potential ranges of spatial autocorrelation cannot be identified.
- iii) The correlograms suggest that a pure nugget model may be more appropriate to describe the data from plot 6. Plot 4, on the other hand, shows a significant change in spatial structure at a lag distance of approximately 25m.

a)



b)

Lag increment codes	Plot 4	Plot 6	Plot 7
1	0 > to ≤ 4.5	0 > to ≤ 2	0 > to ≤ 4
2	4.5 > to ≤ 9	2 > to ≤ 4	4 > to ≤ 8
3	9 > to ≤ 13.5	4 > to ≤ 6	8 > to ≤ 12
4	13.5 > to ≤ 18	6 > to ≤ 8	12 > to ≤ 16
5	18 > to ≤ 22.5	8 > to ≤ 10	16 > to ≤ 20
6	22.5 > to ≤ 27	10 > to ≤ 12	20 > to ≤ 24
7	27 > to ≤ 31.5	12 > to ≤ 14	24 > to ≤ 28
8	31.5 > to ≤ 36	14 > to ≤ 16	28 > to ≤ 32
9	36 > to ≤ 40.5	16 > to ≤ 18	32 > to ≤ 36
10	40.5 > to ≤ 45	18 > to ≤ 20	36 > to ≤ 40
11	45 > to ≤ 49.5	20 > to ≤ 22	40 > to ≤ 44
12	49.5 > to ≤ 54	22 > to ≤ 24	44 > to ≤ 48
13	54 > to ≤ 58.5	24 > to ≤ 26	48 > to ≤ 52
14	58.5 > to ≤ 63	26 > to ≤ 28	52 > to ≤ 56
15	63 > to ≤ 67.5	28 > to ≤ 30	56 > to ≤ 60

**Figure 6.38** a) Moran's I and Geary's C correlograms for the available calcium in the badland plots. b) provides the key to the lag increments used in the correlograms for each plot.

## Potassium

### a) Test of normality, descriptive statistics and inter-plot variation

The frequency distributions displayed by the boxplots (figure 6.39) show that all three plots are considered to be highly positively skewed. Outliers are evident in all datasets although significantly more are evident in plot 6.

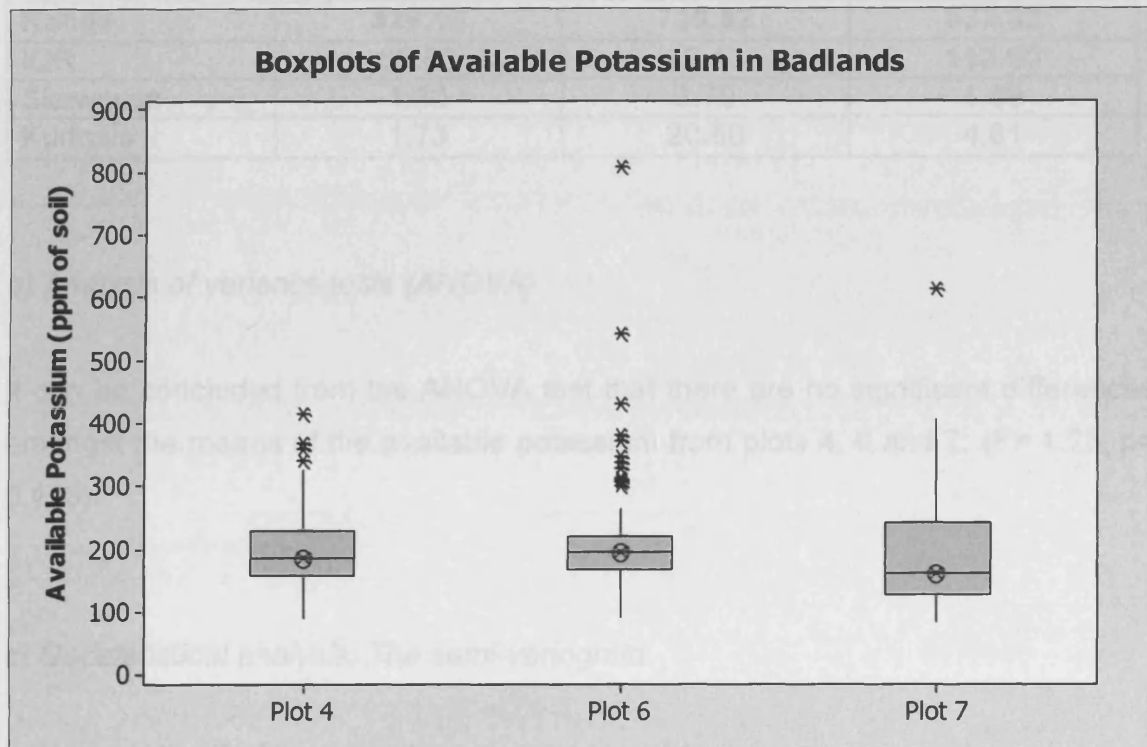


**Figure 6.39** Boxplots representing the sample distribution of available potassium in the shrubland plots.

Inter-plot comparisons (table 6.13) show that the mean values of available potassium are similar in all the plots. However, both the ranges and coefficients of variation differ across the three plots. Plot 4 has the smallest range and smallest within-plot variation, plot 7 has the highest within-plot variation and plot 6 has the greatest range of values.

**Table 6.13** Inter-plot comparisons of descriptive statistics: Available potassium in ppm of soil

Descriptive Statistic	Plot 4 (Karoo)	Plot 6 (Karoo)	Plot 7 (Karoo)
<b>Mean</b>	<b>199.65</b>	<b>209.70</b>	<b>189.58</b>
Median	187.70	197.14	161.66
SE of Mean	5.63	8.64	8.39
St Dev	58.54	88.73	86.40
Variance	3426.45	7873.32	7464.76
<b>Coef Var</b>	<b>29.32</b>	<b>42.31</b>	<b>45.57</b>
Minimum	89.69	89.75	83.22
Maximum	415.82	809.37	615.24
<b>Range</b>	<b>326.13</b>	<b>719.62</b>	<b>532.02</b>
IQR	69.53	52.43	113.60
Skewness	1.20	3.70	1.69
Kurtosis	1.73	20.50	4.61

*b) Analysis of variance tests (ANOVA)*

It can be concluded from the ANOVA test that there are no significant differences amongst the means of the available potassium from plots 4, 6 and 7. ( $F = 1.73$ ,  $p = 0.178$ ).

*c) Geostatistical analysis: The semi-variogram*

Pre-processing of the datasets resulted in one outlier being removed from plot 6. All three distributions are highly positively skewed therefore log transformations were applied to all three datasets. No trends were identified. None of the available potassium datasets could be modelled using the simple models available, thus only the experimental semi-variogram graphs are presented (figure 6.40).

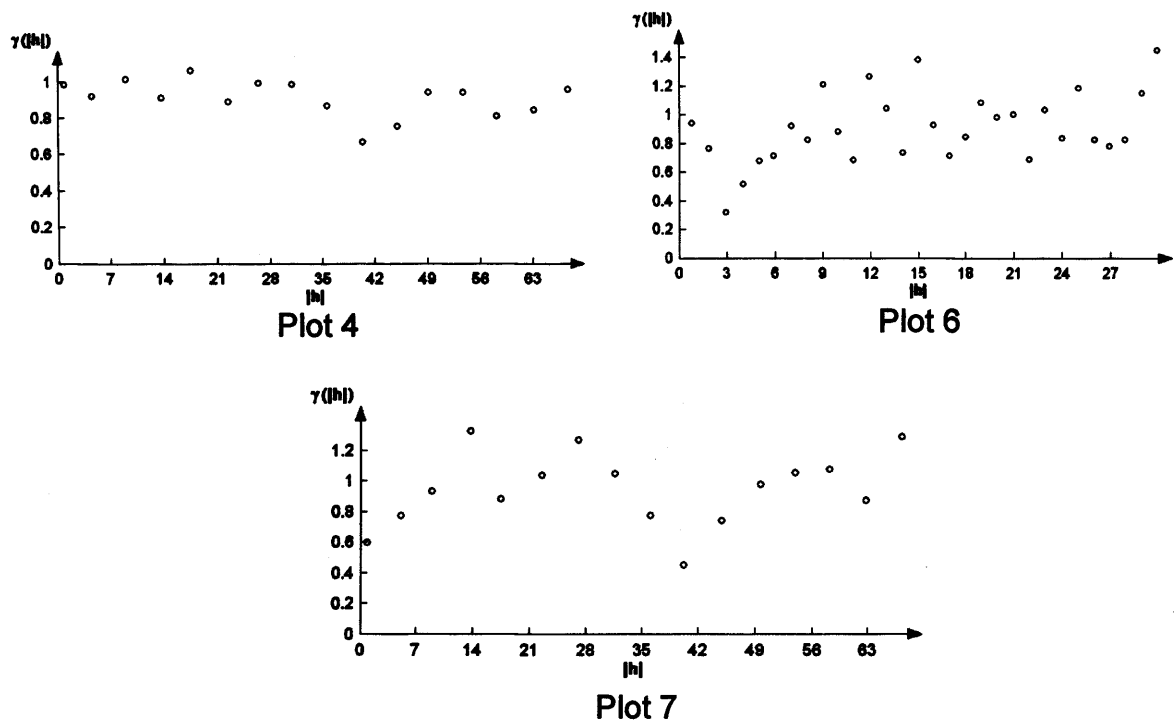


**Figure 6.40** Modelled semi-variograms for the available potassium in badland plots.

The results are as follows:

- i) The experimental variograms show that none of the datasets can be accurately represented by simple models.
- ii) The most accurate simple model applicable to plots 4 and 6 would be a pure nugget model thus suggesting no spatial patterns exist. However, these variograms display evidence of periodicity albeit at different scales thus suggesting that some spatial patterns exist (see figure 6.41).
- iii) Plot 4 also demonstrates a fluctuating downward trend in variance with an increasing lag distance. This may represent a checkerboard pattern.
- iv) Although it may be possible to apply a spherical model to plot 7, the results would not fully represent the spatial patterns of available potassium in this plot. Cyclic behaviour is evident and can be seen in figure 6.41.

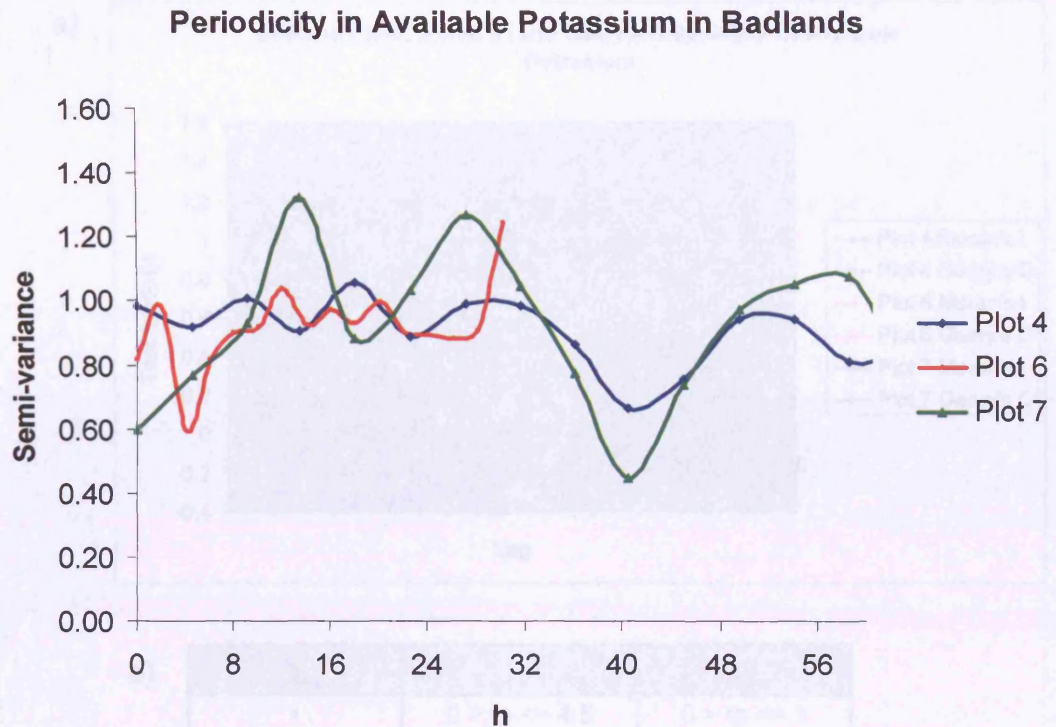


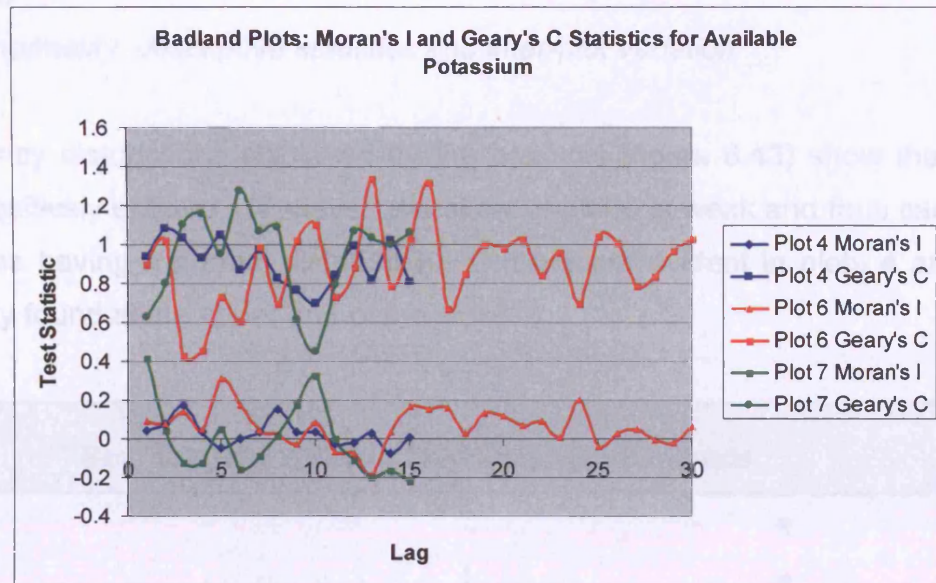
**Figure 6.41** Semi-variograms with connecting lines to show periodicity in the available potassium data in badland plots.

*d) Geostatistical analysis: Moran's I and Geary's C statistics*

The results are as follows: (see figure 6.42)

- i) The Moran's I and Geary's C correlograms correspond relatively well, and the results display similar fluctuating patterns to those evident in the experimental semi-variograms.
- ii) Although generally similar, the correlograms of both plots 4 and 6 display greater fluctuation than the semi-variograms.
- iii) Despite the fluctuating nature of plots 4 and 6, no specific spatial patterns are obvious. There appears to be no significant changes in spatial structure evident from the two correlograms.
- iv) A significant change in spatial structure is evident in plot 7 at a lag distance of approximately 40m.

a)



b)

Lag increment codes	Plot 4 & 7	Plot 6
1	0 > to <= 4.5	0 > to <= 1
2	4.5 > to <= 9	1 > to <= 2
3	9 > to <= 13.5	2 > to <= 3
4	13.5 > to <= 18	3 > to <= 4
5	18 > to <= 22.5	4 > to <= 5
6	22.5 > to <= 27	5 > to <= 6
7	27 > to <= 31.5	6 > to <= 7
8	31.5 > to <= 36	7 > to <= 8
9	36 > to <= 40.5	8 > to <= 9
10	40.5 > to <= 45	9 > to <= 10
11	45 > to <= 49.5	10 > to <= 11
12	49.5 > to <= 54	11 > to <= 12
13	54 > to <= 58.5	12 > to <= 13
14	58.5 > to <= 63	13 > to <= 14
15	63 > to <= 67.5	14 > to <= 15
16		15 > to <= 16
17		16 > to <= 17
18		17 > to <= 18
19		18 > to <= 19
20		19 > to <= 20
21		20 > to <= 21
22		21 > to <= 22
23		22 > to <= 23
24		23 > to <= 24
25		24 > to <= 25
26		25 > to <= 26
27		26 > to <= 27
28		27 > to <= 28
29		28 > to <= 29
30		29 > to <= 30

**Figure 6.42** a) Moran's I and Geary's C correlograms for the available potassium in the badland plots. b) provides the key to the lag increments used in the correlograms for each plot.

## Magnesium

### a) Test of normality, descriptive statistics and inter-plot variation

The frequency distributions displayed by the boxplots (figure 6.43) show that all plots are positively skewed. However, the skew of plot 6 is weak and thus can be described as having a normal distribution. Outliers are evident in plots 4 and 7 and are only found at the upper end of the scale.

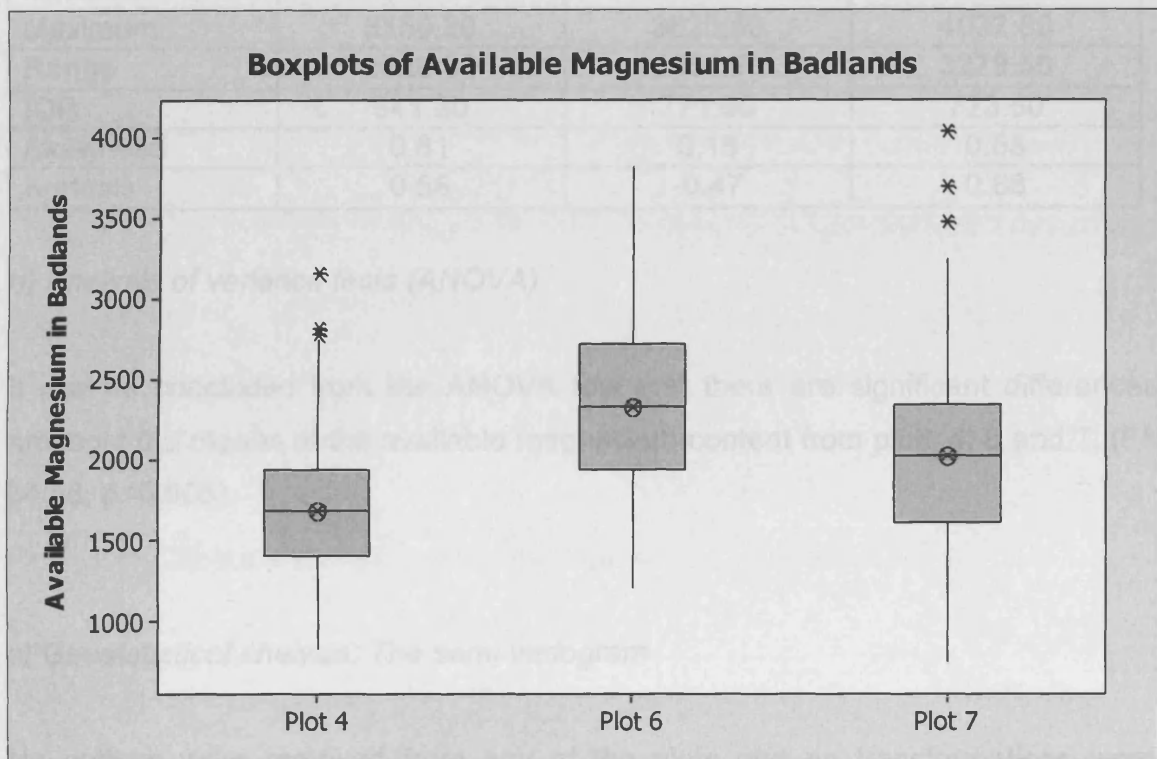


**Figure 6.43** Boxplots representing the sample distribution of available magnesium in the badland plots.

Although the means fluctuate across the three badland plots (table 6.14), the general distribution characteristics are relatively similar. Relative to the mean, the intra-plot variability is similar for all three plots.

**Table 6.14** Inter-plot comparisons of descriptive statistics: Available magnesium in ppm of soil

Descriptive Statistic	Plot 4 (Karoo)	Plot 6 (Karoo)	Plot 7 (Karoo)
Mean	1736.60	2353.10	2040.30
Median	1693.00	2331.50	2030.70
SE of Mean	42.30	56.30	58.20
St Dev	439.80	584.90	599.10
Variance	193430.30	342071.50	358945.70
Coef Var	25.33	24.86	29.36
Minimum	838.40	1216.00	753.30
Maximum	3159.20	3820.50	4032.80
Range	2320.80	2604.50	3279.50
IQR	541.30	771.90	723.50
Skewness	0.81	0.18	0.58
Kurtosis	0.58	-0.47	0.88

*b) Analysis of variance tests (ANOVA)*

It can be concluded from the ANOVA test that there are significant differences amongst the means of the available magnesium content from plots 4, 6 and 7. ( $F=34.46$ ,  $p<0.005$ ).

*c) Geostatistical analysis: The semi-variogram*

No outliers were removed from any of the plots and no transformations were performed before geostatistical analysis was carried out. Table 6.15 shows the numerical results and the associated semi-variogram graphs are presented in figure 6.44.

**Table 6.15** Geostatistical analysis of the available magnesium in badland plots

Parameter: Magnesium						
No.	Plot	Fitted Model	Nugget Value (Co)	Sill (Co+C <sub>1</sub> )	Range (a)	Nugget-to-sill Ratio (Co)/(Co+C <sub>1</sub> )
4	Karoo	Gaussian	0.56	1.36	28.2	0.41
6	Karoo	Spherical	0.4	1.06	7.2	0.38
7	Karoo	Spherical	0.45	1.41	32.64	0.32

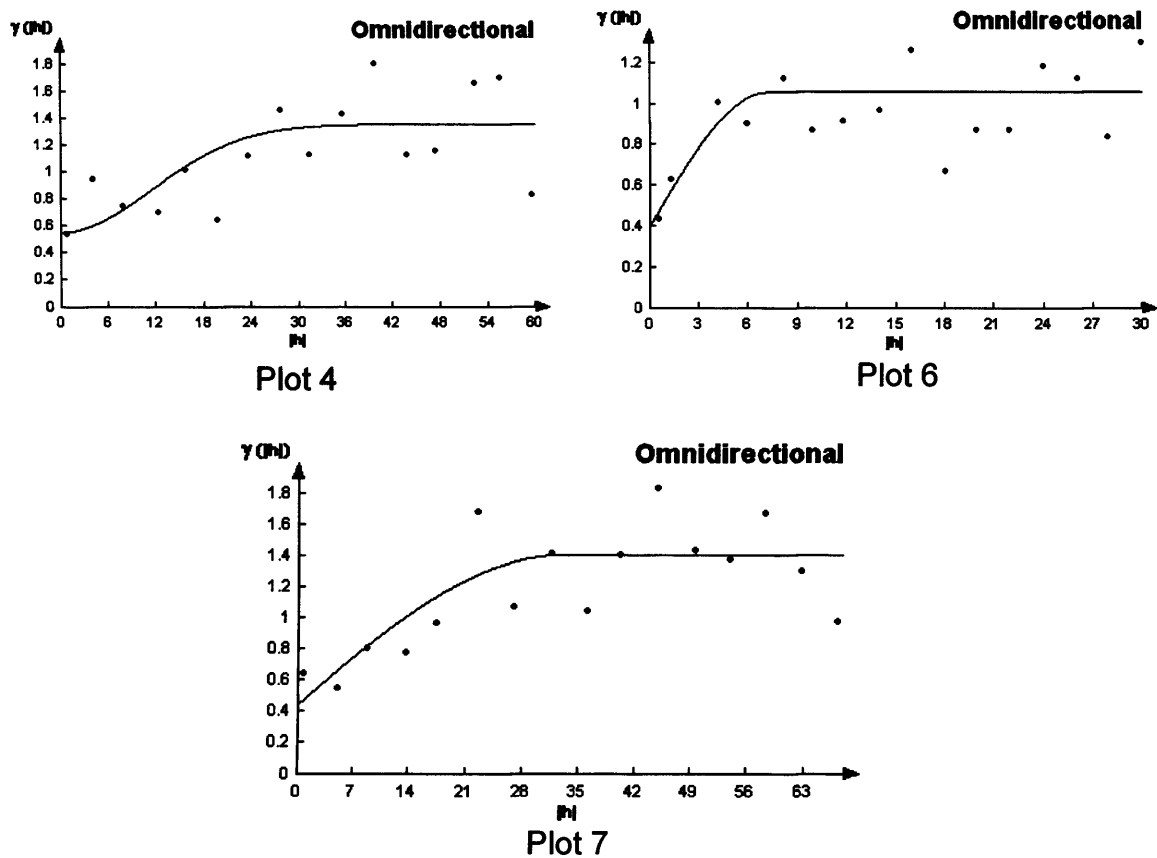


**Figure 6.44** Modelled semi-variograms for the available magnesium in badland plots.

The results are as follows:

- i) Plots 4, 6 and 7 show evidence of spatial autocorrelation. Plots 6 and 7 were best represented by a spherical model and show ranges of 7.2m and 32.64m, respectively. A Gaussian model was applied to plot 4 and a range of 28.2m was derived.
- ii) The nugget-to-sill ratios suggest that all three plots show moderate spatial dependency.
- iii) The cyclic patterns evident in the three plots are shown in figure 6.45. Plots 4 and 7, the two plots measured using the same scale, display similar wavelengths. Plot 6, which has a maximum lag of 30m displays smaller-scale fluctuation but generally follows a similar wave pattern to plots 4 and 7.

### Periodicity in Available Magnesium Data in Badlands

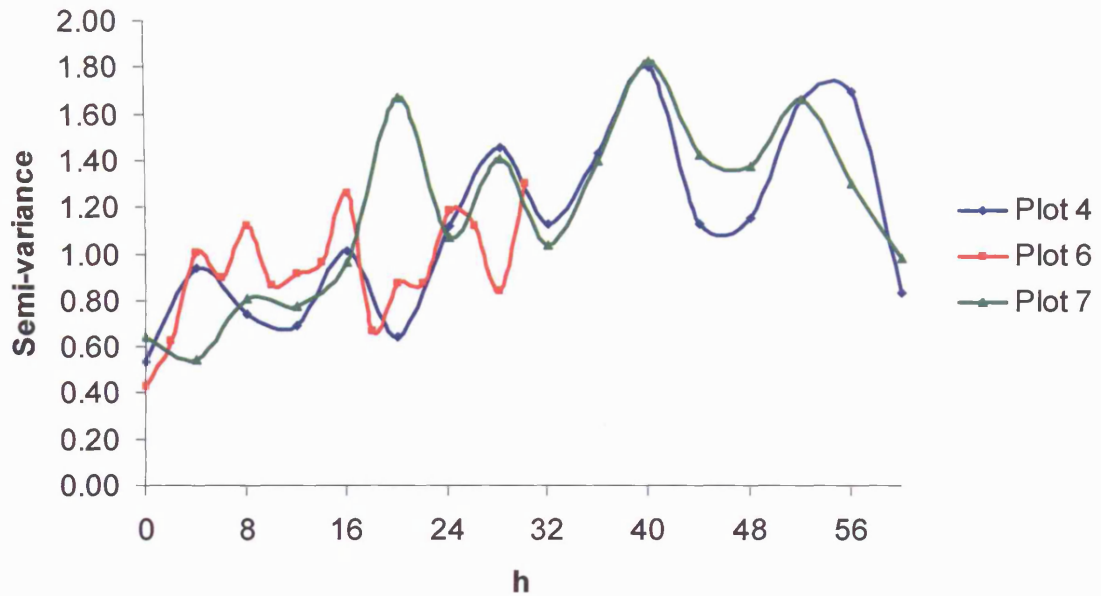


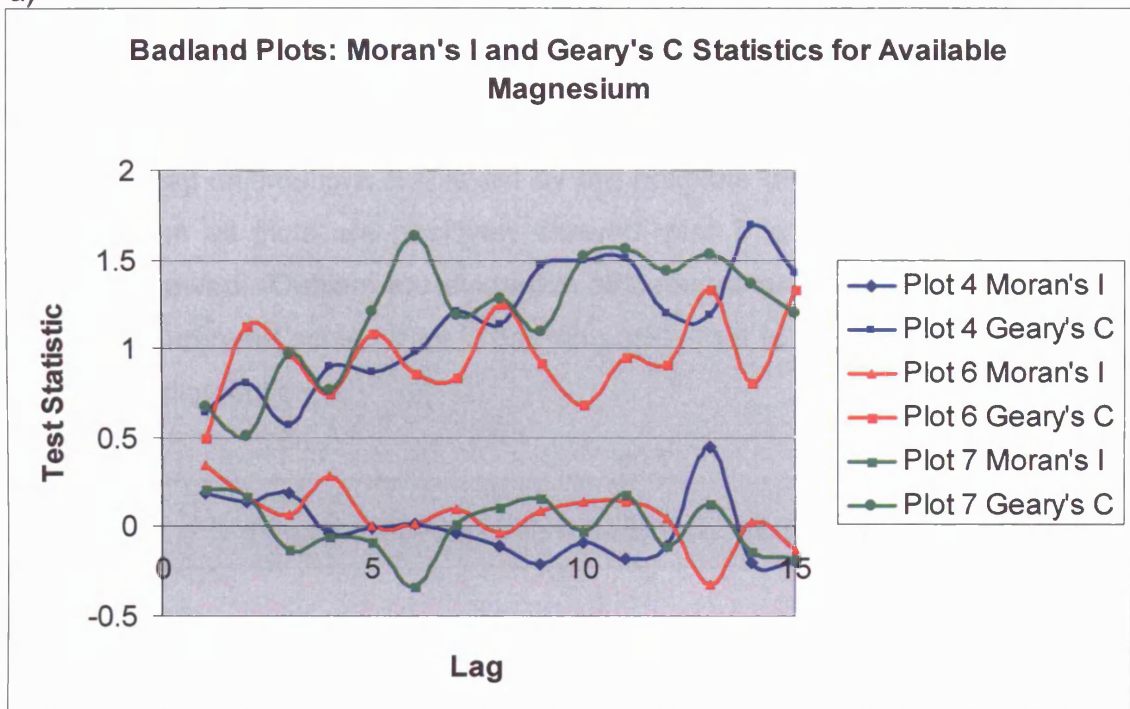
**Figure 6.45** Semi-variograms with connecting lines to show periodicity in the available magnesium data in badland plots.

#### d) Geostatistical analysis: Moran's I and Geary's C statistics

The results are as follows: (see figure 6.46)

- i) Although the Moran's I and Geary's C correlograms correspond relatively well, the results do not reflect the same ranges of spatial autocorrelation derived from the semi-variograms.
- ii) The results from the correlograms suggest that the changes in spatial structure occur at lag distances less than the ranges of spatial autocorrelation derived by the semi-variograms.
- iii) The correlograms for plot 6 indicate that no significant spatial pattern is evident for available magnesium.
- iv) The similarities between the periodicities evident in the semi-variograms of plots 4 and 7 are not reflected in the correlograms.

a)



b)

Lag increment codes	Plot 4	Plot 6	Plot 7
1	0 > to <= 4	0 > to <= 2	0 > to <= 4.5
2	4 > to <= 8	2 > to <= 4	4.5 > to <= 9
3	8 > to <= 12	4 > to <= 6	9 > to <= 13.5
4	12 > to <= 16	6 > to <= 8	13.5 > to <= 18
5	16 > to <= 20	8 > to <= 10	18 > to <= 22.5
6	20 > to <= 24	10 > to <= 12	22.5 > to <= 27
7	24 > to <= 28	12 > to <= 14	27 > to <= 31.5
8	28 > to <= 32	14 > to <= 16	31.5 > to <= 36
9	32 > to <= 36	16 > to <= 18	36 > to <= 40.5
10	36 > to <= 40	18 > to <= 20	40.5 > to <= 45
11	40 > to <= 44	20 > to <= 22	45 > to <= 49.5
12	44 > to <= 48	22 > to <= 24	49.5 > to <= 54
13	48 > to <= 52	24 > to <= 26	54 > to <= 58.5
14	52 > to <= 56	26 > to <= 28	58.5 > to <= 63
15	56 > to <= 60	28 > to <= 30	63 > to <= 67.5

**Figure 6.46** a) Moran's I and Geary's C correlograms for the available magnesium in the badland plots. b) provides the key to the lag increments used in the correlograms for each plot.

**Sodium***a) Test of normality, descriptive statistics and inter-plot variation*

The frequency distributions displayed by the boxplots (figure 6.47) show that the datasets from all plots are positively skewed, plot 7 is considered to be highly positively skewed. Outliers are evident in all datasets and occur at the upper end of the measurement scale. Plot 7 has an outlier that is significantly greater than the general distribution.

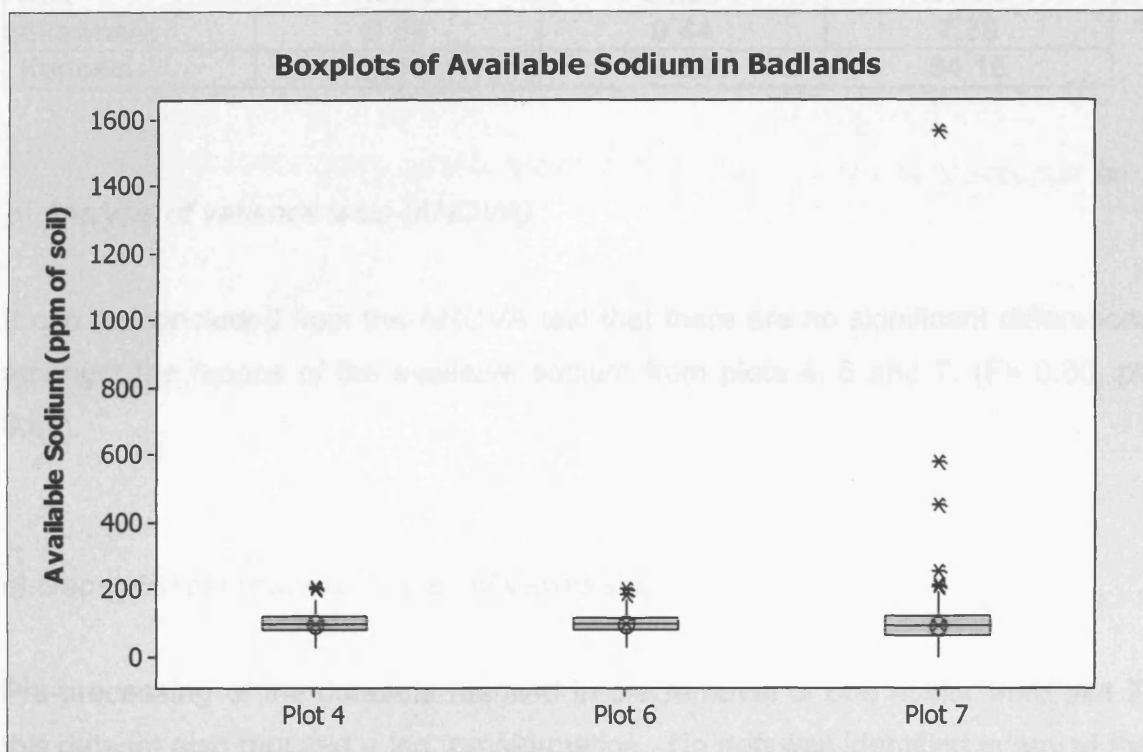


**Figure 6.47** Boxplots representing the sample distribution of available sodium in the badland plots.

The descriptive statistics presented in table 6.16 show that the mean values of available sodium are similar in all three badland plots. Plots 4 and 6 also have very similar ranges and intra-plot variability. Plot 7, in contrast, has a much greater range and coefficient of variation, these results are a consequence of the extreme value at the upper end of the scale. Ignoring this value, plot 7 still can be seen to have a greater range than the other two plots.

**Table 6.16** Inter-plot comparisons of descriptive statistics: Available sodium in ppm of soil

Descriptive Statistic	Plot 4 (Karoo)	Plot 6 (Karoo)	Plot 7 (Karoo)
Mean	<b>102.49</b>	<b>96.07</b>	<b>112.50</b>
Median	98.93	95.16	90.50
SE of Mean	3.19	2.84	15.60
St Dev	33.12	29.46	160.90
Variance	1097.08	868.12	25875.90
Coef Var	<b>32.32</b>	<b>30.67</b>	<b>142.97</b>
Minimum	30.75	27.54	0.00
Maximum	205.85	199.50	1561.00
Range	<b>175.10</b>	<b>171.96</b>	<b>1561.00</b>
IQR	43.10	36.94	57.00
Skewness	0.54	0.44	7.39
Kurtosis	0.44	1.16	64.15

*b) Analysis of variance tests (ANOVA)*

It can be concluded from the ANOVA test that there are no significant differences amongst the means of the available sodium from plots 4, 6 and 7. ( $F = 0.80$ ,  $p = 0.45$ ).

*c) Geostatistical analysis: The semi-variogram*

Pre-processing of the datasets resulted in the removal of one outlier from plot 7, this dataset also required a log transformation. No drift was identified in any of the datasets. None of the available sodium datasets could be modelled using the simple models available, thus only the experimental semi-variogram graphs are presented (figure 6.48).

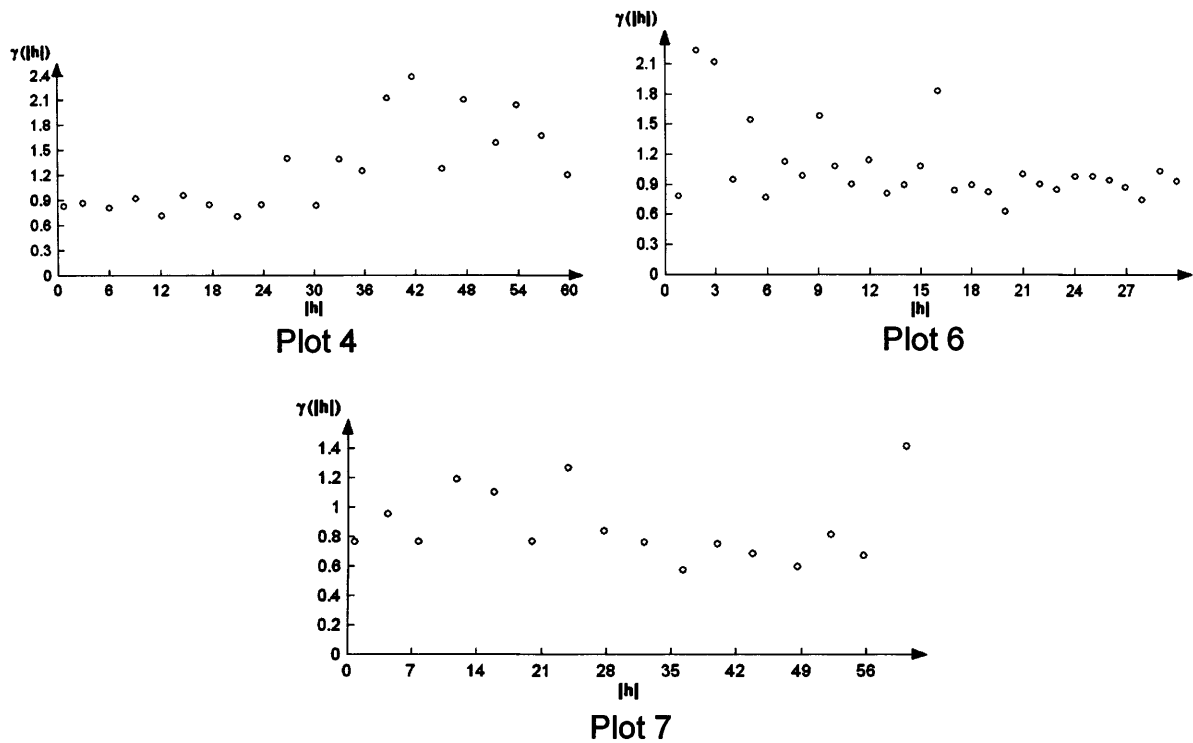


**Figure 6.48** Modelled semi-variograms for the available sodium in badland plots.

The results are as follows:

- i) The experimental variograms show that none of the datasets can be accurately represented by simple models.
- ii) Plots 6 and 7 demonstrate a fluctuating downward trend in variance with an increasing lag distance. This is more pronounced in plot 6 and may represent a checkerboard pattern.
- iii) In contrast to plots 6 and 7, plot 4 demonstrates a significant increase in variance at approximately 26m. This may represent part of spatial pattern that occurs at distances larger than those measured in this study. This could also explain the downward trend in variance evident in plots 6 and 7.
- iv) Figure 6.49 show the periodicity evident in the semi-variogram data. The wavelengths appear relatively similar in the datasets from all three plots.

## Periodicity in Available Sodium Data in Badlands

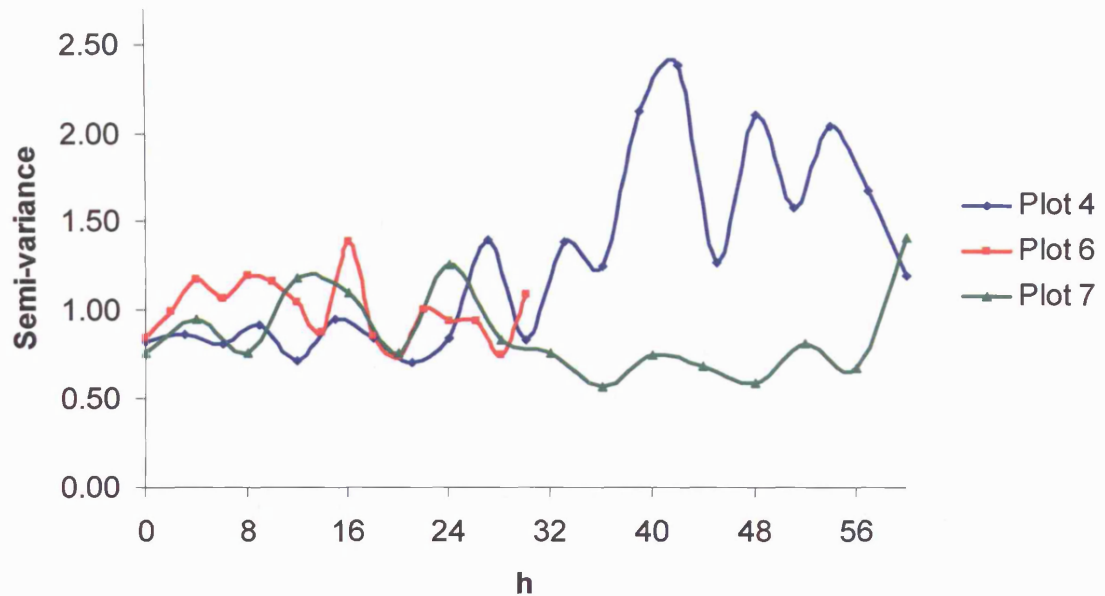
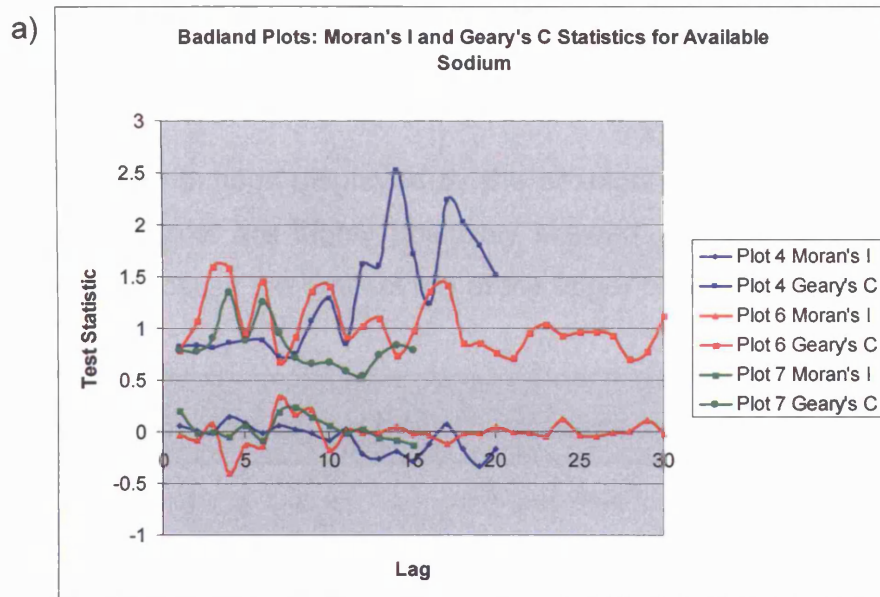


**Figure 6.49** Semi-variograms with connecting lines to show periodicity in the available sodium data in shrubland plots.

*d) Geostatistical analysis: Moran's I and Geary's C statistics*

The results are as follows: (see figure 6.50)

- i) Although the results of the Moran's I and Geary's C correlograms are similar, the Moran's I response appears to be much weaker than the Geary's C.
- ii) Plots 4 and 7 demonstrate the mirroring behaviour of the Geary's C and Moran's I data only at the smaller lags.
- iii) Plot 4 is the only plot that displays evidence of a significant change in spatial structure. This occurs at a lag distance of approximately 27m. This is similar to the results produced by the semi-variogram.
- iv) Although no significant changes in spatial structure are obvious from the correlograms of plots 6 and 7, periodicity can be seen in the results, particularly in the data from plot 6.



b)

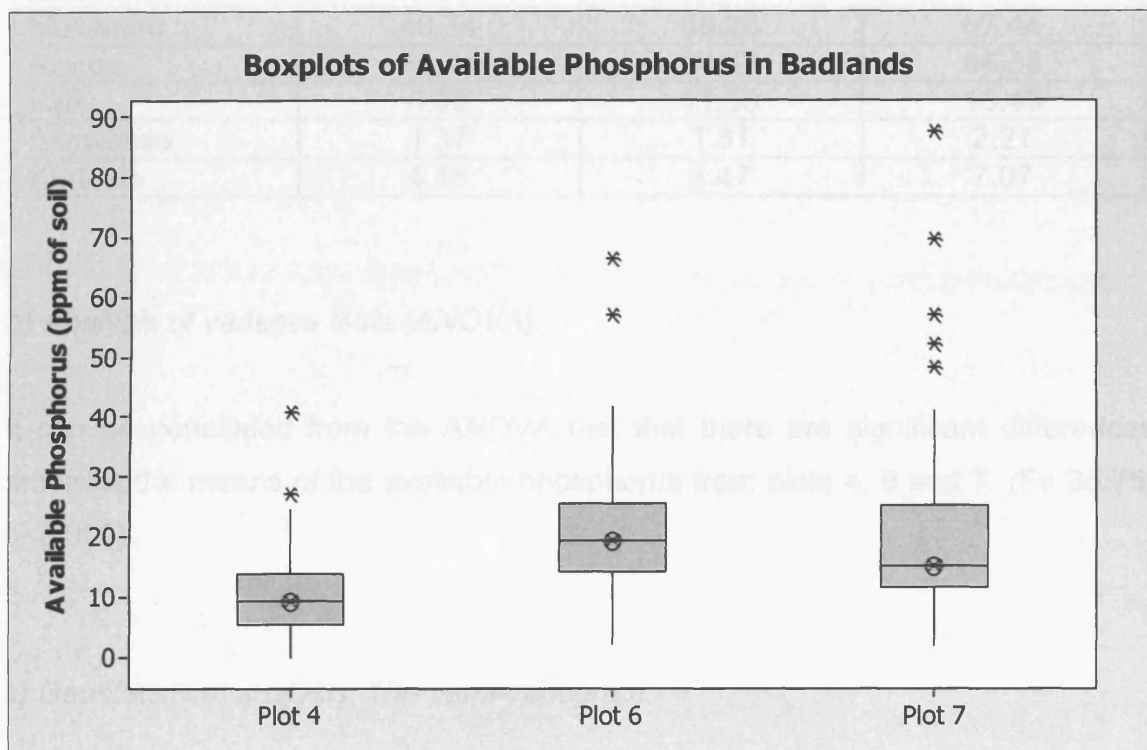
Lag increment codes	Plot 4	Plot 6	Plot 7
1	0 > to <= 3	0 > to <= 1	0 > to <= 4
2	3 > to <= 6	1 > to <= 2	4 > to <= 8
3	6 > to <= 9	2 > to <= 3	8 > to <= 12
4	9 > to <= 12	3 > to <= 4	12 > to <= 16
5	12 > to <= 15	4 > to <= 5	16 > to <= 20
6	15 > to <= 18	5 > to <= 6	20 > to <= 24
7	18 > to <= 21	6 > to <= 7	24 > to <= 28
8	21 > to <= 24	7 > to <= 8	28 > to <= 32
9	24 > to <= 27	8 > to <= 9	32 > to <= 36
10	27 > to <= 30	9 > to <= 10	36 > to <= 40
11	30 > to <= 33	10 > to <= 11	40 > to <= 44
12	33 > to <= 36	11 > to <= 12	44 > to <= 48
13	36 > to <= 39	12 > to <= 13	48 > to <= 52
14	39 > to <= 42	13 > to <= 14	52 > to <= 56
15	42 > to <= 45	14 > to <= 15	56 > to <= 60
16	45 > to <= 48	15 > to <= 16	
17	48 > to <= 51	16 > to <= 17	
18	51 > to <= 54	17 > to <= 18	
19	54 > to <= 57	18 > to <= 19	
20	57 > to <= 60	19 > to <= 20	
21		20 > to <= 21	
22		21 > to <= 22	
23		22 > to <= 23	
24		23 > to <= 24	
25		24 > to <= 25	
26		25 > to <= 26	
27		26 > to <= 27	
28		27 > to <= 28	
29		28 > to <= 29	
30		29 > to <= 30	

Figure 6.50 a) Moran's I and Geary's C correlograms for the available sodium in the badland plots. b) provides the key to the lag increments used in the correlograms for each plot.

## Phosphorus

### a) Test of normality, descriptive statistics and inter-plot variation

The frequency distributions displayed by the boxplots (figure 6.51) show that the datasets from all plots are highly positively skewed. Outliers are evident in all datasets and in all cases the outliers are at the upper end of the measurements.



**Figure 6.51** Boxplots representing the sample distribution of available phosphorus in the badland plots.

The descriptive statistics presented in table 6.17 show that the mean values of available phosphorus from plots 6 and 7 are approximately double that of plot 4. The range of values in plot 4 is also significantly less than plots 6 and 7, although relative to the mean, the within-plot variability is similar to the other two plots. Plot 7 demonstrates the greatest amount of variability within the plot.

**Table 6.17** Inter-plot comparisons of descriptive statistics: Available phosphorus in ppm of soil

Descriptive Statistic	Plot 4 (Karoo)	Plot 6 (Karoo)	Plot 7 (Karoo)
<b>Mean</b>	<b>10.12</b>	<b>21.07</b>	<b>19.74</b>
Median	9.30	19.35	15.28
SE of Mean	0.61	0.99	1.30
St Dev	6.34	10.26	13.38
Variance	40.14	105.16	179.07
<b>Coef Var</b>	<b>62.64</b>	<b>48.68</b>	<b>67.79</b>
Minimum	0.00	2.11	1.86
Maximum	40.74	66.28	87.44
<b>Range</b>	<b>40.74</b>	<b>64.17</b>	<b>85.58</b>
IQR	8.66	11.38	13.45
Skewness	1.37	1.31	2.21
Kurtosis	4.16	3.47	7.07

*b) Analysis of variance tests (ANOVA)*

It can be concluded from the ANOVA test that there are significant differences amongst the means of the available phosphorus from plots 4, 6 and 7. ( $F = 35.75$ ,  $p < 0.005$ ).

*c) Geostatistical analysis: The semi-variogram*

Pre-processing of the datasets resulted in log transformations of all three datasets. No outliers were removed and no trends were detected. None of the available phosphorus datasets could be modelled using the simple models available, thus only the experimental semi-variogram graphs are presented (figure 6.52).

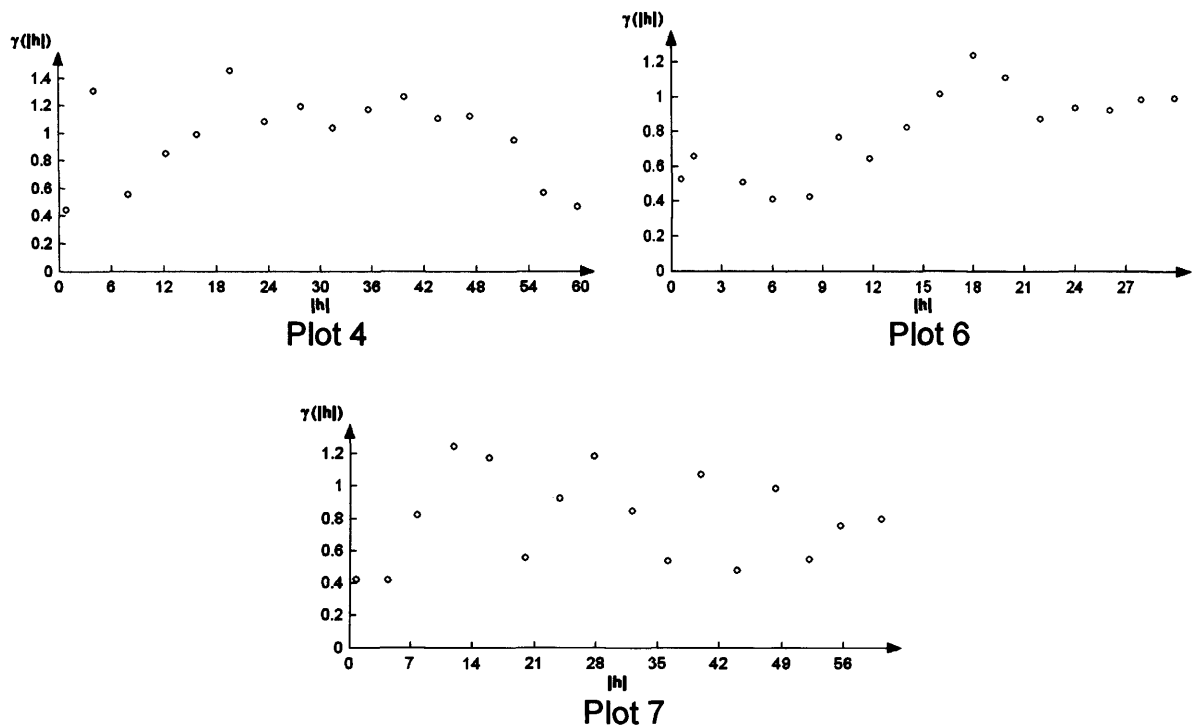


**Figure 6.52** Modelled semi-variograms for the available phosphorus in badland plots.

The results are as follows:

- i) The experimental variograms show that none of the datasets can be accurately represented by simple models.
- ii) Plot 4 may be best represented by a pure nugget model, however, the decrease in variance at the smallest and largest lags suggest that this may represent part of larger-scale periodicity.
- iii) Plot 6, the plot with a maximum lag of 30m, shows some cyclic patterns although these are more pronounced across plot 7, which has a maximum lag distance of 60m (see figure 6.53).
- iv) Although the amplitudes of the waves shown in figure 6.53 are different, the wavelengths are relatively similar in each of the three datasets.

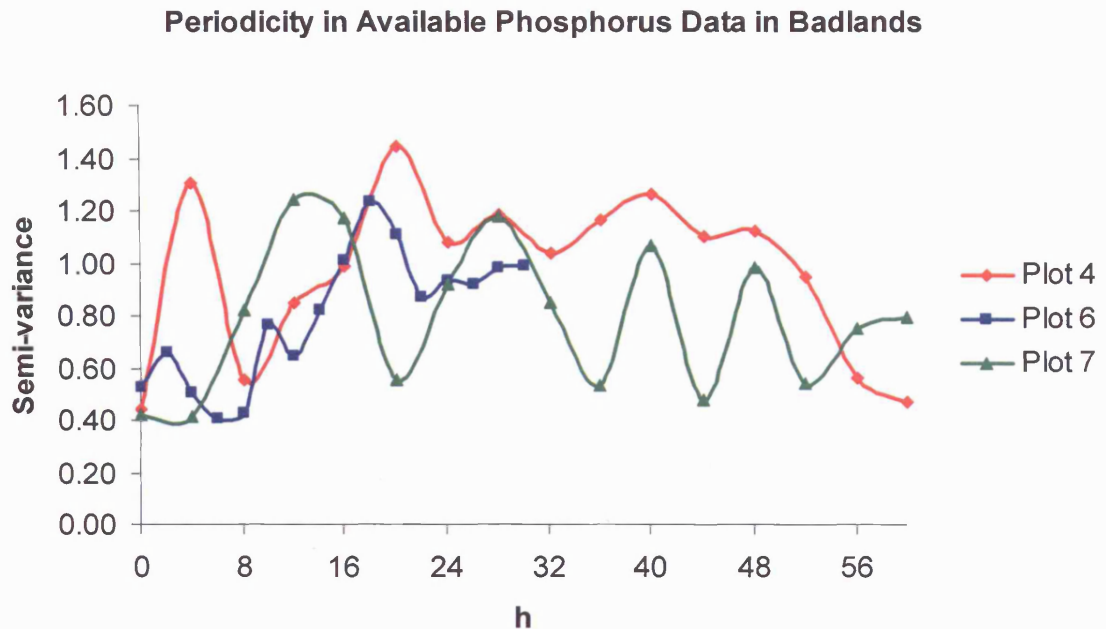


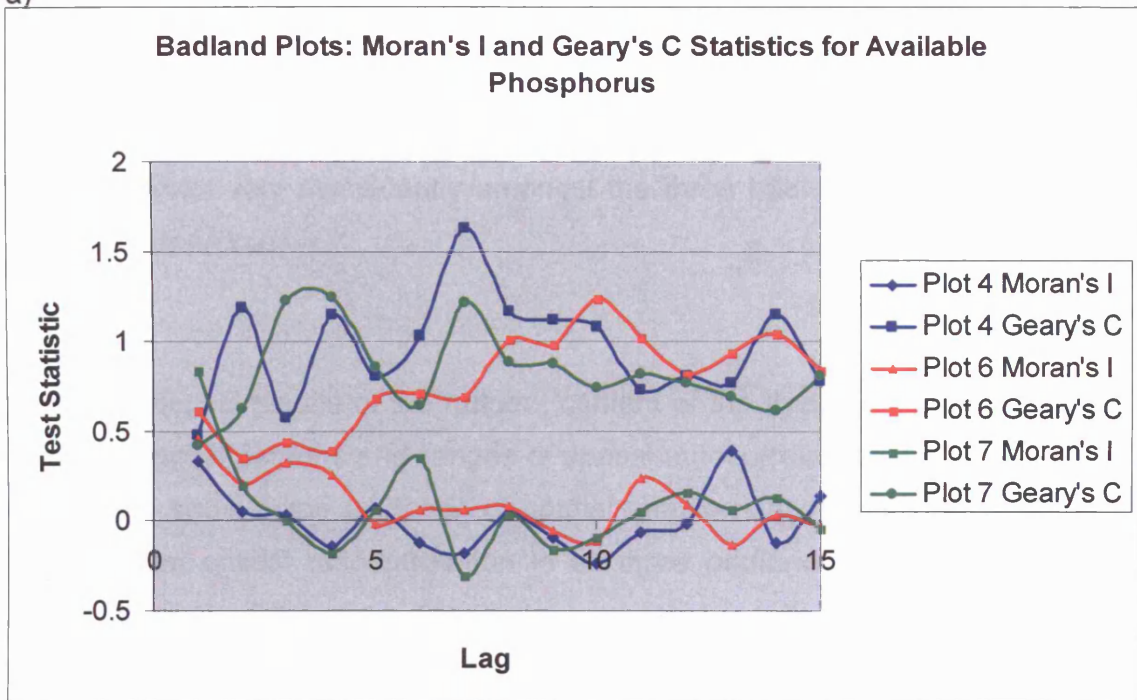
**Figure 6.53** Semi-variograms with connecting lines to show periodicity in the available phosphorus data in shrubland plots.

*d) Geostatistical analysis: Moran's I and Geary's C statistics*

The results are as follows: (see figure 6.54)

- i) Comparisons made between the Moran's I and Geary's C statistics show that the results mirror each other relatively well with the exception of the smaller lag distances of plot 6.
- ii) Cyclic patterns are evident in both correlograms for all three plots.
- iii) Only plot 4 displays a significant change in spatial structure at a lag distance of approximately 22m. Nevertheless, this is only evident in the Geary's C correlogram and not the Moran's I correlogram.

a)



b)

Lag increment codes	Plot 4 & 7	Plot 6
1	0 > to ≤ 4	0 > to ≤ 2
2	4 > to ≤ 8	2 > to ≤ 4
3	8 > to ≤ 12	4 > to ≤ 6
4	12 > to ≤ 16	6 > to ≤ 8
5	16 > to ≤ 20	8 > to ≤ 10
6	20 > to ≤ 24	10 > to ≤ 12
7	24 > to ≤ 28	12 > to ≤ 14
8	28 > to ≤ 32	14 > to ≤ 16
9	32 > to ≤ 36	16 > to ≤ 18
10	36 > to ≤ 40	18 > to ≤ 20
11	40 > to ≤ 44	20 > to ≤ 22
12	44 > to ≤ 48	22 > to ≤ 24
13	48 > to ≤ 52	24 > to ≤ 26
14	52 > to ≤ 56	26 > to ≤ 28
15	56 > to ≤ 60	28 > to ≤ 30

**Figure 6.54** a) Moran's I and Geary's C correlograms for the available phosphorus in the badland plots. b) provides the key to the lag increments used in the correlograms for each plot.

### 6.10.2 Summary

The descriptive statistics show that the distribution characteristics and nutrient contents do not vary significantly amongst the three badland plots located in the Karoo, South Africa.

The geostatistical results of the nutrient content of the three badland plots show a variety of spatial patterns and ranges of spatial autocorrelation. Only calcium and magnesium show some evidence of spatial autocorrelation and only magnesium demonstrates spatial autocorrelation in all three badland plots. Of the ranges derived for each of the two nutrients, no consistent results were evident. Calcium produced ranges of 4.8m and 27.45m and magnesium produced ranges of 28.2m, 7.2m and 32.64m.

Although none of the other experimental variograms had models applied to them, this does not mean that these nutrients exhibit no spatial patterns. Periodicity is evident in the majority of the unmodelled variograms therefore this cyclic behaviour can be classed as a characteristic of badland landscapes. In addition, there is evidence that the scale of measurement may be a significant factor when attempting to determine the spatial patterns of nutrients. Both available calcium and potassium in plot 6 display fine-scale periodicity; this plot was measured using a maximum lag of 30m compared to a maximum lag of 60m used for plots 4 and 7. The two levels of periodicity therefore indicate that fine-scale patterns exist in conjunction with a more general, larger-scale, fluctuating distribution. In contrast, available phosphorus demonstrated a similar pattern of periodicity for all three plots thus indicating that the spatial patterns of phosphorus are not a function of scale.

Some of the experimental variograms of both potassium and sodium display evidence of a downward trend in variance with an increasing lag distance. Although this would generally suggest that the distribution of these nutrients follow

a checkerboard pattern, it could be argued that this characteristic is actually only representing part of a larger-scale cyclic pattern beyond the scale of measurement in this study.

### **6.11 Key findings from the badland plots**

- Complex spatial structures are evident for many of the badland soil parameters, thus making it difficult to represent them accurately with the simple models utilised in this study. Where possible the most representative models have been applied, however, fluctuation of the variance suggests that these models may be misrepresenting the spatial patterns evident in badlands.
- Periodicity is evident in the majority of the badland datasets.
- As periodicity is evident in plot 6 and plots 4 and 7, which were measured using different maximum lag distances, this suggests that the scale of measurement is important when determining the spatial patterns of soil parameters in badland landscapes.
- A decrease in variance with an increasing lag distance is displayed by some of the plots for organic matter content, bulk density and conductivity. Generally, this would suggest a checkerboard pattern is present, however, because of the cyclic patterns evident in the other plots this downward trend may just be representing part of a larger pattern of periodicity.
- Of the plots that demonstrated spatial autocorrelation, the ranges are as follows:

- Organic Matter: 7.20m - 7.48m
  - Dry bulk density: none determined
  - Soil moisture: none determined
  - Shear strength: 14.03m – 16.62m
  - Particle size: none determined
  - pH: none determined
  - Conductivity: 8.54m
  - Calcium: 4.80m – 27.45m
  - Magnesium: 7.20m – 32.64m
  - Potassium: none determined
  - Sodium: none determined
  - Phosphorus: none determined
- Apart from the organic matter content, the ranges of spatial autocorrelation from the badland plots vary significantly. This would suggest that the spatial patterns of each plot are potentially a response of the features in the landscape.
  - In general, the distribution characteristics of the three badland plots are relatively similar. Only the soil shear strength and the pH show significantly different distributions.
  - Soil shear strength varies as a result of some of the sample locations being impenetrable with the shear vane. A maximum value was applied to these locations. More of these locations are evident in plot 4 forcing the median to increase to this maximum value. However, this may not be a true representation of the distribution of the shear strength.
  - The soil pH also varies across the Karoo, plots 4 and 6 are classed as being acidic whereas plot 7 is slightly alkali. This indicates that the soil types are different and that this should be considered when interpreting the results of other soil parameters.

The relationships among the soil parameters will be investigated further in chapters 7 and 8, followed by a detailed interpretation and discussion of the results.

## **CHAPTER SEVEN**

### **Discussion:**

#### **1. Changing Landscapes: the impact of vegetation change**

---

---

##### ***7.1 Comparing soil parameter characteristics in grasslands and shrublands: a discussion on the impact of vegetation change***

***7.1.1 Grasslands and shrublands: a comparison of soil parameters.***

***7.1.2 Soil heterogeneity and vegetation type: changing spatial patterns or changing scale?***

##### ***7.2 The global applicability of soil parameter characteristics in semi-arid environments: a comparison between the Karoo, South Africa and the Sevilleta NWR, New Mexico.***

***7.2.1 Comparison of soil properties between two semi-arid environments***

***7.2.2 Spatial patterns: globally applicable or locally attributable?***

##### ***7.3 Badlands – a progressive evolution?***

***7.3.1 Badlands - a fair description? Characterising the soil properties in badlands and assessing the progressive nature of badland development***

***7.3.2 Identifying spatial patterns of soil properties in badlands and assessing the shrubland-badland connectivity***

---

---

## **7.1 Comparing soil parameter characteristics in grasslands and shrublands: a discussion on the impact of vegetation change**

### **7.1.1 Grasslands and shrublands: a comparison of soil parameters.**

In order to assess the impact of vegetation change on physical and chemical soil parameters, the grassland data from chapter 4 and the shrubland data from chapter 5 were compared. In this section the impact of geographical location is not considered as it can be hypothesised that soil characteristics are characteristic of all semi-arid environments. In addition, any significant but consistent differences associated with the region will not affect this comparison as there are an equal number of grass and shrub plots from each location. Hence, in this section the emphasis is on identifying whether differences exist and their general nature, rather than what the specific differences are. The influence of geographical location will be addressed in section 7.2.

The means of the soil parameters from the grassland and shrubland plots can be seen in table 7.1. The coefficients of variation are also presented to provide an indication of the amount of variation evident in each vegetation community. To statistically test whether differences exist between the two vegetation communities, Mann-Whitney analysis was performed on all the datasets (table 7.2).

**Table 7.1** Means and coefficients of variation [(SD ÷ mean) x 100] of all the soil parameters from the combined grassland and shrubland plots

Soil Parameter	Grasslands		Shrublands	
	Mean	CoV	Mean	CoV
Organic matter (%) *	2.87	35.89	2.25	28.44
Bulk density (g/cm <sup>3</sup> ) *	1.23	13.8	1.3	13.8
Soil moisture (%) *	5.81	72.29	2.29	69
Shear strength (KPa) *	19.14	67.14	9.92	74.7
Clay content (%) **	0.72	30.56	*	*
Silt content (%) **	19.79	36.58	*	*
Sand content (%) **	79.5	9.36	*	*
pH *	7.23	16.74	7.38	16.4
Conductivity (dS/m) *	0.18	38.89	0.15	40.00
Available calcium (ppm of soil) ***	5222	66.87	5722	56.96
Available potassium (ppm of soil) ***	386.32	47.34	314.98	31.97
Available magnesium (ppm of soil) ***	1250.4	37.68	1044.3	30.69
Available sodium (ppm of soil) ***	76.23	60.42	95.2	35.26
Available phosphorus (ppm of soil) ***	39.64	30.9	37.97	36.34

\*(Grass n= 432, Shrub n=431) \*\*(Grass n=104) \*\*\*(Grass n= 427, Shrub n=429)

**Table 7.2** Mann-Whitney analysis between each soil parameter from the combined grassland and shrubland plots (the parameters in blue present significant results).

Soil Parameter	All grassland & shrubland plots	
	Mann-Whitney	
	U	Sign.
Organic matter (%)	225127.0	<0.005
Bulk density (g/cm <sup>3</sup> )	165433.0	<0.005
Soil moisture (%)	247310.5	<0.005
Shear strength (KPa)	234095.0	<0.005
pH	170646.0	<0.005
Conductivity (dS/m)	211230.0	<0.005
Available calcium (ppm of soil)	181064.0	0.598
Available potassium (ppm of soil)	199564.0	<0.005
Available magnesium (ppm of soil)	205843.5	<0.005
Available sodium (ppm of soil)	157119.0	<0.005
Available phosphorus (ppm of soil)	189725.0	0.0618

Statistically, only available calcium and phosphorus display evidence of having no significant differences between the grassland and shrubland plot means. By studying the mean values of the physical properties, soil shear strength exhibits the most significant difference between the means of the two vegetation types, displaying higher means in the grassland landscapes. This may be due to a number of reasons such as soil moisture, texture and the presence of rootmats in the grasslands. Further investigation of the soil moisture demonstrates differences

in the means and thus should be considered when interpreting the shear strength results. Nevertheless, these two parameters also have the highest coefficients of variation, in both vegetation types, indicating that they exhibit greater variability within the plots. Despite this, the majority of soil parameters do not appear to exhibit great differences between the two vegetation types.

Although significant differences between the means are displayed by only three of the soil nutrients, the response of each nutrient may be important to note. Both the mean values of available calcium and sodium are greater in the shrubland plots, whereas the magnesium, potassium and phosphorus mean contents are greater in the grasslands. Although this may potentially be significant in terms of the links between vegetation type and soil erodibility with regards to the relationship between the dispersive behaviour of soil particles and sodium and calcium, the high coefficients of variation suggest this observation should be made with caution.

The coefficients of variation (CoV) provide an overall index of soil parameter variation within each vegetation community. Of the parameters that display a shrubland CoV value greater than a difference of 10% of the grassland CoV, only shear strength and available phosphorus show more variation in the shrubland plots. Thus, in general, the results suggest that the grassland plots exhibit more variation than the shrubland plots. As shrubland landscapes are considered to be more heterogeneous in nature (Schlesinger *et al.*, 1990; 1996, Tongway and Ludwig, 1994) it would be expected that less variation would be evident in grassland plots, contrary to what the results demonstrate. Despite this, analysis of the CoV results of soil nutrients from three sites across the American Southwest show that this result is not unusual (Schlesinger *et al.*, 1996). These results showed that, out of the nutrients that were measured in this study, only phosphate (as an indicator of phosphorus) and sodium varied more in the shrubland plots.

The higher variability evident in the grassland plots could be attributed to two main factors. Firstly, the results of four individual plots have been amalgamated to produce a single grassland dataset. Thus, large-scale spatial differences may be responsible for an increase in parameter variation. Secondly, although grasslands are generally considered to have a more uniform vegetation cover than shrublands (de Soyza *et al.*, 1998), grassland 'patchiness' is a common feature in semi-arid landscapes (Cerdà, 1997; Blomqvist *et al.*, 2000). This 'patchiness' can vary in size, from small mosaics created as a result of grass tussocks to areas a couple of metres across; the cause of such patches is greatly debated but often attributed to overgrazing and climatic factors (Cerdà, 1997). However, grazing cannot be attributed as the cause of grassland 'patches' in the Sevilleta NWR as this site has not been grazed in over 100 years.

Maestre and Cortina (2002) demonstrated that the soil properties of these bare mosaics vary from the soil under their surrounding grass community. Differences in surface crusting and stone contents were identified suggesting bulk density and infiltration characteristics will also vary between the grass cover and patches. Evidence from Puigdefabregas and Sanchez, (1996) and Bochet *et al.*, (1999) also support this view. Thus, the high variability exhibited by the soil parameters from the grassland plots can be partially attributed to the presence of bare mosaics, which are present in both the Karoo and Sevilleta NWR.

As previously mentioned, discounting shear strength and soil moisture, the mean values do not appear to vary greatly between the grass and shrub plots, despite a relatively large amount of within-plot variation displayed by some of the soil parameters, particularly calcium and sodium (grassland only). The mean values indicate that the transition from a grassland to shrubland vegetation community does not necessarily lead to an increase or decrease in a landscape's total quantity of soil resources. However, the statistical comparisons suggest that significant differences do exist between the distributions of most parameters from the two vegetation types.

This indicates that further analysis is needed to identify firstly, whether the distributions of soil resources are different in the two vegetation communities and, if so, secondly, to explain why they are different.

### **7.1.2 Soil heterogeneity and vegetation type: changing spatial patterns or changing scale?**

The geostatistical analysis provides evidence to support the idea that a redistribution of soil parameters occurs concurrently with a grass to shrub vegetation change. Table 7.3 provides the minimum and maximum ranges derived from all the grass and shrub plots. The minimum ranges are the most significant in terms of identifying the influence of the different types of vegetation. In all cases, apart from bulk density, the minimum ranges are less in the shrubland plots. Discounting the properties that display the 'nugget effect' or no spatial patterns as their minimum, only organic matter and bulk density have grassland ranges less than the maximum shrubland range of 7.5m. With the majority of ranges greater than this level it implies that the grassland plots do display relatively homogeneous distributions of most soil parameters.

Although the presence of autocorrelation in grasslands suggests that some spatial patterns are present, the majority of ranges are greater than 10m. This indicates that local landscape variation, such as subtle changes in slope or soil type, may be responsible rather than the autocorrelation being directly related to vegetation. However, the presence of 'patches' mentioned in section 7.1.1 may be a more likely explanation for the development of areas of spatially autocorrelated parameters. The majority of properties do not present maximum ranges per se, but present datasets best represented by a pure nugget model. This implies that these properties can be described as having no spatial patterns and are thus relatively homogenous in nature.

**Table 7.3** Minimum and maximum ranges of spatial autocorrelation derived from semi-variograms of soil parameters from grassland and shrubland plots.

Soil Parameter	Grasslands		Shrublands	
	Minimum Range (m)	Maximum Range (m)	Minimum Range (m)	Maximum Range (m)
Organic matter (%)	5.98	Nugget	4.5	Nugget
Bulk density (g/cm <sup>3</sup> )	6.6	11.55	6.82	Nugget
Soil moisture (%)	10.73	25.11	6.6	15.84
Shear strength (KPa)	8.51	Nugget	4.2	Expo*
Clay content (%)	Nugget	Nugget	*	*
Sand & Silt content (%)	Nugget	Nugget	*	*
pH	16.56	Nugget	5.89	15.54
Conductivity (dS/m)	19.47	Nugget	5.27	Nugget
Available calcium (ppm of soil)	10.5	Nugget	6.6	Nugget
Available potassium (ppm of soil)	12.58	Nugget	7.5	Nugget
Available magnesium (ppm of soil)	12.95	Nugget	5.58	Expo*
Available sodium (ppm of soil)	Nugget	Nugget	Nugget	Nugget
Available phosphorus (ppm of soil)	19.61	Nugget	5.27	Nugget

Expo\*: the dataset increases exponentially, no sill is reached and therefore no range exists.

The minimum ranges of spatial autocorrelation displayed by the organic matter content and bulk density from the grasslands are comparable with those derived from the shrublands. This is particularly surprising for the organic matter content as this parameter is controlled by the presence/absence of vegetation. Kelly *et al.*, (1996) found that a reduced root biomass accounted for up to 90% of variation in soil organic matter content, therefore, as a consequence of a more uniform cover and rootmat, greater ranges would be expected in the grassland plots.

However, the minimum organic matter range reported is perhaps not a true representation of pure grasslands as this value was derived from a plot that would be more accurately described as a mixed vegetation plot. Although the dominant vegetation of this plot was grassland, the influence of the shrubs within it may be responsible for the shorter range of spatial autocorrelation. Although the individual plot results will be discussed in the next section, if the mixed plot result is excluded the minimum range of organic matter in the grasslands is 14.06m. This value is more consistent with the results of the other soil parameters in the grassland landscapes.

The minimum range of autocorrelation derived for bulk density from the grasslands cannot be attributed to the influence of mixed vegetation as this was recorded from a pure grassland landscape. This suggests that, as with the majority of soil parameters, the bulk density distribution of soil in grasslands is sensitive to bare patches in the plot.

No minimum ranges were derived for the grassland particle size distribution or available sodium content. These parameters are best represented by a pure nugget model which indicates random behaviour. It can therefore be concluded that the distributions of these parameters are relatively homogenous in grassland landscapes.

In contrast to the minimum grassland autocorrelation results, which range from 5.98m to 19.61m, the minimum ranges from the shrublands vary from 4.2m to 7.5m (disregarding the nugget effect displayed by sodium). The differences in these results suggest that a significant redistribution of soil resources accompanies shrub invasion. Schlesinger *et al.*, (1996) found that ranges of spatial autocorrelation of essential plants nutrients coincided with the mean diameter of individual shrubs. However, the ranges presented by Schlesinger *et al.*, are in general, smaller than those calculated in this study. It is therefore proposed that the ranges of autocorrelation presented in this study, which were measured at a coarser scale than that of Schlesinger *et al.*, represent the intershrub areas as opposed to the self-perpetuating shrub units.

Despite the minimum ranges indicating that shrubland soil parameters display smaller-scale spatial autocorrelation than grassland soil parameters, the maximum ranges derived from the shrublands are similar to those presented by the grassland datasets. This is a result of a pure nugget model being applied to the majority of parameters. Although this would normally indicate that some shrubland plots are exhibiting no spatial patterns of selected soil parameters, this is not necessarily true for the shrubland data. The nugget model was applied to datasets

that could not be modelled by the simple models available in VARIOWIN 2.2, i.e. spherical, Gaussian, exponential or power models. However, all parameters produced at least one semi-variogram that displayed cyclic behaviour. Despite the pure nugget model being the best fit, the periodicity in the data suggests that a more complex system of soil resource redistribution is in place hence more complex spatial models are needed to accurately explain this type of distribution. More complex functions are created by combining two or more simple models (Webster and Oliver, 2001). However, in this study the fitting of more than one structure to the experimental data was avoided as it complicated the subsequent comparisons with other modelled semi-variograms. In addition, as no further analysis would be carried out using this data, e.g. interpolation techniques, it was deemed unnecessary to fit a model to this type of experimental variogram. Instead, the periodicity evident in the experimental variograms was considered to be adequate for determining the spatial patterns within the plots.

Although the periodicity present in individual plots will be discussed in section 7.2, out of a total of 46 semi-variograms, the grassland plots displayed evidence of cyclic behaviour in 11, whereas out of a total of 44, the shrubland semi-variograms exhibited periodicity in 24. In addition, whilst periodicity is evident to some degree in all the shrubland soil parameters, obvious periodicity is confined to particle size, pH, available sodium and available phosphorus in the grasslands. This may suggest that these parameters are more sensitive to the presence/absence of vegetation cover and thus influenced more by 'patchiness' in the grassland landscape than the other soil parameters.

However, it should be noted that the 'hole effect' is evident in many of the grassland datasets, particularly bulk density, shear strength and available calcium. This presents itself as a decrease in variance then an increase towards the sill, thus producing a 'hole' in the variogram (Webster and Oliver, 2001). The presence of 'holes' in the grassland datasets have largely been ignored for modelling purposes but with regards to characterising the spatial patterns within grassland landscapes, these should be acknowledged as they also can be

attributed to the presence of bare patches within the grass community, although it suggests fewer patches are present than when periodicity is displayed.

Although the grassland soil parameters that display periodicity may be more sensitive to the presence/absence of vegetation, it may be true that the parameters identified as displaying the most prominent 'hole effects' could be linked to an increase in erodibility of the bare patches and thus the potential degradation of grasslands. Bulk density, shear strength and available calcium all show evidence of 'holes' in the datasets and all are considered significant in determining the susceptibility of soil to erosion. The identification of patches using these parameters may therefore be significant in determining potential 'hotspots' of erosion-sensitive areas in grasslands. The influence of the spatial distribution of individual soil properties on the erodibility of soil will be discussed further in chapter 8.

### **Scale & periodicity**

A fundamental change in the way in which the spatial patterns of soil properties in grasslands and shrublands were viewed occurred in the early to mid 1990's. As a result of the work on fine-scale patterns of soil nitrogen in semi-arid grasslands by Hook *et al.*, (1991), Schlesinger *et al.*, (1996) proposed that contrary to the suggestion that soil heterogeneity develops concurrently with shrub encroachment (Tongway and Ludwig, 1994), the patterns evident in shrublands may be a consequence of an *increase* in soil heterogeneity and thus a function of scale. This idea was investigated by Schlesinger *et al.*, (1996) who found that in the Chihuahuan Desert of New Mexico, 35-76% of soil nitrogen variation in the grasslands was found at distances less than 20cm, and thus associated with the tussock size of *Bouteloua eriopoda*. In contrast, the shrublands displayed higher nitrogen concentrations over distances of 1-3m. These values were associated with the mean shrub sizes and therefore attributed to the nutrient cycling of individual shrubs.

The results derived by Schlesinger *et al.*, (1996) provide strong evidence that fine-scale heterogeneity of nutrients is present in grassland plots, hence spatial scale is important when considering the changes that accompany shrub encroachment. In contrast, although the physical properties of semi-arid soil have been studied with respect to grass tussocks and the influence of their canopy cover (e.g. Cerdà, 1997; Bochet *et al.*, 1999), few have studied the fine-scale spatial patterns. However, it can be hypothesised that a similar redistribution to that of the chemical properties will occur due to the relationships that exist between vegetation and soil.

There is little doubt that fine-scale heterogeneity is present in grasslands and amplified heterogeneity is present in shrubland landscapes. However, as scale can be considered a key factor, this research focuses on the spatial characteristics at scales relevant to the grass and shrub communities as a whole, considering them as important as the spatial patterns at an individual plant level. An understanding of the patterns and processes at these coarser scales are particularly important for modelling purposes and will be discussed further in chapter 8.

The results of the spatial analysis, shown in table 7.3, imply that scale of measurement is indeed a significant consideration when determining the spatial patterns of soil parameters. The ranges of spatial autocorrelation derived for the grassland parameters vary for 5.98m to 19.61m and out of 46 semi-variograms, 17 suggest that no spatial patterns exist. These measurements were taken from a 60 x 60m plot and calculated using a maximum lag distance of 30m and a minimum scale of measurement of 0.5m. As previously discussed, the results from this study suggest that, at a scale more representative of a grassland community, the spatial distribution of most soil parameters can be classed as being relatively homogenous. However, these results differ significantly from those presented by Schlesinger *et al.*, (1996) who derived their results from 8 x 12m plots and calculated the semi-variograms using a maximum lag distance of 7m. A comparison of the ranges of autocorrelation of grassland and shrubland nutrients

derived from this study and Schlesinger *et al.* is provided, see tables 7.4 and table 7.5 respectively. It is obvious from these results that scale of measurement strongly influences the derived ranges of spatial autocorrelation in grassland environments and to a lesser degree, shrublands.

**Table 7.4** A comparison of the spatial autocorrelation values (in meters) of nutrients in semi-arid grasslands.

Ranges of spatial autocorrelation for grassland plots						
Nutrient					Sevilleta	Jornada Basin
	Plot 1: Karoo	Plot 2: Karoo	Plot 8: Sevilleta	Plot 10: Sevilleta	(Schlesinger et al., 1996)	(two sites) (Schlesinger et al., 1996)
Ca	na	10.5	na	19.84	1.40	0.72, 1.26
K	na	na	12.58	16.74	1.21	1.37, 1.25
Mg	16.12	na	12.95	na	3.29	1.10, 1.89
Na	na	na	na	na	6.05	1.16, 3.19
P	na	19.61	na	na	na *	2.42, 0.48 *

\* Measurements of PO<sub>4</sub>

na: random variance i.e. no spatial patterns evident.

**Table 7.5** A comparison of the spatial autocorrelation values (in meters) of nutrients in semi-arid grasslands.

Ranges of spatial autocorrelation for shrubland plots						
Nutrient					Sevilleta	Jornada Basin
	Plot 3: Karoo	Plot 5: Karoo	Plot 9: Sevilleta	Plot 11: Sevilleta	(Schlesinger et al., 1996)	(two sites) (Schlesinger et al., 1996)
Ca	nd	na	6.60	na	>7.00	1.22, >7.00
K	na	31.44	7.5	8.06	na	2.13, 2.49
Mg	21.43	8.68	nd**	5.58	1.49	1.14, 2.22
Na	na	nd	nd	na	0.46	na, >7.00
P	8.37	5.27	8.40	na	1.25*	>7.00, 3.49*

\* Measurements of PO<sub>4</sub>

\*\* No range but modelled with a power function

na: random variance i.e. no spatial patterns evident.

nd: not determined

In contrast to the results presented by Schlesinger *et al.*, (1996), the ranges of autocorrelation presented in table 7.3 and 7.5 are too big to be associated with individual grass clumps and the biotic processes linked to them. Instead, the spatial analysis demonstrates that most parameters appear to be sensitive to bare patches resulting in areas where parameters are spatially related.

The impact of scale on the spatial patterns of soil parameters in shrubland landscapes presents itself through the presence of periodicity in the datasets. The study by Schlesinger *et al.*, (1996) attributed the ranges of autocorrelation of essential plant nutrients to the mean shrub size indicating that biotic factors are responsible for the redistribution. In contrast, the ranges of autocorrelation in this study are more likely to be representative of the intershrub zones as values between 4.2m – 7.5m are larger than the average shrubs in the study regions. However, beyond this distance over half the semi-variograms show sinusoidal behaviour. Upon inspection of the semi-variograms derived from shrublands in the study by Schlesinger *et al.*, (1996) some evidence of the 'hole effect' is present in the datasets. This possibly indicates that periodicity would be present if the scale of measurement was increased.

Although there has been some debate over the interpretation of cyclic patterns in ecological datasets, a study by Radeloff *et al.*, (2000) investigated the relationship between periodicity and landscape patches. A number of significant observations were made i) periodic spatial patterns produced periodicity in correlograms ii) the lag distances at which the correlograms peak correspond to the average distances between patch centres iii) the strength of periodicity increases when the diameter of patches is equal to the distance between patch edges. Although the nature and significance of the periodicity displayed by each variogram will be discussed in more detail in section 7.2, it can be concluded that where periodicity in the shrubland data is evident, there is regular variation in the parameter values across the landscape. This is indicative of the differences between the soil parameters in shrub and intershrub zones.

The significance of periodicity has largely been ignored in studies of spatial patterns in landscapes. The importance of this type of pattern is highlighted by Bruckner *et al.*, (1999) who, through the interpretation of sinoidal periodicity in variograms, attributed a mesoscale pattern of soil properties to the influence of tree distribution in a temperate coniferous forest. Although a better understanding of periodicity in datasets is needed, there is potential for the application of this

pattern to assist in the identification of 'sensitive' land. However, Radeloff *et al.*, (2000) also highlight that caution is needed when interpreting the periodicity of variograms, particularly omni-directional variograms, as different complex spatial structures can sometimes produce similarly-shaped variograms and thus be misinterpreted.

## **7.2 The global applicability of soil parameter characteristics in semi-arid environments: a comparison between the Karoo, South Africa and the Sevilleta NWR, New Mexico.**

Although section 7.1 discussed the impact of vegetation change on soil characteristics and concluded that although the total mean quantities of soil resources did not change significantly, vegetation change can be associated with a significant redistribution of both physical and chemical properties of soil.

However, these conclusions were based on an amalgamation of results from a number of grassland and shrubland plots and thus does not account for local and global variation amongst the datasets. As mentioned in chapter 2, factors that may influence soil parameter characteristics range from the climatic regime of the area to variations in soil type as a result of the underlying geology. Despite this, it could be argued that these factors also control vegetation, thus, if vegetation change is observed in these areas, similarities in the behaviour of soil parameters must exist amongst different semi-arid environments.

Although the accuracy of this statement has major implications on the global applicability of process-based models, no study comparing the spatial patterns of soil properties from semi-arid regions in different continents has been identified. Therefore, in order to assess whether the conclusions reached in section 7.1 are accurate and globally applicable, this section compares the results derived from the Karoo site, situated in South Africa with the results from the Sevilleta NWR

site, located in New Mexico, U.S. Detailed descriptions of the two study regions are provided in chapter 3.

### 7.2.1 Comparison of soil properties between two semi-arid environments

The individual plot characteristics of each soil parameter from the two study regions are presented in the respective grassland or shrubland results chapters. To provide a summary of these findings, the overall mean values and coefficients of variation of the soil parameters from both vegetation types and both study regions are presented in table 7.6. Table 7.7 indicates the parameters (highlighted in blue) that have been identified as being statistically similar in both study regions by Mann-Whitney analyses.

**Table 7.6** Means and coefficients of variation [(SD ÷ mean) x 100] of all the soil parameters from the grassland and shrubland plots situated in the Karoo, S.A. and the Sevilleta NWR, N.M.

Soil Parameter	Grasslands				Shrublands			
	Karoo		Sevilleta NWR		Karoo		Sevilleta NWR	
	Mean	CoV	Mean	CoV	Mean	CoV	Mean	CoV
Organic matter (%)	3.42*	30.12	2.33*	30.04	2.57**	28.02	1.93*	15.54
Bulk density (g/cm <sup>3</sup> )	1.18*	17.8	1.27*	8.66	1.24**	17.7	1.35*	9.63
Soil moisture (%)	8.24*	55.1	3.39*	51.03	3.01**	60.8	1.58*	50.63
Shear strength (KPa)	24.53*	58.62	13.75*	58.98	14.36**	56.62	5.47*	38.21
Clay content (%)	0.72***	30.56	-	-	-	-	-	-
Silt content (%)	19.79***	36.58	-	-	-	-	-	-
Sand content (%)	79.5***	9.36	-	-	-	-	-	-
pH	6.08*	8.06	8.38*	1.79	6.27**	10.69	8.49*	1.88
Conductivity (dS/m)	0.20*	36.25	0.16*	36.02	0.15**	40	0.15*	33.33
Av. Ca (ppm of soil)	1818.7***	49.06	8641.8 <sup>^</sup>	5.88	2914*	76.97	8570.2 <sup>^</sup>	4.61
Av. K (ppm of soil)	302.34***	32.96	470.7 <sup>^</sup>	44.04	282.15*	42.64	348.28 <sup>^</sup>	17.18
Av. Mg (ppm of soil)	992.4***	38.24	1509.6 <sup>^</sup>	27.05	995.6*	41.21	1093.7 <sup>^</sup>	16.31
Av. Na (ppm of soil)	75.8***	79.97	76.66 <sup>^</sup>	31.18	96.46*	33.95	93.93 <sup>^</sup>	36.62
Av. P (ppm of soil)	38.52***	36.68	40.76 <sup>^</sup>	24.36	31.65*	38.61	44.38 <sup>^</sup>	27.67

(\*n=216, \*\*n=215, \*\*\*n=214, ^ n= 213)

**Table 7.7** Mann-Whitney analysis of each soil parameter from the Karoo grassland and shrubland plots and the Sevilleta NWR grassland and shrubland plots (the parameters in blue present significant results).

Soil Parameter	Karoo grass & shrub		Sevilleta NWR grass & shrubs	
	T-statistic	Sign.	T-statistic	Sign.
Organic matter (%)	60244.0	<0.005	54664.0	<0.005
Bulk density (g/cm <sup>3</sup> )	43378.0	0.0113	38517.0	<0.005
Soil moisture (%)	64162.0	<0.005	63494.0	<0.005
Shear strength (KPa)	57170.0	<0.005	64930.0	<0.005
pH	42031.5	0.0003	35519.5	<0.005
Conductivity (dS/m)	70092.0	<0.005	70092.0	<0.005
Available calcium (ppm of soil)	42491.0	0.0049	46985.0	<b>0.235</b>
Available potassium (ppm of soil)	49427.0	0.0102	53005.0	<0.005
Available magnesium (ppm of soil)	45440.5	<b>0.5998</b>	60643.0	<0.005
Available sodium (ppm of soil)	39473.0	<0.005	40131.0	<0.005
Available phosphorus (ppm of soil)	39932.0	<0.005	41081.0	0.0001

The results presented in tables 7.6 and 7.7 assist in addressing the global significance of the response of soil parameters to a grass-shrub transition.

*Do the soil parameters in the two study regions respond differently to a grassland-shrubland transition?*

From table 7.6 it is evident that the mean contents of three soil parameters are strongly influenced by geographical location. Shear strength, pH and available calcium show consistent variation between the study regions in both the grassland and shrubland plots. These differences have been attributed to the impact of different soil types. Therefore, in order to investigate whether soil type influences the response of soil parameters to a grassland-shrubland transition, comparisons have been made between the grasslands and shrublands from the Karoo and the Sevilleta NWR separately.

Mann-Whitney analysis, shown in table 7.7, demonstrates that only available calcium in the Sevilleta NWR and available magnesium in the Karoo are statistically similar in both the grasslands and shrublands. However, the mean

values indicate that only shear strength varies significantly between vegetation types in both regions. Despite the differences being relatively insignificant, the responses of the physical properties to vegetation change appear to be consistent in both study regions. The organic matter content, soil moisture and shear strength all demonstrate a decrease in mean values from the shrubland plots whereas bulk density increases. In contrast, the chemical properties are less consistent. Although pH and available sodium both demonstrate an increase, and potassium a decrease in the shrublands, the other properties produce conflicting responses from the two study regions.

The similar responses shown by the physical properties demonstrate that the same plant-soil interactions occur in both semi-arid regions albeit at different scales. As discussed in chapter 2, organic matter is a fundamental soil constituent as it controls and interacts with many other soil properties (Tisdall and Oades, 1982), it is therefore unsurprising that as organic matter decreases concurrently with shrub invasion, the bulk density increases. This is just one example of the plant-soil interactions observed, but highlights the complexities of cause and effect and thus makes the interpretation of the effects of vegetation change on soil difficult.

When comparing the grassland and shrubland data, the consistent response of the physical properties from the two study regions implies that a change in vegetation type is responsible for the differences observed. However, due to the inconsistent nature of the chemical properties, vegetation change may be considered less significant when attributing the cause of differences in the means. Perhaps with the exception of available sodium, which has consistently greater values in the shrubland plots, the influence of soil type may be a more important factor in controlling the response of nutrients in different geographical locations, despite the type of vegetation.

### **7.2.2 Spatial patterns: globally applicable or locally attributable?**

In order to analyse the local and global differences in spatial continuity of soil parameters in different semi-arid environments, the ranges of spatial autocorrelation and semi-variogram characteristics for all grassland and shrubland plots are presented in table 7.8 (see end of chapter). The semi-variograms and the detailed results of the spatial analyses can be found in the respective grassland and shrubland results chapters.

The results of the spatial analyses imply that the *changes* in spatial patterns are consistent with the hypothesis that these results are globally applicable in a general sense. Apart from the autocorrelation values of available potassium and shear strength, the study regions do not display characteristic ranges. Despite a relatively high variability, the ranges show more significant differences between the two vegetation types.

Available potassium, on the other hand, demonstrates greater differences between the two study regions than between the vegetation types. The Karoo produced three semi-variograms that were best modelled by a pure nugget model, and one that displayed a range of 31.44m. In contrast, the Sevilleta NWR produced ranges of 12.58m and 16.74m for the grasslands and 7.5m and 8.06m for the shrublands. Shear strength also produced results that imply that the spatial patterns appear to be influenced by locational differences as well as vegetation type. The Karoo grasslands produced ranges significantly less than the Sevilleta NWR and the Sevilleta NWR shrublands produced ranges of autocorrelation whereas no results were derived for the Karoo.

Although many of the parameters appear to show no evidence of spatial autocorrelation, semi-variograms that demonstrate evidence of periodicity have been highlighted in table 7.6. These parameters do in fact show some evidence of

spatial patterns in the landscape and, as discussed in section 7.1, are likely to represent patches in the grasslands and the intershrub zones in the shrublands.

The periodicity evident in the grasslands appears to be related to the soil parameter rather than geographical location. Soil pH and available sodium demonstrate periodicity in both the Karoo plots and the Sevilleta NWR plots, this suggests that these parameters may be a) more sensitive to the presence/absence of grass or b) sensitive to local variation in soil type. However, as both parameters have semi-variograms that show some evidence of a decrease in variance with an increase in lag distance, the former statement may be more likely as this variogram behaviour indicates that a checkerboard pattern may exist. This could be associated with the tussocky nature of grass in semi-arid environments.

In general, more periodicity is evident in the shrubland plots. The implications of this have been discussed in section 7.1; however, the global applicability of this 'cyclic' characteristic may not be appropriate. Although the Sevilleta NWR plots show similarities in the periodic responses of soil parameters, the Karoo plots display fewer accounts of periodic behaviour, particularly plot 5. The reason for this is likely to be linked to the specific species of shrub and the general shrubland community characteristics. In the Sevilleta NWR, creosotebush is the predominant shrub. Other species are few in number resulting in distinct shrub and intershrub zones. In the Karoo, in contrast, a number of karroid *Merxmullera* mountain veldt species are dominant (Keay-Bright and Boardman, 2006) and grass is often interspersed throughout the landscape. As a consequence, less defined intershrub areas are evident and thus this provides a likely explanation for the weaker periodicity evident in the variograms.

The results from this section suggest that the conclusions reached in section 7.1.2 concerning the differences in spatial patterns evident in grasslands and shrublands are relatively accurate. The spatial structures of the soil properties in the

grasslands of both study regions are similar. The majority of derived ranges of autocorrelation are greater than 8m and approximately half of all the semi-variograms in both study regions showed no evidence of distinct spatial patterns. Although there is some variation amongst the derived ranges of spatial autocorrelation between the two study regions, this is also evident within the study regions thus implying that local patches in the grassland structure are likely to influence the results. However, it can be concluded that the spatial patterns of soil properties in grasslands in semi-arid regions can be classed as being characteristically homogenous.

In terms of the shrublands, the global applicability is harder to determine as direct comparisons are more difficult due to the complex structures displayed in the variograms. However, of the ranges of autocorrelation that were derived, the majority are less than 10m in both study regions. The global applicability of the spatial patterns in shrublands is more evident from the physical properties of soil as cyclic behaviour is displayed in both the Karoo and the Sevilleta NWR sites. The chemical properties show more spatial similarities within each of the study regions with the exception of phosphorus and magnesium. This suggests that abiotic factors such as soil type may be significant in controlling the spatial patterns of non-plant limiting nutrients. The spatial behaviour of phosphorus, however, is similar in both sites and as an essential plant nutrient, can be used as a relatively reliable indicator that the influence of vegetation on plant-limiting nutrients is applicable to both study regions.

However, the key to determining whether the changes in soil properties which accompany grass-shrub transitions are globally applicable lie in the *response* of the spatial patterns in each of the study regions. Despite the difficulty in comparing the ranges of spatial autocorrelation due to the number of shrubland variograms that were best represented by nugget models but displayed evidence of periodicity, the general patterns can be considered as being similar. Apart from conductivity, available calcium and available sodium content, the responses of the soil parameters to a grass-shrub transition in both regions can be characterised by

either a decrease in range of spatial autocorrelation and/or the development of periodicity. This indicates that semi-arid grassland to shrubland transitions can be associated with an increase in soil parameter heterogeneity. However, the different responses evident for the three chemical properties suggest that local abiotic factors are more significant in controlling the spatial patterns of these properties compared to vegetation.

The results therefore show that a redistribution of physical soil parameters and some chemical parameters can be classed as a characteristic process which accompanies grassland to shrubland transitions in semi-arid environments. However, it is acknowledged that the data is necessarily limited and thus, in the future, more study regions should be investigated to support these findings.

### **7.3 Badlands – a progressive evolution?**

As discussed in chapter 2, shrub encroachment is often considered a form of land degradation. However, geomorphological studies generally focus on the impact different vegetation structures have on the hydrological response of a landscape (e.g. Abrahams *et al.*, 1995; Parsons *et al.*, 1996; Wainwright *et al.*, 2000; 2002), rather than how the autogenic response of plants may influence the susceptibility of soil to erosion.

Although some shrubland landscapes are considered as being relatively stable (Westoby *et al.*, 1989), as the Sevilleta NWR shrublands appear to be, it is proposed that if the right conditions exist, shrublands may degrade further to produce badland landscapes such as those observed in the Karoo. This progressive degradation is highlighted by the conceptual model of arid rangeland degradation developed by Milton *et al.*, (1994). This model describes arid degradation as 'a stepwise process'. Although the model focuses on changing

agricultural practices and their effect on land productivity, it is largely based on vegetation change leading to 'desertified patches' and ultimately 'a human-made desert'.

The following discussion aims to determine whether badland development is an extension of the changes to soil properties that occur in the grassland to shrubland transition. Firstly, the mean values will be compared to those of the Karoo grassland and shrublands in order to identify any significant changes or similarities, secondly, the spatial patterns of the soil properties will be compared to those of the shrublands. If further heterogeneity is identified the response of each parameter will be investigated to assess the progressive nature of soil parameter redistribution.

### **7.3.1 Badlands - a fair description? Characterising the soil properties in badlands and assessing the progressive nature of badland development**

The results presented in chapter 6 indicate that the distribution characteristics of the three badland plots located in the Karoo, South Africa do not vary significantly, thus the combined mean values of the soil parameters from the three badland plots are presented in table 7.9. This table presents the changes in mean values associated with the 'stepwise progression' of land degradation in the semi-arid Karoo. All parameters demonstrating a consistent increase or decrease in mean value are displayed in bold, if the change is an increase in mean value, the parameter is highlighted in blue.

Discounting the particle size data, all parameters but shear strength and available calcium show a consistent change in mean content through the transition of the three vegetation stages. This would initially suggest that badland development can be classed as part of the progressive process of land degradation induced by vegetation change.

Interestingly, for the two parameters that did not conform to this progressive change valid reasons can be put forward for their differing responses. The highest mean shear strength value is found in the badlands, nevertheless, table 7.10 indicates that, statistically, the grasslands display a similar mean value. Despite this similarity in value, the reasons for the higher shear strength in these two landscapes are different. In the grasslands, vegetation type controls the shear strength. The relatively uniform vegetation cover and the influence of rootmats improve the strength and stability of the soil. In contrast, it is the lack of vegetation that causes the higher shear strength values in badlands due to higher bulk densities, lower soil moisture and lower organic matter contents which combine to produce very compact soils. However, the shear strength values were measured in dry conditions. If the measurements had been taken under saturated conditions it is likely that the shear strength values of the badlands would be very low, in contrast to the results from this study. This type of measurement would represent the conditions under which soil detachment occurs and therefore reflect the increased susceptibility of soil to erosion expected to be seen in badland landscapes more accurately. Future studies dealing specifically with soil erosion should use the latter method of shear strength measurement.

The shrublands display a mean shear strength value that is significantly less than the other two communities. This suggests that a threshold value must exist that determines whether the presence or absence of vegetation is more significant in controlling the shear strength of soil. Despite the higher shear strength value in the badlands, it should also be noted that the coefficient of variation is also highest in this landscape. This indicates that the variability of shear strength values is greater in the badlands.

Available calcium, the other parameter that does not respond in a consistent manner, demonstrates mean values from the shrublands and badlands that are considered statistically similar (see table 7.10). The grassland plots, however, have a lower mean content. As concluded in section 7.2, the calcium content may be attributable to the underlying soil type and thus less significantly influenced by

the processes involved in vegetation change. Due to the similarities in location of the shrubland and badland sites the soil type would also be expected to be similar. The grassland plots, on the other hand, were located a significant distance from these communities and thus may be displaying calcium contents controlled by local variations in soil type.

**Table 7.9** Means and coefficients of variation  $[(SD \div \text{mean}) \times 100]$  of all the soil parameters from the combined grassland, shrubland and badlands plots in the Karoo.

Soil Parameter	Karoo: Grass		Karoo: Shrub		Karoo: Badlands	
	Mean	CoV	Mean	CoV	Mean	CoV
Organic matter (%) *	3.42	30.12	2.57	28.02	2.44	18.44
Bulk density (g/cm <sup>3</sup> ) *	1.18	17.8	1.24	17.7	1.3	10.77
Soil moisture (%) *	8.24	55.1	3.01	60.8	2.22	39.64
Shear strength (KPa) *	24.53	58.62	14.36	56.62	26.97	70.71
Clay content (%) **	0.72	30.56	*	*	0.47	40.43
Silt content (%) **	19.79	36.58	*	*	8.1	41.98
Sand content (%) **	79.5	9.36	*	*	91.43	3.89
pH *	6.08	8.06	6.27	10.69	6.89	7.69
Conductivity (dS/m) *	0.20	36.25	0.15	40	0.14	65.81
Available calcium (ppm of soil) ***	1818.7	49.06	2914	76.97	2434.5	40.08
Available potassium (ppm of soil) ***	302.34	32.96	282.15	42.64	199.71	39.67
Available magnesium (ppm of soil) ***	992.4	38.24	995.6	41.21	2043.4	29.36
Available sodium (ppm of soil) ***	75.8	79.97	96.46	33.95	103.63	92.38
Available phosphorus (ppm of soil) ***	38.52	36.68	31.65	38.61	16.96	67.51

\*(Grass n= 432, Shrub n=431) \*\*(Grass/Badland n=104) \*\*\*(Grass n= 427, Shrub n=429)  
All badlands n= 322)

**Table 7.10** Mann-Whitney analysis between each soil parameter from the combined grassland, shrubland and badland plots (the parameters in blue present significant results).

Soil Parameter	Karoo grass & badlands		Karoo shrub & badlands	
	U	Sign.	U	Sign.
Organic matter (%)	82923.0	<0.005	<b>59490.0</b>	<b>0.3477</b>
Bulk density (g/cm <sup>3</sup> )	47114.0	<0.005	52358.0	0.002
Soil moisture (%)	90964.0	<0.005	64120.0	0.001
Shear strength (KPa)	<b>58361.0</b>	<b>0.97</b>	45793.5	<0.005
Clay content (%)	7420.0	<0.005	*	*
Silt content (%)	6036.0	<0.005	*	*
Sand content (%)	15669.5	<0.005	*	*
pH	32625.0	<0.005	41290.0	<0.005
Conductivity (dS/m)	77181.0	<0.005	23436.0	<0.005
Available calcium (ppm of soil)	44887.0	<0.005	<b>58969.0</b>	<b>0.6686</b>
Available potassium (ppm of soil)	79495.0	<0.005	74005.0	<0.005
Available magnesium (ppm of soil)	26910.0	<0.005	27035.0	<0.005
Available sodium (ppm of soil)	47649.0	<0.005	<b>57619.0</b>	<b>0.7375</b>
Available phosphorus (ppm of soil)	84691.0	<0.005	63598.5	<0.005

Although the statistical analyses implies that the organic matter contents and available sodium contents are also similar in the shrubland and badlands plots, the response of organic matter content is the most surprising. As sodium is not an essential plant nutrient, differences in the mean contents between the two types of landscape were not expected, organic matter in contrast, is dependent on the presence of vegetation (Kelly *et al.*, 1996). It would therefore be expected that significantly less organic matter would be present in the badlands.

However, some aspects of the soil chemistry demonstrate a change concurrent with the presence of badlands. Available magnesium, potassium, phosphorus and soil pH all demonstrate a significant change. Soil pH and magnesium show an increase in the badlands whereas potassium and phosphorus decrease. The decrease in phosphorus is consistent with loss of fine particles and potassium can possibly be linked to the low clay content, soil moisture and organic matter content of the badlands (Fixen and Grove, 1990; Haby *et al.*, 1990). High magnesium levels, in contrast, have been found to be a characteristic of many arid and semi-arid regions (Haby *et al.*, 1990). However, these interactions will be discussed further in chapter 8.

Statistical analysis of the particle size data also suggests significant differences exist between the grassland and badland sites. However, due to the lack of datasets, the impact of vegetation change on changes of particle size distribution is difficult to determine. A review of the literature provided a number of grassland and shrubland datasets derived from various sites in New Mexico, a summary is found in table 7.11. Comparisons made from these datasets suggest that the response of particle size to vegetation transitions is highly variable. Although not directly comparable, the results derived from this study show that the responses of particle size in grassland and badland environments in the Karoo behave in the opposite manner to the responses of particle size in grasslands and shrublands recorded by Schlesinger *et al.*, (2000), but they did respond in a similar fashion to those derived by Müller (Unpublished thesis). Notwithstanding the lack of comparable badland data, the disparities in the results between grass – shrub transitions suggest that particle size cannot necessarily be used as evidence that badland landscapes are a continuation of the development of soil parameter heterogeneity caused by shrubland invasion.

**Table 7.11** Summary of particle sizes derived from grassland and shrubland environments in New Mexico. Where second values are given this indicate inter-vegetation areas apart from Müller where this indicates a second fieldsite.

	Kieft <i>et al.</i> , 1998		Schlesinger <i>et al.</i> , 2000		Neave & Rayburg, 2006		Müller (Unpub thesis)	
	Grass	Shrub	Grass	Shrub	Grass	Shrub	Grass	Shrub
Sand	68, 68	64, 55	89	79	78	87, 71	9	40, 67*
Silt	22, 22	26, 32	7	11	10	8, 22	65	26, 12*
Clay	9, 9	8, 11	4	10	12	5, 7	25	7, 4*

Although the results from this study reflect that further erosion in badland landscapes preferentially removes finer particles, the influence of possible differences in soil type between the grassland and badland sites cannot be ruled out without further analysis.

### 7.3.2 Identifying spatial patterns of soil properties in badlands and assessing the shrubland-badland connectivity

No evidence of the use of geostatistics in determining the spatial patterns of soil parameters in badland landscapes has been found. The semi-variograms and the detailed results can be found in chapter 6, however, the ranges and semi-variogram characteristics are summarised in table 7.12.

As Radeloff *et al.*, (2000) provide a detailed discussion on the interpretation of spatial patterns, periodicity and the implications of stationarity in ecological datasets, this will not be discussed here.

**Table 7.12** Ranges of spatial autocorrelation (in meters) derived from semi-variograms for all shrubland and badland plots in the Karoo.

Soil Parameter	Karoo Shrublands		Karoo Badlands		
	Ranges of spatial autocorrelations				
	Plot 3	Plot 5	Plot 4	Plot 6	Plot 7
Organic matter (%)	4.5*	Nugget	na*	7.2	7.48
Bulk density (g/cm <sup>3</sup> )	Nugget	6.82	na*	na	na*
Soil moisture (%)	6.6	15.84	na	na	na
Shear strength (KPa)	na	Expo	16.62	Nugget	14.03
Clay content (%)	*	*	-	na	-
Sand & Silt content (%)	*	*	-	na	-
pH	15.54	5.89	na	na	na
Conductivity (dS/m)	Nugget	Nugget	na	na*	8.54
Available calcium (ppm of soil)	na	Nugget	na	4.8	27.45
Available potassium (ppm of soil)	Nugget*	31.44	na*	na	na
Available magnesium (ppm of soil)	21.43	8.68	28.2	7.2	32.64
Available sodium (ppm of soil)	Nugget	na*	na	na*	na*
Available phosphorus (ppm of soil)	8.37	5.27	na	na	na

Values highlighted in blue exhibit periodicity in their semi-variograms

\* Semi-variogram displays a decrease in variance with an increase in lag distance

The results show that out of a total of 35 badland semi-variograms, only 10 display evidence of spatial autocorrelation. These are: organic matter content, shear strength, conductivity, available calcium and available magnesium.

An examination of the ranges shows that there are no obvious relationships between the ranges from the shrublands and badlands. In addition, a comparison of the results from the three individual plots indicates that, in most cases, the responses seem to be site specific.

The upper ranges of mean available calcium and magnesium are c. 30m. These distances imply that variation in local soil type is, again, the most likely dominant factor in controlling the spatial patterns of these properties. However, both these parameters have minimum ranges of 4.8m and 7.2m, respectively. Apart from shear strength, these values are similar to the ranges of the other properties that display evidence of spatial autocorrelation. These ranges suggest that the parameters may in fact be subject to spatial reorganisation that is consistent with the presence of rills and gullies, and thus represent the interfluvial areas.

One of the problems associated with the geostatistical analyses implemented in this study is that due to the complex nature of the spatial structures, particularly evident in the badland datasets, it was impossible to describe accurately the spatial patterns using the simple models available. However, in these cases the general shape of the semi-variogram was interpreted, providing an indication of the spatial characteristics of each parameter.

Over 80% of the semi-variograms displayed some evidence of periodicity. As Radeloff *et al.*, (2000) found that the lag distances at which correlograms or variograms peak correspond to the average distances between patch centres, the wavelengths of the different parameters were analysed to identify the likely cause of the periodicity. A number of observations were made:

- i) An average wavelength of c. 8m was found for a number of parameters; organic matter, bulk density, conductivity, available magnesium, available sodium and available phosphorus. Despite some plot

variation, this is a relatively consistent result that may be significant in characterising the spatial patterns of parameters in badlands.

- ii) The impact of scale may be significant due to the differences in wavelengths observed between plot 6, which had a maximum lag distance of 30m and plots 4 and 7, which had maximum lag distances of 60m. Finer-scale periodicity was demonstrated in plot 6 for soil moisture, shear strength, available calcium and available magnesium.
- iii) In all three plots water content, available sodium, available calcium and available magnesium follow similar cyclic patterns as does pH and conductivity.

Although the complex nature of soil interactions makes the interpretation of the periodicity relatively difficult, the results suggest that a further redistribution of soil parameters occurs in badland landscapes. Some parameters exhibit similar patterns of variation thus indicating that the mechanism of redistribution could potentially be linked to the presence of vegetation, which is only found on the badland 'peaks' or interfluvial areas. However, the scale of measurement may be an important factor when determining the spatial patterns of some parameters.

As Radeloff *et al.*, (2000) state that the peaks are related to the centre of the patches, a wavelength of approximately 8m could potentially be related to the undulating nature of the badland landscape and thus be associated with gully frequency. As no data on gully frequency is available for this study this hypothesis should be investigated in future studies. However, due to the complex relationship between vegetation, badland development and the hydrological response, the influence of the individual parameters is difficult to determine. In addition, some semi-variograms (see table 7.10) display evidence of a decrease in variance with an increasing lag distance, this suggests more complex patterns are evident in the badlands. Although initially this was thought to be related to a checkerboard pattern, the cyclic patterns revealed by the other plots for the same parameters suggest that the downward trends evident in the badland data are, in fact, displaying partial periodicity and thus are a function of scale.

Although no characteristic relationships can be identified between the ranges of spatial autocorrelation from the shrublands and badlands, the significant increase in parameters displaying evidence of cyclic patterns in the badlands show that progressive heterogeneity occurs concurrently with the development of these landscapes. A common wavelength of c. 8m is evident in approximately half of all soil parameters, these patterns are most likely reflecting the gullied nature of the landscape, representing the differences between gully floors and interfluvial areas.

As finer-scale periodicity was demonstrated in plot 6 for soil moisture, shear strength, available calcium and available magnesium, and some larger scale patterns also appear to be evident in plots 4 and 7, this suggests that spatial patterns in badlands appear to occur on a number of spatial scales. Again, this would imply that the distribution of soil parameters may be a function of the morphology of the gully network e.g. the frequency or density of the rills.

**Table 7.8** Ranges of spatial autocorrelation (in meters) derived from semi-variograms for all shrubland and grassland plots in the Karoo and the Sevilleleta NWR.

Soil Parameter	Grasslands				Shrublands			
	Karoo		Sevilleleta NWR		Karoo		Sevilleleta NWR	
	Plot 1	Plot 2	Plot 8	Plot 10	Plot 3	Plot 5	Plot 9	Plot 11
Organic matter (%)	5.98	21.09	14.06	Nugget	4.5*	Nugget	Nugget*	Nugget
Bulk density (g/cm <sup>3</sup> )	8.6	11.55	6.6	9.3	Nugget	6.82	Nugget*	Nugget
Soil moisture (%)	16.17	19.47	10.73	25.11	6.6	15.84	9.6	7.44
Shear strength (KPa)	8.51	9.24	17.16	Nugget	na	Expo	4.2	9.61
Clay content (%)	-	Nugget	-	-	-	-	-	-
Sand & Silt content (%)	-	Nugget	-	-	-	-	-	-
pH	Nugget	Nugget	Nugget*	16.56	15.54	5.89	na*	na
Conductivity (dS/m)	Nugget	19.47	Nugget	Nugget	Nugget	Nugget	8.1	5.27
Available calcium (ppm of soil)	Nugget	10.5	Nugget	19.84	na	Nugget	6.6	Nugget
Available potassium (ppm of soil)	Nugget	Nugget	12.58	16.74	Nugget*	31.44	7.5	8.06
Available magnesium (ppm of soil)	16.12	Nugget*	12.95	Nugget	21.43	8.68	Expo	5.58
Available sodium (ppm of soil)	Nugget*	Nugget*	Nugget*	Nugget	Nugget	na*	na*	Nugget
Available phosphorus (ppm of soil)	Nugget	19.61	Nugget	Nugget	8.37	5.27	8.4	Nugget

Values highlighted in blue exhibit periodicity in their semi-variograms

\* Semi-variogram displays a decrease in variance with an increase in lag distance

## CHAPTER EIGHT

### Discussion:

#### **2. Linking vegetation change and erosion: physical and chemical soil property interactions**

---

##### ***8.1 Vegetation and the susceptibility of soil to erosion***

##### ***8.2 The consequences for modelling***

---

##### ***8.1 Vegetation change and the susceptibility of soil to erosion***

The previous chapter has identified and discussed the evidence that shows that a grassland to shrubland transition is associated with a redistribution of soil parameters. In the Karoo, spatial heterogeneity is then seen to increase further with the development of badlands. In order to understand the link between vegetation change and soil erosion, it is imperative to understand the relationships that exist amongst both physical and chemical properties of soil.

Using the aggregate stability measurements as an initial indicator of the erodibility of soil (Barthès and Roose, 2002), the results suggest that the grassland plots are generally more stable than the shrubland plots. The differences in aggregate stability between the two vegetation types suggest that the erodibility of soil may increase concurrently with shrub encroachment. This reflects the findings of Boix-Fayos *et al.*, (2001) who found that the stability of macroaggregates is positively correlated with organic matter. As a consequence, greater aggregate stability would be expected in grasslands due to the more uniform vegetation cover and thus organic matter production. The Karoo sites were also shown to be significantly more stable than the Sevilleta NWR plots. The difference between

the two study regions reflects the well established fact that soil type is also a significant controlling factor of aggregate stability.

These findings raise two important questions;

- i) Do other soil parameters also indicate that an increase in erodibility can be associated with vegetation change, and therefore, what causes the erodibility of soil to vary with vegetation type?
- ii) How do the changing spatial patterns of soil properties influence the erodibility of the soil?

*Do other soil parameters also indicate that an increase in erodibility can be associated with vegetation change, and therefore, what causes the erodibility of soil to vary with vegetation type?*

Interactions of the physical properties of soil largely determine the structure and hence the erodibility of soil. A general indicator of the soil structure is the shear strength. This parameter combines the effects bulk density, organic matter content and soil moisture and is commonly used as an index of soil erodibility (Torri *et al.*, 1987). Measurements of the shear strength show that the mean values decrease significantly in the shrubland plots compared to the grasslands, however, the means are then observed to rise in the badlands to values comparable with the grasslands.

The reduction in shear strength from the grasslands to the shrublands implies that the structure of the soil in the shrublands is weaker than that of the grassland communities. As weaker structures can be more susceptible to the erosive forces of water this would imply that, as with the aggregate stability measurements, the shear strength of soil is influenced by vegetation change. However, according to Gyssels and Poesen (2003) and Gyssels *et al.*, (2005), rather than the vegetation canopy, it is the belowground biomass that is the significant controlling factor of the stability of soil due to its ability to provide mechanical reinforcement and

influence other soil properties that control soil erodibility. Roots have been shown to have positive effects on soil aggregate stability (Amezketta, 1999), infiltration capacity (Li *et al.*, 1992), soil bulk density (Li *et al.*, 1992), soil texture (Sakkar *et al.*, 1979), organic content (Tisdall and Oades, 1982; Kelly *et al.*, 1996) and soil chemistry (Glinski and Lipiec, 1990).

The importance of root systems on shear strength is explained in detail by Gyssels *et al.*, (2005). In summary, the soil-root matrix is thought to be significantly stronger than the two separate entities because soil is strong in compression but weak in tension, whereas plant roots are weak in compression but strong in tension. However, the importance of the root characteristics is also highlighted. Grasses provide the greatest protection due to their shallow and dense root network, shrubs in contrast, will display a deeper and more heterogeneous root system that can result in poorer soil stability.

Therefore, according to research undertaken by Maestre and Cortina (2002), Gyssels and Poesen (2003), Gyssels *et al.*, (2005) and de Baets *et al.*, (2005), the reduction in near-surface root mass associated with shrub invasion will increase the soil's susceptibility to erosion. However, they argue that only sheet and rill erosion are affected as deeper roots associated with shrubs can, in fact, provide resistance to gully erosion. Unfortunately, no quantitative data for root density is available for the fieldsites in this study. However, through correlation analysis (see table 8.1 and appendices) and mean value comparisons of the physical properties of soil, the extent to which the physical presence of biomass (above and below) controls the shear strength was considered.

Of the physical properties of soil, only soil moisture demonstrated significant variability in mean values throughout the two vegetation communities. Despite this, no consistent or significant relationships were identified between soil moisture and shear strength. Similar results were derived for bulk density. Although positive correlations were found between organic matter and shear strength in all

vegetation types in both study regions, none of the correlations were strong (above 0.5).

The above results suggest that the differences in shear strength between the grassland and shrubland plots are therefore a consequence of the stabilising function of plant roots rather than the direct effect of changes in mean contents of organic matter, bulk density or soil moisture. However, both Zhang *et al.*, (2001) and Nearing *et al.*, (1991) evaluated the effects of soil bulk density and soil moisture content on shear strength of soil. Both concluded that the strength of a soil decreases with decreasing bulk density and increasing water content. This may suggest that relationships amongst these factors do exist but due to the spatial variability within the plots, the interactions are difficult to identify.

In contrast to the grasslands, the high shear strength values evident in the badlands cannot be attributed to the influence of rootmats due to the general lack of vegetation cover. Instead, it is proposed that in the badlands the absence of vegetation cover causes compaction of the soil through raindrop action, and combined with the dispersion of clay particles, causes the development of a concrete-like crust on the soil surface. These crusts are associated with stronger shear strengths but can have an ambivalent effect on gully development (Valentin *et al.*, 2005). Cracks in the surface crusts may initiate the development of gullies (Prasad and Römken, 2004) whereas a uniform crust may inhibit soil detachment and reduce sediment transport by overland flow (Neave and Abrahams, 2001). Again, it should be highlighted that in order for shear strength to provide a direct indication of the erodibility of soil, the measurements must be taken when the soil is saturated. As these conditions were not met in this study, the interpretation of shear strength results must be made with caution.

In the Karoo badlands, physical crusts are widespread. These are usually characterised as having greater bulk densities, smaller pore spaces and lower

hydraulic conductivities (Shainberg and Singer, 1985). The ability of a soil to develop a physical crust is largely a function of the texture of the soil. The soil in the Karoo badlands is classed as having a loamy sand texture and thus is considered to be highly susceptible to crust development (Poesen, 1992).

Spatial and temporal aspects of the development of the Karoo badlands have been studied recently by Keay-Bright and Boardman (2006). Using aerial photographs to monitor changes in the same gully systems measured in this study, they found that, in contrast to the expected increase in degradation, there has been a 15% reduction in the extent of severely degraded badlands areas between 1945 and 2002. The formation of new gully networks were not identified in the area, however, an increase in the density of some existing gully systems was noted. These results suggest that the badlands in the Karoo have stabilised to some extent. The presence of extensive crusting and the high shear strength values derived from this study would also support this conclusion.

Although no significant correlations were found between any soil parameters and shear strength in the badlands, this may be due to the presence of extreme values which were common in many of the datasets. However, a more likely explanation for the absence of a significant relationship between shear strength and bulk density is provided by Roth (1997). Through studying the bulk density of surface crusts and soil texture, Roth found that the bulk density of soil decreases with depth from the surface. In this study, bulk density measurements were taken from approximately the top 8cm of soil to be consistent with the other vegetation communities, however, in badlands, bulk density measurements of the surface crust may be more relevant to understanding the behaviour of soil properties and their response to erosion. The importance of the surface crust conditions on the hydrological response and thus the susceptibility of badlands to erosion is further emphasised by Kuhn and Yair (2004). They attributed the generation of concentrated runoff and thus the development of badlands to changes in soil properties that influence the infiltration characteristics of the soil. In future studies,

the influence of the surface crust should be considered as well as the behaviour of the underlying soil properties.

Although it is commonly thought that only the physical and biological properties of soil are significant in determining indices of erodibility, the soil chemistry also plays a significant role (e.g. Mamedov *et al.*, 2002; Faulkner *et al.*, 2004). As discussed in chapter 2, the calcium and sodium content of soil are significant determining factors of the dispersive behaviour of the soil particles. Sodium is known to increase the dispersibility of clay particles whereas calcium is known to have the opposite effect. However, as the sodium and calcium contents did not display significant differences between the shrublands and badlands in the Karoo, nor did they display significant correlations with the clay content, neither can be attributed to influencing the increased erodibility that has led to the development of badlands.

*How do the changing spatial patterns of soil properties influence the erodibility of the soil?*

The evidence presented so far shows that there appears to be an increase in the erodibility of soil associated with vegetation change. Despite this, apart from the parameters that are directly affected by the structural influence of above and below-ground biomass, the mean values of the physical soil parameters do not change significantly through the vegetation transitions. This implies that increased erosion is a function of the spatial patterns, and ultimately the degree of heterogeneity, determined by the structure of the vegetation community.

In order to understand the importance of the spatial patterns of soil parameters in relation to erosion, the interconnected nature of the soil properties were analysed using the Spearman's Rank correlation coefficient test. Table 8.1 presents the parameters that displayed strong correlations (greater than 0.5) for each of the three vegetation types. The full tables of results can be found in appendix 2.

Although cause and effect cannot be determined from correlation analysis, assumptions about these relationships can be made on the basis of known soil interactions.

The results demonstrate that many complex interactions are likely to be influencing the susceptibility of soil to erosion as a result of changes in plant distribution. However, the results also demonstrate that the correlations vary across the three vegetation types and are particularly weak in the badland landscapes. This highlights the problems associated with understanding the processes and interactions of soil properties in landscapes that display increased heterogeneity.

**Table 8.1** F-values of Spearman's Rank correlation between soil parameters in grasslands, shrublands and badlands.

Soil Parameter Correlations		Grasslands		Shrublands		Badlands
		Karoo	Sevilleta NWR	Karoo	Sevilleta NWR	Karoo
Organic matter	Bulk density	-0.626	-0.581	-0.571	*	*
	pH	-0.516	*	*	*	*
	Water content	*	0.821	*	*	*
	Conductivity	*	0.622	0.505	*	*
	Potassium	*	0.776	*	*	*
Bulk density	Conductivity	-0.546	*	*	*	*
	Water content	*	-0.587	-0.642	-0.512	*
	Magnesium	*	-0.507	*	*	*
	Potassium	*	-0.562	*	*	*
	Sodium	*	*	*	-0.511	*
Water content	Conductivity	0.533	0.587	*	*	*
	Magnesium	*	0.728	-0.522	*	*
	Potassium	*	0.677	*	*	*
	Sodium	*	*	*	0.611	*
	Calcium	*	*	-0.685	*	*
	pH	*	*	-0.632	*	*
Shear strength	Magnesium	*	0.559	*	*	*
	Potassium	*	0.644	*	*	*
pH	Conductivity	*	-0.55	*	-0.586	*
	Magnesium	*	*	0.587	*	*
	Calcium	*	*	0.698	*	*
Conductivity	Magnesium	*	0.512	*	*	*
	Potassium	*	0.507	*	*	*
Calcium	Magnesium	0.76	*	0.766	*	0.887
	Sodium	0.546	*	*	*	*
	Potassium	0.551	*	*	*	*
Sodium	Potassium	0.502	*	*	*	*
	Magnesium	*	*	*	-0.584	*
Potassium	Magnesium	0.519	0.866	*	*	*
	Phosphorus	0.658	*	0.531	*	*

In all cases the p-value indicated that the correlation was different from zero.

It is proposed that organic matter is the key component in the plant-soil relationship and hence is the starting point in understanding how the spatial distribution of plants affects the erodibility of soil. Although Geddes and Dunkerley (1999) show that leaf litter and organic matter are redistributed throughout the shrubland landscape by rainsplash, the spatial patterns showed evidence of autocorrelation and periodicity suggesting that this process does not redistribute the organic matter significantly. Instead, it is proposed that a change in organic matter content acts as a catalyst to further changes in the physical and chemical nature of the soil.

As this study focuses on identifying the spatial patterns of the shrubland landscape as a whole rather than specifically investigating the differences in soil properties between shrub and intershrub areas, the interpretation of what the ranges of spatial autocorrelation represent has to be made with caution. However, the work undertaken by Schlesinger *et al.*, (1996) and Müller (Unpublished thesis) in New Mexico show that the ranges of autocorrelation can be compared to the mean size of the dominant shrub in order to determine the significance of the results. Müller reported ranges of up to 4.5m for ammonium and nitrate content in creosotebush sites and attributed them as representing the shrub zones. Schlesinger *et al.*, on the other hand, generally attributed shrub zones as encompassing ranges under 3m. These findings suggest that the majority of ranges derived from the shrubland sites in this study do represent the intershrub regions as all are greater than 4.5m. Further evidence to this are the similarities in the ranges and periodic nature between the two Sevilleta NWR plots. The vegetation structure is such that the shrub/intershrub zones are well defined. This is reflected in the ranges derived in the Sevilleta NWR in comparison to the Karoo. The intershrub zones in the Karoo are not as distinct due to the presence of other plant species, therefore it is not surprising that there are greater ranges and greater variations between the ranges derived from the two Karoo plots. The smaller ranges evident in the shrubland plots and the increased periodicity are therefore representative of areas that are low in organic matter content and thus the associated adverse soil conditions.

The results in table 8.1 show that organic matter content is strongly negatively correlated with bulk density and pH whereas it is strongly positively correlated with water content, conductivity and potassium. This demonstrates that areas consisting of high organic matter also have higher water contents, lower bulk densities and greater available potassium, a plant-limiting nutrient. Combined, these factors create more favourable growing conditions, not only for existing plants but for the germination of seeds. These conditions have been found to occur under plant canopies (e.g. Schlesinger *et al.*, 1996, Bochet *et al.*, 1999). In contrast, areas low in organic matter will not only have weaker structures due to a decrease in particle binding agents but it will be affected by higher bulk densities

resulting in poorer infiltration capabilities and thus making it more susceptible to runoff and erosion (e.g. Abrahams *et al.*, 1995, Neave and Rayburg, 2006). These conditions are representative of the intershrub regions. The susceptibility to erosion will be further exacerbated due to the lack of stabilising roots in these areas, as discussed previously.

The catalyst effect is further demonstrated by observing the relationships amongst bulk density and a number of other parameters. Strong negative correlations are evident between bulk density and conductivity, water content, potassium, magnesium and sodium. Water content is then seen to be strongly negatively correlated with calcium and pH, in addition to the previously mentioned parameters. This cycle continues, with every soil parameter being related to another. The highly complex nature of these interactions makes disaggregating the individual effects of the parameters on the erodibility of soil extremely difficult.

Positive correlations exist amongst the soil nutrients demonstrating the interconnected nature of both the plant limiting nutrients (P, K, Mg) and the non-limiting nutrients (Ca and Na). However, the spatial patterns are the significant element when considering these relationships with respect to the erodibility of the soil. As all the nutrients demonstrate an increase in spatial heterogeneity or periodicity throughout the transition from grassland to shrublands, it suggests that vegetation controls the redistribution. However, as no data is provided on where the high and low values are in relation to vegetation it cannot be concluded that greater quantities of plant-limiting nutrients are under the shrubs and greater quantities of sodium and calcium are in the intershrub areas. Nevertheless, assumptions can be made about the nature of the distributions as studies by Schlesinger *et al.*, (1996), Bochet *et al.*, (1999) and Titus *et al.*, (2002), all suggest that vegetation regulates the cycling of biologically limiting nutrients whereas abiotic factors control the cycling of non-limiting nutrients.

It is therefore proposed that areas of preferential erosion are created as a consequence the complex interactions between biotic and abiotic processes. Increased heterogeneity in vegetation cover, a shrubland characteristic, induces fundamental changes in the structure of the soil. The influence of increased root heterogeneity inferred through the organic matter content, and consequently established by the decrease in autocorrelation ranges and increase in plots demonstrating periodicity, creates areas of weaker soil structure and poorer infiltration capabilities. These are demonstrated through the similar responses of bulk density, soil moisture and shear strength that have been shown to accompany grass-shrub transitions. The response of these soil parameters combine to create conditions that encourage overland flow. The increase in runoff then washes fine particles downslope and, as a consequence, causes a depletion of essential plant nutrients. The geostatistics reflect this as significantly lower ranges of autocorrelation of available phosphorus in the shrublands are evident compared to the grasslands. This highlights the increase in spatial heterogeneity of plant essential nutrients and thus shows that some areas are experiencing significant phosphorus depletion.

The poorer soil structure makes these regions more susceptible to particle detachment through physical erosional processes and the changes in soil chemistry may cause an increase in the dispersion of clay particles through increased sodium contents. If the correct combination of soil and environmental conditions exist, then the heterogeneity of soil parameters can increase and exacerbate erosion. The increase in periodicity of all soil parameters in the badland plots demonstrate this increase in heterogeneity and show that badlands can be classed as a progressive evolution of degrading shrublands. Figure 8.1 summarises the processes, patterns and interactions that are considered significant in semi-arid land degradation.

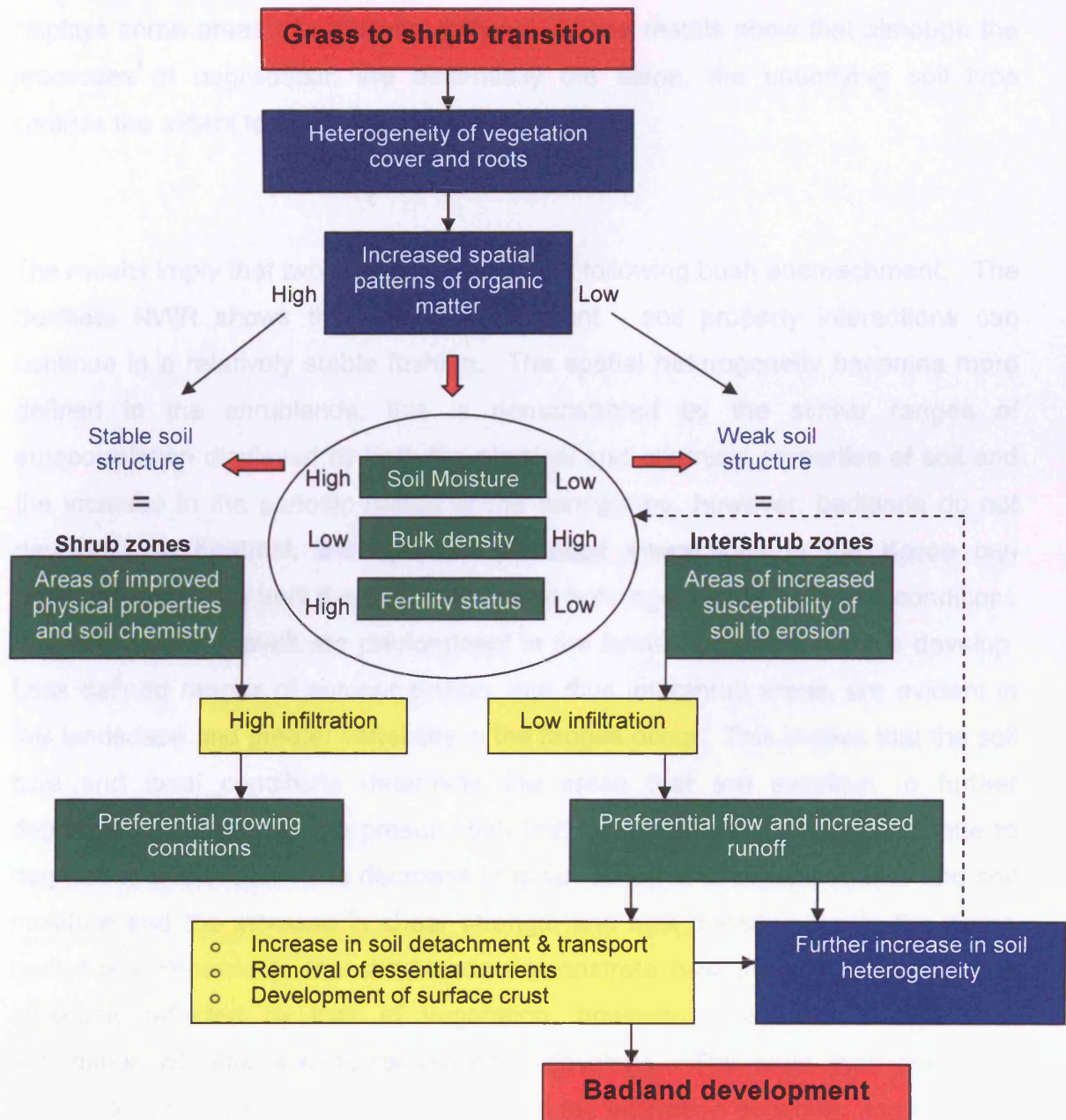


**Figure 8.1** Conceptual model of processes, patterns and interactions connecting vegetation change to the susceptibility of soil to erosion in semi-arid environments

This continuing cycle explains the processes linking vegetation change and increased erosion, and provides a possible mechanism to explain the development of badlands in some semi-arid environments. Despite the shrubland plots in the Sevilleta NWR showing greater evidence of spatial heterogeneity, as established through the smaller ranges of autocorrelation and greater occurrences of

periodicity, badlands have not developed in this region. In contrast, the Karoo displays some areas of extensive gullying. These results show that although the processes of degradation are essentially the same, the underlying soil type controls the extent to which the degradation occurs.

The results imply that two scenarios can occur following bush encroachment. The Sevilleta NWR shows that the cycle of plant - soil property interactions can continue in a relatively stable fashion. The spatial heterogeneity becomes more defined in the shrublands, this is demonstrated by the similar ranges of autocorrelation displayed by both the physical and chemical properties of soil and the increase in the periodic nature of the variograms, however, badlands do not develop. In contrast, the cycle of plant-soil interactions in the Karoo can potentially continue until the extent of spatial heterogeneity is such that conditions that inhibit plant growth are predominant in the landscape and badlands develop. Less defined ranges of autocorrelation, and thus intershrub areas, are evident in this landscape and greater variability in the ranges occur. This implies that the soil type and local conditions determine the areas that are sensitive to further degradation rather than the presumption that all intershrub areas will continue to degrade to this extent. The decrease in mean contents of organic matter and soil moisture and the increase in shear strength and bulk density seen in the Karoo badlands compared to the shrublands demonstrate how the soil properties are adversely affected by loss of vegetation, however, it is the soil type that determines whether a concrete-like crust develops. The crust itself creates a dense soil structure that will not only reduce the infiltration capability and increase surface runoff but also makes it difficult for plants to become re-established. These factors all contribute to the increase in erosion evident in badland landscapes.

## **8.2 The consequences for modelling**

The results of this study have number of implications for the future development of process-based erosion prediction models for semi-arid environments. There are three main factors to consider; spatial patterns in the landscape, the influence of scale and the global applicability of erosion prediction models.

Although many authors have attempted to model the hydrological response and their effect on the erosional process (e.g. EUROSEM, Morgan *et al.*, 1998; WEPP, Lane and Nearing, 1989), the importance of the spatial variability and the interactions amongst the soil parameters has been neglected in many attempts, particularly when modelling rill initiation and interrill erosion. The results of this research, however, demonstrate that the spatial distribution of vegetation controls the soil parameters that ultimately control the surface hydrology. It is proposed that complex interactions between plants and soil, and amongst the soil parameters themselves, influence the spatial distributions that determine the areas that are sensitive to erosion in the landscape. The results imply that shrubland and badland landscapes cannot be represented in a model as a uniform landscape, and thus cannot be represented by a single 'index of erodibility' which is often applied to soils in such models.

Although some attempts have been made to incorporate spatial patterns of landscapes into prediction models (e.g. Goodrich *et al.*, 1991; Moore and Grayson, 1991; Scoging *et al.*, 1992; Smith *et al.*, 1995), the accuracy and therefore their applicability is subject to debate. Neave and Rayburg (2006), for example, modelled runoff and erosion on grassland and shrubland communities using the KINEROS2 prediction model (Smith *et al.*, 1995). Although this model has the capability to route flow over varying soil and surface conditions, these are confined to shrub and intershrub units only and thus do not fully represent the dynamics of spatial variability. Van Oost *et al.*, (2005), on the other hand, discuss the sensitivity of process-based and hydrological models to parameter estimations and

choice of input parameters thus highlighting the need for improved evaluation and parameterisation of spatially distributed soil erosion models.

Parsons *et al.*, (1997) emphasise the importance of having an understanding of the interacting parameters that influence erosion. Information on rainfall distribution and energy, overland flow hydraulics and soil properties are all acknowledged as being significant, however, the quantity of data required is such that it is unrealistic to incorporate all parameters. Instead, Parsons and Wainwright (2006) suggest a probabilistic approach to model rill initiation. However, despite the fact that this model takes into account the spatial variability of soil shear strength amongst other hydrological factors, the spatial variability is not captured explicitly.

The influence of soil properties on erosion prediction are often neglected in favour of overland flow hydraulics, thus the significance of the spatial reorganisation of soil parameters in different plant communities is underestimated. The complex interactions between physical and chemical properties discourage the incorporation of these factors into prediction models, however, the spatial patterns displayed in this study suggest that for the simplified purposes of modelling, the distribution of organic matter could be used as an indicator of the spatial patterns of the physical soil parameters. The spatial patterns of most soil parameters derived from the different vegetation communities demonstrated a characteristic response to vegetation change, therefore, the susceptibility of soil to erosion could be inferred by this parameter due to its relationship with aggregate stability, bulk density and soil moisture. The chemical properties of soil, however, would need more experimental input as soil type significantly affects the mean quantities and thus the strength of response to vegetation change.

However, perhaps the most important finding of this study is the influence of scale on the spatial patterns of soil parameters. The sampling technique utilised in this study was designed to produce quantitative spatial data of soil parameters that

were representative of the different vegetation communities found in semi-arid environments and relate the patterns to the erodibility of the landscape.

The geostatistical results differ from those derived by Schlesinger *et al.*, (1996) and Hook *et al.*, (1991) who found fine-scale heterogeneity in grassland environments. The differences in results are a function of the scale of measurement. This indicates that at a scale more representative of vegetation communities and thus for modelling landscapes, fine-scale patterns may be insignificant. However, if the results of both this study and the work of Schlesinger *et al.*, (1996) are considered together, it demonstrates that the spatial patterns in semi-arid grasslands occur at multi-scales. As suggested by de Soyza *et al.*, (1998), fine-scale patterns, combined with the presence of bare mosaics may be significant to both the susceptibility of grasslands to shrub invasion and the sensitivity of the grassland to erosion.

Although the shrubland data appeared to be less affected by the scale of measurement, the interpretation of the data strongly relies on knowledge of the study area. Shrub and intershrub units can be attributed to causing areas of spatial autocorrelation of soil parameters in shrubland landscapes. At the individual shrub scale, clear ranges of spatial autocorrelation can be derived, as demonstrated by the patterns of nutrients presented by Schlesinger *et al.*, (1996). However, at a scale that incorporates a shrub community, the spatial patterns present themselves through periodicity in the spatial data.

Some evidence of patterns occurring at multi-scales was also presented in the badland data. Two parameters in particular, shear strength and soil moisture, demonstrated fine-scale and coarse-scale periodicity. These patterns are vital in determining the erodibility of the badlands and thus should be considered when developing badland erosion models. However, it is acknowledged that understanding patterns and processes across scales is an extremely complex

problem and an ongoing task (Bellehumeur and Legendre 1998; Wu *et al.*, 2000; Peters and Havstad, 2006).

Although mapping the study areas using interpolation techniques is not part of this thesis, the geostatistical results raise some important issues. Firstly, it was observed that some experimental semi-variograms could not be modelled using simple models, however, this did not mean no spatial patterns existed. In some cases the 'best fit' model was applied but often this did not represent the data adequately. Although this was not a significant issue for this study as the experimental variograms themselves could be interpreted, interpolation techniques require the data to be fitted with a variogram model. Visual and automatic fitting of a model each have advantages and disadvantages but it is unlikely that either would produce a representative result, especially if periodicity is evident in the data. Unless complex, multi-structured models are applied to the semi-variograms, interpolation of the data may be too generalised and therefore invalid.

Often the fitting of variograms is not seen as an important step due to the development of interpolation software. A significant amount of research relies on this process. For example, Müller (Unpublished thesis) studied the significance of scaling approaches to modelling water, sediment and nutrient fluxes in semi-arid New Mexico. By studying the spatial variability of soil parameters, their significance in the scaling of hydrological/sediment transport models was noted. However, only simple models were applied to the data and periodicity was ignored. It is therefore suggested that the validity of the fitted variograms may have significant consequences on the accuracy of the models developed from these datasets.

Although accurately representing the results derived from semi-variograms is a problem associated with models that incorporate spatial data, other issues should also be considered when interpreting spatial results. Firstly, the method of quantifying the spatial variability is important. Intra-plot analysis using the means

and standard deviations generally produced results that were contrary to those derived from the geostatistics. This indicates that research that infers spatial patterns using techniques other than geostatistics should be treated with caution. However, the geostatistical methods employed can have an indirect impact on the accuracy of models. Many different techniques are available and although the semi-variogram is commonly used to determine the spatial patterns of soil parameters, many geostatisticians emphasise the importance of using more than one method in order to assess the accuracy of the results (Dale *et al.*, 2002; Perry *et al.*, 2002). The Geary's C and Moran's I correlograms were calculated in this study. In general, the results were comparable to those derived from the semi-variograms, however, as an ancillary resource, these were particularly useful in determining whether periodicity was significant or whether a pure nugget model was a more accurate description of the data. Despite this, some disparities were evident amongst the methods, suggesting that caution is needed when comparing spatial results derived from different techniques.

By comparing the response of spatial patterns of soil parameters in the Karoo, South Africa and the Sevilleta National Wildlife Refuge, New Mexico, the global applicability of models based on the influence of vegetation change on soil erosion was assessed. The results conclude that the response of soil parameters to vegetation change is essentially the same in both study regions. Although this is a promising finding with regards to the development and applicability of process-based erosion prediction models to semi-arid regions, the results also indicate that the strength of the response appears to vary between the regions. Both the soil type and the species of vegetation are thought to influence the extent of the spatial patterns and also potentially determine whether or not badlands will develop. The extent of the influence of plant species was not determined in this study as direct shrub and intershrub comparisons were not made. However, the significance of plant species was highlighted by Bochet *et al.*, (1999) who found different spatial responses of soil parameters under three different shrub species, similar findings were presented by Andreu *et al.*, (1998). These variables should be factored into the development of the models to allow the appropriate erosional response to be represented.

Although Baird (2004) emphasises the difficulties in conceptualising 'real' hillslope processes, demonstrating the inappropriate use of laboratory simulations and the problems associated with scale, the results of this study highlight the importance of understanding of the underlying mechanisms and characteristics of the erosion process. Without this knowledge deterministic, process-based models will never be able to realistically represent the hydrologic response of a hillslope or accurately predict erosion.

## **CHAPTER NINE**

### **Conclusion**

---

---

This study demonstrates the changes to the physical and chemical properties of soil that accompany vegetation change, how these properties are related to each other and consequently how they interact to modify the erodibility of the landscape.

By investigating the spatial characteristics of the physical and chemical properties of soil in grassland, shrublands and badlands communities, the effects of vegetation structure on controlling land degradation processes in semi-arid environments were assessed. This research highlights the importance of spatial patterns in the landscape and the influence of scale.

The results show that soil parameters in grassland landscapes can be classed as having a relatively uniform distribution. However, a number of grassland semi-variograms displayed evidence of 'the hole effect' thus indicating that bare patches are distributed in grassland landscapes. These patches may be responsible for the shorter ranges of spatial autocorrelation of organic matter and bulk density

evident in some of the grassland plots. In a study by Schenk *et al.*, (2003) it was found that even relatively subtle differences in edaphic characteristics can cause differences in the spatial organisation of plant communities. It is therefore proposed that this characteristic may be responsible for creating areas that are more sensitive to both erosion and shrub invasion.

The spatial patterns evident in the shrubland landscapes demonstrate that the self-perpetuating nature of semi-arid shrubs causes a redistribution of soil properties. In the cases where clear spatial autocorrelation was evident, both the physical and chemical soil parameters demonstrated significantly smaller ranges of spatial autocorrelation than those derived from the grassland plots. As the ranges are greater than the mean diameters of the shrubs themselves, they are most likely to represent the intershrub areas in the landscape. Although a significant number of semi-variograms were best represented by pure nugget models, which under normal circumstances would indicate that no significant spatial patterns exist, periodicity was identified in the majority of the datasets. This pattern represents the variation of the shrub and intershrub zones across the landscape and is therefore a function of scale.

Despite many studies investigating the influence of shrubs on local soil parameter changes, few have considered the spatial patterns at scales that are representative of vegetation communities. As a consequence of this, the importance of the cyclic spatial patterns of soil parameters in shrubland landscapes has never been considered. According to Radeloff *et al.*, (2000) the peaks and troughs of the variances displayed by the semi-variograms are representative of regular patches in the landscape. It is therefore proposed that the frequency of these peaks and troughs may be significant with regards to assessing the degree of degradation in the shrublands.

Periodicity was even more prevalent in the badland landscapes. Every soil parameter demonstrated some degree of cyclic behaviour. Organic matter, bulk

density, conductivity, available magnesium, sodium and phosphorus all displayed an average wavelength of approximately 8m. The consistency of these results suggests that the spatial patterns of soil properties may be strongly related to the gullied nature of the badlands.

It is proposed that the spatial patterns of soil parameters link vegetation change with the degradation of semi-arid landscapes. The soil with the most stable structure, demonstrated through the aggregate stability and shear strength, was found to be in the grasslands. The uniform plant cover and near-surface rootmats increase the stability of this environment, reflected in the relatively homogenous patterns of the physical soil parameters. The shrublands, in contrast, demonstrate a decrease in structural stability. Increased heterogeneity in plant cover, rootmats and thus organic matter are thought to significantly influence the structure of the soil. These factors act as a catalyst, inducing changes in other soil parameters. The spatial patterns demonstrate that there are areas of poorer soil structure adjacent to areas of stronger soil structures and therefore, through correlation analysis, it can be seen that some areas are more likely to be susceptible to erosion.

Due to the general absence of vegetation in badlands, direct links between the impact of vegetation and physical soil parameters are not made. In these landscapes abiotic processes take over as the mechanisms of spatial reorganisation of soil parameters. The significance of the development of badlands in relation to vegetation change is therefore not presented through the spatial patterns themselves but through the differences in responses between the shrublands and badlands. Both the mean values and spatial patterns suggest that badland landscapes represent an extension of the redistribution of soil parameters seen in shrublands. This implies that if the correct conditions exist, shrubland landscapes can continue to degrade until the intershrub regions become the dominant landform; the landscape becomes inhospitable to plants and hydrological processes lead to conditions that propagate rills and gullies.

The influence of the chemical properties of soil is more significant in the badland landscapes. The absence of vegetation is reflected in the decline of available phosphorus. The decrease is a consequence of the interrelated nature of soil parameters; the phosphorus binds to the clay particles, which are commonly dispersed in the presence of sodium, and are then washed downslope. In the absence of vegetation the phosphorus is not replenished. The dispersive nature of sodium is also thought to contribute to the development of a crust on the soil surface of badlands. Compaction caused by raindrops increases the bulk density and thus changes the infiltration characteristics of the soil creating areas that are more susceptible to the erosive power of overland flow.

Comparisons between the soil parameters derived from the Karoo, South Africa and the Sevilleta National Wildlife Refuge, New Mexico, show that the same patterns and processes accompany the invasion of shrubs into grassland landscapes in both semi-arid environments.

Despite some variation amongst the derived ranges of spatial autocorrelation between the grassland landscapes in the two study regions, differences are also evident within the study regions thus implying that local patches in the grassland structure are likely to influence the results. However, it can be concluded that the spatial patterns of soil properties in grasslands in semi-arid regions can be classed as being characteristically homogenous.

The global applicability of the spatial patterns in shrubland landscapes is harder to determine as direct comparisons are more difficult due to the complex structures displayed in the variograms. However, of the ranges of autocorrelation that were derived, the majority are less than 10m in both study regions, which supports the idea that increased heterogeneity of soil parameters accompanies shrub invasion. The global applicability is more evident from the physical properties of soil; a characteristic cyclic pattern is displayed in all parameters both in the Karoo and the Sevilleta NWR semi-variograms. The presence of this periodic pattern in both

datasets is particularly significant as the redistribution of the physical properties reflect the influential nature of the presence/absence of vegetation. It is proposed that the shear strength, bulk density and soil moisture are closely related to the organic matter content of the soil and thus is considered a significant controlling factor of the structural stability of the soil.

The chemical properties show more spatial similarities within each of the study regions with the exception of phosphorus and magnesium. This suggests that abiotic factors such as soil type may be significant in controlling the spatial patterns of non-plant limiting nutrients. The spatial behaviour of phosphorus, however, is similar in both sites and as an essential plant nutrient, shows that vegetation change has a significant impact on the redistribution of plant-limiting nutrients in semi-arid regions.

However, the key to determining whether the changes in soil properties which accompany grass-shrub transitions are globally applicable is associated with the *response* of the spatial patterns within each of the study regions. Apart from conductivity, available calcium and available sodium content, the responses of the soil parameters to a grass-shrub transition in both regions can be characterised by either a decrease in range of spatial autocorrelation and/or the development of periodicity. This indicates that semi-arid grassland to shrubland transitions can be associated with an increase in soil parameter heterogeneity. However, the different responses evident for the three chemical properties suggest that local abiotic factors are more significant in controlling the spatial patterns of these properties.

As gully development is only present in the Karoo and not the Sevilleta NWR, it can be concluded that abiotic factors control the extent to which land degradation occurs and therefore the development of badlands cannot be considered as a characteristic of all semi-arid environments.

The Sevilleta NWR shows that the cycle of plant - soil property interactions can continue in a relatively stable fashion. The spatial heterogeneity becomes more defined in the shrublands, but badlands have not developed. In contrast, the cycle of plant-soil interactions in the Karoo can, in some cases, continue until the extent of spatial heterogeneity is such that conditions that inhibit plant growth are predominant in the landscape and badlands develop. The decrease in mean contents of organic matter and soil moisture and the increase in shear strength and bulk density, evident in the Karoo badlands compared to the shrublands, demonstrate how the soil properties are adversely affected by loss of vegetation. However, it is the soil type and local conditions that determine whether badlands will develop, and in particular, whether a concrete-like crust will develop. The crust creates a dense soil structure that not only reduces the infiltration capability and increases surface runoff but also makes it difficult for plants to become re-established. The interactions of these factors contribute to the increase in erosion evident in badland landscapes.

The results of this study show that although the processes of vegetation change and land degradation are essentially the same in semi-arid regions, the underlying soil type and local conditions determine the areas that are sensitive to further degradation and the extent to which the degradation occurs.

One of the objectives of this research was to assess the importance of scale of measurement on the spatial patterns attributed to a landscape. The geostatistical results indicate that at a scale more representative of vegetation communities and thus for modelling landscapes, fine-scale patterns may be insignificant. However, if the results of both this study and the work of Schlesinger *et al.*, (1996), for example, are considered together, it demonstrates that the spatial patterns in semi-arid grasslands occur at multi-scales. Although the shrubland data appeared to be less affected by the scale of measurement, the interpretation of the data strongly relies on knowledge of the study area. Shrub and intershrub units can be attributed to causing areas of spatial autocorrelation of soil parameters in shrubland landscapes. At the individual shrub scale, clear ranges of spatial

autocorrelation can be derived, as demonstrated by the patterns of nutrients presented by Schlesinger *et al.*, (1996). However, at a scale that incorporates a shrub community, the spatial patterns present themselves through periodicity in the spatial data thus indicating that regular patterns of high and low values of soil properties exist in this landscape. The relationships identified amongst the soil parameters support the idea that increased heterogeneity in shrublands creates areas that are more susceptible to soil erosion. The implications of these findings on advancing erosion models are significant. The geostatistical results show that shrubland and badland landscapes cannot be represented in a model as a uniform landscape, and thus cannot be represented by a single 'index of erodibility' which is often applied to soils in such models.

By understanding the spatial patterns of soil properties that influence the soil's susceptibility to erosion in different vegetation communities, probabilistic models of soil erosion can be improved. Although it is acknowledged that it is impractical to measure all physical and chemical properties, the results of this study show that the organic matter content could be used as an indicator of the areas of the landscape that may be more sensitive to erosion.

The influence of soil properties on erosion prediction is often neglected in favour of overland flow hydraulics, however, the results of this research show that the reorganisation of soil parameters that accompanies shrub invasion will create areas that are more susceptible to erosion and areas of preferential flow. These patterns may usefully be incorporated into models to identify areas that are potentially susceptible to rill initiation. This research shows that the significance of the spatial patterns of vegetation structure and the associated distribution of soil parameters and plant roots has been underestimated with regards to existing erosion prediction models.

### Further work

This research furthers the understanding of land degradation processes in semi-arid environments by highlighting the importance of spatial patterns in the landscape and the influence of scale. By utilising this knowledge in the development of erosion prediction models their validity may be improved as the response of a landscape to erosive processes will be better represented. Continuing research on the behaviour of soil properties and their interactions is needed to fully understand the feedback mechanisms of the plant-soil relationships, however, this research emphasises that a multi-faceted approach is required if a comprehensive explanation of the patterns and processes is desired.

The use of geostatistics has great potential in developing the understanding of the spatial organisation of both vegetation and soil parameters and as such, the interactions between the two. Further research on the importance of periodicity in spatial data could potentially provide another means of assessing the extent of land degradation or erosion sensitive areas in semi-arid environments. In addition, the significance of 'patches' in grassland landscapes should be investigated in more detail. 'Hole effects' displayed by semi-variograms are thought to represent these characteristic patches and therefore may be used to identify areas that are potentially more sensitive to erosion and/or the invasion of shrubs.

One aspect of the land degradation process that has not been considered in this study is the temporal aspect. Both short-term and long-term temporal variation may affect the spatial distribution of soil parameters and thus influence the susceptibility of soil to erosion. Through seasonal climatic variations, the vegetation structure may differ, influencing soil parameters such as organic matter content, soil moisture and the soil chemistry. Long-term temporal aspects such as the period of time since the establishment of shrubs and thus the stage of soil parameter redistribution may also be significant. It is therefore suggested that the rates of transition and the significance of the 'stage' of degradation would aid the

understanding of vegetation change and its influence on the susceptibility of soil to erosion.

## Bibliography

- Abrahams, A. D., Parsons, A. J. and Luk, S. H. (1989) Distribution of depth of overland flow on desert hillslopes and implications for modelling soil erosion. *Journal of Hydrology* **106**: 177-184.
- Abrahams, A. D., Parsons, A. J. and Hirsch, P. J. (1992) Field and laboratory studies of resistance to interrill overland flow on semi-arid hillslopes, southern Arizona *In* A. J. Parsons and A. D. Abrahams (Eds.) *Overland flow: Hydraulics and erosion mechanics* UCL Press Ltd: London
- Abrahams, A. D., Parsons, A. J. and Wainwright, J. (1995) Effects of vegetation change on interrill runoff and erosion, Walnut Gulch, southern Arizona. *Geomorphology* **13**: 37-48.
- Abrahams, A. D., Parsons, A. J. and Wainwright, J. (2003) Disposition of rainwater under creosotebush. *Hydrological Processes* **17**(13): 2555-2566.
- Acocks, J. P. H. (1953) Veld types of South Africa. *Memoirs of the botanical survey of South Africa* **28**: 1-192.
- Acocks, J. P. H. (1988) Veld types of South Africa (3rd Edition). *Memoirs of the botanical survey of South Africa* **57**.
- Allison, F. E. (1973) *Soil organic matter and its role in crop production*. : Elsevier Scientific: Amsterdam.
- Amezketta, E. (1999) Soil aggregate stability: a review. *Journal of Sustainable Agriculture* **14**(2-3): 83-151.
- Andreu, V., Rubio, J. L., Gimeno-García, E. and Llinares, J. V. (1998) Testing three Mediterranean shrub species in runoff reduction and sediment transport. *Soil and Tillage Research* **45**: 411-454.
- Anselin, L. (2003) Spatial autocorrelation (3), Global spatial autocorrelation. <http://sal.agecon.uiuc.edu>. Accessed: 08/08/2006.
- Asner, G. P., Elmore, A. J., Olander, L. P., Martin, R. E. and Harris, A. T. (2004) Grazing systems, ecological responses, and global change. *Annual Reviews of Environment and Resources* **29**: 261-299.

- Asner, G. P. and Heidebrecht, K. B. (2005) Desertification alters regional ecosystem-climate interactions. *Global Change Biology* **11**: 182-194.
- Baird, A. J., Thornes, J. B. and Watts, G. P. (1992) Extending overland-flow models to problems of slope evolution and the representation of complex slope-surface topographies *In* A. J. Parsons and A. D. Abrahams (Eds.) *Overland flow: Hydraulics and erosion mechanics* UCL Press Ltd: London.
- Ball, D. F. (1964) Loss-on-ignition as an estimate of organic matter and organic carbon in noncalcareous soils. *Journal of Soil Science* **15**: 84-92.
- Barthès, B. and Roose, E. (2002) Aggregate stability as an indicator of soil susceptibility to runoff and erosion; validation at several levels. *Catena* **47**(2): 133-149.
- Bellehumeur, C. and Legendre, P. (1998) Multiscale sources of variation in ecological variables: modelling spatial dispersion, elaborating sampling designs. *Landscape Ecology* **13**(1): 15-25.
- Bestelmeyer, B. T., Trujillo, D. A., Tugel, A. J. and Havstad, K. M. (2006) A multi-scale classification of vegetation dynamics in arid lands: What is the right scale for models, monitoring, and restoration? *Journal of Arid Environments* **65**: 296-318.
- Blomqvist, M. M., Olf, H., Blaauw, M. B., Bongers, T. and van der Putten, W. H. (2000) Interactions between above- and belowground biota: importance for small-scale vegetation mosaics in a grassland ecosystem. *OIKOS* **90**: 582-598.
- Boardman, J., Parsons, A. J., Holland, R., Holmes, P. J. and Washington, R. (2003) Development of badlands and gullies in the Sneeuwberg, Great Karoo, South Africa. *Catena* **50**(2-4): 165-184.
- Bochet, E., Rubio, J. L. and Poesen, J. (1999) Modified topsoil islands within patchy Mediterranean vegetation in SE Spain. *Catena* **38**(1): 23-44.
- Böhm, P. and Gerold, G. (1995) Pedo-hydrological and sediment responses to simulated rainfall on soils of the Konya Uplands (Turkey). *Catena* **25**(1-4): 63-76.
- Boix-Fayos, C., Calvo-Cases, A., Imeson, A. C. and Soriano-Soto, M. D. (2001) Influence of soil properties on the aggregation of some Mediterranean soils and the use of aggregate size and stability as land degradation indicators. *Catena* **44**(1): 47-67.

- Bouma, N. A. and Imeson, A. C. (2000) Investigation of relationships between measured field indicators and erosion processes on badland surfaces at Petrer, Spain. *Catena* **40**(2): 147-171.
- Bradford, J. M., Truman, C. C. and Huang, C. (1992) Comparison of three measures of resistance of soil surface seals to raindrop splash. *Soil Technology* **5**: 47-56.
- Bruckner, A., Kandeler, E. and Kampichler, C. (1999) Plot-scale spatial patterns of soil water, pH, substrate-induced respiration and N mineralisation in a temperate coniferous forest. *Geoderma* **93**: 207-223.
- Brus, D. J. and de Gruijter, J. J. (1997) Random sampling or geostatistical modelling? Choosing between design-based and model -based sampling strategies for soil (with discussion). *Geoderma* **80**: 1-44.
- Bryan, R. B. (2000) Soil erodibility and processes of water erosion on hillslope. *Geomorphology* **32** (3-4): 385-415.
- Buffington, L. C. and Herbel, C. H. (1965) Vegetational changes on a semi-desert grassland range from 1858 to 1963. *Ecological Monographs* **35**(2): 139-164.
- Buurman, P., Pape, T. and Muggler, C. C. (1997) Laser grain-size determination in soil genetic studies. 1. Practical problems. *Soil Science* **162**: 211-218.
- Cambardella, C. A., Moorman, T. B., Novak, J. M., Parkin, T. B., Karlen, D. L., Turco, R. F. and Konopka, A. E. (1994) Field scale variability of soil properties in central Iowa soils. *Soil Science Society of America Journal* **58**: 1501-1511.
- Cambardella, C. A. and Karlen, D. L. (1999) Spatial analysis of fertility parameters. *Precision Agriculture* **1**: 5-14.
- Carroll, Z. L. and Oliver, M. A. (2005) Exploring the spatial relations between soil physical properties and apparent electrical conductivity. *Geoderma* **128**(3-4): 354-374.
- Cerdà, A. (1997) The effect of patchy distribution of *Stipa tenacissima* L. on runoff and erosion. *Journal of Arid Environments* **36**: 37-51.
- Charley, J. L. and West, N. E. (1975) Plant-induced soil chemical patterns in some shrub-dominated semi-desert ecosystems of Utah. *Journal of Ecology* **63**(3): 945-963.

- Christopher, T. B. S. (2003) *Aggregate stability of different aggregate sizes*.  
[http://www.agri.upm.edu.my/~chris/as/om\\_fractions.html](http://www.agri.upm.edu.my/~chris/as/om_fractions.html).  
Accessed: 10/08/2003.
- Cowling, R. M., Roux, P. W. and Pieterse, A. J. H. (1986) Report of the Committee for Terrestrial Ecosystems National Programme for Ecosystem Research.
- Dale, M. R. T., Dixon, P., Fortin, M. J., Legendre, P., Myers, D. E. and Rosenberg, M. S. (2002) Conceptual and mathematical relationships among methods for spatial analysis. *Ecography* **25**: 558-577.
- de Baets, S., Poesen, J., Gysels, G. and Knapen, A. (2005) Effects of grass roots on the erodibility of topsoils during concentrated flow. *Geomorphology* **76**: 54-67.
- de Lima, J. L. M. P. (1992) Model KININF for overland flow on pervious surfaces *In* A. J. Parsons and A. D. Abrahams (Eds.) *Overland flow: Hydraulics and erosion mechanics* UCL Press Ltd: London.
- de Soyza, A. G., Whitford, W. G., Herrick, J. E., Van Zee, J. W. and Havstad, K. M. (1998) Early warning indicators of desertification: examples of tests in the Chihuahuan Desert. *Journal of Arid Environments* **39**: 101-112.
- Dean, W. R. J., Hoffman, M. T., Meadows, M. E. and Milton, S. J. (1995) Desertification in the semi-arid Karoo, South Africa: review and reassessment. *Journal of Arid Environments* **30**: 247-264.
- Dexter, A. R. and Chan, K. Y. (1991) Soil mechanical properties as influenced by exchangeable cations. *Journal of Soil Science* **42**: 219-226.
- Doudill, A. J., Heathwaite, A. L. and Thomas, D. S. G. (1998) Soil water movement and nutrient cycling in semi-arid rangeland: vegetation change and system resilience. *Hydrological Processes* **12**: 443-459.
- Eshel, G., Levy, G. J., Mingelgrin, U. and Singer, M. J. (2004) Critical evaluation of the use of laser diffraction for particle-size distribution analysis. *Soil Science Society of America Journal* **68**: 736-743.
- Faulkner, H., Alexander, R. T. and Zukowskyj, P. (2004) Variations in soil dispersivity across a gully head displaying shallow sub-surface pipes, and the role of shallow pipes in rill initiation *Earth Surface Processes and Landforms* **29**(9): 1143-1160.



- Favis-Mortlock, D. T., Boardman, J., Parsons, A. J. and Lascelles, B. (2000) Emergence and erosion: a model for rill initiation and development. *Hydrological Processes* **14**: 2173-2205.
- Fixen, P. E. and Grove, J. H. (1990) Testing soils for phosphorus *In* R. L. Westerman (Ed.) *Soil testing and plant analysis (Third Edition)* Soil Science Society of America, Inc.: Madison, Wisconsin (141-172).
- Flaate, K. (1966) Factors influencing the results of vane tests. *Canadian Geotechnical Journal* **3**(1): 18-31.
- Franzluebbers, A. J. (2002) Water infiltration and soil structure related to organic matter and its stratification with depth. *Soil and Tillage Research* **66**(2): 197-205.
- Friedel, M. H. (1991) Range condition assessment and the concept of thresholds: A Viewpoint. *Journal of Range Management* **44**: 422-426.
- Gaston, L. A., Locke, M. A., Zablutowicz, R. M. and Reddy, K. N. (2003) *Spatial relationships among soil properties and weed population in Beasley Lake Watershed*. <http://199.133.10.189/Services/docs.htm?docid=8411>  
Accessed: 12/03/2003.
- Geddes, N. and Dunkerley, D. L. (1999) The influence of organic litter on the erosive effects of raindrops and of gravity drops released from desert shrubs. *Catena* **36**: 303-313.
- Gibbens, R. P., McNeely, R. P., Havstad, K. M., Beck, R. F. and Nolen, B. (2005) Vegetation changes in the Jornada Basin from 1858 to 1998. *Journal of Arid Environments* **61**: 651-668.
- Gifford, G. F. (1985) Cover allocation in rangeland watershed management: A review *In* E. B. Jones and T. J. Ward (Eds.) *Watershed Management in the Eighties: Proceedings of a Symposium* ASCE: New York.
- Gilley, J. E., Elliot, W. J., Laflen, J. M. and Simanton, J. R. (1993) Critical shear stress and critical flow rates for initiation of rilling. *Journal of Hydrology* **142**(1-4): 251-271.
- Glinski, J. and Lipiec, J. (1990) *Soil physical conditions and plant roots*. Boca Raton, FL: CRC Press.
- Gonzalez, P. and Zak, D. R. (1994) Geostatistical analysis of soil properties in a secondary tropical dry forest, St. Lucia, West Indies *Plant and Soil* **163**(1): 45-54.

- Goodrich, D. C., Woolhiser, D. A. and Keefer, T. O. (1991) Kinematic routing using finite elements on a triangular irregular network. *Water Resources Research* **27**: 995-1003.
- Goovaerts, P. (1999) Geostatistics in soil science: state-of-the-art and perspectives. *Geoderma* **89**: 1-45.
- Greig-Smith, P. (1952) The use of random and contiguous quadrats in the study of the structure of plant communities. *Annals of Botany* **16**: 293-316.
- Gringarten, E. and Deutsch, C. V. (2001) Teacher's Aide: Variogram interpretation and modelling. *Mathematical Geology* **33**(4): 507-534.
- Guardia, R., Gallart, F. and Ninot, J. M. (2000) Soil seed bank and seedling dynamics in badlands of the Upper Llobregat basin (Pyrenees). *Catena* **40**(2): 189-202.
- Gutierrez, J. and Hernandez, I. I. (1996) Runoff and interrill erosion as affected by grass cover in a semi-arid rangeland of northern Mexico. *Journal of Arid Environments* **34**: 287-295.
- Gyssels, G. and Poesen, J. (2003) The importance of plant root characteristics in controlling concentrated flow erosion rates. *Earth Surface Processes and Landforms* **28**: 371-384.
- Gyssels, G., Poesen, J., Bochet, E. and Li, Y. (2005) Impact of plant roots on the resistance of soils to erosion by water: a review. *Progress in Physical Geography* **29**(2): 189-217.
- Haby, V. A., Russelle, M. P. and Skogley, R. O. (1990) Testing soils for potassium, calcium, and magnesium *In* R. L. Westerman (Ed.) *Soil testing and plant analysis (Third Edition)* Soil Science Society of America, Inc.: Madison, Wisconsin (p. 181-221).
- Havstad, K., Gibbens, R. P., Knorr, C. A. and Murray, L. W. (1999) Long-term influences of shrub removal and lagomorph exclusion on Chihuahuan Desert vegetation dynamics. *Journal of Arid Environments* **42**: 155-166.
- Hjulstrom, F. (1935) The Morphological activity of rivers as illustrated by river Fyris. *Bulletin of the Geological Institute, Uppsala* **25**: 89-122.
- Hoffman, T., Todd, S., Ntshona, Z. and Turner, S. (1999) *Land degradation in South Africa*. National Botanical Institute, Kirstenbosch Research Centre: Cape Town.

- Hook, P. B., Burke, I. C. and Lauenroth, W. K. (1991) Heterogeneity of soil and plant N and C associated with individual plants and openings in North America shortgrass steppe. *Plant and Soil* **138**: 247-256.
- Horton, R. E. (1945) Erosional development of streams and their drainage basins: hydrophysical approach to quantitative morphology. *Bulletin of the Geological Society of America* **56**: 370-375.
- Huang, C., Gascuel-Oudou, C. and Cros-Cayot, S. (2002) Hillslope topographic and hydrologic effects on overland flow and erosion. *Catena* **46**(2-3): 177-188.
- Jackson, M. L. (1958) *Soil chemical analysis*. Prentice-Hall: Englewood Cliffs, NJ.
- Keay-Bright, J. and Boardman, J. (2006) Changes in the distribution of degraded land over time in the central Karoo, South Africa. *Catena* **67**: 1-14.
- Kelly, R. H., Burke, I. C. and Lauenroth, W. K. (1996) Soil Organic Matter and Nutrient Availability Responses to Reduced Plant Inputs in Shortgrass Steppe. *Ecology* **77**(8): 2516-2527.
- Kershaw, K. A. (1957) The use of cover and frequency in the detection of pattern in plant communities. *Ecology* **38**(2): 291-299.
- Kieft, T. L., White, C. S., Loftin, S. R., Aguilar, R., Craig, J. A. and Skaar, D. A. (1998) Temporal dynamics in soil carbon and nitrogen resources at a grassland-shrubland ecotone. *Ecology* **79**(2): 671-683.
- Kirkby, M. J. and Bull, L. J. (2000) Some factors controlling gully growth in fine-grained sediments: a model applied in southeast Spain. *Catena* **40**(2): 127-146.
- Kosmas, C., Danalatos, N. G. and Gerontidis, S. (2000) The effect of land parameters on vegetation performance and degree of erosion under Mediterranean conditions. *Catena* **40**(1): 3-17.
- Kraaij, T. and Milton, S. J. (2006) Vegetation changes (1995-2004) in semi-arid Karoo shrubland, South Africa: Effects of rainfall, wild herbivores and change in land use. *Journal of Arid Environments* **64**: 174-192.
- Kuhn N. J. and Yair, A. (2004) Spatial distribution of surface conditions and runoff generation in small arid watersheds, Zin Valley Badlands, Israel. *Geomorphology* **57**(3): 183-200.

- Lane, L. J. and Nearing, M. (1989) USDA-Water Erosion Prediction Project: Hillslope profile version *In NSERL Report No. 2* USDA-ARS National Soil Erosion Laboratory: West Lafayette.
- Lane, L. J., Nearing, M. A., Laflen, J. M., Foster, G. R. and Nichols, M. H. (1992) Description of the US Department of Agriculture water erosion prediction project (WEPP) model *In* A. J. Parsons and A. D. Abrahams (Eds.) *Overland flow: Hydraulics and erosion mechanics* UCL Press Ltd: London.
- Lang, R. D. (1979) The effects of ground cover on surface runoff from experimental plots. *Journal of Soil Conservation*, **35**: 108–114. **35**: 108-114.
- Léonard, J. and Richard, G. (2004) Estimation of runoff critical shear stress for soil erosion from soil shear strength **57**: 233-249. *Catena* **57**(3): 233-249.
- Li, Y., Xu, X. Q. and Zhu, X. M. (1992) Preliminary study on the mechanism of plant roots to increase the anti-scourability of soil on the Loess Plateau. *Science in China* **35**: 1085-1092.
- Low, A. B. and Rebelo, T. G. (1996) *Vegetation of South Africa, Lesotho and Swaziland*. Pretoria, South Africa: Department of Environmental Affairs and Tourism: Pretoria.
- Ludwig, J. A., Tongway, D. J., Eager, R. W., Williams, R. J. and Cook, G. D. (1999) Fine-scale vegetation patches decline in size and cover with increasing rainfall in Australian savannas. *Landscape Ecology* **14**: 557-566.
- Maestre, F. T. and Cortina, J. (2002) Spatial patterns of surface soil properties and vegetation in a Mediterranean semi-arid steppe. *Plant and Soil* **241**: 279-291.
- Mamedov, A. I., Shainberg, I. and Levy, G. J. (2002) Wetting rate and sodicity effects on interrill erosion from semi-arid Israeli soils. *Soil and Tillage Research* **68**(2): 121-132.
- Martinez-Mena, M., Rogel, J. A., Albaladejo, J. and Castillo, V. M. (1999) Influence of vegetal cover on sediment particle-size distribution in natural rainfall conditions in a semi-arid environment. *Catena* **38**: 175-190.
- Mbagwu, J. S. C., Piccolo, A. and Mbila, M. O. (1993) Water-stability of aggregates of some tropical soils treated with humic substances. *Pedologie* **43**: 269-284.



- Meadows, M. E. and Hoffman, M. T. (2002) The nature, extent and causes of land degradation in South Africa: legacy of the past, lessons for the future? *Area* **34**(428-437).
- Meyer, L. D. and Wischmeier, W. H. (1969) Mathematical simulation of the process of soil erosion by water. *Transactions of the American Society of Agricultural Engineers* **12**: 754-758, 762.
- Middleton, H. E. (1930) Properties of soils which influence soil erosion. *USDA Technical Bulletin No.178*.
- Milne, B.T., Moore, D.I., Betancourt, J.L., Parks, J.A., Swetnam, T. W., Parmenter, R. R. and Pockman, W. T. (2003) *Multidecadal drought cycles in south-central New Mexico: patterns and consequences. Climate variability and ecosystem response at long term ecological research (LTER) sites* (Eds D. Greenland, D. Goodin and R. Smith). 286-307. Oxford University Press, Oxford.
- Milton, S. J., Dean, W. R. J., du Plessis, M. A. and Siegfried, W. R. (1994) A Conceptual Model of Arid Rangeland Degradation *BioScience* **44**(2): 70-76.
- Moore, I. D. and Grayson, R. B. (1991) Terrain-based prediction of runoff with vector elevation data. *Water Resources Research* **27**: 1177-1191.
- Morgan, R. P. C., Quinton, J. N. and Rickson, R. J. (1993) *EUROSEM: A user guide*. Silsoe College: Silsoe-Bedford.
- Morgan, R. P. C. (1995) *Soil Erosion and Conservation. (2<sup>nd</sup> Edition)*. Longman Group: Harlow.
- Morgan, R. P. C., Quinton, J. N., Smith, R. E., Govers, G., Poesen, J. W. A., Auerswald, K., Chisci, G. , Torri, D. and Styczen M. E. (1998) The European Soil Erosion Model (EUROSEM): a dynamic approach for predicting sediment transport from fields and small catchments. *Earth Surface Processes and Landforms* **23**(6): 527-544.
- Müller, E. N. (Unpublished thesis) *Scaling approaches to the modelling of water, sediment and nutrient fluxes within semi-arid landscapes, Jornada Basin, New Mexico*. University of London: London.
- Nearing, M. A., Bradford, J. M. and Parker, S. C. (1991) Soil detachment by shallow flow at low slope. *Soil Science Society of America Journal* **55**: 339-344.

- Neave, M. and Abrahams, A. D. (2001) Impact of small mammal disturbances on sediment yield from grassland and shrubland ecosystems in the Chihuahuan Desert. . *Catena* **44**: 285-303.
- Neave, M. and Abrahams, A. D. (2002) Vegetation influences on water yields from grassland and shrubland ecosystems in the Chihuahuan Desert. *Earth Surface Processes and Landforms* **27**: 1011-1020.
- Neave, M. and Rayburg, S. (2006) Nonlinear biofluvial responses to vegetation change in a semiarid environment  
*Geomorphology* doi:10.1016/j.geomorph.2006.07.018.
- Nogueras, P., Burjachs, F., Gallart, F. and Puigdefabregas, J. (2000) Recent gully erosion in the El Cautivo badlands (Tabernas, SE Spain). *Catena* **40**(2): 203-215.
- Oades, J. M. (1984) Soil organic matter and structural stability: Mechanisms and implications for management. *Plant Soil* **76**: 319-337.
- Okin, G. S., Gillette, D. A. and Herrick, J. E. (2006) Multi-scale controls on and consequences of aeolian processes in landscape change in arid and semi-arid environments. *Journal of Arid Environments* **65**: 253-275.
- Olea, R. A. (1999) *Geostatistics for engineers and earth scientists*. Kluwer Academic Publishers: Massachusetts.
- Orr, H. K. (1970) *Runoff and erosion control by seeded and native vegetation on a forest burn, Black Hills, South Dakota*. U.S. Forest Service, Rocky Mountain Forest and Range Experiment Station: Research paper RM-60.
- Pannatier, Y. (1996) *VARIOWIN Software for spatial data analysis in 2D*. Springer: New York.
- Parsons, A. J. and Abrahams, A. D. (1992) Field investigations of sediment removal in interrill overland flow In A. J. Parsons and A. D. Abrahams (Eds.) *Overland flow: Hydraulics and erosion mechanics* UCL Press Ltd: London.
- Parsons, A. J., Abrahams, A. D. and Simanton, J. R. (1992) Microtopography and soil-surface materials on semi-arid piedmont hillslopes, southern Arizona. *Journal of Arid Environments* **22**: 107-115.
- Parsons, A. J., Abrahams, A. D. and Wainwright, J. (1996) Responses of interrill runoff and erosion rates to vegetation change in southern Arizona. *Geomorphology* **14**: 311-317.



- Parsons, A. J., Wainwright, J., Abrahams, A. D. and Simanton, J. R. (1997) Distributed dynamic modelling of interrill overland flow. *Hydrological Processes* **11**: 1833-1859.
- Parsons, A. J. and Wainwright, J. (in press) Depth distribution of interill overland flow and the formation of rills. *Hydrological Processes*.
- Perry, J. N., Liebhold, A. M., Rosenberg, M. S., Dungan, J. L., Miriti, M., Jakomulska, A. and Citron-Pousty, S. (2002) Illustrations and guidelines for selecting statistical methods for quantifying spatial pattern in ecological data. *Ecography* **25**: 578-600.
- Peters, D. P. C. (2002) Plant species dominance at a grassland-shrubland ecotone: an individual-based gap dynamics model of herbaceous and woody species. *Ecological Modelling* **152**(1): 5-32.
- Peters, D. P. C. and Havstad, K. M. (2006) Nonlinear dynamics in arid and semi-arid systems: Interactions among drivers and processes across scales. *Journal of Arid Environments* **65**: 196-206.
- Poesen, J. (1981) Rainwash experiments on the erodibility of loose sediments. *Earth Surface Processes and Landforms* **6**: 285-307.
- Poesen, J. (1992) Mechanisms of overland flow generation and sediment production on loamy and sandy soils with and without rock fragments *In* A. J. Parsons and A. D. Abrahams (Eds.) *Overland flow: Hydraulics and erosion mechanics* UCL Press Ltd: London.
- Pons, Y., Capillon, A. and Cheverry, C. (2000) Water movement and stability of profiles in drained, clayey and swelling soils: at saturation, the structural stability determines the profile porosity. *European Journal of Agronomy* **12**(3-4): 269-279.
- Prasad, S. and Romkens, M. J. M. (2004) Mechanic energy and subsurface hydrologic effect in head-cut processes. *In* Li., Y., Poesen, J., Valentin, C. (Eds.), *Gully erosion under global change*, Sichuan Science and Technology Press, Chengdu, China, pp. 109-120.
- Prosser, I. A., Dietrich, W. E. and Stevenson, J. (1995) Flow resistance and sediment transport by concentrated overland flow in a grassland valley. *Geomorphology* **13**: 71-86.



- Puigdefabregas, J. and Sanchez, G. (1996) *Geomorphological implications of vegetation patchiness in semi-arid slopes. In: M. Anderson and S. Brooks (eds.), Advances in Hillslope Processes, 2: 1027-1060. John Wiley.*
- Qi, Y. and Wu, J. (1996) Effects of changing spatial resolution on the results of landscape pattern analysis using autocorrelation indices. *Landscape Ecology* **11**(1): 39-49.
- Radeloff, V. C., Miller, T. F., He, H. S. and Mladenoff, D. J. (2000) Periodicity in spatial data and geostatistical models: autocorrelation between patches *Ecography* **23**: 81-91.
- Rango, A., Tartowski, S. L., Laliberte, A., Wainwright, J. and Parsons, A. J. (2006) Islands of hydrologically enhanced biotic productivity in natural and managed arid ecosystems. *Journal of Arid Environments* **65**: 235-252.
- Rawling, (2004) *Sevilleta LTER data*  
<http://sevilleta.unm.edu/data/archive/gis/#soils>. Accessed:10/06/05.
- Regues, D., Guardia, R. and Gallart, F. (2000) Geomorphic agents versus vegetation spreading as causes of badland occurrence in a Mediterranean subhumid mountainous area. *Catena* **40**(2): 173-187.
- Rienks, S. M., Botha, G. A. and Hughes, J. C. (2000) Some physical and chemical properties of sediments exposed in a gully (donga) in northern KwaZulu-Natal, South Africa and their relationship to the erodibility of the colluvial layers. *Catena* **39**(1): 11-31.
- Rietkerk, M., Ouedraogo, T., Kumar, L., Sanou, S., Langevelde, F. v., Kiema, A., Koppel, J. v. d., Andel, J. v., Hearne, J., Skidmore, A. K., Ridder, N. d., Stroosnijder, L. and Prins, H. H. T. (2002) Fine-scale spatial distribution of plants and resources on a sandy soil in the Sahel. *Plant and Soil* **239**: 69-77.
- Roth, C. H. (1997) Bulk density of surface crusts: depth functions and relationships to texture *Catena* **29**(3): 223-237.
- Roux, P. W. and Theron, G. K. (1987) Vegetation change in the Karoo Biome *In R. M. Cowling and P. W. Roux (Eds.) The Karoo Biome: a preliminary synthesis, Part 2 - Vegetation and history. South African National Scientific Programmes Report (70-95).*
- Rowell, D. L. (1994) *Soil Science: Methods and Applications*. Longman: Harlow.

- Sakkar, A. N., Jenkins, D. A. and Wyn Jones, R. G. (1979) Modification to mechanical and mineralogical composition of soil within the rhizosphere. In Harley, J.L. and Russel, R. S. (Eds.) *The soil-plant interface*, London: Academic Press.
- Schaffers, A. P. (2002) Soil, biomass, and management of semi-natural vegetation. *Plant Ecology* **158**: 229-246.
- Schenk, J. H., Holzapfel, C., Hamilton, J. G. and Mahall, B. E. (2003) Spatial ecology of a small desert shrub on adjacent geological substrates. *Journal of Ecology* **91**: 383-395.
- Schlesinger, W. H., Reynolds, J. F., Cunningham, G. L., Huenneke, L. F., Jarrell, W. M., Virginia, R. A. and Whitford, W. G. (1990) Biological feedbacks in global desertification. *Science* **247**: 1043-1048.
- Schlesinger, W. H., Raikes, J. A., Hartley, A. E. and Cross, A. F. (1996) On the spatial pattern of soil nutrients in desert ecosystems. *Ecology* **77**(2): 364-374.
- Schlesinger, W. H. and Pilmanis, A. M. (1998) Plant-soil interactions in deserts. *Biogeochemistry* **42**: 169-187.
- Schlesinger, W. H., Abrahams, A. D., Parsons, A. J. and Wainwright, J. (1999) Nutrient losses in run-off from grassland and shrubland habitats in Southern New Mexico: 1. rainfall simulation experiments. *Biogeochemistry* **45**: 21-34.
- Schlesinger, W. H., Ward, T. J. and Anderson, J. (2000) Nutrient losses in runoff from grassland and shrubland habitats in southern New Mexico: II. Field plots. *Biogeochemistry* **49**: 69-86.
- Schmidt, J. (1992) Modelling long-term soil loss and landform change In A. J. Parsons and A. D. Abrahams (Eds.) *Overland flow: Hydraulics and erosion mechanics* UCL Press Ltd: London
- Schulte, E. E., Kaufman, C. and Peters, J. B. (1991) The influence of sample size and heating time on soil weight loss-on-ignition. *Communications in Soil Science and Plant Analysis* **22**: 159-168.
- Schulze, B. R. (1980) *Climate of South Africa*. General Survey. Weather Bureau. Department of Transport: Pretoria.



- Scoging, H. (1992) Modelling overland-flow hydrology for dynamic hydraulics *In* A. J. Parsons and A. D. Abrahams (Eds.) *Overland flow: Hydraulics and erosion mechanics* UCL Press Ltd: London.
- Scoging, H., Parsons, A. J. and Abrahams, A. D. (1992) Application of a dynamic overland-flow model to a semi-arid hillslope, Walnut Gulch, Arizona *In* A. J. Parsons and A. D. Abrahams (Eds.) *Overland flow: Hydraulics and erosion mechanics* UCL Press Ltd: London.
- Sevilleta LTER data (2005) <http://sevilleta.unm.edu/data/archive/gis/#soils>. Accessed: 10/06/03.
- Shainberge, I. and Singer, M. J. (1985) Effect of electrolytic concentration on the hydraulic properties of depositional crust. *Soil Science Society of America Journal* **49**: 1260-1263.
- Smith, A. B. (1999) Hunters and herders in the Karoo landscape. *In* W. R. J. Dean and S. Dean (Eds.) *The Ecology of the Karoo*. Cambridge University Press, Cambridge, pp. 243-256.
- Smith, D. D. and Wischmeier, W. H. (1962) Rainfall erosion. *Advances in Agronomy* **14**: 109-148.
- Smith, R. E., Goodrich, D. C. and Quinton, J. N. (1995) Dynamic, distributed simulation of watershed erosion: The KINEROS2 and EUROSEM models. *Journal of Soil and Water Conservation* **50**(5): 57-520.
- Snelder, D. J. and Bryan, R. B. (1995) The use of rainfall simulation tests to assess the influence of vegetation density on soil loss on degraded rangelands in the Baringo District, Kenya. *Catena* **25**(1-4): 105-116.
- Soil Analysis: Handbook of reference methods. (2000) Soil and Plant Analysis Council, Inc. 1999. CRC Press.
- Sugden, J. M. (1989) *Palaeoecology of the Central and Marginal Uplands of the Karoo, South Africa*. University of Cape Town: Cape Town.
- Sun, B., Zhou, S. and Zhao, Q. (2003) Evaluation of spatial and temporal changes of soil quality based on geostatistical analysis in the hill region of subtropical China. *Geoderma* **115**: 85-99.
- Thomas, D. S., Holmes, P. J., Bateman, M. D. and Marker, M. E. (2002) Geomorphic evidence for late Quaternary environmental change from the eastern Great Karoo margin, South Africa. *Quaternary International* **89**: 151-164.

- Thomas, D. S. G. and Twyman, C. (2004) Good or bad rangeland? Hybrid knowledge, science, and local understandings of vegetation dynamics in the Kalahari. *Land Degradation and Development* **15**: 215-231.
- Thornes, J. B. (2005) Coupling erosion, vegetation and grazing. *Land Degradation and Development* **16**: 127-138.
- Tisdall, J. M. and Oades, J. M. (1982) Organic matter and water-stable aggregates in soils. *Journal of Soil Science* **33**: 141-163.
- Titus, J. H., Nowak, R. S. and Smith, S. D. (2002) Soil resource heterogeneity in the Mojave Desert. *Journal of Arid Environments* **52**: 269-292.
- Tongway, D. J. and Ludwig, J. A. (1994) Small-scale resource heterogeneity in semi-arid landscapes. *Pacific Conservation Biology* **1**: 201-208.
- Torri, D., Sfalanga, M. and Chisci, G. (1987) Threshold conditions for incipient rilling. *Catena supplement* **8**: 97-105.
- Torri, D., Costanza, C. and Rodolfi, G. (2000) Badlands in changing environments: an introduction. *Catena* **40**: 119-125.
- United Nations Convention to Combat Desertification: International Year of Deserts and Desertification* UNCCD (2006) <http://www.iydd.org/> Accessed: 02/11/06.
- Vaidya, P. H. and Pal, D. K. (2002) Microtopography as a factor in the degradation of Vertisols in Central India. *Land Degradation and Development* **13**: 429-445.
- Valentin, C., Poesen, J. and Li, Y. (2005) Gully erosion: Impacts, factors and control. *Catena* **63**: 132-153.
- Van Oost, K., Govers, G., Cerdan, O., Thauré, D., Van Rompaey, A., Steegen, A., Nachtergaele, J., Takken, I. and Poesen, J. (2005) Spatially distributed data for erosion model calibration and validation: The Ganspoel and Kinderveld datasets *Catena* **61**(2-3): 105-121.
- Vandekerckhove, L., Poesen, J., Oostwoud Wijdenes, D., Gysels, G., Beuselinck, L. and de Luna, E. (2000) Characteristics and controlling factors of bank gullies in two semi-arid mediterranean environments. *Geomorphology* **33**(1-2): 37-58.
- Wackernagel, H. (2003) *Multivariate Geostatistics: An introduction with applications*. Springer-Verlag Berlin and Heidelberg GmbH & Co.



- Wainwright, J., Parsons, A. J. and Abrahams, A. D. (1999) Rainfall energy under creosotebush. *Journal of Arid Environments* **43**: 111-120.
- Wainwright, J., Parsons, A. J. and Abrahams, A. D. (2000) Plot-scale studies of vegetation, overland flow and erosion interactions: case studies from Arizona and New Mexico. *Hydrological Processes* **14**: 2921-2943.
- Wang (2000) In Müller, E. N. (Unpublished thesis) *Scaling approaches to the modelling of water, sediment and nutrient fluxes within semi-arid landscapes, Jornada Basin, New Mexico*. University of London: London.
- Warren, A. (1998) Environmental science and desertification at the frontier, in *The arid frontier: interactive management of environment and development*, Eds. Bruins, H.J. and Lithwick, H., Kluwer, Dordrecht, 117-127.
- Watkeys, M. K. (1999) Soils of the arid south-western zone of Africa *In* W. R. J. Dean and S. J. Milton (Eds.) *The Karoo: Ecological patterns and processes* Cambridge University Press: Cambridge.
- Webster, R. and Oliver, M. A. (2001) *Geostatistics for Environmental Scientists*. John Wiley and Son, Ltd: Chichester.
- Westerman, R. L. (Ed.) (1991) *Soil testing and plant analysis (Third Edition)* Soil Science Society of America, Inc.: Madison, Wisconsin.
- Western, A. W., Bloschl, G. and Grayson, R. B. (1998) Geostatistical characterisation of soil moisture patterns in the Tarrawarra catchment. *Journal of Hydrology* **205**(1): 20-37.
- Westoby, M., Walker, B. and Noy-Meir, I. (1989) Opportunistic management for rangelands not at equilibrium. *Journal of Range Management* **42**(4): 266-274.
- Wiegand, T. and Jeltsch, F. (2000) Long-term dynamics in arid and semiarid ecosystems- synthesis of a workshop. *Plant Ecology* **150**: 3-6.
- Wild, A. (2001) *Soils and the Environment: An Introduction*. Cambridge University Press.
- Wright, D. and Rajper, I. (2000) An assessment of the relative effects of adverse physical and chemical properties of sodic soil on the growth and yield of wheat (*Triticum aestivum* L.). *Plant and Soil* **223**: 277-285.
- Wu, J., Gao, W. and Tueller, P. T. (1997) Effects of changing spatial scale on the results of statistical analysis with landscape data: A case study. *Geographical Information Sciences* **3**: 30-41.



- Wu, J., Jelinski, D. E., Luck, M. and Tueller, P. T. (2000) Multiscale analysis of landscape heterogeneity: Scale variance and pattern metrics. *Geographical Information Sciences* **6**(1): 6-19.
- Zak, D. R., Tilman, D., Parmenter, R. R., Rice, C. W., Fisher, F. M., Vose, J., Milchunas, D. and Martin, C. W. (1994) Plant Production and Soil Microorganisms in Late-Successional Ecosystems: A Continental-Scale Study. *Ecology* **75**(8): 2333-2347.
- Zhang, B., Zhao, Q. G., Horn, R. and Baumgartl, T. (2001) Shear strength of surface soil as affected by soil bulk density and soil water content. *Soil and Tillage Research* **59**(3-4): 97-106.